frontiers | Research Topics

Women in terrestrial microbiology 2022

Edited by
Katharina Kujala, Paola Grenni and
Anna Barra Caracciolo

Published in
Frontiers in Microbiology

ISSN 1664-8714
ISBN 978-2-8325-4096-1
DOI 10.3389/978-2-8325-4096-1

About Frontiers

Frontiers is more than just an open access publisher of scholarly articles: it is a pioneering approach to the world of academia, radically improving the way scholarly research is managed. The grand vision of Frontiers is a world where all people have an equal opportunity to seek, share and generate knowledge. Frontiers provides immediate and permanent online open access to all its publications, but this alone is not enough to realize our grand goals.

Frontiers journal series

The Frontiers journal series is a multi-tier and interdisciplinary set of open-access, online journals, promising a paradigm shift from the current review, selection and dissemination processes in academic publishing. All Frontiers journals are driven by researchers for researchers; therefore, they constitute a service to the scholarly community. At the same time, the *Frontiers journal series* operates on a revolutionary invention, the tiered publishing system, initially addressing specific communities of scholars, and gradually climbing up to broader public understanding, thus serving the interests of the lay society, too.

Dedication to quality

Each Frontiers article is a landmark of the highest quality, thanks to genuinely collaborative interactions between authors and review editors, who include some of the world's best academicians. Research must be certified by peers before entering a stream of knowledge that may eventually reach the public - and shape society; therefore, Frontiers only applies the most rigorous and unbiased reviews. Frontiers revolutionizes research publishing by freely delivering the most outstanding research, evaluated with no bias from both the academic and social point of view. By applying the most advanced information technologies, Frontiers is catapulting scholarly publishing into a new generation.

What are Frontiers Research Topics?

Frontiers Research Topics are very popular trademarks of the *Frontiers journals series*: they are collections of at least ten articles, all centered on a particular subject. With their unique mix of varied contributions from Original Research to Review Articles, Frontiers Research Topics unify the most influential researchers, the latest key findings and historical advances in a hot research area.

Find out more on how to host your own Frontiers Research Topic or contribute to one as an author by contacting the Frontiers editorial office: frontiersin.org/about/contact

Women in terrestrial microbiology: 2022

Topic editors

Katharina Kujala — University of Oulu, Finland

Paola Grenni — Water Research Institute, National Research Council, Italy

Anna Barra Caracciolo — National Research Council - Water Research Institute, Italy

Citation

Kujala, K., Grenni, P., Barra Caracciolo, A., eds. (2023). *Women in terrestrial microbiology: 2022*. Lausanne: Frontiers Media SA.

doi: 10.3389/978-2-8325-4096-1

Table of contents

frontiers | Frontiers in Microbiology

TYPE Editorial
PUBLISHED 27 November 2023
DOI 10.3389/fmicb.2023.1326145

OPEN ACCESS

EDITED AND REVIEWED BY
Jeanette M. Norton,
Utah State University, United States

*CORRESPONDENCE
Paola Grenni
paola.grenni@irsa.cnr.it

RECEIVED 22 October 2023
ACCEPTED 06 November 2023
PUBLISHED 27 November 2023

CITATION
Grenni P, Kujala K and Barra Caracciolo A (2023) Editorial: Women in terrestrial microbiology: 2022. *Front. Microbiol.* 14:1326145. doi: 10.3389/fmicb.2023.1326145

Editorial: Women in terrestrial microbiology: 2022

Paola Grenni[1,2]*, Katharina Kujala[3] and Anna Barra Caracciolo[1]

[1]Water Research Institute of the National Research Council, Montelibretti, Italy, [2]National Biodiversity Future Center (NBFC), Palermo, Italy, [3]Water, Energy, and Environmental Engineering Research Unit, University of Oulu, Oulu, Finland

KEYWORDS

PGPB, bioplastic, hyperarid soil microbiome, fungal decomposition, sustainable horticultural substrates, biodeteriogens in Egyptian pyramids, soil rare bacteria

Editorial on the Research Topic
Women in terrestrial microbiology: 2022

Although we have been discussing gender equality for many decades, in 2023 we have not yet reached it. When looking at science, and especially STEM (science, technology, engineering, and mathematics) research, it is clear that more efforts are needed to achieve gender equality. Women are still underrepresented in STEM research fields, with only 30% of the world's researchers being women, according to the UNESCO Institute for Statistics. Higher dropout rates, resulting in shorter academic careers, are common for women (Huang et al., 2020). While the share of female authors in scientific publications has increased over the last few decades (Huang et al., 2020; Sarabi and Smith, 2023), male authors still dominate the publishing landscape, and even when male and female authors have contributed equally to a publication (i.e., shared first authorship), it is more common to see the male author's name mentioned before the female author's (Broderick and Casadevall, 2019). Women are overall less likely to receive credit for their work than their male counterparts, as male researchers more often receive co-authorship than female researchers for similar tasks (Ross et al., 2022). This brings on a vicious cycle of lower visibility, lower impact, and, in consequence, lower funding and career opportunities (Van den Besselaar and Sandström, 2017). In particular, the higher career ranks, such as full professors, are still very much male-dominated (Van den Besselaar and Sandström, 2017).

There is evidence that gender-diverse teams tend to produce research output with a higher degree of novelty and impact (Sarabi and Smith, 2023). While the reasons for this are still unclear, it is likely that the integration and empowerment of women (i.e., acknowledgment and incorporation of their expertise) rather than strict gender ratios are the keys to high-impact research (Love et al., 2022). It is therefore in the interest of science and society to promote gender equality in STEM fields. To leverage female authors in STEM fields and give them a platform to promote their findings, Frontiers has launched a series of Research Topics celebrating International Women's Day. All publications on these Research Topics have a female researcher as the first author and, for some papers, also as the corresponding author. Our Research Topic, Women in Terrestrial Microbiology: 2022, features eight articles covering a wide range of terrestrial microbiology topics in which female researchers played the main role.

The articles presented discuss microbes from extreme habitats (Aguilera-Torres et al.; Demergasso et al.), microbes beneficial to plants (Boak et al.; Cuartero et al.; Pot et al.), microbes involved in organic matter degradation (Brabcová et al.; Bandini et al.), and microbial threats to ancient monuments (Rizk et al.).

Extreme environments such as the arid Atacama Desert or the exposed slopes of the Andes challenge microbial communities with various stressors such as desiccation, large temperature fluctuations, and changes in moisture. Demergasso et al. demonstrated in a simulated rainfall event that bacterial communities in the Atacama Desert have the potential to respond quickly to the improved conditions and initiate growth. In the Andes, plant growth-promoting bacteria were shown by Aguilera-Torres et al. to alleviate the environmental stress on xerophytic plants. Plant-beneficial bacteria were also the focus of Boak et al., who found that the type-II secretion systems of *Pseudomonas chloroaphis* are a valuable weapon against competitors and predators, thus helping to shape the microbial communities of the rhizosphere. Cuartero et al., on the other hand, investigated the impact of the sustainable farming practice of intercropping on soil microbial diversity and soil C and N cycling. Their study demonstrated the beneficial effects of intercropping on both microbial diversity and the abundance of plant-beneficial microbes. More sustainable practices were also the inspiration for the study by Pot et al., who looked into materials to replace peat, a popular growing substrate in horticulture, with more sustainable alternatives. They found that many of the tested options, e.g., green or vegetable composts, showed higher numbers of potentially plant-beneficial microbes than the traditional peat-based substrates. Microbial communities involved in organic matter degradation were the focus of the study by Brabcová et al.. They showed how fungal communities in decaying deadwood change over the course of the decay process. Moreover, these changes can be linked to microclimate factors such as pH and temperature in the wood. On a similar topic, but from a more applied perspective, Bandini et al. focused on how bioplastics, which are widely advocated as sustainable alternatives to traditional plastics, affect microbial communities during anaerobic digestion and aerobic composting. Indeed, the authors found a pronounced impact, which may indicate a need to adjust process parameters for digestion and composting if bioplastics are to be degraded in these systems in the future. The last study in our Research Topic dedicated to women researchers in Terrestrial microbiology takes us to Egypt, where Rizk et al. set out to characterize potential microbial threats to the pyramids. They found that the microbial communities in and on the stones of the pyramids also comprise such microbes that could increase the risk of physical and chemical deterioration of these valuable cultural heritage monuments, which needs to be considered in conservation efforts.

This Research Topic is a valid example of how women are able to coordinate high-level research.

Author contributions

PG: Writing—original draft, Writing—review & editing. KK: Writing—original draft, Writing—review & editing. ABC: Writing—review & editing.

Funding

The author(s) declare that no financial support was received for the research, authorship, and/or publication of this article.

Conflict of interest

The authors declare that the research was conducted in the absence of any commercial or financial relationships that could be construed as a potential conflict of interest.

The author(s) declared that they were an editorial board member of Frontiers, at the time of submission. This had no impact on the peer review process and the final decision.

Publisher's note

References

Broderick, N. A., and Casadevall, A. (2019). Gender inequalities among authors who contributed equally. *eLife* 8, e36399. doi: 10.7554/eLife.36399

Huang, J., Gates, A. J., Sinatra, R., and Barabási, A. L. (2020). Historical comparison of gender inequality in scientific careers across countries and disciplines. *Proc. Natl. Acad. Sci. U.S.A.* 177, 4609–4616. doi: 10.1073/pnas.1914221117

Love, H. B., Stephens, A., Fosdick, B. K., Tofany, E., and Fisher, E. R. (2022). The impact of gender diversity on scientific research teams: a need to broaden and accelerate future research. *Human. Soc. Sci. Commun.* 9, 386. doi: 10.1057/s41599-022-01389-w

Ross, M. B., Glennon, B. M., Murciano-Goroff, R., Berkes, E. G., Weinberg, B. A., and Lane, J. I. (2022). Women are credited less in science than men. *Nature* 608, 135–145. doi: 10.1038/s41586-022-04966-w

Sarabi, Y., and Smith, M. (2023). Gender diversity and publication activity – an analysis of STEM in the UK. *Res. Eval.* 32, 321–331. doi: 10.1093/reseval/rvad008

Van den Besselaar, P., and Sandström, U. (2017). Vicious circles of gender bias, lower positions, and lower performance: gender differences in scholarly productivity and impact. *PLoS ONE* 12, e0183301. doi: 10.1371/journal.pone.0183301

frontiers | Frontiers in Microbiology

ORIGINAL RESEARCH
published: 07 April 2022
doi: 10.3389/fmicb.2022.843092

The Type VI Secretion Systems in Plant-Beneficial Bacteria Modulate Prokaryotic and Eukaryotic Interactions in the Rhizosphere

*Emily N. Boak[1], Sara Kirolos[2], Huiqiao Pan[1,3], Leland S. Pierson III[4] and Elizabeth A. Pierson[1,4]**

[1] Department of Horticultural Sciences, Texas A&M University, College Station, TX, United States, [2] Department of Biology, Texas A&M University, College Station, TX, United States, [3] Department of Embryology, Carnegie Institution for Science, Baltimore, MD, United States, [4] Department of Plant Pathology and Microbiology, Texas A&M University, College Station, TX, United States

OPEN ACCESS

Edited by:
Eoin L. Brodie,
Lawrence Berkeley National Laboratory, United States

Reviewed by:
Jose Antonio Ibarra,
Instituto Politécnico Nacional (IPN), Mexico
Sophie Gaudriault,
Institut National de la Recherche Agronomique Centre Montpellier, France

***Correspondence:**
Elizabeth A. Pierson
elizabeth.pierson@ag.tamu.edu

Specialty section:
This article was submitted to Terrestrial Microbiology, a section of the journal Frontiers in Microbiology

Received: 24 December 2021
Accepted: 04 March 2022
Published: 07 April 2022

Citation:
Boak EN, Kirolos S, Pan H, Pierson LS III and Pierson EA (2022) The Type VI Secretion Systems in Plant-Beneficial Bacteria Modulate Prokaryotic and Eukaryotic Interactions in the Rhizosphere. Front. Microbiol. 13:843092. doi: 10.3389/fmicb.2022.843092

Rhizosphere colonizing plant growth promoting bacteria (PGPB) increase their competitiveness by producing diffusible toxic secondary metabolites, which inhibit competitors and deter predators. Many PGPB also have one or more Type VI Secretion System (T6SS), for the delivery of weapons directly into prokaryotic and eukaryotic cells. Studied predominantly in human and plant pathogens as a virulence mechanism for the delivery of effector proteins, the function of T6SS for PGPB in the rhizosphere niche is poorly understood. We utilized a collection of *Pseudomonas chlororaphis* 30–84 mutants deficient in one or both of its two T6SS and/or secondary metabolite production to examine the relative importance of each T6SS in rhizosphere competence, bacterial competition, and protection from bacterivores. A mutant deficient in both T6SS was less persistent than wild type in the rhizosphere. Both T6SS contributed to competitiveness against other PGPB or plant pathogenic strains not affected by secondary metabolite production, but only T6SS-2 was effective against strains lacking their own T6SS. Having at least one T6SS was also essential for protection from predation by several eukaryotic bacterivores. In contrast to diffusible weapons that may not be produced at low cell density, T6SS afford rhizobacteria an additional, more immediate line of defense against competitors and predators.

Keywords: T6SS, PGPB (plant growth-promoting bacteria), bacterivores, competition, *Pseudomonas*, rhizosphere ecology, GacS/GacA

INTRODUCTION

The rhizosphere, the area surrounding plant roots that is directly influenced by root exudates and the associated microorganisms that comprise the rhizosphere microbiome, is an important source of plant-beneficial microorganisms (Bakker et al., 2012; Berendsen et al., 2012; Pascale et al., 2020). The rhizosphere niche is shaped by a complex community of bacteria, archaea, fungi, protists and viruses and the cooperative, competitive, and predatory interactions among members and with the plant root. Bacteria employ many different strategies to buffer and protect themselves from abiotic and biotic stresses, especially competition with other microorganisms and

grazing by predators (Matz and Kjelleberg, 2005; Matz et al., 2005; Hibbing et al., 2010). These include multicellular behavior and formation of a biofilm community (Costerton, 1995; Yin et al., 2019) and the utilization of diverse secretion systems to deploy an arsenal of diffusible products enabling bacteria to defend or modify their "space" (Hibbing et al., 2010; Ghoul and Mitri, 2016; Stubbendieck and Straight, 2016; Dorosky et al., 2017; Granato et al., 2019). Many bacteria also have short-range mechanisms for the delivery of weapons or other products when in direct contact with sister cells or cells of other rhizosphere inhabitants of which the Type VI Secretion System (T6SS) is one of the best studied examples (Basler, 2015; Cianfanelli et al., 2016; Smith et al., 2020). It is becoming increasingly clear that T6SS mediate interactions important for competitive fitness in a variety of environments (Gallegos-Monterrosa and Coulthurst, 2021), although their roles in rhizosphere community dynamics and benefits to plant-beneficial bacteria is not well understood.

T6SS are needle-like injection systems and the encoding genes have been found in approximately 25% of Proteobacteria (Basler et al., 2013). T6SS have been shown to be important for the delivery of effector proteins into neighboring prokaryotic and eukaryotic cells and other intercellular interactions (Barret et al., 2011; Basler et al., 2013; Abby et al., 2016; Bernal et al., 2017b). Consequently, the primary focus of T6SS research has been on pathogenic bacteria and the role of T6SS in bacterial virulence and pathogenesis. A role for T6SS in virulence was first demonstrated using *Vibrio cholerae* and the bacterial predator *Dictyostelium discoideum* (Pukatzki et al., 2006). T6SS have been further implicated in virulence and killing of other eukaryotes such as *Caenorhabditis elegans*, an important bacterial predator and animal model organism (Vaitkevicius et al., 2006). T6SS have been shown to be important among human pathogens such as *Burkholderia pseudomallei, Pseudomonas aeruginosa, Vibrio cholerae,* and *Salmonella enterica* serovar Typhimurium and their T6SS have been linked directly to their virulence (Pukatzki et al., 2006; Basler et al., 2013; Aubert et al., 2016; Sana et al., 2016). T6SS are also important virulence factors among plant pathogens such as *Ralstonia solanacearum* and *Erwinia amylovora* (Tian et al., 2017; Asolkar and Ramesh, 2020). Although, T6SS have been well studied in pathogenic systems, much less information exists for their importance in the lifestyle of non-pathogenic organisms. Interestingly, many plant growth promoting bacteria (PGPB) also possess one or more T6SS (Loper et al., 2012; Marchi et al., 2013; Bernal et al., 2017a). Thus, it is likely that T6SS in PGPB may be involved in other functions related to their host-associated niche or plant beneficial activities.

Generally, T6SS are composed of 13–15 structural proteins divided into three interlocking structures: the intermembrane anchor, the baseplate, and the needle/sheath. The length of the entire structure has been shown to be determined by the width of the cell, which can measure up to 1 μm in length, allowing it to interact with both prokaryotes and eukaryotes (Basler et al., 2013; Abby et al., 2016; Bernal et al., 2017b; Santin et al., 2019). This needle is topped with a valine-glycine repeat protein G (VgrG) trimer, which is in turn topped by one proline-alanine-alanine-arginine (PAAR) repeat protein using hydrogen bonds (Shneider et al., 2013) and the PAAR protein acts as a sharpener enabling the end to penetrate neighboring cells (Ho et al., 2014; Basler, 2015). ClpV "recycles" the system by detaching the proteins and allowing them to reform elsewhere (Kapitein et al., 2013; Zoued et al., 2014). Other genes such as the serine/threonine kinase and phosphatase (*ppkA* and *pppA*) are associated with the genes encoding structural proteins, and PpkA and PppA are involved in the regulation of the firing of the system (Kulasekara and Miller, 2007; Chen et al., 2015).

A great deal of genetic diversity has been found among the operons encoding T6SS and many bacterial species have multiple T6SS-encoding operons that differ in terms of their genetic organization, the presence or absence of certain effectors, or their regulation (Chen et al., 2011, 2015; Loper et al., 2012; Spiewak et al., 2019). Efforts to characterize this diversity has led to T6SS-encoding operons being partitioned into five clades (Boyer et al., 2009; Bernal et al., 2017b). Characterization of T6SS using this clade system illustrates both the diversity in bacterial taxa having T6SS as well as the diversity of systems found within a single species. For example, *Burkholderia thailandensis* possesses five different T6SS and these systems have been shown to perform different roles (Schwarz et al., 2010). In *Pseudomonas*, T6SS may differ in terms of the type of stimuli that causes firing, e.g., contact-dependent firing or random firing. Contact-dependent firing is regulated by the signaling cascade TagQRST. This signaling cascade alerts the cell when damage has been caused to its membrane and triggers the formation of the T6SS in what is known as dueling behavior (Basler et al., 2013). In contrast, to fire randomly the TagQRST signaling cascade is not needed. Some *Pseudomonas* may have both dueling and random firing behavior, such as *P. fluorescens* Q287, which contains three T6SS clusters, one of which contains the TagQRST signaling cascade (Loper et al., 2012; Basler et al., 2013, this study). A direct method to predict T6SS function has not been established based purely on sequence analysis, but the genetic organization, effector types, and firing regulation are all possible determinants of functionality (Bernal et al., 2017b). Consequently, when more than one system is present within a species, it is possible that the systems perform different, non-redundant functions, increasing the repertoire of functionalities provided (Schwarz et al., 2010).

To gain a better understanding of the importance of T6SS for the rhizosphere lifestyle, we focused on *Pseudomonas chlororaphis* subsp. *aureofaciens* 30–84, a well-characterized plant PGPB that is an effective rhizosphere colonizer. Previous research demonstrated that production of phenazines, diffusible anti-microbial compounds, contributes to biofilm formation, rhizosphere competence, inhibition of fungal plant pathogens, plant disease suppression, and mediation of wheat seedling water and salt stress (Mazzola et al., 1992; Pierson and Thomashow, 1992; Maddula et al., 2006; Yu et al., 2018; Mahmoudi et al., 2019; Yuan et al., 2020). *P. chlororaphis* 30–84 also produces other diffusible weapons including hydrogen cyanide, several types of extracellular enzymes, and multiple R-tailocin particles, antibacterial proteins that resemble bacteriophage tails and target and kill other pseudomonads (Loper et al., 2012; Wang et al., 2013; Dorosky et al., 2017, 2018). The genome of *P. chlororaphis* 30-84 also encodes two genetically distinct T6SS (Loper et al., 2012, this study). With a diverse spectrum of diffusible protective

mechanisms already at its disposal, we questioned whether the two T6SS, close-range defensive weapons were important for competitive rhizosphere fitness. We hypothesized, if both T6SS were functional, they may serve non-redundant functions that contribute to the ability of this PGPB to survive the rhizosphere niche and promote plant health. To test this hypothesis, we created mutants defective in one or both T6SS and used these derivatives to characterize the role of each T6SS in rhizosphere competence, bacterial competition, and protection from bacterivores. To examine the role of the T6SS in the context of the entire arsenal of competitive mechanisms, we used an existing collection of mutants including derivatives deficient in the production of phenazines (but not T6SS activity) and a global regulatory mutant *P. chlororaphis* 30–84 GacA (Chancey et al., 1999). The expression of T6SS-encoding genes in *P. chlororaphis* 30–84 are notably down regulated in *gacS* and *gacA* mutants (Wang et al., 2013), as observed in other *Pseudomonas* species (Hassan et al., 2010; Records and Gross, 2010; Chen et al., 2015). The GacS/GacA two component system also controls the production of secondary metabolites (including phenazines), bacteriocins, and extracellular enzymes in *P. chlororaphis* 30–84 (Wang et al., 2013) as observed in other PGPB (Heeb and Haas, 2001; Jousset et al., 2009). Having derivatives deficient in specific competitive mechanisms enabled us to distinguish the role of each T6SS from other mechanisms that contribute to competitive fitness and protection from bacterivores.

MATERIALS AND METHODS

Bacterial Strains and Media

The bacterial strains and plasmids used in this study are described in **Table 1**. A spontaneous rifampin-resistant derivative of *P. chlororaphis* 30–84 was used in all studies, hereafter referred to as wild type (30–84 WT). *P. chlororaphis* and wheat rhizosphere test strains were grown at 28°C in the following media: Luria-Bertani (LB) (Fisher BioReagents, Hampton, NH, United States), AB minimal (2% glucose) (Chilton et al., 1974) amended with 2% casamino acids (AB + CAA) (CAA is from BD Bacto, San Jose, CA, United States) or King's medium B (KMB) (King et al., 1954). *Escherichia coli* was grown at 37°C in LB medium, unless otherwise noted. *E. coli* and *Pseudomonas* strains were grown in liquid culture with agitation (200 rotations/min) or on solid medium (amended with agar at 15 g/l). Antibiotics were used in the following concentrations for *E. coli:* kanamycin (Km), gentamicin (Gm), carbenicillin (Cb), and 5-bromo-4-chloro-3-indolyl-β-D-galactopyranoside (X-gal) at 50, 15, 100, and 40 μg/ml, respectively; and for *P. chlororaphis:* Km, Gm, Cb, rifampicin (Rif), and cycloheximide at 50, 50, 100, 100, and 100 μg/ml, respectively.

Phylogenetic Analysis of Chromosomal Regions Containing Two Putative T6SS

Pseudomonas chlororaphis 30–84 genes annotated as encoding two T6SS are shown in **Figure 1**. We determined how these two T6SS compared to clades established by Boyer et al. (2009) and expanded by Bernal et al. (2017b). The amino acid sequences encoded by four highly conserved genes, *tssB, tssC, tssK,* and *tssM,* from each of the two *P. chlororaphis* 30–84 T6SS and the corresponding sequences from five species representing each clade were retrieved from the National Center for Biotechnology Information (NCBI) database and compared using BLASTp (Altschul et al., 1990). Based on levels of amino acid sequence identity, the *P. chlororaphis* 30–84 proteins were most similar to proteins in clades 3, 1.1, and 4A. The same *P. chlororaphis* 30–84 amino acid sequences were then compared to the corresponding amino acid sequences of 12 other plant-associated species belonging to clade 1.1, 3, or 4A. Also included were corresponding amino acid sequences from several biological control strains (Loper et al., 2012). The sequences were aligned using MUSCLE (MUltiple Sequence Comparison by Log-Expectation) through the program MEGA7 (Kumar et al., 2016). Once aligned, the Jones, Taylor, and Thorton (JTT) model in MEGA7 and bootstrap analysis with 1000 bootstrap replicates was used to build a maximum likelihood (ML) tree for each of the conserved genes. The program FigTree v1.4.4 (Rambaut, 2009; Gardner and Hall, 2013) was used to visually represent the ML trees.

Generation of Single and Double T6SS Mutants

A derivative of *P. chlororaphis* 30-84 containing a *tssA-2* deletion mutation (ΔTssA2) was generated using the suicide vector pEX18Ap and using methods described previously (Hmelo et al., 2015). Briefly, DNA sequences (1,000 nucleotides [nt]) flanking the gene *tssA-2* were amplified by two-step PCR using the primer pairs TssA2KO-UP-F-*Eco*RI and TssA2KO-UP-R-*Kpn*I, and TssA2KO-DWN-F-*Kpn*I and TssA2KO-DWN-R-*Hin*dIII, respectively (**Supplementary Table S1**). Amplification using primers TssA2KO-UP-F-*Eco*RI and TssA2KO-DWN-R-*Hin*dIII and using the product of the previous PCRs as a template resulted in a construct that contained the upstream fragment separated from the downstream fragment by a *Kpn*I restriction site. This fragment was ligated into the *Eco*RI and *Hin*dIII restriction enzyme sites in the multiple-cloning region of pEX18a to create plasmid pEX18A + TSSA2. A kanamycin resistance cassette with its promoter was obtained via PCR amplification using pUC4K as the template and the primers TssA2KO-UP-R-*Kpn*I and TssA2KO-DWN-F-*Kpn*I and ligated between the upstream and downstream fragments at the *Kpn*I site in pEX18Ap. The final construct (pEX18A + TSSA2/KMR) was transformed into *E. coli* DH5α, and transformants were selected on LB amended with Km and Xgal. After conjugation, double-crossover mutants into *P. chlororaphis* were obtained by counterselection on LB amended with Rif, Km, and 6% sucrose and confirmed using PCR primers specific to the internal regions of *tssA-2.* PCR was performed using GoTaq® Green Master Mix (Promega, Madison, WI, United States) according to manufacturer recommendations. *E. coli* transformation and *P. chlororaphis* conjugation were performed as described previously (Pierson and Thomashow, 1992; Wang et al., 2012).

A derivative of *P. chlororaphis* 30-84 containing a *tssA-1* deletion mutation (ΔTssA1) was generated using the

TABLE 1 | Bacteria strains and plasmids used in this study.

Strain	Description	References
Pseudomonas		
P. chlororaphis 30–84 WT	"Wild type," Rif^r	Pierson and Thomashow, 1992
P. chlororaphis 30–84 ZN	Phz$^-$, Rif^r, *phzB:lacZ* genomic fusion	Pierson et al., 1994
P. chlororaphis 30–84 GacA	Phz$^-$ Rif^r spontaneous *gacA* mutant	Chancey et al., 1999
P. chlororaphis 30–84 I/I2	*phzI:npt* and *csaI:uidA-Gm* genomic fusion, Gm^r	Zhang and Pierson, 2001
P. chlororaphis 30–84 ΔTssA1	T6SS-1 mutant: Pchl3084_RS17705 replaced with Km^r cassette	This study
P. chlororaphis 30–84 ΔTssA2	T6SS-2 mutant: Pchl3084_RS00080 replaced with Km^r cassette	This study
P. chlororaphis 30–84 ΔTssA1/2	T6SS-1/2 mutant with Pchl3084_RS17705 replaced with Km^r and Pchl3084_RS00080 replaced with Gm^r cassette	This study
***Pseudomonas* rhizosphere colonizing, biocontrol strains**		
P. protegens Pf-5	Rhizosphere associated PGPB (formerly *P. fluorescens* Pf-5) with T6SS-encoding genes	Howell, 1979
P. synxantha 2-79	Rhizosphere associated PGPB (formerly *P. fluorescens* 2-79) without T6SS-encoding genes	Weller and Cook, 1983
P. fluorescens Q2-87	Rhizosphere associated PGPB with T6SS-encoding genes	Pierson and Weller, 1994
Environmental and Plant Pathogenic Strains		
Pseudomonas putida F1	Environmental isolate, without T6SS-encoding genes	https://genome.jgi.doe.gov/portal/psepu/psepu.home.html
Pseudomonas syringae pv. *tomato* DC3000	Plant pathogen with functional T6SS	Petnicki-Ocwieja et al., 2002
Agrobacterium tumefaciens C58	Plant pathogen with functional T6SS	Ma et al., 2014
Pectobacterium carotovorum subsp. *carotovorum*	Plant pathogen with T6SS-encoding genes	Lei et al., 2019
Escherichia coli		
E. coli DH5α	*F$^-$recA1 endA1 hsdR17 supE44 thi-1 gyrA96 relA1* Δ(argF-lacZYA) Iq69 Φ80lacZΔM15λ$^-$	GIBCO-BRL
E. coli HB101	F$^-$ *hsds20*($r_B^-m_B^-$)*supE44recA1 ara14 proA2 lacY1 galK2 rpsL20 xyl-5 mtl-5*λ$^-$	GIBCO-BRL
*E. coli delta*B	*D. discoideum* food source	*Dictyostelium* Stock Center
E. coli OP50	*C. elegans* food source	Brenner, 1974
Plasmids	**Description**	**References**
pEX18Ap	Ap^r	Hoang et al., 1998
pUC4K	Km^r, Ap^r	Grindley and Joyce, 1981
pUCP20Gm	Gm^r, pUCp20 derivative containing constitutive promoter P_{lac} with *Sma*I-flanked Gm^r cassette inserted into the unique *Sca*I site within *bla*	Chiang and Burrows, 2003
pEX18A + TSSA2	pEX18A containing *tssA-2* upstream and downstream sequences separated by a *Kpn*I restriction site	This study
pEX18A + TSSA2/KMR	pEX18A containing *tssA-2* upstream and downstream sequences separated by a Km resistance cassette	This study
pEX18A + TSSA1/KMR	pEX18A containing *tssA-1* upstream and downstream sequences separated by a Km resistance cassette	This study
pEX18A + TSSA2/GMR	pEX18A containing *tssA-2* upstream and downstream sequences separated by a Gm resistance cassette	This study

Ap^r, Km^r, Gm^r, Rif^r indicate ampicillin, kanamycin, gentamicin, and rifampin, respectively.

suicide vector pEX18Ap. Briefly, DNA sequences upstream (∼1200 nt) and downstream (∼1,100 nt) flanking *tssA-1* were amplified via PCR using the primer pairs TssA1KO-repliQa-UP-F and TssA1KO-repliQa-UP-R, and TssA1KO-repliQa-DWN-F and TssA1KO-repliQa-DWN-R, respectively (**Supplementary Table S1**). The kanamycin resistance cassette with its promoter was amplified via PCR using pUC4K as the template and primers TssA1KO-repliQa-KmR-F and TssA1KO-repliQa-KmR-R. The final construct (pEX18A + TSSA1/KMR) was obtained using repliQa HiFi Assembly according to the manufacturer ("RepliQa HiFi ToughMix | Superior Speed and Inhibitor Tolerance | Quantabio, 2021"). DH5α transformants were selected on LB

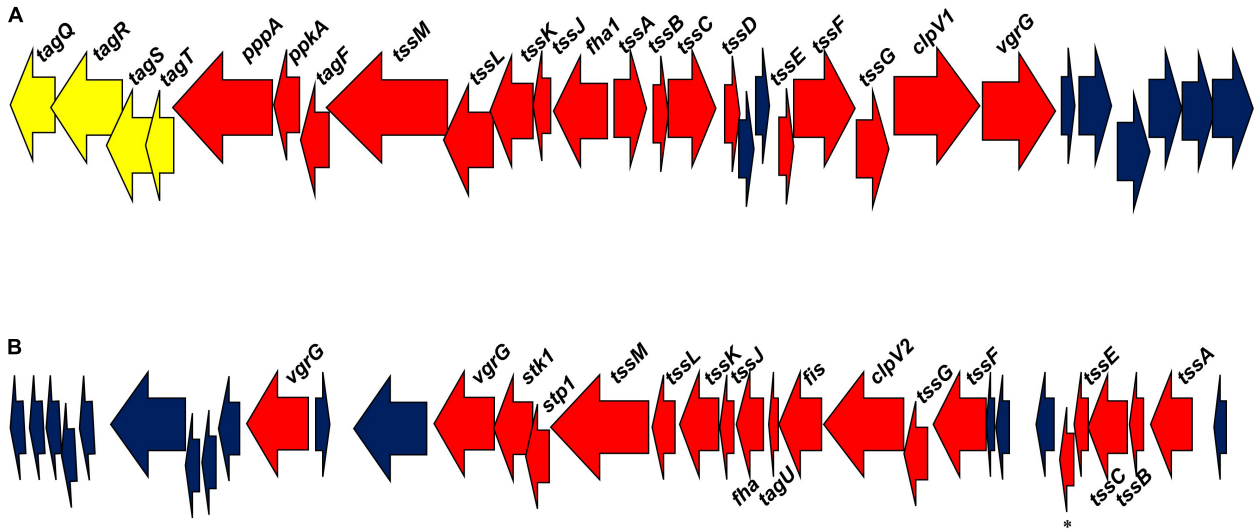

FIGURE 1 | *Pseudomonas chlororaphis* 30–84 T6SS gene clusters. **(A)** The T6SS-1 cluster of genes. **(B)** The T6SS-2 cluster of genes. Red arrows designate genes encoding conserved proteins involved in T6SS structure and function. Blue arrows designate genes encoding hypothetical proteins. Yellow arrows designate genes encoding proteins associated with the TagQRST system in T6SS-1. *Refers to a gene encoding a T6SS protein with a PAAR domain.

amended with Km and Xgal. *P. chlororaphis* double-crossover mutants were obtained by counterselection on LB amended with Rif, Km and 6% sucrose and confirmed using PCR primers specific to the internal regions of *tssA-1*.

To generate the double mutant ΔTssA1/2, a gentamicin resistant cassette with its promoter was amplified using the plasmid pUCP20Gm as the template and the primer pairs DoubleKO-GnR + A2UP-R and DoubleKO-GnR + A2DWN-F. The plasmid pEX18A + TSSA2 was digested with *Kpn*I. The final construct containing the gentamicin resistance cassette (pEX18A + TSSA2/GMR) inserted at the *Kpn*I site was obtained using repliQa HiFi Assembly. The plasmid pEX18A + TSSA2/GMR was transformed into *E. coli* DH5α and transformants were selected on LB amended with Gm and Xgal. *P. chlororaphis* double-crossover mutants in ΔTssA1 were obtained by counter selection on LB amended with Rif, Km, Gm and 6% sucrose and confirmed using PCR primers specific to the internal regions of *tssA-1* and *tssA-2*.

Growth in Planktonic Culture and Surface Attached Biofilms

The strains 30-84 WT, ΔTssA1, ΔTssA2, and ΔTssA1/2 were grown in LB medium at 28°C with agitation and the optical density (OD_{620}) was measured at one-hour intervals until 8 h and then at two-hour intervals between 24 and 30 h The experiment was performed with two biological replicates and repeated three times.

Surface attached biofilm formation was quantified via 96-well microtiter assay routinely used in our lab (Maddula et al., 2006) with slight modifications. Briefly, pre-cultures were grown in LB medium (28°C, with agitation, 16 h). These cultures were resuspended in fresh LB medium and grown to a final cell density of OD_{620} = 0.8. Each strain (1.2 μL) was inoculated into 120 μL AB + CAA in separate wells of a 96 well polystyrene cell culture plate (Corning Inc., Corning, NY, United States). The plate was incubated at 28°C for 72 h without agitation in a sealed container to minimize evaporation. Unattached cells were removed by inversion of the plate with vigorous tapping. The adherent bacteria were fixed to the plate (20 min, 50°C) and stained (1 min, 150 μL of 0.1% crystal violet). Excess stain was removed by inversion of the plate followed by two washings with sterile distilled water. The adherent cells were decolorized (to release the dye) with a 20% acetone/80% ethanol solution (200 μL, 5 min, room temperature). A sample (100 μL) of each well was transferred to a new 96-well plate and the amount of dye (proportional to the density of adherent cells) was quantified (OD_{540}). The experiment was performed with two biological replicates (separate colonies) and five technical replicates and repeated three times.

Rhizosphere Colonization and Persistence Assay

We used repeated planting/harvest cycles to evaluate rhizosphere persistence as described previously (Mazzola et al., 1992). The assay was performed using methods described previously (Dorosky et al., 2017) with minor modifications. Soil used for rhizosphere experiments was a Pullman clay loam collected from the USDA-ARS, Bushland, TX dryland wheat plots at a depth of 1–15 cm. Prior to use in experiments, it was necessary to sieve (2 mm mesh) and mix the soil with sand (soil:sand, 2:1, v:v) to facilitate drainage as described previously (Mahmoudi et al., 2019). The soil-sand mix is hereafter referred to as soil. The hard red winter wheat cultivar TAM 304 (Rudd et al., 2015) was used for all rhizosphere studies.

Bacteria were grown overnight with antibiotic selection, washed twice with sterile water, and resuspended in sterile water at a final concentration of 1×10^9 CFU/mL. Inoculum was added to either steam-sterilized soil (autoclaved twice: 121°C, 15 psi, 45 min, 24 h pause between cycles) or untreated (field) soil. Final bacterial concentrations were adjusted to 10^6 CFU/g by dilution using sterile water, adding the diluted suspension to soil (20 mL solution per 500 g), and mixing thoroughly daily for four days. Soil was then added to clean conical plastic growth tubes (Ray Leach Cone-tainers, 4 cm diameter, 21 cm height).

Wheat seeds (TAM 304) were surface disinfested by incubation in 10% bleach (10 min.) and then washed with sterile water (five times for 1 min. each). Disinfested seeds were pregerminated on germination paper for 48 h. The seedlings were planted in the growth tubes four days after the soil was inoculated with bacteria. A total of 50 plants were sown at the start of the experiment. Plants were grown on a light bench (8 h:16 h dark/light cycle, room temperature) and given sterile water (10 mL) every five days. After 20 days of growth, 10 of the 50 plants from each treatment were randomly selected and harvested and rhizosphere populations determined. The unharvested plants (remaining 40 of the 50 plants/treatment) were removed individually from their containers, the shoot system was excised and discarded, and the soil and root system were transferred to a clean paper cup, mixed by shaking, and returned to the conical growth tube from which they were obtained. This soil was then replanted with disinfested, pregerminated wheat seeds to initiate the second 20-day planting/harvest cycle. At each harvest, 10 of the remaining plants from each treatment were harvested and rhizosphere populations determined. The planting to harvest cycle was repeated for a total of five cycles. The entire experiment was repeated three times.

In vitro and Rhizosphere Competition Assays

Competitive fitness assays compared the populations of competitors grown separately and in 50:50 mixed cultures *in vitro*. Briefly, bacterial strains were grown overnight in LB at 28°C with agitation (200 rpm), harvested, washed, and resuspended in fresh medium (cell densities were adjusted to OD_{620} = 0.5) before creating the single strain or mixed starting cultures. Mixed cultures were prepared using equal volumes of competitors. A total of 10 μl per treatment was placed onto ∼ 1 cm^2 pieces of nitrocellulose filter paper on LB plates, and plates were incubated at 28°C for 5 h. Nitrocellulose papers then were transferred separately to sterile tubes containing 1 mL sterile water (sufficient to cover filter paper), and cells were collected by vortexing for 30 s twice with a 5 min. rest in between. Bacterial populations were enumerated via serial dilution plating on LB after 48 h. *P. chlororaphis* 30–84 and derivative appear bright orange on plates making them easy to distinguish from competitors. A competitive ratio was calculated by standardizing the population size of each strain in mixture to the population size of that strain without a competitor. The experiment was performed with five biological replicates and repeated three times.

Competitive fitness assays comparing the growth of competitors grown separately and in 50:50 mixed cultures in the wheat root rhizosphere were performed similar to previous methods (Dorosky et al., 2017). The inoculum was prepared as described for the *in vitro* assay, but the final total cell density used to inoculate seeds was 10^9 CFU/ml (OD_{620} = ∼1.0). Wheat seeds were surface disinfested and pregerminated (as described above) and then suspended in bacterial inoculum for 10 min. The seeds were sown into steam-sterilized soil (prepared as above). Plants were grown and maintained as above. After 28 days, the entire root system and loosely adhering soil was transferred to a sterile plastic tube (15 mL), immersed in 5 mL of sterile water and sonicated and vortexed three times (10 s each). Serial dilutions were plated onto LB amended with cycloheximide and bacterial populations quantified after 48 h. The roots were dried for 48 h at 65°C and populations were standardized to root dry weight. Competitive ratios were calculated as above. The experiment was performed with 8–10 replicates/treatment and repeated three times.

Predator-Prey Studies

Dictyostelium discoideum

Dictyostelium discoideum strain AX2 was purchased from the *Dictyostelium* stock center (Fey et al., 2013). *D. discoideum* cells were grown in SIH medium (Formedium, Hunstanton, United Kingdom) with agitation as described previously (Brock and Gomer, 1999; Rijal et al., 2019). *D. discoideum* cells were collected by centrifugation (500 × *g*, 3 min.), resuspended/washed in fresh SIH twice, and resuspended at a final concentration of 1×10^6 cells/mL in SIH (determined via direct counts using a hemocytometer). *D. discoideum* cells (1 mL/well) were added to 24-well plates (Cat. #353047, Corning, NY, United States), allowed to adhere for 30 min., and then the liquid medium was replaced with low nutrition PBM or high nutrition HL5 (Phillips and Gomer, 2012).

Bacterial cultures were grown in LB media for 16 h, and bacterial cells were collected by centrifugation (2,000 × g, 1 min.) and resuspended in PBM. Bacterial cultures were then standardized to a low cell density (OD_{600} = 0.1) and added to the wells containing *D. discoideum* cells. Bacteria used as prey in the feeding assay included 30–84 WT, ΔTssA1, ΔTssA2, ΔTssA1/2, and *P. chlororaphis* derivatives 30–84 GacA, 30–84 I/I2, or 30–84 ZN. *D. discoideum* cells growing without bacteria as a food source or with *E. coli*ΔB (used in lab as a preferred prey source) were used as controls. After 24 h, the mixed cultures were slowly resuspended with a pipettor to detach the *D. discoideum* cells from the wells and 200 μL from each well was transferred into a 96-well microtiter-plate suitable for microscopy (#160822/1, ibidi, Martinsried, Germany). The *D. discoideum* cells were left to adhere for 30 min. Differential Interference Contrast (DIC) images were obtained using a Nikon Ti2 Eclipse Microscope (40X, 100X oil). Another 200 μL

from each well was used for serial dilutions to determine bacterial populations.

To measure Contact Site A protein (CsA) and Discoidin I levels in D. discoideum cells, the phagocytosis assay was performed as above. After 24 h, the supernatant was removed from each well and 200 mL of 2X SDS sample buffer was added to each well. The cells were collected by pipetting up and down repeatedly. The collected material was then heated to 95°C for 5 min. Samples were electrophoresed and blotted as described previously (Bakthavatsalam et al., 2008) except that the blots were blocked in 5% non-fat skim milk (Difco, Franklin Lakes, NJ, United States) in PBST [Phosphate Buffered Saline (pH 7.4) + 0.1% Tween-20] for 1 h and stained as previously described (Rijal et al., 2019) with either 1:500 #20-121-1-s anti-CsA (Developmental Studies Hybridoma Bank, Iowa City, IA, United States), 1:500 #80-52-13-s anti-Discoidin I (Developmental Studies Hybridoma Bank, Iowa City, IA, United States) or 1:1000 #13E5 beta-Actin (Cell Signaling Technology, Danvers, MA, United States) and then using a a secondary antibody 1:2500 #715-036-150 peroxidase-conjugated donkey anti-Mouse IgG (Jackson ImmunoResearch, West Grove, PA, United States) or 1:2500 #711-036-152 peroxidase-conjugated donkey anti-Rabbit IgG (Jackson ImmunoResearch, West Grove, PA, United States). Staining was detected with Supersignal West Pico PLUS Chemiluminescent Substrate for 10 min. (Cat # 34087, Thermo, Waltham, MA, United States). Images of the membranes were taken using a BioRad ChemiDoc XRS system and quantified using the Image Lab software (Bio-Rad, Hercules, CA, United States). Band intensities were normalized to the corresponding total actin band intensity.

To determine the effect of predation on bacterial fitness, a bacterial clearing assay was performed as described previously (Phillips and Gomer, 2010). Briefly, bacterial cultures and *D. discoideum* cells were grown and collected as described above but the final concentration of *D. discoideum* was adjusted to 500,000 cells/mL. 100 μL of each bacterial culture were spread onto SM/5 (pH = 6.5) medium plates and 10 μL of *D. discoideum* was then transferred to the center of the plate. Plates were incubated at 22°C for 5 days and the diameter of the zone of clearing was measured after 2 and 5 days. The experiment was repeated using four biological replicates.

Tetrahymena thermophila

For the feeding assay, *T. thermophila* CU427 (*Tetrahymena* Stock Center, Cornell University, Ithaca, NY, United States) were grown according to a previous protocol with minor modifications (Wilson et al., 1999). Briefly, *T. thermophila* was grown in PPYS (2% proteose peptone, 90 μM sequestrene, 0.2% yeast extract) liquid medium overnight with agitation (200 rpm, 30°C) and then transferred to 200 mL fresh media. Populations were adjusted to 3×10^5 cells/20 mL via direct population counts using a hemocytometer and Leitz (Epivert) microscope (100X). Bacterial cultures were grown in LB for 16 h, and bacterial cells were collected by centrifugation (3,000 × *g*, 15 min) and washed with an equal amount of sterile water. Bacterial cultures were then standardized to a low cell density (OD_{620} = 0.1). Bacteria used as prey in the feeding assay included 30–84 WT, ΔTssA1, ΔTssA2, ΔTssA1/2, 30–84 GacA, 30–84 I/I2, or 30–84 ZN. *T. thermophila* without prey bacteria was used as a control. Bacterial and *T. thermophila* cultures were mixed (5 mL, 20 mL, respectively) and grown in 50 mL tubes with agitation (200 rpm, 27°C). After 4 h and 24 h, *Tetrahymena* populations in mixed cultures were enumerated via direct counts using a hemocytometer.

For the mating assay, *T. thermophila* with different germlines, CU427 and CU330, were selected. These were selected as they are non-self-cells of different germlines and will reproduce together (Cervantes et al., 2013). CU427 and CU330 (*Tetrahymena* Stock Center, Cornell University) were grown in PPYS liquid media overnight (200 rpm, 30°C) and collected via centrifugation (3,000 × *g*, 10 min.) and washed in an equal amount of 10 mM Tris Buffer (pH = 7.4) twice. *T. thermophila* were grown overnight (200 rpm, 30°C) in 10 mM Tris Buffer to induce starvation and then populations were standardized to a cell density of $1.5 - 2 \times 10^5$/10 mL (via direct counts). Bacterial cultures were prepared as described above and standardized to OD_{620} = 0.1. *T. thermophila* CU427 and CU330 cultures were mixed in equal amounts (10 mL each) with 1 mL of the bacterial culture. After 4 h the treatments were viewed under the Leitz (Epivert) microscope, and the frequency of mated cell pairs (number of mated pairs/total number of observations) determined. Mating is defined by the joining to two *T. thermophila* cells vs. cells that remain single. This experiment was repeated three times.

Caenorhabditis elegans

Caenorhabditis elegans N2 hermaphrodites (*Caenorhabditis* Genetics Center, University of Minnesota, Minneapolis, MN, United States) were partially synchronized by allowing the nematodes to crowd a Nematode Growth Media (NGM) plate (Brenner, 1974) and consume all of their food source. Once the eggs produced on this plate hatched to stage L1 they were removed to a fresh NGM plate with *E. coli* OP50 for food and allowed to grow (20°C) to stage L4. Once mature, five L4 adult nematodes were selected and placed onto new NGM plates inoculated with one of the different prey bacteria: *E coli* OP50 (control), 30–84 WT, ΔTssA1, ΔTssA2, ΔTssA1/2, 30–84 GacA, 30–84 I/I2, or 30–84 ZN. Nematodes were allowed to lay eggs for 1 h (at room temperature) and then transferred to a new prey-containing plate. This transfer protocol was repeated until there were four plates per treatment, with the original nematodes being removed from the fourth plate. The plates were observed every 24 h for 72 h. The numbers of immature and mature nematodes were enumerated, and the percentage of adult nematodes calculated. Images of the plates were taken after 72 h using a Zeiss Stemi SV11 scope (26X magnification) and a Hamamatsu ImagEM EM-CCD camera. Bacterial clearing was estimated from total space occupied by *C. elegans* at the end of 72 h. Experiments were replicated three times.

Statistical Analyses

All data presented are the mean ± the standard error from at least two experiments. Unless otherwise indicated, multiple comparisons were analyzed ($\alpha = 0.05$) using ANOVA and either Tukey HSD or Student's *t* tests and significant differences ($P < 0.05$) are indicated by lowercase letters. All data were

analyzed using JMP Version 16 Software (SAS Institute Inc., Cary, NC, United States).

RESULTS

Pseudomonas chlororaphis 30–84 Has Two Putative T6SS

Pseudomonas chlororaphis 30–84 contains two separate T6SS gene clusters, T6SS-1 and T6SS-2 (**Figure 1**), both of which contain genes encoding at least 12 of the 13 conserved T6SS proteins (*tssA-tssM*). These proteins combine into subunits that make the three structures necessary for T6SS formation: the intermembrane structure (composed of the proteins TssJ, TssL, and TssM); the baseplate structure (composed of TssE, TssF, TssG, and TssK); and the sheath and needle-like structure (TssB, TssC and Hcp/TssD) with TssA coordinating the assembly of the final structure (Planamente et al., 2016; Zoued et al., 2017). The gene encoding Hcp is not present in the T6SS-2 cluster, but an additional putative *hcp* gene is found elsewhere in the genome. The needle-like structure is topped with a valine-glycine repeat protein G (VgrG/TssI) trimer that in most cases is associated with effector proteins (Ho et al., 2014). The proline-alanine-alanine-arginine (PAAR) repeat protein sits atop VgrG and acts as a sharpener enabling the end to penetrate neighboring cells (Shneider et al., 2013; Ho et al., 2014; Basler, 2015). Both T6SS-1 and T6SS-2 have genes encoding putative VgrG proteins associated with their clusters (one and two genes, respectively), and an additional seven putative VgrG-encoding genes are found elsewhere in the genome. Only the T6SS-2 contains a gene encoding PAAR protein in its cluster, with nine more putative PAAR protein-encoding genes occurring elsewhere in the genome. ClpV (TssH) is involved in recycling the system (Kapitein et al., 2013; Zoued et al., 2014) and is found in both T6SS clusters. Hcp, VgrG, and PAAR proteins are associated with the delivery of effectors (Ho et al., 2014) and effectors are frequently identified based on their proximity to the encoding genes in the genome (Spiewak et al., 2019). The locations of these genes in the genome were used to search for putative effectors associated with both T6SS.

The two T6SS differ in organization. In T6SS-1, the structural genes are divergently transcribed whereas in T6SS-2 the genes are transcribed in the same direction. Additionally, the genes encoding the regulation cascade system TagQRST, shown previously to be responsible for contact-dependent firing used in T6SS dueling (Basler et al., 2013) are found only within T6SS-1 gene cluster, suggesting this system may be fired in a contact-dependent manner. Genes encoding a serine/threonine kinase (PpkA) required to phosphorylate the protein Fha for the dueling signal to be received and induce T6SS formation and a serine/threonine phosphatase (PppA) required to dephosphorylate Fha allowing the T6SS to be dismantled and recycled by ClpV (Casabona et al., 2013; Ho et al., 2014) are also present in T6SS-1. Although the T6SS-2 cluster lacks the Tag regulatory cascade, it contains genes encoding a serine/threonine kinase (Stk1), Fha, and a serine/threonine phosphatase (Stp1), suggesting random firing as seen in other systems (Basler and Mekalanos, 2012). Based on the differences in the organization and regulation of these systems, we hypothesized that they respond to different stimuli and potentially serve non-redundant functions.

We compared the two *P. chlororaphis* 30-84 T6SS clusters to the genetic clades established by Boyer et al. (2009) and expanded by Bernal et al. (2017b). The predicted amino acid sequences of four highly conserved structural genes, *tssB, tssC, tssK,* and *tssM* from T6SS-1 and T6SS-2 and the corresponding sequences from five species representing each clade were compared using BLASTp. Based on the levels of amino acid sequence identity, the proteins in T6SS-1 were most similar to clade 3, whereas the amino acid sequences in T6SS-2 were similar to both clades 1.1 and 4A. The predicted amino acid sequences of these genes in T6SS-1 and T6SS-2 were then compared to corresponding sequences from 12 other plant-associated species belonging to clade 1.1, 3, or 4A. Maximum likelihood trees were constructed for each protein and confirmed that the amino acid sequences in T6SS-1 group aligned optimally with clade 3. Clade 3 includes T6SS from a wide variety of genera, including the *P. aeruginosa* T6SS involved in contact-dependent dueling (Basler et al., 2013). The amino acid sequences in T6SS-2 predominately align with clade 1.1 (although a single strain belonging to 4A clustered nearby), which includes T6SS from many different pseudomonads such as *P. fluorescens* strains that appear to be random firing systems (Bernal et al., 2017b). The maximum likelihood tree for TssB (also used for clade analysis by Bernal et al., 2017b) appears in **Supplementary Figure S1**.

Growth of *Pseudomonas chlororaphis* T6SS Mutants

To study the function of each T6SS, mutants were generated to disrupt T6SS assembly via deletion of *tssA* in each system and double mutants generated in both systems. In planktonic culture, there was no difference in the growth rates of 30–84 WT or the single T6SS mutants (ΔTssA1 and ΔTssA2), although the double mutant (ΔTssA1/2) consistently grew somewhat slower and reached a slightly lower cell density after 30 h (**Supplementary Figure S2A**). However, in surface-attached biofilms, population levels of 30-84 WT and the single or double T6SS mutants were no different after 72 h (**Supplementary Figure S2B**).

We also looked at the ability of 30–84 WT, ΔTssA1, ΔTssA2, and ΔTssA1/2 to colonize and persist in the wheat rhizosphere after multiple plant/harvest cycles in steam-sterilized and untreated field soil. No differences in the rhizosphere populations of strains were observed at the end of one harvest cycle in either sterile or field soil (**Figure 2**), indicating no loss in colonizing ability by the mutants. In the steam-sterilized soil, although the rhizosphere populations were slightly smaller at the end of five plant harvest cycles compared to the first harvest, there were still no statistical differences among treatments. In contrast, in natural soil the rhizosphere populations of ΔTssA1/2 were significantly reduced compared to 30–84 WT, whereas populations of ΔTssA2 were intermediate (**Figure 2**). These data

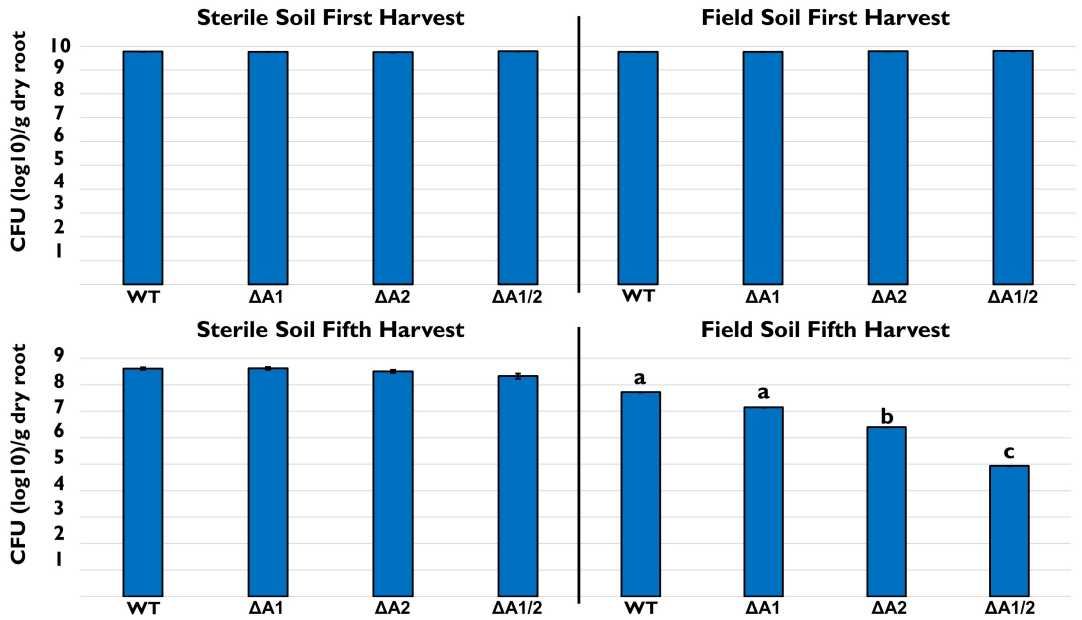

FIGURE 2 | Rhizosphere persistence over repeat harvests. Bacterial populations (log10 CFU/g root dry weight) in sterile and field soil after the first and fifth harvest. Strains tested included 30–84 WT, the single T6SS mutants ΔTssA1 and ΔTssA2, and the double mutant ΔTssA1/2. Data are the mean and standard errors (bars may be too small to see for some treatments) from three replicate experiments (n = 10/per replicate). Lettering indicates significant differences. Data were analyzed using a one-way ANOVA and Tukey's tests and significant differences are indicated, $p < 0.05$.

suggested that having a T6SS is not necessary for rhizosphere colonization but is important for competitive persistence.

Bacterial Competition Assays

We explored the hypothesis that disruption of either or both T6SS alters competitive fitness using single strain competition assays *in vitro*. For this assay, 30–84 WT and each of the T6SS mutants were grown separately or in 50:50 mixtures with other well-characterized rhizosphere colonizing *Pseudomonas* PGPB strains shown in this study or previous work to be completely or partially resistant to phenazines or bacteriocins (Dorosky et al., 2017, 2018). These included strains for which there was information about their T6SS and the sequence similarity of their T6SS to the *P. chlororaphis* 30–84 T6SS clusters. Rhizosphere competitors included *P. synxantha* 2–79 (no T6SS), *P. protegens* Pf-5 (a T6SS-1 homolog), and *P. fluorescens* Q2–87 (three T6SS, including T6SS-1 and T6SS-2 homologs) (Loper et al., 2012; **Supplementary Figure S1**). For mixed strain treatments, strains were grown independently then mixed and applied to filter paper on solid LB medium, whereas for single strain treatments the same total volume of the one strain was applied. The population of each strain in mixture was compared to the populations of their single strain counterparts to observe any effect on growth. Competition with 30–84 WT, ΔTssA1, ΔTssA2, or ΔTssA1/2 are shown as separate analyses (**Figure 3**). All strains grew well when cultured separately on filters ($\sim 10^8$, and did not differ statistically, $p < 0.05$). In competition with *P. synxantha* 2–79, 30–84 WT and ΔTssA1 reduced *P. synxantha* 2–79 populations, whereas ΔTssA2 and ΔTssA1/2 permitted substantial growth of *P. synxantha* 2–79 in mixed cultures and the growth of both *P. chlororaphis* 30–84 derivatives was reduced. These results suggest T6SS-2 (which may be randomly firing), but not TSS6-1 (which may be contact dependent) confers a competitive advantage to *P. chlororaphis* 30-84 over *P. synxantha* 2-79 (which lacks a T6SS). In contrast, neither of the T6SS had an appreciable effect on the growth of *P. protegens* Pf-5, whereas *P. protegens* was able to reduce the growth ΔTssA1/2 in mixed culture. In competition with *P. fluorescens* Q2–87, 30–84 WT and both single T6SS mutants virtually eliminated *P. fluorescens* Q2–87, whereas ΔTssA1/2 permitted growth of *P. fluorescens* Q2–87 in mixed culture, indicating having at least one T6SS conferred a competitive advantage to 30–84 WT (**Figure 3**).

In the rhizosphere, in mixed treatments with *P. chlororaphis* 30–84 WT or either of the single T6SS mutants and one of the biological control treatments, none of the competitor strains (*P. synxantha* 2–79, *P. protegens* Pf-5, or *P. fluorescens* Q2–87) had a competitive advantage (**Figure 4**). However, ΔTssA1/2 populations were reduced substantially in the presence of *P. protegens* Pf-5 and *P. fluorescens* Q2–87 and reduced somewhat in the presence of *P. synxantha* 2–79, suggesting that at least one T6SS is needed for competitive fitness in mixtures, especially with the biological control agents having at least one T6SS.

We also examined the importance of one or both T6SS using the wild type and T6SS mutants in competition assays with several environmental isolates or plant pathogens (**Supplementary Figure S3**). We found that the environmental isolate *P. putida* F1 (no T6SS-encoding genes) performed similarly to *P. synxantha* 2–79 in mixed culture being inhibited by *P. chlororaphis* 30–84 WT and ΔTssA1, whereas ΔTssA2 and ΔTssA1/2 permitted substantial growth. *Agrobacterium*

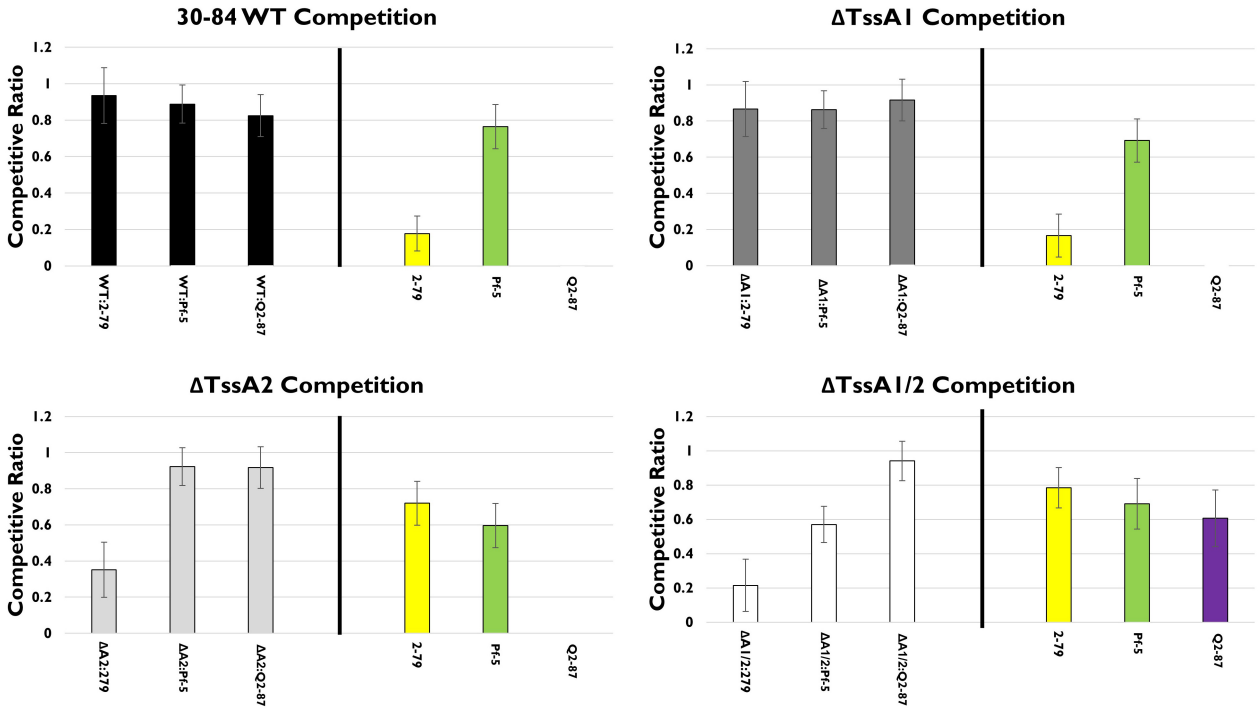

FIGURE 3 | *In vitro* competition assays. The competitive fitness of 30–84 WT, the single T6SS mutants, ΔTssA1 and ΔTssA2, and the double mutant, ΔTssA1/2 were evaluated by comparing their populations when grown separately or in 50:50 mixtures with other *Pseudomonas* rhizosphere colonizing bacteria in liquid media. Data are expressed as competitive ratios (population in mixture/population when grown separately). Gray scale bars (left) indicate performance of 30–84 WT and derivatives, and colored bars (right) indicate performance of competitors, including *P. fluorescens* 2–79 (yellow color, having no T6SS), *P. protegens* Pf-5 (green color, having a T6SS-1 homolog), and *P. fluorescens* Q2–87 (purple color, having three T6SS, including T6SS-1 and T6SS-2 homologs). Individual bacterial cultures or mixture cultures were spotted onto nitrocellulose filters on LB plates and incubated at 28°C, 5 h. Bacterial cells were washed from filters, collected via centrifugation, and populations were enumerated after 48 h via serial dilution plating. Data are the mean competitive ratios of five replicates pooled across three experiments (n = 15) and standard errors are indicated.

tumefaciens C58 and *Pseudomonas syringae* pv. tomato DC3000, each have functional T6SS (Petnicki-Ocwieja et al., 2002; Ma et al., 2014, respectively) but their populations were reduced substantially when grown with 30–84 WT or either of the single mutants. When grown with the double mutants both of these pathogen competitors were able to maintain high populations. *Pectobacterium carotovorum* subsp. *carotovorum* inhibited the double mutant, but the wild type and the single mutants were able to coexist with the pathogen (**Supplementary Figure S3**). These results indicate that having at least one T6SS is important for competition against plant pathogens, with T6SS-2 being important for competition against strains lacking their own T6SS.

T6SS as an Anti-predation Mechanism Against Different Types of Bacterivores

In these studies, we employed three different bacterivores having different feeding styles, including *Dictyostelium discoideum* a soil dwelling amoeba that feeds on bacteria at the soil surface via phagocytosis (Dunn et al., 2018; Williams and Kay, 2018), *Tetrahymena thermophila* a ciliate filter/phagocytosis feeder (Gavin, 1980; Luan et al., 2012; Dürichen et al., 2016), and the soil-dwelling nematode *Caenorhabditis elegans* (Avery and You, 2018). Bacteria used as prey in all feeding assay included 30–84 WT, ΔTssA1, ΔTssA2, ΔTssA1/2, and *P. chlororaphis* derivatives deficient specifically in the production of phenazines (Phz), quorum sensing (QS) signal production, or one or both T6SS system, e.g., 30–84 WT (Phz^+, QS^+, $T6SS^+$), 30–84 ZN (Phz^-, QS^+, $T6SS^+$), 30–84 I/I2 (Phz^-, QS^-, $T6SS^+$), ΔTssA1, ΔTssA2, ΔTssA1/2 (Phz^+, QS^+), and 30–84 GacA (Phz^-, QS^-, $T6SS^{reduced}$).

Dictyostelium discoideum

To test our hypothesis that one or both of the T6SS function in anti-predation defense against *D. discoideum* amoeba cells, we observed the behavior of *D. discoideum* amoebae when the food source offered as prey consisted of 30–84 WT, 30–84 ZN, 30–84 I/I2 ΔTssA1, ΔTssA2, ΔTssA1/2, or 30–84 GacA. We performed the assay in two different types of medium: low nutrition (PBM) and high nutrition (HL5) medium. Because starvation stress in this amoeba results in aggregation and formation of multicellular fruiting bodies, we assessed aggregation behavior (Kessin, 2001). In low nutrition medium, we observed that after 24 h, *D. discoideum* cells growing without a bacterium food source (control) began to thin and stream and formed extensive aggregates (**Figure 5**). Similarly, when offered 30-84

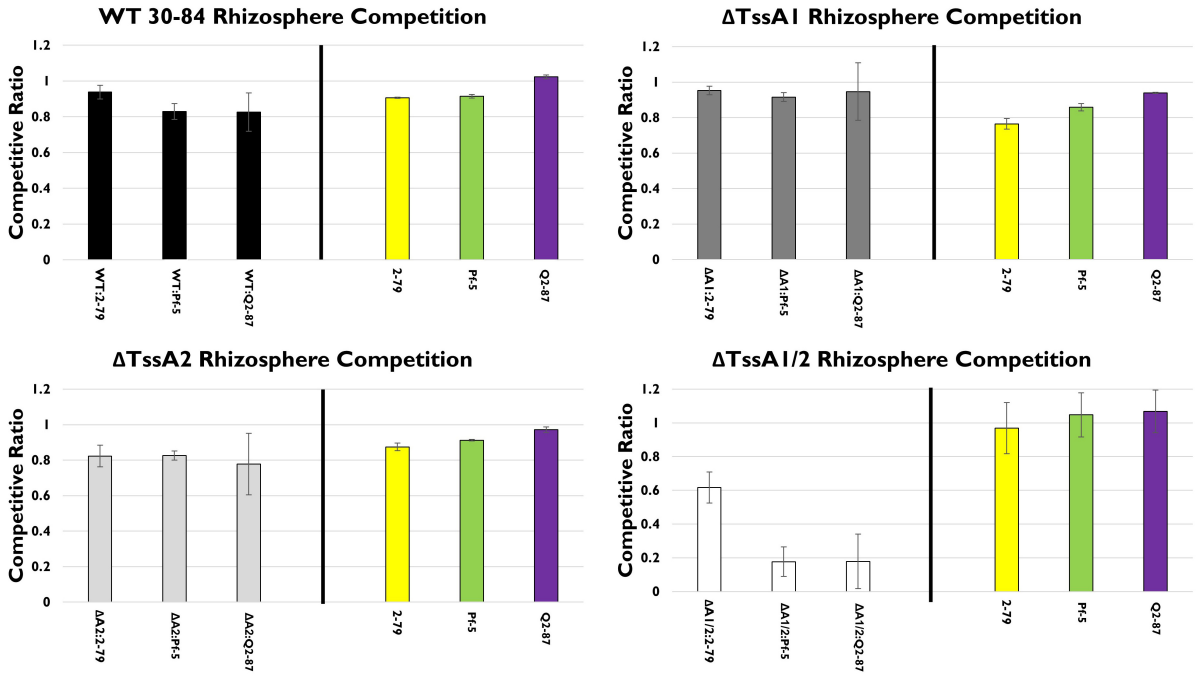

FIGURE 4 | Rhizosphere competition assays. The competitive fitness 30–84 WT, the single T6SS mutants, ΔTssA1 and ΔTssA2, and the double mutant, ΔTssA1/2 were evaluated by comparing their populations when grown separately or in 50:50 mixtures with other *Pseudomonas* rhizosphere colonizing bacteria in the rhizosphere. Data are expressed as competitive ratios (population in mixture/population when grown separately). Gray scale bars (left) indicate performance of 30–84 WT and derivatives, and colored bars (right) indicate performance of competitors, including *P. fluorescens* 2–79 (yellow color, having no T6SS), *P. protegens* Pf-5 (green color, having a T6SS-1 homolog), and *P. fluorescens* Q2–87 (purple color, having three T6SS, including T6SS-1 and T6SS-2 homologs). After 28 days, bacterial populations from the entire root system and loosely adhering soil were collected and enumerated via serial dilution plating. Populations were standardized to root dry weight. Data are the mean competitive ratios of at least eight replicates pooled across three experiments (n = 24) and standard errors are indicated.

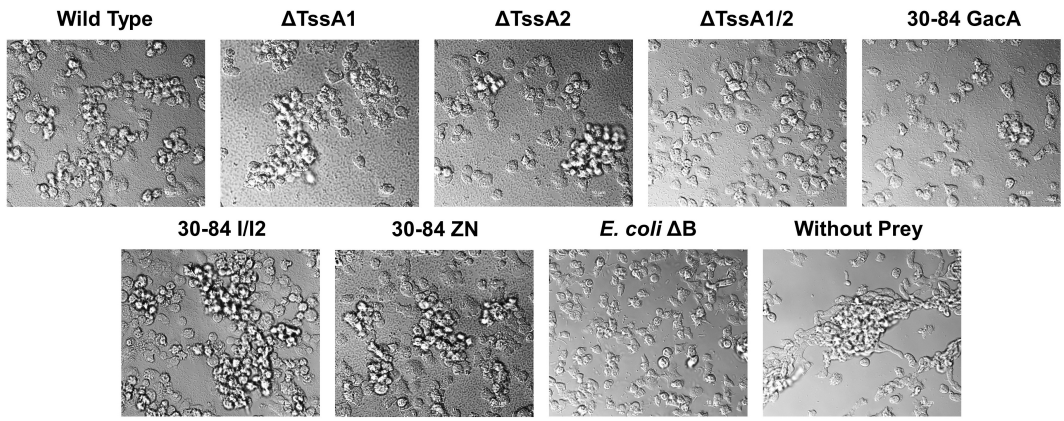

FIGURE 5 | Aggregation behavior of *Dictyostelium discoideum* grown with different bacterial strains as a food source. Bacteria used as prey in the feeding assay included 30–84 WT, ΔTssA1, ΔTssA2, ΔTssA1/2, 30–84 GacA, 30–84 I/I2, or 30–84 ZN and *E. coli* ΔB (used as a preferred prey in the lab). *D. discoideum* without prey bacteria was used as a negative control. *D. discoideum* cells were grown in 24-well plates in low nutrient PBM media for 24 h and aggregation behavior was observed using DIC microscopy (100X oil). The *D. discoideum* control (without prey) showed high levels of aggregation caused by stress due to the lack of nutrition in the media. *D. discoideum* growing with 30–84 WT, ΔTssA1, ΔTssA2, 30–84 I/I2, and 30–84 ZN displayed a similar level of aggregation, indicating that *D. discoideum* cannot eat these strains. *D. discoideum* grown with *E. coli* ΔB showed little to no aggregation. *D. discoideum* growing with ΔTssA1/2 and 30–84 GacA treatments showed similarly low levels of aggregation. Two replicate experiments were performed, and representative images from the same replicate are presented.

WT or derivatives 30–84 ZN, 30–84 I/I2, ΔTssA1, or ΔTssA2, all having at least one intact T6SS, extensive aggregation resulted. In contrast, *D. discoideum* cells growing with *E. coli* ΔB (used in lab as a preferred prey source) showed no aggregation. *D. discoideum* growing with ΔTssA1/2 and 30–84 GacA treatments showed no aggregation, similar to cells grown on *E. coli* ΔB, indicating that

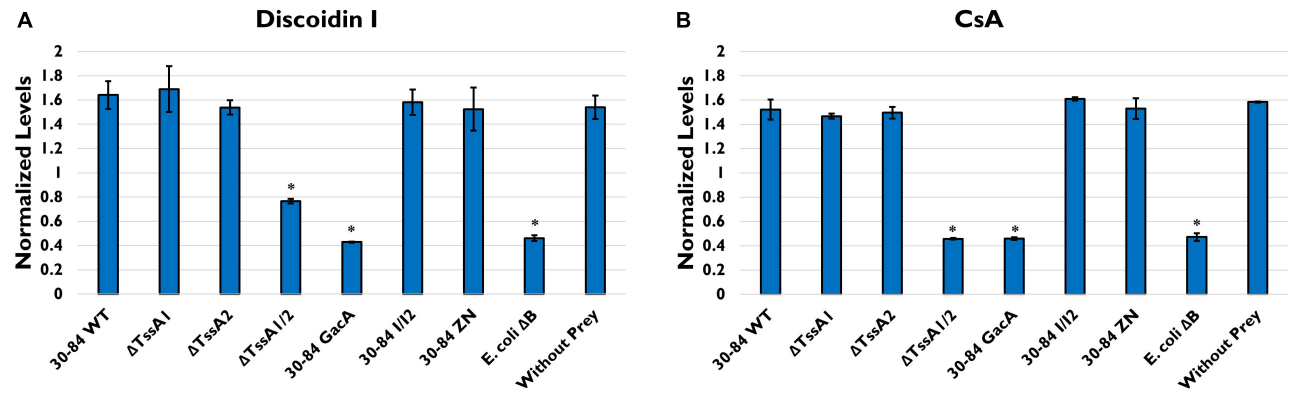

FIGURE 6 | Levels of two starvation markers in *Dictyostelium discoideum*. *D. discoideum* AX2 cells were incubated in PBM with the indicated prey strains (30–84 WT, ΔTssA1, ΔTssA2, ΔTssA1/2, 30–84 GacA, 30–84 I/I2, or 30–84 ZN and *E. coli* ΔB) or without prey (negative control) for 24 h. Western blots were stained with anti-Discoidin I, anti-CsA, or anti-beta-Actin antibodies. Graphs show the levels of **(A)** Discoidin I or **(B)** CsA normalized to total actin. Values are mean and standard error of 2 independent experiments. * Indicates $p < 0.01$ compared to *D. dictyostelium* AX2 control (Unpaired *t*-tests, Welch's correction).

the *D. discoideum* was able to gain adequate nutrition by using these strains as a food source (**Figure 5**). In HL5 media, little to no aggregation behavior was seen, consistent with *D. discoideum* having adequate nutrition (**Supplementary Figure S4**). These results suggest that having at least one functional T6SS causes *D. discoideum* stress behavior typically associated with starvation in low nutrition media, whereas neither the lack of phenazine or quorum sensing signal production reduced the aggregation behavior, indicating neither play a significant role in promoting the stress response.

To confirm that bacterial T6SS induce stress during feeding, we measured the production of *D. discoideum* development markers Discoidin I and Contact site A (CsA). Discoidin I is a protein involved in adhesion that is detectable at low levels in vegetative amoeba cells but is expressed at high levels during aggregation (Springer et al., 1984). CsA is a glycoprotein involved in cell-cell binding that is expressed at very low levels in growing cells and is then expressed during development (Harloff et al., 1989). We found that when grown without prey (negative control) in low nutrition media, *D. discoideum* produced high levels of both Discoidin I and CsA (**Figure 6**). When grown with *E. coli* ΔB (preferred prey) the production of both proteins was significantly lower compared to the negative control. When grown with 30–84 WT, 30–84 I/I2, or 30–84 ZN as the prey, levels of Discoidin I and CsA were comparable to the negative control, indicating that phenazines were not the driving mechanism behind this response. *D. discoideum* also produced high levels of both development markers when grown with ΔTssA1 and ΔTssA2. When *D. discoideum* was grown with ΔTssA1/2 or 30–84 GacA, levels of both proteins were comparable to the *E. coli* ΔB control (**Figure 6**). Taken together these results indicate that bacteria having one or both T6SS causes stress in *D. discoideum*, which deters predation.

To determine how *D. discoideum* predation effects bacterial fitness, a plate clearing assay was performed in which the size of the zone of clearing (and *D. discoideum* spread) after 5 days was used as a measure of bacterial cell death due to predation. On all plates, the initial colony of *D. discoideum* resulted in a clear zone ∼1 cm in diameter after 2 days. After 5 days, the clearing zone on plates containing 30–84 WT, ΔTssA1, ΔTssA2, 30–84 I/I2, and 30–84 ZN did not increase significantly i.e., the zones were within 0.05 cm of the clearing diameter measured at day 2 (**Figure 7**). The clearing zone on plates containing the preferred prey *E. coli*ΔB or 30–84 GacA grew to 3.0 $\pm$0.2 and 3.8 $\pm$0.02 cm, respectively, and on ΔTssA1/2 grew to 1.7 $\pm$0.06 cm. These results indicate that 30–84 GacA and ΔTssA1/2 populations suffered greater losses due to *D. discoideum* feeding (**Figure 7**).

Tetrahymena thermophila

As above, in the feeding assay using the model ciliate *Tetrahymena thermophila* CU427, predators were offered the same single prey choice strains (30–84 WT, ΔTssA1, ΔTssA2, ΔTssA1/2, 30–84 GacA, 30–84 I/I2, 30–84 ZN), and population densities of the predator in mixed culture were measured after 4 and 24 h. No significant differences in *T. thermophila* population densities were found even after 24 h (**Supplementary Figure S5**). However, we also assessed stress related behaviors of *T. thermophila* when offered the different prey choices via a mating assay. Two *T. thermophila* of different mating types, CU427 and CU330, were selected for this assay as they are recognized as "non-self" cells with different germlines, and will therefore reproduce (Cervantes et al., 2013). In the mating assay, *T. thermophila* were starved prior to their exposure to the different prey. If *T. thermophila* continued to experience starvation stress, this would increase instances of mating (Cole, 2000-2013). After 4 h, the frequency of mating was ∼55% for the control (no food source) and the frequency of mating for 30–84 WT, 30–84 I/I2, or 30–84 ZN as the food source was similar (62, 53, and 62%, respectively; **Figure 8**). Since all three of these derivatives have wild type T6SS expression, but differ in their ability to produce phenazines, these data demonstrate that the production of phenazines did not enhance mating. In contrast, the frequency of mating was significantly lower for *T. thermophila*

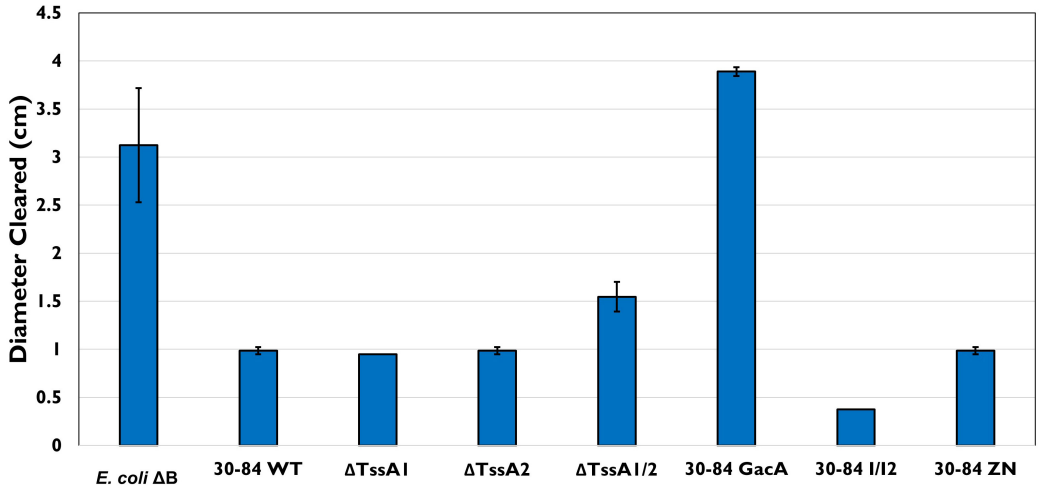

FIGURE 7 | Bacterial plate clearing by *Dictyostelium discoideum.* Bacteria used as prey in the feeding assay included 30–84 WT, ΔTssA1, ΔTssA2, ΔTssA1/2, 30–84 GacA, 30–84 I/I2, or 30–84 ZN and *E. coli* ΔB (used as a preferred prey in the lab). The diameter of bacterial lawn cleared by *D. discoideum* was measured in cm after 72 h. Lettering indicates significant differences. *D. discoideum* colonies grown on 30–84 WT, both single mutants, 30–84 I/I2, and 30–84 ZN showed little to no clearing, indicating low to no bacterial cell death. *D. discoideum* growing on *E. coli* ΔB showed significant levels of clearing. When grown on 30–84 GacA, levels of clearing similar to the control were observed. When grown on ΔTssA1/2, less clearing was observed than on the control, but levels were still significantly higher than clearing on 30–84 WT and the single mutants, indicating a decrease in bacterial fitness when lacking at least one functional T6SS. Data are the means and standard error (may be too small to see for some treatments) of four biological replicate experiments ($n = 4$). Data were analyzed using one-way ANOVA and Student *t*-tests, $p < 0.05$.

growing with ΔTssA1/2 or 30-84 GacA (19%, 36%, respectively, **Figure 8**). Observations support the hypothesis that having an intact T6SS causes predator stress, resulting in reduced levels of bacterivory.

Caenorhabditis elegans

As in the previous experiments, the bacterivorous nematode *C. elegans* was offered different prey choices. In this experiment, 5 *C. elegans* adults were allowed to graze for 1 h on a lawn of each bacterial strain and then moved successively to a fresh prey-containing plate every 1 h three more times, enabling nematodes to lay eggs on each of the plates. Plates were then observed for 72 h at 24 h intervals and adult and juvenile nematodes maturing from eggs were counted. Well-fed nematodes will mature from eggs within 72 h.

After 72 h, a large percentage (∼45%) of nematodes grown on *E. coli* OP50, the *C. elegans* normal laboratory food source, were mature (**Figure 9**). The percentages of adult nematodes observed on plates having ΔTssA1/2 and 30–84 GacA as food sources were also high (∼55%), whereas the percentages were lower when *C. elegans* was grown on plates having 30–84 WT, ΔTssA1, ΔTssA2, 30–84 I/I2, or 30-84 ZN as the food source (2, 2, 0, 9.5, and 0.03% adults, respectively) (**Figure 9**). Moreover, for plates containing 30–84 WT, 30–84 I/I2, or 30–84 ZN as the food source, *C. elegans* avoided the center of the plates where the bacterial density was greatest, instead moving to the edges of the plate (**Supplementary Figure S6**). On plates containing these prey sources, less than 25% of the plate was cleared (where clearing indicates bacterial consumption, **Supplementary Table S2**). Since these three derivatives have wild type T6SS expression, but differ in their production of phenazines, these data demonstrate that the production of phenazines was not the primary feeding deterrent. Similarly, the nematodes moved to the outside of the plate and generally cleared less than 25% of the plate when grown on plates containing ΔTssA1 or ΔTssA2 as the food source. On ΔTssA1/2 and 30–84 GacA, nematodes were found in the center of the plates and often cleared greater than 90% of the plate (**Supplementary Figure S6** and **Supplementary Table S2**). Data indicate that having either T6SS is a deterrent to *C. elegans* feeding, and that *C. elegans* prefer prey lacking expression of both.

In silico Identification of Putative T6SS-Dependent Effectors and Immunity Proteins

Given the importance of both systems for defense against competitors and predators, we used a bioinformatics approach to identify potential T6SS effectors and their predicted modes of action that may contribute to defense. Neither of the T6SS clusters in *P. chlororaphis* 30–84 contain genes previously annotated as encoding T6SS-dependent effectors. However, since T6SS-dependent effector genes are often located in close proximity to genes encoding VgrG, Hcp, or PAAR proteins, we analyzed the predicted protein sequences of genes closely associated with all copies of these genes using BLASTp (Lien and Lai, 2017; Spiewak et al., 2019). Putative effectors and immunity proteins were identified based on predicted functional domains and homology to proteins within established T6SS effector superfamilies. Using this approach, a diversity of putative T6SS effectors and associated proteins were discovered and all VgrG- or Hcp-encoding genes, whether

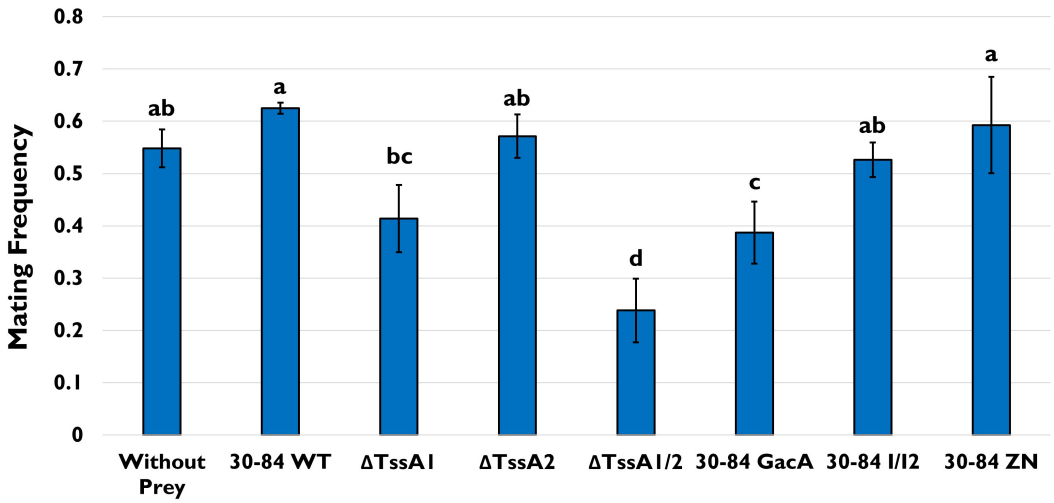

FIGURE 8 | *Tetrahymena* mating assay. *T. thermophila* CU427 and CU330 were grown separately overnight in Tris Buffer (pH = 7.4) to induce starvation. Populations were standardized to a cell density of 1.5 – 2 × 10^5/10 mL (via direct counts) in fresh Tris Buffer and mixed together with only the bacterial strain as a food source. Bacteria used as prey included 30–84 WT, ΔTssA1, ΔTssA2, ΔTssA1/2, 30–84 GacA, 30–84 I/I2, or 30–84 ZN, and the *T. thermophila* pairs without prey was used as a negative control. After 4 h, the treatments were viewed using a Leitz (Epivert) microscope (100X magnification), and the frequency of mated cell pairs (number of mated pairs/total number of observations) determined. Mean frequencies and standard errors are shown. This experiment was repeated three times (n = 3). Letters denote significant differences. Data were analyzed using one-way ANOVA and Student t-tests, $p < 0.05$.

located within a T6SS gene cluster or elsewhere in the genome, were associated with at least one putative effector (**Supplementary Table S3**).

Not surprisingly the two T6SS gene clusters harbored genes encoding different putative effectors. Within the T6SS-1 cluster, adjacent to an Hcp encoding gene is a gene encoding a Tae4-like protein (RS17725). Tae (type VI amidase effectors) family effectors have peptidoglycan amidase activity and are typically located adjacent to a cognate immunity protein (Zhang et al., 2013). However, the adjacent gene encoding a hypothetical protein bears no amino acid sequence homology to the known Tae4 immunity protein Tai4 and has no well characterized conserved domains. Also within the T6SS-1 cluster and adjacent to a VgrG-encoding gene (RS17755) are two genes encoding hypothetical proteins, one with a DUF2169 domains. Adapter proteins with the DUF2169 domain were shown to be necessary for the efficient secretion of T6SS effectors in *A. tumefaciens* (Bondage et al., 2016). Located nearby the T6SS-1 gene cluster and associated with a VgrG-encoding gene (RS17845) are genes encoding three hypothetical proteins predicted to have lipase (class 3) activity, be a cytoplasm-localized lipoprotein, or contain a DUF4123 domain. Proteins having a DUF4123 domain may serve as T6SS effector chaperones (Liang et al., 2015). In the T6SS-2 cluster, a gene encoding a hypothetical protein (RS29475) having a lysozyme-like domain similar to the C-terminal domain of pesticin is flanked by two VgrG encoding genes. Pesticin is an antibacterial toxin involved in hydrolysis of the peptidoglycan in the periplasm. Proteins with a pesticin C-terminal domain are typically involved in the hydrolysis of beta-1,4- linked polysaccharides (Patzer et al., 2012). Also in the T6SS-2 cluster and adjacent to one of the VgrG encoding genes are genes encoding three hypothetical proteins, one with a DUF4123 domain, one encoding a Tli1-like immunity protein with a DUF3304 domain shown to be associated with immunity proteins (Crisan et al., 2019), and one encoding a Tle1-like phospholipase protein (Ma et al., 2017) with a DUF2235 domain shown to be common in proteins containing a MIX (marker for type six effectors) sequence (Salomon et al., 2014).

Elsewhere in the genome, we discovered genes encoding putative effectors with predicted activities related to the breakdown of phospholipids or the production of toxins. Including the Tle-like effector associated with T6SS-2, we discovered three putative effectors predicted to have phospholipase activity, belonging to different phospholipase effector families: Tle, Tpl, and Pld. A gene encoding a TplE-like protein (RS20065) is located in a cluster with genes encoding a VgrG, two putative immunity protein pairs (paralogs), and a PAAR protein. A gene encoding a putative type VI secretion phospholipase D effector (Pld) in the same ortholog group as *tle5B* in *P. aeruginosa* PAO1 (RS20580) was located adjacent to another VgrG encoding gene. In *P. aeruginosa* PAO1, adjacent to *tle5B* are genes encoding three immunity proteins, each were found to have four, three, or two Sel1-like repeats (SLR) (Wen et al., 2020). No genes encoding similar immunity proteins were found in *P. chlororaphis* 30–84, however, the gene adjacent to *pld* in *P. chlororaphis* 30–84 encodes a hypothetical protein with three SLR repeats. Elsewhere in the genome, a gene encoding a RhsA- like protein (RS01885) was found within a four gene cluster containing genes encoding a putative TAP (T6 adaptor protein) protein with unknown function, VgrG and Hcp. Rhs (rearrangement hotspot) proteins, typically have multiple repeats of RHS

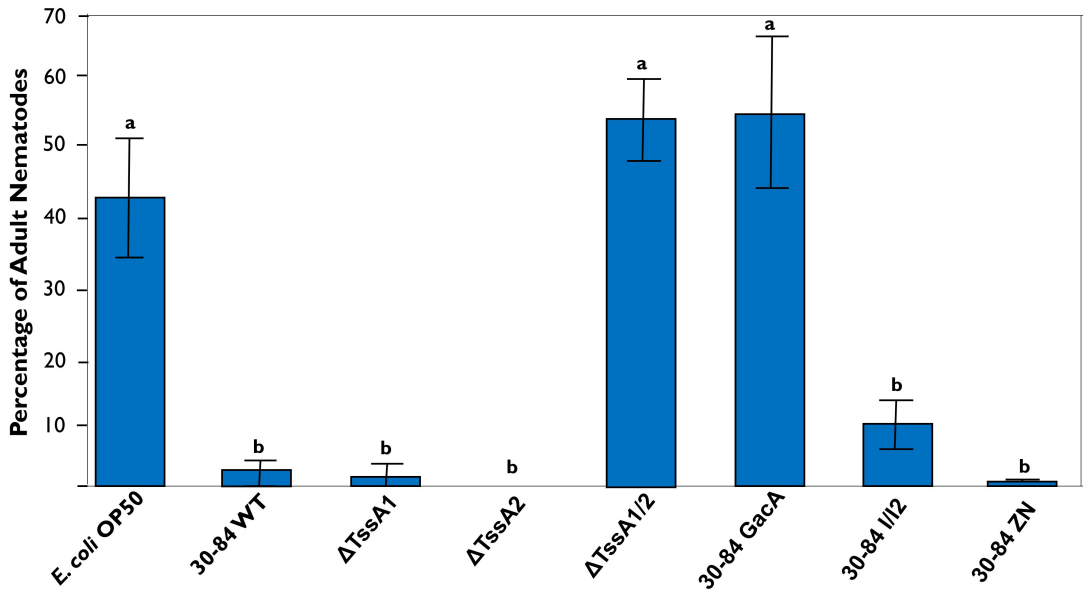

FIGURE 9 | Percentage of *C. elegans* that reach maturity after 72 h. Five adult *C. elegans* were transferred at 1-h intervals to new prey-containing plates to facilitate egg laying (a total of four successive transfers), and then the percentage of nematodes maturing to adults were measured every 24 h over a 72-h period. Plates contained either 30–84 WT, ΔTssA1, ΔTssA2, ΔTssA1/2, 30–84 GacA, 30–84 I/I2, 30–84 ZN, or *E. coli* OP50 (control) as a food source. Data are the mean and standard errors of three replicate experiments (four plates/replicate). Data were analyzed using one-way ANOVA and Tukey tests. Letters indicate significant differences, $p < 0.01$.

sequences and have been associated with toxicity and bacterial competition (Koskiniemi et al., 2013; Vacheron et al., 2019). The arrangement of the four genes is the same as the RhsP2-containing cluster in *P. aeruginosa* PA14 previously shown to be involved in T6SS secretion (Jones et al., 2014). Other putative effectors and their predicted function are also described in **Supplementary Table S3**.

DISCUSSION

Type VI Secretion Systems (T6SS) are known to be involved in many different types of bacterial interactions with prokaryotes and eukaryotes, and previous studies showed that in comparison to bacterial strains lacking T6SS, the presence of a T6SS confers greater fitness to bacteria in their environments (Haapalainen et al., 2012; Bernal et al., 2017b). Many bacterial species possess one to several T6SS and the different T6SS can be involved in different types of interactions (Chen et al., 2011). Consequently, possessing more than one T6SS can increase the repertoire of potential benefits to the strain (Schwarz et al., 2010). Plant growth promoting pseudomonads may either lack T6SS or possess one to several different T6SS, but their importance in activities related to their plant-associated habitat are not well studied. In the present study, we describe the structure and organization of two separate T6SS gene clusters in the PGPB strain *P. chlororaphis* 30–84 and provide evidence to support a role for both in competition against other bacterial species, including other PGPB and phytopathogens, and protection against different types of bacterivorous predators.

Bioinformatic analysis revealed that *P. chlororaphis* 30–84 has two separate T6SS clusters, each of which contain at least 12 of the 13 conserved T6SS structural proteins, but that the two clusters are quite different in terms of their organization and regulation. Comparative genomic analyses suggested that the two systems are not redundant and differ in their potential for responding to environmental stimuli. The T6SS-1 gene cluster contains putative Tag protein-encoding genes, which are involved in contact dependent firing, and was organizationally similar to the gene cluster encoding the *P. aeruginosa* T6SS previously shown to display dueling behavior (Basler et al., 2013). Together, these findings led us to hypothesize that T6SS-1 is fired in a contact dependent manner. The absence of the Tag-encoding genes in the T6SS-2 cluster led us to hypothesize random firing of this T6SS (i.e., not contact-dependent). Consistent with these hypotheses, *P. chlororaphis* 30-84 derivatives lacking a functional T6SS-2 (ΔTssA2 and ΔTssA1/2), and thus lacking random firing, permitted substantial growth of *P. synxantha* 2–79 (which lacks a T6SS) in mixed cultures, whereas derivatives having the T6SS-2 cluster (30–84 WT and ΔTssA1) competitively reduced *P. synxantha* 2–79 *in vitro*. We saw the same pattern of behavior in competition assays using *P. putida* F1, which also lacks a T6SS.

Previous studies showed that T6SS are important for the inhibition of competitors. For example, Bernal et al. (2017a) showed the biological control strain *P. putida* KT2440 possesses three different T6SS and, when all three were disrupted, control of certain plant pathogens was lost. In the present

study, we examined competitive fitness both in terms of the ability of the *P. chlororaphis* mutants to limit the growth of challengers and to resist the impact of challenges on their own growth. We found that *P. chlororaphis* wild type was significantly more effective than the double mutant in inhibiting the growth of several different plant pathogens and even different rhizosphere-colonizing biological control strains in mixed cultures *in vitro*. Moreover, in competition with certain strains (*P. synxantha* 2–79, *P. protegens* Pf-5, *Pectobacterium carotovorum*), the population of the double mutant was reduced, indicating inability to protect itself. Competition assays utilizing the single mutants showed that, in most cases, having either system was sufficient for competitor inhibition, although as noted above there were some exceptions demonstrating that T6SS-2 was effective against a broader spectrum of competitors (including those having no T6SS) than T6SS-1. It was interesting that derivatives having either T6SS system significantly inhibited *P. fluorescence* Q2–87 (having three T6SS, including T6SS-1 and T6SS-2 homologs) in mixed cultures *in vitro*, whereas *P. fluorescence* Q2–87 was able to grow in the presence of the double mutant. These observations are consistent with the hypothesis that despite having multiple T6SS systems, Q2–87 may not have immunity to *P. chlororaphis* 30–84 T6SS effectors. In some cases, pathogens (*Pseudomonas marginalis*) or biological control agents (*Pseudomonas putida* KT2440) that were chosen for competition assays were highly sensitive to phenazine or bacteriocin production and would not grow in the competition assay even with ΔTssA1/2. In other cases, strains (*P. putida* F1, *P. syringae* DC3000) that were shown previously to be sensitive to bacteriocins produced by *P. chlororaphis* 30–84 (Dorosky et al., 2017) were able to sustain somewhat higher populations in mixed culture with the double mutant compared to wild type, indicating both types of weapons contribute to competitive fitness against certain *Pseudomonas* strains. However, the majority of biological control strains tested (*P. synxantha* 2–79, *P. protegens* Pf-5, *P. fluorescens* Q2–87) were neither sensitive to phenazines nor bacteriocins, highlighting the importance of contact-dependent mechanisms in a rhizosphere where the antibiotic "resistome," the collection of all the antibiotic resistance genes, may be well established (O'Brien and Wright, 2011).

Interestingly, the rhizosphere habitat offered some protection from competition, presumably because strains could escape interaction spatially. In general, ΔTssA1/2 was less competitive than wild type. This deficit is unlikely to be the result of insufficiency in colonization ability, because ΔTssA1/2 colonized the rhizosphere as well as 30–84 WT in sterile and field soil in our persistence assay. However, after five harvest cycles ΔTssA1/2 populations were significantly smaller than 30–84 WT populations, but only in field soil. The populations of ΔTssA2 were also reduced under these conditions, suggesting that the putatively random-firing T6SS-2 is slightly more important than the putatively contact-dependent firing T6SS-1 for *P. chlororaphis* 30–84 competitive persistence in the rhizosphere. In this study, we purposely looked at competition between *P. chlororaphis* 30–84 and other well-characterized PGPB strains because these are also known to be good rhizosphere colonists. Our results highlight the importance of considering T6SS compatibility when considering multi-strain mixtures of PGPB.

We also examined the importance of T6SS for protecting *P. chlororaphis* 30–84 from predators with different feeding styles including, *D. discoideum, T. thermophila,* and *C. elegans.* Previous studies using these organisms as host model systems demonstrated that bacterial T6SS play a vital role in virulence against *D. discoideum* and *C. elegans* and protection against predation by *Tetrahymena* (Pukatzki et al., 2006; Sana et al., 2013; Wang et al., 2018). Our study is unique in that we examined the effect of each T6SS on the feeding and behavior of the predators and the impact of predation on bacterial populations rather than focusing on virulence and killing. For all three predators, we found that being grown with a bacterial food source with least one T6SS reduced predator feeding, increased predator stress, and altered predator behavior relative to the double mutant. For example, when grown with 30–84 WT or the single mutants as the primary food source, *D. discoideum* formed extensive aggregates, a common stress response (Kessin, 2001). Levels of developmental proteins related to aggregation behavior (Discoidin I and CsA) were also high in *D. discoideum* populations grown on 30–84 WT or the single mutants as the primary food source. In contrast, when grown with the double mutant or 30–84 GacA as the primary food source, no aggregation was observed, and development protein levels were reduced. When grown together with the different prey strains in high nutritional medium, there were no differences in predator behavior or stress levels, indicating no limitations to co-existence when there was sufficient food for the predator. In assays using pre-starved *T. thermophila,* mating, a stress related behavior (Cole, 2000-2013), was observed at high levels only when *T. thermophila* was grown with 30–84 WT or the single mutants as the primary food source. *C. elegans* also displayed behavior indicating its avoidance of 30-84 WT or single mutants, moving away from where the bacteria were spotted to the edges of the plates. In contrast, when grown with the double T6SS mutant or 30–84 GacA as the primary food source, nematodes were found in the center of the plates and matured at higher rates. Having at least one T6SS also had important consequences for bacterial fitness, resulting in less herbivory of those derivatives with at least one T6SS than for those without a functional T6SS as determined from clearing zones in assays with *D. discoideum* and *C. elegans*.

Phenotypic variation resulting from spontaneous mutation in *gacS/gacA* is a common problem among *Pseudomonas* biological control agents (van den Broek et al., 2005). Spontaneous *gacS* or *gacA* mutants arising in fermentation culture may outcompete the antibiotic producing wild type, causing a deficiency in secondary metabolites essential for biological control activity (Duffy and Defago, 2000). However, in the rhizosphere *P. chlororaphis* 30–84 wild type and *gac* mutants survive better together than apart (Chancey et al., 2002) and interact mutualistically in biofilms (Driscoll et al., 2011), indicating a benefit to maintaining phenotypic variation for competitive rhizosphere fitness. As in our

study, previous work by Jousset et al., 2009 demonstrated that *C. elegans* and the amoeba, *Acanthamoeba castellanii*, preferentially consumed a *Pseudomonas protegens* (previously *fluorescens*) CHA0 *gacS* mutant – although in their study they used mixed populations of mutants with wild type. Jousset et al. (2009) suggested that predator preference for the *gacS* mutant was due to loss of quorum sensing and antibiotic production. Like *P. chlororaphis* 30–84, *P. protegens* CHA0 possesses a diverse arsenal of diffusible weapons as well T6SS-encoding genes. In the present study, having a collection of phenazine, quorum sensing, and T6SS mutants enabled us to demonstrate that the T6SS had an important role in altering predator feeding and behavior. However as determined from the plate clearing assays with *D. discoideum* and *C. elegans*, *P. chlororaphis* 30–84 GacA was somewhat more aggressively attacked than ΔTssA1/2, indicating that other GacS/GacA controlled phenotypes contribute to defense against these predators.

Previous work demonstrated a role for T6SS in the delivery of effectors important for competition and virulence (Russell et al., 2011; Chen et al., 2015; Bernal et al., 2017b). All effectors delivered by T6SS studied to date are associated with the needle-like structure, specifically with either VgrG, Hcp or PAAR proteins (Ho et al., 2014). We identified a number of potential effector-encoding genes in the *P. chlororaphis* 30–84 genome that could be delivered via T6SS based on their proximity to genes encoding VgrG, Hcp or PAAR proteins, a method commonly used for effector discovery (English et al., 2012; Spiewak et al., 2019). Notably the putative effectors identified included several genes that may encode proteins with lipase or phospholipase activity, although the functionality of these was not specifically addressed in this study. Previous studies showed that predicted lipases are often encoded adjacent to *vgrG* homologs and those associated with T6SS may function to degrade bacterial membrane phospholipids (Russell et al., 2013). T6SS secreted phospholipase effectors were shown to increase virulence against amoebae (Pukatzki et al., 2006; MacIntyre et al., 2010), and some studies have attributed this to effectors specifically targeting lipids in the membrane of eukaryotes (Miyata et al., 2011; Durand et al., 2014; Jiang et al., 2014). The presence of potential phospholipase effectors in *P. chlororaphis* 30–84 suggests a potential mechanism for the interaction observed with eukaryotic bacterivores. Furthermore, the gene encoding the putative Pld effector is adjacent to a gene encoding a protein with multiple Sel1-like repeats (SLR). Sel1, first described in *C. elegans*, and proteins with SLRs were shown to be important for signal transduction in both prokaryotes and eukaryotes (Mittl and Schneider-Brachert, 2007). An effector with multiple SLRs could indicate another potential mechanism by which *P. chlororaphis* 30–84 effectors interact with eukaryotic predators. In addition, we also found possible effectors with potential amidase, lysozyme, and peptidoglycan degrading activity as well as an Rhsp2 homolog. Rhs effectors were shown to have antibacterial properties and are involved in bacterial competition (Hachani et al., 2014; Whitney et al., 2014; Alcoforado Diniz and Coulthurst, 2015). Notably, adjacent to genes encoding VgrG genes we often found genes encoding proteins with DUF4123 or DUF2169 domains. These domains were shown to be utilized in effector chaperoning (Liang et al., 2015) or secretion (Bondage et al., 2016), suggesting they may be important for cargo loading and secretion in *P. chlororaphis* 30-84 T6SS. Although demonstrating the efficacy of potential effectors was outside the scope of this study, their association with genes encoding VgrG and proteins with predicted chaperone domains strongly indicates their potential role as effectors. The diversity of effectors found and their predicted activities, portrays likely mechanisms for targeting both prokaryotic and eukaryotic systems.

In summary, our results demonstrate that in *P. chlororaphis* 30–84 both T6SS-1 and T6SS-2 serve as defensive weapons against other rhizosphere colonists that may be completely or partially resistant to the production of diffusible antimicrobials and bacteriocins, with T6SS-2 being more important for competition against strains lacking their own T6SS. Having at least one T6SS was also necessary for predator defense whereas loss of phenazine production had little effect on predation or predator behavior, indicating a greater role for T6SS than phenazines in defense against the predators we studied. Interestingly, having only one functional T6SS typically provided the same level and spectrum of protection as wild type. One possible explanation is that both T6SS systems may be capable of interchangeably delivering the repertoire of effectors, although this remains to be tested. Consequently, it is noteworthy that most of the groups of *vgrG*-associated potential effector genes are widely distributed throughout the genome rather than being localized within T6SS gene clusters, and typically one of the associated proteins encoded within each group shares a conserved domain previously shown to serve as a T6SS effector chaperone. We speculate that in contrast to diffusible weapons that may not be produced at low cell density or that function only after attaining a sufficient concentration in the environment, T6SS afford rhizosphere colonizing bacteria an additional more immediate line of defense against competitors and predators.

DATA AVAILABILITY STATEMENT

The original contributions presented in the study are included in the article/**Supplementary Material**, further inquiries can be directed to the corresponding author/s.

AUTHOR CONTRIBUTIONS

EB, EP, and SK designed the experiments. EB and SK performed the experiments, generated original data, and performed the data analysis. EB and EP wrote the manuscript. EP provided project supervision and major contribution to the final draft. All authors contributed to the interpretation of results and revisions of the manuscript, read and approved the submitted version.

FUNDING

This research was supported by funding from the DOE-Office of Energy Efficiency and Renewable Energy-EERE (DE-EE0007104); the Root Rhizosphere Interface Project, Department of Plant Pathology and Microbiology, Texas A&M University; the Graduate Assistant-Teaching Fellowship from the Department of Horticultural Sciences, Texas A&M University; and the Willie Mae Harris Teaching Excellence Fellowship, Texas A&M University.

ACKNOWLEDGMENTS

We thank current and former members of the Pierson research group including Jun Myoung Yu, Robert Dorosky, Peiguo Yuan, Julien Levy, and Jeroen Versteegen. We are grateful for expertise and use of facilities for some experiments provided by: Richard Gomer (*D. discoideum* assays), Geoffrey Kapler and Quang Hung Dang (*T. thermophila* assays), and Luis Garcia (*C. elegans* assays). We thank Sanjay Babu for use of some laboratory equipment. We thank Patricia Klein, Terry Gentry, and Hisashi Kiowa for helpful discussions and suggestions to improve the manuscript. We also thank all reviewers for their thoughtful suggestions that improved our manuscript.

SUPPLEMENTARY MATERIAL

The Supplementary Material for this article can be found online at: https://www.frontiersin.org/articles/10.3389/fmicb.2022.843092/full#supplementary-material

Supplementary Figure S1 | Phylogenetic tree comparing TssB from *P. chlororaphis* T6SS-1 and T6SS-2 clusters to known homologs. The amino acid sequences for TssB from both *P. chlororaphis* 30–84 T6SS clusters were compared to the corresponding sequences from individuals within each established clade referenced in Bernal et al. (2017b) using NCBI BLASTp. The *P. chlororaphis* 30–84 amino acid sequences and representative TssB amino acid sequences from these clades were aligned and a maximum likelihood tree was constructed using MEGA7. The program FigTree was used to convert the MEGA7 tree into figure format. TssB in the *P. chlororaphis* 30–84 cluster 1 (indicated by stars) aligned with sequences in clade 3 whereas the TssB from *P. chlororaphis* 30-84 cluster 2 (indicated by triangles) aligned predominately with sequences in clade 1.1 (although a single strain belonging to 4A clustered with it).

Supplementary Figure S2 | Planktonic growth curve and attached biofilm production. **(A)** Planktonic growth: bacteria were grown in LB medium at 28°C with agitation and populations were measured (OD_{620}) every hour up to 8 h and then every 2 h from 24 h to 30 hours. Data are the mean and standard error of six replicates. **(B)** Attached biofilms: separate wells of 96-well plates were inoculated with bacteria and grown at 28°C without agitation for 72 h. After removal of non-adhering cells, surface-attached biofilms were stained with crystal violet. The optical density (540 nm) of crystal violet released from the biofilms was used as a relative measure of biofilm population density. Data are the means and standard errors of two biological replicates per strain (started from separate colonies) and five technical replicates performed three times. Strains tested included 30–84 WT, the single T6SS mutants ΔTssA1 and ΔTssA2, and the double mutant ΔTssA1/2. Data were analyzed using a one-way ANOVA and Tukey's tests, $p < 0.05$. No significant differences were found.

Supplementary Figure S3 | *In vitro* competition assays against environmental isolates and pathogens. The competitive fitness of 30–84 WT and T6SS mutants against environmental isolates and pathogenic strains were evaluated by comparing their populations when grown separately or in 50:50 mixtures in liquid medium. Data are expressed as competitive ratios (population in mixture/population when grown separately). Gray scale bars (left) indicate performance of 30–84WT and derivatives, and colored bars (right) indicate performance of competitors, including *P. putida* F1 (blue), *Agrobacterium tumefaciens* C58 (orange), *P. syringae* DC3000 (red), and *Pectobacterium carotovorum* (green). Individual bacterial cultures or mixed cultures were spotted onto nitrocellulose filters on LB plates and incubated at 28°C, 5 h. Bacterial cells were washed from filters, collected via centrifugation, and populations were enumerated after 48 h via serial dilution plating. Data are the means (log10 CFU/1 mL) of at least five biological replicates/treatment pooled across at least two experiments and standard errors are indicated.

Supplementary Figure S4 | Aggregation behavior of *Dictyostelium discoideum* grown with different bacterial strains in high nutrition HL5 medium. Bacteria used as prey in the feeding assay included 30–84 WT, ΔTssA1, ΔTssA2, ΔTssA1/2, 30–84 GacA, 30–84 I/I2, or 30–84 ZN and *E. coli* ΔB (used as a preferred prey in the lab). *D. discoideum* without prey bacteria was used as a negative control. *D. discoideum* cells were grown in 24 well plates in high nutrient HL5 media for 24 h and aggregation behavior was observed using DIC microscopy (100X oil). All treatments showed no aggregation behavior, indicating no stress. Two replicate experiments were performed, and representative images are presented from the same replicate are presented.

Supplementary Figure S5 | *Tetrahymena* populations after 24 h feeding assay. Bacteria used as prey in the feeding assay included 30–84 WT, ΔTssA1, ΔTssA2, ΔTssA1/2, 30–84 GacA, 30–84 I/I2, or 30–84 ZN. *T. thermophila* without prey bacteria was used as a negative control. Bacterial and *T. thermophila* cultures were mixed (5 mL, 20 mL, respectively) and grown in 50 ml tubes with agitation (200 rpm, 27°C). After 24 h, *T. thermophila* populations in mixed cultures were enumerated via direct counts using a hemocytometer. Data are the means and standard errors of six replicate experiments. Data were analyzed using a one-way ANOVA and Student *t*-tests ($p < 0.05$). No significant differences were found.

Supplementary Figure S6 | Images of *C. elegans* on plates containing different prey after 72 h. Five adult *C. elegans* were transferred at 1-hour intervals to new prey-containing plates to facilitate egg laying (a total of four successive transfers), and then images were taken at 72 h. Images are of the center of the plate where bacterial cultures were applied. Plates contained either 30–84 WT, ΔTssA1, ΔTssA2, ΔTssA1/2, 30–84 GacA, 30–84 I/I2, 30–84 ZN, or *E. coli* OP50 (control) as a food source. Images were obtained using a Zeiss Stemi SV11 scope (26X magnification) and a Hamamatsu ImagEM EM-CCD camera. Adult nematodes can be seen on the plates containing ΔTssA1/2, 30-84 GacA or *E. coli* OP50 (ΔTssA1/2 image contains air bubble), whereas no or only a few, immature nematodes can be seen on plates with the other prey sources. The experiment and imaging were repeated three times with four plates/replicate ($n = 12$) and representative images from the same replicate are shown.

REFERENCES

Abby, S. S., Cury, J., Guglielmini, J., Néron, B., Touchon, M., and Rocha, E. P. C. (2016). Identification of protein secretion systems in bacterial genomes. *Sci. Rep.* 6:23080. doi: 10.1038/srep23080

Alcoforado Diniz, J., and Coulthurst, S. J. (2015). Intraspecies competition in *Serratia marcescens* is mediated by type VI-secreted Rhs effectors and a conserved effector-associated accessory protein. *J. Bacteriol.* 197, 2350–2360. doi: 10.1128/JB.00199-15

Altschul, S. F., Gish, W., Miller, W., Myers, E. W., and Lipman, D. J. (1990). Basic local alignment search tool. *J. Mol. Biol.* 215, 403–410. doi: 10.1016/S0022-2836(05)80360-2

Asolkar, T., and Ramesh, R. (2020). The involvement of the type six secretion system (T6SS) in the virulence of *Ralstonia solanacearum* on brinjal. *3 Biotech* 10:324. doi: 10.1007/s13205-020-02311-4

Aubert, D. F., Xu, H., Yang, J., Shi, X., Gao, W., Li, Lin, et al. (2016). A *Burkholderia* type VI effector deamidates Rho GTPases to activate the Pyrin inflammasome and trigger inflammation. *Cell Host Microbe* 19, 664–674. doi: 10.1016/j.chom.2016.04.004

Avery, L., and You, Y. J. (2018). "*C. elegans* feeding," in *WormBook: The Online Review of C. elegans* Biology, ed. The C. elegans Research Community (Pasadena, CA: WormBook).

Bakker, M. G., Manter, D. K., Sheflin, A. M., Weir, T. L., and Vivanco, J. M. (2012). Harnessing the rhizosphere microbiome through plant breeding and agricultural management. *Plant Soil* 360, 1–13. doi: 10.1007/s11104-012-1361-x

Bakthavatsalam, D., Brock, D. A., Nikravan, N. N., Houston, K. D., Hatton, R. D., and Gomer, R. H. (2008). The secreted *Dictyostelium* protein CfaD is a chalone. *J. Cell Sci.* 121, 2473–2480. doi: 10.1242/jcs.026682

Barret, M., Egan, F., Fargier, E., Morrissey, J. P., and O'Gara, F. (2011). Genomic analysis of the type VI secretion systems in *Pseudomonas* spp.: novel clusters and putative effectors uncovered. *Microbiology* 157, 1726–1739. doi: 10.1099/mic.0.048645-0

Basler, M. (2015). Type VI secretion system: secretion by a contractile nanomachine. *Philos. Trans. R. Soc. Lond. B Biol. Sci.* 370:20150021. doi: 10.1098/rstb.2015.0021

Basler, M., and Mekalanos, J. J. (2012). Type 6 secretion dynamics within and between bacterial cells. *Science* 337:815. doi: 10.1126/science.1222901

Basler, M., Ho, B. T., and Mekalanos, J. J. (2013). Tit-for-tat: type VI secretion system counterattack during bacterial cell-cell interactions. *Cell* 152, 884–894. doi: 10.1016/j.cell.2013.01.042

Berendsen, R. L., Pieterse, C. M. J., and Bakker, P. A. H. M. (2012). The rhizosphere microbiome and plant health. *Trends Plant Sci.* 17, 478–486. doi: 10.1016/j.tplants.2012.04.001

Bernal, P., Llamas, M. A., and Filloux, A. (2017b). Type VI secretion systems in plant-associated bacteria. *Environ. Microbiol.* 20, 1–15. doi: 10.1111/1462-2920.13956

Bernal, P., Allsopp, L. P., Filloux, A., and Llamas, M. A. (2017a). The *Pseudomonas putida* T6SS is a plant warden against phytopathogens. *ISME J.* 11, 972–987. doi: 10.1038/ismej.2016.169

Bondage, D. D., Lin, J. S., Ma, L. S., Kuo, C. H., and Lai, E. M. (2016). VgrG C terminus confers the type VI effector transport specificity and is required for binding with PAAR and adaptor-effector complex. *Proc. Natl. Acad. Sci. U.S.A.* 113, 3931–3940. doi: 10.1073/pnas.1600428113

Boyer, F., Fichant, G., Berthod, J., Vandenbrouch, Y., and Attree, I. (2009). Dissecting the bacterial type VI secretion system by a genome wide in silico analysis: what can be learned from available microbial genomic resources? *BMC Genomics* 10:104. doi: 10.1186/1471-2164-10-104

Brenner, S. (1974). The Genetics of *Caenorhabditis elegans*. *Genetics* 77, 71–94. doi: 10.1093/genetics/77.1.71

Brock, D. A., and Gomer, R. H. (1999). A cell-counting factor regulating structure size in *Dictyostelium*. *Genes Dev.* 13, 1960–1969. doi: 10.1101/gad.13.15.1960

Casabona, M. G., Silverman, J. M., Sall, K. M., Boyer, F., Couté, Y., Poirel, J., et al. (2013). An ABC transporter and an outer membrane lipoprotein participate in posttranslational activation of type VI secretion in *Pseudomonas aeruginosa*. *Environ. Microbiol.* 15, 471–486. doi: 10.1111/j.1462-2920.2012.02816.x

Cervantes, M. D., Hamilton, E. P., Xiong, J., Lawson, M. J., Yuan, D., Hadjithomas, M., et al. (2013). Selecting one of several mating types through gene segment joining and deletion in *Tetrahymena thermophila*. *PLoS Biol.* 11:e1001518. doi: 10.1371/journal.pbio.1001518

Chancey, S. T., Wood, D. W., and Pierson, L. S. III (1999). Two-component transcriptional regulation of N-acyl-homoserine lactone production in *Pseudomonas aureofaciens*. *Appl. Environ. Microbiol.* 65, 2294–2299. doi: 10.1128/AEM.65.6.2294-2299.1999

Chancey, S. T., Wood, D. W., Pierson, E. A., and Pierson, L. S. III (2002). Survival of GacS/GacA mutants of the biological control bacterium *Pseudomonas aureofaciens* 30-84 in the wheat rhizosphere. *Appl. Environ. Microbiol.* 68, 3308–3314. doi: 10.1128/AEM.68.7.3308-3314.2002

Chen, L., Zou, Y., She, P., and Wu, Y. (2015). Composition, function, and regulation of T6SS in *Pseudomonas aeruginosa*. *Microbiol. Res.* 172, 19–25. doi: 10.1016/j.micres.2015.01.004

Chen, Y., Wong, J., Sun, G. W., Liu, Y., Gladys Tan, G. Y., and Gan, Y. H. (2011). Regulation of type VI secretion system during *Burkholderia pseudomallei* infection. *Infect. Immun.* 79, 3064–3074. doi: 10.1128/IAI.05148-11

Chiang, P., and Burrows, L. L. (2003). Biofilm formation by hyperpiliated mutants of *Pseudomonas aeruginosa*. *J. Bacteriol.* 185, 2374–2378. doi: 10.1128/JB.185.7.2374-2378.2003

Chilton, M. D., Currier, T. C., Farrand, S. K., Bendich, A. J., Gordon, M. P., and Nester, E. W. (1974). *Agrobacterium tumefaciens* DNA and PS8 bacteriophage DNA not detected in crown gall tumors. *Proc. Natl. Acad. Sci. U.S.A.* 71, 3672–3676. doi: 10.1073/pnas.71.9.3672

Cianfanelli, F. R., Monlezun, L., and Coulthurst, S. J. (2016). Aim, load, fire: the type VI secretion system, a bacterial nanoweapon. *Trends Microbiol.* 24, 51–62. doi: 10.1016/j.tim.2015.10.005

Cole, E. S. (2000-2013). "The *Tetrahymena* conjugation junction," in *Madame Curie Bioscience Database [Internet]*, (Austin, TX: Landes Bioscience). Available online at: https://www.ncbi.nlm.nih.gov/books/NBK6002/ (accessed December 24, 2021).

Costerton, J. W. (1995). Overview of microbial biofilms. *J. Ind. Microbiol.* 15, 137–140. doi: 10.1007/BF01569816

Crisan, C. V., Chande, A. T., Williams, K., Raghuram, V., Rishishwar, L., Steinback, G., et al. (2019). Analysis of *Vibrio cholerae* genomes identifies new type VI secretion system gene clusters. *Genome Biol.* 20:163. doi: 10.1186/s13059-019-1765-5

Dorosky, R. J., Pierson, L. S. III, and Pierson, E. A. III (2018). *Pseudomonas chlororaphis* produces multiple R-tailocin particles that broaden the killing spectrum and contribute to persistence in rhizosphere communities. *Appl. Environ. Microbiol.* 84:e01230-18. doi: 10.1128/AEM.01230-18

Dorosky, R. J., Yu, J. M., Pierson, L. S. III, and Pierson, E. A. (2017). *Pseudomonas chlororaphis* produces two distinct R-tailocins that contribute to bacterial competition in biofilms and on roots. *Appl. Environ. Microbiol.* 83, e706–e717. doi: 10.1128/AEM.00706-17

Driscoll, W. W., Pierson, L. S. III, and Pierson, E. A. (2011). Spontaneous Gac mutants of *Pseudomonas* biological control strains: cheaters or mutualists? *Appl. Environ. Microbiol.* 77, 7227–7235. doi: 10.1128/AEM.00679-11

Duffy, B. K., and Defago, G. (2000). Controlling instability in *gacS-gacA* regulatory genes during inoculant production of *Pseudomonas fluorescens* biocontrol strains. *Appl. Environ. Microbiol.* 66, 3142–3150. doi: 10.1128/aem.66.8.3142-3150.2000

Dunn, J. D., Bosmani, C., Barisch, C., Raykov, L., Lefrancois, L. H., Cardenal-Munoz, E., et al. (2018). Eat, prey, live: *Dictyostelium discoideum* as a model for cell-autonomous defenses. *Front. Immunol.* 8:1906. doi: 10.3389/fimmu.2017.01906

Durand, E., Cambillau, C., Cascales, E., and Journet, L. (2014). VgrG, Tae, Tle, and beyond: the versatile arsenal of type VI secretion effectors. *Trends Microbiol.* 22, 498–507. doi: 10.1016/j.tim.2014.06.004

Dürichen, H., Siegmund, L., Burmester, A., Fischer, M. S., and Wöstemeyer, J. (2016). Ingestion and digestion studies in *Tetrahymena pyriformis* based on chemically modified microparticles. *Eur. J. Protistol.* 52, 45–57. doi: 10.1016/j.ejop.2015.11.004

English, G., Trunk, K., Rao, V. A., Srikannathasan, V., Hunter, W. N., and Coulthurst, S. J. (2012). New secreted toxins and immunity proteins encoded within the type VI secretion system gene cluster of *Serratia marcescens*. *Mol. Microbiol.* 86, 921–936. doi: 10.1111/mmi.12028

Fey, P., Dodson, R. J., Basu, S., and Chisholm, R. L. (2013). "One stop shop for everything *Dictyostelium*: dictyBase and the dicty stock center in 2012," in *Dictyostelium discoideum Protocols. Methods in Molecular Biology (Methods and Protocols)*, Vol. 983, eds L. Eichinger and F. Rivero (Totowa, NJ: Humana Press), doi: 10.1007/978-1-62703-302-2_4

Gallegos-Monterrosa, R., and Coulthurst, S. J. (2021). The ecological impact of a bacterial weapon: microbial interactions and the Type VI secretion system. *FEMS Microbiol. Rev.* 45:fuab033. doi: 10.1093/femsre/fuab033

Gardner, S. N., and Hall, B. G. (2013). When whole-genome alignments just won't work: kSNP v2 software for alignment-free SNP discovery and phylogenetics of hundreds of microbial genomes. *PLoS One* 8:e81760. doi: 10.1371/journal.pone.0081760

Gavin, R. H. (1980). The oral apparatus of *Tetrahymena* V. Oral apparatus polypeptides and their distribution. *J. Cell Sci.* 44, 317–333. doi: 10.1242/jcs.44.1.317

Ghoul, M., and Mitri, S. (2016). The ecology and evolution of microbial competition. *Trends Microbiol.* 24, 833–845. doi: 10.1016/j.tim.2016.06.011

Granato, E. T., Meiller-Legrand, T. A., and Foster, K. R. (2019). The evolution and ecology of bacterial warfare. *Curr. Biol.* 29, 521–537. doi: 10.1016/j.cub.2019.04.024

Grindley, N. D. F., and Joyce, C. M. (1981). Analysis of the structure and function of the kanamycin-resistance transposon Tn903. *Cold Spring Harb. Symp. Quant. Biol.* 45, 125–133. doi: 10.1101/SQB.1981.045.01.021

Haapalainen, M., Mosorin, H., Dorati, F., Wu, R. F., Roine, E., Taira, S., et al. (2012). Hcp2, a secreted protein of the phytopathogen *Pseudomonas syringae* pv. tomato DC3000, is required for fitness for competition against bacteria and yeasts. *J. Bacteriol.* 194, 4810–4822. doi: 10.1128/JB.00611-12

Hachani, A., Allsopp, L. P., Oduko, Y., and Filloux, A. (2014). The VgrG proteins are 'a la carte' delivery systems for bacterial type VI effectors. *J. Biol. Chem.* 289, 17872–17884. doi: 10.1074/jbc.M114.563429

Harloff, C., Gerisch, G., and Noegel, A. A. (1989). Selective elimination of the contact site A protein of *Dictyostelium discoideum* by gene disruption. *Genes Dev.* 3, 2011–2019. doi: 10.1101/gad.3.12a.2011

Hassan, K. A., Johnson, A., Shaffer, B. T., Ren, Q., Kidarsa, T. A., Elbourne, L. D. H., et al. (2010). Inactivation of the GacA response regulator in *Pseudomonas fluorescens* Pf-5 has far-reaching transcriptomic consequences. *Environ. Microbiol.* 12, 899–915. doi: 10.1111/j.1462-2920.2009.02134.x

Heeb, S., and Haas, D. (2001). Regulatory roles of the GacS/GacA two-component system in plant-associated and other gram-negative bacteria. *Mol. Plant Microbe Interact.* 14, 1351–1363. doi: 10.1094/MPMI.2001.14.12.1351

Hibbing, M. E., Fuqua, C., Parsek, M. R., and Peterson, S. B. (2010). Bacterial competition: surviving and thriving in the microbial jungle. *Nat. Rev. Microbiol.* 8, 15–25. doi: 10.1038/nrmicro2259

Hmelo, L. R., Borlee, B. R., Almblad, H., Love, M. E., Randall, T. E., Tseng, B. S., et al. (2015). Precision-engineering the *Pseudomonas aeruginosa* genome with two-step allelic exchange. *Nat. Protoc.* 10, 1820–1841. doi: 10.1038/nprot.2015.115

Ho, B. T., Dong, T. G., and Mekalanos, J. J. (2014). A view to a kill: the bacterial type VI secretion system. *Cell Host Microbe* 15, 9–21. doi: 10.1016/j.chom.2013.11.008

Hoang, T. T., Karkhoff-Schweizer, R. R., Kutchma, A. J., and Schweizer, H. P. (1998). A broad-host-range Flp-FRT recombination system for site-specific excision of chromosomally-located DNA sequences: application for isolation of unmarked *Pseudomonas aeruginosa* mutants. *Gene* 212, 77–86. doi: 10.1016/s0378-1119(98)00130-9

Howell, C. R. (1979). Control of *Rhizoctonia solani* on cotton seedlings with *Pseudomonas fluorescens* and with an antibiotic produced by the bacterium. *Phytopathology* 69:480. doi: 10.1094/Phyto-69-480

Jiang, F., Waterfield, N. R., Yang, J., Yang, G., and Jin, Q. (2014). A *Pseudomonas aeruginosa* type VI secretion phospholipase D effector targets both prokaryotic and eukaryotic cells. *Cell Host Microbe* 15, 600–610. doi: 10.1016/j.chom.2014.04.010

Jones, C., Hachani, A., Manoli, E., and Filloux, A. (2014). An *rhs* gene linked to the second type VI secretion cluster is a feature of the *Pseudomonas aeruginosa* strain PA14. *J. Bacteriol.* 196, 800–810. doi: 10.1128/JB.00863-13

Jousset, A., Rochat, L., Pechy-Tarr, M., Keel, C., Scheu, S., and Bonkowski, M. (2009). Predators promote defence of rhizosphere bacterial populations by selective feeding on non-toxic cheaters. *ISME J.* 3, 666–674. doi: 10.1038/ismej.2009.26

Kapitein, N., Bonemann, G., Pietrosiuk, A., Seyffer, F., Hausser, I., Locker, J. K., et al. (2013). ClpV recycles VipA/VipB tubules and prevents non-productive tubule formation to ensure efficient type VI protein secretion. *Mol. Microbiol.* 87, 1013–1028. doi: 10.1111/mmi.12147

Kessin, R. H. (2001). *Dictyostelium: Evolution, Cell Biology, and the Development of Multicellularity*. Cambridge: Cambridge University Press, 294.

King, E. O., Ward, M. K., and Raney, D. E. (1954). Two simple media for the demonstration of pyocyanin and fluorescin. *J. Lab. Clin. Med.* 44, 301–307. doi: 10.5555/uri:pii:002221435490222X

Koskiniemi, S., Lamoureux, J. G., Nikolakakis, K. C., Roodenbeke, C., Kaplan, M. D., Low, D. A., et al. (2013). Rhs proteins from diverse bacteria mediate intercellular competition. *Proc. Nat. Acad. Sci. U.S.A.* 110, 7032–7037. doi: 10.1073/pnas.1300627110

Kulasekara, H. D., and Miller, S. I. (2007). Threonine phosphorylation times bacterial secretion. *Nat. Cell Biol.* 9, 734–736. doi: 10.1038/ncb0707-734

Kumar, S., Stecher, G., and Tamura, K. (2016). MEGA7: molecular evolutionary genetics analysis version 7.0 for bigger datasets. *Mol. Biol. Evol.* 33, 1870–1874. doi: 10.1093/molbev/msw054

Lei, L., Yuan, L., Shi, Y., Xie, X., Chai, A., Wang, Q., et al. (2019). Comparative genomic analysis of *Pectobacterium carotovorum* subsp. *brasiliense* SX309 provides novel insights into its genetic and phenotypic features. *BMC Genomics* 20:486. doi: 10.1186/s12864-019-5831-x

Liang, X., Moore, R., Wilton, M., Wong, M. J. Q., Lam, L., and Dong, T. G. (2015). Identification of divergent type VI secretion effectors using a conserved chaperone domain. *Proc. Nat. Acad. Sci. U.S.A.* 112, 9106–9111. doi: 10.1073/pnas.1505317112

Lien, Y. W., and Lai, E. M. (2017). Type VI secretion effectors: methodologies and biology. *Front. Cell. Infect. Microbiol.* 7:254. doi: 10.3389/fcimb.2017.00254

Loper, J. E., Hassan, K. A., Mavrodi, D. V., Davis, E. W., Lim, C. K., Shaffer, B. T., et al. (2012). Comparative genomics of plant-associated *Pseudomonas* spp.: insights into diversity and inheritance of traits involved in multitrophic interactions. *PLoS Genet.* 8:e1002784. doi: 10.1371/journal.pgen.1002784

Luan, E., Miller, G., Ngui, C., and Siddiqui, F. (2012). The effect of temperature on food vacuole formation by *Tetrahyemna thermophila*. *Expedition* 2.

Ma, J., Pan, Z., Huang, J., Sun, M., Lu, C., and Yao, H. (2017). The Hcp proteins fused with diverse extended-toxin domains represent a novel pattern of antibacterial effectors in type VI secretion systems. *Virulence* 8, 1189–1202. doi: 10.1080/21505594.2017.1279374

Ma, L. S., Hachani, A., Lin, J. S., Filloux, A., and Lai, E. M. (2014). Agrobacterium tumefaciens deploys a superfamily of type VI secretion DNase effectors as weapons for interbacterial competition *in planta*. *Cell Host Microbe* 16, 94–104. doi: 10.1016/j.chom.2014.06.002

MacIntyre, D. L., Miyata, S. T., Kitaoka, M., and Pukatzki, S. (2010). The *Vibrio cholerae* type VI secretion system displays antimicrobial properties. *Proc. Natl. Acad. Sci. U.S.A.* 107, 19520–19524. doi: 10.1073/pnas.1012931107

Maddula, V. S. R. K., Zhang, Z., Pierson, E. A., and Pierson, L. S. III (2006). Quorum sensing and phenazines are involved in biofilm formation by *Pseudomonas chlororaphis (aureofaciens)* strain 30-84. *Microb. Ecol.* 52, 289–301. doi: 10.1007/s00248-006-9064-6

Mahmoudi, T. R., Yu, J. M., Liu, S., Pierson, L. S. III, and Pierson, E. A. (2019). Drought-stress tolerance in wheat seedlings conferred by phenazine-producing rhizobacteria. *Front. Microbiol.* 10:1590. doi: 10.3389/fmicb.2019.01590

Marchi, M., Boutin, M., Gazengel, K., Rispe, C., Gauthier, J. P., Guillerm-Erckelboudt, A. Y., et al. (2013). Genomic analysis of the biocontrol strain *Pseudomonas fluorescens* Pf29Arp with evidence of T3SS and T6SS gene expression on plant roots. *Environ. Microbiol. Rep.* 5, 393–403. doi: 10.1111/1758-2229.12048

Matz, C., and Kjelleberg, S. (2005). Off the hook – how bacteria survive protozoan grazing. *Trends Microbiol.* 13, 302–307. doi: 10.1016/j.tim.2005.05.009

Matz, C., McDougald, D., Moreno, A. M., Yung, P. Y., Yildiz, F. H., and Kielleberg, S. (2005). Biofilm formation and phenotypic variation enhance predation-driven persistence of *Vibrio cholerae*. *Proc. Natl. Acad. Sci. U.S.A.* 102, 16819–16824. doi: 10.1073/pnas.0505350102

Mazzola, M., Cook, R. J., Thomashow, L. S., Weller, D. M., and Pierson, L. S. III (1992). Contribution of phenazine antibiotic biosynthesis to the ecological competence of fluorescent pseudomonads in soil habitats. *Appl. Environ. Microbiol.* 58, 2616–2624. doi: 10.1128/aem.58.8.2616-2624.1992

Mittl, P. R. E., and Schneider-Brachert, W. (2007). Sel1-like repeat proteins in signal transduction. *Cell. Signal.* 19, 20–31. doi: 10.1016/j.cellsig.2006.05.034

Miyata, S. T., Kitaoka, M., Brooks, T. M., McAuley, S. B., and Pukatzki, S. (2011). Vibrio cholerae requires the type VI secretion system virulence factor VasX to kill *Dictyostelium discoideum*. *Infect. Immun.* 79, 2941–2949. doi: 10.1128/IAI.01266-10

O'Brien, J., and Wright, G. D. (2011). An ecological perspective of microbial secondary metabolism. *Curr. Opin. Biotechnol.* 22, 552–558. doi: 10.1016/j.copbio.2011.03.010

Pascale, A., Proietti, S., Pantelides, I. S., and Stringlis, I. A. (2020). Modulation of the root microbiome by plant molecules: the basis for targeted disease suppression and plant growth promotion. *Front. Plant Sci.* 10:1741. doi: 10.3389/fpls.2019.01741

Patzer, S. I., Albrecht, R., Braun, V., and Zeth, K. (2012). Structural and mechanistic studies of pesticin, a bacterial homolog of phage lysozymes. *J. Biol. Chem.* 287, 23381–23396. doi: 10.1074/jbc.M112.362913

Petnicki-Ocwieja, T., Schneider, D. J., Tam, V. C., Chancey, S. T., Shan, L., Jamir, Y., et al. (2002). Genomewide identification of proteins secreted by the Hrp type III protein secretion system of *Pseudomonas syringae* pv. tomato DC3000. *Proc. Natl. Acad. Sci. U.S.A.* 99, 7652–7657. doi: 10.1073/pnas.112183899

Phillips, J. E., and Gomer, R. H. (2010). The ROCO kinase QkgA is necessary for the proliferation inhibition by autocrine signals in *Dictyostelium discoideum*. *Eukaryot. Cell* 9, 1557–1565. doi: 10.1128/EC.00121-10

Phillips, J. E., and Gomer, R. H. (2012). A secreted protein is an endogenous chemorepellant in *Dictyostelium discoideum*. *Proc. Nat. Acad. Sci. U.S.A.* 109, 10990–10995. doi: 10.1073/pnas.1206350109

Pierson, E. A., and Weller, D. M. (1994). Use of mixtures of fluorescent pseudomonads to suppress take-all and improve the growth of wheat. *Phytopathology* 84, 940–947. doi: 10.1094/Phyto-84-940

Pierson, L. S. III, and Thomashow, L. S. (1992). Cloning and heterologous expression of the phenazine biosynthetic locus from *Pseudomonas aureofaciens* 30-84. *Mol. Plant Microbe Interact.* 5, 330–339. doi: 10.1094/mpmi-5-330

Pierson, L. S. III, Keppenne, V. D., and Wood, D. W. (1994). Phenazine antibiotic biosynthesis in *Pseudomonas aureofaciens* 30-84 is regulated by PhzR in response to cell density. *J. Bacteriol.* 176, 3966–3974. doi: 10.1128/jb.176.13.3966-3974.1994

Planamente, S., Salih, O., Manoli, E., Ablesa-Jove, D., Freemont, P. S., and Filloux, A. (2016). TssA forms a gp6-like ring attached to the type VI secretion sheath. *EMBO J.* 35, 1613–1627. doi: 10.15252/embj.201694024

Pukatzki, S., Ma, A. T., Sturtevant, D., Krastins, B., Sarracino, D., Nelson, W. C., et al. (2006). Identification of a conserved bacterial protein secretion system in *Vibrio cholerae* using the *Dictyostelium* host model system. *Proc. Natl. Acad. Sci. U.S.A* 103, 1528–1533. doi: 10.1073/pnas.0510322103

Quantabio (2021). *RepliQa HiFi ToughMix. Superior Speed and Inhibitor Tolerance*. Available online at: https://www.quantabio.com/repliqa-hifi-toughmix (accessed May 14, 2021).

Rambaut, A. (2009). *FigTree v1.3.1*. Available online at: https://ci.nii.ac.jp/naid/10030433668/#cit (accessed June 1, 2021).

Records, A. R., and Gross, D. C. (2010). Sensor kinases RetS and LadS regulate *Pseudomonas syringae* Type VI secretion and virulence factors. *J. Bacteriol.* 192, 3584–3596. doi: 10.1128/JB.00114-10

Rijal, R., Consalvo, K. M., Lindsey, C. K., and Gomer, R. H. (2019). An endogenous chemorepellent directs cell movement by inhibiting pseudopods at one side of cells. *Mol. Biol. Cell* 30, 242–255. doi: 10.1091/mbc.E18-09-0562

Rudd, J. C., Devkota, R. N., Ibrahim, A. M., Marshall, D., Sutton, R., Baker, J. A., et al. (2015). 'TAM 304' wheat, adapted to the adequate rainfall or high-input irrigated production system in the southern Great Plains. *J. Plant Regist.* 9, 331–337.

Russell, A. B., Hood, R. D., Bui, N. K., LeRoux, M., Vollmer, W., and Mougous, J. D. (2011). Type VI secretion delivers bacteriolytic effectors to target cells. *Nature* 475, 343–347. doi: 10.1038/nature10244

Russell, A. B., LeRoux, M., Hathazi, K., Agnello, D. M., Ishikawa, T., Wiggins, P. A., et al. (2013). Diverse type VI secretion phospholipases are functional plastic antibacterial effectors. *Nature* 496, 508–512. doi: 10.1038/nature12074

Salomon, D., Kinch, L. N., Trudgian, D. C., Guo, X., Klimko, J. A., Grishin, N. V., et al. (2014). Marker for type VI secretion system effectors. *Proc. Natl. Acad. Sci. U.S.A.* 111, 9271–9276. doi: 10.1073/pnas.1406110111

Sana, T. G., Flaugnatti, N., Lugo, K. A., Lam, L. H., Jacobson, A., Baylot, V., et al. (2016). *Salmonella typhimurium* utilizes a T6SS-mediated antibacterial weapon to establish in the host gut. *Proc. Natl. Acad. Sci. U.S.A.* 113, e5044–e5051. doi: 10.1073/pnas.1608858113

Sana, T. G., Soscia, C., Tonglet, C. M., Garvis, S., and Bleves, S. (2013). Divergent control of two type VI secretion systems by RpoN in *Pseudomonas aeruginosa*. *PLoS One* 8:e76030. doi: 10.1371/journal.pone.0076030

Santin, Y. G., Doan, T., Journet, L., and Cascales, E. (2019). Cell width dictates type VI secretion tail length. *Curr. Biol.* 29, 3707–3713. doi: 10.1016/j.cub.2019.08.058

Schwarz, S., West, T. E., Boyer, F., Chiang, W. C., Carl, M. A., Hood, R. D., et al. (2010). *Burkholderia* type VI secretion systems have distinct roles in eukaryotic and bacterial cell interactions. *PLoS Pathog.* 6:e1001068. doi: 10.1371/journal.ppat.1001068

Shneider, M. M., Buth, S. A., Ho, B. T., Basler, M., Mekalanos, J. J., and Leiman, P. G. (2013). PAAR-repeat proteins sharpen and diversify the type VI secretion system spike. *Nature* 500, 350–353. doi: 10.1038/nature12453

Smith, W. P. J., Vettiger, A., Winter, J., Ryser, T., Comstock, L. E., Basler, M., et al. (2020). The evolution of the type VI secretion system as a disintegration weapon. *PLoS Biol.* 18:e3000720. doi: 10.1371/journal.pbio.3000720

Spiewak, H. L., Shastri, S., Zhang, L., Schwager, S., Eberl, L., Vergunst, A. C., et al. (2019). *Burkholderia cenocepacia* utilizes a type VI secretion system for bacterial competition. *Microbiologyopen* 8:e774. doi: 10.1002/mbo3.774

Springer, W. R., Cooper, D. N. W., and Barondes, S. H. (1984). Discoidin I is implicated in cell-substratum attachment and ordered cell migration of *Dictyostelium discoideum* and resembles fibronectin. *Cell* 39, 557–564. doi: 10.1016/0092-8674(84)90462-8

Stubbendieck, R. M., and Straight, P. D. (2016). Multifaceted interfaces of bacterial competition. *J. Bacteriol.* 198, 2145–2155. doi: 10.1128/JB.00275-16

Tian, Y., Zhao, Y., Shi, L., Cui, Z., Hu, B., and Zhao, Y. (2017). Type VI secretion systems of *Erwinia amylovora* contribute to bacterial competition, virulence, and exopolysaccharide production. *Phytopathology* 107, 654–661. doi: 10.1094/PHYTO-11-16-0393-R

Vacheron, J., Pechy-Tarr, M., Brochet, S., Heimann, C. M., Stojilijkovic, M., Maurhofer, M., et al. (2019). T6SS contributes to gut microbiome invasion and killing of an herbivorous pest insect by plant-beneficial *Pseudomonas protegens*. *ISME J.* 13, 1318–1329. doi: 10.1038/s41396-019-0353-8

Vaitkevicius, K., Lindmark, B., Ou, G., Song, T., Toma, C., Iwanaga, M., et al. (2006). A *Vibrio cholerae* protease needed for killing of *Caenorhabditis elegans* has a role in protection from natural predator grazing. *Proc. Natl. Acad. Sci. U.S.A.* 103, 9280–9285. doi: 10.1073/pnas.0601754103

van den Broek, D., Bloemverg, G. V., and Lugtenberg, B. (2005). The role of phenotypic variation in rhizosphere *Pseudomonas* bacteria. *Environ. Microbiol.* 7, 1686–1697. doi: 10.1111/j.1462-2920.2005.00912.x

Wang, D., Lee, S. H., Seeve, C., Yu, J. M., Pierson, L. S. III, and Pierson, E. A. (2013). Roles of the Gac-Rsm pathway in the regulation of phenazine biosynthesis in *Pseudomonas chlororaphis* 30-84. *MicrobiololgyOpen* 2, 505–524. doi: 10.1002/mbo3.90

Wang, D., Yu, J. M., Pierson, L. S. III, and Pierson, E. A. (2012). Differential regulation of phenazine biosynthesis by RpeA and RpeB in *Pseudomonas chlororaphis* 30-84. *Microbiology* 158, 1745–1757. doi: 10.1099/mic.0.059352-0

Wang, N., Liu, J., Pang, M., Wu, Y., Awan, F., Liles, M. R., et al. (2018). Diverse roles of Hcp family proteins in the environmental fitness and pathogenicity of *Aeromonas hydrophila* Chinese epidemic strain NJ-35. *Appl. Microbiol. Biotechnol.* 102, 7083–7095. doi: 10.1007/s00253-018-9116-0

Weller, D. M., and Cook, R. J. (1983). Suppression of take-all of wheat by seed treatments with fluorescent pseudomonads. *Phytopathology* 73, 463–469. doi: 10.1094/Phyto-73-463

Wen, H., Geng, Z., Gao, Z., She, Z., and Dong, Y. (2020). Characterization of the *Pseudomonas aeruginosa* T6SS PldB immunity proteins PA5086, PA5087, and PA5088 explains a novel stockpiling mechanism. *Acta Crystallogr. F:Struct. Biol. Commun.* 76, 222–227. doi: 10.1107/S2053230X2000566X

Whitney, J. C., Beck, C. M., Goo, Y. A., Russell, A. B., Harding, B. N., De Leon, J. A., et al. (2014). Genetically distinct pathways guide effector export through the type VI secretion system. *Mol. Microbiol.* 92, 529–542. doi: 10.1111/mmi.12571

Williams, T. D., and Kay, R. R. (2018). The physiological regulation of macropinocytosis during *Dictyostelium* growth and development. *J. Cell Sci.* 131:jcs213736. doi: 10.1242/jcs.213736

Wilson, L., Matsudaira, P. T., Asai, D. J., and Forney, J. D. (1999). *Tetrahymena thermophila of Methods in Cell Biology*, Vol. 62. Cambridge, MA: Academic Press.

Yin, W., Wang, Y., Liu, L., and He, J. (2019). Biofilms: the microbial 'protective clothing' in extreme environments. *Int. J. Mol. Sci.* 20:3423. doi: 10.3390/ijms20143423

Yu, J. M., Wang, D., Pierson, L. S. III, and Pierson, E. A. (2018). Effect of producing different phenazines on bacterial fitness and biological control in *Pseudomonas chlororaphis* 30-84. *Plant Pathol. J.* 34, 44–58. doi: 10.5423/PPJ.FT.12.2017.0277

Yuan, P., Pan, H., Boak, E. N., Pierson, L. S. III, and Pierson, E. A. (2020). Phenazine-producing rhizobacteria promote plant growth and reduce redox and osmotic stress in wheat seedlings under saline conditions. *Front. Plant Sci.* 11:575314. doi: 10.3389/fpls.2020.575314

Zhang, H., Gao, Z. Q., Wang, W. J., Liu, G. F., Xu, J. H., Su, X. D., et al. (2013). Structure of the type VI effector-immunity complex (Tae4-Tai4) provides novel insights into the inhibition mechanisms of the effector by its immunity protein. *J. Biol. Chem.* 288, 5928–5939. doi: 10.1074/jbc.M112.434357

Zhang, Z., and Pierson, L. S. III (2001). A second quorum-sensing system regulates cell surface properties but not phenazine antibiotic production in *Pseudomonas aureofaciens*. *Appl. Environ. Microbiol.* 67, 4305–4315. doi: 10.1128/AEM.67.9.4305-4315.2001

Zoued, A., Brunet, Y. R., Durand, E., Aschtgen, M. S., Logger, L., Douzi, B., et al. (2014). Architecture and assembly of the type VI secretion system. *Acta. Bioch. Biophys.* 1843, 1664–1673. doi: 10.1016/j.bbamcr.2014.03.018

Zoued, A., Durand, E., Santin, Y. G., Journet, L., Roussel, A., Cambillau, C., et al. (2017). TssA: the cap protein of the type VI secretion system tail. *BioEssays* 39:1600262. doi: 10.1002/bies.201600262

Conflict of Interest: The authors declare that the research was conducted in the absence of any commercial or financial relationships that could be construed as a potential conflict of interest.

frontiers | Frontiers in Microbiology

ORIGINAL RESEARCH
published: 13 April 2022
doi: 10.3389/fmicb.2022.835274

Fungal Community Development in Decomposing Fine Deadwood Is Largely Affected by Microclimate

Vendula Brabcová[1†], Vojtěch Tláskal[1†], Clémentine Lepinay[1], Petra Zrůstová[1], Ivana Eichlerová[1], Martina Šťursová[1], Jörg Müller[2,3], Roland Brandl[4], Claus Bässler[3,5] and Petr Baldrian[1]*

[1] Laboratory of Environmental Microbiology, Institute of Microbiology of the Czech Academy of Sciences, Prague, Czechia, [2] Department of Animal Ecology and Tropical Biology, University of Würzburg, Würzburg, Germany, [3] Bavarian Forest National Park, Grafenau, Germany, [4] Animal Ecology, Department of Ecology, Faculty of Biology, Philipps-Universität Marburg, Marburg, Germany, [5] Department of Conservation Biology, Faculty of Biological Sciences, Institute for Ecology, Evolution and Diversity, Goethe University Frankfurt, Frankfurt, Germany

Fine woody debris (FWD) represents the majority of the deadwood stock in managed forests and serves as an important biodiversity hotspot and refuge for many organisms, including deadwood fungi. Wood decomposition in forests, representing an important input of nutrients into forest soils, is mainly driven by fungal communities that undergo continuous changes during deadwood decomposition. However, while the assembly processes of fungal communities in long-lasting coarse woody debris have been repeatedly explored, similar information for the more ephemeral habitat of fine deadwood is missing. Here, we followed the fate of FWD of *Fagus sylvatica* and *Abies alba* in a Central European forest to describe the assembly and diversity patterns of fungal communities over 6 years. Importantly, the effect of microclimate on deadwood properties and fungal communities was addressed by comparing FWD decomposition in closed forests and under open canopies because the large surface-to-volume ratio of FWD makes it highly sensitive to temperature and moisture fluctuations. Indeed, fungal biomass increases and pH decreases were significantly higher in FWD under closed canopy in the initial stages of decomposition indicating higher fungal activity and hence decay processes. The assembly patterns of the fungal community were strongly affected by both tree species and microclimatic conditions. The communities in the open/closed canopies and in each tree species were different throughout the whole succession with only limited convergence in time in terms of both species and ecological guild composition. Decomposition under the open canopy was characterized by high sample-to-sample variability, showing the diversification of fungal resources. Tree species-specific fungi were detected among the abundant species mostly during the initial decomposition, whereas fungi associated with certain canopy cover treatments were present evenly during decomposition. The species diversity of forest stands and the variability in microclimatic conditions both promote the diversity of fine woody debris fungi in a forest.

Keywords: decomposition, deadwood, fungal community, succession, canopy cover, microclimate, temperate forest, ecology

OPEN ACCESS

Edited by:
Marja Tiirola,
University of Jyväskylä, Finland

Reviewed by:
Ari Mikko Hietala,
Norwegian Institute of Bioeconomy Research (NIBIO), Norway
Gábor M. Kovács,
Eötvös Loránd University, Hungary

***Correspondence:**
Vendula Brabcová
brabcova@biomed.cas.cz

† These authors have contributed equally to this work

Specialty section:
This article was submitted to Terrestrial Microbiology, a section of the journal Frontiers in Microbiology

Received: *14 December 2021*
Accepted: *11 March 2022*
Published: *13 April 2022*

Citation:
Brabcová V, Tláskal V, Lepinay C, Zrůstová P, Eichlerová I, Šťursová M, Müller J, Brandl R, Bässler C and Baldrian P (2022) Fungal Community Development in Decomposing Fine Deadwood Is Largely Affected by Microclimate. Front. Microbiol. 13:835274. doi: 10.3389/fmicb.2022.835274

INTRODUCTION

Temperate forests represent a significant global sink of carbon (C) (Harris et al., 2021). Part of the C removed from the atmosphere is incorporated into tissues of the trees—wood, leaves, and roots. The amount of C stored in deadwood varies considerably among natural temperate forests of Central Europe, reaching up to 550 m^3 ha^{-1} (Christensen et al., 2005; Král et al., 2010; Seibold et al., 2021). Beech (*Fagus sylvatica*) forests with a variable proportion of fir (*Abies alba*) are among the most common forests in Central Europe (Krah et al., 2018), where they represent the natural vegetation of submontane to montane forests (Bolte et al., 2007). Fine woody debris (FWD, deadwood of diameter < 10 cm) represents only a small portion of deadwood stocks in natural forests where snags and coarse wood of fallen trees are present (Baldrian, 2017; Ricker et al., 2019). Although the amount of fine deadwood in temperate forests estimated typically at 2–9 m^3 ha^{-1} (Nordén et al., 2004; Domke et al., 2016) appears moderate, it represents the dominant stock of deadwood in managed forests where tree stems are harvested. Whereas coarse woody debris (CWD) decomposes slowly and persists over multiple decades (Přívětivý et al., 2018), FWD shows rapid turnover due to fast decomposition (Müller-Using and Bartsch, 2009). Moreover, fragmentation of the FWD resource creates a high variety of habitats and a high number of habitat patches, leading to a high diversity of fungi (Heilmann-Clausen and Christensen, 2004). FWD decomposition might be affected by multiple factors, including tree species, size, and climatic conditions at a site (Berbeco et al., 2012; Ricker et al., 2016), with reported rates of mass loss of 0.17–0.25 $year^{-1}$ (Fasth et al., 2011; Ostrogović et al., 2015).

In forest ecosystems, deadwood decomposition represents one of the paths of nutrient input into soils (Peršoh and Borken, 2017; Šamonil et al., 2020). These nutrients originate in the plant biomass (Šamonil et al., 2020) or, in the case of nitrogen, are fixed from the atmosphere by deadwood bacteria (Rinne et al., 2017; Tláskal et al., 2021) and enter topsoil after full deadwood decomposition. Deadwood is also one of the most important factors contributing to the maintenance of biodiversity in forests (Stokland et al., 2012; Seibold et al., 2015). Namely, it is a habitat and a nutrient source for a wide range of organisms, including microorganisms, fungi and bacteria (Johnston et al., 2016; Větrovský et al., 2020; Tláskal and Baldrian, 2021). Due to filamentous growth, possession of extracellular enzymes and the ability to acidify their substrate, fungi are efficient in the colonization of large patches of wood and its utilization, despite the recalcitrance, fluctuating moisture content and low nitrogen content of this substrate.

The study of fungi on decomposing wood in the past typically targeted CWD (Rajala et al., 2012; Arnstadt et al., 2016; Baldrian et al., 2016), except for the pioneering studies analyzing microbes on decomposing *Salix caprea* twigs (Angst et al., 2018) or substrate preferences of fungi on deadwood of various sizes (Juutilainen et al., 2017). Fungal communities of FWD were typically studied by fruitbody surveys, although the fruitbody approach has several important limitations, such as limited sporocarp production on small woody resources (Ovaskainen et al., 2013). FWD was reported to support higher fungal diversity than the CWD of a corresponding volume (Heilmann-Clausen and Christensen, 2004; Nordén et al., 2004; Bässler et al., 2010). In a comparative survey, 75% of Ascomycota and 30% of Basidiomycota species were found exclusively on FWD (Nordén et al., 2004), and the majority of wood-inhabiting basidiomycetes were found on branches with diameters < 5 cm (Küffer and Senn-Irlet, 2005). Conventional forest management practices remove CWD and change microclimate conditions due to manipulation of the canopy (Bässler et al., 2014). Under such conditions, FWD at clearcuts and in forest stands can serve as an important refuge for wood fungi (Nordén et al., 2004; Küffer and Senn-Irlet, 2005; Juutilainen et al., 2014).

Multiple factors affect fungal communities on deadwood, including tree species, deadwood size or wood decay stage (Juutilainen et al., 2014; Atrena et al., 2020), but among stand-level variables, canopy gaps are also important (Krah et al., 2018; Atrena et al., 2020). The effect of tree species is broadly attributed to the species-specific differences in deadwood properties, namely, in density, content of nitrogen or the amounts and origins of phenolics and other extractives such as resins. These factors lead to different decomposition rates, organismic diversity and successive changes in the compositions and activities of wood decomposing fungal communities (Kahl et al., 2017; Angst et al., 2019). pH and the carbon/nitrogen ratio are strong predictors of the fungal community composition affecting the abundance of dominant fungal taxa (Lepinay et al., 2021a), and their changes goes hand-in-hand with successional changes in fungal communities. Fungi with different morphological traits inhabit deadwood of different qualities, leading to the specialization of the fungal communities and organismic diversity of fungal colonizers (Purhonen et al., 2020). The canopy openness of forests is closely related to their temperature buffering capacity (Frey et al., 2016; De Frenne et al., 2019). Forest gaps are characterized by an increased respiration rate (Forrester et al., 2012), elevated summer temperatures, higher solar radiation, and changed soil water content (Scharenbroch and Bockheim, 2007). Considering that climatic factors are the primary drivers of fungal distribution (Větrovský et al., 2019), FWD seems to be especially sensitive to actual microclimatic conditions due to its high surface-to-volume ratio (Bässler et al., 2010). However, the extent to which microclimate affects fungi in decomposing FWD is not known.

In this study, we set up an experiment where the fates of the FWD of beech (*Fagus sylvatica*) and fir (*Abies alba*), the two main tree species of the temperate forests of central Europe at elevations of 750–900 m a. s. l., were followed for 6 years under open and closed canopies. The aim was to determine the factors affecting the assembly of fungal communities during decomposition and assess the size and relative importance of the effects of microclimate and the host tree. Experimental plots with sunny gaps surrogated the changed microclimatic conditions caused by natural disturbances such as windstorms, insect outbreaks, or forest management. The frequency of these events has increased in the temperate zone, and they have more pronounced effects in managed forests than in unmanaged forests (Sommerfeld et al., 2018). The length of the experiment covered

an extended part of FWD decomposition and lasted until 2017, when mass loss and fragmentation made it impossible to follow FWD at certain locations.

We hypothesized that beech and fir FWDs are inhabited by a substantial share of tree species-specific fungal taxa and tree species are therefore the key factor affecting fungal community. Host tree species were reported as an important driver of fungal community development on coarse deadwood (Nordén et al., 2004; Baber et al., 2016; Krah et al., 2018; Atrena et al., 2020), although not equally strong in all cases (Baldrian et al., 2016). We expected a high share of *r*-selected species, namely, molds and yeasts (Mašínová et al., 2018; Algora Gallardo et al., 2021), in the earlier stages of fine deadwood decomposition, similar to the decomposition of leaf and plant litter (Voříšková and Baldrian, 2013). We further hypothesized that higher canopy openness results in decreased decomposition due to harsher conditions and selection of specific taxa adapted to the actual microclimatic conditions. To evaluate the importance of the FWD as an ecosystem component, we also quantified the amount of FWD present in the temperate forest of the study area representing the typical managed forest in the mountains of Central Europe.

MATERIALS AND METHODS

Study Area and Experimental Design

The experimental sites were located in the management zone of the Bavarian Forest NP in Germany (48.9° N, 13.3°E). The management zone covers an area of 6,000 ha that surrounds the 18,000 ha core zone of the national park. The area is characterized by montane mixed forest consisting of European beech (*Fagus sylvatica* L.), Silver fir (*Abies alba* Mill.) and Norway spruce [*Picea abies* (L.) H. Karst] (Bässler et al., 2010). The sampling design was a part of the broader experimental design described in Krah et al. (2018). In autumn 2011, freshly cut branches of fir and beech were deposited on 64 plots and arranged in a random block design with four spatially independent blocks. The branches (fine woody debris, FWD) had diameters of 3.2 ± 1.3 cm and lengths of 2.7 ± 0.9 m. These branches were taken from trees of the same age that were harvested from the same forest stand. The origin of the branches was identical and branches were randomly distributed across study sites to mitigate the potential effect of communities of fungal endophytes inhabiting individual branches on fungal community development. Each block contained randomly located sets of plots with either fir or beech branches or both. The mixture of fir and beech deadwood represented the factor of forest stand tree diversity. Within each block, two plots per treatment (fir, beech, or mixed) were set under open or closed canopies (**Supplementary Figure 1**). Canopy openness was used as a surrogate for stand microclimates (Müller et al., 2015; Seibold et al., 2015; Krah et al., 2018; De Frenne et al., 2019). The sunny open canopy plots were the result of clearings where an area of 0.1 ha was freed from living and dead trees. To avoid shading by a dense grass layer surrounding the deadwood on sunny plots, each plot was mowed once a year during the growing season as described previously (Seibold et al., 2016a,b). The daily peak temperatures of the deadwood surfaces in summer were measured in the sunny and shady plots. The mean values were much higher in sunny plots (∼30°C) than in the closed canopies (∼15°C) (Müller et al., 2020). All experimental plots were sampled annually in October from 2012 to 2017.

Fine Woody Debris Census

To quantify the local stock of FWD within the unmanaged forest, FWD was collected from the litter surface and organic horizon of soil in thirty-six 2×2 m squares located close to the experimental sites. All FWD inside the square was collected, as well as the FWD intersecting the eastern and southern borders of the square, while the FWD intersecting the western and northern borders was disregarded. The FWD was classified into three size categories (diameters of the thicker end of the FWD of 0.5–1.5, 1.6–5.0, and 5.1–10.0 cm). Per-square counts and masses of the FWD were recorded. FWD from each size category was subsampled and weighed before and after air-drying to assess dry mass content. The per-square FWD mass was estimated by multiplying the wet mass per plot by the relative dry mass content of each size category. Collected FWD was not used in set experiment as it included FWD of different decay length.

Sampling, Sample Processing, and Analysis

One composite FWD sample was obtained from each selected branch. It was obtained from two vertical drillings of the branch in its center using an electric drill equipped with a 10 mm diameter auger across the entire diameter of the branch. The drilling points were placed evenly along the branch, avoiding the close proximity of the ends of the branch. The auger was sterilized between drillings, and the dust from all drilling points was collected in sterile plastic bags and frozen within a few hours after drilling. In total, 2 beech or 2 fir samples were taken from each block from plots containing only beech or fir, and 2 beech and 2 fir samples were taken from plots containing mixed deadwood, resulting in 4 beech and 4 fir composite samples per canopy type. Thus 64 samples in total were taken annually (**Supplementary Figure 1**), resulting in a total of 384 samples in the study.

The drilled materials were weighed in the laboratory and freeze-dried to estimate the deadwood dry mass. Next, it was milled using an Ultra Centrifugal Mill ZM 200 (Retsch, Germany), and the resulting fine powder was used for the subsequent analyses. Dry mass content was based on the loss of mass during freeze-drying, and pH was measured after mixing with distilled water (1:10 w:vol). The wood C and N contents were measured using an elemental analyzer in an external laboratory of the Institute of Botany of the Czech Academy of Sciences, Průhonice, Czech Republic, as described previously (Větrovský and Baldrian, 2015). C was measured using sulfochromic oxidation, and the nitrogen content was estimated by sulfuric acid mineralization with the addition of selenium and sodium sulfate and conversion to ammonium ions, which were measured by a segmented flow analyzer (SFA), Skalar. To

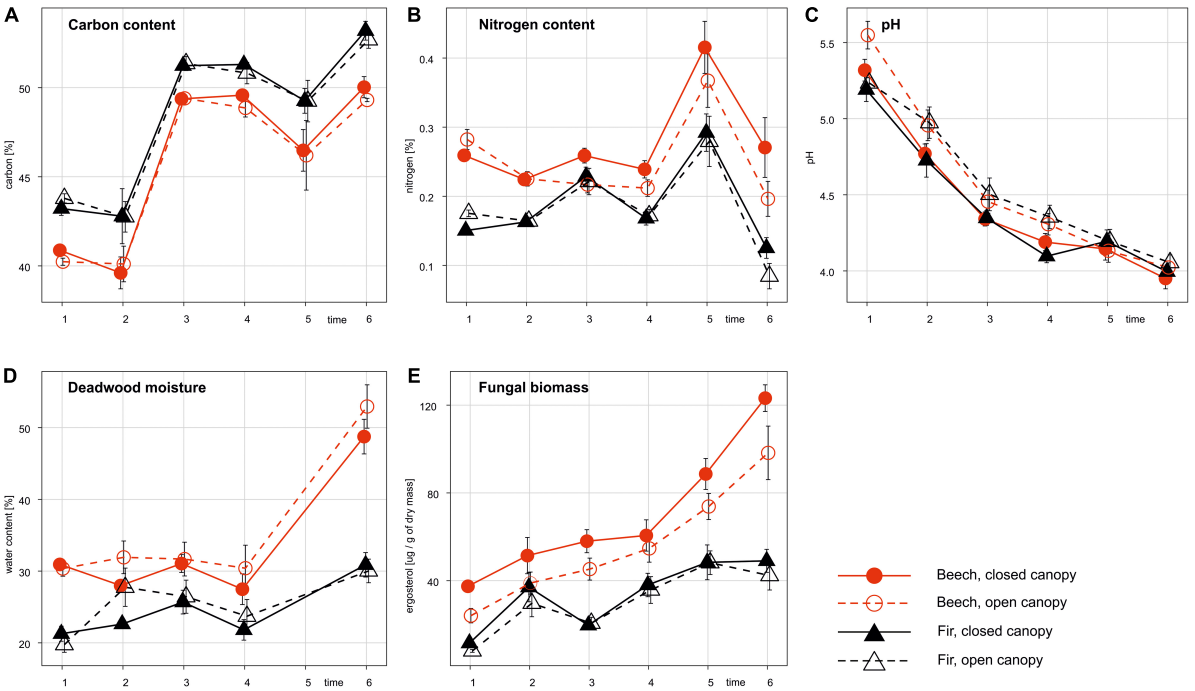

FIGURE 1 | Fungal biomass **(E)** and changes in physicochemical compositions **(A–D)** of fine beech and fir deadwoods during decomposition in a natural temperate forest. Data represent the mean ± SE of 16 samples per treatment and timepoint (years).

quantify fungal biomass, total ergosterol was extracted using 10% KOH in methanol and analyzed by HPLC (Šnajdr et al., 2008).

Extraction and Analysis of Environmental DNA

Total genomic DNA was extracted from 200 mg of freeze-dried material using the NucleoSpin Soil Kit (Macherey-Nagel, Germany) according to the manufacturer's instructions (Baldrian et al., 2016). Briefly, cells were lysed using SL1 lysis buffer. Enhancer SX was added prior to lysis. The samples were homogenized using FastPrep-24 (MP Biomedicals, Santa Anna, United States) at 5 m s^{-1} for 2 × 30 s. In the last step, DNA was eluted from the columns using 50 µl of deionized water. One extraction per sample was performed.

For the microbial community analysis, PCR amplification of the fungal ITS2 region was performed using barcoded gITS7 and ITS4 primers (Ihrmark et al., 2012) in triplicate PCRs per sample as described previously (Baldrian et al., 2016). PCRs contained 2.5 µl of 10 × buffer for DyNAzyme DNA Polymerase, 0.75 µl of BSA (20 mg ml^{-1}), 1 µl of each primer (0.01 mM), 0.5 µl of PCR Nucleotide Mix (10 mM each), 0.75 µl polymerase (2 U $µl^{-1}$ DyNAZyme II DNA polymerase 1: 24 Pfu DNA polymerase) and 1 µl of template DNA. Cycling conditions were 94°C for 5 min, 35 cycles of 94°C for 1 min, 62°C for 1 min, and 72°C for 1 min, and a final extension at 72°C for 10 min. PCR triplicate reaction products were pooled and purified, and amplicon libraries prepared with the TruSeq DNA PCR-Free Kit (Illumina) were sequenced in house on the Illumina MiSeq (2 × 250-base reads).

The amplicon sequencing data were processed using the pipeline SEED 2.1.1 (Větrovský et al., 2018). Briefly, paired-end reads were merged using fastq-join (Aronesty, 2013). The ITS2 region was extracted using ITS Extractor 1.0.11 (Bengtsson-Palme et al., 2013) before processing. Chimeric sequences were detected using Usearch 11.0.667 (Edgar, 2010) and deleted, and sequences were clustered using UPARSE implemented within Usearch (Edgar, 2013) at a 97% similarity level. The most abundant sequences were selected from each cluster, and the closest hits at the species level were identified using BLASTn against UNITE (Nilsson et al., 2019). Where the best hit showed lower similarity than 97 with 95% coverage, the best genus-level hit was identified. Species-level analyses were performed on a dataset where OTUs belonging to the same species were combined and all other OTUs were combined into the genus of the best hit and designated "sp." Sequences identified as *Fagus* sp. or *Abies* sp. were discarded similarly as well as non-fungal sequences. Sequencing data have been deposited in the SRA database under BioProject accession number PRJNA671809.

To assign putative ecological functions to the fungal OTUs, the fungal genera of the best hit were classified into ecological categories (e.g., white rot, brown rot, saprotroph, plant pathogen, ectomycorrhiza) based on (Põlme et al., 2020). Fungal OTUs not assigned to a genus with known ecophysiology and those assigned to genera with unclear ecology remained unclassified.

Data Processing and Statistics

Succession time was defined as the average position of a taxon in succession considering its relative abundance over time, and

the duration of occurrence was defined as the time span covering 90% of the taxon relative abundance as defined and calculated previously (Štursová et al., 2020). Tree or canopy specificity was defined as the strength of association of the taxon with one particular tree or canopy type and calculated as the sum of abundances in beech deadwood (closed canopy deadwood) divided by the sum of abundances in all samples. A value of 1 corresponds to a taxon exclusively found on beech deadwood. A value of 0.5 assigned to a taxon indicates that it is equally abundant on beech and fir deadwood. A value of 0 assigned to a taxon indicates that it is exclusively found on fir deadwood. For canopy openness, a value of 1 corresponds to a taxon exclusively found under the closed canopy and 0 corresponds to a taxon exclusively found under the open canopy. Taxa with tree specificities between 1.0 and 0.95 were considered beech-specific (or closed canopy-specific, respectively), and those with specificities between 0.05 and 0.00 were considered fir-specific (or open canopy-specific, respectively).

Statistical analyses were performed in PAST 4.03[1] and R (R Core Team, 2020). Two-dimensional non-metric multidimensional scaling (NMDS) ordination analysis on Euclidean distances was used to address the dissimilarity of the fungal community compositions based on Hellinger-transformed relative abundances. NMDS was performed in R with the package *vegan*, function metaMDS (Oksanen et al., 2020; R Core Team, 2020). Variables were fitted to the ordination diagram as vectors with 999 permutations and included pH, as well as the C and N and ergosterol contents. Diversity estimates (Shannon–Wiener index, OTU richness, Chao 1, and evenness) were calculated for a dataset containing the relative abundance of 2,000 randomly selected sequences from each sample in SEED 2.1.1 (Větrovský et al., 2018). Differences in the environmental variables (pH, C, N, C/N, ergosterol, and water contents) were tested using a linear mixed model (LMM, function lmer) with log-transformed data. For the LMM, the effect of explanatory variables, i.e., tree species, canopy openness and their interaction, over decomposition time were tested by considering time and plot identifiers (the same plots were repeatedly measured over time) as random effects. Differences between the explanatory variables were also tested for each time separately using two-way ANOVA or the non-parametric Kruskal–Wallis test and Tukey–Kramer HSD test on log-transformed data. Mantel tests with 99,999 permutations were used to examine the correlations between data matrices, and Euclidean distances were used for all variables except community data. One-way or two-way PERMANOVA tests with 9,999 permutations were used to examine the effects of treatments on fungal communities. Spearman rank correlations were used as a measure of the relationships between variables. Variation partitioning analyses on Hellinger-transformed OTU abundances were performed to identify the parts of the variance explained by tree species and canopy openness for the whole dataset and with length of decomposition, canopy openness and wood chemistry (i.e., N, C, C/N and pH) for each tree species independently. Data were rarefied to 2,000 sequences. The "varpart" function from the "vegan" R package was used (Oksanen et al., 2020). The importance values of the obtained variances were determined with Monte Carlo permutation tests. In all cases, differences at $P < 0.05$ were considered statistically significant.

[1]https://www.nhm.uio.no/english/research/infrastructure/past/

RESULTS

Abundance and Moisture of Fine Woody Debris

The abundance of fine woody debris at the tested small-scale plots of 2 × 2 m exhibited high spatial variability, and their masses ranged from 1.4 to 11.50 t ha^{-1} dry mass (90,000–230,000 pieces per ha). On average, 5.3 ± 2.8 t ha^{-1} fine woody debris was recorded. This was composed of 1.0 ± 0.5 t ha^{-1} (19%) of twigs with diameters of < 1.5 cm, 1.9 ± 1.3 t ha^{-1} (35%) of branches with diameters between 1.6 and 5 cm, and 2.4 ± 2.7 t ha^{-1} (46%) of branches with diameters between 5.1 and 10 cm. The mean moisture content of fine woody debris was 26.2 ± 1.8% and it was almost equivalent in all size classes (**Supplementary Figure 2**).

Properties of Fine Woody Debris During Six Years of Decomposition

The chemical and nutritional compositions of FWD differed considerably between tree species. Beech and fir were characterized by different C:N ratios in the first year of decomposition [beech C:N = 154 ± 5, fir C:N = 270 ± 7, $F_{(1,\ 57)} = 231.66$, $P < 0.001$] due to the lower content of N in fir deadwood [0.27 ± 0.01% in beech, 0.16 ± 0.00% in fir, $F_{(1,\ 57)} = 145.70$, $P < 0.001$]. Overall, the carbon contents increased during decomposition (LMM: $\chi^2 = 5.89$, $P = 0.015$), while the N contents fluctuated over time (LMM: $\chi^2 = 0.04$, $P = 0.834$). Beech deadwood had, on average, higher moisture content over the whole experiment, and increased in time. Canopy cover had no effect on deadwood moisture content at the time of sampling in October (**Figure 1**). The pH of both tree species decreased steadily from 5.3 to 4.0 during decomposition (LMM: $\chi^2 = 14.56$, $P < 0.001$). Beech deadwood differed in pH from fir deadwood only in the first year [$F_{(1,\ 57)} = 9.41$, $P = 0.003$]. The pH was significantly lower under the closed canopy in years 2 and 4 of decomposition [$F_{(1,\ 58)} = 4.97$, $P = 0.030$ and $F_{(1,\ 58)} = 8.49$, $P = 0.005$, respectively]. The diversity of the deadwood in the plots (single tree or mixed species) had no effect on the deadwood pH, deadwood moisture, or nutrient contents [$F_{(1,\ 58)} < 0.56$, $P > 0.457$ for all estimates].

Fungal Biomass and Community Compositions in the Different Types of Fine Woody Debris

The fungal biomass content quantified as ergosterol was significantly higher in beech than in fir deadwood throughout the whole experiment (LMM: $\chi^2 = 16.61$, $P < 0.001$). On average it was twice as high (**Figure 1**). While the ergosterol content in beech deadwood increased steadily during the whole experiment from 31 μg g^{-1} in year 1 to 110 μg g^{-1} in year 6, in fir deadwood, it increased only within the first 5 years from 10 to 48 μg g^{-1}

and then remained stable. The canopy cover effect was important after 1 year of decomposition, with higher fungal biomass under the closed canopy [$F_{(1,\ 58)} = 24.13$, $P < 0.001$; **Figure 1**]; higher diversity of deadwood origin on the plot had no effect on fungal biomass [$F_{(1,\ 58)} = 2.51$, $P = 0.115$ for fir and $F_{(1,\ 58)} < 0.01$, $P = 0.949$ for beech].

The fungal diversity estimated as species richness or the Chao-1 index was significantly higher in fir FWD in canopy gaps than under closed canopy gaps ($P < 0.0001$). The species richness overall was highest in beech FWD after 5 years of decomposition, and in fir FWD after 4 years of decomposition while it decreased later (**Supplementary Figure 3**). Among the potential drivers of fungal community composition, one-way PERMANOVA and variation partitioning analyses showed that tree species, canopy cover and time were all significant ($P < 0.0001$, one-way PERMANOVA). Most of the variation was explained by tree species (8.3%) and canopy cover (8.0%) (**Supplementary Figure 4**). Within the separate beech and fir deadwoods, the canopy type and time as well as their interaction had significant effects on fungal communities ($P < 0.0001$, two-way PERMANOVA). Time had clearly a lower impact on fungal community composition than tree species and canopy type (tree $F = 24.3$, canopy $F = 26.6$, time $F = 5.2$, all $P < 0.0001$). Canopy cover explained 11.8 and 12.7% of the detected variability in beech and fir FWD, respectively (**Supplementary Figures 4B,C**).

Based on the data of all OTUs with relative abundances over 0.5% in three or more samples, fungal communities detected in beech and fir FWD clustered separately, as well as in the case of the different canopy types (**Figure 2A**). Although the stress value of NMDS was high, the results were supported by other statistical results. Over time, fungal communities underwent changes but remained treatment-specific. The most important differences were detected in the initial stage of decomposition. Although the composition of communities tended to converge, treatments remained clearly separated even after 6 years of decomposition (**Figure 2A**). The increased diversity of deadwood origin present on site did not clearly affect the community structure. However, detailed PERMANOVA revealed a marginal effect of increased FWD diversity on fungal community structure composition in fine beech deadwood ($P = 0.054$) but not in fine fir deadwood ($P = 0.275$).

The fungal communities in fine beech and fir deadwoods were characterized by continuous changes in the relative abundances of Ascomycota and Basidiomycota. Among other fungal phyla, only Mucoromycota were more abundant in fir deadwood under the closed canopy in approximately the middle of the decomposition, where the share of their sequences was approximately 7%. The fungal community in beech FWD in year 1 was dominated by the sequences of Ascomycota (75%). With time, it initially decreased to 35% and later increased to 57% at the end of the experiment. The share of Basidiomycota sequences reached its maximum in the middle part of the experiment at 64% (**Figure 3A**). The share of Ascomycota was substantially higher, by 19–52% under the open canopy during the whole course of the experiment.

At the order level, beech deadwood under the closed canopy was dominated by *Xylariales*, which were gradually replaced by

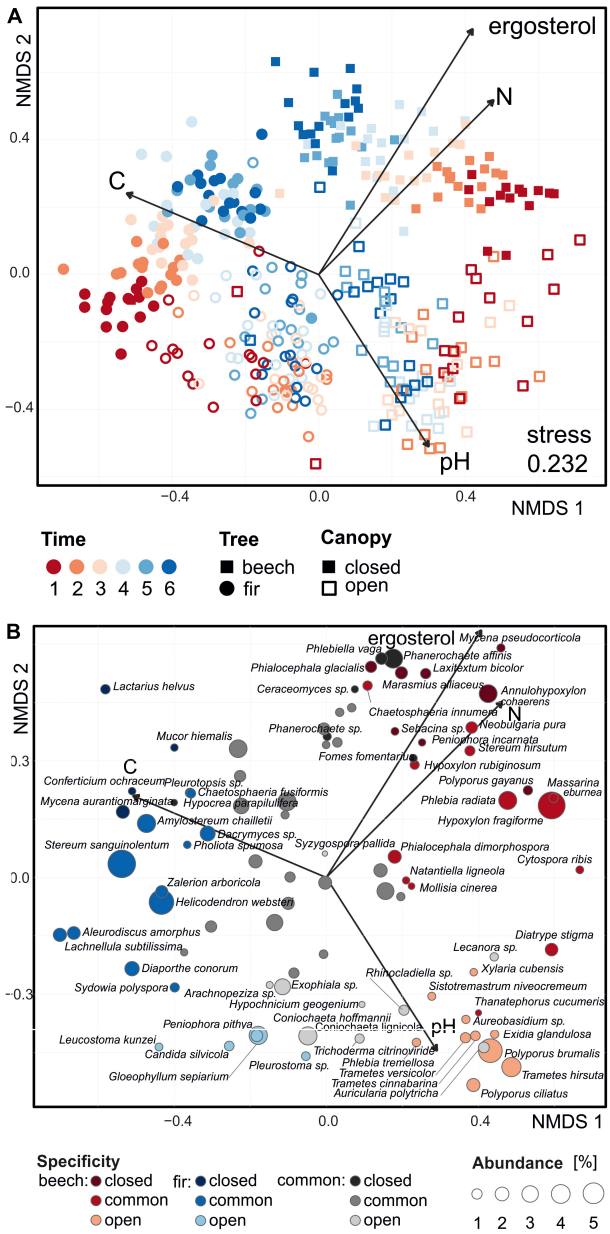

FIGURE 2 | Non-metric multidimensional scaling of decomposing fine deadwood of beech and fir under different microclimatic conditions in a natural temperate forest based on dissimilarities among samples. Analysis was based on Euclidean distances on Hellinger-transformed relative abundances. Vectors indicate environmental variables with significant correlations with NMDS results ($P < 0.05$). **(A)** Samples are represented by points. OTUs with relative abundances over 0.5% in at least three samples were included. **(B)** Each point represents the abundant species and its specificity for substrate and microclimatic conditions. The size of the point is scaled based on the relative average abundances in all samples. Species with maximal abundances over 5% in at least three samples are displayed.

Polyporales, whereas a high share of *Coniochaetales* or *Helotiales* was observed at the end of the experiment under the open canopy (**Figure 3B**). Fir FWD under the closed canopy was initially dominated by *Helotiales* and *Russulales*, while the shares

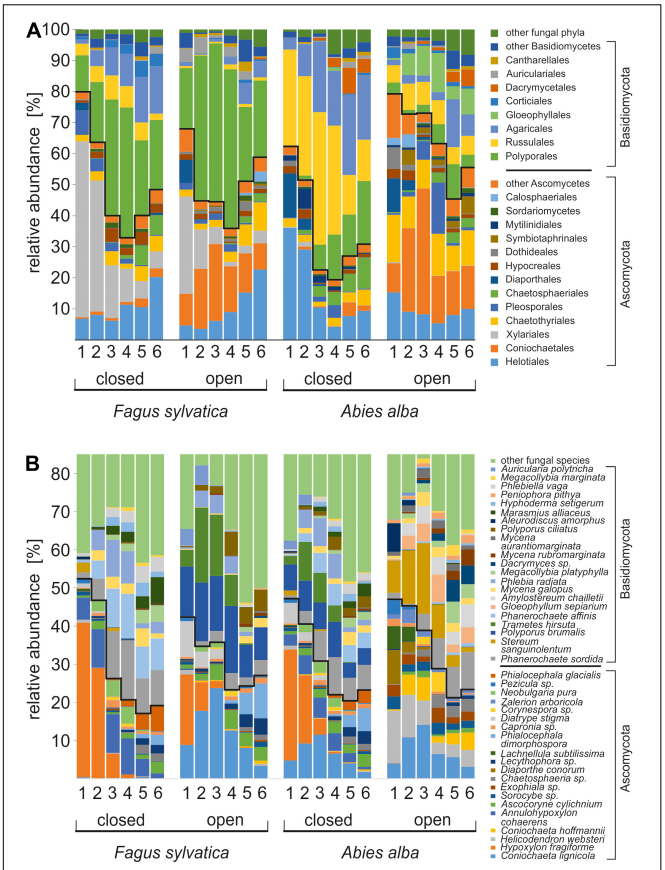

FIGURE 3 | Succession of fungi in decomposing fine beech and fir deadwoods in a natural temperate forest. The data represent the means of 16 samples per treatment for fungal orders **(A)** and species **(B)**. Fungal orders and species with average abundances over 0.5% are included. Lines separate Ascomycota and Basidiomycota.

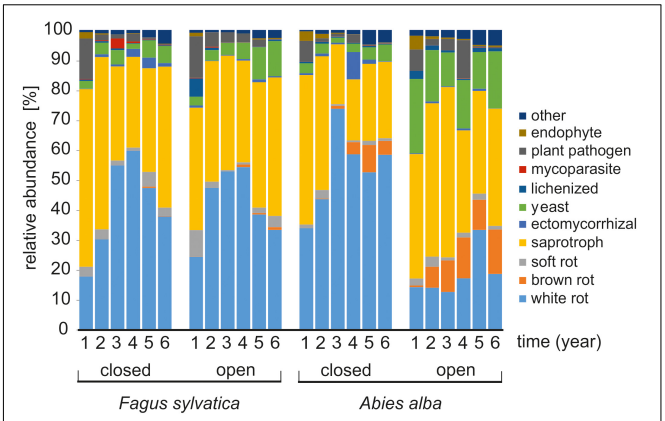

FIGURE 4 | Diversity of fungal ecophysiological groups in fine beech (*Fagus sylvatica*) and fir (*Abies alba*) deadwoods decomposing in a natural temperate forest. Data represent means from 16 samples from 4 sampling sites.

of *Agaricales* and *Polyporales* increased with time. In contrast, the fungal community of fir deadwood decomposing under the open canopy was phylogenetically diverse, with higher shares of *Coniochaetales*, *Chaetotriales*, *Helotiales*, *Russulales,* and *Gloephyllales* (**Figure 3**).

Initially, both tree species were mainly colonized by fungi classified as saprotrophs (60% beech and 50% fir deadwood) with some share of white-rot fungi (18 and 34%, respectively) and plant pathogens (14 and 7%, respectively) under the closed canopy. Later, white-rot fungi dominated the decomposition of both deadwood species. Relatively higher shares of ectomycorrhizal fungi (up to 4% in beech and 9% in fir) were occasionally observed in the later phases of the experiment under a closed canopy. Brown-rot fungi increased in the later phases of fir decomposition, where their sequences represented up to 9% (**Figure 4**). The abundance of yeasts was clearly increased in fir deadwood under the open canopy, by an average of 2.6-fold compared to the closed canopy, and the same was observed in beech deadwood at the end of the experiment. Two-way PERMANOVA (Bray–Curtis distance, 9,999 permutations) revealed that in beech deadwood, only the time of decomposition (P = 0.0001) but not the canopy type (P = 0.1852) affected the share of fungi with different ecologies. In contrast, on fir, time (P = 0.0001), canopy (P = 0.0001) and their interaction (P = 0.0005) had significant effects. The increased diversity of the mixed FWD did not affect the fungi share of ecological groups.

The vast majority of fungal taxa were detected only over a limited timeframe in succession (**Figure 5**). The durations of occurrence were variable among the fungi but very often they were limited to a few years, indicating fast community turnover. Regardless of the deadwood species or canopy type, the fungi present in the initial decomposition had low occurrence durations (typically 1–2 years), while those fungi that first appeared at intermediate and late stages of the experiment were sometimes present for 4 or more years (**Figure 5**). Most of the highly abundant fungi were restricted to only beech deadwood (34%) or to only fir deadwood (23%). The vast majority of the fungi did not prioritize according to the canopy type (58% in beech, 73% in fir deadwood), yet as much as 19 and 10% of the fungi were closed canopy-specific in beech and fir deadwoods, respectively (**Figure 2B**). Tree species-specific fungi were present throughout the decomposition. However, their highest shares were observed at the beginning of decomposition, where tree-unspecific fungal species with calculated specificity <0.95 are largely missing. Canopy-specific fungi were present in equal shares over the decomposition (**Figure 6**). The calculated succession times of the commonly present fungal species did not significantly differ in beech or fir deadwoods, nor under open or closed canopies (**Supplementary Figure 5**).

Among fungi with high relative sequence abundances in beech deadwood under a closed canopy, *Hypoxylon fragiforme, Polyporus gayanus,* and *Massarina eburnea* were typical during early decomposition. Later, those and *Phanerochaete sordida, Phanerochaete affinis, Annulohypoxylon cohaerens,* and *Phlebia radiata* were replaced by *Marasmius alliaceus* and *Phialocephala glacialis* at the end of the decomposition. Decomposing fir deadwood under closed canopy was in the early phase dominated by *Helicodendron websteri, Stereum sanguinolentum,*

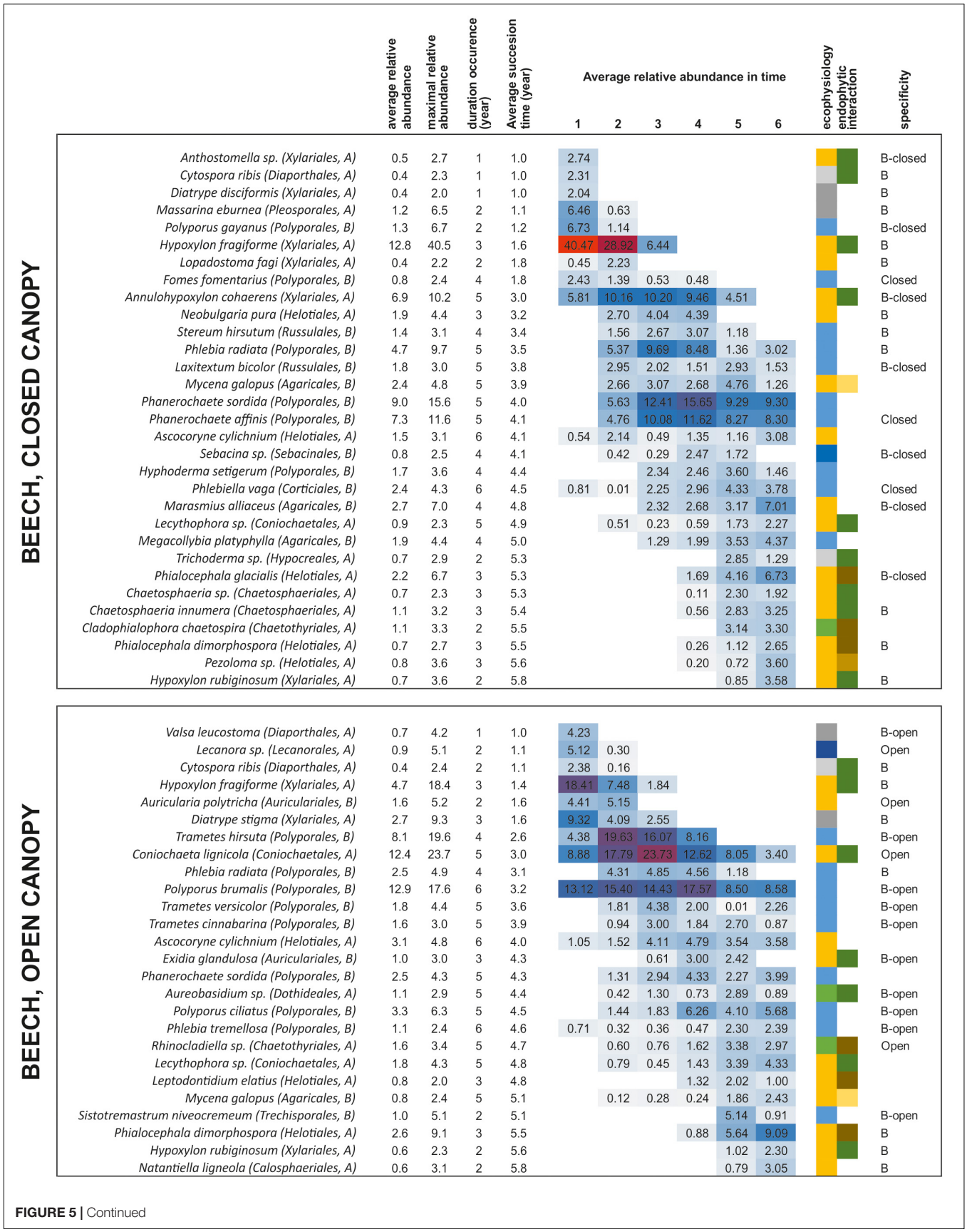

FIGURE 5 | Continued

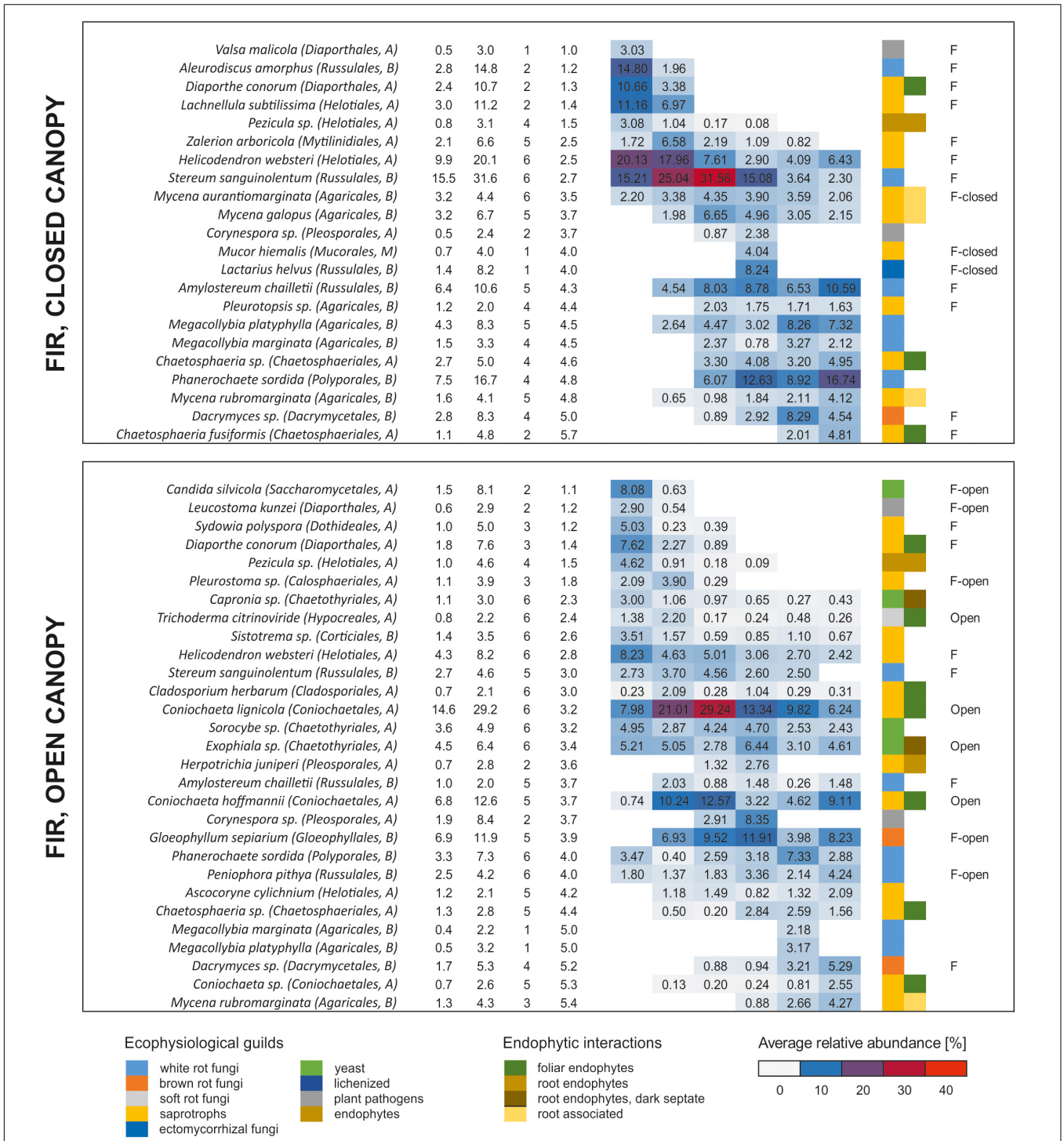

FIGURE 5 | Successional development of the fungal communities in beech *(Fagus sylvatica)* and fir *(Abies alba)* fine deadwoods decomposing under closed and open canopies in a natural temperate forest. All taxa with abundances above 1% in 3 yearly observations or maximum relative abundances in any single year over 2% were considered.

Aleurodiscus amorphus, Lachnellula subtilissima, Diaporthe conorum followed by *Zalerion arboricola*. From the second year of decomposition, *Stereum sanguinolentum* dominated the fungal community and was later accompanied by *Amylostereum chailletii, Lactarius helvus,* and *Mycena galopus*. The late phase community typically had higher shares of sequences of *Phanerochaete sordida, Dacrymyces* sp. and *Megacollybia platyphylla*. Under the open canopy, *Hypoxylon fragiforme* is a

typical fungus in the first years of decomposition, but in addition to this, *Trametes hirsuta*, *Diatrype stigma*, *Auricularia polytricha,* and *Lecanora* sp. were also found at high sequence abundances. The late phase of decomposition under the open canopy typically contained *Phialocephala dimorphospora, Polyporus ciliatus,* and *Sistotremastrum niveocremeum*. The fir deadwood under the open canopy initially showed a higher diversity of abundant fungal taxa with high shares of *Candida silvicola*, *Diaporthe conorum* and *Sydowia polyspora*. Further on, *Coniochaeta lignicola*, *Coniochaeta hoffmannii,* and *Gloeophyllum sepiarium* dominated the fungal community, along with *Corynespora* sp., *Helicodendron websteri,* and *Exophiala* sp. These taxa were replaced by *Phanerochaete sordida* and *Dacrymyces* sp. at the end of the decomposition (**Figure 5**).

Only a few highly abundant taxa exhibited low substrate specificity and were present in both deadwood species. This was the case for *Coniochaeta lignicola*, *Phanerochaete sordida*, *Mycena galopus,* and *Megacollybia platyphylla* (**Supplementary Figure 6**). The share of fungi common to both tree species increased over time and declined shortly before the end of the experiment, which was similar to the diversity of the fungal decomposer community overall. Their preferences for certain succession stages were mostly similar in beech and fir deadwoods ($P < 0.0001$, $R^2 = 0.6999$). Similarly, the succession times of fungi without canopy specificity did not differ ($P < 0.0001$, $R^2 = 0.8994$, beech deadwood; $P < 0.0001$, $R^2 = 0.6842$, fir deadwood) (**Figure 6**).

DISCUSSION

Fine Woody Debris in the Forest Ecosystem

The stock of fine woody debris present in the management zone of the Bavarian Forest NP was estimated at 5.3 t ha^{-1} (∼17.5 m^3 ha^{-1}), which is within the range previously reported in temperate broadleaf forests (Nordén et al., 2004). However, this estimated deadwood mass is considerably smaller than that estimated for natural beech-dominated forest reserves that is rich in dead tree trunks (coarse woody debris, CWD) and can have 130–300 m^3 of woody debris per hectare (Christensen et al., 2005; Král et al., 2018). Calculated amount of FWD roughly corresponds to the recently reported quantity of coarse woody debris in European forests across all management types that reached only 11.5 m^3 ha^{-1} (Forest Europe, 2015). This is the consequence of intensive forest management, where the total amount of deadwood is limited to 10–20% of its original mass. That is caused mainly by extracting the CWD (Müller-Using and Bartsch, 2009). Fine woody debris (with diameters < 10 cm) thus currently represents the bulk of the deadwood stock in the majority of the managed forest ecosystems in Europe. More importantly, the C flux through FWD is much faster than that through CWD. A recent analysis showed that 50% of mass from beech CWD is lost within 25–38 years in warm humid climates corresponding to the Bavarian Forest NP. The higher value is for CWD with diameters > 55 cm, while the lower value is for CWD with diameters of 10–25 cm (Přívětivý et al., 2016). The values for fir wood are comparable (Přívětivý et al., 2018). Compared to that, 50% of the mass loss of FWD is achieved considerably faster, within 7 years (Angst et al., 2018; Přívětivý et al., 2018). The FWD turnover is thus roughly 5 times faster than of CWD and we observe only one fifth of the deposited FWD over the time equal to lifespan of CWD. Therefore, the stock of 5.3 t ha^{-1} of FWD recorded in the Bavarian Forest NP would thus correspond, in terms of yearly production, to a stock of 26.5 t ha^{-1} (or approximately 90 m^3 ha^{-1}) of CWD, which is approximately half of the values observed in unmanaged forests (Král et al., 2010). Undoubtedly, the contribution of FWD to the flow of complex C compounds and other nutrients temporarily stored in wood into soil is highly important.

Fine Woody Debris Decomposition

Our experiment allowed us to analyze the FWD decomposition until the branches at certain locations disintegrated and thus it covered a large proportion of the FWD lifespan. The rapid decay progress was demonstrated by the increasing ergosterol content, deadwood moisture and wood pH decrease, both of which reflect the activity of fungal wood decomposers (Baldrian et al., 2016; Lepinay et al., 2021a,b; Přívětivý and Šamonil, 2021). The higher ergosterol contents and moisture of beech FWD suggest their faster decomposition, as already described for identical tree species (Přívětivý et al., 2016; Kahl et al., 2017; Lepinay et al., 2021a; Přívětivý and Šamonil, 2021). The tree specificity of deadwood moisture was previously described for *A. abies* and *F. sylvatica* (Přívětivý and Šamonil, 2021). The tree specificity in deadwood moisture may reflect the different retention capacity of deadwood based on its physiochemical properties. The rapid advance of beech FWD decomposition was also indicated by the presence of ectomycorrhizal species that typically occur in the latest stages of succession (Rajala et al., 2012; Baldrian et al., 2016).

The consistent changes in deadwood chemistry reflected its initial composition and set the stage for a functionally even decomposition process regardless of the deadwood origin and microclimatic conditions. In detail, the open canopy slowed initial fungal colonization, as demonstrated by the significantly lower amounts of ergosterol in year 1 and slower acidification, but this canopy effect disappeared later. The changing pH of the FWD was likely one of the factors affecting fungal community assembly since it is a strong predictor of fungal community composition on deadwood (Purahong et al., 2018), and many deadwood fungi show specific pH preferences (Lepinay et al., 2021a).

Fungal Community Composition and Its Drivers

The compositions of the fine deadwood fungal communities were strongly affected by both tree species and microclimatic conditions. Our results are thus in line with observations on coarse deadwood that identified substrate quality (tree species) and climate (temperature and moisture) as the key factors affecting fungal communities (Rayner and Boddy, 1988; Rajala et al., 2012; Abrego et al., 2017; Bani et al., 2018;

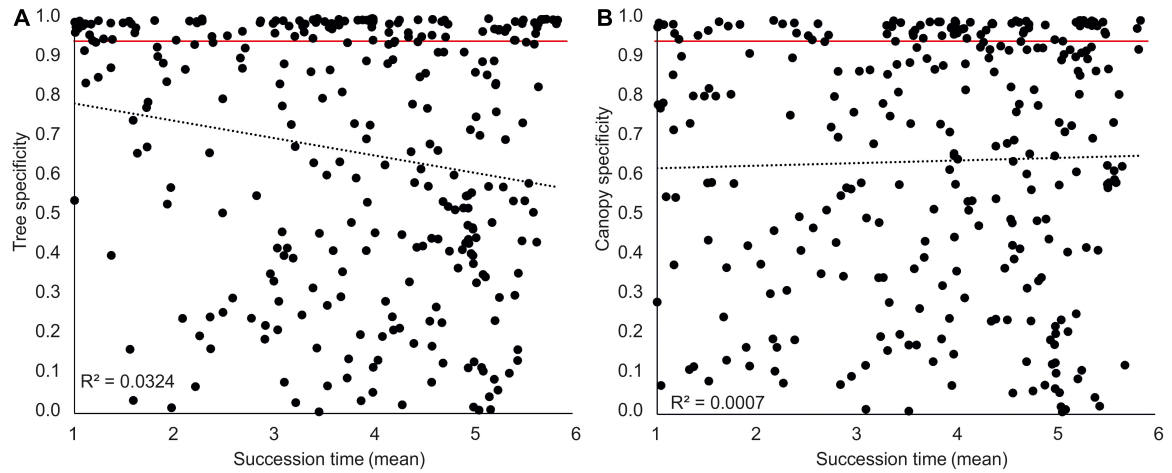

FIGURE 6 | Specificity of fungal taxa to FWD type and microclimatic conditions during succession on beech (*Fagus sylvatica*) and fir (*Abies alba*) fine woody debris (FWD) in a natural temperate forest. All taxa with abundances above 0.5% in at least 3 samples and above 1% in a single sample are represented by a dot. Species were considered specific if a minimum of 95% of the detected sequences were found in one FWD type or under one of the defined microclimatic conditions (marked with full red line). Correlations between succession time (in years) and **(A)** the level of specificity to a FWD type (Spearman R = -0.1304, P = 0.0246) or **(B)** microclimatic conditions—canopy manipulation (Spearman R = 0. 0359, P = 0.5380).

Purahong et al., 2018; Harmon et al., 2020). Beyond the seasonal climate, microclimate extremes cause more variability in the environment. Importantly, both the tree species and microclimatic conditions influenced the whole successional development of fine woody debris fungal communities, thus confirming the sensitivity of the FWD fate to microclimates.

Fungal communities on beech and fir FWD underwent successional development but remained distinct throughout the whole experiment. Previously, certain fungal species were reported to prefer beech or fir CWD in mixed forests (Lepinay et al., 2021a), but the differences were often indistinct (Baldrian et al., 2016). The level of tree species specificity on FWD observed here was considerably higher. The observed specialization of Ascomycota to FWD or deadwood of smaller size is in line with previous reports (Nordén et al., 2004; Rajala et al., 2012). The colonization of FWD is certainly easier than that of CWD due to its large surface-to-volume ratio and allows the establishment of Ascomycota, whose ability to decompose recalcitrant wood components is limited (Eichlerová et al., 2015). The high share of Ascomycota in the initial phase of deadwood and litter decomposition is typical (Voříšková and Baldrian, 2013; Baldrian et al., 2016; Štursová et al., 2020; Lepinay et al., 2021a) and reflects the high share of opportunists in this fungal phylum that prefer to utilize the less recalcitrant components of the plant biomass (Algora Gallardo et al., 2021). Detection of Mucoromycota in the fourth year of decomposition may indicate their involvement in the decomposition of the mycelia of early fungal colonizers since these fungi are frequently associated with decomposing fungal biomass (Brabcová et al., 2018; Algora Gallardo et al., 2021).

In both deadwood species, the initial community of saprotrophs, white-rot fungi and plant pathogens was later replaced and dominated by various white-rot fungi. Similar to our finding, brown-rot fungi are most frequently found in the intermediate stage of CWD decomposition (Rajala et al., 2012). Brown-rot fungi are considered to have adapted to decompose wood where there is lower competitive pressure (Song et al., 2017), which is clearly contrasting with the many cord-forming white-rot soil fungi with combative life-history strategies (Rayner and Boddy, 1988; Boddy and Hiscox, 2017). We found that white-rot fungi were commonly present on both substrates. Ectomycorrhizal fungi were more represented only in the later decomposition of FWD. They are frequently found on tree seedlings commonly growing on dead tree trunks and their low frequency in FWD is likely due to the fact that this is impossible on FWD.

Experimental opening of the canopy in our experiment resulted in considerably different penetration rates of solar radiation, which were, on average, sevenfold higher in cleared plots on an area of 0.5 ha (Krah et al., 2018), and the summer temperatures on deadwood surfaces were on average twofold higher under open canopies than under closed canopies (Müller et al., 2020). The dense canopy acts as a thermal buffer, possibly mitigating the severity of the impacts of climate change on forest biodiversity and functioning (De Frenne et al., 2019). Canopy gaps can promote the diversity of wood-inhabiting fungi on CWD (Brazee et al., 2014) as well as arthropods (Horák et al., 2016; Seibold et al., 2018). An increase in fungal diversity was observed only in the fir FWD in the present study, but the open canopy clearly prioritize different FWD fungi than the closed canopy. We assume that fungal taxa presence is driven by a combination of nutritional and climatic factors. Interestingly, the fir FWD decomposition under the harsh open canopy environment was dominated by Ascomycota throughout the whole process (**Figure 3**). Some ascomycetes are endophytes or pioneer species that can rapidly colonize new and competition-free woody substrates (Menkis et al., 2004; Parfitt et al., 2010). Their presence may indicate lower competitive forces being present in fir FWD.

Broad niche differentiation in FWD (Bässler et al., 2010) is further supported by the diversity of fungal guilds detected in canopy gaps, with a high abundance of plant pathogens, yeasts (in both FWD types) and brown-rot and soft-rot fungi observed in fir (**Figure 4**). This may also indicate a lower ability of otherwise highly competitive white-rot fungi to cope with stressful environmental conditions leading to the phylogenetic diversification of the fungal community.

In general, the guild of foliar endophytes was very abundant in the early decomposition regardless of the tree species, which confirms that they are priority colonizers initiating wood decomposition (Song et al., 2017). As already proposed, there is a strong priority effect in fungal community assembly in deadwood (Boddy, 2000; Hiscox et al., 2015; Krah et al., 2018). An increased abundance of yeasts was typical for advanced decomposition. These fungi are known to utilize various substrates (Mašínová et al., 2018), including fungal mycelium (Brabcová et al., 2018). A high proportion of the recorded fungi were dark septate endophytes recently detected in decomposing roots (Kohout et al., 2021), a type of substrate that is similar in size and composition to FWD.

Individual taxa showed various levels of preferences for tree species, microclimatic conditions and certain decomposition stages. Regardless of the conditions, fungal species were typically present over only a limited timeframe, typically 1–2 years for the early colonizers and a longer time for later inhabitants. Such a fast turnover of taxa is rather typical of litter (Voříšková and Baldrian, 2013; Urbanová et al., 2015) and less pronounced on coarse deadwood, where many fungal taxa persist for a long time during the deadwood lifecycle (Baldrian et al., 2016). Fungal taxa associated with both beech and fir appeared at a similar timepoint, demonstrating that the succession time of common taxa is an equally stable trait of FWD-associated fungi as that for litter decomposers (Štursová et al., 2020). Tree-specific fungi were detected over the whole decomposition and were most abundant during the initial decomposition. This is likely a consequence of the tree specificity of fungal endophytes and their priority in colonization or a result of filtering by nutrient availability (Bhatnagar et al., 2018). The microclimatic conditions seem to be a weaker filter of the initial colonization, and canopy-specific fungi were rather evenly distributed in time with a slightly higher share in later decomposition.

The contribution of the FWD to the forest biodiversity pool has not been frequently addressed. Forest fungal biodiversity is broadly limited by deadwood manipulation during forest management (Juutilainen et al., 2014), which also includes FWD manipulation (Sandström et al., 2019). Follow up studies emphasized, that particularly CWD of a smaller diameter is highly important in the preservation of fungal biodiversity in managed forests (Heilmann-Clausen and Christensen, 2004). Nonetheless, the very fine (<5 cm diameter) and fine woody debris (5–10 cm diameter) may harbor 75% of the total fungal diversity (Abrego et al., 2017; Juutilainen et al., 2017). Comparing our results with an equally detailed study of fungal communities that are important in the CWD decomposition of *Fagus sylvaticus* and *Abies alba* (Lepinay et al., 2021b), we enumerated identical overall numbers of fungal OTUs. We confirmed that FWD is very important for the diversity of Ascomycota, whereas CWD must also be present to ensure the occurrence of many basidiomycete species (Nordén et al., 2004). The assemblage of CWD fungal communities is mainly determined by tree species and deadwood stage (Müller et al., 2020), while we stress that microclimatic factors are another key determinant of FWD fungal biodiversity.

CONCLUSION

This study highlights the importance of FWD in forest carbon stock, biodiversity and high variability of microclimatic conditions in mitigating the impact of conventional forest management. In agreement with our hypothesis, tree species were an important driver of fungal community assembly in FWD. Microclimatic conditions represented another, almost equally strong determinant of the fungal community. Combinations of these factors resulted in typical succession series during FWD decomposition. Increased deadwood species diversity did not affect the fungal communities of unique FWDs. Ascomycota were the main fungal group involved in FWD decomposition. Depending on tree species and environmental factors, these fungi may dominate the whole decomposition process in contrast to the dominant role of Basidiomycota in coarse deadwood. Tree-specific fungal species were common during initial decomposition, whereas canopy-specific fungi were less frequent and rather evenly distributed over time. The presence of a sufficient amount of FWD, forest stand diversity and microclimatic conditions are important factors in the maintenance of fungal diversity. Moreover, fine woody debris represents an important input of recalcitrant plant biomass whose decomposition liberates wood nutrients into soil. Fine deadwood production is comparable in size to that of coarse deadwood in natural forests and represents the bulk of deadwood turnover in the majority of European forests that are managed and thus devoid of coarse deadwood.

DATA AVAILABILITY STATEMENT

The datasets presented in this study can be found in online repositories. The names of the repository/repositories and accession number(s) can be found below: https://www.ncbi.nlm.nih.gov/sra, PRJNA671809.

AUTHOR CONTRIBUTIONS

CB, PB, JM, and RB: conceptualization. CB, VT, PZ, PB, and VB: experimental design and methodology. VT, PZ, IE, CL, MŠ, and VB: performance of experimental work, data evaluation, and statistical analyses. CB, PB, and VB: validation. VB: writing—original draft preparation. VT, CL, CB, JM, PB, and VB: writing—review and editing. PB and VB: supervision, project administration, and funding acquisition. All authors have read and agreed to the published version of the manuscript.

FUNDING

This research was funded by the Czech Science Foundation (21-09334J).

ACKNOWLEDGMENTS

We thank Tomáš Větrovský for retrieving and providing the raw sequencing data. The members of the Laboratory of Environmental Microbiology are acknowledged for help with the fine woody debris census.

SUPPLEMENTARY MATERIAL

The Supplementary Material for this article can be found online at: https://www.frontiersin.org/articles/10.3389/fmicb.2022.835274/full#supplementary-material

Supplementary Figure 1 | Experimental design, based on a figure from Krah et al. (2018).

Supplementary Figure 2 | Amount of deadwood present on the forest floor of a Bavarian Forest NP and moisture levels of the fine woody debris (FWD), log scale. Small FWD: 0.5–1.5 cm in diameter, mid-size FWD: 1.6–5.0 cm in diameter, large FWD: 5.1–10.0 cm in diameter, parts with minimum lengths of 10 cm. Boxes indicate the lower and upper quartiles, and individual points represent separate 2 × 2 m sampling plots.

Supplementary Figure 3 | Diversity of fungi during the decomposition of the FWD of beech and fir in a temperate natural forest expressed as OTU richness and Chao 1 estimates. Development of diversity estimated over time (left), overall differences not considering community development over time (right).

Supplementary Figure 4 | Venn diagram representing the results of variation partitioning analyses on Hellinger-transformed OTU abundances. **(A)** Tree species and canopy cover calculated using all FWD samples, **(B)** canopy cover, time and deadwood chemism for beech FWD, C: canopy, time and deadwood chemism for fir FWD.

Supplementary Figure 5 | Occurrence of fungal taxa during succession on beech and fir fine woody debris (FWD) in a montane forest according to FWD type and microclimatic conditions. Correlations between succession time (in years) of each fungal taxon present on mixed beech and fir FWD (**A**, $P < 0.0001$), detected under open and closed canopies in beech (**B**, $P < 0.0001$) or fir (**C**, $P < 0.0001$) fine woody debris. All taxa with abundances above 0.5% in three or more samples and above 1% in at least one sample were considered.

Supplementary Figure 6 | Commonly present fungal species and their succession during fine woody debris decomposition. The figure includes species present in at least three samples over 1%, with maximal abundance in a single year over 2% or an average abundance over 0.5%. **(A)** Fungal species common in beech and fir deadwoods, **(B)** beech deadwood, both canopy types, **(C)** fir deadwood, both canopy types.

REFERENCES

Abrego, N., Norberg, A., and Ovaskainen, O. (2017). Measuring and predicting the influence of traits on the assembly processes of wood-inhabiting fungi. *J. Ecol.* 105, 1070–1081. doi: 10.1111/1365-2745.12722

Algora Gallardo, C., Baldrian, P., and López-Mondéjar, R. (2021). Litter-inhabiting fungi show high level of specialization towards biopolymers composing plant and fungal biomass. *Biol. Fertil. Soils* 57, 77–88. doi: 10.1007/S00374-020-01507-3

Angst, Š, Baldrian, P., Harantová, L., Cajthaml, T., and Frouz, J. (2018). Different twig litter (*Salix caprea*) diameter does affect microbial community activity and composition but not decay rate. *FEMS Microbiol. Ecol.* 94:fiy126. doi: 10.1093/femsec/fiy126

Angst, Š, Harantová, L., Baldrian, P., Angst, G., Cajthaml, T., Straková, P., et al. (2019). Tree species identity alters decomposition of understory litter and associated microbial communities: a case study. *Biol. Fertil. Soils* 55, 525–538. doi: 10.1007/s00374-019-01360-z

Arnstadt, T., Hoppe, B., Kahl, T., Kellner, H., Krüger, D., Bauhus, J., et al. (2016). Dynamics of fungal community composition, decomposition and resulting deadwood properties in logs of *Fagus sylvatica*, *Picea abies* and *Pinus sylvestris*. *For. Ecol. Manage.* 382, 129–142. doi: 10.1016/j.foreco.2016.10.004

Aronesty, E. (2013). Comparison of sequencing utility programs. *Open Bioinform. J.* 7, 1–8. doi: 10.2174/1875036201307010001

Atrena, A., Banelytė, G. G., Læssøe, T., Riis-Hansen, R., Bruun, H. H., Rahbek, C., et al. (2020). Quality of substrate and forest structure determine macrofungal richness along a gradient of management intensity in beech forests. *For. Ecol. Manage.* 478:118512. doi: 10.1016/j.foreco.2020.118512

Baber, K., Otto, P., Kahl, T., Gossner, M. M., Wirth, C., Gminder, A., et al. (2016). Disentangling the effects of forest-stand type and dead-wood origin of the early successional stage on the diversity of wood-inhabiting fungi. *For. Ecol. Manage.* 377, 161–169. doi: 10.1016/j.foreco.2016.07.011

Baldrian, P. (2017). Forest microbiome: diversity, complexity and dynamics. *FEMS Microbiol. Rev.* 41, 109–130. doi: 10.1093/femsre/fuw040

Baldrian, P., Zrůstová, P., Tláskal, V., Davidová, A., Merhautová, V., and Vrška, T. (2016). Fungi associated with decomposing deadwood in a natural beech-dominated forest. *Fungal Ecol.* 23, 109–122. doi: 10.1016/j.funeco.2016.07.001

Bani, A., Pioli, S., Ventura, M., Panzacchi, P., Borruso, L., Tognetti, R., et al. (2018). The role of microbial community in the decomposition of leaf litter and deadwood. *Appl. Soil Ecol.* 126, 75–84. doi: 10.1016/j.apsoil.2018.02.017

Bässler, C., Ernst, R., Cadotte, M., Heibl, C., and Müller, J. (2014). Near-to-nature logging influences fungal community assembly processes in a temperate forest. *J. Appl. Ecol.* 51, 939–948. doi: 10.1111/1365-2664.12267

Bässler, C., Müller, J., Dziock, F., and Brandl, R. (2010). Effects of resource availability and climate on the diversity of wood-decaying fungi. *J. Ecol.* 98, 822–832. doi: 10.1111/j.1365-2745.2010.01669.x

Bengtsson-Palme, J., Ryberg, M., Hartmann, M., Branco, S., Wang, Z., Godhe, A., et al. (2013). Improved software detection and extraction of ITS1 and ITS2 from ribosomal ITS sequences of fungi and other eukaryotes for analysis of environmental sequencing data. *Methods Ecol. Evol.* 4, 914–919. doi: 10.1111/2041-210X.12073

Berbeco, M. R., Melillo, J. M., and Orians, C. M. (2012). Soil warming accelerates decomposition of fine woody debris. *Plant Soil* 356, 405–417. doi: 10.1007/s11104-012-1130-x

Bhatnagar, J. M., Peay, K. G., and Treseder, K. K. (2018). Litter chemistry influences decomposition through activity of specific microbial functional guilds. *Ecol. Monogr.* 88, 429–444. doi: 10.1002/ecm.1303

Boddy, L. (2000). Interspecific combative interactions between wood-decaying basidiomycetes. *FEMS Microbiol. Ecol.* 31, 185–194. doi: 10.1016/S0168-6496(99)00093-8

Boddy, L., and Hiscox, J. (2017). "Fungal ecology: principles and mechanisms of colonization and competition by saprotrophic fungi," in *The Fungal Kingdom*, eds B. J. Howlett, E. H. Stukenbrock, J. Heitman, N. A. R. Gow, P. W. Crous, and T. Y. James (Washington, DC: American Society of Microbiology), 293–308. doi: 10.1128/microbiolspec.funk-0019-2016

Bolte, A., Czajkowski, T., and Kompa, T. (2007). The north-eastern distribution range of European beech – a review. *Forestry* 80, 413–429. doi: 10.1093/forestry/cpm028

Brabcová, V., Štursová, M., and Baldrian, P. (2018). Nutrient content affects the turnover of fungal biomass in forest topsoil and the composition of associated microbial communities. *Soil Biol. Biochem.* 118, 187–198. doi: 10.1016/j.soilbio.2017.12.012

Brazee, N. J., Lindner, D. L., D'Amato, A. W., Fraver, S., Forrester, J. A., and Mladenoff, D. J. (2014). Disturbance and diversity of wood-inhabiting fungi:

effects of canopy gaps and downed woody debris. *Biodivers. Conserv.* 23, 2155–2172. doi: 10.1007/s10531-014-0710-x

Christensen, M., Hahn, K., Mountford, E. P., Ódor, P., Standovár, T., Rozenbergar, D., et al. (2005). Dead wood in European beech (*Fagus sylvatica*) forest reserves. *For. Ecol. Manage.* 210, 267–282. doi: 10.1016/j.foreco.2005.02.032

De Frenne, P., Zellweger, F., Rodríguez-Sánchez, F., Scheffers, B. R., Hylander, K., Luoto, M., et al. (2019). Global buffering of temperatures under forest canopies. *Nat. Ecol. Evol.* 3, 744–749. doi: 10.1038/s41559-019-0842-1

Domke, G. M., Perry, C. H., Walters, B. F., Woodall, C. W., Russell, M. B., and Smith, J. E. (2016). Estimating litter carbon stocks on forest land in the United States. *Sci. Total Environ.* 557–558, 469–478. doi: 10.1016/j.scitotenv.2016.03.090

Edgar, R. C. (2010). Search and clustering orders of magnitude faster than BLAST. *Bioinformatics* 26, 2460–2461. doi: 10.1093/bioinformatics/btq461

Edgar, R. C. (2013). UPARSE: highly accurate OTU sequences from microbial amplicon reads. *Nat. Methods* 10, 996–998. doi: 10.1038/nmeth.2604

Eichlerová, I., Homolka, L., Žifčáková, L., Lisá, L., Dobiášová, P., and Baldrian, P. (2015). Enzymatic systems involved in decomposition reflects the ecology and taxonomy of saprotrophic fungi. *Fungal Ecol.* 13, 10–22. doi: 10.1016/j.funeco.2014.08.002

Fasth, B. G., Harmon, M. E., Sexton, J., and White, P. (2011). Decomposition of fine woody debris in a deciduous forest in North Carolina. *J. Torrey Bot. Soc.* 138, 192–206. doi: 10.3159/TORREY-D-10-00009.1

Forest Europe (2015). *State of Europe's Forests. Ministerial Conference on the Protection of Forests in Europe*. Madrid: Forest Europe, Liaison Unit Madrid.

Forrester, J. A., Mladenoff, D. J., Gower, S. T., and Stoffel, J. L. (2012). Interactions of temperature and moisture with respiration from coarse woody debris in experimental forest canopy gaps. *For. Ecol. Manage.* 265, 124–132. doi: 10.1016/j.foreco.2011.10.038

Frey, S. J. K., Hadley, A. S., Johnson, S. L., Schulze, M., Jones, J. A., and Betts, M. G. (2016). Spatial models reveal the microclimatic buffering capacity of old-growth forests. *Sci. Adv.* 2:e1501392. doi: 10.1126/sciadv.1501392

Harmon, M. E., Fasth, B. G., Yatskov, M., Kastendick, D., Rock, J., and Woodall, C. W. (2020). Release of coarse woody detritus-related carbon: a synthesis across forest biomes. *Carbon Balance Manage.* 15:1. doi: 10.1186/s13021-019-0136-6

Harris, N. L., Gibbs, D. A., Baccini, A., Birdsey, R. A., de Bruin, S., Farina, M., et al. (2021). Global maps of twenty-first century forest carbon fluxes. *Nat. Clim. Chang.* 11, 234–240. doi: 10.1038/s41558-020-00976-6

Heilmann-Clausen, J., and Christensen, M. (2004). Does size matter? On the importance of various dead wood fractions for fungal diversity in Danish beech forests. *For. Ecol. Manage.* 201, 105–117. doi: 10.1016/j.foreco.2004.07.010

Hiscox, J., Savoury, M., Müller, C. T., Lindahl, B. D., Rogers, H. J., and Boddy, L. (2015). Priority effects during fungal community establishment in beech wood. *ISME J.* 9, 2246–2260. doi: 10.1038/ismej.2015.38

Horák, J., Kout, J., Vodka, Š, and Donato, D. C. (2016). Dead wood dependent organisms in one of the oldest protected forests of Europe: investigating the contrasting effects of within-stand variation in a highly diversified environment. *For. Ecol. Manage.* 363, 229–236. doi: 10.1016/j.foreco.2015.12.041

Ihrmark, K., Bödeker, I. T. M., Cruz-Martinez, K., Friberg, H., Kubartova, A., Schenck, J., et al. (2012). New primers to amplify the fungal ITS2 region – evaluation by 454-sequencing of artificial and natural communities. *FEMS Microbiol. Ecol.* 82, 666–677. doi: 10.1111/j.1574-6941.2012.01437.x

Johnston, S. R., Boddy, L., and Weightman, A. J. (2016). Bacteria in decomposing wood and their interactions with wood-decay fungi. *FEMS Microbiol. Ecol.* 92:fiw179. doi: 10.1093/femsec/fiw179

Juutilainen, K., Mönkkönen, M., Kotiranta, H., and Halme, P. (2014). The effects of forest management on wood-inhabiting fungi occupying dead wood of different diameter fractions. *For. Ecol. Manage.* 313, 283–291. doi: 10.1016/j.foreco.2013.11.019

Juutilainen, K., Mönkkönen, M., Kotiranta, H., and Halme, P. (2017). Resource use of wood-inhabiting fungi in different boreal forest types. *Fungal Ecol.* 27, 96–106. doi: 10.1016/j.funeco.2017.03.003

Kahl, T., Arnstadt, T., Baber, K., Baessler, C., Bauhus, J., Borken, W., et al. (2017). Wood decay rates of 13 temperate tree species in relation to wood properties, enzyme activities and organismic diversities. *For. Ecol. Manage.* 391, 86–95. doi: 10.1016/j.foreco.2017.02.012

Kohout, P., Sudová, R., Brabcová, V., Vosolsobě, S., Baldrian, P., and Albrechtová, J. (2021). Forest microhabitat affects succession of fungal communities on decomposing fine tree roots. *Front. Microbiol.* 12:541583. doi: 10.3389/fmicb.2021.541583

Krah, F. S., Seibold, S., Brandl, R., Baldrian, P., Müller, J., and Bässler, C. (2018). Independent effects of host and environment on the diversity of wood-inhabiting fungi. *J. Ecol.* 106, 1428–1442. doi: 10.1111/1365-2745.12939

Král, K., Daněk, P., Janík, D., Krůček, M., and Vrška, T. (2018). How cyclical and predictable are Central European temperate forest dynamics in terms of development phases? *J. Veg. Sci.* 29, 84–97. doi: 10.1111/JVS.12590

Král, K., Janík, D., Vrška, T., Adam, D., Hort, L., Unar, P., et al. (2010). Local variability of stand structural features in beech dominated natural forests of Central Europe: implications for sampling. *For. Ecol. Manage.* 260, 2196–2203. doi: 10.1016/j.foreco.2010.09.020

Küffer, N., and Senn-Irlet, B. (2005). Influence of forest management on the species richness and composition of wood-inhabiting Basidiomycetes in Swiss forests. *Biodivers. Conserv.* 14, 2419–2435. doi: 10.1007/s10531-004-0151-z

Lepinay, C., Jiráska, L., Tláskal, V., Brabcová, V., Vrška, T., and Baldrian, P. (2021a). Successional development of fungal communities associated with decomposing deadwood in a natural mixed temperate forest. *J. Fungi* 7:412. doi: 10.3390/jof7060412

Lepinay, C., Tláskal, V., Vrška, T., Brabcová, V., and Baldrian, P. (2021b). Successional development of wood-inhabiting fungi associated with dominant tree species in a natural temperate floodplain forest. *Fungal Ecol.* 2021:101116. doi: 10.1016/j.funeco.2021.101116

Mašínová, T., Yurkov, A., and Baldrian, P. (2018). Forest soil yeasts: decomposition potential and the utilization of carbon sources. *Fungal Ecol.* 34, 10–19. doi: 10.1016/j.funeco.2018.03.005

Menkis, A., Allmer, J., Vasiliauskas, R., Lygis, V., Stenlid, J., and Finlay, R. (2004). Ecology and molecular characterization of dark septate fungi from roots, living stems, coarse and fine woody debris. *Mycol. Res.* 108, 965–973. doi: 10.1017/S0953756204000668

Müller, J., Brustel, H., Brin, A., Bussler, H., Bouget, C., Obermaier, E., et al. (2015). Increasing temperature may compensate for lower amounts of dead wood in driving richness of saproxylic beetles. *Ecography (Cop.).* 38, 499–509. doi: 10.1111/ecog.00908

Müller, J., Ulyshen, M., Seibold, S., Cadotte, M., Chao, A., Bässler, C., et al. (2020). Primary determinants of communities in deadwood vary among taxa but are regionally consistent. *Oikos* 129, 1579–1588. doi: 10.1111/oik.07335

Müller-Using, S., and Bartsch, N. (2009). Decay dynamic of coarse and fine woody debris of a beech (*Fagus sylvatica* L.) forest in Central Germany. *Eur. J. For. Res.* 128, 287–296. doi: 10.1007/s10342-009-0264-8

Nilsson, R. H., Larsson, K. H., Taylor, A. F. S., Bengtsson-Palme, J., Jeppesen, T. S., Schigel, D., et al. (2019). The UNITE database for molecular identification of fungi: handling dark taxa and parallel taxonomic classifications. *Nucleic Acids Res.* 47, D259–D264. doi: 10.1093/nar/gky1022

Nordén, B., Ryberg, M., Götmark, F., and Olausson, B. (2004). Relative importance of coarse and fine woody debris for the diversity of wood-inhabiting fungi in temperate broadleaf forests. *Biol. Conserv.* 117, 1–10. doi: 10.1016/S0006-3207(03)00235-0

Oksanen, J., Blanchet, F. G., Friendly, M., Kindt, R., Legendre, P., McGlinn, D., et al. (2020). *Vegan: Community Ecology Package. R Package Version 2.5-7*. Available online at: https://cran.r-project.org/package=vegan

Ostrogović, M. Z., Marjanović, H., Balenović, I., Sever, K., and Jazbec, A. (2015). Decomposition of fine woody debris from main tree species in lowland oak forests. *Polish J. Ecol.* 63, 247–259. doi: 10.3161/15052249PJE2015.63.2.008

Ovaskainen, O., Schigel, D., Ali-Kovero, H., Auvinen, P., Paulin, L., Nordén, B., et al. (2013). Combining high-throughput sequencing with fruit body surveys reveals contrasting life-history strategies in fungi. *ISME J.* 7, 1696–1709. doi: 10.1038/ismej.2013.61

Parfitt, D., Hunt, J., Dockrell, D., Rogers, H. J., and Boddy, L. (2010). Do all trees carry the seeds of their own destruction? PCR reveals numerous wood decay fungi latently present in sapwood of a wide range of angiosperm trees. *Fungal Ecol.* 3, 338–346. doi: 10.1016/j.funeco.2010.02.001

Peršoh, D., and Borken, W. (2017). Impact of woody debris of different tree species on the microbial activity and community of an underlying organic horizon. *Soil Biol. Biochem.* 115, 516–525. doi: 10.1016/j.soilbio.2017.09.017

Põlme, S., Abarenkov, K., Henrik Nilsson, R., Lindahl, B. D., Clemmensen, K. E., Kauserud, H., et al. (2020). FungalTraits: a user-friendly traits database of fungi

and fungus-like stramenopiles. *Fungal Divers.* 105, 1–16. doi: 10.1007/s13225-020-00466-2

Přívětivý, T., Adam, D., and Vrška, T. (2018). Decay dynamics of *Abies alba* and *Picea abies* deadwood in relation to environmental conditions. *For. Ecol. Manage.* 427, 250–259. doi: 10.1016/J.FORECO.2018.06.008

Přívětivý, T., and Šamonil, P. (2021). Variation in downed deadwood density, biomass, and moisture during decomposition in a natural temperate forest. *Forests* 12:1352. doi: 10.3390/F12101352

Přívětivý, T., Janík, D., Unar, P., Adam, D., Král, K., and Vrška, T. (2016). How do environmental conditions affect the deadwood decomposition of European beech (*Fagus sylvatica* L.)? *For. Ecol. Manage.* 381, 177–187. doi: 10.1016/j.foreco.2016.09.033

Purahong, W., Wubet, T., Krüger, D., and Buscot, F. (2018). Molecular evidence strongly supports deadwood-inhabiting fungi exhibiting unexpected tree species preferences in temperate forests. *ISME J.* 12, 289–295. doi: 10.1038/ismej.2017.177

Purhonen, J., Ovaskainen, O., Halme, P., Komonen, A., Huhtinen, S., Kotiranta, H., et al. (2020). Morphological traits predict host-tree specialization in wood-inhabiting fungal communities. *Fungal Ecol.* 46:100863. doi: 10.1016/j.funeco.2019.08.007

R Core Team (2020). *R: A Language and Environment for Statistical Computing*. Vienna: R Foundation for Statistical Computing.

Rajala, T., Peltoniemi, M., Pennanen, T., and Mäkipää, R. (2012). Fungal community dynamics in relation to substrate quality of decaying *Norway spruce* (*Picea abies* [L.] Karst.) logs in boreal forests. *FEMS Microbiol. Ecol.* 81, 494–505. doi: 10.1111/j.1574-6941.2012.01376.x

Rayner, A. D. M., and Boddy, L. (1988). *Fungal Decomposition of Wood: Its Biology And Ecology*. Hoboken. NJ: John Wiley & Sons Ltd.

Ricker, M. C., Blosser, G. D., Conner, W. H., and Lockaby, B. G. (2019). Wood biomass and carbon pools within a floodplain forest of the Congaree River, South Carolina, USA. *Wetlands* 39, 1003–1013. doi: 10.1007/s13157-019-01150-1

Ricker, M. C., Lockaby, B. G., Blosser, G. D., and Conner, W. H. (2016). Rapid wood decay and nutrient mineralization in an old-growth bottomland hardwood forest. *Biogeochemistry* 127, 323–338. doi: 10.1007/s10533-016-0183-y

Rinne, K. T., Rajala, T., Peltoniemi, K., Chen, J., Smolander, A., and Mäkipää, R. (2017). Accumulation rates and sources of external nitrogen in decaying wood in a Norway spruce dominated forest. *Funct. Ecol.* 31, 530–541. doi: 10.1111/1365-2435.12734

Šamonil, P., Daněk, P., Tláskal, V., Tejneckě, V., and Drěbek, O. (2020). Convergence, divergence or chaos? Consequences of tree trunk decay for pedogenesis and the soil microbiome in a temperate natural forest. *Geoderma* 376:114499. doi: 10.1016/j.geoderma.2020.114499

Sandström, J., Bernes, C., Junninen, K., Lõhmus, A., Macdonald, E., Müller, J., et al. (2019). Impacts of dead wood manipulation on the biodiversity of temperate and boreal forests. A systematic review. *J. Appl. Ecol.* 56, 1770–1781. doi: 10.1111/1365-2664.13395

Scharenbroch, B. C., and Bockheim, J. G. (2007). Impacts of forest gaps on soil properties and processes in old growth northern hardwood-hemlock forests. *Plant Soil* 294, 219–233. doi: 10.1007/s11104-007-9248-y

Seibold, S., Bässler, C., Baldrian, P., Reinhard, L., Thorn, S., Ulyshen, M. D., et al. (2016a). Dead-wood addition promotes non-saproxylic epigeal arthropods but effects are mediated by canopy openness. *Biol. Conserv.* 204, 181–188. doi: 10.1016/j.biocon.2016.09.031

Seibold, S., Bässler, C., Brandl, R., Büche, B., Szallies, A., Thorn, S., et al. (2016b). Microclimate and habitat heterogeneity as the major drivers of beetle diversity in dead wood. *J. Appl. Ecol.* 53, 934–943. doi: 10.1111/1365-2664.12607

Seibold, S., Bässler, C., Brandl, R., Gossner, M. M., Thorn, S., Ulyshen, M. D., et al. (2015). Experimental studies of dead-wood biodiversity - A review identifying global gaps in knowledge. *Biol. Conserv.* 191, 139–149. doi: 10.1016/j.biocon.2015.06.006

Seibold, S., Hagge, J., Müller, J., Gruppe, A., Brandl, R., Bässler, C., et al. (2018). Experiments with dead wood reveal the importance of dead branches in the canopy for saproxylic beetle conservation. *For. Ecol. Manage.* 409, 564–570. doi: 10.1016/j.foreco.2017.11.052

Seibold, S., Rammer, W., Hothorn, T., Seidl, R., Ulyshen, M. D., Lorz, J., et al. (2021). The contribution of insects to global forest deadwood decomposition. *Nature* 597, 77–81. doi: 10.1038/S41586-021-03740-8

Šnajdr, J., Valášková, V., Merhautová, V., Herinková, J., Cajthaml, T., and Baldrian, P. (2008). Spatial variability of enzyme activities and microbial biomass in the upper layers of *Quercus petraea* forest soil. *Soil Biol. Biochem.* 40, 2068–2075. doi: 10.1016/j.soilbio.2008.01.015

Sommerfeld, A., Senf, C., Buma, B., D'Amato, A. W., Després, T., Díaz-Hormazábal, I., et al. (2018). Patterns and drivers of recent disturbances across the temperate forest biome. *Nat. Commun.* 9:4355. doi: 10.1038/s41467-018-06788-9

Song, Z., Kennedy, P. G., Liew, F. J., and Schilling, J. S. (2017). Fungal endophytes as priority colonizers initiating wood decomposition. *Funct. Ecol.* 31, 407–418. doi: 10.1111/1365-2435.12735

Stokland, J. N., Siitonen, J., and Jonsson, B. G. (2012). *Biodiversity in Dead Wood*. Cambridge: Cambridge University Press.

Štursová, M., Šnajdr, J., Koukol, O., Tláskal, V., Cajthaml, T., and Baldrian, P. (2020). Long-term decomposition of litter in the montane forest and the definition of fungal traits in the successional space. *Fungal Ecol.* 46:100913. doi: 10.1016/j.funeco.2020.100913

Tláskal, V., and Baldrian, P. (2021). Deadwood-inhabiting bacteria show adaptations to changing carbon and nitrogen availability during decomposition. *Front. Microbiol.* 12:685303. doi: 10.3389/FMICB.2021.685303

Tláskal, V., Brabcová, V., Větrovský, T., Jomura, M., López-Mondéjar, R., Oliveira Monteiro, L. M., et al. (2021). Complementary roles of wood-inhabiting fungi and bacteria facilitate deadwood decomposition. *mSystems* 6:e01078–20. doi: 10.1128/mSystems.01078-20

Urbanová, M., Šnajdr, J., and Baldrian, P. (2015). Composition of fungal and bacterial communities in forest litter and soil is largely determined by dominant trees. *Soil Biol. Biochem.* 84, 53–64. doi: 10.1016/j.soilbio.2015.02.011

Větrovský, T., and Baldrian, P. (2015). An in-depth analysis of actinobacterial communities shows their high diversity in grassland soils along a gradient of mixed heavy metal contamination. *Biol. Fertil. Soils* 51, 827–837. doi: 10.1007/s00374-015-1029-9

Větrovský, T., Baldrian, P., and Morais, D. (2018). SEED 2: a user-friendly platform for amplicon high-throughput sequencing data analyses. *Bioinformatics* 34, 2292–2294. doi: 10.1093/bioinformatics/bty071

Větrovský, T., Kohout, P., Kopecký, M., Machac, A., Man, M., Bahnmann, B. D., et al. (2019). A meta-analysis of global fungal distribution reveals climate-driven patterns. *Nat. Commun.* 10:5142. doi: 10.1038/s41467-019-13164-8

Větrovský, T., Morais, D., Kohout, P., Lepinay, C., Algora, C., Awokunle Hollá, S., et al. (2020). GlobalFungi, a global database of fungal occurrences from high-throughput-sequencing metabarcoding studies. *Sci. Data* 7:228. doi: 10.1038/s41597-020-0567-7

Voříšková, J., and Baldrian, P. (2013). Fungal community on decomposing leaf litter undergoes rapid successional changes. *ISME J.* 7, 477–486. doi: 10.1038/ismej.2012.116

Conflict of Interest: The authors declare that the research was conducted in the absence of any commercial or financial relationships that could be construed as a potential conflict of interest.

Publisher's Note: All claims expressed in this article are solely those of the authors and do not necessarily represent those of their affiliated organizations, or those of the publisher, the editors and the reviewers. Any product that may be evaluated in this article, or claim that may be made by its manufacturer, is not guaranteed or endorsed by the publisher.

frontiers | Frontiers in Microbiology

TYPE Original Research
PUBLISHED 26 September 2022
DOI 10.3389/fmicb.2022.983855

OPEN ACCESS

EDITED BY
Raj Boopathy,
Nicholls State University,
United States

REVIEWED BY
Achmad Syafiuddin,
Nahdlatul Ulama University of Surabaya,
Indonesia
Spyridon Ntougias,
Democritus University of Thrace, Greece

*CORRESPONDENCE
Steffi Pot
steffi.pot@kuleuven.be

†These authors share last authorship

SPECIALTY SECTION
This article was submitted to Terrestrial Microbiology, a section of the journal Frontiers in Microbiology

RECEIVED 01 July 2022
ACCEPTED 01 September 2022
PUBLISHED 26 September 2022

CITATION
Pot S, De Tender C, Ommeslag S, Delcour I, Ceusters J, Vandecasteele B, Debode J and Vancampenhout K (2022) Elucidating the microbiome of the sustainable peat replacers composts and nature management residues.
Front. Microbiol. 13:983855.
doi: 10.3389/fmicb.2022.983855

Elucidating the microbiome of the sustainable peat replacers composts and nature management residues

Steffi Pot[1,2]*, Caroline De Tender[2,3], Sarah Ommeslag[2], Ilse Delcour[4], Johan Ceusters[5,6], Bart Vandecasteele[2], Jane Debode[2†] and Karen Vancampenhout[1†]

[1]Division Forest, Nature and Landscape, Department of Earth and Environmental Sciences, KU Leuven, Geel, Belgium, [2]Plant Sciences Unit, Flanders Research Institute for Agriculture, Fisheries and Food (ILVO), Merelbeke, Belgium, [3]Department of Plant Biotechnology and Bioinformatics, Ghent University, Zwijnaarde, Belgium, [4]PCS Ornamental Plant Research, Destelbergen, Belgium, [5]Division of Crop Biotechnics, Department of Biosystems, Research Group for Sustainable Crop Production & Protection, KU Leuven, Geel, Belgium, [6]Centre for Environmental Sciences, Environmental Biology, UHasselt, Diepenbeek, Belgium

Sustainable peat alternatives, such as composts and management residues, are considered to have beneficial microbiological characteristics compared to peat-based substrates. Studies comparing microbiological characteristics of these three types of biomass are, however, lacking. This study examined if and how microbiological characteristics of subtypes of composts and management residues differ from peat-based substrates, and how feedstock and (bio) chemical characteristics drive these characteristics. In addition, microbiome characteristics were evaluated that may contribute to plant growth and health. These characteristics include: genera associated with known beneficial or harmful microorganisms, microbial diversity, functional diversity/activity, microbial biomass, fungal to bacterial ratio and inoculation efficiency with the biocontrol fungus *Trichoderma harzianum*. Bacterial and fungal communities were studied using 16S rRNA and ITS2 gene metabarcoding, community-level physiological profiling (Biolog EcoPlates) and PLFA analysis. Inoculation with *T. harzianum* was assessed using qPCR. Samples of feedstock-based subtypes of composts and peat-based substrates showed similar microbial community compositions, while subtypes based on management residues were more variable in their microbial community composition. For management residues, a classification based on pH and hemicellulose content may be relevant for bacterial and fungal communities, respectively. Green composts, vegetable, fruit and garden composts and woody composts show the most potential to enhance plant growth or to suppress pathogens for non-acidophilic plants, while grass clippings, chopped heath and woody fractions of compost show the most potential for blends for calcifuge plants. Fungal biomass was a suitable predictor for inoculation efficiency of composts and management residues.

KEYWORDS

microbiology, composts, Biolog EcoPlates, PLFA analysis, sustainable horticultural substrates, nature management residues, metabarcoding

Introduction

In horticulture, peat is a major constituent of diverse substrates. Its low pH, low bulk density, optimal EC, high porosity, high water holding capacity and homogeneity make peat an ideal substrate for growing many ornamental plants (Schmilewski, 2008; Michel, 2010). However, environmental concerns regarding peat extraction and utilization are rapidly growing. Peatlands are valuable habitats for protected animal and plant species, are important carbon sinks, and provide environmental services, such as regulation of local water quality and flood protection (Alexander et al., 2008). Moreover, draining of peatlands and extraction of peat accelerates peat decomposition to such an extent that peatlands become a major source of greenhouse gasses (Bonn et al., 2016).

Hence, there is an urgent need to find sustainable alternatives for peat in horticulture. A promising avenue in the search for more sustainable peat alternatives may be the use of residual biomass, such as composts and nature management residues. Studies have shown that composts can have physicochemical and (bio)chemical properties that make them suitable peat alternatives for multiple types of plants (Hernandez-Apaolaza et al., 2005; Bustamante et al., 2008; Herrera et al., 2008; Vandecasteele et al., 2021). Management residues, such as sods and chopped biomass from heathland management efforts, can replace 40% of peat in growing media for calcifuge ornamental plants without loss of plant quality (Miserez et al., 2019a).

Apart from supporting plant growth, horticultural substrates also provide a habitat for microorganisms. The interaction between plants and their rhizosphere microbiome can be beneficial and even critical to plant health, growth and productivity (Chaparro et al., 2012; Quiza et al., 2015). Rhizosphere microorganisms can improve nutrient availability, reduce biotic and abiotic stress, and increase plant defenses (Figueiredo et al., 2011). Microbial communities in the rhizosphere can contribute to the reduction of biotic stress and the suppression of plant pathogens by several types of interaction between microorganisms and pathogens, including competition for nutrients and ecological niches, antibiosis, predation, parasitism, and the activation of disease resistance in plants (Ntougias et al., 2008). Various rhizosphere microorganisms are known for their beneficial effects on plant growth and health, including nitrogen-fixing bacteria, mycorrhizal fungi, plant growth promoting rhizobacteria (PGPR) and fungi (PGPF), and biocontrol agents (Berendsen et al., 2012). Beneficial microorganisms present in horticultural substrates may thus contribute positively to the rhizosphere microbiome and enhance plant growth and resistance to plant pathogens. Additionally, substrates with higher general microbial biomass or diversity may be less susceptible for colonization by other organisms due to stronger competition for nutrients and niches, and may therefore be more suppressive to pathogens (Chaparro et al., 2012; Bongiorno et al., 2019). Studies have also shown a positive effect of microbial biomass and diversity on plant growth and productivity (Wagg et al., 2011; Weidner et al., 2015; Shen et al., 2016; Kolton et al., 2017). Higher metabolic activity and functional diversity can be associated with disease suppression and plant growth promotion (Brussaard et al., 2007; Mendes et al., 2011; Alam et al., 2014; Kolton et al., 2017; Neher et al., 2022). However, horticultural substrates may also harbor potential plant or human pathogens, which poses a risk for plant and human health, but also for the environment (Cartwright, 1995; Waller et al., 2008; Al-Sadi et al., 2011, 2016).

Despite their importance in terms of plant growth and health, the microbiological characteristics of peat alternatives have not received much attention in scientific literature. The current understanding of the microbial communities in peat-based substrates and peat alternatives, such as composts and management residues, is still limited. It is assumed that peat does not provide a suitable food base for microorganisms to grow as it has a high amount of strongly polymerized organic matter, and therefore a low energy reserve (Hoitink and Boehm, 1999). Hence, peat is often considered as an ineffective medium to harbor (beneficial) microorganisms and to support sustained biological control (Hoitink and Boehm, 1999; Krause et al., 2001), yet data to support such assumption are few. Peat alternatives are assumed to be more suitable media for (beneficial) microorganisms because of the higher amount of available energy reserves. Composts and management residues have been shown to have a higher microbial biomass than peat (Vandecasteele et al., 2021), and are expected to have a higher diversity and activity as compared to peat. Accordingly, composts and management residues may have a positive effect on plant growth and resistance to pathogens. Additionally, several known biocontrol agents, such as *Bacillus* spp., *Pseudomonas* spp., and *Trichoderma* spp., have been retrieved from composts, which may contribute to a possible disease suppressive effect in composts (Dukare et al., 2011; Chen et al., 2012; Antoniou et al., 2017; Lutz et al., 2020). Other biocontrol agents associated with disease suppression in composts include non-pathogenic *Fusarium* spp. (Kavroulakis et al., 2007; Blaya et al., 2016), *Zopfiella* spp. (Blaya et al., 2016), *Enterobacter* spp. (Kwok et al., 1987; Chen et al., 2012), *Xanthomonas* spp. (Kwok et al., 1987), *Aeromonas* spp. (Oberhänsli et al., 2017), *Flavobacterium* spp. (Kwok et al., 1987) and non-pathogenic *Verticllium* spp. (Postma et al., 2003). In addition to biocontrol agents naturally occurring in composts, composts have been shown to improve colonization and consequently the efficacy of commercial biocontrol organisms (Krause et al., 2001; Joos et al., 2020).

Another important requirement for the use of peat alternatives in horticultural substrates is the absence of human and plant pathogens, as this may pose a potential risk for plant and human health (Jones and Martin, 2003). Several studies have shown the presence of pathogenic fungi that can infect plants *via* the roots, such as *Fusarium* spp., *Rhizoctonia* spp., and *Pythium* spp., in horticultural substrates (Cartwright, 1995; Waller et al., 2008). Potential human pathogens that have been reported to be present

in substrates include *Salmonella* spp., *Escherichia* spp., *Shigella* spp., and *Klebsiella* spp. (Epstein, 2001; Jones and Martin, 2003).

A range of different feedstocks and processing methods make composts and management residues very heterogenous materials. Microbiological characteristics are also expected to show a large heterogeneity. Pot et al. (2021a,b) showed that the initial microbiological composition is paramount in obtaining a favorable microbiome in substrates, as possibilities for adaptation or optimization of microbiological characteristics of composts and management residues are limited. Hence, it is important to understand what properties drive the microbial composition of peat alternatives. Feedstock, pH, mineral N content and organic matter content have been suggested as potential drivers of microbial communities in composts (Neher et al., 2013; Sun et al., 2020; Wu et al., 2020). It is, however, unclear which properties drive the microbial composition in other types of composts and other peat alternatives.

The objective of this study is to compare microbiological characteristics of subtypes of composts and management residues to peat-based substrates using a classification based on feedstock that is also used by commercial suppliers. Specifically, this study focusses on how the microbiological characteristics of feedstock-based subtypes of composts and management residues differ from peat-based substrates, and how feedstock and (bio)chemical characteristics drive these microbiological characteristics. Moreover, this study assesses if these different subtypes of composts and management residues can be regarded as good peat alternatives based on different characteristics that may indicate plant growth and health promotion. These characteristics include presence of genera associated with known beneficial microorganisms, absence of genera known to include pathogens, high microbial diversity, high functional diversity and activity, high microbial biomass, high fungal to bacterial ratio and the potential to increase the inoculation efficiency of the biocontrol fungus *Trichoderma harzianum*. Finally, it was determined which microbiological characteristics may predict inoculation efficiency.

Materials and methods

Set of materials

The set of materials consisted of 10 peat-based substrates, 16 composts from different installations and feedstocks, and 12 management residues from various locations and vegetation types (Table 1). Composts and management residues were each divided into subtypes based on feedstock, as is common practice in the sector. For composts, four feedstock-based subtypes could be distinguished: green composts (C1), vegetable, fruit and garden (VFG) composts (C2), woody composts (C3), and peat composts (i.e., composts based on spent substrates; C4). For management residues, four feedstock-based subtypes could be distinguished: grass clippings (M1), chopped heath (M2), forest sods (M3) and woody fractions of composts (M4). Peat-based substrates were divided into two subtypes based on whether they were treated with lime. The two subtypes were classified as pure peat-based substrates (P1) and limed peat-based substrates (P2). An overview of (bio)chemical characteristics (determined and described by Vandecasteele et al. (2021)) of the different samples can also be found in Table 1.

16S rRNA and ITS2 gene metabarcoding

The different materials were each sampled three times (250 mg per sample), resulting in three technical replicates for each sample. DNA was extracted from each sample using the DNeasy Powersoil Pro Kit (QIAGEN, Germantown, MD, United States), according to the manufacturer's instructions, and stored at −20°C until use for metabarcoding, as described below.

Metabarcoding of the bacterial and fungal populations was done on the V3-V4 fragment of the 16S rRNA gene and the ITS2 gene fragment, respectively, as described in detail in De Tender et al. (2016a). Reads are available for download at the NCBI sequence read archive (SRA) under project numbers PRJNA624053, PRJNA715731 and PRJNA767265.

Demultiplexing of the metabarcoding dataset was performed by the sequencing provider. Primers were removed using Trimmomatic version 0.32 (Bolger et al., 2014). Adapters were already removed by the sequencing provider. For the ITS2-sequences, some adapters were still present and were removed using Cutadapt version 2.7 (Martin, 2011). Quality of the pre-processed sequences was checked using FastQC version 0.11.8 (Andrews, 2010). Further processing of the sequences was done using the DADA2 pipeline version 1.12.1 (Callahan et al., 2015), as described in detail in Pot et al. (2021a). Briefly, low quality reads were trimmed, sequences were dereplicated and amplicon sequence variants (ASVs) were inferred based on the parametric model of errors calculated by the algorithm. Inferred sequences were merged, chimeras were removed and taxonomy was assigned by the SILVA database v132 (bacteria; Quast et al., 2012; Yilmaz et al., 2013; Glöckner et al., 2017) and UNITE database v020219 (fungi; Nilsson et al., 2018).

Two sequence tables (bacterial and fungal) were constructed. For each biological replicate ($n = 10$ for peat-based substrates, $n = 16$ for composts and $n = 12$ for management residues), the mean of the absolute ASV counts of the tree technical replicates was calculated. All analyses were done for both the bacterial and fungal sequence tables. To remove low abundant reads, first, ASVs with less than three counts per million in at least three samples were removed from the datasets. Second, the table was used as input to calculate the Shannon diversity index applying the diversity function of the vegan package (version 2.5.7) in R (version 4.0.4; Oksanen et al., 2020), to determine alpha diversity. To find significant differences in mean diversity between the different subtypes of composts, management residues and peat-based substrates, a linear model including subtype as main effect was used. Linearity, homogeneity of variances and normality were

TABLE 1 (Bio)chemical characteristics of the different samples of composts (C), management residues (M) and peat-based substrates (P).

Sample	Description	Type	Subtype	Cellulose (%/OM)	Hemicellulose (%/OM)	Lignin (%/OM)	pH-H_2O	EC	NO_3-N (mg/L)	NH_4-N (mg/L)	N_{min} (mg/L)	SO_4 (mg/L)	Cl (mg/L)	OM (%/DM)	P_{water} (mg/L)	C_{water} (mg/L)	C/N	N_{immob} (%)	OUR (mmol O_2/kg OM/h)	Cum. CO_2 release (mol CO_2/kg OM)
BW01	Grass clippings	M	M1	16.3	10.1	15.6	5.6	39.0	<5.0	<5.0	<5.0	<11.7	11.1	50.7	<4.7	77.5	27.5	−11.0	8.3	0.8
BW02	Chopped heath	M	M2	27.5	17.9	27.0	5.6	24.0	<5.0	<5.0	<5.0	<11.7	<10	86.7	<4.7	47.7	32.3	3.0	7.7	1.4
BW03	Grass clippings	M	M1	33.4	38.2	8.6	7.1	189.0	<5.0	21.4	21.4	31.6	92.8	94.5	11.4	225.2	23.6	−8.0	24.6	2.4
BW04	Grass clippings	M	M1	7.9	8.4	7.6	4.8	198.0	63.9	5.4	69.3	<11.7	27.9	31.7	33.3	58.1	17.7	−7.0	4.2	1.4
BW05	Forest sods	M	M3	17.6	9.1	31.4	4.3	28.0	<5.0	<5.0	<5.0	<11.7	<10	77.9	<4.7	36.1	22.4	−2.0	2.2	0.6
BW06 #	Green compost	C	C1	8.8	3.3	7.8	8.8	851.0	6.3	<5.0	6.3	247.0	529.6	25.5	13.0	220.5	13.0	4.0	6.4	1.3
BW08 #	Green compost	C	C1	12.1	4.2	12.6	8.5	1156.0	<5.0	14.0	14.0	378.5	807.3	43.3	21.2	393.8	15.9	6.0	11.7	3.5
BW09 #	Wood chip compost	C	C3	9.6	7.8	11.8	7.6	2430.0	668.2	16.3	684.5	820.5	483.1	54.6	38.8	298.7	13.9	−5.0	1.6	0.3
BW10 #	Wood chip compost	C	C3	9.4	5.4	15.2	5.8	1209.0	367.9	40.8	408.7	400.6	175.0	43.3	78.1	129.9	15.9	−1.0	1.8	0.6
BW11 #	Peat compost	C	C4	13.2	9.4	16.0	6.4	2100.0	586.9	26.8	613.7	990.8	266.6	65.0	110.5	222.8	18.0	13.0	1.1	0.3
BW12 #	Peat compost	C	C4	28.1	10.7	31.7	6.9	1253.0	401.0	<5.0	401.0	1041.4	165.6	82.3	12.9	38.0	24.0	10.0	1.2	0.5
BW13 #	Poplar bark compost	C	C3	30.3	11.9	29.4	5.4	461.0	<5.0	<5.0	<5.0	28.1	66.2	88.4	42.0	352.7	46.5	63.0	7.8	4.8
BW14 #	Fungus-dominant woody compost	C	C3	8.1	5.2	11.3	7.5	361.0	<5.0	<5.0	<5.0	201.8	180.8	37.2	<4.7	87.3	16.8	21.0	2.8	1.6
BW15	Woody fraction of green compost	M	M4	46.8	19.3	23.3	6.9	234.0	<5.0	<5.0	<5.0	32.6	76.1	95.2	28.3	174.8	72.1	45.0	5.6	3.1
BW16 #	Green compost	C	C1	5.4	2.8	11.6	7.9	1273.0	193.0	10.9	203.9	96.9	640.9	30.9	28.9	274.5	11.1	−3.0	3.1	1.0
BW19 #	VFG compost	C	C2	7.1	5.4	11.1	8.5	3030.0	418.6	649.9	1068.5	1073.4	975.2	38.1	19.8	485.9	9.7	36.0	7.2	1.9
BW22	Woody fraction of green compost	M	M4	32.5	12.5	24.9	7.8	918.0	<5.0	15.3	15.3	173.7	710.8	79.8	29.9	379.8	37.6	38.0	11.1	3.7
BW24	Soft rush	M	M1	29.5	32.7	13.3	7.9	448.0	<5.0	30.4	30.4	156.0	266.2	89.2	23.6	159.9	21.7	7.0	15.7	3.5
BW25	Chopped heath	M	M2	16.7	11.7	17.2	6.0	31.0	<5.0	<5.0	<5.0	<11.7	<10	52.1	<4.7	92.7	30.8	78.0	12.0	2.6
BW26	Chopped heath	M	M2	5.5	4.0	9.7	4.5	333.0	88.4	101.4	189.8	79.5	17.5	36.2	13.9	71.3	16.8	−4.0	0.3	0.2
BW27	VFG compost	C	C2	7.8	3.2	11.6	8.5	2200.0	241.7	122.3	364.0	166.5	1663.9	32.9	27.9	308.9	8.6	−58.3	2.4	1.1
BW28	Woody fraction of green compost	C	C1	13.8	4.8	16.0	7.5	804.0	<5.0	8.4	8.4	168.1	363.7	48.1	23.3	563.7	15.9	44.0	16.0	5.6
BW29	Green compost	C	C1	12.1	4.9	17.4	8.1	894.0	77.2	7.7	84.9	108.5	477.5	50.0	34.2	265.3	12.1	−38.0	2.2	1.2

(Continued)

10.3389/fmicb.2022.983855

TABLE 1 (Continued)

Sample	Description	Type	Subtype	Cellulose (%/OM)	Hemicellulose (%/OM)	Lignin (%/OM)	pH-H_2O	EC	NO_3-N (mg/L)	NH_4-N (mg/L)	N_{min} (mg/L)	SO_4 (mg/L)	Cl (mg/L)	OM (%/DM)	P_{water} (mg/L)	C_{water} (mg/L)	C/N	N_{immob} (%)	OUR (mmol O_2/kg OM/h)	Cum. CO_2 release (mol CO_2/kg OM)
BW30	VFG compost mixed with green compost	C	C2	9.1	5.8	14.9	8.3	1490.0	170.7	76.5	247.2	401.7	986.1	44.8	31.5	242.3	9.8	−34.0	5.4	1.2
BW31	Green compost	C	C1	8.7	6.1	14.3	8.3	1721.0	225.1	6.1	231.2	330.1	1075.2	39.0	29.6	272.6	10.2	−27.9	3.0	1.3
BW32	Green compost	C	C1	10.3	4.4	11.9	8.9	1558.0	7.7	225.5	233.2	223.0	1276.2	41.0	56.0	415.7	10.8	43.7	4.8	2.2
BW34	Forest sods	M	M3	14.1	7.1	14.2	4.7	100.0	<5.0	<5.0	<5.0	<11.7	37.6	41.1	<4.7	89.0	27.0	−6.0	5.7	1.1
BW53	Chopped heath	M	M2	8.6	5.3	12.9	5.9	226.0	24.3	6.8	31.1	42.2	106.5	36.8	69.1	98.3	20.1	52.7	6.1	1.1
BWr61 *	White peat	P	P1	49.7	23.3	13.1	4.7	26.0	<5.0	<5.0	<5.0	<11.7	<10	97.8	<4.7	49.5	68.2	3.8	0.5	0.2
BWr62 *	Peat mixture	P	P2	31.0	18.3	24.5	6.1	231.0	50.6	<5.0	50.6	159.8	25.9	89.9	55.5	96.4	44.6		0.9	0.2
BWr67 *	Black peat	P	P1	21.6	9.1	32.1	4.7	272.0	17.5	<5.0	17.5	468.8	27.3	89.0	<4.7	31.5	37.7		1.2	0.1
BWr65	Peat mixture	P	P1	−160.0	17.5	21.5	4.0	164.0	20.7	34.8	55.5	173.7	21.5	97.6	<4.7	32.9	55.0	21.3	0.7	0.1
BWr66	Black peat	P	P1	28.6	17.3	31.2	4.7	33.0	<5.0	5.0	<5.0	27.8	22.5	95.9	4.7	60.4	36.9	7.0	0.7	0.3
BWr46	Peat mixture	P	P2	26.0	14.3	18.1	6.6	68.0	8.9	<5.0	8.9	63.3	23.7	69.1	<4.7	51.9	38.7		0.3	
BWr47	Peat mixture	P	P2	26.2	9.2	21.7	6.0	702.0	275.8	<5.0	275.8	486.4	26.4	69.5	78.2	26.4	42.0		0.1	0.2
BWr48	Peat mixture	P	P2	16.3	7.2	11.5	6.4	86.0	8.6	<5.0	8.6	80.7	26.5	33.7	17.5	53.1	28.3		0.6	
BWr49	Peat mixture	P	P2	28.2	10.0	31.6	6.7	128.0	10.6	<5.0	10.6	159.8	23.8	80.6	<4.7	41.8	47.5		0.3	
BWr419	White peat	P	P1	−124.1	14.3	19.2	4.9	129.0	<5.0	5.7	5.7	<11.7	<10	97.2	<4.7	52.8	47.3	20.6	0.2	0.3

P1 = pure peat-based substrates ($n = 5$); P2 = limed peat-based substrates ($n = 5$); C1 = green composts ($n = 7$); C2 = VFG composts ($n = 3$); C3 = woody composts ($n = 4$); C4 = peat composts ($n = 2$); M1 = grass clippings ($n = 4$); M2 = chopped heath ($n = 4$); M3 = forest sods ($n = 2$); M4 = woody fractions of composts ($n = 2$). Asterisks indicate reference samples used for community-level physiological profiling (Biolog EcoPlates). Hashtags indicate compost samples used for inoculation efficiency. VFG compost, vegetable, fruit and garden compost; EC, electrical conductivity; N_{min}, mineral N = NO_3–N + NH_4–N; OM, organic matter; DM, dry matter; P_{water}, water-extractable P; C_{water}, water-extractable C; N_{immob}, N immobilization; OUR, oxygen uptake rate.

10.3389/fmicb.2022.983855

checked prior to analysis by plotting residuals vs. fitted values, a QQ plot of the standardized residuals and a scale-location plot. Pairwise comparisons were made using least square means. *p*-Values <0.05 were considered significant. Third, beta diversity was studied. Absolute ASV counts were transformed to relative abundances, and a dissimilarity matrix (based on the Bray–Curtis dissimilarity index) was calculated from the ASV table. Homogeneity of the variances was checked on this dissimilarity matrix using the betadisper function. The effect of type of biomass and subtype on the community composition was studied by doing a PERMANOVA analysis on the dissimilarity matrix. To visualize the observed differences, principal coordinate analysis (PCoA) on the dissimilarity matrix was done. Fourth, heatmaps were made using the heatmap.2 function of the gplots package (version 3.1.1) in R for each type of biomass to visualize similarities between different samples. As input for these heatmaps, bacterial and fungal genera with a relative abundance equal to or larger than 1% in at least one of the samples were used. Fifth, (bio)chemical characteristics of the different samples, were fitted onto the PCoA ordinations for each type of biomass using the envfit function of the vegan package (version 2.5.7). More specifically, cellulose, hemicellulose, pH-H_2O, electroconductivity (EC), nitrates (NO_3-N), ammonium (NH_4-N), mineral N (N_{min}), sulfates (SO_4), chlorine (Cl), organic matter (OM), water extractable phosphor (P_{water}) and carbon (C_{water}), carbon:nitrogen ratio (C/N), nitrogen immobilization (N_{immob}), oxygen uptake rate (OUR) and cumulative CO_2 release, that were determined and described in detail by Vandecasteele et al. (2021) and that can be found in Table 1, were used for this analysis. Significance of the correlations between the (bio)chemical characteristics and the PCoA ordination on the other hand was tested using a permutation test with 999 permutations. Significant correlations ($p < 0.05$) were plotted on the PCoA plots with the length of the arrows proportional to the correlation. Sixth, the presence of potential beneficial microorganisms was studied, focusing on genera known to include plant growth promoting microorganisms and biocontrol agents, including *Penicillium*, *Serratia*, *Paenibacillus*, *Burkholderia*, *Trichoderma*, *Bacillus*, *Pseudomonas*, and *Streptomyces* (Bhattacharyya and Jha, 2012; Neher et al., 2022). Additionally, the different samples were screened for the presence of genera including potential pathogens, focusing on genera known to include human pathogens, including *Salmonella*, *Escherichia*, *Klebsiella*, *Shigella*, and *Enterobacter*, or plant pathogens that can infect the plant roots *via* the growing medium, including *Verticillium*, *Rhizoctonia*, *Fusarium*, *Pythium*, *Sclerotinia*, and *Plasmodiaphora*. Seventh, the effect of subtype of biomass on abundance was tested using the edgeR package (version 3.32.1; Robinson et al., 2010) as described in Pot et al. (2021a). The analyses were done upon clustering the bacterial and fungal ASV table with absolute sample counts at phylum, family, and genus level. Normalization based on the trimmed mean of M-values (TMM) was applied to correct for differences in library size of the count table. A design matrix was defined based on the experimental design, with a main effect for subtype. The dispersion parameter was calculated. Following, a negative binomial model was fitted for every ASV and then combined. Likelihood-ratio tests were conducted on the contrast of the model parameters to assess differential abundances. *p*-Values <0.05 were considered significant. Correction for multiple testing was included by adopting the Benjamini-Hochberg False Discovery Rate procedure.

Community-level physiological profiling using Biolog EcoPlates

The different materials were each sampled once (3 g per sample) and analyzed using Biolog EcoPlates (Biolog, Inc., CA, United States) as described in detail in Pot et al. (2021a). For peat-based substrates, only three samples were used (see Table 1). The average well color development (AWCD) and Shannon diversity index (functional diversity) were calculated as described in Pot et al. (2021a). For each biological replicate, the average AWCD and Shannon diversity index was calculated from the three technical replicates.

To determine differences in overall AWCD and AWCD of the different carbon sources and the functional diversity (Shannon diversity index) between the subtypes of biomass, a linear model including subtype as main effect was used after checking the assumptions. Pairwise comparisons were made using least square means. Furthermore, relative optical density values after 7 days were divided by the AWCD to minimize the influence of inoculum density differences between plates (Garland and Mills, 1991; Graham and Haynes, 2005). To visualize differences in functional community composition, principal component analysis (PCA) was done on these values. The effect of subtype of biomass was studied by doing a PERMANOVA analysis.

Phospholipid fatty acid analysis

Phospholipid fatty acid (PLFA) analysis was performed by Vandecasteele et al. (2021). Seventeen PLFAs were selected because of their use of biomarker fatty acids for six distinct microbial groups: Gram-positive bacteria (i-C15:0, a-C15:0, i-C16:0, i-C17:0), Gram-negative bacteria (C16:1c9, C17:0cy, C19:0cy), bacteria (non-specific; C14:0, C15:0, C16:0, C17:0, C18:0), actinomycetes (10Me-C16:0, 10Me-C18:0), fungi (C18:2n9,12) and mycorrhiza (C16:1c11), and summed up together with C18:1c9 to calculate total microbial biomass. In addition, fungal to bacterial ratio was determined.

To determine differences in total microbial biomass and fungal to bacterial ratio between subtypes, a linear model was used with subtype as main effect after checking the assumptions. Pairwise comparisons were made using least square means. To visualize differences in microbial biomass between subtypes, principal component analysis (PCA) was done on the microbial biomass of different microbial groups and total microbial biomass.

The effect of subtype of biomass was studied by doing a PERMANOVA analysis.

Inoculation efficiency of *Trichoderma harzianum*

Inoculation efficiency by the biocontrol fungus *T. harzianum* was assessed by qPCR as described in Vandecasteele et al. (2021). Differences in inoculation efficiency between subtypes of composts, management residues and peat-based substrates were determined using a linear model with subtype as a main effect after checking the assumptions. Pairwise comparisons were made using least square means. Spearman correlations were used to determine correlations between the inoculation efficiency and the initial microbiological characteristics of the samples (bacterial and fungal diversity, biomass of different microbial groups, metabolic activity, and functional diversity).

All statistical tests were conducted in RStudio 1.2.5001.

Results

Comparison between peat-based substrates, composts and management residues

Differences in bacterial and fungal community composition between composts, management residues and peat-based substrates were visualized by principal coordinate analysis (PCoA; Supplementary Figure S1). For bacteria, the first and second principal coordinate (PCo) represented 12.9% and 8.1%, respectively, of the variance in the dataset, whereas for the fungal communities, these values were 10.8% and 9.8%, respectively. Particularly for bacteria, PCo1 represented variation between the different types of biomass (i.e., composts, management residues and peat-based substrates), while PCo2 represented variation between the individual samples within the three types of biomass. PERMANOVA analysis showed a significant shift in the bacterial communities ($p = 0.001$) and fungal communities ($p = 0.001$) between the types of biomass. Composts and management residues both show large variation in their bacterial and fungal community composition, indicating high heterogeneity within the microbial communities of each type of biomass.

Comparison between subtypes of peat-based substrates and composts and management residues

Differences in microbial community composition

Redoing the PCoA with the subtypes as input, differences in bacterial and fungal community composition were still observed between the subtypes of composts, management residues and peat-based substrates, for both bacteria and fungi ($p = 0.001$ and $p = 0.001$, respectively; Figure 1). However, the condition of homogeneity of variances was not fulfilled for fungi ($p < 0.001$), indicating that the division in subtypes might be not sufficient to deal with the high sample heterogeneity.

Next to the differences between peat-based substrates, composts and management residues, also within each type of biomass differences in bacterial and fungal community composition were found (Supplementary Figure S2). PERMANOVA analysis showed a significant difference in the bacterial and fungal community composition between the different subtypes within composts ($p = 0.001$ and $p = 0.003$, respectively) and peat-based substrates ($p = 0.02$ and $p = 0.02$,

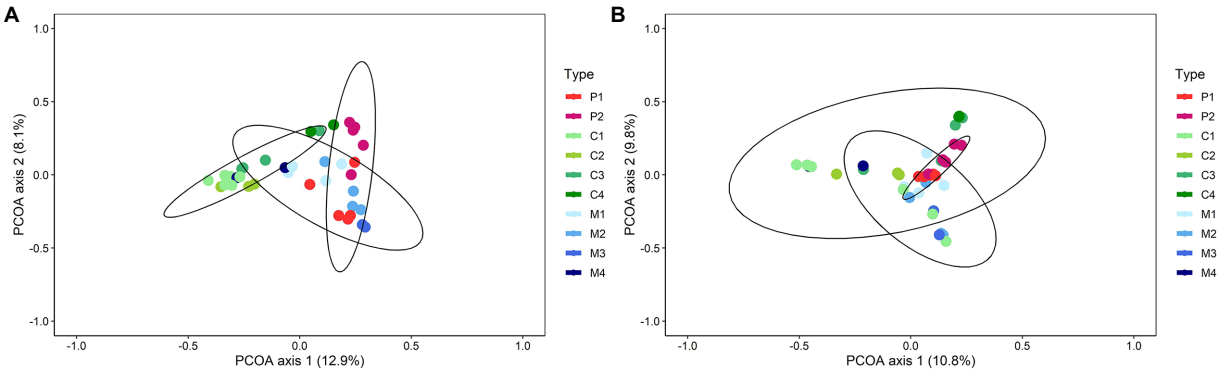

FIGURE 1
Shifts in bacterial **(A)** and fungal **(B)** community composition between the subtypes of peat-based substrates, composts, and management residues. Both figures represent Principal Coordinate Analysis (PCoA) profiles of pairwise community dissimilarity (Bray-Curtis) indices of either bacterial (16S V3-V4 rRNA gene) or fungal (ITS2 gene) sequencing data, respectively. Colors indicate the different subtypes of peat-based substrates, composts, and management residues. P1=pure peat-based substrates (n=5); P2=limed peat-based substrates (n=5); C1=green composts (n=7); C2=VFG composts (n=3); C3=woody composts (n=4); C4=peat composts (n=2); M1=grass clippings (n=4); M2=chopped heath (n=4); M3=forest sods (n=2); M4=woody fractions of composts (n=2).

respectively). For management residues, a significant difference in bacterial community composition was found between the subtypes ($p = 0.01$).

To verify whether this heterogeneity in the community is indeed dependent on feedstock-based subtypes within each type of biomass, heatmaps were produced based on the genera with a relative abundance of at least 1% in one of the samples to visualize similarities between the different samples (Supplementary Figures S3, S4). For peat-based substrates, the two feedstock-based subtypes – pure and limed peat-based substrates – showed a similar clustering based on bacterial and fungal community composition. Only one sample of the pure peat-based substrates clustered more closely to the limed peat-based substrates than to the other pure peat-based substrates, which could also be noted in the PCoA plots. For composts, no real clustering on feedstock could be noted, either for the bacterial and fungal community. This is in contrast of what could be observed in the PCoA plots (Supplementary Figure S4): samples of the different feedstock-based subtypes clustered relatively closely together for both bacterial and fungal sequences, indicating samples belonging to feedstock-based subtypes show similar bacterial and fungal community composition. Green composts (C1) and VFG composts (C2) showed similar bacterial and fungal community compositions. Woody composts (C3) and peat composts (C4) also showed similar bacterial and fungal community compositions. For management residues, samples of the different feedstock-based subtypes showed less similarity in their bacterial and fungal community composition. Samples belonging to forest sods (M3) or woody fractions of composts (M4) each showed similar bacterial and fungal community composition. However, samples of grass clippings (M1) and samples of chopped heath (M2) showed large variation in bacterial and fungal community compositions, which could be noted in the bacterial and fungal heatmaps as well as in the PCoA plots. Except for the composts, the heatmaps and PCoA plots showed the same patterns. The differences between the PCoA plots and the heatmaps for composts may be due to differences in the determination of similarities between samples. In the PCoA plots, the total bacterial and fungal community composition is considered, while the heatmaps are based on genera that have a relative abundance of at least 1% in at least one sample.

Linking microbial community composition with chemical characteristics

Within each type of biomass, the correlations between the bacterial and fungal community composition and chemical characteristics were determined (Figure 2; Supplementary Table S1). For peat-based substrates, no (bio) chemical characteristics were significantly correlated with the bacterial community composition. Fungal community composition in peat-based substrates was significantly correlated with N immobilization ($p = 0.04$, $r^2 = 0.99$). For composts, bacterial community composition was significantly correlated with pH-H_2O ($p = 0.003$), EC ($p = 0.004$), NO_3-N ($p = 0.002$), NH_4-N ($p = 0.05$), N_{min} ($p = 0.004$), SO_4 ($p = 0.02$), Cl ($p = 0.001$), P_{water} ($p = 0.03$), C/N ratio ($p = 0.03$), oxygen uptake rate (OUR; $p = 0.05$) and cumulative CO_2 release ($p = 0.04$), for which Cl had the highest influence on the bacterial community composition in composts ($r^2 = 0.85$). Fungal community composition in composts was significantly correlated with hemicellulose content ($p = 0.02$), pH-H_2O ($p = 0.008$), NO_3-N ($p = 0.006$), SO_4 ($p = 0.05$), Cl ($p = 0.009$) and oxygen uptake rate (OUR; $p = 0.05$), for which NO_3-N had the highest influence on the bacterial community composition in composts ($r^2 = 0.57$). For management residues, the bacterial community composition was significantly correlated with pH-H_2O ($p = 0.006$, $r^2 = 0.74$) and C_{water} ($p = 0.04$, $r^2 = 0.48$), and the fungal community composition was solely correlated with hemicellulose ($p = 0.02$, $r^2 = 0.51$).

Differences in characteristics of the microbial community

To study the difference in microbial community between the subtypes of the three biomass types in more detail, (1) differential abundances between peat-based substrates and management residues/composts, (2) the presence of beneficial microorganisms and pathogens, and (3) bacterial and fungal diversity were investigated.

First, the differential abundances of bacterial and fungal phyla, families, and genera between the subtypes of composts and management residues on one hand and peat-based substrates on the other hand were studied (Supplementary Tables S2, S3). For bacteria, the number of differentially abundant taxa in subtypes of composts and management residues was larger when compared to limed peat-based substrates than to pure peat-based substrates, indicating that bacterial community composition in subtypes of composts and management residues is more similar to pure peat-based substrates. For fungi, the number of differentially abundant taxa in subtypes of composts and management residues was similar when compared to either pure or limed peat-based substrates, indicating that subtypes of composts and management residues show a similar level of (dis)similarity as compared to pure or limed peat-based substrates. The relative number of significantly differential abundant taxa in compost and management residues is considerable smaller for fungi than for bacteria, indicating the fungal community composition of composts and management residues is more similar to that of peat-based substrates than the bacterial community composition. For composts, green composts (C1) showed the largest number of differentially abundant bacterial genera as compared to pure (P1; 76 genera) and limed peat-based substrates (P2; 268 genera), while woody composts (C3) showed the largest number of differentially abundant fungal genera as compared to pure (P1; 7 genera) and limed peat-based substrates (P2; 6 genera). For management residues, woody fractions of composts (M4) showed the largest number of differentially abundant bacterial genera as compared to pure (P1; 26 genera) and limed peat-based substrates (P2; 129 genera). Grass clippings (M1) showed the largest number of

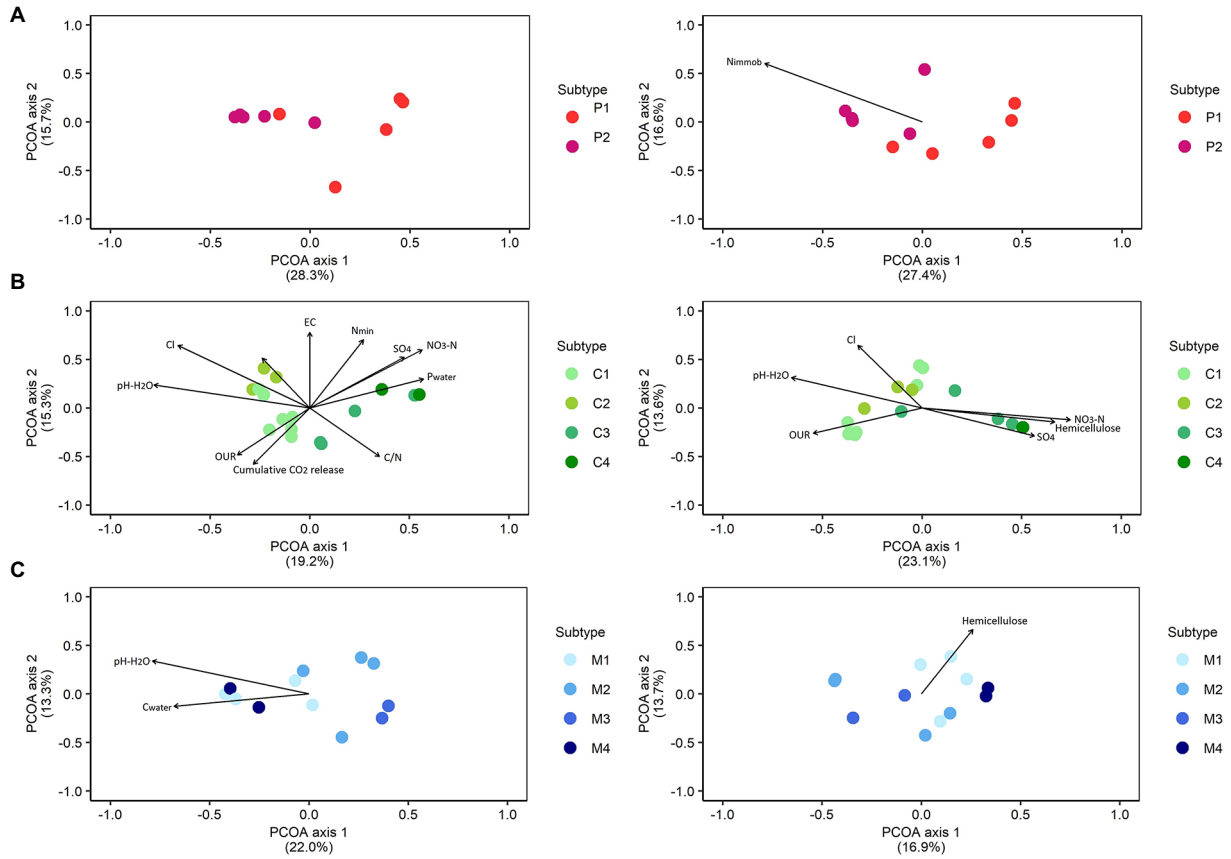

FIGURE 2
Correlations between bacterial and fungal community composition and chemical characteristics. Principal Coordinate Analysis (PCoA) profile of pairwise community dissimilarity (Bray-Curtis) indices of bacterial (16S V3-V4 rRNA gene; left) and fungal (ITS2 gene; right) sequencing data in peat-based substrates **(A)**, composts **(B)**, and management residues **(C)**. Arrows indicate significant correlations between corresponding variables and microbial community composition. The segments are scaled to the r^2 value, so that variables with a longer segment are more strongly correlated with the data than those with a shorter segment. Nimmob=N immobilization; Pwater=water extractable P; Fungi=total biomass fungi; Actinomycetes=total biomass actinomycetes; Gram − bact.=total biomass Gram-negative bacteria; Gram+bact.=total biomass of Gram-positive bacteria; Non-specific bact.=total biomass of non-specific bacteria. P1=pure peat-based substrates (n=5); P2=limed peat-based substrates (n=5); C1=green composts (n=7); C2=VFG composts (n=3); C3=woody composts (n=4); C4=peat composts (n=2); M1=grass clippings (n=4); M2=chopped heath (n=4); M3=forest sods (n=2); M4=woody fractions of composts (n=2).

differentially abundant fungal genera as compared to pure peat-based substrates (P1; 8 genera), while chopped heath (M2) showed the largest number of differentially abundant fungal genera compared to limed peat-based substrates (P2; 14 genera).

A detail of the differentially abundant bacterial genera (relative abundance >1%) and fungal genera between subtypes of peat-based substrates P1 and P2 on one hand and subtypes of composts and management residues on the other hand is shown in Supplementary Tables S4–S7. There were no bacterial genera that were significantly increased or decreased compared to pure peat-based substrates (P1) in all subtypes of composts. All subtypes of composts showed a significant increase in the relative abundances of *Flavobacterium* as compared to limed peat-based substrates (P2). No fungal genera were significantly increased or decreased compared to pure (P1) or limed (P2) peat-based substrates in all subtypes of composts. No bacterial or fungal genera were significantly increased or decreased compared to pure (P1) or limed (P2) peat-based substrates in all subtypes of management residues.

Second, the presence of genera known to include beneficial microorganisms and genera known to include human and/or plant pathogens was determined. The genera associated with the potential beneficial microorganisms *Bacillus*, *Paenibacillus*, *Pseudomonas* and *Serratia* were differentially abundant in several subtypes of composts and management residues as compared to the subtypes of peat-based substrates (Supplementary Table S8; Figure 3). The relative abundance of *Bacillus* was significantly higher in woody composts (C3) than in pure peat-based substrates (P1; $p < 0.001$) and in green composts (C1; $p = 0.003$), VFG composts (C2; $p = 0.006$), woody composts (C3; $p < 0.001$) and woody fractions of composts (M4; $p = 0.003$) than in limed peat-based substrates (P2). *Paenibacillus* was significantly more abundant in green composts (C1; $p < 0.001$), woody composts (C3; $p < 0.001$) and woody fractions

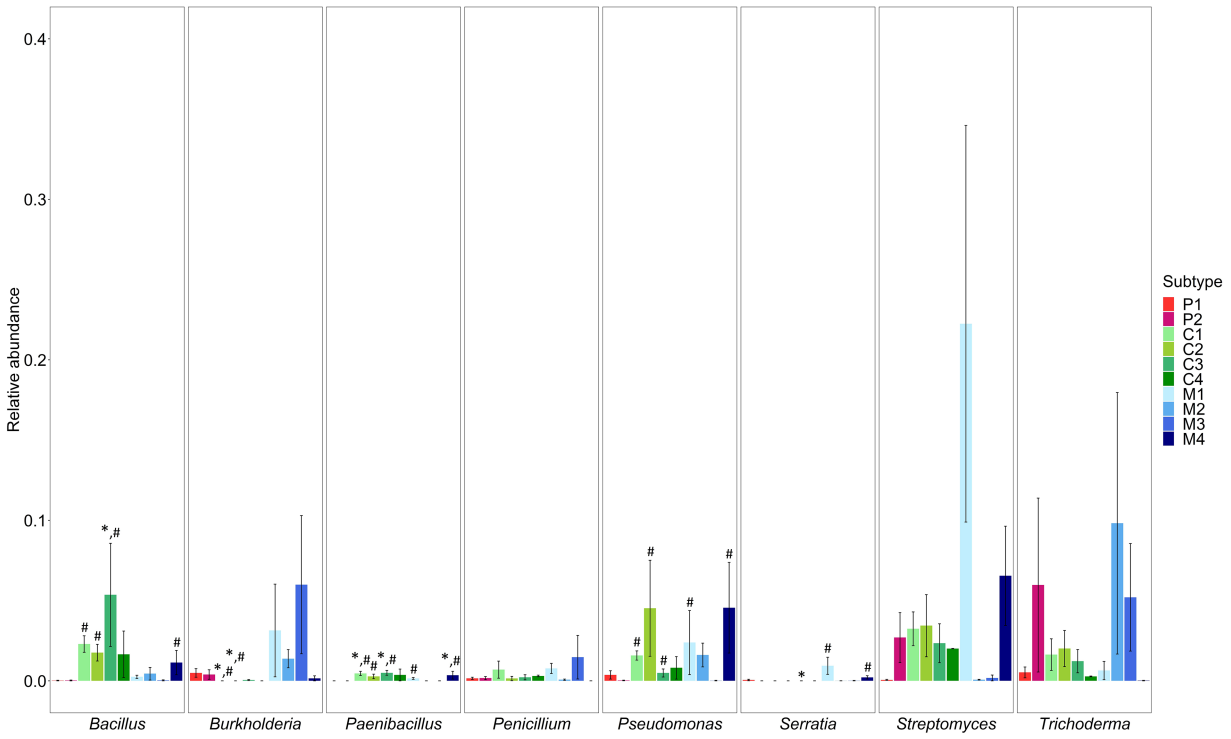

FIGURE 3
Mean relative abundances (proportions)±SE of genera known to include beneficial microorganisms *Bacillus*, *Burkholderia*, *Paenibacillus*, *Pseudomonas*, *Serratia*, *Streptomyces*, *Penicillium* and *Trichoderma* in the different subtypes of peat-based substrates, composts, and management residues. Colors represent the different subtypes in each type of biomass. P1=pure peat-based substrates (n=5); P2=limed peat-based substrates (n=5); C1=green composts (n=7); C2=VFG composts (n=3); C3=woody composts (n=4); C4=peat composts (n=2); M1=grass clippings (n=4); M2=chopped heath (n=4); M3=forest sods (n=2); M4=woody fractions of composts (n=2). Asterisk indicates a significant difference as compared to P1. Hashtag indicates a significant difference as compared to P2.

of composts (M4; $p < 0.001$) than in pure peat-based substrates (P1) and in green composts (C1; $p < 0.001$), VFG composts (C2; $p < 0.001$), woody composts (C3; $p < 0.001$), grass clippings (M1; $p = 0.001$) and woody fractions of composts (M4; $p < 0.001$) than in limed peat-based substrates (P2). *Pseudomonas* was significantly more abundant in green composts (C1; $p = 0.006$), VFG composts (C2; $p = 0.002$), woody composts (C3; $p = 0.01$), grass clippings (M1; $p = 0.005$) and woody fractions of composts (M4; $p = 0.002$) than in limed peat-based substrates (P2). The relative abundance of *Serratia* was significantly lower in woody composts (C3) than in pure peat-based substrates (P1; $p < 0.001$) and significantly higher in grass clippings (M1; $p < 0.001$) and woody fractions of composts (M4; $p < 0.001$) than in limed peat-based substrates (P2). *Burkholderia* was significantly less abundant in green composts (C1) and VFG composts (C2) than in pure (P1; $p < 0.001$ and $p = 0.005$, respectively) and limed peat-based substrates (P2; $p < 0.001$ and $p = 0.005$, respectively). *Streptomyces*, *Penicillium* and *Trichoderma* were not differential abundant in the subtypes of composts and management residues compared to the subtypes of peat-based substrates. Other genera that were significantly more abundant in at least one subtype of composts or management residues also have been found in literature to include beneficial species. Supplementary Table S9 shows an overview of these genera and the species that have been found to have a positive effect on disease suppression of plant pathogens in horticulture or to have plant growth promoting characteristics in horticultural plants. Most of these genera were significantly more abundant in green composts (C1), VFG composts (C2) and woody composts (C3) and in grass clippings (M1) and woody fractions of composts (M4). A larger number of these genera was significantly more abundant in the subtypes of composts and management residues when compared to limed peat-based substrates (P2) than compared to pure peat-based substrates (P1; see Supplementary Tables S4–S7).

Genera known to include potential human and/or plant pathogens *Klebsiella*, *Enterobacter* and *Escherichia/Shigella* were differentially abundant in several subtypes of composts and management residues as compared to the subtypes of peat-based substrates (Supplementary Table S10). *Klebsiella* was significantly more abundant in grass clippings (M1; $p = 0.005$) and woody fractions of composts (M4; $p = 0.009$) than in limed peat-based substrates. The relative abundance of *Enterobacter* was significantly higher in grass clippings (M1; $p < 0.001$ and $p < 0.001$) than in the two subtypes of peat-based substrates. Moreover, *Enterobacter* was significantly more abundant in green composts (C1; $p = 0.02$) and

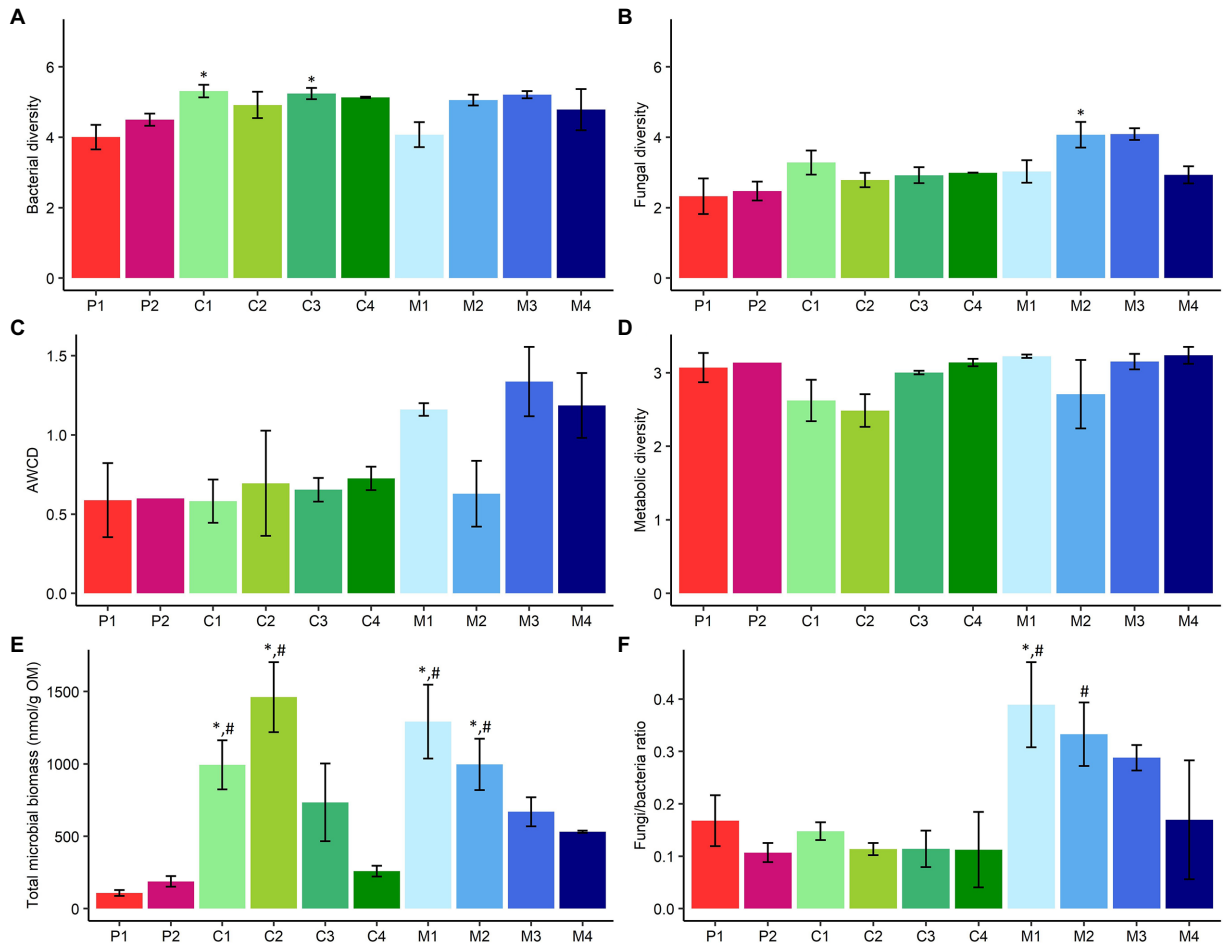

FIGURE 4
Comparison of microbiological characteristics of subtypes of peat-based substrates, composts, and management residues. **(A)** Mean bacterial diversity±SE, calculated as the Shannon Diversity Index, based on 16S V3-V4 rRNA gene metabarcoding data. **(B)** Mean fungal diversity±SE, calculated as the Shannon Diversity Index, based on ITS2 gene metabarcoding data. **(C)** Mean metabolic activity±SE, expressed as AWCD (average well color development), based on data from community-level physiological profiling using Biolog EcoPlates. **(D)** Mean metabolic diversity±SE, calculated as the Shannon diversity index, based on data from community-level physiological profiling using Biolog EcoPlates. **(E)** Mean total microbial biomass±SE (nmol/g OM), based on PLFA analysis data. **(F)** Mean fungal to bacterial ratio (F/B)±SE, based on PLFA analysis data. P1=pure peat-based substrates (n=5); P2=limed peat-based substrates (n=5); C1=green composts (n=7); C2=VFG composts (n=3); C3=woody composts (n=4); C4=peat composts (n=2); M1=grass clippings (n=4); M2=chopped heath (n=4); M3=forest sods (n=2); M4=woody fractions of composts (n=2). Asterisk indicates a significant difference as compared to P1, and hashtag indicates a significant difference as compared to P2.

woody fractions of composts (M4; $p<0.001$) than in limed peat-based substrates. The relative abundance of *Escherichia/Shigella* was significantly higher in grass clippings (M1; $p=0.001$ and $p=0.001$, respectively) and woody fractions of composts (M4; $p=0.006$ and $p=0.006$, respectively) than in pure (P1) and limed peat-based substrates (P2).

Third, bacterial and fungal diversity in the different subtypes of composts, management residues and peat-based substrates were determined (Figures 4A,B). Green composts (C1; $p=0.05$) and woody composts (C3; $p=0.04$) showed a significant higher bacterial diversity than pure peat-based substrates (P1). Fungal diversity was significantly higher in chopped heath (M2; $p=0.04$) than in pure peat-based substrates (P1).

Differences in functional characteristics of microbial community

Functional community composition was not significantly different between the different subtypes of biomass (Supplementary Figure S5). Metabolic activity, expressed as AWCD, showed no significant differences between the subtypes of peat-based substrates and subtypes of composts and management residues (Figure 4C). Metabolic diversity did not significantly differ between the subtypes of peat-based substrates and subtypes of composts and management residues (Figure 4D). No significant differences in AWCD of different C-sources were found between subtypes of composts and management residues and subtypes of peat-based substrates (Supplementary Figure S6).

Differences in microbial biomass

PCA showed a significant difference in microbial biomass between the different subtypes of biomass (Supplementary Figure S7). Green composts (C1; $p = 0.009$ and $p = 0.02$, respectively), VFG composts (C2; $p < 0.001$ and $p = 0.001$, respectively) have a significant higher microbial biomass than pure (P1) and limed peat-based substrates (P2). Grass clippings (M1; $p < 0.001$ and $p = 0.002$, respectively) and chopped heath (M2; $p = 0.02$ and $p = 0.05$, respectively) have a significant higher microbial biomass than pure (P1) and limed peat-based substrates (P2; Figure 4E).

Grass clippings (M1; $p = 0.04$ and $p = 0.004$, respectively) have a significant higher fungi/bacteria ratio than pure (P1) and limed peat-based substrates (P2). Chopped heath (M2) has a significant higher fungi/bacteria ratio than limed peat-based substrates (P2; $p = 0.04$; Figure 4F).

Inoculation with *Trichoderma harzianum*

No significant differences in inoculation efficiency were found between the different subtypes of composts and management residues (Supplementary Figure S8).

For peat-based substrates, net inoculation was not significantly correlated with the initial microbial characteristics. Net inoculation in composts was significantly correlated with the initial biomass of non-specific bacteria ($p = 0.01$; rho = −0.82), Gram-positive bacteria ($p = 0.01$; rho = −0.78), Actinomycetes ($p = 0.02$; rho = −0.73), Gram-negative bacteria ($p = 0.02$; rho = −0.73), fungi ($p = 0.001$; rho = −0.89), and the total initial microbial biomass ($p = 0.01$; rho = −0.77). In management residues, net inoculation was significantly correlated with the initial biomass of fungi ($p = 0.04$; rho = −061; Figure 5).

Discussion

Composts, management residues and peat-based substrates showed differences in their microbial community composition. However, even within each type of biomass, a high in-between sample variability in the bacterial and fungal community could be noted. To look deeper into this variability, the three types of

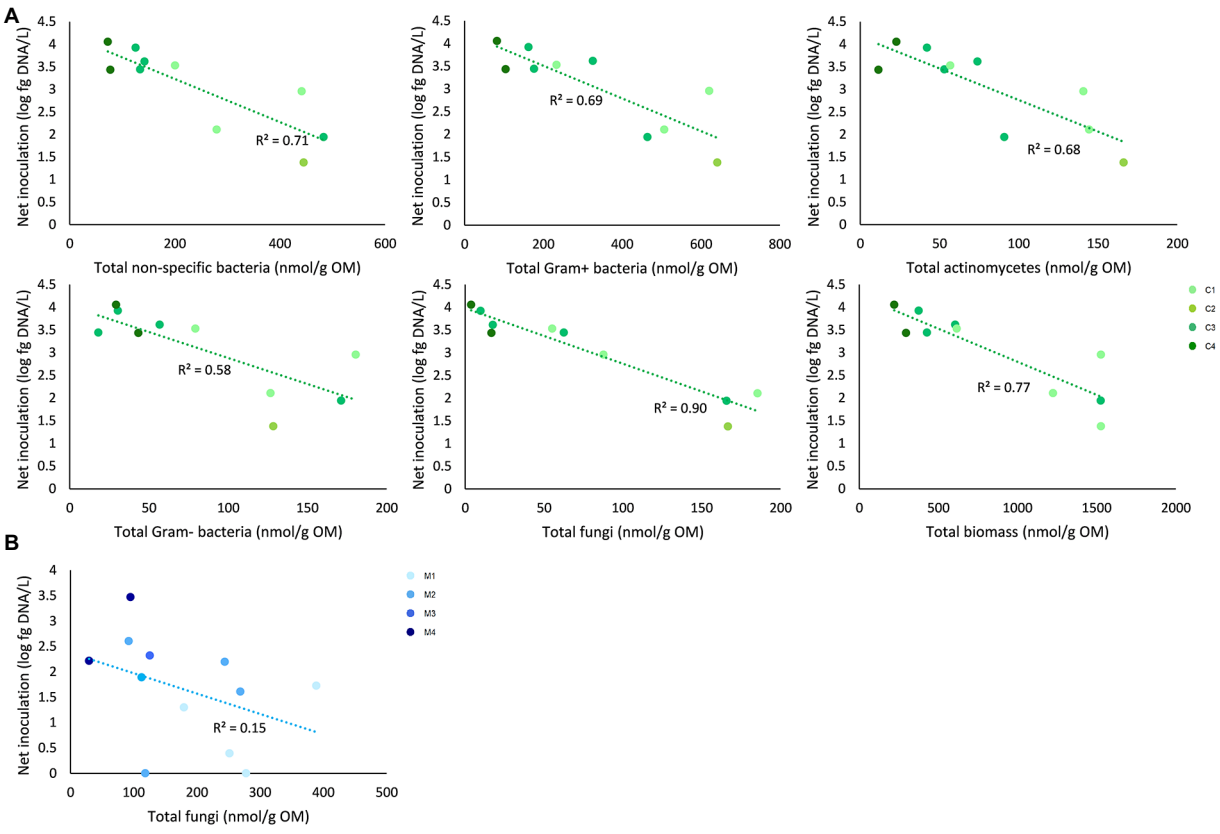

FIGURE 5
Correlations between initial microbial characteristics of composts and management residues and net inoculation of *Trichoderma harzianum*. **(A)** Net inoculation in composts was significantly correlated with the initial biomass of non-specific bacteria, Gram-positive bacteria, Actinomycetes, Gram-negative bacteria, fungi, and the total initial microbial biomass. **(B)** Net inoculation in management residues was significantly correlated with biomass of fungi. Determination coefficients (R^2) are shown. Colors indicate the different subtypes of composts and management residues. C1=green composts (n=3); C2=VFG composts (n=1); C3=woody composts (n=4); C4=peat composts (n=2); M1=grass clippings (n=4); M2=chopped heath (n=4); M3=forest sods (n=2); M4=woody fractions of composts (n=2).

biomass were classified in subtypes using a feedstock-based classification that is also used by commercial suppliers. Based on these subtypes, the microbiological characteristics of composts, management residues were studied in comparison to peat-based substrates in three ways.

First, it was assessed how feedstock and (bio)chemical characteristics drive microbiological characteristics of subtypes of peat-based substrates, composts, and management residues and how these subtypes of compost and management residues differ from peat-based substrates.

Samples of pure peat-based substrates showed a different microbial community than limed peat-based substrates, indicating that liming of the substrates influences the microbiome. Therefore, for microbiological characteristics, the classification based on liming of the peat-based substrates seems relevant. Bacterial community composition was not related to any other (bio)chemical characteristics. Differences in fungal community composition were related to nitrogen immobilization. Jezile et al. (2009) showed that the addition of lime to soil can cause an increase in nitrogen immobilization caused by a higher microbial activity, which may explain differences in nitrogen immobilization between pure and limed peat-based substrates. Differences in N immobilization in soils can also be linked to differences in microbial community composition (Schimel et al., 2005).

For composts, samples of feedstock-based subtypes clustered relatively closely together, indicating a similar microbiological composition within each feedstock-based subtype. For other types of compost, Ashraf et al. (2007) and Neher et al. (2013) also showed that bacterial and fungal communities responded to feedstock, resulting in distinct types of microbial communities in composts produced from different materials. In this study, there was, however, considerable overlap between several feedstock-based subtypes of composts. Microbial community composition of green composts and VFG composts showed large overlap, especially for fungal community composition. These similarities in microbial community composition may be due to similarities in feedstock, as there is a large diversity of source materials for both subtypes. Reyes-Torres et al. (2018) showed high variability in the composition of green composts due to the diversity of source materials. Woody composts and peat composts also showed large overlap, for both bacterial and fungal community composition. Again, similarities in feedstock may cause the similarities in microbial community composition for both subtypes of compost. Differences in bacterial community composition between different composts were most strongly related to chlorine content and nitrate, while differences in fungal community composition were most strongly related to nitrate. Other studies also reported that bacterial and fungal community composition were affected by nitrate (Zhang et al., 2011; Wu et al., 2020). Other chemical characteristics that have been reported to be related to bacterial community composition in composts include pH, organic matter and water soluble carbon, while fungal community composition can be related to organic carbon, water soluble carbon, and C/N (Zhang et al., 2011; Huhe et al., 2017; Sun et al., 2020; Wu et al., 2020). The chemical characteristics that were relatively strongly related to both bacterial and fungal community composition in this study were nitrate and Cl.

For nature management residues, feedstock-based subtypes were more difficult to distinguish based on microbiological community composition, with relative high dispersion between samples of feedstock-based subtypes. Miserez et al. (2019b) showed that management techniques, such as plaggen and chopping the heath vegetation, are an important determinant for chemical and physical characteristics of nature management residues. However, considerable variation in physical characteristics was seen between samples of chopped heath, which may be caused by variation in the amount of mineral material that is removed during chopping. Variation in management techniques may also cause variation in microbiological characteristics of feedstock-based subtypes observed in this study. Differences in bacterial community composition between management residues were mainly related to pH, while differences in fungal community composition were mainly related to hemicellulose content. Miserez et al. (2019b) reported that management residues show considerable differences in hemicellulose content. The fungal community may be influenced by hemicellulose, as saprotrophic fungi are efficient degraders of hemicellulose and other recalcitrant fractions of plant residues (van der Wal et al., 2013). No (bio) chemical characteristics were related to both bacterial and fungal community composition.

Previous studies already showed that composts and woody materials, such as wood fiber, display distinct microbial community profiles compared to peat (Green et al., 2004; Montagne et al., 2015, 2017). Montagne et al. (2015, 2017) reported that the microbial community in horticultural substrates is strongly dependent on substrate characteristics such as the origin of the material and physical structure due to the production process, resulting in globally distinct microbial communities in distinct types of substrates. Pot et al. (2022) showed that a microbial community diverging from that of peat-based substrates may be most favorable in disease suppressive growing media. Based on this information, for composts, green composts and woody composts have the most opportunity as these show the largest difference in either bacterial or fungal community compared to peat-based substrates. For management residues, woody fractions of composts showed the largest difference in bacterial community composition as compared to peat-based substrates. Grass clippings and chopped heath showed the largest difference in fungal community composition compared to pure and limed peat-based substrates, respectively.

Second, to look more into detail in the differences between subtypes of composts and management residues, different microbiological characteristics that have been reported in

literature as indicators for plant growth and health promotion in horticultural substates or soils were evaluated, i.e., presence of genera associated with known beneficial microorganisms, absence of genera with known pathogens, microbial diversity, functional diversity and metabolic activity, microbial biomass, and fungal to bacterial ratio.

Some subtypes of composts and management residues showed a significantly higher abundance for genera known to be associated with beneficial microorganisms. Compared to pure peat-based substrates, only green composts, woody composts, and woody fractions of composts showed a significant increase in the relative abundance of at least one genus associated with beneficial microorganisms. Compared to limed peat-based substrates, more subtypes showed a significant increase in these genera and more of these genera were significantly increased in relative abundance. Green composts, VGF composts, woody composts, grass clippings, and woody fractions of composts showed an increase in at least three beneficial genera. The higher abundance of these genera in composts and management residues may be a benefit as compared to peat-based substrates. Several studies have shown high abundances of plant growth promoting microorganisms and biocontrol agents, such as *Bacillus* spp., *Pseudomonas* spp., *Serratia* spp., *Paenibacullus* spp., and *Trichoderma* spp., in composts, leading to better plant growth and higher disease suppressiveness (Dukare et al., 2011; Chen et al., 2012; Antoniou et al., 2017; Lutz et al., 2020; Neher et al., 2022). Mendes et al. (2011) showed that the relative abundance of genera associated with beneficial microorganisms (i.e., significant higher abundance) is an important indicator for disease suppressiveness. The important remark should be made, however, that metabarcoding does not allow to reliably identify microorganisms at species level and that their function is unknown. It is therefore not sure if beneficial species or strains are present and functional in the samples. Further analysis, such as isolation of these strains, would therefore be necessary to confirm the presence of beneficial strains in the samples. However, studies have shown that relative abundances at genus level can also give an indication of disease suppression (Mendes et al., 2011; Liu et al., 2016, 2019).

Besides beneficial microorganisms, also pathogens may be present in composts and management residues, including human pathogens, belonging to genera such as *Salmonella, Escherichia, Klebsiella*, *Shigella*, and *Enterobacter*, or plant pathogens that can infect the plant roots *via* the growing medium, belonging to genera such as *Verticillium*, *Rhizoctonia*, *Sclerotinia,* and *Plasmodiaphora*. The genera *Klebsiella*, *Enterobacter,* and *Escherichia*/*Shigella* were present in some subtypes of peat-based substrates, composts, and management residues, specifically in pure peat-based substrates, green composts, grass clippings, and woody fractions of composts. However, again, the remark should be made that metabarcoding cannot confirm the presence and function of pathogenic strains in the samples. Further analysis, such as isolation *via* plating, would be necessary to confirm this. Moreover, several of the species included in these genera even have been shown to be non-pathogenic or even to have positive effects on plants. Several strains in the *Escherichia/Shigella* genus have been reported to be non-pathogenic (Welch, 2006; Liu, 2019). *Enterobacter* sp. and *Klebsiella* sp. have been reported to have plant growth promoting or disease suppressive effects in different plants (Chelius and Triplett, 2000; Ngamau et al., 2012; Marcos et al., 2015; Anzuay et al., 2017; Neher et al., 2022). Further analysis at species level would be needed to study the presence of pathogenic species. In addition, although relative abundances of some of these genera were significantly increased is subtypes in composts and management residues, they were in general found in very small abundances. Other genera that may include human and/or plant pathogens, such as *Salmonella, Verticillium*, *Rhizoctonia*, *Sclerotinia* or *Plasmodiaphora*, were not found in any of the subtypes. Based on those results, it may be concluded that the different subtypes of composts and management residues are relatively safe for use in substrates.

Based on estimations of bacterial diversity in composts and peat by Neher et al. (2013) and De Tender et al. (2016a), respectively, it was hypothesized that composts are more diverse than peat. Green composts and woody composts showed a significant higher bacterial diversity than pure peat-based substrates, while chopped heath showed a significant higher fungal diversity than pure peat-based substrates. However, none of the subtypes of composts or management residues showed a significantly higher bacterial or fungal diversity than limed peat-based substrates. A higher microbial diversity may be considered to be positive for the use in substrates, as this may outcompete pathogens by niche saturation, leading to a higher disease suppressiveness (Chaparro et al., 2012; van Elsas et al., 2012; Bongiorno et al., 2019). In addition, studies have also shown a positive effect of microbial diversity on plant growth (Wagg et al., 2011; Weidner et al., 2015; Kolton et al., 2017).

Subtypes of composts and management residues were expected to have a higher functional diversity and metabolic activity than peat-based substrates (Pane et al., 2011; Lutz et al., 2020). However, subtypes of composts and management residues did not show a significant higher functional diversity or metabolic activity than subtypes of peat-based substrates.

Vandecasteele et al. (2021) showed that composts and management residues in general have a higher microbial biomass compared to peat-based substrates. The present study showed that this is not the case for all subtypes of composts and management residues. For composts, only green composts and VGF composts showed a significantly higher microbial biomass than pure and limed peat-based substrates. For management residues, grass clippings and chopped heath showed a significant higher microbial biomass than pure and limed peat-based substrates. In addition, Vandecasteele et al. (2021) showed that management residues showed in general a higher fungal to bacterial ratio than peat-based substrates. However, for the subtypes of management residues, only grass clippings and chopped heath showed a significant higher fungal to bacterial ratio. A high microbial biomass and fungal to bacterial ratio may be related to higher disease suppression (Bongiorno et al., 2019; De Corato, 2020; Neher et al., 2022). Microbial biomass has also been associated with increased yield (Shen et al., 2016).

To assess if the different beneficial microbiological characteristics of subtypes of composts and management residues result in enhanced plant growth and/or disease suppression, the data of this study should be linked to plant-pathogens experiments in which different subtypes are used as a peat replacer.

Third, it was assessed if different types of composts and management residues can increase inoculation efficiency of *T. harzianum*, a biocontrol fungus, and which microbiological characteristics of composts and management residues can be used to predict inoculation efficiency. Joos et al. (2020) showed that different composts are suitable carrier media for *T. harzianum*. In addition, Vandecasteele et al. (2021) showed that composts have a significant higher inoculation efficiency than peat-based substrates. However, when the subtypes of composts or management residues were compared to pure and limed peat-based substrates, no significant differences were found in inoculation efficiency. A possible explanation for this may be that there were no significant differences in the organic matter content between the subtypes of composts and management residues, which is positively correlated with the survival rate of *T. harizanum* (Kibaki et al., 2006). Net inoculation of *T. harzianum* was significantly correlated with initial microbiological characteristics of composts and management residues. For composts, the initial biomass of non-specific bacteria, Gram-positive bacteria, Actinomycetes, Gram-negative bacteria, fungi, and the total initial microbial biomass was significantly correlated with net inoculation of the biocontrol fungus. Fungal biomass showed the strongest correlation. For management residues, fungal biomass was significantly correlated with net inoculation of the biocontrol fungus. These results show that fungal biomass may be a suitable predictor for inoculation efficiency with *T. harzianum* for both composts and management residues. This may be due to lower competition for nutrients and niches in substrates with a low initial fungal biomass (Fliessbach et al., 2009; Quiza et al., 2015). In further research, the relation between fungal biomass and inoculation efficiency of a biocontrol fungus could be studied for different biocontrol products and in other horticultural substrates.

Conclusion

For composts and peat-based substrates, a classification based on feedstock is relevant for bacterial and fungal community compositions, while for nature management residues feedstock-based subtypes may be less relevant for microbiology, as these subtypes were more difficult to distinguish based on microbial community composition. For composts, differences in bacterial community composition were related to chlorine and nitrate, while fungal community composition was related to nitrate. Bacterial and fungal community composition between management residues were mainly related to pH and hemicellulose content, respectively. Based on the microbiological characteristics, the subtypes showing the most potential to enhance plant growth and/or health are green composts, VFG composts, and woody composts in horticultural substrates for non-acidophilic plants and grass clippings, chopped heath, and woody fractions of compost for horticultural substrates for calcifuge plants. Further research should link these data to plant-pathogen experiments. Fungal biomass may be a suitable predictor for inoculation efficiency with *T. harzianum* for both composts and management residues. Further research should focus on evaluating this for different biocontrol products and other horticultural substrates.

Data availability statement

The datasets presented in this study can be found in online repositories. The names of the repository/repositories and accession number(s) can be found at: https://www.ncbi.nlm.nih.gov/, PRJNA624053; https://www.ncbi.nlm.nih.gov/, PRJNA715731; https://www.ncbi.nlm.nih.gov/, PRJNA767265.

Author contributions

JD, BV, ID, KV, CT, and JC were involved in the design and supervision of the study. SO conducted the metabarcoding, PLFA analysis, and inoculation experiment. SP conducted the Biolog EcoPlates experiment, conducted the statistical analysis of the data, and wrote the first draft and finalized the manuscript. SO and SP conducted the bio-informatics of the NGS data. All authors contributed to the article and approved the submitted version.

Funding

This work was supported by Flanders Innovation & Entrepreneurship (HBC.2017.0815) (Bi-o-ptimal@work – Sustainable cultivation in container and open field by using innovative and local materials with enhanced microbial life, ready for use and implementation by ornamental growers). CT received a grant of the Research Foundation Flanders (FWO) with application number (12S9418N). KV received an FWO sabbatical bench fee (number VWH-E1313-SAB/22/016).

Conflict of interest

The authors declare that the research was conducted in the absence of any commercial or financial relationships that could be construed as a potential conflict of interest.

Publisher's note

All claims expressed in this article are solely those of the authors and do not necessarily represent those

of their affiliated organizations, or those of the publisher, the editors and the reviewers. Any product that may be evaluated in this article, or claim that may be made by its manufacturer, is not guaranteed or endorsed by the publisher.

Supplementary material

The Supplementary material for this article can be found online at: https://www.frontiersin.org/articles/10.3389/fmicb.2022.983855/full#supplementary-material

References

Alam, M. Z., Braun, G., Norrie, J., and Mark Hodges, D. (2014). Ascophyllum extract application can promote plant growth and root yield in carrot associated with increased root-zone soil microbial activity. *Can. J. Plant Sci.* 94, 337–348. doi: 10.4141/cjps2013-135

Alexander, P., Bragg, N., Meade, R., Padelopoulos, G., and Watts, O. (2008). Peat in horticulture and conservation: the UK response to a changing world. *Mires and Peat* 3.

Al-Sadi, A. M., Al-Said, F. A., Al-Jabri, A. H., Al-Mahmooli, I. H., Al-Hinai, A. H., and de Cock, A. W. A. M. (2011). Occurrence and characterization of fungi and oomycetes transmitted via potting mixtures and organic manures. *Crop Prot.* 30, 38–44. doi: 10.1016/j.cropro.2010.09.015

Al-Sadi, A. M., Al-Zakwani, H. A., Nasehi, A., Al-Mazroui, S. S., and Al-Mahmooli, I. H. (2016). Analysis of bacterial communities associated with potting media. *Springerplus* 5:74. doi: 10.1186/s40064-016-1729-0

Andrews, S. (2010). FastQC: A quality control tool for high throughput sequence data. Available at: http://www.bioinformatics.babraham.ac.uk/projects/fastqc/

Antoniou, A., Tsolakidou, M.-D., Stringlis, I. A., and Pantelides, I. S. (2017). Rhizosphere microbiome recruited from a suppressive compost improves plant fitness and increases protection against vascular wilt pathogens of tomato. *Front. Plant Sci.* 8:2022. doi: 10.3389/fpls.2017.02022

Anzuay, M. S., Ciancio, M. G. R., Ludueña, L. M., Angelini, J. G., Barros, G., Pastor, N., et al. (2017). Growth promotion of peanut (*Arachis hypogaea* L.) and maize (*Zea mays* L.) plants by single and mixed cultures of efficient phosphate solubilizing bacteria that are tolerant to abiotic stress and pesticides. *Microbiol. Res.* 199, 98–109. doi: 10.1016/j.micres.2017.03.006

Ashraf, R., Shahid, F., and Ali, T. (2007). Association of fungi, bacteria and actinomycetes with different composts. *Pak. J. Bot.* 39, 2141–2151.

Berendsen, R. L., Pieterse, C. M. J., and Bakker, P. A. H. M. (2012). The rhizosphere microbiome and plant health. *Trends Plant Sci.* 17, 478–486. doi: 10.1016/j.tplants.2012.04.001

Bhattacharyya, P. N., and Jha, D. K. (2012). Plant growth-promoting rhizobacteria (PGPR): emergence in agriculture. *World J. Microbiol. Biotechnol.* 28, 1327–1350. doi: 10.1007/s11274-011-0979-9

Blaya, J., Marhuenda, F. C., Pascual, J. A., and Ros, M. (2016). Microbiota characterization of compost using omics approaches opens new perspectives for *Phytophthora* root rot control. *PLoS One* 11:e0158048. doi: 10.1371/journal.pone.0158048

Bolger, A. M., Lohse, M., and Usadel, B. (2014). Trimmomatic: a flexible trimmer for Illumina sequence data. *Bioinformatics* 30, 2114–2120. doi: 10.1093/bioinformatics/btu170

Bongiorno, G., Postma, J., Bünemann, E. K., Brussaard, L., de Goede, R. G. M., Mäder, P., et al. (2019). Soil suppressiveness to *Pythium ultimum* in ten European long-term field experiments and its relation with soil parameters. *Soil Biol. Biochem.* 133, 174–187. doi: 10.1016/j.soilbio.2019.03.012

Bonn, A., Allott, T., Evans, M., Joosten, H., and Stoneman, R. (2016). *Peatland Restoration and Ecosystem Services: Science, Policy and Practice*. Cambridge, UK: Cambridge University Press.

Brussaard, L., de Ruiter, P. C., and Brown, G. G. (2007). Soil biodiversity for agricultural sustainability. *Agric. Ecosyst. Environ.* 121, 233–244. doi: 10.1016/j.agee.2006.12.013

Bustamante, M., Paredes, C., Moral, R., Agulló, E., Murcia, P., and Abad, M. (2008). Composts from distillery wastes as peat substitutes for transplant production. *Resour. Conserv. Recycl.* 52, 792–799. doi: 10.1016/j.resconrec.2007.11.005

Callahan, B. J., McMurdie, P. J., Rosen, M. J., Han, A. W., Johnson, A. J., and Holmes, S. P. (2015). DADA2: high resolution sample inference from amplicon data. Bio RXiv, 024034. doi: 10.1101/024034

Cartwright, D. K. (1995). Commercial potting medium as the source of Pythium causing a disease on tobacco transplants. *Plant Dis.* 79:538. doi: 10.1094/PD-79-0538A

Chaparro, J. M., Sheflin, A. M., Manter, D. K., and Vivanco, J. M. (2012). Manipulating the soil microbiome to increase soil health and plant fertility. *Biol. Fertil. Soils* 48, 489–499. doi: 10.1007/s00374-012-0691-4

Chelius, M. K., and Triplett, E. W. (2000). Immunolocalization of dinitrogenase reductase produced by Klebsiella pneumoniae in association with *Zea mays* L. *Appl. Environ. Microbiol.* 66, 783–787. doi: 10.1128/AEM.66.2.783-787.2000

Chen, M.-H., Jack, A. L. H., McGuire, I. C., and Nelson, E. B. (2012). Seed-colonizing bacterial communities associated with the suppression of Pythium seedling disease in a municipal biosolids compost. *Phytopathology* 102, 478–489. doi: 10.1094/PHYTO-08-11-0240-R

De Corato, U. (2020). Disease-suppressive compost enhances natural soil suppressiveness against soil-borne plant pathogens: a critical review. *Rhizosphere* 13:100192. doi: 10.1016/j.rhisph.2020.100192

De Tender, C., Debode, J., Vandecasteele, B., D'Hose, T., Cremelie, P., Haegeman, A., et al. (2016a). Biological, physicochemical and plant health responses in lettuce and strawberry in soil or peat amended with biochar. *Appl. Soil Ecol.* 107, 1–12. doi: 10.1016/j.apsoil.2016.05.001

Dukare, A. S., Prasanna, R., Chandra Dubey, S., Nain, L., Chaudhary, V., Singh, R., et al. (2011). Evaluating novel microbe amended composts as biocontrol agents in tomato. *Crop Prot.* 30, 436–442. doi: 10.1016/j.cropro.2010.12.017

Epstein, E. (2001). "Human pathogens: hazards, controls, and precautions in compost," in *Compost Utilization in Horticultural Cropping Systems*. eds. P. J. Stofella and B. A. Kahn (Boca Raton, Florida, USA: CRS Press LLC).

Figueiredo, M. D. V. B., Seldin, L., De Araujo, F. F., and Mariano, R. D. L. R. (2011). "Plant growth promoting rhizobacteria: fundamentals and applications," in *Plant Growth and Health Promoting Bacteria*. ed. D. K. Maheshwari (Heidelberg, Germany: Springer), 21–43.

Fliessbach, A., Winkler, M., Lutz, M. P., Oberholzer, H.-R., and Mäder, P. (2009). Soil amendment with Pseudomonas fluorescens CHA0: lasting effects on soil biological properties in soils low in microbial biomass and activity. *Microb. Ecol.* 57, 611–623. doi: 10.1007/s00248-009-9489-9

Garland, J. L., and Mills, A. L. (1991). Classification and characterization of heterotrophic microbial communities on the basis of patterns of community-level sole-carbon-source utilization. *Appl. Environ. Microbiol.* 57, 2351–2359. Pub Med. doi: 10.1128/AEM.57.8.2351-2359.1991

Glöckner, F. O., Yilmaz, P., Quast, C., Gerken, J., Beccati, A., Ciuprina, A., et al. (2017). 25 years of serving the community with ribosomal RNA gene reference databases and tools. *J. Biotechnol.* 261, 169–176. doi: 10.1016/j.jbiotec.2017.06.1198

Graham, M. H., and Haynes, R. (2005). Catabolic diversity of soil microbial communities under sugarcane and other land uses estimated by biolog and substrate-induced respiration methods. *Appl. Soil Ecol.* 29, 155–164. doi: 10.1016/j.apsoil.2004.11.002

Green, S. J., Michel, F. C., Hadar, Y., and Minz, D. (2004). Similarity of bacterial communities in sawdust- and straw-amended cow manure composts. *FEMS Microbiol. Lett.* 233, 115–123. doi: 10.1016/j.femsle.2004.01.049

Hernandez-Apaolaza, L., Gasco, A. M., Gasco, J. M., and Guerrero, F. (2005). Reuse of waste materials as growing media for ornamental plants. *Bioresour. Technol.* 96, 125–131. doi: 10.1016/j.biortech.2004.02.028

Herrera, F., Castillo, J. E., Chica, A. F., and Lopez Bellido, L. (2008). Use of municipal solid waste compost (MSWC) as a growing medium in the nursery production of tomato plants. *Bioresour. Technol.* 99, 287–296. doi: 10.1016/j.biortech.2006.12.042

Hoitink, H. A. J., and Boehm, M. J. (1999). Biocontrol within the context of soil microbial communities: a substrate-dependent phenomenon. *Annu. Rev. Phytopathol.* 37, 427–446. doi: 10.1146/annurev.phyto.37.1.427

Huhe, , Jiang, C., Wu, Y., and Cheng, Y. (2017). Bacterial and fungal communities and contribution of physicochemical factors during cattle farm waste composting. *Microbiol. Open* 6:e00518. doi: 10.1002/mbo3.518

Jezile, G. G., Westfall, D. G., Peterson, G., Child, D. R., Turner, D. P., and Averbeke, W. V. (2009). Effects of liming on microbial activity and N mineralization in broiler manure-amended soils from Bizana, eastern cape, South Africa. *S. Afr. J. Plant Soil* 26, 18–23. doi: 10.1080/02571862.2009.10639927

Jones, P., and Martin, M. (2003). *A Review of the Literature on the Occurrence and Survival of Pathogens of Animals and Humans in Garden Compost*. The Waste and Resources Action Programme. Oxford, UK: Banbury.

Joos, L., Herren, G. L., Couvreur, M., Binnemans, I., Oni, F. E., Höfte, M., et al. (2020). Compost is a carrier medium for *Trichoderma harzianum*. *Biol. Control* 65, 737–749. doi: 10.1007/s10526-020-10040-z

Kavroulakis, N., Ntougias, S., Zervakis, G. I., Ehaliotis, C., Haralampidis, K., and Papadopoulou, K. K. (2007). Role of ethylene in the protection of tomato plants against soil-borne fungal pathogens conferred by an endophytic *Fusarium solani* strain. *J. Exp. Bot.* 58, 3853–3864. doi: 10.1093/jxb/erm230

Kibaki, J., Hau, B., and Waiganjo, M. M. (2006). "Growth and survival of *Trichoderma harzianum* as influenced by substrate compost content," in *Proceedings of 10th KARI Biennial Scientific Conference, I*.

Kolton, M., Graber, E. R., Tsehansky, L., Elad, Y., and Cytryn, E. (2017). Biochar-stimulated plant performance is strongly linked to microbial diversity and metabolic potential in the rhizosphere. *New Phytol.* 213, 1393–1404. doi: 10.1111/nph.14253

Krause, M. S., Madden, L. V., and Hoitink, H. A. (2001). Effect of potting mix microbial carrying capacity on biological control of rhizoctonia damping-off of radish and Rhizoctonia crown and root rot of poinsettia. *Phytopathology* 91, 1116–1123. doi: 10.1094/PHYTO.2001.91.11.1116

Kwok, O. C. H., Fahy, P. C., Hoitink, H. A. J., and Kuter, G. A. (1987). Interactions between bacteria and *Trichoderma hamatum* in suppression of *Rhizoctonia* damping-off in bark compost media. *Phytopathology* Available at: https://scholar.google.com/scholar_lookup?title=Interactions+between+bacteria+and+Trichoderma+hamatum+in+suppression+of+Rhizoctonia+damping-off+in+bark+compost+media&author=Kwok%2C+O.C.H.&publication_year=1987

Liu, D. (2019). "*Escherichia coli*," in *Encyclopedia of Microbiology*. *4th* edn. ed. T. M. Schmidt. (Cambridge, UK: Academic Press), 171–182.

Liu, L., Huang, X., Zhao, J., Zhang, J., and Cai, Z. (2019). Characterizing the key agents in a disease-suppressed soil managed by reductive soil disinfestation. *Appl. Environ. Microbiol.* 85, e02992–e02918. doi: 10.1128/AEM.02992-18

Liu, X., Zhang, S., Jiang, Q., Bai, Y., Shen, G., Li, S., et al. (2016). Using community analysis to explore bacterial indicators for disease suppression of tobacco bacterial wilt. *Sci. Rep.* 6:36773. doi: 10.1038/srep36773

Lutz, S., Thuerig, B., Oberhaensli, T., Mayerhofer, J., Fuchs, J. G., Widmer, F., et al. (2020). Harnessing the microbiomes of suppressive composts for plant protection: from metagenomes to beneficial microorganisms and reliable diagnostics. *Front. Microbiol.* 11:1810. doi: 10.3389/fmicb.2020.01810

Marcos, F., Freitas Iório, R., Silveira, A., Ribeiro, R., Machado, E., and Lagôa, A. (2015). Endophytic bacteria affect sugarcane physiology without changing plant growth. *Bragantia* 75, 1–9. doi: 10.1590/1678-4499.256

Martin, M. (2011). Cutadapt removes adapter sequences from high-throughput sequencing reads. *EMBnet. J.* 17, 10–12. doi: 10.14806/ej.17.1.200

Mendes, R., Kruijt, M., de Bruijn, I., Dekkers, E., van der Voort, M., Schneider, J. H. M., et al. (2011). Deciphering the rhizosphere microbiome for disease-suppressive bacteria. *Science* 332, 1097–1100. doi: 10.1126/science.1203980

Michel, J.-C. (2010). The physical properties of peat: a key factor for modern growing media. *Mires and Peat* 6.

Miserez, A., Nelissen, V., Pauwels, E., Schamp, B., Grunert, O., Veken, B., et al. (2019b). Characteristics of residues from heathland restauration and management: implications for their sustainable use in agricultural soils or growing media. *Waste Biomass Valorization* 11, 4341–4358. doi: 10.1007/s12649-019-00765-z

Miserez, A., Pauwels, E., Schamp, B., Reubens, B., De Nolf, W., De Nolf, L., et al. (2019a). The potential of management residues from heathland and forest as a growing medium constituent and possible peat alternative for containerized ornamentals. *Acta Hortic.* 1266, 395–404. doi: 10.17660/ActaHortic.2019.1266.55

Montagne, V., Capiaux, H., Barret, M., Cannavo, P., Charpentier, S., Grosbellet, C., et al. (2017). Bacterial and fungal communities vary with the type of organic substrate: implications for biocontrol of soilless crops. *Environ. Chem. Lett.* 15, 537–545. doi: 10.1007/s10311-017-0628-0

Montagne, V., Charpentier, S., Cannavo, P., Capiaux, H., Grosbellet, C., and Lebeau, T. (2015). Structure and activity of spontaneous fungal communities in organic substrates used for soilless crops. *Sci. Hortic.* 192, 148–157. doi: 10.1016/j.scienta.2015.06.011

Neher, D. A., Hoitink, H. A., Biala, J., Rynk, R., and Black, G. (2022). "Chapter 17—compost use for plant disease suppression," in *The Composting Handbook*. ed. R. Rynk (Cambridge, UK: Academic Press), 847–878.

Neher, D. A., Weicht, T. R., Bates, S. T., Leff, J. W., and Fierer, N. (2013). Changes in bacterial and fungal communities across compost recipes, preparation methods, and composting times. *PLoS One* 8:e79512. doi: 10.1371/journal.pone.0079512

Ngamau, C., Matiru, V., Tani, A., and Wangari, C. (2012). Isolation and identification of endophytic bacteria of bananas (*Musa* spp.) in Kenya and their potential as biofertilizers for sustainable banana production. *Afr. J. Microbiol. Res.* 6, 6414–6422.

Nilsson, R. H., Larsson, K.-H., Taylor, A. F. S., Bengtsson-Palme, J., Jeppesen, T. S., Schigel, D., et al. (2018). The UNITE database for molecular identification of fungi: handling dark taxa and parallel taxonomic classifications. *Nucleic Acids Res.* 47, D259–D264. doi: 10.1093/nar/gky1022

Ntougias, S., Papadopoulou, K. K., Zervakis, G. I., Kavroulakis, N., and Ehaliotis, C. (2008). Suppression of soil-borne pathogens of tomato by composts derived from agro-industrial wastes abundant in Mediterranean regions. *Biol. Fertil. Soils* 44, 1081–1090. doi: 10.1007/s00374-008-0295-1

Oberhänsli, T., Hofer, V., Tamm, L., Fuchs, J., Koller, M., Herforth Rahmé, J., et al. (2017). *Aeromonas* media in compost amendments contributes to suppression of *Pythium ultimum* in cress. *Acta Hortic.* 1164, 353–360. doi: 10.17660/ActaHortic.2017.1164.45

Oksanen, J., Blanchet, F. G., Friendly, M., Kindt, R., and Wagner, H. H. (2020). vegan: community ecology package. – R package ver. 2.5-7. Available at: https://cran.rproject.org/web/packages/vegan/

Pane, C., Spaccini, R., Piccolo, A., Scala, F., and Bonanomi, G. (2011). Compost amendments enhance peat suppressiveness to *Pythium ultimum*, *Rhizoctonia solani* and *Sclerotinia minor*. *Biol. Control* 56, 115–124. doi: 10.1016/j.biocontrol.2010.10.002

Postma, J., Montanari, M., and van den Boogert, P. H. J. F. (2003). Microbial enrichment to enhance the disease suppressive activity of compost. *Eur. J. Soil Biol.* 39, 157–163. doi: 10.1016/S1164-5563(03)00031-1

Pot, S., De Tender, C., Ommeslag, S., Delcour, I., Ceusters, J., Gorrens, E., et al. (2021a). Understanding the shift in the microbiome of composts that are optimized for a better fit-for-purpose in growing media. *Front. Microbiol.* 12:643679. doi: 10.3389/fmicb.2021.643679

Pot, S., De Tender, C., Ommeslag, S., Delcour, I., Ceusters, J., Gorrens, E., et al. (2021b). Shifts in the microbiome of management residues that are optimized for a better fit in growing media. *Acta Hortic.* 1317, 107–114. doi: 10.17660/ActaHortic.2021.1317.13

Pot, S., De Tender, C., Ommeslag, S., Delcour, I., Ceusters, J., Vandecasteele, B., et al. (2022). Suppression of *Phytophthora* on *Chamaecyparis* in sustainable horticultural substrates depends on fertilization and is linked to the rhizobiome. *Phytobiomes J.* doi: 10.1094/PBIOMES-05-22-0029-R

Quast, C., Pruesse, E., Yilmaz, P., Gerken, J., Schweer, T., Yarza, P., et al. (2012). The SILVA ribosomal RNA gene database project: Improved data processing and web-based tools. *Nucleic Acids Res.* 41, D590–D596. doi: 10.1093/nar/gks1219

Quiza, L., St-Arnaud, M., and Yergeau, E. (2015). Harnessing phytomicrobiome signaling for rhizosphere microbiome engineering. *Front. Plant Sci.* 6:507. doi: 10.3389/fpls.2015.00507

Reyes-Torres, M., Oviedo-Ocaña, E. R., Dominguez, I., Komilis, D., and Sánchez, A. (2018). A systematic review on the composting of green waste: feedstock quality and optimization strategies. *Waste Manag.* 77, 486–499. doi: 10.1016/j.wasman.2018.04.037

Robinson, M. D., McCarthy, D. J., and Smyth, G. K. (2010). Edge R: a Bioconductor package for differential expression analysis of digital gene expression data. *Bioinformatics* 26, 139–140. doi: 10.1093/bioinformatics/btp616

Schimel, J., Bennett, J., and Fierer, N. (2005). "Microbial community composition and soil nitrogen cycling: is there really a connection?" in *Biological Diversity and Function in Soils*. eds. R. Bardgett, M. Usher and D. Hopkins (Cambridge: Cambridge University Press), 171–188.

Schmilewski, G. (2008). The role of peat in assuring the quality of growing media. *Mires and Peat* 3.

Shen, Y., Chen, Y., and Li, S. (2016). Microbial functional diversity, biomass and activity as affected by soil surface mulching in a semiarid farmland. *PLoS One* 11:e0159144. doi: 10.1371/journal.pone.0159144

Sun, L., Han, X., Li, J., Zhao, Z., Liu, Y., Xi, Q., et al. (2020). Microbial community and its association with physicochemical factors during compost bedding for dairy cows. *Front. Microbiol.* 11:254. doi: 10.3389/fmicb.2020.00254

van der Wal, A., Geydan, T. D., Kuyper, T. W., and de Boer, W. (2013). A thready affair: linking fungal diversity and community dynamics to terrestrial decomposition processes. *FEMS Microbiol. Rev.* 37, 477–494. doi: 10.1111/1574-6976.12001

van Elsas, J. D., Chiurazzi, M., Mallon, C. A., Elhottovā, D., Krištůfek, V., and Salles, J. F. (2012). Microbial diversity determines the invasion of soil by a bacterial pathogen. *Proc. Natl. Acad. Sci. U. S. A.* 109, 1159–1164. doi: 10.1073/pnas.1109326109

Vandecasteele, B., Pot, S., Maenhout, K., Delcour, I., Vancampenhout, K., and Debode, J. (2021). Acidification of composts versus woody management residues: optimizing biological and chemical characteristics for a better fit in growing media. *J. Environ. Manag.* 277:111444. doi: 10.1016/j.jenvman.2020.111444

Wagg, C., Jansa, J., Schmid, B., and van der Heijden, M. G. A. (2011). Belowground biodiversity effects of plant symbionts support aboveground productivity. *Ecol. Lett.* 14, 1001–1009. doi: 10.1111/j.1461-0248.2011.01666.x

Waller, P. L., Thornton, C. R., Farley, D., and Groenhof, A. (2008). Pathogens and other fungi in growing media constituents. *Acta Hortic.* 779, 361–366. doi: 10.17660/ActaHortic.2008.779.45

Weidner, S., Koller, R., Latz, E., Kowalchuk, G., Bonkowski, M., Scheu, S., et al. (2015). Bacterial diversity amplifies nutrient-based plant–soil feedbacks. *Funct. Ecol.* 29, 1341–1349. doi: 10.1111/1365-2435.12445

Welch, R. (2006). "The genus Escherichia," in *The Prokaryotes*. *Vol. 6*. eds. M. Dworkin, S. Falkow, E. Rosenberg, K.-H. Schleifer and E. Stackebrandt (New York, USA: Springer), 60–71.

Wu, X., Ren, L., Luo, L., Zhang, J., Zhang, L., and Huang, H. (2020). Bacterial and fungal community dynamics and shaping factors during agricultural waste composting with zeolite and biochar addition. *Sustainability* 12:7082. doi: 10.3390/su12177082

Yilmaz, P., Parfrey, L. W., Yarza, P., Gerken, J., Pruesse, E., Quast, C., et al. (2013). The SILVA and "All-species Living Tree Project (LTP)" taxonomic frameworks. *Nucleic Acids Res.* 42, D643–D648. doi: 10.1093/nar/gkt1209

Zhang, J., Zeng, G., Chen, Y., Yu, M., Yu, Z., Li, H., et al. (2011). Effects of physico-chemical parameters on the bacterial and fungal communities during agricultural waste composting. *Bioresour. Technol.* 102, 2950–2956. doi: 10.1016/j.biortech.2010.11.089

frontiers | Frontiers in Microbiology

TYPE Original Research
PUBLISHED 07 November 2022
DOI 10.3389/fmicb.2022.1004593

OPEN ACCESS

EDITED BY
Leonardo Erijman,
Consejo Nacional de Investigaciones Científicas y Técnicas (CONICET), Argentina

REVIEWED BY
Weijun Shen,
Guangxi University, China
Wayan Wangiyana,
University of Mataram, Indonesia

*CORRESPONDENCE
Margarita Ros
margaros@cebas.csic.es

SPECIALTY SECTION
This article was submitted to Terrestrial Microbiology, a section of the journal Frontiers in Microbiology

RECEIVED 27 July 2022
ACCEPTED 17 October 2022
PUBLISHED 07 November 2022

CITATION
Cuartero J, Pascual JA, Vivo J-M, Özbolat O, Sánchez-Navarro V, Weiss J, Zornoza R, Martínez-Mena M, García E and Ros M (2022) Melon/cowpea intercropping pattern influenced the N and C soil cycling and the abundance of soil rare bacterial taxa. *Front. Microbiol.* 13:1004593. doi: 10.3389/fmicb.2022.1004593

Melon/cowpea intercropping pattern influenced the N and C soil cycling and the abundance of soil rare bacterial taxa

Jessica Cuartero[1], Jose Antonio Pascual[1], Juana-María Vivo[2], Onurcan Özbolat[3], Virginia Sánchez-Navarro[3], Julia Weiss[3], Raúl Zornoza[3,4], María Martínez-Mena[1], Eloisa García[1] and Margarita Ros[1]*

[1]Centre of Edaphology and Applied Biology of the Segura (CSIC), University Campus of Espinardo, Murcia, Spain, [2]Department of Statistics and Operations Research, CMN & IMIB-Arrixaca, University of Murcia, Murcia, Spain, [3]Institute of Plant Biotechnology, Plaza del Hospital s/n, Technical University of Cartagena, Cartagena, Spain, [4]Department of Agricultural Science, Polytechnic University of Cartagena, Cartagena, Spain

The high use of pesticides, herbicides, and unsustainable farming practices resulted in losses of soil quality. Sustainable farming practices such as intercropping could be a good alternative to traditional monocrop, especially using legumes such as cowpea (*Vigna unguiculata L. Walp*). In this study, different melon and cowpea intercropping patterns (melon mixed with cowpea in the same row (MC1); alternating one melon row and one cowpea row (MC2); alternating two melon rows and one cowpea row (MC3)) were assayed to study the intercropping effect on soil bacterial community through 16S rRNA region in a 3-year experiment. The results indicated that intercropping showed high content of total organic carbon, total nitrogen and ammonium, melon yield, and bacterial diversity as well as higher levels of beneficial soil microorganisms such a *Pseudomonas*, *Aeromicrobium*, *Niastella*, or *Sphingomonas* which can promote plant growth and plant defense against pathogens. Furthermore, intercropping showed a higher rare taxa diversity in two (MC1 and MC2) out of the three intercropping systems. In addition, N-cycling genes such as *nirB*, *nosZ,* and *amoA* were more abundant in MC1 and MC2 whereas the *narG* predicted gene was far more abundant in the intercropping systems than in the monocrop at the end of the 3-year experiment. This research fills a gap in knowledge about the importance of soil bacteria in an intercropping melon/cowpea pattern, showing the benefits to yield and soil quality with a decrease in N fertilization.

KEYWORDS

intercropping, cowpea, melon, 16S rRNA, nitrogen cycle, PICRUSt2, carbon cycle

Introduction

Soil is a diverse, complex, and yet widely unknown ecosystem in the world, but it is crucial for life because it produces more than 98% of human food (Kopittke et al., 2019). That food production is being compromised, however, mainly due to soil degradation and environmental changes, erosion, loss of soil organic ca rbon, loss of soil fertility, nutrient imbalance, acidification, salinization, and loss of microbial diversity, which are some of soil degradation processes (Dai et al., 2018; Zhou et al., 2018; Gedamu, 2020). There are many factors that affect soil degradation, although it is well known that agricultural management is one of the major contributors (Lal, 2015) through the use of fertilizers, pesticides, herbicides, and other types of practices such as tillage or monoculture (Tetteh, 2015). Therefore, one of the greatest challenges of this century is changing these practices into more sustainable ones such as intercropping.

Crops selected for intercropping normally have different abilities to use the resources available for growth, which leads to yield advantages and increased stability of crop yield compared to a single crop in a low input system (Wang et al., 2015; Dong et al., 2018). However, the use of intercrops has largely focused on the cereal-legume combination (Padhi and Panigrahi, 2006; Dwivedi et al., 2015), and there is still a significant lack of knowledge regarding other types of intercropping, especially with *Cucurbitaceae* plants Melon (*Cucumis melo L.*) is a fruit of great importance around the globe Spain is one of the largest melon exporters in the world, and most of these melons are grown in Murcia (OEC, 2019). Intensive melon cultivation can generate soil and water degradation due to the excessive use of pesticides to reduce the impact of pathogens, and to the necessary application of synthetic fertilizers, due to nutrient depletion (Li et al., 2001). Cowpea (*Vigna unguiculata L. Walp*) is a legume adapted to drought stress (Franke et al., 2018) that is frequently used in intercropping systems with maize (*Zea mays L.*), shorghum (*Sorghum bicolor L. Moench*) and pearl millet (*Pennisetum glaucum LRBr*) (Namatsheve et al., 2021). Legumes have a symbiotic relationship with nitrogen-fixing bacteria through the increased abundance of the gene *nifH*. They can capture nitrogen from the air, so intercropping with legumes allows neighboring crops to absorb more nitrogen from the soil, thus constituting a natural form of biofortification (Zuo and Zhang, 2009; Xue et al., 2016). This helps increase the quality of the fruits and soil (Ritchie and Roser, 2017). In addition, previous studies have reported that the planting patterns could also affect the soil and yield (Xianhai et al., 2012; Raza et al., 2019), so it is necessary to study different intercropping as well as plant distribution.

The influence of intercropping on soil microbial communities has been studied in several agriculture systems (Chen et al., 2018; Lian et al., 2019). In an intercropping system, the roots of different plant species interact with each other and subsequently affect root exudation, which undoubtedly alters the microbial diversity, structure, and functionality (Broeckling et al., 2008; Lian et al., 2019) and affects nutrient transport and mineralization (Rashid et al., 2016). The changed microbial community and activity could affect C and N dynamics, probably due to the ability of microbial communities to regulate C and N use efficiency (Mooshammer et al., 2014). Soil microbial communities are highly diverse and contain both abundant and rare taxa that are crucial for regulating multiple soil processes (Fuhrman, 2009; Delgado-Baquerizo et al., 2018). These rare taxa could be key in certain soil functions, and since their numbers are low, small changes in the soil ecosystem can affect them and even cause them to disappear (Zhou and Wu, 2021). Dominant taxa, on the other hand, would need more soil disturbance to vanish Studying the rare taxa could, thus, indicate changes in soil quality. Relatively little is known about how abundant and rare taxa respond to intercropping drivers, or how microbial community drives biogeochemical cycles.

A three-year intercropping experiment (melon/cowpea) with different patterns was conducted to evaluate the impact on the soil bacterial community (abundant and rare taxa), functionality, and associated ecosystems, by analysis of high-throughput sequencing and soil properties. We hoped to find out (a) whether intercropping patterns affect microbial diversity in the same order for overall microbial community, abundant and rare bacterial taxa; (b) if the intercropping patterns influenced the bacterial community composition differently; and (c) whether the intercropped system enhanced soil macronutrients through changes in predicted microbial genes involved in C- and N-cycling.

Materials and methods

Experimental design and sampling

The soil used in this study was classified as Haplic Haplic Calcisol (Loamic, hypercalcic) IUSS (IUSS Working Group WRB, 2015) from La Palma, Cartagena, (37° 41′18″N 0° 56′60″ W), a province of Murcia (SE Spain), in May-August 2018 The detailed experiment is related to Cuartero et al. (2022). Briefly, the treatments used were: (i) melon (*Cucumis melo*) monocrop (M); (ii) mixed intercropping, with melon mixed with cowpea in the same row (MC1); (iii) row intercropping at a ratio of 1:1 (melon:cowpea), alternating one melon row and one cowpea row (MC2); and (iv) row intercropping at a ratio of 2:1 (melon:cowpea), alternating two melon rows and one cowpea row (MC3) (Supplementary Figure 1). All crops were drip irrigated and grown under organic management. The melon plot (M) received the equivalent

of 3,000 kg ha-1 of organic fertilizer (N org) (3.2% N and 7% K_2O). The intercropped plots (MC1, MC2, and MC3) received 30% less Norg than the melon monocrop to assess the efficiency of the intercropping in reducing external fertilization needs.

Five random soil subsamples (0–10 cm depth) were collected in the first and third year of the melon/cowpea intercropping treatments corresponding to 10 August 2018 (referred to as first) and 11 September 2020 (referred to as third). Samples were labeled and immediately brought to the lab where they were separated into two aliquots. The soil was sieved through 2 mm mesh, and the major part was stored at −20°C for biological analysis; a sub-sample was air-dried for chemical analyses.

Soil DNA extraction, PCR amplification, and sequencing

Soil DNA extraction and Next-Generation-Sequencing of bacterial 16S hypervariable regions were performed according to Cuartero et al. (2022). Briefly, soil DNA was extracted from 1 g of soil (wet weight) using DNeasy Power Soil Kit (Qiagen). Quantity and quality of DNA were tested through Qubit 2.0 fluorometer (Invitrogen, Thermo Fisher Scientific, USA) and NanoDrop 2000 (Thermo Fisher Scientific, Waltham, MA, USA). Ion TorrentTM Personal Genome MachineTM (PGM) was employed to amplify 16S hypervariable region using Ion XpressTM Plus Fragment Library Kit in combination with Ion XpressTM Barcode adapter (Thermo Fisher Scientific), the detailed process is described in Cuartero et al. (2022).

Sequencing data processing

Bacterial raw sequences, barcodes, and primers were trimmed according to the BaseCaller application. The sequences were denoised with ACACIA (Bragg et al., 2012), and imported to QIIME2 v20202 (Bolyen et al., 2019). Then, sequences were denoised using the DADA2 algorithm with sequences truncated with a $Q > 30$ (Callahan et al., 2016) on average. Amplicon Sequence Variants (ASV) obtained from DADA2 were classified using the "classify-consensus-vsearch" command against the SILVA 132 (Quast et al., 2012) database. Functional analysis of the bacterial community was carried out using the PICRUSt2 (Phylogenetic investigation of communities by reconstruction of unobserved states) algorithm (Douglas et al., 2020). Some of the predicted functional genes were then selected to study the effects of intercropping on N- and C-cycling in the soil.

The sequences were uploaded to the European Nucleotide Archive (ENA) with the study accession code PRJEB42624.

Soil properties

The soil pH, Electrical Conductivity (EC), Total Organic Carbon (TOC), Total Nitrogen (TN), and Ammonia (NH_4^+) were measured according to Cuartero et al. (2022), briefly, EC was measured in deionized water (1:5 w/v), TOC and TN were determined using CHNS-O analyzer (EA-1108, Carlo Erba). NH_4^+ was extracted with 2M KCL in a 1:10 soil: extractant ratio and measured by colorimetric assay.

Statistical analysis

Random forest (RF) analysis was used to test the most important microbial taxa across the intercropping systems at the two sampling times by the randomForest package v 4.7-1 (Liaw and Wiener, 2002). Establishing an RF classifier, which contains a multitude of decision trees based on the threshold abundance of the critical genus (Yu et al., 2021). To enhance the RF classification performance, the optimal three RF hyper-parameters were searched through the "train" function from the caret package v 6.0-91 (Kuhn et al., 2020). The number of variables selected as a splitting parameter at each node (mtry), the number of decision trees (ntree), and the maximal number of nodes (maxnodes) in the forest An 18-fold cross-validation was employed to assess the performance of the classification using the "rfcv" function, as suggested by Zhang et al. (2019). All samples ($n = 20$) were used as the training set and RF classification (proximity = TRUE, importance = TRUE). Finally, the "varImpPlot" and "MDSplot" functions were used to show the importance of taxa and performance in classification, respectively Prior to the test, the differences among cropping systems, normality, and homogeneity of variance assumptions were assayed by Shapiro-Wilk and Levene's tests using the package car (Fox et al., 2007). Mean comparisons were performed with a one-way analysis of variance (ANOVA), followed by the *post-hoc* test of Tukey's honestly significant difference (HSD) when the null hypothesis was rejected Non-parametric Kruskal–Wallis test was applied when data did not fit a normal distribution and, if the assayed data were significant, a multiple comparison Z-values test was performed using the "dunnTest" function with Benjamini-Hochberg corrections in the FSA package (Ogle and Ogle, 2017). To test the treatment effects in paired-measures data, the non-parametric rank-based model "nparLD" was performed through the nparLD package v 21 (Noguchi et al., 2012) using f1ldf1 design.

To study the effects of intercropping systems on bacterial community, the ASV data table was split into rare or more abundant taxa being (> 01%) abundant taxa, (< 01%) rare taxa, and total taxa. A Principal Coordinates Analysis (PCoA) was used to visualize the variation of the community composition based on the Bray-Curtis distance. To test the differences between the cropping systems, a Permutational Multivariate Analysis of Variance (PERMANOVA) was conducted using the "betadisper" and "adonis" functions with 999 permutations from the vegan package v 2.5-7 (Oksanen et al., 2020). Alpha diversity as the Shannon index was calculated using the vegan package A Venn diagram was made to study the total ASVs shared among cropping systems Canonical Correspondence Analysis (CCA) using the "cca", and "envfit" functions from the vegan package was performed to study the correlation of microbial top ten abundance genera with soil properties. A Non-metric Multidimensional Scaling was performed using the "metaMDS" function from the vegan package with the Bray-Curtis distance to visualize the predicted functional genus. All tests were performed using R language (R Core Team, 2020) and plots were made using mainly the ggplot2 package v 3.3.5 (Gómez-Rubio, 2017).

Results

Effect of intercropping on physicochemical soil properties and melon yield

The pH and EC were not affected by the interaction between treatment and sampling time (Table 1). The pH diminished significantly in the third year, and it was lower in the intercropped systems (MC1, MC2, and MC3) than in monoculture (M). EC increased significantly in the third year of the experiment, and the highest EC was recorded in MC1. The interaction between the cropping system and sampling time did not affect TOC and TN (Table 1). TOC and TN increased in intercropping systems compared to monoculture and the values were higher in the third year. NH_4^+ was significantly higher in the intercropped systems than in the monocrop (M) and its levels dropped significantly in the third year (Table 1). The melon yield average was greater in the intercropping systems (MC1, MC2, and MC3) than in the monocrop (M) and was significantly lower value in the third year than in the first year.

A canonical correspondence analysis at both sampling times (Supplementary Figure 2) revealed the influence of soil properties on the microbial community at the genus level. Constrained CCA explained 85 and 60% of the inertia for the first and third years of the experiment, respectively. The top ten genera were highly affected by NH_4^+, EC, pH, TN, and TOC (p-value: 0.002, 0.044, 0.003, 0.001, and 0.001, respectively), in the first year of the experiment, but by the third year of the experiment, they were only significantly affected by pH, TOC, EC and TN (p-value: 0.029, 0.011, 0.061, and 0.002, respectively).

Effect of intercropping on whole, abundant, and rare bacterial diversity

At both sampling times, the different intercropping had a total of 2,140,702 reads ranging from ≈ 28,000 to 66,000 reads per sample which had a total of 9,558 different ASV ranging from 217 to 1,025 ASV per sample. Data were rarefied to 27,978 reads and the rarefaction curve constructed by randomly selected sequences from samples indicating that the number of sequences was representative of the bacterial community (Supplementary Figure 3).

The ASV obtained were classified into 31 phyla, 394 families, and 638 genera. A Venn diagram showed that all the cropping systems shared 670 (13%) and the intercropped systems 119 (4%). ASV respectively in the first year of the cropping system (Figures 1A,B). However, this number decreased to 141 ASV (4%) for all crop systems and 119 (4%) between intercropped systems in the third year of the cropping system (Figures 1A,B). In general, the effect of intercropping systems showed large differences with monocrop, where MC1 and MC2 shared with monocrop (M) only 1 and 2% of ASVs respectively in both samplings, and MC3 shared with monocrop around 2 and 1% of ASVs in both samplings (Figures 1A,B).

Large differences were found in the ASVs counts from different cropping systems. The ASV data table was split into (> 0.1%) abundant taxa, (< 0.1%) rare taxa, and total taxa. In the first year, intercropping systems (MC1, MC2, and MC3) showed a higher composition of rare taxa (ranging from 5,107 to 6,020%) than the most abundant taxa (ranging from 3,980 to 4,983%). Compared to the monocrop, the intercropping MC3 showed the highest number of total ASVs, and rare taxa (897/540) followed by MC1 (851/490) and MC2 (748/382) respectively, compared to monocrop (M) (Supplementary Table S1). However, in the third year of the experiment intercropping system showed a higher proportion of most abundant taxa (76.61–62.17%) compared to rare taxa (23.39–35.44%), MC2 showed the highest values of total ASVs, and rare taxa (415/157) followed by MC1 (364/129) (Supplementary Table S1).

The Shannon index for the total, most abundant, and rare taxa diminished in the third year (Figure 2; Supplementary Table 2). In the first year of the cropping system, MC1 and MC3 showed the highest total and rare taxa diversity compared to monocrop (M) (Figure 2). In the third year, however, MC1 and MC2 showed higher values than the monocrop (M) while MC3 showed the lowest Shannon index (Figure 2, Supplementary Table 2).

The β-microbial diversity represented by PCA analysis of the whole, most abundant, and rare taxa at both sampling

TABLE 1 Different soil properties and harvest in different sampling times and cropping systems.

	First				Third					
	M	MC1	MC2	MC3	M	MC1	MC2	MC3		*P*-value
pH	8.48 ± 0.02	8.40 ± 0.02	8.43 ± 0.03	8.42 ± 0.02	7.98 ± 0.07	7.73 ± 0.12	7.83 ± 0.15	7.96 ± 0.06	G	***
									T	***
									GxT	ns
EC (dS m^{-1})	0.290 ± 0.001	0.336 ± 0.023	0.297 ± 0.013	0.303 ± 0.028	0.496 ± 0.015	0.555 ± 0.069	0.537 ± 0.040	0.505 ± 0.026	G	***
									T	***
									GxT	ns
TOC (g kg^{-1})	9.5 ± 0.1	11.2 ± 0.4	11.1 ± 0.2	11.9 ± 0.2	9.86 ± 0.9	12.3 ± 0.4	11.0 ± 0.6	12.1 ± 1.2	G	***
									T	*
									GxT	ns
TN (g kg^{-1})	1.10 ± 0.00	1.30 ± 0.00	1.30 ± 0.00	1.30 ± 0.00	1.08 ± 0.04	1.36 ± 0.06	1.34 ± 0.11	1.34 ± 0.06	G	***
									T	*
									GxT	ns
NH_4^+ (mg kg^{-1})	0.83 ± 0.13 b	1.83 ± 0.07 a	3.47 ± 0.49 a	4.63 ± 0.56 a	0.76 ± 0.15 b	0.94 ± 0.30 a	0.91 ± 0.19 a	1.06 ± 0.39 a	G	***
									T	***
									GxT	***
Yield (kg ha^{-1})	15,092 ± 230	26,271 ± 3,339	20,287 ± 3,038	24,759 ± 2,049	8,561 ± 428	9,637 ± 2,599	10,600 ± 2,330	10,843 ± 2,451	G	ns
									T	***
									GxT	ns

(mean±sd; $n = 5$) G, Group (which corresponds to cropping system); *T*, Time; *GxT*, interaction of Group x Time; *M*, Melon monocrop; MC1, Mixed intercropping; MC2, Intercropping row 1:1 melon:cowpea; MC2, Intercropping row 2:1 melon:cowpea; *EC*, Electrical conductivity; *TOC*, Total organic carbon; *TN*, Total nitrogen; NH_4^+ total ammonium; Yield; Melon Yield Letters represent the significant differences between the cropping system and sampling time. *P* value: *** < 0.001; ** < 0.01; * < 0.05.

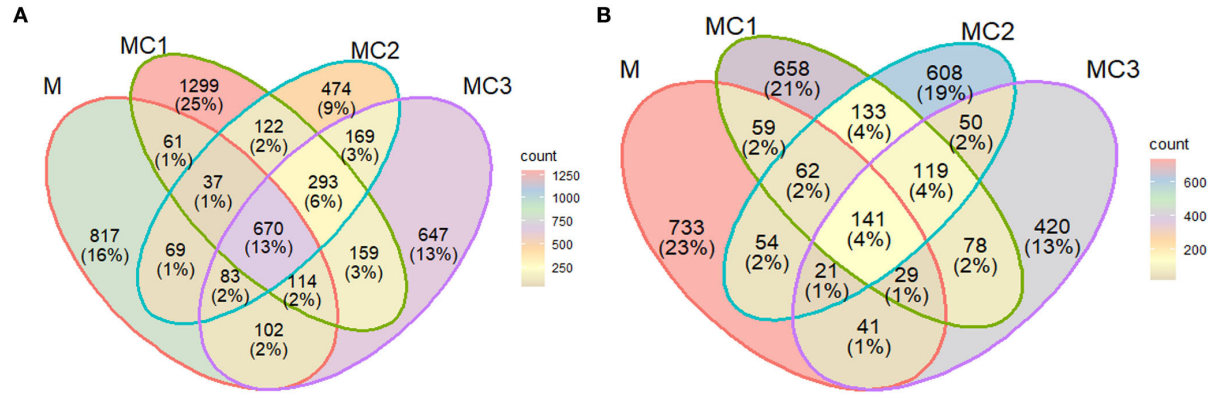

FIGURE 1
Venn diagram based on ASVs at the first **(A)** and third **(B)** year of the experiment. M, melon monocrop; MC1, mixed intercropping; MC2, intercropping row 1:1 melon:cowpea; MC3, intercropping row 2:1 melon:cowpea. The numbers (percentages) of the abundant bacteria in different systems are indicated in the overlapping and non-overlapping areas.

times showed significant changes (PERMANOVA; $P < 0.05$) in the intercropped treatments compared to the monocrop (M) (Figure 3). In the first year of the experiment, no significant differences were observed between intercropped systems in any of diversity indices, while in the third year, only the rare taxa showed significant differences between the intercropped systems, with MC3 showing different values from MC1 and MC2 (Figure 3).

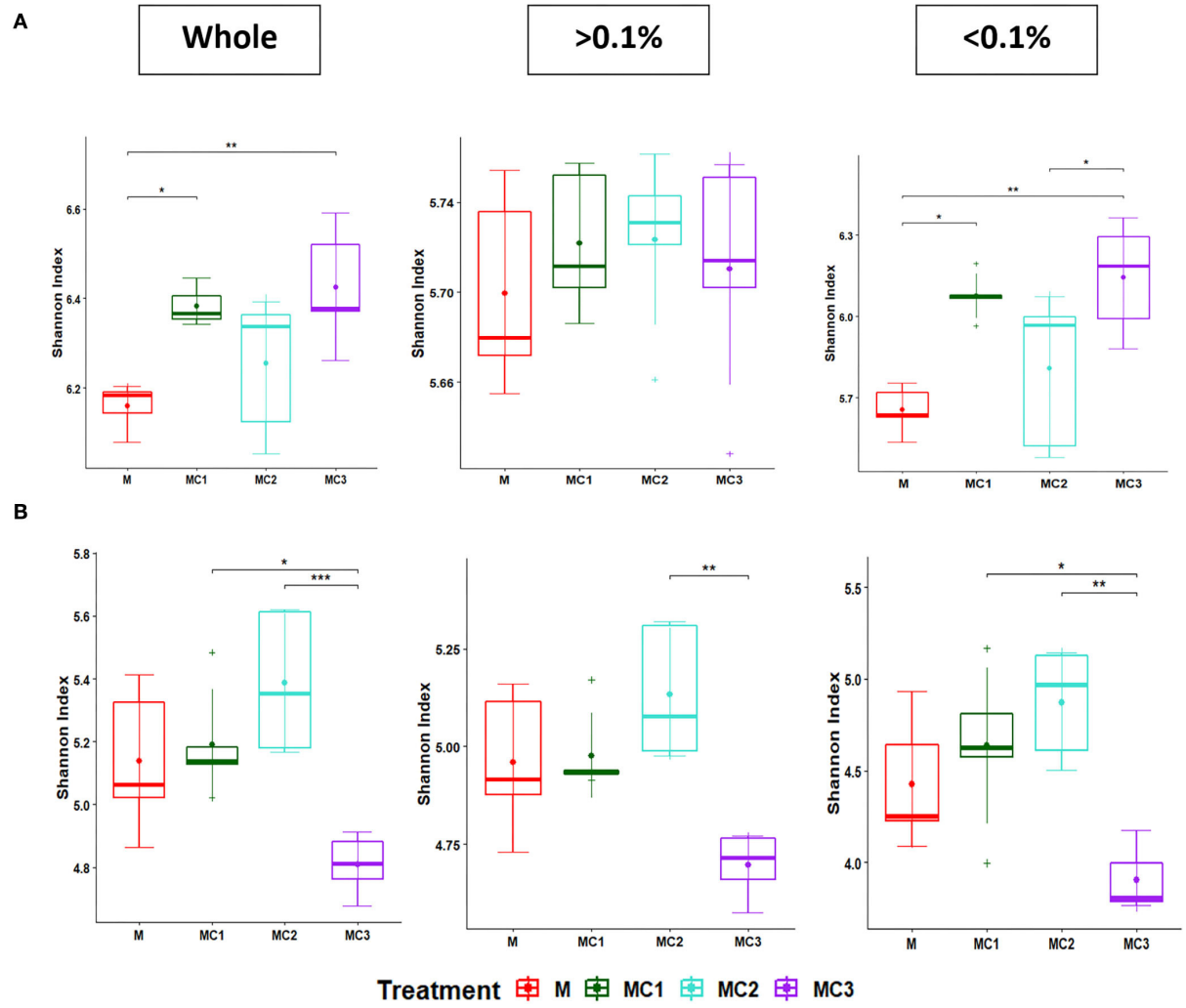

FIGURE 2
Boxplot of Shannon diversity index of the whole, more abundant, and rare bacterial taxa at the first **(A)** and third **(B)** years under the cropping systems. The "●" and line inside the box plot respectively represent the mean and median, ($n = 5$). "+" outside the box plot are outliers. Significant differences between cropping systems (Kruskal–Wallis test followed by *post-hoc*) are indicated by "*", < 0.05: "**", < 0.01; "***", < 0.001. The "> 0.1%" represents the abundant taxa; "< 0.1%" represents the rare taxa; whole, total. M, melon monocrop; MC1, mixed intercropping; MC2, intercropping row 1:1 melon:cowpea; MC3, intercropping row 2:1 melon:cowpea.

Effect of intercropping on responsive bacterial genera

The top 10 most abundant genera cover ≈70% of the evaluated taxa, being identified as *Pseudomonas* (11.60%), *Bacillus* (9.45%), *Sphingomonas* (8.26%), *Skermanella* (7.46%), *MND1* (7.28%), *Streptomyces* (6.97%) *Nocardioides* (6.52%), *SWB02* (4.51%) *Blastococcus* (4.12%) and *Ammoniphilus* (2.66%); all were affected by the type of cropping systems and sampling times (Figure 4, Supplementary Table 3). The relative abundance of *Pseudomonas*, *Sphingomonas*, *Nocardioides*, *SWB02,* and *Streptomyces* was significantly higher in the three intercropped systems, whereas, the relative abundance of *Bacillus*, *Skermanella*, *Ammoniphilus*, and *Blastococcus*, was significantly lower compared to monocrop (M) (Figure 4A). Differences were also observed by sampling time, in which *Pseudomonas*, *Skermanella*, *MND1*, *SWB02,* and *Blastoccus* showed higher relative abundance in the third year of the experiment; whereas the relative abundance of *Bacillus*, *Sphingomonas*, *Nocardioides*, *Amoniphilus*, and *Streptomyces* decreased (Figure 4B).

To identify the representative microbes in the cropping systems, random forest analyses with all genera were

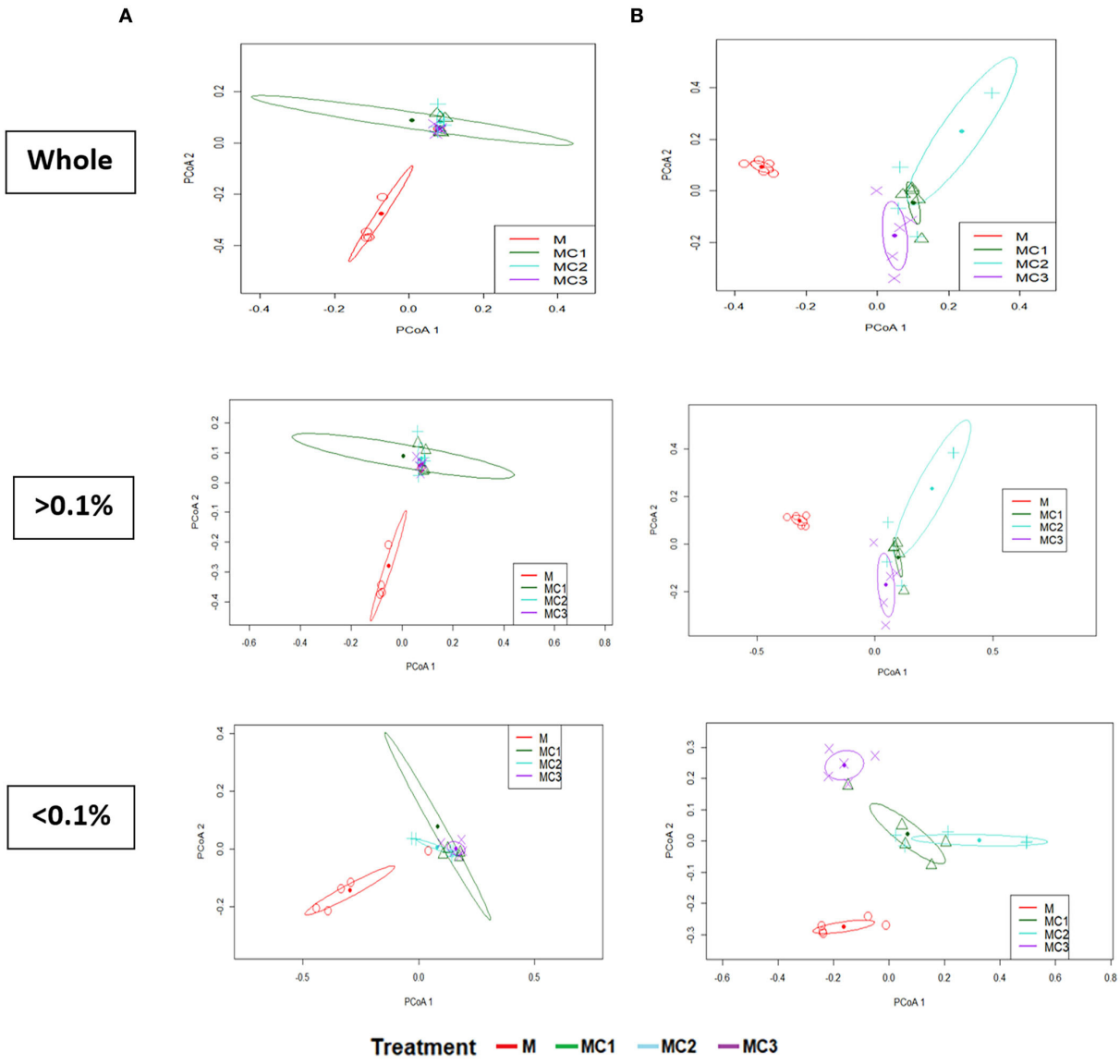

FIGURE 3
Principal Coordinate Analysis of soil bacteria community (β-Diversity) using Bray-Curtis distance for whole, most abundant, and rare taxa at the first **(A)** and the third **(B)** year under the cropping systems. > 0.1% represents the abundant taxa; < 0.1 represent the rare taxa; whole, total, M, melon monocrop; MC1, mixed intercropping; MC2, intercropping row 1:1 melon:cowpea; MC3, intercropping row 2:1 melon:cowpea.

conducted at both sampling times to find the most important genera (Supplementary Figures 4A,B). The MDS showed how all cropping systems at both sampling times can be clearly differentiated by the selected genera (Supplementary Figures 4C,D). Of the 15 most important genera in the first year of the experiment, *Microvirga*, *Nonomuraea*, *Micromonospora*, *Kribella*, *Roseomonas*, and *Rubrobacter* were highly enriched in monocrop (M); *Mesorhizobium*, *Gemmata*, *SWB02*, *Iamia*, and *Pontibacter* were highly enriched in MC1 and *Nocardioides*, *Agromyces*, *Aeromicrobium*, and *Hypomicrobium* were highly enriched in MC3 (Supplementary Figure 4A). In the third year of the experiment, however, different genera were observed for cropping system, in which *Ammoniphilus*, *Lysobacter*, and *Bradyrhizobium* were highly enriched in the monocrop (M), *Thauera*, *Nannocystis*, *Aeromicrobium*, *Nonomuraea*, and *Sphingomonas* were highly enriched in MC1; *SM1A02*, *Niastella*, *Ensifer*, and *Bryobacter* in MC2, and *Vogesella*, *Streptomyces*, and *Policyclovorans* were highly enriched in MC3 (Supplementary Figure 5B).

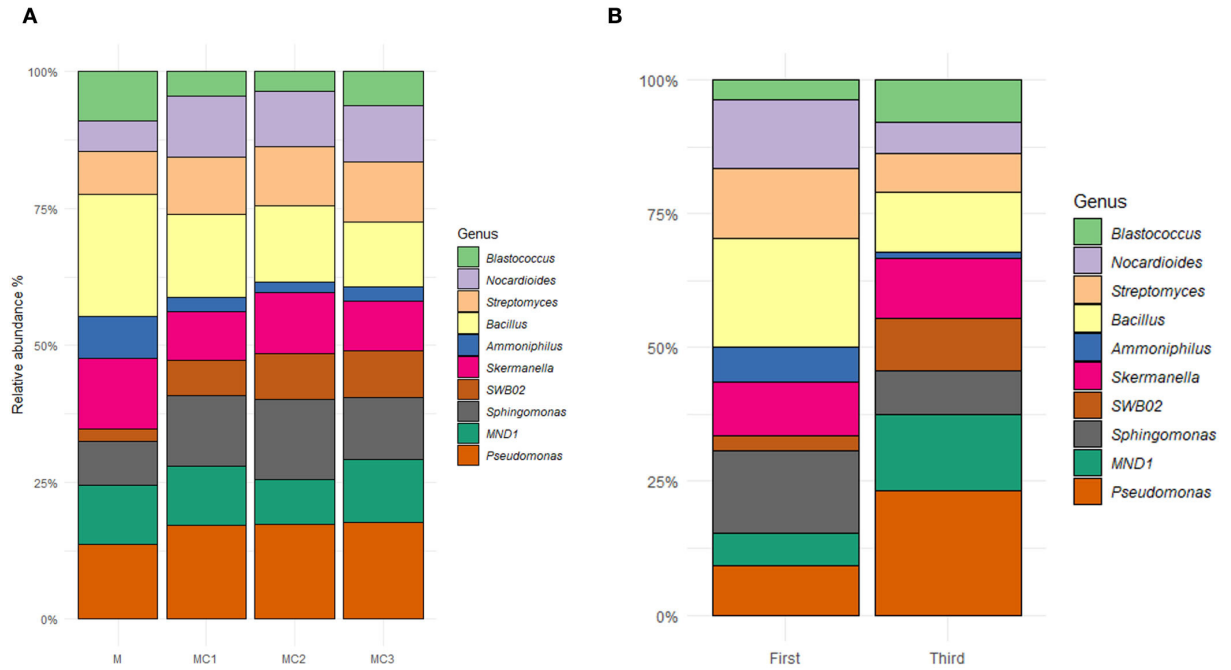

FIGURE 4
Top ten more abundant genera in **(A)** different cropping systems and **(B)** different sampling times. M, melon monocrop; MC1, mixed intercropping; MC2, intercropping row 1:1 melon:cowpea; MC3, intercropping row 2:1 melon:cowpea; Initial, the first year; final, the last year.

Effect of intercropping systems on predictive functional profiling of soil microbial communities

To understand the phylogenetic or taxonomic composition of bacterial communities, it is necessary to study the predictive community functions of 16S rRNA sequencing data. Most pathways did not show the interaction between cropping systems and sampling time except for Citrate Cycle (TCA) (Supplementary Table S4). Bacterial secretion, nitrogen metabolism, energy metabolism, and transporters increased significantly in the third year, whereas the TCA cycle and protein export decreased. In general, all the intercropped systems showed higher values of the different studied pathways compared to monoculture (M) showing the highest values in MC1 and MC2 (Supplementary Table S4).

Functional predicted N-cycling genes

In general, the predicted N-Cycling genes were highly affected by the cropping system, sampling time, and their interaction (Supplementary Table S5). In the third year, potential nitrogen fixation—identified by *nifT* and *nifX* genes—was highest in MC1 and was significantly lower in MC2 and MC3 than in the monocrop (M) (Supplementary Table S5). Dissimilatory nitrogen reduction genes (*narG* and *nirB*) involved in the denitrification process were significantly more abundant in the third year and showed higher values in the intercropping systems, among which MC1 and MC2 showed the highest values (Supplementary Table S5). The abundance of *amoA* and *amoC* genes involved in the nitrification process was higher in the first year than in the third. At the end of the experiment, MC2 showed the highest values. The predicted gene *nosZ* showed higher values in the third year than in the first year For this gene, the intercropping systems had significantly higher values than the monocrop (M) and MC1 and MC2 showed the highest values (Supplementary Table S5).

The NMDS plot of predicted N-Cycling genes showed no observable differences among cropping systems in the first year (Figure 5A). This trend changed in the third year of the experiment, however, when the cropping systems were clearly differentiated (NMDS Stress = 0.039).

Functional predicted C-cycling genes

To evaluate the carbon availability to soil bacteria under different cropping systems, the predicted genes *glcD* (Glycolate oxidase subunit), *xylA*, *alpha-amylase*, *glucokinase*, and *pyruvate kinase* were studied. The results showed that all genes were highly affected by the cropping system, sampling time, and

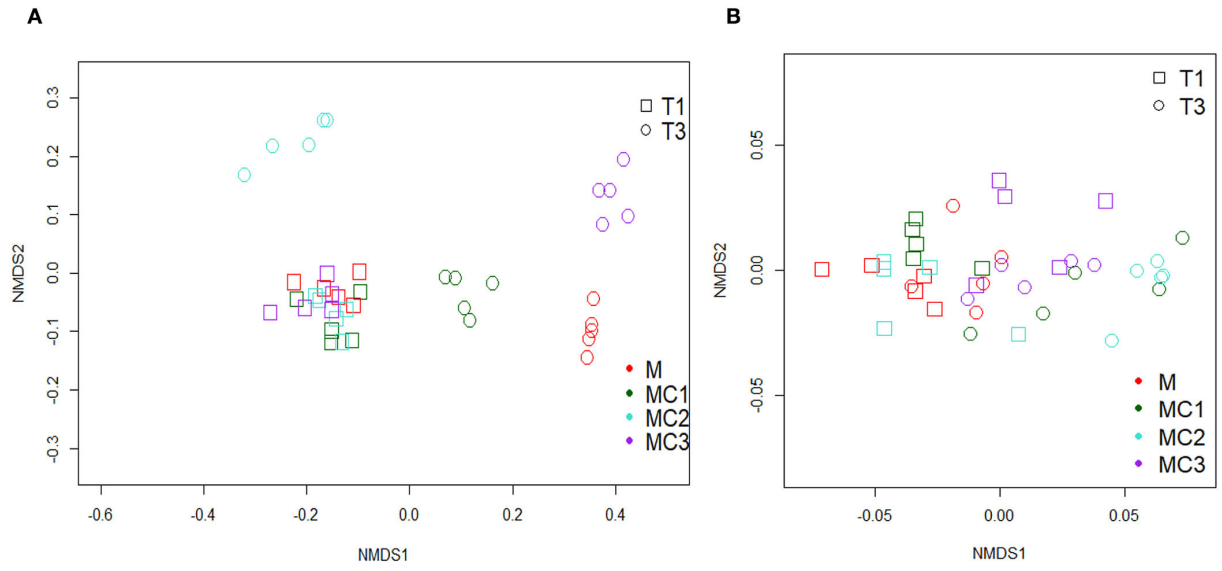

FIGURE 5
A Non-metric Multi-dimensional Scaling (NMDS) of predicted nitrogen cycle genes **(A)** and predicted carbon cycle genes **(B)** M, melon monocrop; MC1, mixed intercropping; MC2, intercropping row 1:1 melon:cowpea; MC3, intercropping row 2:1 melon:cowpea; T1, First year; T3, Third year.

their interaction (Supplementary Table S6). All predictive genes increased in the third year of the experiment compared to the first year (Supplementary Table S6). In the first year, the highest values were found in MC3 followed by MC1 and MC2 compared to Monocrop, while, in the third year the highest values were found in MC1 and MC2 compared to monocrop (M) (Supplementary Table 6). NMDS from C-Cycling predicted genes (Figure 5B) showed that predicted carbon genes clustered together (NMDS Stress = 0.08) in all treatments at different times.

Discussion

Intercropping is an environmentally friendly method that plays an important role in improving soil quality and in controlling pests and disease occurrence (Dai et al., 2019). The degree of improvement depends on the crop species, the intercropping combinations, and their spatial distribution (Raseduzzaman and Jensen, 2017; Ren et al., 2017; Zhang et al., 2018b; Salgado et al., 2021). Studies are scarce, however, concerning melon/cowpea intercropping and patterns Our results revealed that the bacterial communities were altered by the intercropping system and pattern, a fact that is attributed to the root interactions between the different plant species, which subsequently affects root exudation (Broeckling et al., 2008; Lian et al., 2019). This undoubtedly alters the microbial diversity, structure, and functionality (Li and Wu, 2018; Zeng et al., 2019). Bacteria have been linked to C acquisition strategies and their interactions can contribute to soil stabilization through the biopolymers they exuded (Chenu, 1989; Deng et al., 2015) which act as binding agents in which bacteria are causal factors in enhancing soil aggregation (Lehmann et al., 2017). It highlighted the changes in those members contributing to the "rare biosphere" (Pascoal et al., 2021) increasing the sensitivity of detecting effects on microbiomes as having been observed by other studies (Jiao and Lu, 2020a; Ji et al., 2020), where they suggested that abundant taxa play a dominant role in the stability and maintenance of agro-soils whereas rare taxa have a high influence under environmental disturbances (Jiao and Lu, 2020b). In our study, the increase in bacterial diversity (Supplementary Table S1, Figure 2) was due principally to the increase of rare bacterial diversity (oligotrophic and synergistic bacteria) instead of the most abundant (copiotrophics and competitive) bacteria, as was observed by Liu et al. (2022). It is possible that rare bacteria had to perform synergistic activities for extracting energy and carbon from more complex organic substrates during the 3-year experiment. This would enable rare bacteria community members to carry out more elaborated interactions than the abundant bacteria, which get their nutrients and energy from roots, whose exudates would promote competition between fast-growing copiotrophs (Fierer et al., 2012; Liu et al., 2022). Rare taxa could have a more important role in functionality, which can help to crop growth (Chen et al., 2020; Liang et al., 2020; Xiong et al., 2021). The Bacterial diversity of this study could be affected after 3 years of intercropping by the decrease in pH since the acidification can change the stability of bacterial cell membranes and thus inhibits

bacterial growth (Feng et al., 2014; Zarafshar et al., 2020). Beta diversity—which represents the extent of change in community composition, or the degree of community differentiation—showed differences between monocrop (M) and intercropped systems (Figure 3) in whole bacteria and the most abundant taxa However, in the third year, if we focus only on the rare taxa, beta diversity showed differences according to the pattern—MC1 and MC2 grouped separately from MC3 and M. This could indicate that higher plant biomass in MC1 and MC2 induce higher soil organic matter fraction levels, intercropped systems can induce higher soil organic matter fraction contents which could act as major sources of energy for microorganisms (Tian et al., 2013).

The Intercropping systems showed an increase in beneficial microorganisms (*Pseudomonas*, *Sphigomonas*, *Streptomyces*, *Nocardioides,* and *SWB02*) (Supplementary Table S3, Figure 4), as other authors have observed in different intercropping systems (Yu et al., 2019; Zhao et al., 2022) *Sphingomonas* promote nitrogen fixation and dehydrogenation (Leys et al., 2004) and has also been found to increase plant growth hormone production (Asaf et al., 2020). Some species of *Pseudomonas* can enhance nutrient uptake and thus plant growth (Franke-Whittle et al., 2015; Lami et al., 2020) *SWB02*, on the other hand, has been linked to the capacity to oxidize nitrite to nitrate (Fumasoli et al., 2015; Gao et al., 2021), while *Niastella* (Supplementary Figure 4B) can mitigate N_20 emissions (Nishizawa et al., 2014) *Aeromicrobium* (Supplementary Figures 4A,B) has been linked to plant biomass (Nuzzo et al., 2020) and has a greater capability to produce secondary compounds with antimicrobial capacities (Miller et al., 1991). These bacteria were highly correlated with TN, TOC, and pH at both sampling times (Supplementary Figure 2). Cong et al. (2015) observed that the increases in aboveground productivity by enhancing soil C and N should occur due to the microbial species complementarity, as our results showed (Supplementary Figure 2).

Nitrogen is an essential element for plant growth and development, and it is the element most closely related to yield (Zhao et al., 2022). Our results showed significantly higher TN and NH_4^+ (Table 1) in intercropped than in the monocrop (M), even considering that 30% less fertilization was used in the intercropped systems than in the monocrop. An increase in melon yield was observed in intercropping systems at both sampling times. In previous studies, Cuartero et al. (2022) observed higher yield in intercropped systems probably due to low N fertilizer addition (Yu et al., 2018). This fact has previously been observed in other cowpea intercrop relationships, such as cowpea-maize (Latati et al., 2014), cowpea-sorghum (Oseni, 2010), and cowpea-cassava (Sikirou and Wydra, 2008). Also, this finding may be due to the complex biological diversity under intercropping systems that resulted in the transfer of N to soil *via* ions and root exudates and further facilitated the accumulation and decomposition of soil N fractions. In legume-mixed intercropping, legumes increase N_2 fixation, thus providing higher N levels for the adjacent crop, thus yielding a growth advantage for the intercropped plant (Subedi and Ma, 2005; Yu et al., 2018). In addition, the higher plant litter and root exudates by intercropping compared to monoculture may have been responsible for the increase in TOC content (Table 1). Castellano et al. (2015) suggested that plant litter is the primary source of all SOM. No differences were observed between intercropped systems probably due to the use of only one intercrop species because according to Zhang et al. (2021) different intercropped resulted in differences in the N cycle predicted genes, and these differences might be caused by variations in the quantity and quality of plant litter and root exudates among intercrops.

Biological factors, such as microorganisms, could indicate the environmental balance through biotic indexes derived from the observation of taxa. Therefore, in this study, random forest analysis (Supplementary Figure 4) identified specific genera as possible indicators of different intercropping systems, where only 13% of the genera belonged to the most abundant genera in intercropping systems, and the sampling time showed a stronger influence of these biomarkers than the different intercropping patterns.

When a bacterial community structure is altered due to a disturbance (Figure 3), as in this study (intercropping), functional redundancy (an overlap in the ecological functions of various species) is very important for maintaining the functionality of the community (Wohl et al., 2004; Comte and del Giorgio, 2010; Baho et al., 2012) and this fact does not produce a relationship between disturbance and microbial structure. However, our results (Supplementary Table S4) indicated an increase of prediction functional genes principally in MC1 and MC2, such as bacterial secretion system, protein export, transporter, and energy metabolism that could indicate a higher activity of soil bacteria and a higher secretion of protein and agents promoting soil aggregation (Oliveira et al., 2019). Also, an increase in carbon fixation and the TCA cycle and N metabolism could indicate an acceleration of nutrient conversion (Shi et al., 2017). The TCA cycle, also known as the Krebs cycle and citric cycle, is the main source of energy for cells and essential for aerobic respiration to deal with oxidative stress and produce energy for secreting defense compounds (Zhang et al., 2018a).

Six prediction genes (Supplementary Table S5) involved in different steps of the Nitrogen cycle showed, by NMDS (Figure 5A), differences between cropping systems in the third year of the experiment which could indicate that although bacterial abundance and diversity diminished this cycle is not N-limited and each intercropped system have system-specific bottlenecks in the N cycle N_2 fixation gene expression is strongly dependent on the level of mineral N in soil (Li et al., 2016). Intercropping system with cowpea in the third year showed, in general, higher nitrogen fixation genes principally in MC1 with less inorganic fertilization than melon monocrop (M).

Root-derived compounds may induce nodulation *via* hormone signaling and stimulate N_2 fixation by increasing the activities of proteins involved in N_2 fixation at the gene expression and physiological levels (Li et al., 2016). However, more than half of the increased N_2 fixation under intercropping could be also attributed to soil micro-organisms including members of the phyla Actinobacteria (*Arthrobacter* and *Agromyces*), Bacteroidetes, Firmicutes (*Bacillus* and *Psychrobacillus*) and Proteobacteria (Rilling et al., 2018) some of them observed in our intercropping systems. Ammonia, which is considered a regulatory signal of symbiosis in the nodules (Patriarca et al., 2002), could be one of the different ways to carry the nitrogen captured in nodules to the rhizosphere of melon since ammonia can diffuse in soil due to its positive charge then it could be oxidized again by nitrifying bacteria like *SM1A02* or *Sphingomonas* (Xie and Yokota, 2006) or uptake by plants.

Genes involved in the denitrification process were higher than nitrification in all cropping systems. Denitrification is the process of dissimilatory reduction of nitrate and nitrite, producing gaseous end products of nitric oxide (NO), N_2O, and dinitrogen (N_2). The process of denitrification relies on a series of enzymes that were produced when *narG* and *nirB* genes are expressed. They were highly increased in intercropping systems principally MC1 and MC2 indicating higher emission of N_2O from soil (Shaw et al., 2006), probably due to excess inorganic fertilization being incorporated However, the increase of gen *nosZ* could indicate the greater conversion of N_2O–N_2 and decreased greenhouse gas production (Krause et al., 2017). Nitrification is a biochemical process important for soil fertility in which nitrifying bacteria transform the ammonium into nitrates (NO_3) to be used by plants (Kant, 2018), where gen as *amoA* and *amoC* are involved and MC1 and MC2 showed the highest values.

In addition, a higher content of alpha-amylase, xylose, and glycolate oxidase (Supplementary Table S5) abundance potential genes (belonging to carbon and glycolate cycle) related mainly with *Bacillus*, *Caulobacter*, *Streptomyces,* and other decomposers genera (Wijbenga et al., 1991; Stephens et al., 2007; Gubbens et al., 2017; Luang-In et al., 2019; Ibrahim et al., 2021) could help to increase the availability of nutrients for plants Fernández-Bayo et al. (2019) showed that organic exudates from the rhizosphere can increase these C degrading pathways. According to these results, intercropping systems MC1 and MC2 have a greater diversity of energy and carbon sources so cowpea could lead to a more complex and capable microbial community than traditional monoculture, as it was pointed out by Li et al. (2022). Carbon fixation was also enhanced (Supplementary Table S4) in soils with higher cowpea plants density which is commonly incorporated into soils through microorganisms (Berg et al., 2010) and is one of the most important steps in the carbon cycle, a crucial step for CO_2 assimilation and sequestration and it has been previously related with soils with high bacteria diversity (Lynn et al., 2017).

Conclusion

The study of beta diversity using the rare taxa instead of the whole taxa was able to show differences between intercropped patterns (MC1 and MC2 compared to MC3). Intercropping systems showed higher value content of total organic carbon (TOC), total nitrogen (TN), melon yield, and bacterial diversity as well as a higher content of beneficial soil microorganisms such as *Pseudomonas*, *Aeromicrobium*, *Niastella* or *Sphingomonas* which can promote plant growth and its protection against different pathogens. Predictive N and C cycling genes showed higher abundance in the intercropped system than in monocrop, and also showed differences between intercropped systems, where MC1 and MC2 showed higher abundance than MC3.

Data availability statement

The datasets presented in this study can be found in online repositories. The names of the repository/repositories and accession number(s) can be found in the article/Supplementary material.

Author contributions

Conceptualization: JC, VS-N, RZ, JW, JP, J-MV, MM-M, EG, and MR. Methodology: JC, OÖ, VS-N, JW, RZ, JP, J-MV, EG, MM-M, and MR. Validation: RZ, JP, and MR. Formal analysis and data curation: JC and J-MV. Investigation and resources: JC, OÖ, VS-N, JW, RZ, JP, J-MV, and MR. Writing—original draft preparation: JC. Writing—review and editing and supervision: JP, J-MV, and MR. Visualization: JC and J-MV. Project administration and funding acquisition: JP and MR. All authors have read and agreed to the published version of the manuscript.

Funding

This study was supported by the AsociaHortus project [AGL2017-83975-R] funded by the Spanish Ministry of Science, Innovation and Universities, and the European Commission Horizon 2020 project Diverfarming [Grant agreement 728003].

Acknowledgments

RZ acknowledges the financial support received from the Spanish Ministry of Science, Innovation and Universities through the Ramón y Cajal Program [RYC-2015-18758]. Thanks to Ansley Evans for the English editing.

Conflict of interest

The authors declare that the research was conducted in the absence of any commercial or financial relationships that could be construed as a potential conflict of interest.

Publisher's note

All claims expressed in this article are solely those of the authors and do not necessarily represent those of their affiliated organizations, or those of the publisher, the editors and the reviewers. Any product that may be evaluated in this article, or claim that may be made by its manufacturer, is not guaranteed or endorsed by the publisher.

Supplementary material

The Supplementary Material for this article can be found online at: https://www.frontiersin.org/articles/10.3389/fmicb.2022.1004593/full#supplementary-material

References

Asaf, S., Numan, M., Khan, A. L., and Al-Harrasi, A. (2020). Sphingomonas: from diversity and genomics to functional role in environmental remediation and plant growth. *Crit. Rev. Biotechnol.* 40, 138–152. doi: 10.1080/07388551.2019.1709793

Baho, D. L., Peter, H., and Tranvik, L. J. (2012). Resistance and resilience of microbial communities–temporal and spatial insurance against perturbations. *Environ. Microbiol.* 14, 2283–2292. doi: 10.1111/j.1462-2920.2012.02754.x

Berg, I. A., Kockelkorn, D., Ramos-Vera, W. H., Say, R. F., Zarzycki, J., Hügler, M., et al. (2010). Autotrophic carbon fixation in archaea. *Nat. Rev. Microbiol.* 8, 447–460. doi: 10.1038/nrmicro2365

Bolyen, E., Rideout, J. R., Dillon, M. R., Bokulich, N. A., Abnet, C., Al-Ghalith, G. A., et al. (2019). Reproducible, interactive, scalable, and extensible microbiome data science using QIIME2. *Nat. Biotech*. 37, 852–857. doi: 10.1038/s41587-019-0209-9

Bragg, L., Stone, G., Imelfort, M., Hugenholtz, P., and Tyson, G. W. (2012). Fast, accurate error-correction of amplicon pyrosequences using Acacia. *Nat. Methods* 9, 425–426. doi: 10.1038/nmeth.1990

Broeckling, C. D., Broz, A. K., Bergelson, J., Manter, D. K., and Vivanco, J. M. (2008). Root exudates regulate soil fungal community composition and diversity. *Appl. Environ. Microbiol.* 74, 738–744. doi: 10.1128/AEM.02188-07

Callahan, B. J., McMurdie, P. J., Rosen, M. J., Han, A. W., Johnson, A. J. A., and Holmes, S. P. (2016). DADA2: high-resolution sample inference from Illumina amplicon data. *Nat. Methods.* 13, 581–583. doi: 10.1038/nmeth.3869

Castellano, M. J., Mueller, K. E., Olk, D. C., Sawyer, J. E., and Six, J. (2015). Integrating plant litter quality, soil organic matter stabilization, and the carbon saturation concept. *Glob. Chang. Biol.* 21, 3200–3209. doi: 10.1111/gcb.12982

Chen, G., Kong, X., Gan, Y., Zhang, R., Feng, F., Yu, A., et al. (2018). Enhancing the systems productivity and water use efficiency through coordinated soil water sharing and compensation in strip-intercropping. *Sci. Rep.* 8, 1–11. doi: 10.1038/s41598-018-28612-6

Chen, Q.-L., Ding, J., Zhu, D., Hu, H.-W., Delgado-Baquerizo, M., Ma, Y.-B., et al. (2020). Rare microbial taxa as the major drivers of ecosystem multifunctionality in long-term fertilized soils. *Soil. Biol. Biochem.* 141, 107686. doi: 10.1016/j.soilbio.2019.107686

Chenu, C. (1989). Influence of a fungal polysaccharide, scleroglucan, on clay microstructures. *Soil. Biol. Biochem.* 21, 299–305. doi: 10.1016/0038-0717(89)90108-9

Comte, J., and del Giorgio, P. A. (2010). Linking the patterns of change in composition and function in bacterioplankton successions along environmental gradients. *Ecology* 91, 1466–1476. doi: 10.1890/09-0848.1

Cong, W., Hoffland, E., Li, L., Six, J., Sun, J., Bao, X., et al. (2015). Intercropping enhances soil carbon and nitrogen. *Glob. Chang. Biol.* 21, 1715–1726. doi: 10.1111/gcb.12738

Cuartero, J., Pascual, J. A., Vivo, J.-M., Özbolat, O., Sánchez-Navarro, V., Egea-Cortines, M., et al. (2022). A first-year melon/cowpea intercropping system improves soil nutrients and changes the soil microbial community. *Agric. Ecosyst. Environ.* 328, 107856. doi: 10.1016/j.agee.2022.107856

Dai, J., Qiu, W., Wang, N., Wang, T., Nakanishi, H., and Zuo, Y. (2019). From Leguminosae/Gramineae intercropping systems to see benefits of intercropping on iron nutrition. *Front. Plant Sci.* 10, 605. doi: 10.3389/fpls.2019.00605

Dai, Z., Su, W., Chen, H., Barberán, A., Zhao, H., Yu, M., et al. (2018). Long-term nitrogen fertilization decreases bacterial diversity and favors the growth of Actinobacteria and Proteobacteria in agro-ecosystems across the globe. *Glob. Chang. Biol.* 24, 3452–3461. doi: 10.1111/gcb.14163

Delgado-Baquerizo, M., Oliverio, A. M., Brewer, T. E., Benavent-González, A., Eldridge, D. J., Bardgett, R. D., et al. (2018). A global atlas of the dominant bacteria found in soil. *Science* 359, 320–325. doi: 10.1126/science.aap9516

Deng, J., Orner, E. P., Chau, J. F., Anderson, E. M., Kadilak, A. L., Rubinstein, R. L., et al. (2015). Synergistic effects of soil microstructure and bacterial EPS on drying rate in emulated soil micromodels. *Soil. Biol. Biochem.* 83, 116–124. doi: 10.1016/j.soilbio.2014.12.006

Dong, K., Sun, R., and Dong, X. (2018). CO_2 emissions, natural gas and renewables, economic growth: assessing the evidence from China. *Sci. Total Environ.* 640, 293–302. doi: 10.1016/j.scitotenv.2018.05.322

Douglas, G. M., Maffei, V. J., Zaneveld, J. R., Yurgel, S. N., Brown, J. R., Taylor, C. M., et al. (2020). PICRUSt2 for prediction of metagenome functions. *Nat. Biotechnol.* 38, 685–688. doi: 10.1038/s41587-020-0548-6

Dwivedi, A., Dev, I., Kumar, V., Yadav, R. S., Yadav, M., Gupta, D., et al. (2015). Potential role of maize-legume intercropping systems to improve soil fertility status under smallholder farming systems for sustainable agriculture in India. *Int. J. Life Sci. Biotechnol. Pharm. Res.* 4, 145.

Feng, Y., Grogan, P., Caporaso, J. G., Zhang, H., Lin, X., Knight, R., et al. (2014). pH is a good predictor of the distribution of anoxygenic purple phototrophic bacteria in Arctic soils. *Soil. Biol. Biochem.* 74, 193–200. doi: 10.1016/j.soilbio.2014.03.014

Fernández-Bayo, J. D., Hestmark, K. V., Claypool, J. T., Harrold, D. R., Randall, T. E., Achmon, Y., et al. (2019). The initial soil microbiota impacts the potential for lignocellulose degradation during soil solarization. *J. Appl. Microbiol.* 126, 1729–1741. doi: 10.1111/jam.14258

Fierer, N., Lauber, C. L., Ramirez, K. S., Zaneveld, J., Bradford, M. A., and Knight, R. (2012). Comparative metagenomic, phylogenetic and physiological analyses of soil microbial communities across nitrogen gradients. *ISME J.* 6, 1007–1017. doi: 10.1038/ismej.2011.159

Fox, J., Friendly, G. G., Graves, S., Heiberger, R., Monette, G., Nilsson, H., et al. (2007). *The Car Package*. Vienna: R Foundation for Statistical computing.

Franke, A. C., van den Brand, G. J., Vanlauwe, B., and Giller, K. E. (2018). Sustainable intensification through rotations with grain legumes in Sub-Saharan Africa: a review. *Agric. Ecosyst. Environ.* 261, 172–185. doi: 10.1016/j.agee.2017.09.029

Franke-Whittle, I. H., Manici, L. M., Insam, H., and Stres, B. (2015). Rhizosphere bacteria and fungi associated with plant growth in soils of three replanted apple orchards. *Plant Soil.* 395, 317–333. doi: 10.1007/s11104-015-2562-x

Fuhrman, J. A. (2009). Microbial community structure and its functional implications. *Nature* 459, 193–199. doi: 10.1038/nature08058

Fumasoli, A., Morgenroth, E., and Udert, K. M. (2015). Modeling the low pH limit of *Nitrosomonas eutropha* in high-strength nitrogen wastewaters. *Water Res.* 83, 161–170. doi: 10.1016/j.watres.2015.06.013

Gao, J., Duan, C., Huang, X., Yu, J., Cao, Z., and Zhu, J. (2021). The Tolerance of Anoxic-Oxic (A/O) Process for the Changing of Refractory

Organics in Electroplating Wastewater: Performance, Optimization and Microbial Characteristics. *Processes* 9, 962. doi: 10.3390/pr9060962

Gedamu, M. T. (2020). Soil degradation and its management options in Ethiopia: a review. *Int. J. Res. Innov. Earth Sci.* 7, 59–76.

Gómez-Rubio, V. (2017). ggplot2-elegant graphics for data analysis. *J. Stat. Softw.* 77, 1–3. doi: 10.18637/jss.v077.b02

Gubbens, J., Janus, M. M., Florea, B. I., Overkleeft, H. S., and van Wezel, G. P. (2017). Identification of glucose kinase-dependent and-independent pathways for carbon control of primary metabolism, development and antibiotic production in Streptomyces coelicolor by quantitative proteomics. *Mol. Microbiol.* 105, 175. doi: 10.1111/mmi.13714

Ibrahim, A. M., Hamouda, R. A., El-Naggar, N. E.-A., and Al-Shakankery, F. M. (2021). Bioprocess development for enhanced endoglucanase production by newly isolated bacteria, purification, characterization and *in vitro* efficacy as anti-biofilm of *Pseudomonas aeruginosa*. *Sci. Rep.* 11, 1–24. doi: 10.1038/s41598-021-87901-9

IUSS Working Group WRB (2015). *World Reference Base for Soil Resources 2014 (Update 2015), International Soil Classification System for Naming Soils and Creating Legends for Soil Maps*. World Soil Resources Reports, FAO, Rome.

Ji, X., Wang, Y., and Lee, P.-H. (2020). Evolution of microbial dynamics with the introduction of real seawater portions in a low-strength feeding anammox process. *Appl. Microbiol. Biotechnol.* 104, 5593–5604. doi: 10.1007/s00253-020-10598-9

Jiao, S., and Lu, Y. (2020a). Abundant fungi adapt to broader environmental gradients than rare fungi in agricultural fields. *Glob. Chang. Biol.* 26, 4506–4520. doi: 10.1111/gcb.15130

Jiao, S., and Lu, Y. (2020b). Soil pH and temperature regulate assembly processes of abundant and rare bacterial communities in agricultural ecosystems. *Environ. Microbiol.* 22, 1052–1065. doi: 10.1111/1462-2920.14815

Kant, S. (2018). Understanding nitrate uptake, signaling and remobilisation for improving plant nitrogen use efficiency. *Semin. Cell Dev. Biol.* 74, 89–96. doi: 10.1016/j.semcdb.2017.08.034

Kopittke, P. M., Menzies, N. W., Wang, P., McKenna, B. A., and Lombi, E. (2019). Soil and the intensification of agriculture for global food security. *Environ. Int.* 132, 105078. doi: 10.1016/j.envint.2019.105078

Krause, H.-M., Thonar, C., Eschenbach, W., Well, R., Mäder, P., Behrens, S., et al. (2017). Long term farming systems affect soils potential for N_2O production and reduction processes under denitrifying conditions. *Soil. Biol. Biochem.* 114, 31–41. doi: 10.1016/j.soilbio.2017.06.025

Kuhn, M., Wing, J., Weston, S., Williams, A., Keefer, C., Engelhardt, A., et al. (2020). *caret: Classification and Regression Training. R Package Version 6.0–86*. Cambridge, MA: Astrophysics Source Code Library.

Lal, R. (2015). Restoring soil quality to mitigate soil degradation. *Sustainability* 7, 5875–5895. doi: 10.3390/su7055875

Lami, M. J., Adler, C., Caram-Di Santo, M. C., Zenoff, A. M., de Cristóbal, R. E., Espinosa-Urgel, M., et al. (2020). Pseudomonas stutzeri MJL19, a rhizosphere-colonizing bacterium that promotes plant growth under saline stress. *J. Appl. Microbiol.* 129, 1321–1336. doi: 10.1111/jam.14692

Latati, M., Blavet, D., Alkama, N., Laoufi, H., Drevon, J.-J., Gerard, F., et al. (2014). The intercropping cowpea-maize improves soil phosphorus availability and maize yields in an alkaline soil. *Plant Soil.* 385, 181–191. doi: 10.1007/s11104-014-2214-6

Lehmann, A., Zheng, W., and Rillig, M. C. (2017). Soil biota contributions to soil aggregation. *Nat. Ecol. Evol.* 1, 1828–1835. doi: 10.1038/s41559-017-0344-y

Leys, N. M. E. J., Ryngaert, A., Bastiaens, L., Verstraete, W., Top, E. M., and Springael, D. (2004). Occurrence and phylogenetic diversity of Sphingomonas strains in soils contaminated with polycyclic aromatic hydrocarbons. *Appl. Environ. Microbiol.* 70, 1944–1955. doi: 10.1128/AEM.70.4.1944-1955.2004

Li, B., Li, Y.-Y., Wu, H.-M., Zhang, F.-F., Li, C.-J., Li, X.-X., et al. (2016). Root exudates drive interspecific facilitation by enhancing nodulation and N-2 fixation. *Proc. Natl. Acad. Sci. USA* 113, 6496. doi: 10.1073/pnas.1523580113

Li, K., Shiraiwa, T., Inamura, T., Saitoh, K., and Horie, T. (2001). Recovery of 15N-labeled ammonium by barley and maize grown on the soils with long-term application of chemical and organic fertilizers. *Plant Prod. Sci.* 4, 29–35. doi: 10.1626/pps.4.29

Li, S., and Wu, F. (2018). Diversity and co-occurrence patterns of soil bacterial and fungal communities in seven intercropping systems. *Front. Microbiol.* 9, 1521. doi: 10.3389/fmicb.2018.01521

Li, Y., Han, C., Dong, X., Sun, S., and Zhao, C. (2022). Soil microbial communities of dryland legume plantations are more complex than non-legumes. *Sci. Total Environ.* 822, 153560. doi: 10.1016/j.scitotenv.2022.153560

Lian, T., Mu, Y., Jin, J., Ma, Q., Cheng, Y., Cai, Z., et al. (2019). Impact of intercropping on the coupling between soil microbial community structure, activity, and nutrient-use efficiencies. *PeerJ.* 7, e6412. doi: 10.7717/peerj.6412

Liang, Y., Xiao, X., Nuccio, E. E., Yuan, M., Zhang, N., Xue, K., et al. (2020). Differentiation strategies of soil rare and abundant microbial taxa in response to changing climatic regimes. *Environ. Microbiol.* 22, 1327–1340. doi: 10.1111/1462-2920.14945

Liaw, A., and Wiener, M. (2002). Classification and regression by randomForest. *R News* 2, 18–22.

Liu, B., Arlotti, D., Huyghebaert, B., and Tebbe, C. C. (2022). Disentangling the impact of contrasting agricultural management practices on soil microbial communities–Importance of rare bacterial community members. *Soil. Biol. Biochem.* 166, 108573. doi: 10.1016/j.soilbio.2022.108573

Luang-In, V., Yotchaisarn, M., Saengha, W., Udomwong, P., Deeseenthum, S., and Maneewan, K. (2019). Isolation and identification of amylase-producing bacteria from soil in Nasinuan Community Forest, Maha Sarakham, Thailand. *Biomed. Pharmacol. J.* 12, 1061–1068. doi: 10.13005/bpj/1735

Lynn, T. M., Ge, T., Yuan, H., Wei, X., Wu, X., Xiao, K., et al. (2017). Soil carbon-fixation rates and associated bacterial diversity and abundance in three natural ecosystems. *Microb. Ecol.* 73, 645–657. doi: 10.1007/s00248-016-0890-x

Miller, E. S., Woese, C. R., and Brenner, S. (1991). Description of the erythromycin-producing bacterium Arthrobacter sp. strain NRRL B-3381 as Aeromicrobium erythreum gen. nov., sp. nov. *Int. J. Syst. Evol. Microbiol.* 41, 363–368. doi: 10.1099/00207713-41-3-363

Mooshammer, M., Wanek, W., Hämmerle, I., Fuchslueger, L., Hofhansl, F., Knoltsch, A., et al. (2014). Adjustment of microbial nitrogen use efficiency to carbon: nitrogen imbalances regulates soil nitrogen cycling. *Nat. Commun.* 5, 1–7. doi: 10.1038/ncomms4694

Namatsheve, T., Chikowo, R., Corbeels, M., Mouquet-Rivier, C., Icard-Vernière, C., and Cardinael, R. (2021). Maize-cowpea intercropping as an ecological intensification option for low input systems in sub-humid Zimbabwe: Productivity, biological N2-fixation and grain mineral content. *Field. Crops Res.* 263, 108052. doi: 10.1016/j.fcr.2020.108052

Nishizawa, T., Quan, A., Kai, A., Tago, K., Ishii, S., Shen, W., et al. (2014). Inoculation with N 2-generating denitrifier strains mitigates N 2 O emission from agricultural soil fertilized with poultry manure. *Biol. Fertil. Soils* 50, 1001–1007. doi: 10.1007/s00374-014-0918-7

Noguchi, K., Gel, Y. R., Brunner, E., and Konietschke, F. (2012). nparLD: an R software package for the nonparametric analysis of longitudinal data in factorial experiments. *J. Stat. Softw.* 50, 1–23. doi: 10.18637/jss.v050.i12

Nuzzo, A., Satpute, A., Albrecht, U., and Strauss, S. L. (2020). Impact of soil microbial amendments on tomato rhizosphere microbiome and plant growth in field soil. *Microb. Ecol.* 80, 398–409. doi: 10.1007/s00248-020-01497-7

OEC (2019). *Melons*. Available online at: https://oec.world/en/profile/hs92/melons (accessed February 11, 2022).

Ogle, D., and Ogle, M. D. (2017). Package "FSA." *CRAN Repos*, 1–206 (accessed Jun 5, 2022).

Oksanen, J., Blanchet, F. G., Friendly, M., Kindt, R., Legendre, P., McGlinn, D., et al. (2020). *vegan: Community Ecology Package. R package version 2.5-7*. Available online at: https://CRAN.R-project.org/package=vegan (accessed May 1, 2022).

Oliveira, M., Barre, P., Trindade, H., and Virto, I. (2019). Different efficiencies of grain legumes in crop rotations to improve soil aggregation and organic carbon in the short-term in a sandy Cambisol. *Soil Tillage Res.* 186, 23–35. doi: 10.1016/j.still.2018.10.003

Oseni, T. O. (2010). Evaluation of sorghum-cowpea intercrop productivity in savanna agro-ecology using competition indices. *J. Agric. Sci.* 2, 229. doi: 10.5539/jas.v2n3p229

Padhi, A. K., and Panigrahi, R. K. (2006). Effect of intercrop and crop geometry on productivity, economics, energetics and soil-fertility status of maize (Zea mays)-based intercropping systems. *Indian J. Agron.* 51, 174–177. Available online at: https://www.indianjournals.com/ijor.aspx?target=ijor:ija&volume=51&issue=3&article=005

Pascoal, F., Costa, R., and Magalhães, C. (2021). The microbial rare biosphere: current concepts, methods and ecological principles. *FEMS Microbiol. Ecol.* 97, fiaa227. doi: 10.1093/femsec/fiaa227

Patriarca, E. J., Tatè, R., and Iaccarino, M. (2002). Key role of bacterial NH4+ metabolism in Rhizobium-plant symbiosis. *Microbiol. Mol. Biol. Rev.* 66, 203–222. doi: 10.1128/MMBR.66.2.203-222.2002

Quast, C., Pruesse, E., Yilmaz, P., Gerken, J., Schweer, T., Yarza, P., et al. (2012). The SILVA ribosomal RNA gene database project: improved data processing and web-based tools. *Nucleic. Acids Res.* 41, D590–D596. doi: 10.1093/nar/gks1219

R Core Team (2020). *R: A Language and Environment for Statistical Computing*. Vienna.

Raseduzzaman, M. D., and Jensen, E. S. (2017). Does intercropping enhance yield stability in arable crop production? A meta-analysis. *Eur. J. Agron.* 91, 25–33. doi: 10.1016/j.eja.2017.09.009

Rashid, M. I., Mujawar, L. H., Shahzad, T., Almeelbi, T., Ismail, I. M. I., and Oves, M. (2016). Bacteria and fungi can contribute to nutrients bioavailability and aggregate formation in degraded soils. *Microbiol. Res.* 183, 26–41. doi: 10.1016/j.micres.2015.11.007

Raza, A., Razzaq, A., Mehmood, S. S., Zou, X., Zhang, X., Lv, Y., et al. (2019). Impact of climate change on crops adaptation and strategies to tackle its outcome: a review. *Plants* 8, 34. doi: 10.3390/plants8020034

Ren, Y. Y., Wang, X. L., Zhang, S. Q., Palta, J. A., and Chen, Y. L. (2017). Influence of spatial arrangement in maize-soybean intercropping on root growth and water use efficiency. *Plant Soil* 415, 131–144. doi: 10.1007/s11104-016-3143-3

Rilling, J. I., Acuña, J. J., Sadowsky, M. J., and Jorquera, M. A. (2018). Putative nitrogen-fixing bacteria associated with the rhizosphere and root endosphere of wheat plants grown in an andisol from southern Chile. *Front. Microbiol.* 9, 2710. doi: 10.3389/fmicb.2018.02710

Ritchie, H., and Roser, M. (2017). *Micronutrient Deficiency. Our World in Data*. Available online at: https://ourworldindata.org/micronutrient-deficiency?utm_medium=syndication (accessed April 8, 2022).

Salgado, G. C., Ambrosano, E. J., Rossi, F., Otsuk, I. P., Ambrosao, G. M. B., Patri, P., et al. (2021). Yield and nutrient concentrations of organic cherry tomatoes and legumes grown in intercropping systems in rotation with maize. *Biol. Agric. Hortic.* 38, 1–19. doi: 10.1080/01448765.2021.1992796

Shaw, L. J., Nicol, G. W., Smith, Z., Fear, J., Prosser, J. I., and Baggs, E. M. (2006). *Nitrosospira* spp. can produce nitrous oxide *via* a nitrifier denitrification pathway. *Environ. Microbiol.* 8, 214–222. doi: 10.1111/j.1462-2920.2005.00882.x

Shi, L., Huang, Y., Zhang, M., Yu, Y., Lu, Y., and Kong, F. (2017). Bacterial community dynamics and functional variation during the long-term decomposition of cyanobacterial blooms *in vitro*. *Sci. Total Environ.* 598, 77–86. doi: 10.1016/j.scitotenv.2017.04.115

Sikirou, R., and Wydra, K. (2008). Effect of intercropping cowpea with maize or cassava on cowpea bacterial blight and yield. *J. Plant Dis. Prot.* 115, 145–151. doi: 10.1007/BF03356262

Stephens, C., Christen, B., Watanabe, K., Fuchs, T., and Jenal, U. (2007). Regulation of D-xylose metabolism in *Caulobacter crescentus* by a LacI-type repressor. *J. Bacteriol.* 189, 8828–8834. doi: 10.1128/JB.01342-07

Subedi, K. D., and Ma, B. L. (2005). Nitrogen uptake and partitioning in stay-green and leafy maize hybrids. *Crop. Sci.* 45, 740–747. doi: 10.2135/cropsci2005.0740

Tetteh, R. N. (2015). Chemical soil degradation as a result of contamination: a review. *J. Soil. Sci. Environ. Manag.* 6, 301–308. doi: 10.5897/JSSEM15.0499

Tian, Y., Cao, F., and Wang, G. (2013). Soil microbiological properties and enzyme activity in Ginkgo–tea agroforestry compared with monoculture. *Agrofor. Syst.* 87, 1201–1210. doi: 10.1007/s10457-013-9630-0

Wang, Y., Cheng, S., Fang, H., Yu, G., Xu, X., Xu, M., et al. (2015). Contrasting effects of ammonium and nitrate inputs on soil CO2 emission in a subtropical coniferous plantation of southern China. *Biol. Fertil. Soils* 51, 815–825. doi: 10.1007/s00374-015-1028-x

Wijbenga, D.-J., Beldman, G., Veen, A., and Binnema, D. J. (1991). Production of native-starch-degrading enzymes by a *Bacillus firmus*/lentus strain. *Appl. Microbiol. Biotechnol.* 35, 180–184. doi: 10.1007/BF00184683

Wohl, D. L., Arora, S., and Gladstone, J. R. (2004). Functional redundancy supports biodiversity and ecosystem function in a closed and constant environment. *Ecology* 85, 1534–1540. doi: 10.1890/03-3050

Xianhai, Z., Mingdao, C., and Weifu, L. (2012). Improving planting pattern for intercropping in the whole production span of rubber tree. *Afr. J. Biotechnol.* 11, 8484–8490. doi: 10.5897/AJB11.3811

Xie, C.-H., and Yokota, A. (2006). Sphingomonas azotifigens sp. nov., a nitrogen-fixing bacterium isolated from the roots of *Oryza sativa*. *Int. J. Syst. Evol. Microbiol.* 56, 889–893. doi: 10.1099/ijs.0.64056-0

Xiong, C., He, J., Singh, B. K., Zhu, Y., Wang, J., Li, P., et al. (2021). Rare taxa maintain the stability of crop mycobiomes and ecosystem functions. *Environ. Microbiol.* 23, 1907–1924. doi: 10.1111/1462-2920.15262

Xue, Y., Xia, H., Christie, P., Zhang, Z., Li, L., and Tang, C. (2016). Crop acquisition of phosphorus, iron and zinc from soil in cereal/legume intercropping systems: a critical review. *Ann. Bot.* 117, 363–377. doi: 10.1093/aob/mcv182

Yu, D., Zhang, Q., de Jaegher, B., Liu, J., Sui, Q., Zheng, X., et al. (2021). Effect of proton pump inhibitor on microbial community, function, and kinetics in anaerobic digestion with ammonia stress. *Bioresour. Technol.* 319, 124118. doi: 10.1016/j.biortech.2020.124118

Yu, H., Chen, S., Zhang, X., Zhou, X., and Wu, F. (2019). Rhizosphere bacterial community in watermelon-wheat intercropping was more stable than in watermelon monoculture system under Fusarium oxysporum f. *sp. niveum invasion. Plant Soil* 445, 369–381. doi: 10.1007/s11104-019-04321-5

Yu, Z., Liu, J., Li, Y., Jin, J., Liu, X., and Wang, G. (2018). Impact of land use, fertilization and seasonal variation on the abundance and diversity of nirS-type denitrifying bacterial communities in a Mollisol in Northeast China. *Eur. J. Soil Biol.* 85, 4–11. doi: 10.1016/j.ejsobi.2017.12.001

Zarafshar, M., Bazot, S., Matinizadeh, M., Bordbar, S. K., Rousta, M. J., Kooch, Y., et al. (2020). Do tree plantations or cultivated fields have the same ability to maintain soil quality as natural forests? *Appl. Soil Ecol.* 151, 103536. doi: 10.1016/j.apsoil.2020.103536

Zeng, P., Guo, Z., Xiao, X., and Peng, C. (2019). Dynamic response of enzymatic activity and microbial community structure in metal (loid)-contaminated soil with tree-herb intercropping. *Geoderma* 345, 5–16. doi: 10.1016/j.geoderma.2019.03.013

Zhang, H., Du, W., Peralta-Videa, J. R., Gardea-Torresdey, J. L., White, J. C., Keller, A., et al. (2018a). Metabolomics reveals how cucumber (Cucumis sativus) reprograms metabolites to cope with silver ions and silver nanoparticle-induced oxidative stress. *Environ. Sci. Technol.* 52, 8016–8026. doi: 10.1021/acs.est.8b02440

Zhang, J., Liu, Y.-X., Zhang, N., Hu, B., Jin, T., Xu, H., et al. (2019). NRT1. 1B is associated with root microbiota composition and nitrogen use in field-grown rice. *Nat. Biotechnol.* 37, 676–684. doi: 10.1038/s41587-019-0104-4

Zhang, Y., Han, M., Song, M., Tian, J., Song, B., Hu, Y., et al. (2021). Intercropping with aromatic plants increased the soil organic matter content and changed the microbial community in a pear orchard. *Front. Microbiol.* 12, 241. doi: 10.3389/fmicb.2021.616932

Zhang, Y., Li, X., Gregorich, E. G., McLaughlin, N. B., Zhang, X., Guo, Y., et al. (2018b). No-tillage with continuous maize cropping enhances soil aggregation and organic carbon storage in Northeast China. *Geoderma* 330, 204–211. doi: 10.1016/j.geoderma.2018.05.037

Zhao, X., Dong, Q., Han, Y., Zhang, K., Shi, X., Yang, X., et al. (2022). Maize/peanut intercropping improves nutrient uptake of side-row maize and system microbial community diversity. *BMC Microbiol.* 22, 1–16. doi: 10.1186/s12866-021-02425-6

Zhou, X., and Wu, F. (2021). Land-use conversion from open field to greenhouse cultivation differently affected the diversities and assembly processes of soil abundant and rare fungal communities. *Sci. Total Environ.* 788, 147751. doi: 10.1016/j.scitotenv.2021.147751

Zhou, Z., Wang, C., and Luo, Y. (2018). Effects of forest degradation on microbial communities and soil carbon cycling: a global meta-analysis. *Glob. Ecol. Biogeogr.* 27, 110–124. doi: 10.1111/geb.12663

Zuo, Y., and Zhang, F. (2009). Iron and zinc biofortification strategies in dicot plants by intercropping with gramineous species. A review. *Agron. Sustain. Dev.* 29, 63–71. doi: 10.1051/agro:2008055

frontiers | Frontiers in Microbiology

TYPE Original Research
PUBLISHED 11 November 2022
DOI 10.3389/fmicb.2022.1035561

OPEN ACCESS

EDITED BY
Rasheed Adeleke,
North-West University, South Africa

REVIEWED BY
Marina Basaglia,
University of Padua, Italy
Obinna Tobechukwu Ezeokoli,
University of the Free State,
South Africa

*CORRESPONDENCE
Edoardo Puglisi
edoardo.puglisi@unicatt.it

SPECIALTY SECTION
This article was submitted to Terrestrial Microbiology, a section of the journal Frontiers in Microbiology

RECEIVED 02 September 2022
ACCEPTED 17 October 2022
PUBLISHED 11 November 2022

CITATION
Bandini F, Vaccari F, Soldano M, Piccinini S, Misci C, Bellotti G, Taskin E, Cocconcelli PS and Puglisi E (2022) Rigid bioplastics shape the microbial communities involved in the treatment of the organic fraction of municipal solid waste. *Front. Microbiol.* 13:1035561. doi: 10.3389/fmicb.2022.1035561

Rigid bioplastics shape the microbial communities involved in the treatment of the organic fraction of municipal solid waste

Francesca Bandini[1], Filippo Vaccari[1], Mariangela Soldano[2], Sergio Piccinini[2], Chiara Misci[1], Gabriele Bellotti[1], Eren Taskin[1], Pier Sandro Cocconcelli[1] and Edoardo Puglisi[1]*

[1]Department for Sustainable Food Process, Università Cattolica del Sacro Cuore, Piacenza, PC, Italy, [2]Centro Ricerche Produzioni Animali S.p.A. (CRPA), Reggio Emilia, RE, Italy

While bioplastics are gaining wide interest in replacing conventional plastics, it is necessary to understand whether the treatment of the organic fraction of municipal solid waste (OFMSW) as an end-of-life option is compatible with their biodegradation and their possible role in shaping the microbial communities involved in the processes. In the present work, we assessed the microbiological impact of rigid polylactic acid (PLA) and starch-based bioplastics (SBB) spoons on the thermophilic anaerobic digestion and the aerobic composting of OFMSW under real plant conditions. In order to thoroughly evaluate the effect of PLA and SBB on the bacterial, archaeal, and fungal communities during the process, high-throughput sequencing (HTS) technology was carried out. The results suggest that bioplastics shape the communities' structure, especially in the aerobic phase. Distinctive bacterial and fungal sequences were found for SBB compared to the positive control, which showed a more limited diversity. *Mucor racemosus* was especially abundant in composts from bioplastics' treatment, whereas *Penicillium roqueforti* was found only in compost from PLA and *Thermomyces lanuginosus* in that from SBB. This work shed a light on the microbial communities involved in the OFMSW treatment with and without the presence of bioplastics, using a new approach to evaluate this end-of-life option.

KEYWORDS

biofilm, microbial ecology, anaerobic digestion, composting, metagenomics

Introduction

Conventional petroleum-based plastics cover a wide range of applications (Koch and Mihalyi, 2018), and the annual European production in 2019 exceeded 57.9 million tonnes (Plastics Europe, 2020), leading to serious environmental pollution concerns due to the high amount of disposable items, reaching 29.1 million tonnes of post-consumer waste (Geyer et al., 2017; Rhodes, 2019). Consequently, micro- and nano-plastics, which

are plastic particles derived from macro-plastics' degradation with a diameter <5 mm and <100 nm, respectively (Karbalaei et al., 2018; Ng et al., 2018; Wang et al., 2019), are accumulating rapidly and have been already identified in different environments and places, such as Arctic ice, air, food and drinking water, soils, glaciers, and oceans, and also in human and animal bodies (Toussaint et al., 2019; Kanhai et al., 2020; Paul et al., 2020). While the possible impacts of micro- and nano-plastics on human health are still being investigated (Jiang et al., 2020), the increasing levels of plastic residues in the environment pose a new set of potential threats. To deal with these problems, bioplastics, including materials based on renewable sources, have arisen as possible beneficial alternatives (Abe et al., 2021) to reduce carbon footprint and dependency on fossil fuel, and to limit greenhouse gas emissions (Shamsuddin et al., 2017). Moreover, these polymers can be more easily biodegraded by a combination of abiotic processes, such as UV, temperature, moisture, and pH, as well as biotic parameters, mainly microbial activities (Mohee et al., 2008; Karamanlioglu et al., 2017; Harrison et al., 2018). According to European Bioplastics (2020), the current global bioplastics production slightly exceeds 0.6% of global plastic production, but the market is expected to grow in the upcoming years. Biodegradable plastics labeled as "compostable" must follow rigorous criteria as described in the European Standard EN 13432 (EN13432, 2002), in which, for instance, the breakdown under industrial composting conditions must occur in less than 12 weeks.

Among the different end-of-life options (i.e., recycling, landfill, etc.), the biological waste treatment, such as anaerobic digestion and the following aerobic composting of the organic fraction of municipal solid waste (OFMSW), is an environmentally safe and economically feasible treatment for bioplastics waste management (Butbunchu and Pathom-Aree, 2019). The industrial plants provide appropriate conditions for the efficient conversion of organic carbon into nutrient-rich compost that can be used as soil amender (i.e., compost). Moreover, energy recovery through anaerobic digestion is among the benefit of these worldwide developed processes (Song et al., 2009). However, the end-of-life options depend on the available waste management system in each country (Gómez and Michel Jr, 2013). In detail, anaerobic digestion leads to the production of biogas (mainly CH_4 and CO_2), water, hydrogen, sulfide, ammonia, and digestate through microbial metabolism and in absence of oxygen (Shrestha et al., 2020). The four microbiological reactions occurring, namely, hydrolysis, acidogenesis, acetogenesis, and methanogenesis, have been already extensively studied (Fernández-Rodríguez et al., 2013; Micolucci et al., 2016, 2018). On the one hand, the correct deterioration of organic matter, as well as bioplastics, may be influenced by process parameters, such as time and temperature. On the other hand, the aerobic composting process of the digestate consists of solid waste valorization (Kale et al., 2007; Spaccini et al., 2016) to obtain a homogeneous organic-rich and stable compost. This product, used as a soil amendment, has high microbial diversity (Song et al., 2009; Karamanlioglu and Robson, 2013; Sisto et al., 2018) and in composting plants the appropriate conditions for microorganisms growth are provided (Gu et al., 1993; Mohee et al., 2008; Sarasa et al., 2009; Gómez and Michel Jr, 2013; Javierre et al., 2015). The degradability of bioplastics is affected by different factors, such as their chemical and physical structures (Massardier-nageotte et al., 2006; Endres, 2017) and the high variety of biopolymer blends. The microbial diversity to which the bioplastics are exposed is among the most influential factors in degradation together with the operating conditions (Folino et al., 2020). For instance, according to the literature, the rates of degradation differ under aerobic and anaerobic conditions (Thakur et al., 2018), highlighting the relevance of microbial activity. Since the existing plants processing the OFMSW were not designed to also treat bioplastics, they may not be totally effective in the management and deterioration of these materials (Calabrò and Grosso, 2019). Furthermore, bioplastics may also play a key role in shaping the microbial communities involved during the processes (Bandini et al., 2020).

We reproduced at pilot-scale the anaerobic digestion and the following aerobic composting of the OFMSW treatment under real industrial conditions for time and temperature (25 days HRT at 52 ± 0.5°C and 22 days at 65 ± 0.2°C, respectively) (Bandini et al., 2022). Polylactic acid (PLA) and starch-based bioplastic (SBB) in the final form of rigid spoons, which are supposed to follow the same fate as the OFMSW, were tested at 5% (w/w) concentration on organic waste, separately, according to the latest report provided by Consorzio Italiano Compostatori (CIC-COREPLA, 2020). To monitor the bacterial, archaeal, and fungal communities during the whole process, high-throughput sequencing (HTS) technology of phylogenetic markers was carried out on the digestate used as inoculum, on the OFMSW slurry, on intermediate samples during the anaerobic digestion and on the final composts from each treatment. This study aims (i) to determine the possible influence of biopolymers on the microbial structure during the OFMSW treatment; (ii) to assess in detail the microbial evolution during anaerobic digestion, comparing the positive control (OFMSW only) with the two bioplastics; and (iii) to evaluate the microbiological quality of the final composts obtained from both the tested materials separately.

Materials and methods

Pilot-scale experiment setup and tested materials

The tested materials were compostable and commercially available PLA and SBB spoons with the same weight and thickness, which were broken into 2–5 mm pieces. The OFMSW

slurry was sampled from a full-scale anaerobic and thermophilic plant. This slurry, which was previously subjected to separation from bioplastics and squeezing of the fraction, was further sifted with a 5-mm sieve to remove coarse fractions and plastics and to improve its homogeneity. The inoculum was collected from an OFMSW thermophilic plant and used immediately. All the substrates, including bioplastics, were chemically characterized as reported in a previous study (Bandini et al., 2022).

The anaerobic digestion was performed in three 24 L continuous stirred tank reactors under thermophilic conditions (52 ± 0.5°C). Each digester was filled with (i) OFMSW (positive control or blank) slurry and inoculum, (ii) OFMSW slurry, inoculum, and ground PLA spoons (2–5 mm), and (iii) OFMSW slurry, inoculum, and ground SBB spoons (2–5 mm). To reproduce the current Italian situation, the percentage of bioplastics to OFMSW was set at 5% w/w, and the reactors were daily fed. The hydraulic retention time (HRT) was 25 days, and the organic loading rate (OLR) was set based on chemical analyses. The following aerobic composting of the digestates lasted 22 days at 65 ± 0.2°C. The digestates from the three reactors were recovered by centrifugation and mixed with a green fraction of organic waste in a 1:1 ratio. Three technical replicates were obtained from each digestate for composting. A brief description of the experiment is given as an outline in **Supplementary Figure 1**.

Anaerobic digestion and composting monitoring analyses

On the one hand, during anaerobic digestion, the quantity and quality of the produced biogas were monitored. The percentage in the volume of CH_4, CO_2, O_2, and the concentration of H_2S and organic acids were measured, and the temperature inside the reactors was continuously recorded. On the other hand, after the aerobic composting of the solid digestates, pH, humidity, and inert materials were determined together with the disintegration degree of the tested materials. The measurement of the bioplastic content in the final compost was performed in a fraction between 2 and 10 mm. The quality of the final composts was evaluated through phytotoxicity and ecotoxicity tests on seeds and soil fauna, respectively. Other physicochemical analyses on materials were performed and reported elsewhere (Bandini et al., 2022).

DNA extraction, amplification, and sequencing

The DNA was extracted from the thermophilic anaerobic inoculum, the sieved OFMSW slurry, and the mix of inoculum and slurry. To monitor the microbial activity, intermediate sampling during the anaerobic digestion was carried out, namely at time 0 (T0), approximately one (T1) and two (T2) weeks after the addition of bioplastics to the reactors, and on the last day (Tfinal). The DNA was also extracted from the final composts obtained from the three treatments. The PowerSoil DNA Isolation Kit (Qiagen) was used, according to the manufacturer's instructions. DNA quantification was performed with the Quant-iT HS ds-DNA assay kit (Invitrogen, Paisley, UK) using a QuBitTM fluorometer and stored at −20°C for further analyses. Analyses were carried out using three replicates for each sample.

DNA amplification and Illumina high-throughput sequencing

To assess the bacterial, archaeal, and fungal communities, microbiological analyses based on HTS of 16S rDNA and Internal Transcribed Spacer 1 (ITS1) region of ribosomal RNA (rRNA) amplicons were performed, respectively.

The V3–V4 bacterial regions were amplified by PCR using universal primers 343F (5′-TACGGRAGGCAGCAG-3′) and 802R (5′-TACNVGGGTWTCTAATCC-3′). The PCR amplifications were performed with the Phusion Flash High-Fidelity Master Mix (Thermo Fisher Scientific, Inc., Waltham, MA, USA), and the mixture comprised 12.5 μl of Phusion Flash High-Fidelity Master Mix, 1.25 μl of each primer (10 μM), and 1 ng of DNA template and nuclease-free water, to a final volume of 25 μl. The thermocycler program was used as follows: initial denaturation at 95°C for 5 min, followed by 20 cycles of denaturation at 95°C for 30 s, annealing at 50°C for 30 s, an extension at 72°C for 30 s, and a final extension at 72°C for 10 min.

Differently, to assess the archaeal diversity, the V3–V4 regions were amplified using the primer pair 344F (5′-ACGGGGYGCAGCAGGCGCGA-3′) (Raskin et al., 1994) and 806R (5′-GGACTACVSGGGTATCTAAT-3′) (Takai and Horikoshi, 2000). The PCR reaction mix was composed of 12.5 μl of Phusion Flash High-Fidelity Master Mix, 1.25 μl of each primer (10 μM), 1 ng of DNA template, and nuclease-free water, to a final volume of 25 μl. The thermocycler program was with the following conditions: initial denaturation at 94°C for 5 min; followed by 20 cycles of denaturation at 90°C for 30 s, annealing at 50°C for 30 s, an extension at 72°C for 30 s, and a final extension at 72°C for 10 min.

Finally, the fungal communities were estimated using the universal primers ITS-1 (5′-TCCGTAGGTGAACCTGCGG-3′) and ITS-2 (5′-GCTGCGTTCTTCATCGATGC-3′; White et al., 1990), and PCR reactions were carried out with 12.5 μl of Phusion Flash High-Fidelity Master Mix, 1.25 μl of each primer (10 μM), and 1 ng of DNA template and nuclease-free water, to a final volume of 25 μl. The thermocycler was set with an initial hold at 94°C for 4 min, followed by 28 cycles of 94°C for 30 s,

annealing at 56°C for 30 s, an extension at 72°C for 1 min, and a final extension at 72°C for 7 min.

To allow simultaneous analyses and reduce the generation of anomalous data, an indexing PCR was performed. Amplicons were combined in equimolar ratios and multiplexed into two separate pools, one for Bacteria and Archaea and another for Fungi. The pools were purified throughout the solid-phase reversible immobilization (SPRI) method (Agencourt AMPure XP kit; REF A63880, Beckman Coulter, Milano, Italy) and sequenced by Fasteris S.A. (Geneva, Switzerland). The amplicon libraries were prepared using the TruSeq DNA sample preparation kit (REF 15 026 486, Illumina Inc., San Diego, CA, USA), and the sequencing was carried out with the MiSeq Illumina instrument (Illumina Inc.), generating 300 bp paired-end reads.

Sequence processing and statistical analyses

Data filtering, multiplexing, and preparation for statistical analyses were performed according to previous studies (Berry et al., 2011; Vasileiadis et al., 2015; Bortolini et al., 2016; Puglisi et al., 2019; Bandini et al., 2020). Briefly, the MiSeq Control Software version 2.3.0.3, RTA v1.18.42.0 and CASAVA v1.8.2 were used for base calling, whereas the "pandaseq" script was applied to align raw Illumina sequences (Bartram et al., 2011). Since V3–V4, 16S rRNA and ITS1 gene amplicons are shorter than 500 bp and require 300 bp paired-end reads per amplicon for re-constructing full regions, a minimum overlap of 30 bp between read pairs and two maximum allowed mismatches was set. Fastx-toolkit[1]) was applied to demultiplex the sequences according to sample indexes and primers. According to Bortolini et al. (2016), among the bacterial and archaeal sequences, homopolymers >10 bp (chimeras), sequences outside the regions of interest, and non-targeted taxa were removed. The UCHIME algorithm with the UNITE database v6 was used to identify and discard homopolymers >10 bp, chimeras, and non-fungal sequences among the ITS amplicons. Operational taxonomic units (OTUs) and taxonomy-based approaches were performed on the sequences. Mothur V1.32.1 was applied for the OTUs and taxonomy matrixes for the V3–V4 regions (Schloss et al., 2009), whereas statistical analyses were performed with R[2] supplemented with Vegan package (Dixon, 2003). OTUs were determined in VSEARCH. Mothur was used to perform ITS taxonomy-based analyses with a minimum length of 120 bp and no upper length limit due to ITS variability. The average linkage algorithm was applied at different taxonomic levels to visualize the hierarchical clustering of the sequences, while the unconstrained sample grouping was assessed by principal component analysis (PCA), and the canonical correspondence analysis (CCA) was used to visualize the significance of different treatments on the analyzed diversity (constrained variance).

To estimate the associated α and β diversity, the OTU- and taxonomy-based matrixes were analyzed using R. Moreover, to better estimate any significant differences between samples, α diversity analyses based on Shannon's Index, Observed Richness (S), Simpson's Diversity Index (D), and Chao's Index were performed on bacterial and fungal communities as previously described (Bandini et al., 2020). Good's coverage estimate was calculated to assess the "percentage diversity" captured by sequencing (Good, 1953), whereas to identify significantly different features between samples Metastats coupled to FDR test for the comparison of means was applied (Paulson et al., 2011). The identification of the most abundant OTUs was confirmed with RDP (Ribosomal Database Project) for Bacteria and Archaea and with BLAST (Basic Local Alignment Search) searches of the GenBank database for Fungi. Analysis of variance of means (ANOVA) and Tukey's HSD pairwise comparison test ($\alpha < 0.05$) were performed to assess significant differences between samples. The raw sequences data have been deposited in the Sequence Read Archive of NCBI, and the accession numbers will be assigned.

In the experiment and data analyses, samples were labeled as follows: digestate used as inoculum, "T0_none_initial_digestate"; OFMSW slurry, "T0_none_OFMSW_slurry"; the mixture of digestate and OFMSW slurry as initial time T0, "T0_none_digestate_OFMSW"; intermediate samples at T1, T2, and Tfinal during anaerobic digestion for each treatment, "TX_treatment_anaerobic"; final compost from each treatment, "Tfinal_treatment_compost". Each sample was reported in triplicate.

Results and discussion

Thermophilic anaerobic digestion and aerobic composting of rigid bioplastics with organic fraction of municipal solid waste

Probably, due to the high daily OLR, the specific methane production for bioplastics was lower than the positive control, and biological process problems were found after 2 weeks (Bandini et al., 2022). The process instability also resulted in high H_2S concentration in the gas phase in the last period of the test and in a progressive increase over time in the concentration of organic acids. At the end of the anaerobic digestion with OFMSW, PLA and SBB spoon residues remained in an undegraded form leading to serious risks to clog pipers or the mechanical parts of the reactors. Also, after the aerobic composting, the tested bioplastics did not reach the

1 http://hannonlab.cshl.edu/fastx_toolkit/

2 http://www.R-project.org/

disintegration target imposed by UNI EN 13432 standard, and several residues were found in the final compost. Phytotoxicity tests reported the lowest Germination Index for PLA elutriate, whereas a potential negative effect of SBB on soil fauna was detected.

Overview of the bacterial, archaeal, and fungal communities' structure during organic fraction of municipal solid waste treatment with bioplastics

After the screening and filtering steps, bacterial amplicons resulted in 14,500 high-quality sequences per sample and the dataset revealed a consistent coverage of 99%. Sequences were classified at 51.6% to family level, at 43.1% to genus level, and at 5.9% to species level (data not shown). **Figure 1** shows the hierarchical clustering of classified sequences using the average linkage algorithm at the genus classification level for all the samples. The samples clustered according to treatments, showing differences in bacterial community between the OFMSW slurry and all the other matrixes. The digestate was located between the intermediate samples of T2 and the Tfinal of anaerobic digestion of the PLA treatment, exhibiting nevertheless a unique diversity. Probably due to the microbial richness of the digestate, the initial mixture T0 clustered among the T1 of PLA and the T2 of SBB. The composts were placed together and showed a wider bacterial diversity than the anaerobic digestion samples. Even among the same treatment, some differences further demonstrate the microbial diversity of these samples. However, the final compost from OFMSW showed a different bacterial diversity compared to the two tested bioplastics. The most abundant genera in OFMSW slurry were *Lactobacillus* and *Fusobacterium*, and these were not found in any other treatments. OTUs assigned to the Halanaerobiaceae family were found mainly in the initial digestate and in almost all anaerobic digestion samples, although the abundance decreased from T0 to T2 until it dropped significantly at Tfinal for the three treatments without differences between the positive controls and the bioplastics. This family contains fermenting and cellulolytic bacteria (Simankova et al., 1993) and was already reported in the thermophilic digester (Li et al., 2015). *Caldicoprobacter* was the distinctive genus of the anaerobic digestion Tfinal samples where it was found with higher abundance and without significant differences between OFMSW and bioplastics treatment. Bacteria of this thermophilic genus belonging to the class *Clostridia* are known for fermenting sugars into acetate, lactate, ethanol, hydrogen, and carbon dioxide and were already detected in anaerobic digestion (Ziganshina et al., 2017). Since they are obligate heterotrophic bacteria mainly isolated from hydrothermal hot springs (Bouanane-Darenfed et al., 2013), and their presence at the end of the anaerobic phase may be due to their resistance to high ammonia levels. *Bacillus, Geobacillus,* and *Ureibacillus* were the dominant genera in all compost samples and were already reported in literature for mature substrate after composting (Vajna et al., 2012). These thermophilic bacteria are frequently detected in compost as they contribute to the vigorous degradation of organic compounds (Hanajima et al., 2009), such as *Ureibacillus*, which is capable of degrading lignocellulose (Wang et al., 2011) and was also isolated during thermophilic composting of sludge (Steger et al., 2005). Their mutual presence in the compost from OFMSW, PLA, and SBB may suggest that these microorganisms contribute significantly to the degradation of cellulosic material, and possibly bioplastics, during the thermophilic composting phase of the anaerobic digestates. Differently, *Actinopolymorpha* and *Thermobispora* genera were mainly found in compost obtained from OFMSW, and the second one was already isolated from this substrate (Steger et al., 2007; Cao et al., 2019). *Thermoactinomyces* genus was detected especially in compost obtained from OFMSW and PLA. Since a member of this thermophilic and lipolytic actinomycete was inoculated in compost to more efficiently decompose food waste into mature substrate (Ke et al., 2010), its presence in composts from PLA may be positively evaluated.

Figure 2 shows the taxonomic assignment at the genus level for the 261 archaeal high-quality sequences per sample. The average coverage rate was 98%, and the sequences were classified into family (100%), genus (99.8%), and species (1.2%) levels (data not shown). Such a low taxonomic assignment at the species level could be explained by the scarcity of data deposited in the main database. As will later be shown in **Figure 3**, one OTU was identified at the species level. Since these microorganisms are hardly cultivable under laboratory conditions and are often associated with extreme growth conditions, their knowledge is still limited. In **Figure 2**, the most abundant archaeal genera are shown. *Methanobrevibacter* and *Methanosphaera* were the only genera identified, and no particular differences were observed between the samples in the overall reproduced OFMSW process. *Methanobrevibacter* was the dominant genus in each sample and was positively correlated with biogas yield playing a key role in biogas production (Li et al., 2015). This genus belonging to the Methanobacteriaceae family generally dominates the biogas reactors and was also present in fresh cattle manure (Goberna et al., 2015). High concentration of H_2S detected in the reactors may have significantly modulated the archaea biodiversity during anaerobic digestion (Bandini et al., 2022). As reported in a recently published research, since H_2S is toxic to methanogens, there is a strong correlation between the presence of this compound and the microbial population in the reactors (Olivera et al., 2022). Otherwise, the *Methanosphaera* genus was detected in each sample except some as compost from PLA, T2 for SBB treatment, one replicate of digestate, and Tfinal for SBB. The presence of this methanogenic archaea was already reported

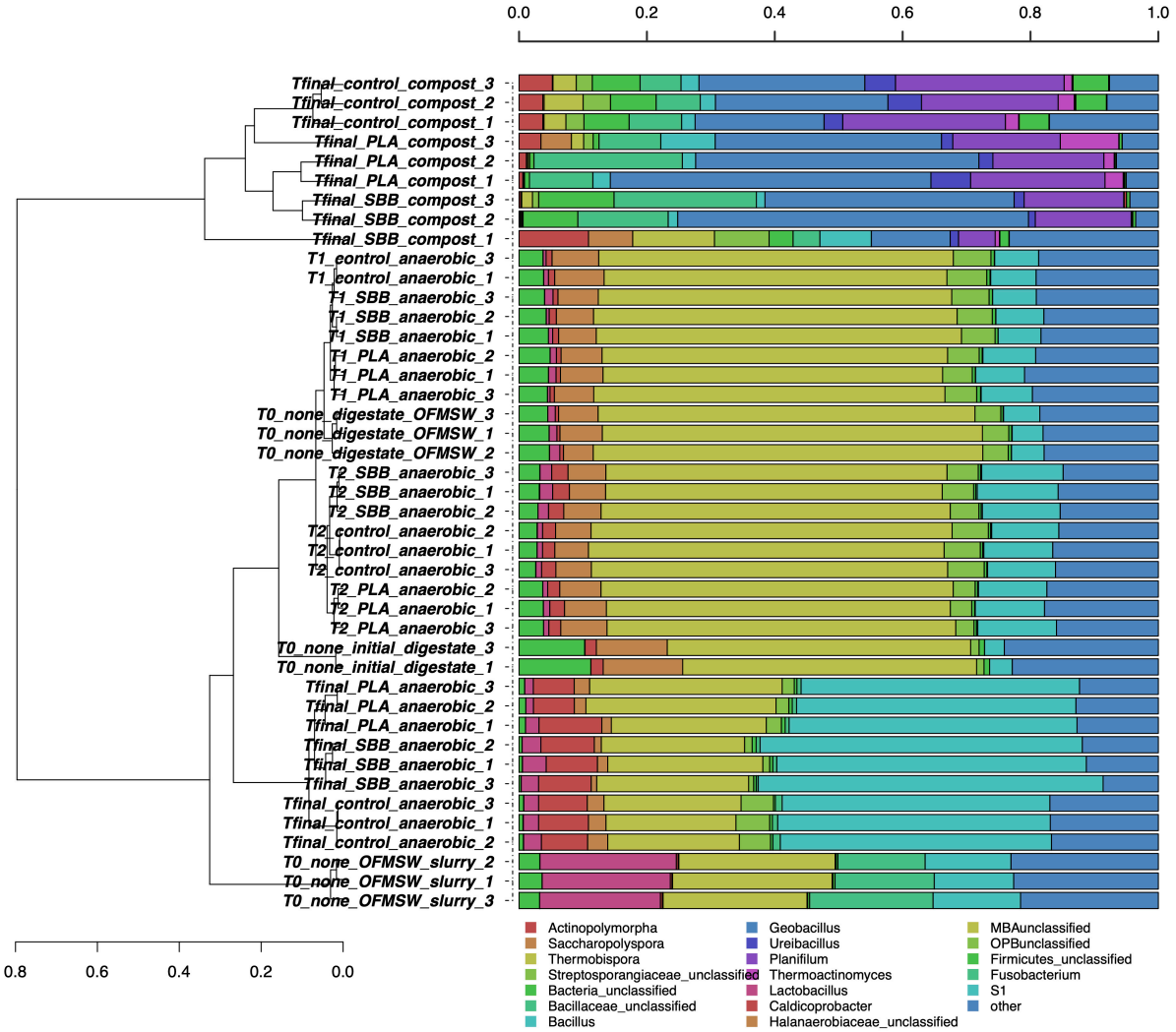

FIGURE 1
Hierarchical clustering of bacterial sequences using the average linkage algorithm at the genus level for taxa with at least ≥5% participation in a single sample. Taxa with low contributions were added to the "other" group. PLA, polylactic acid; SBB, starch-based bioplastic; OFMSW, organic fraction of municipal solid waste.

in literature (Goberna et al., 2015; Achmon et al., 2019) and dominated the active methane production during co-digestion of food waste (Zhang et al., 2016). Members of this genus have one of the most restricted metabolisms since they can neither oxidize methanol to carbon dioxide nor reduce carbon dioxide to methane (Fricke et al., 2006), and methanol- and acetate-rich environments provide the optimum conditions to grow (Facey et al., 2012). However, we cannot exclude the hypothesis that the presence of archaeal DNA in composting samples can be a residue from the anaerobic phase.

Figure 4 shows the taxonomic classification of the 12,500 ITS1 sequences per sample. The Good's coverage result was 99%, and the sequences were classified at 75.9% at the family level, 74.5% at the genus level, and 65.7% at the species level. The OFMSW slurry presented a separate fungal community, dominated by *Penicillium*, *Debaryomyces*, *Kazachstania,* and *Candida* genera. *Penicillium* species usually govern food waste (Torp and Skaar, 1998; Rundberget et al., 2004), whereas *Kazachstania* spp. was already found in food waste slurry (Wang et al., 2020) and traditional fermentation, such as alcohols production, is connected to this genus (Di Cagno et al., 2014; Lhomme et al., 2015). Otherwise, the anaerobic digestion samples, including the initial digestate and intermediate times of all the treatments, did not cluster uniformly between replicates and stages. However, some dominant fungi can be identified only in these samples, such as unclassified *Saccharomycetes*, *Cladosporium,* and *Mortierella*. Due to the high levels of proteins, amino acids, and ammonia food waste is an adequate substrate for the growth of *Saccharomycetes* (Suwannarat and Ritchie, 2015), which was also applied for the anaerobic

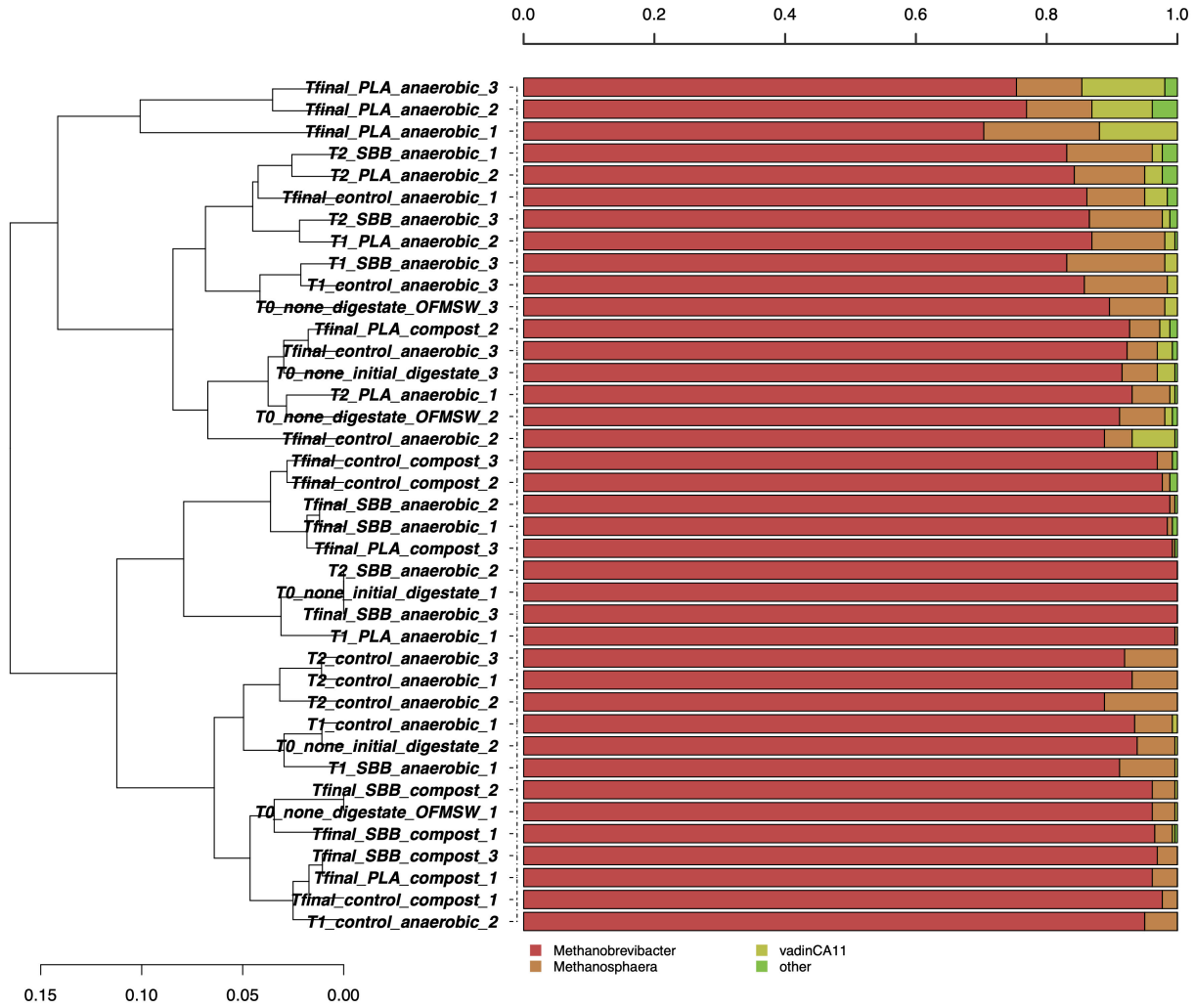

FIGURE 2
Hierarchical clustering of archaeal sequences using the average linkage algorithm at the genus level for taxa with at least ≥5% participation in a single sample. Taxa with low contributions were added to the "other" group. PLA, polylactic acid; SBB, starch-based bioplastic; OFMSW, organic fraction of municipal solid waste.

digestion of kitchen waste (Zheng et al., 2022). Differently, compost samples were grouped into separate clusters, showing a heterogeneous trend. The positive control was distantly related to the two bioplastic-treated composts, exhibiting a completely different fungal community. Fungi are mainly active in an aerobic environment and they also play a crucial role in the polymers' biodegradation process (Folino et al., 2020). In the compost from OFMSW, *Cladosporium*, *Penicillium*, and *Mucor* were the dominant fungal genera. In recent work, *Cladosporium* was found during composting of digestate from food waste and it is associated with the ability to degrade lignocellulose matter (Ryckeboer et al., 2003). The presence of this fungus in compost from OFMSW could be a good indicator. It was also found in compost treated with PLA and SBB, but in lower abundance than the positive control. The unclassified *Sordariaceae* genus was instead a characteristic genus in compost from SBB and PLA, and this membranous or coriaceous ascomata fungus was often found on decaying substrate, such as wood (Zhang et al., 2006; Maharachchikumbura et al., 2016). In conclusion, especially in the final composts, strong differences can be noticed between the positive control and the bioplastics treatments, highlighting a possible effect of these materials in modulating the fungal community involved in the aerobic process.

Based on the HTS results, detailed analyses were carried out in terms of α-diversity, namely, the distribution of the most abundant bacterial, archaeal, and fungal OTUs. Chao, Shannon's, Simpson's (D), and Observed Richness (Sobs) α-diversity indexes were calculated to evaluate the diversity, the evenness, and the dissimilarity in terms of community

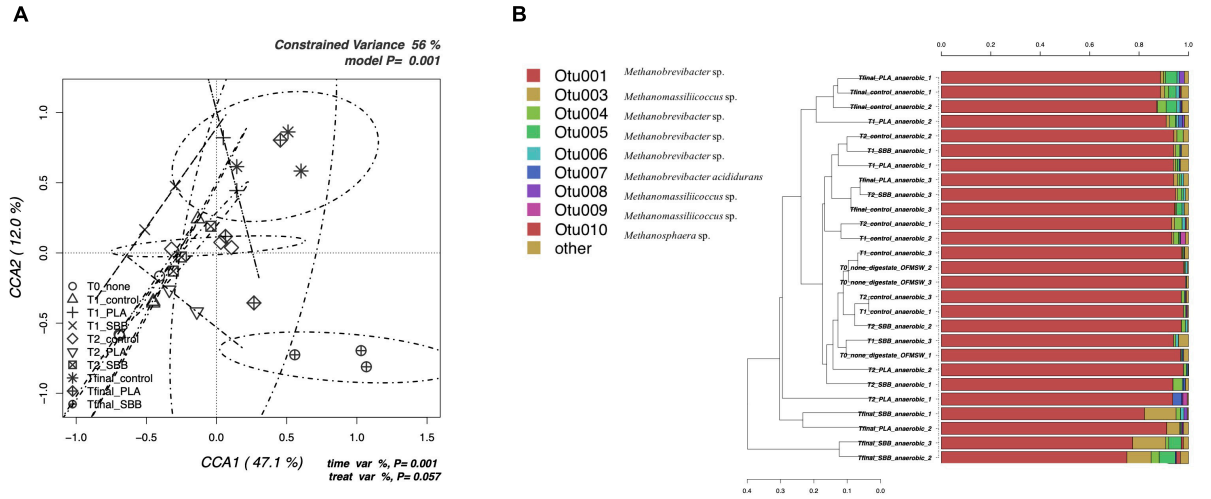

FIGURE 3
Archaeal community during anaerobic digestion. **(A)** Hypothesis-driven canonical correspondence analysis (CCA) model performed on the total archaeal OTUs relative abundance data from anaerobic digestion intermediate samples. **(B)** Overview and identification of the most abundant OTUs comprising 99% of the archaeal diversity in anaerobic digestion intermediate samples. PLA, polylactic acid; SBB, starch-based bioplastic; OFMSW, organic fraction of municipal solid waste.

structure between the microbial communities at different stages and with different treatments. **Supplementary Table 1** reports the average (±SD) of α-diversity indexes and richness of bacterial microbiomes. Based on ANOVA and LSD test ($p < 0.05$) performed, Chao, Sobs, and Shannon indexes on the bacterial α-diversity resulted in significant differences according to *F* values. In particular, the digestate and OFMSW slurry resulted in a different bacterial community compared to all other samples (Chao and Sobs). The intermediate anaerobic digestion samples showed fewer differences between stages and treatments. Otherwise, archaeal α-diversity indexes (**Supplementary Table 2**) resulted in significant differences for Sobs, Simpson, and Shannon. The digestate reported a significantly different archaeal community structure, whereas lower distinctions were appreciated for the other samples. According to Sobs, Shannon, and Chao indexes, the OFMSW and PLA composts were significantly lower compared to SBB. As for bacteria, the fungal Chao, Sobs, and Shannon α-diversity indexes (**Supplementary Table 3**) resulted in significant differences. Composts from PLA and SBB reported significantly lower results for Chao, Sobs, and Shannon indexes compared to the compost from OFMSW. According to the Simpson's Index, the T0 of anaerobic digestion reported significantly higher differences among other samples.

This overview of the bacterial, archaeal, and fungal communities involved in the digestate, in the OFMSW slurry, in different stages of anaerobic digestion, and in the final compost was crucial to assess their dynamics and the hypothetical role of bioplastics in modulating them. According to our knowledge, this is the first study to thoroughly map the microbial communities involved during the OFMSW treatment.

A detailed focus on the bacterial community during thermophilic anaerobic digestion of organic fraction of municipal solid waste and bioplastic

To better evaluate the effects of bioplastics on the bacterial community during anaerobic digestion, a db-RDA model based on OTUs was applied. **Figure 5A** shows the CCA that was significant ($p = 0.001$) and had a high explanation of variance (78.3% of the total variance). The first and the second canonical axes represented 60.2 and 14.6% of the variance, respectively. T0 samples were negatively correlated with both axes and grouped separately, highlighting a distinct bacterial diversity. In the same sector, CCA were also located the samples of T1, showing a similar community between treatments and not very distant from that of T0. The T2 samples clustered together and overlapped the different treatments, whereas Tfinal showed different communities for positive control and bioplastics treatment.

Figure 5B represents the hierarchical cluster of the most abundant OTUs in anaerobic digestion samples and the respective identification confirmed with RDP. OTU0001, which corresponds to Uncultured Clostridiales, was predominant at all stages, but reduced toward the end of the anaerobic process, as reported in a recent study under thermophilic conditions (Jackson et al., 2020). In the early stages, OTU0001 was almost 60% of the total bacterial diversity as described in literature (Granada et al., 2018), reducing to 40–50% at Tfinal for SBB and PLA, and up to 30% in the positive control. In agreement with these results, it appears that both PLA and SBB have an effect on

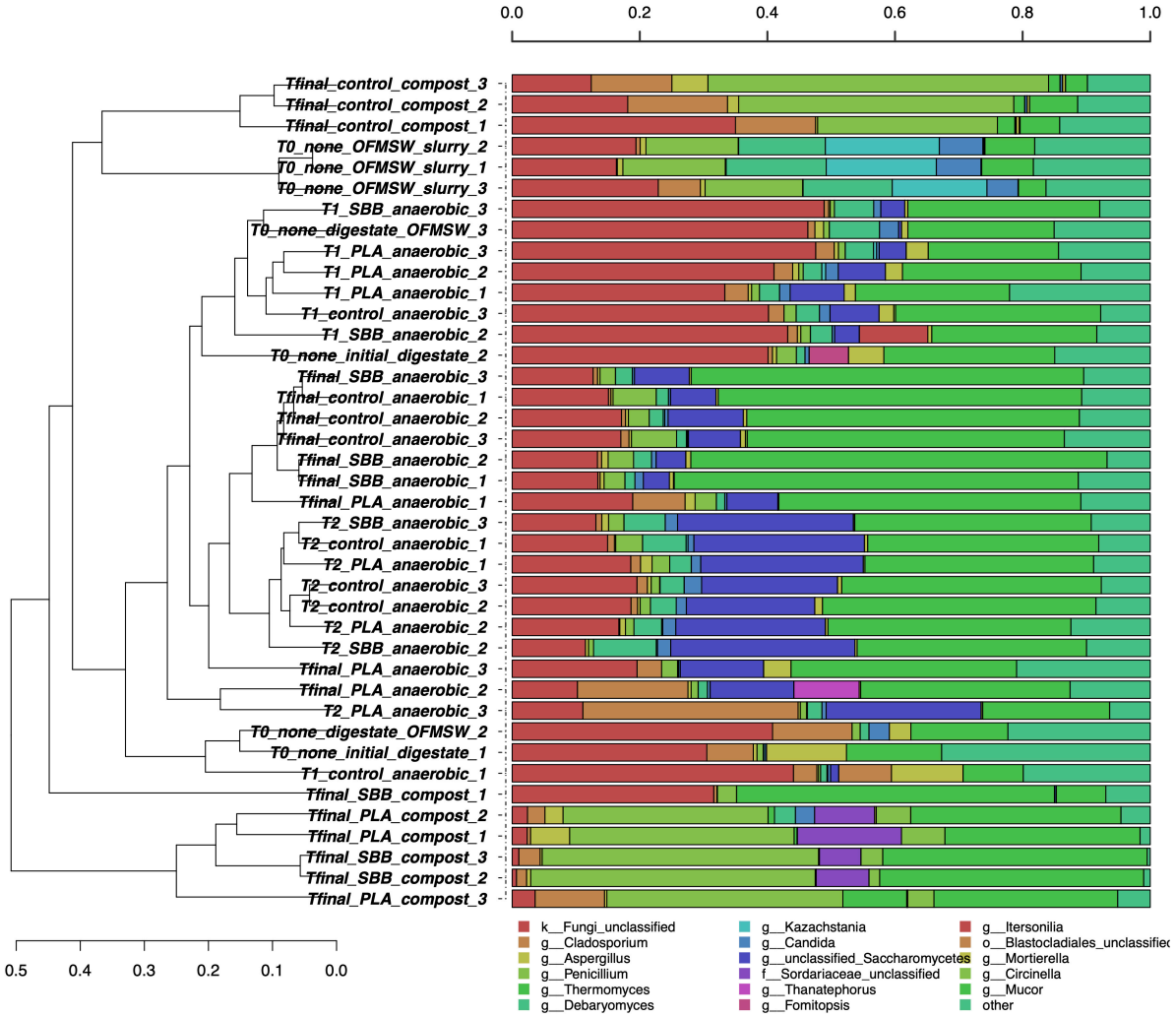

FIGURE 4
Hierarchical clustering of fungal sequences using the average linkage algorithm at the genus level for taxa with at least ≥5% participation in a single sample. Taxa with low contributions were added to the "other" group. PLA, polylactic acid; SBB, starch-based bioplastic; OFMSW, organic fraction of municipal solid waste.

the abundance of Clostridiales, which are decisive performers during hydrolysis, acidogenesis, acetogenesis, and syntrophic acetate oxidation (Ziganshin et al., 2013). Both OTU0006 and OTU0009 were identified as *Hydrogenispora* sp., which are hydrolytic, acidogenic, and acetogenic bacteria already detected in anaerobic digester (Kang et al., 2021). These bacteria are able to ferment carbohydrates such as glucose, maltose, and fructose into acetate, ethanol, and hydrogen, respectively (Yang et al., 2016; Corbellini et al., 2018), and probably for this reason OTU0009 was slightly more abundant in T1 samples, especially in SBB. Otherwise, several strains of *Clostridium* sp. (OTU0015), mainly found in T2 and Tfinal of each sample, are key actors involved in the production of butyric acid as the main product of sugar metabolism (Soh et al., 1991). They also produce hydrogen, carbon dioxide, acetate, ethanol, and lactate (Kim et al., 2010) and, probably due to the ability of any strains to consume starch (Zhang et al., 2020), OTU0010, identified as Uncultured Clostridiales, was mainly found in the Tfinal of SBB treatment. OTU0016, identified as *Acetivibrio saccincola* (synonym: *Herbivorax saccincola*) was detected in all samples, although with a slightly lower abundance in Tfinal for PLA and SBB. This novel thermophilic and anaerobic bacterium was isolated from a lab-scale biogas fermenter and seems to play a key role in the remineralization of plant biomass by hydrolyzing polysaccharides (Koeck et al., 2016). This may also have important implications in the degradation of organic matter in bioplastics, and its lower abundance compared to the positive control may not be a good indicator. Finally, *Defluviitalea* sp. (OTU0044) was mainly found not only in OFMSW Tfinal but also in PLA. This spore-forming and the

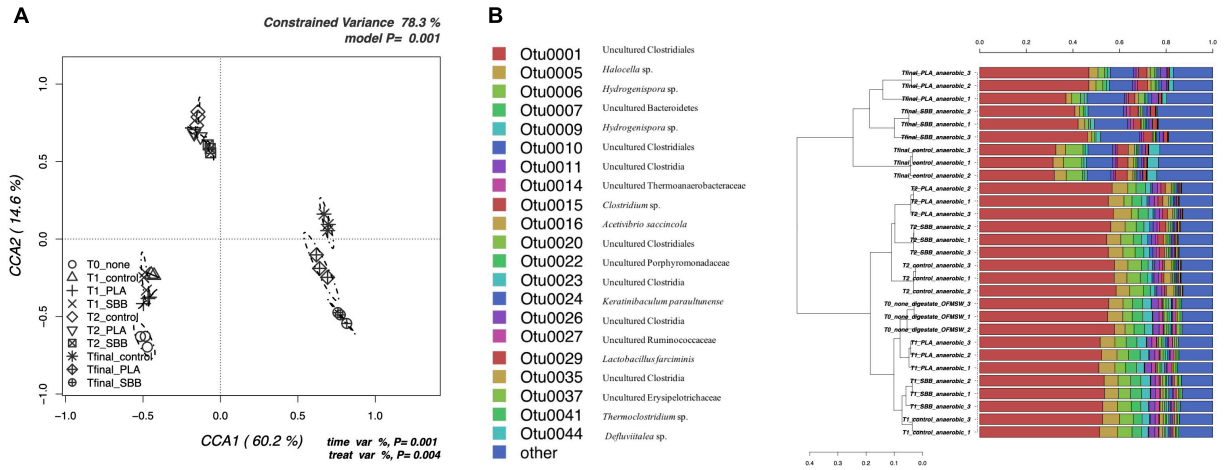

FIGURE 5
Bacterial community during anaerobic digestion. **(A)** Hypothesis-driven canonical correspondence analysis (CCA) model performed on the total bacterial OTUs relative abundance data from anaerobic digestion intermediate samples. **(B)** Overview and identification of the most abundant OTUs comprising 99% of the bacterial diversity in anaerobic digestion intermediate samples. PLA, polylactic acid; SBB, starch-based bioplastic; OFMSW, organic fraction of municipal solid waste.

saccharolytic bacterium were already isolated from an anaerobic digester (Ma et al., 2017) and played a remarkable role in the digestion stage of acidogenesis (Zhang et al., 2017). Its absence in the Tfinal of the SBB treatment may not have a positive implication in the anaerobic digestion and degradation of organic matter processes.

A detailed focus on the archaeal community during thermophilic anaerobic digestion of organic fraction of municipal solid waste and bioplastics

Figure 3A shows the CCA for the archaeal community structure during anaerobic digestion. The CCA model was significant (p = 0.001) and had a high explanation of variance (56% of the total variance). The first and the second canonical axes represented 67.1 and 12.0% of the variance, respectively. However, as reported in a previous study (Bandini et al., 2020), the archaeal population did not follow heterogeneous trend during the anaerobic digestion. Samples were overlapping for both different stages and treatments, with the only exception of the Tfinal for SBB, which showed more distinctive diversity. Indeed, the ellipse is completely confined in the sector positively correlated with the first axis and negatively correlated with the second axis and overlaps only with the archaeal diversity found in the Tfinal for PLA treatment.

The taxonomic assignment of the most abundant OTUs is reported in Figure 3B and, as mentioned in the overview discussed in the previous section, the diversity is limited. OTU001, identified as *Methanobrevibacter* sp., was dominant in each sample, especially in the digestate and in early fermentation samples. The abundance of this OTU was almost 100%, then dropping to about 70% for the SBB Tfinal. This genus is a methanogen responsible for methane production from hydrogen and carbon dioxide inside the process (Sousa et al., 2007; Wang et al., 2018) and was already detected in thermophilic conditions (Lee et al., 2014). The decrease in abundance in the final samples of the process may indicate a complete utilization of the substrates necessary for the growth of these archaea, such as biogas exhaustion. On the one hand, Other OTUs also belong to the *Methanobrevibacter* sp., but the most distinctive ones were OTU004 and OTU005 that were found mainly in the Tfinal of OFMSW and SBB. In general, PLA Tfinal did not show uniform diversity and clustered heterogeneously. On the other hand, Tfinal from PLA (a replicate) and SBB clustered differently compared to the positive control and reported a higher abundance of OTU003 (*Methanomassiliicoccus* sp.). This hydrogenotrophic genus was detected in the thermophilic anaerobic digester (Jackson et al., 2020; Sposob et al., 2020). Other OTUs that corresponded to the same genus were also found especially in the last stages of anaerobic digestion, without distinction between treatments, such as OTU008 which was detected in a replicate in the Tfinal of the positive control. As already reported in a previous study at lab-scale (Bandini et al., 2020) and in a recently published work (Peng et al., 2022), the relative abundance of the archaeal community is strictly related to the *Clostridium* genus. The growth of these hydrogenotrophic and syntrophic acetate-oxidizing (SAO) microorganisms increased in tandem with the *Clostridium* sp.

A detailed focus on the fungal community during thermophilic anaerobic digestion of organic fraction of municipal solid waste and bioplastics

The db-RDA model based on fungal OTUs reported in **Figure 6A** shows the CCA that was significant (p = 0.001) and had a high explanation of variance (51% of the total variance). The first and the second canonical axes represented 32.5 and 17.1% of the variance, respectively. The samples were quite heterogeneously distributed. In particular, the initial digestate was negatively correlated with both axes, almost completely overlapping with the T1 of PLA and SBB, probably showing a similar microbial community. The T1 of the positive control had a wide ellipsis, including both T1 samples from the two bioplastics and all T2 samples. The latter, in fact, were overlaid regardless of treatment, assuming a fairly similar fungal diversity. The final anaerobic digestion samples were positively correlated with the first axis and negatively correlated with the second axis, respectively. Those in the PLA treatment showed a broader community more similar to that of the positive control, whereas those in the SBB treatment reported a narrower and more distinct ellipse.

Figure 6B shows the hierarchical clustering of fungal sequences at the genus level. Studies of fungal populations involved during anaerobic digestion in the literature are scarce. However, given their affinity for acidic environments (Oranusi and Dahunsi, 2013), it is critical to understand whether they too play a key role in the fermentation of organic matter and, especially, whether they are affected by the presence of bioplastics during the process. Moreover, the biodegradation of bioplastics involves, together with prokaryotic, also eukaryotic fungi and protozoa microorganisms (Rujnić-Sokele and Pilipović, 2017). From **Figure 6B**, it can be noticed that not all replicates of the same sample are always grouped together, but in general, the clusters were in accordance with what is shown in **Figure 6A**. OTU1, identified as *Mucor racemosus*, was dominant in all samples but with lower abundance in the anaerobic digestate used as inoculum. Only in the T2 samples from all treatments, this OTU competed with the abundance of OTU2. This genus was already found previously in thermophilic anaerobic digesters treating food waste and human excreta (Oranusi and Dahunsi, 2013; Bandini et al., 2020). Moreover, this species was tested for phosphorous removal during waste stream (Ye et al., 2015) but was mainly isolated from mesophilic and thermophilic composting (Ryckeboer et al., 2003). *Geotrichum candidum* (OTU14) was detected only in Tfinal samples from all treatments, but in greater abundance in the reactor with SBB. This yeast is widely spread in the environment and has the ability to ferment carbohydrates, ethanol, and glycerol in anaerobic conditions (Fisgativa et al., 2017). *G. candidum* is also a plant pathogen, isolated from food waste (Fisgativa et al., 2017), which is particularly relevant for its strong lipase and protease activity on organic matter, and fatty acids and peptides production. Its higher abundance with the SBB treatment may be caused by the higher carbohydrate content of the SBB. OTU2, identified as *Pichia* sp. was detected in T1 and T2 indistinctly, although slightly with less abundance in SBB treatment. However, in general, the abundance of this genus increases greatly from the samples of the third day to those of the seventh day. *Pichia* sp. was found also in Tfinal samples in the same abundance as the T1 samples. This fermentative yeast had a facultative aerobic metabolism and was also found in a recent study focusing on fungal dynamics in the anaerobic digestion of sewage sludge and food waste (Qin et al., 2021). Moreover, this research states that fungal diversity varied in relation to HRT and OLR. *Pichia* sp. was particularly abundant after 34 days of anaerobic digestion, and this result agrees with our data which reported this genus mainly at T2 (after 18 days of reactor stabilization and 14 days after the addition of bioplastics, for a total of 32 days). Differently, *Rhizoctonia solani* (OTU37) and *Itersonilia pannonica* (OTU52) can be outlined among the most distinctive OTUs for one replicate of Tfinal from PLA and one replicate of T1 from SBB, respectively. *R. solani* is a common soil-borne fungal pathogen that was already isolated in feedstock (Bandte et al., 2013). According to this article, the anaerobic digestion at mesophilic conditions reduces most of the phytopathogens infecting plants, and it was remarkable to detect its presence at the end of the thermophilic treatment (Tfinal from PLA treatment). Finally, since one strain of *Cladosporium* sp. was identified as PLA-degrading microorganism (Nair et al., 2016), the abundance of OTU16 and OTU8 in PLA samples may play a key role in the degradation process of this biopolymer during the anaerobic digestion.

Effects of polylactic acid and starch-based bioplastic on bacterial diversity in compost

Composting is an aerobic biodegradative process of organic matter that involves numerous microorganisms. Microbial communities degrade the organic substrates into more stable, humified forms and inorganic products, while their succession is a prerequisite to ensure not only complete biodegradation (Ryckeboer et al., 2003) but also the quality of the final product. **Figure 7A** shows the CCA for the bacterial community structure in composts from the three treatments. The CCA model was significant (p = 0.044) and had a 34.6% of explanation of variance. The first and the second canonical axes represented 59.6 and 40.4% of the variance, respectively. As can be seen, the bacterial diversity differed significantly between samples obtained from OFMSW, OFMSW mixed with PLA,

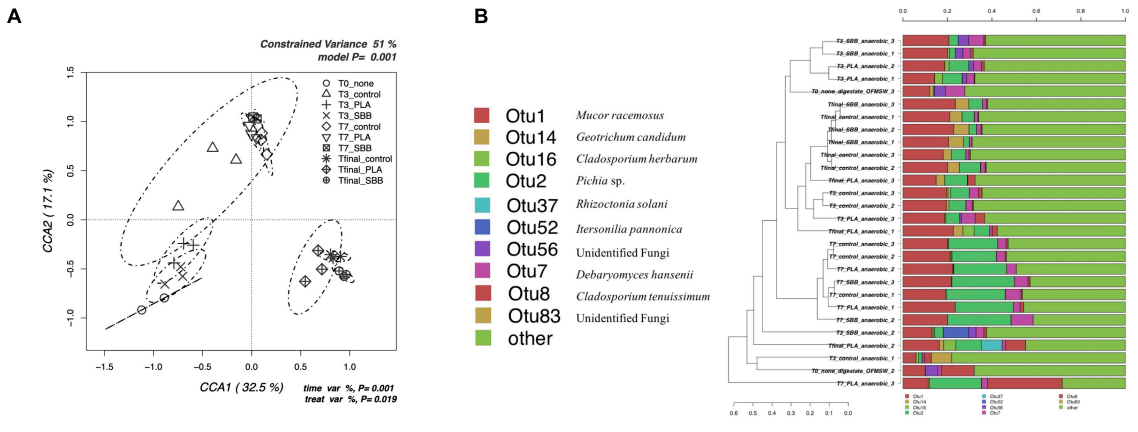

FIGURE 6
Fungal community during anaerobic digestion. **(A)** Hypothesis-driven canonical correspondence analysis (CCA) model performed on the total bacterial OTUs relative abundance data from anaerobic digestion intermediate samples. **(B)** Overview and identification of the most abundant OTUs comprising 95% of the fungal diversity in anaerobic digestion intermediate samples. PLA, polylactic acid; SBB, starch-based bioplastic; OFMSW, organic fraction of municipal solid waste.

and OFMSW mixed with SBB. The positive control clustered negatively with both the axes, whereas the PLA and SBB were both positively correlated with the CCA1, but negatively and positively with the CCA2, respectively.

The Metastats model for the most abundant 15 OTUs is shown in **Figure 7B**. First of all, it is important to underline that after the composting phase no OTU previously identified in the anaerobic phase were found again. This is probably due to the difference between anaerobic and aerobic phases, both occurring at thermophilic conditions, which allowed the selection of different bacteria. Among the OTUs, *Geobacillus thermantarcticus* (OTU0003) was one of the most abundants, accounting for more than 40% of the sequences for composts obtained from both the bioplastics and about 28% for the positive control. To our knowledge, there are no references to this thermophilic strain in composts from the literature. However, its presence may be associated with its optimum growth at 60°C and its strictly aerobic metabolism (Coorevits et al., 2012). Statistically significant difference was found for OTU0004 and identified as *Planifilum fulgidum*. This microorganism, able to degrade hemicellulose, cellulose, and protein, was already detected as dominant in compost containing spent mushroom substrate and a high-nitrogen environment (Zhang et al., 2021). Other species belonging to the genus were found in compost, but its presence may be related to the presence of nitrogen. Indeed, the OTU0008 was also identified as *Geobacillus thermodenitrificans*, a thermophilic bacteria isolated from compost heap which have the ability to convert lignocellulose into lactic acid and reduce nitrate (Daas et al., 2018). This OTU was particularly abundant in the compost from PLA and significantly lower in that obtained from SBB, probably due to the difference in the availability of substrates, such as nitrogen. Moreover, a strain of *Geobacillus* is reported as an L-PLA degrading thermophile (Tomita et al., 2004). *Thermaerobacter composti* (OTU0017), already isolated from compost in Japan (Yabe et al., 2009), was more abundant in positive control and SBB compost compared to PLA, as well as OTU0018 (*Thermobispora bispora*), OTU0019 (*Thermasporomyces composti*), OTU0025 (*T. bispora*), and OTU0028 (*Caldibacillus debilis*). It is important to underline that no abundant sequences of pathogenic bacteria were found. Moreover, there were notably statistically significant differences between the compost samples obtained from the different treatments. In conclusion, the presence of bioplastics may greatly influence aerobic composting.

Effects of polylactic acid and starch-based bioplastic on fungal diversity in compost

Some polymers are mainly, or even only, degraded by fungi (Rujnić-Sokele and Pilipović, 2017), and thus this microbial group will, therefore, play a key role during the aerobic composting of food waste and bioplastics.

To better evaluate the effects of bioplastics on the fungal community during aerobic composting, a db-RDA model based on OTUs was applied. **Figure 8A** shows the CCA that was significant (p = 0.02) and had a 39.3% of explanation of total variance. The first and the second canonical axes represented 75.5 and 24.5% of the variance, respectively. Composts obtained from the OFMSW showed a limited microbial diversity, and its ellipsis was located approximately in the center of the plot.

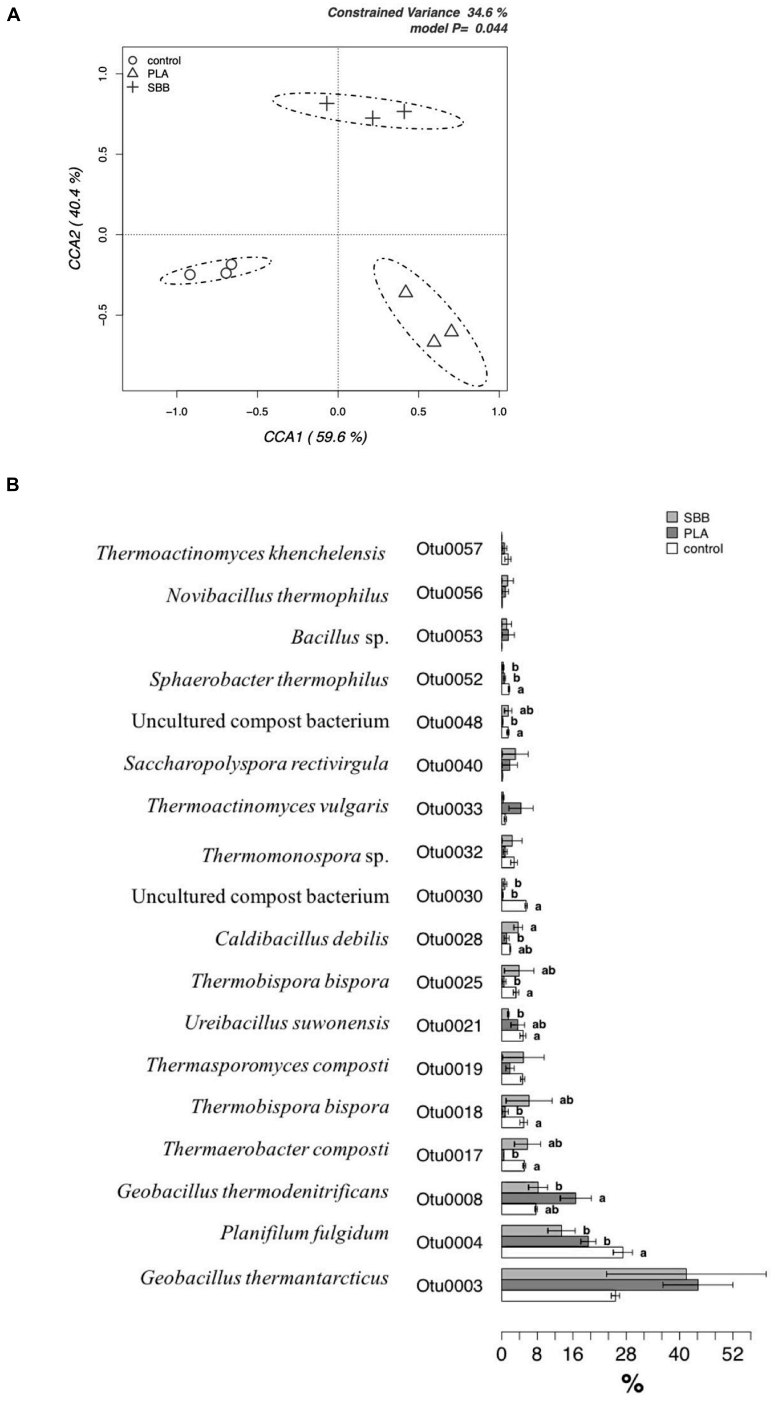

FIGURE 7
The bacterial community in compost. **(A)** Hypothesis-driven canonical correspondence analysis (CCA) model performed on the total bacterial OTUs relative abundance data from composts of each treatment (OFMSW, control; PLA; SBB). **(B)** Metastats model on the relative abundances of genera comprising 99.9% of each treatment's bacterial diversity in composts (OFMSW, control; PLA; SBB). OTUs showing significant differences according to the false discovery rate correction are highlighted with letters. PLA, polylactic acid; SBB, starch-based bioplastic; OFMSW, organic fraction of municipal solid waste.

Otherwise, the composts obtained from the treatment of the two bioplastics reported a wider fungal diversity, which was both positively correlated with the CCA1 axes.

In order to identify any significant differences between composts in terms of their distribution of the most abundant OTUs, a detailed analysis was carried out using a Metastats

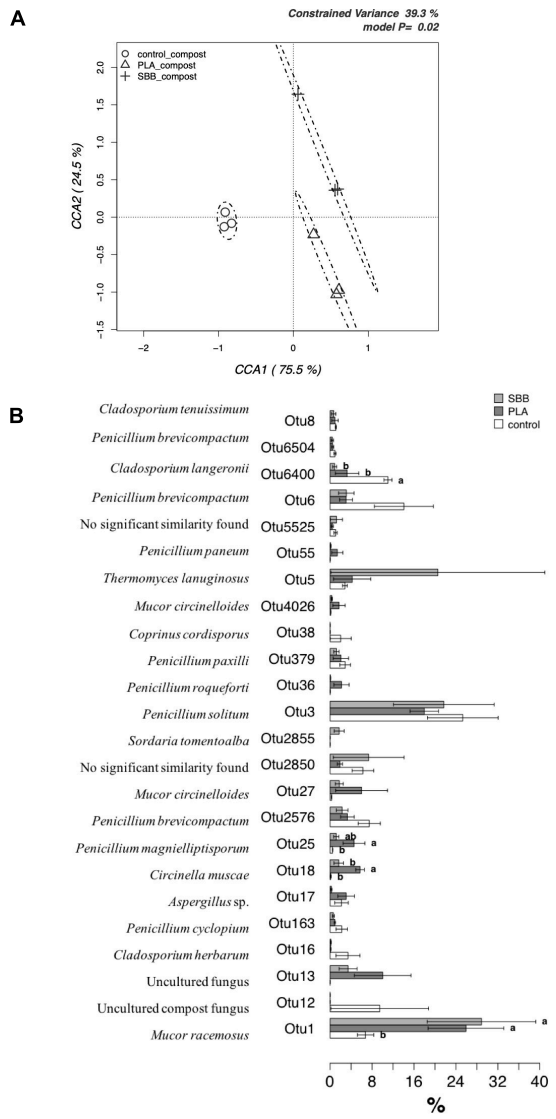

FIGURE 8
Fungal community in compost. **(A)** Hypothesis-driven canonical correspondence analysis (CCA) model performed on the total fungal OTUs relative abundance data from composts of each treatment (OFMSW, control; PLA; SBB). **(B)** Metastats model on the relative abundances of genera comprising 99.9% of each treatment's fungal diversity in composts (OFMSW, control; PLA; SBB). OTUs showing significant differences according to the false discovery rate correction are highlighted with letters. PLA, polylactic acid; SBB, starch-based bioplastic; OFMSW, organic fraction of municipal solid waste.

model (**Figure 8B**). *M. racemosus* (OTU1) was the only fungal OTU detected even in the anaerobic digestion and with a higher abundance than the others in several samples. In the compost from SBB and PLA, it was found with an abundance >24%, resulting statistically different from the positive control. Since different strains can produce lipase, gelatinase, xylanase, amylase, and caseinase enzyme (Silawat et al., 2013), highlighting its biodegradable role in composting process. Its greater abundance in compost from bioplastics treatment may be due to the higher carbon availability from the polymers used. The *Cladosporium* genus has the ability to produce cellulolytic and xylanolytic enzymes (Gupta et al., 2003; Fapohunda, 2006) and was also identified as PLA colonizing fungi (Karamanlioglu et al., 2014), but only the OTU6400 (*Cladosporium langeronii*) was found in abundance in PLA compost. The OTUs identified belonging to the genus *Penicillium*, being a good producer of various extracellular enzymes, is considered a crucial decomposer-recycler of organic matter of all types (Hee-Yeon et al., 2007; Li and Zong, 2010). Furthermore, *Penicillium solitum* (OTU3) was among the most abundant OTU, accounting for more than 16–24% of sequences for the three composts without statistically significant differences. This fungus was isolated from domestic compost and it is exploited for its extracellular lipases, which are more active on longer chained substrates (Chinaglia et al., 2014). However, there are no studies in the literature on the possible relationship of this species with bioplastics. On the contrary, some OTUs were particularly abundant in samples from bioplastics treatment, hypothesizing that they may play a key role in their biodegradation in thermophilic composting environments. On the one hand, OTU18 (*Circinella muscae*), OTU25 (*Penicillium magnielliptisporum*), and OTU27 (*Mucor circinelloides*) were mainly found in PLA compost, but no reference to the possible affinity of these fungi with bioplastics was found in the literature. On the other hand, *Penicillium roqueforti* (OTU36), due to its ability to totally assimilate DL-lactic acid, partially soluble racemic oligomers, and nitrogen source, was isolated as PLA-degrading microorganism (Torres et al., 1996). Since it was found only in the compost obtained from this treatment, its role may be to degrade PLA with promising potentials. In composts obtained from SBB treatment, OTU2855 (*Sordaria tomentoalba*) and OTU5 (*Thermomyces lanuginosus*) were more abundant compared to the other samples. *T. lanuginosus* is a polyester-degrading thermophilic bacterium able to hydrolyze the aromatic poly(trimethylene terephthalate) (PTT) (Eberl et al., 2008) and polyurethane (PU) (Zafar et al., 2014), but there are no references in the literature about this fungus associated with SBB. To summarize, our results suggested that PLA and SBB may influence and modulate the fungal community involved during the thermophilic aerobic composting of OFMSW.

Conclusion

This work gain insight into the microbial structures during the anaerobic digestion and aerobic composting of OFMSW with PLA and SBB, giving a new approach to understanding the microbial activity of bacteria, archaea, and fungi involved and hypothesizing the relationship between these

microorganisms and the different tested materials. Our results suggest that these materials shape microbial communities at different stages of the process, but their effect is most evident in the aerobic composting phase. Distinctive bacteria and fungi were detected in PLA and SBB treatment, suggesting a possible role of these materials in establishing different substrate conditions for their growth probably due to the presence and/or release of additives, chemicals, and plasticizers. Among fungi, *P. roqueforti* was found only in compost from PLA treatment and *T. lanuginosus* in that from SBB. Moreover, through a culturable isolation approach, the microorganisms found on each specific material may be exploited to enhance their biodegradation in contaminated environments. Certainly, a fundamental role is also played by the process parameters, which define the primary conditions for the growth of the different microbial groups involved. To better understand the fate and impacts of these biopolymers, further studies should focus on the microbial activity in the process and the feasibility of allowing these materials in food waste collection management. It is critical to understand whether bioplastics may lead to operational challenges not only in physical biodegradation but also in microbiological aspects, and the full extent of biodegradability of bioplastics must be discussed so that the existing plants can determine how to better process them.

Data availability statement

The datasets presented in this study can be found in online repositories. The names of the repository/repositories and accession number(s) can be found below: NCBI – PRJNA883589.

Author contributions

FB: conceptualization, methodology, formal analysis, and writing—original draft. FV: conceptualization and methodology. MS and SP: methodology—anaerobic digestion tests. CM, GB, and ET: methodology. PC: conceptualization, writing—review and editing, and supervision. EP: conceptualization, software, formal analysis, resources, writing—review and editing, supervision, project administration, and funding acquisition. All authors contributed to the article and approved the submitted version.

Acknowledgments

We are grateful to Sotirios Vasileiadis for a number of scripts used for the analyses of NGS Illumina data.

Conflict of interest

Authors MS and SP were employed by the Centro Ricerche Produzioni Animali S.p.A.

The remaining authors declare that the research was conducted in the absence of any commercial or financial relationships that could be construed as a potential conflict of interest.

Publisher's note

Supplementary material

The Supplementary Material for this article can be found online at: https://www.frontiersin.org/articles/10.3389/fmicb.2022.1035561/full#supplementary-material

References

Abe, M. M., Branciforti, M. C., and Brienzo, M. (2021). Biodegradation of hemicellulose-cellulose-starch-based bioplastics and microbial polyesters. *Recycling* 6:22.

Achmon, Y., Claypool, J. T., Pace, S., Simmons, B. A., Singer, S. W., and Simmons, C. W. (2019). Assessment of biogas production and microbial ecology in a high solid anaerobic digestion of major California food processing residues. *Bioresour. Technol. Rep.* 5, 1–11. doi: 10.1016/j.biteb.2018.11.007

Bandini, F., Misci, C., Taskin, E., Cocconcelli, P. S., and Puglisi, E. (2020). Biopolymers modulate microbial communities in municipal organic waste digestion. *FEMS Microbiol. Ecol.* 96:fiaa183. doi: 10.1093/femsec/fiaa183

Bandini, F., Taskin, E., Vaccari, F., Soldano, M., Piccinini, S., Frache, A., et al. (2022). Anaerobic digestion and aerobic composting of rigid biopolymers in bio-waste treatment: fate and effects on the final compost. *Bioresour. Technol.* 351:126934. doi: 10.1016/j.biortech.2022.126934

Bandte, M., Schleusner, Y., Heiermann, M., Plöchl, M., and Büttner, C. (2013). Viability of plant–pathogenic fungi reduced by anaerobic digestion. *BioEnergy Res.* 6, 966–973.

Bartram, A. K., Lynch, M. D. J., Stearns, J. C., Moreno-Hagelsieb, G., and Neufeld, J. D. (2011). Generation of multimillion-sequence 16S rRNA gene libraries from complex microbial communities by assembling paired-end Illumina reads. *Appl. Environ. Microbiol.* 77, 3846–3852. doi: 10.1128/AEM.02772-10

Berry, D., Mahfoudh, K., Ben, Wagner, M., and Loy, A. (2011). Barcoded primers used in multiplex amplicon pyrosequencing bias amplification. *Appl. Environ. Microbiol.* 77, 7846–7849. doi: 10.1128/AEM.05220-11

Bortolini, C., Patrone, V., Puglisi, E., and Morelli, L. (2016). Detailed analyses of the bacterial populations in processed cocoa beans of different geographic origin, subject to varied fermentation conditions. *Int. J. Food Microbiol.* 236, 98–106. doi: 10.1016/j.ijfoodmicro.2016.07.004

Bouanane-Darenfed, A., Hania, W., Ben, Hacene, H., Cayol, J.-L., Ollivier, B., et al. (2013). Caldicoprobacter guelmensis sp. nov., a thermophilic, anaerobic, xylanolytic bacterium isolated from a hot spring. *Int. J. Syst. Evol. Microbiol.* 63, 2049–2053. doi: 10.1099/ijs.0.043497-0

Butbunchu, N., and Pathom-Aree, W. (2019). Actinobacteria as promising candidate for polylactic acid type bioplastic degradation. *Front. Microbiol.* 10:2834. doi: 10.3389/fmicb.2019.02834

Calabrò, P. S., and Grosso, M. (2019). Bioplastics and waste management. *Waste Manag.* 78, 800–801. doi: 10.1016/j.wasman.2018.06.054

Cao, G., Song, T., Shen, Y., Jin, Q., Feng, W., Fan, L., et al. (2019). Diversity of bacterial and fungal communities in wheat straw compost for Agaricus bisporus cultivation. *Hortscience* 54, 100–109.

Chinaglia, S., Chiarelli, L. R., Maggi, M., Rodolfi, M., Valentini, G., and Picco, A. M. (2014). Biochemistry of lipolytic enzymes secreted by Penicillium solitum and Cladosporium cladosporioides. *Biosci. Biotechnol. Biochem.* 78, 245–254. doi: 10.1080/09168451.2014.882752

CIC-COREPLA (2020). *Studio CIC-COREPLA, 2020: Triplicano le Bioplastiche Compostabili Nella Raccolta Dell'organico. [Study of the the Italian Composting and Biogas Association and the Italian National Consortium for the Collection and Recycling of Plastic Packages: Compostable Bioplastics in the Organic Waste Collection Tripled]*. Italy: COREPLA.

Coorevits, A., Dinsdale, A. E., Halket, G., Lebbe, L., De Vos, P., Van Landschoot, A., et al. (2012). Taxonomic revision of the genus *Geobacillus*: emendation of *Geobacillus*, *G. stearothermophilus*, *G. jurassicus*, *G. toebii*, *G. thermodenitrificans* and *G. thermoglucosidans* (nom. corrig., formerly 'thermoglucosidasius'); transfer of Bacillus thermantarcticus. *Int. J. Syst. Evol. Microbiol.* 62, 1470–1485.

Corbellini, V., Kougias, P. G., Treu, L., Bassani, I., Malpei, F., and Angelidaki, I. (2018). Hybrid biogas upgrading in a two-stage thermophilic reactor. *Energy Convers. Manag.* 168, 1–10.

Daas, M. J. A., Vriesendorp, B., van de Weijer, A. H. P., van der Oost, J., and van Kranenburg, R. (2018). Complete genome sequence of Geobacillus thermodenitrificans T12, a potential host for biotechnological applications. *Curr. Microbiol.* 75, 49–56. doi: 10.1007/s00284-017-1349-0

Di Cagno, R., Pontonio, E., Buchin, S., De Angelis, M., Lattanzi, A., Valerio, F., et al. (2014). Diversity of the lactic acid bacterium and yeast microbiota in the switch from firm-to liquid-sourdough fermentation. *Appl. Environ. Microbiol.* 80, 3161–3172. doi: 10.1128/AEM.00309-14

Dixon, P. (2003). Computer program review VEGAN, a package of R functions for community ecology. *J. Veg. Sci.* 14, 927–930. doi: 10.1111/j.1654-1103.2002.tb02049.x

Eberl, A., Heumann, S., Kotek, R., Kaufmann, F., Mitsche, S., Cavaco-Paulo, A., et al. (2008). Enzymatic hydrolysis of PTT polymers and oligomers. *J. Biotechnol.* 135, 45–51. doi: 10.1016/j.jbiotec.2008.02.015

EN13432 (2002). *Requirements for packaging recoverable through composting and biodegradation-Test scheme and evaluation criteria for the final acceptance of packaging.*

Endres, H.-J. (2017). Bioplastics. *Adv Biochem Eng Biotechnol.* 166, 427–468.

European Bioplastics (2020). *Bioplastics Market Data*. Berlin: Bioplastics Europe.

Facey, H. V., Northwood, K. S., and Wright, A. G. (2012). Molecular diversity of methanogens in fecal samples from captive *S umatran* Orangutans (P ongo abelii). *Am. J. Primatol.* 74, 408–413. doi: 10.1002/ajp.21992

Fapohunda, S. O. (2006). Production of lipase and toxic metabolites by *Cladosporium cladosporioides* under varied conditions. *Mycol. Balc.* 3, 89–93.

Fernández-Rodríguez, J., Pérez, M., and Romero, L. I. (2013). Comparison of mesophilic and thermophilic dry anaerobic digestion of OFMSW: Kinetic analysis. *Chem. Eng. J.* 232, 59–64.

Fisgativa, H., Tremier, A., Le Roux, S., Bureau, C., and Dabert, P. (2017). Understanding the anaerobic biodegradability of food waste: Relationship between the typological, biochemical and microbial characteristics. *J. Environ. Manag.* 188, 95–107. doi: 10.1016/j.jenvman.2016.11.058

Folino, A., Karageorgiou, A., Calabrò, P. S., and Komilis, D. (2020). Biodegradation of wasted bioplastics in natural and industrial environments: A review. *Sustainability* 12:6030.

Fricke, W. F., Seedorf, H., Henne, A., Krüer, , M., Liesegang, H., Hedderich, R., et al. (2006). The genome sequence of *Methanosphaera stadtmanae* reveals why this human intestinal archaeon is restricted to methanol and H2 for methane formation and ATP synthesis. *J. Bacteriol.* 188, 642–658. doi: 10.1128/JB.188.2.642-658.2006

Geyer, R., Jambeck, J. R., and Law, K. L. (2017). Production, use, and fate of all plastics ever made. *Sci. Adv.* 3:e1700782.

Goberna, M., Gadermaier, M., Franke-Whittle, I. H., García, C., Wett, B., and Insam, H. (2015). Start-up strategies in manure-fed biogas reactors: Process parameters and methanogenic communities. *Biomass Bioenergy* 75, 46–56.

Gómez, E. F., and Michel, F. C. Jr. (2013). Biodegradability of conventional and bio-based plastics and natural fiber composites during composting, anaerobic digestion and long-term soil incubation. *Polym. Degrad. Stab.* 98, 2583–2591.

Good, I. J. (1953). The population frequencies of species and the estimation of population parameters. *Biometrika* 40, 237–264.

Granada, C. E., Hasan, C., Marder, M., Konrad, O., Vargas, L. K., Passaglia, L. M. P., et al. (2018). Biogas from slaughterhouse wastewater anaerobic digestion is driven by the archaeal family Methanobacteriaceae and bacterial families *Porphyromonadaceae* and *Tissierellaceae*. *Renew. Energy* 118, 840–846. doi: 10.1016/j.renene.2017.11.077

Gu, J.-D., Eberiel, D. T., McCarthy, S. P., and Gross, R. A. (1993). Cellulose acetate biodegradability upon exposure to simulated aerobic composting and anaerobic bioreactor environments. *J. Environ. Polym. Degrad.* 1, 143–153.

Gupta, R., Rathi, P., Gupta, N., and Bradoo, S. (2003). Lipase assays for conventional and molecular screening: an overview. *Biotechnol. Appl. Biochem.* 37, 63–71. doi: 10.1042/ba20020059

Hanajima, D., Haruta, S., Hori, T., Ishii, M., Haga, K., and Igarashi, Y. (2009). Bacterial community dynamics during reduction of odorous compounds in aerated pig manure slurry. *J. Appl. Microbiol.* 106, 118–129. doi: 10.1111/j.1365-2672.2008.03984.x

Harrison, J. P., Boardman, C., O'Callaghan, K., Delort, A.-M., and Song, J. (2018). Biodegradability standards for carrier bags and plastic films in aquatic environments: a critical review. *R. Soc. Open Sci.* 5:171792. doi: 10.1098/rsos.171792

Hee-Yeon, C. H., Bancerz, R., Ginalska, G., Leonowicz, A., Nam–Seok, C. H. O., and Shoji, O. (2007). Culture conditions of psychrotrophic fungus, Penicillium chrysogenum and its lipase characteristics. *J. Fac. Agr. Kyushu Univ.* 52, 281–286.

Jackson, S. A., Kang, X., O'Shea, R., O'Leary, N., Murphy, J. D., and Dobson, A. D. W. (2020). Anaerobic digestion performance and microbial community structures in biogas production from whiskey distillers organic by-products. *Bioresour. Technol. Rep.* 12:100565.

Javierre, C., Sarasa, J., Claveria, I., and Fernández, A. (2015). Study of the biodisintegration on a painted bioplastic material waste. *Mater. Plast.* 52, 116–121. doi: 10.1016/j.biortech.2008.11.049

Jiang, B., Kauffman, A. E., Li, L., McFee, W., Cai, B., Weinstein, J., et al. (2020). Health impacts of environmental contamination of micro- And nanoplastics: A review. *Environ. Health Prev. Med.* 25, 1–15. doi: 10.1186/s12199-020-00870-9

Kale, G., Kijchavengkul, T., Auras, R., Rubino, M., Selke, S. E., and Singh, S. P. (2007). Compostability of bioplastic packaging materials?: An overview. *Macromol. Biosci.* 7, 255–277. doi: 10.1002/mabi.200600168

Kang, Y.-R., Su, Y., Wang, J., Chu, Y.-X., Tian, G., and He, R. (2021). Effects of different pretreatment methods on biogas production and microbial community in anaerobic digestion of wheat straw. *Environ. Sci. Pollut. Res.* 28, 51772–51785. doi: 10.1007/s11356-021-14296-5

Kanhai, L. D. K., Gardfeldt, K., Krumpen, T., Thompson, R. C., and O'Connor, I. (2020). Microplastics in sea ice and seawater beneath ice floes from the Arctic Ocean. *Sci. Rep.* 10, 1–11. doi: 10.1038/s41598-020-61948-6

Karamanlioglu, M., and Robson, G. D. (2013). The influence of biotic and abiotic factors on the rate of degradation of poly(lactic) acid (PLA) coupons buried in compost and soil. *Polym. Degrad. Stab.* 98, 2063–2071. doi: 10.1016/j.polymdegradstab.2013.07.004

Karamanlioglu, M., Houlden, A., and Robson, G. D. (2014). Isolation and characterisation of fungal communities associated with degradation and growth on the surface of poly (lactic) acid (PLA) in soil and compost. *Int. Biodeterior. Biodegrad.* 95, 301–310.

Karamanlioglu, M., Preziosi, R., and Robson, G. D. (2017). Abiotic and biotic environmental degradation of the bioplastic polymer poly (lactic acid): a review. *Polym. Degrad. Stab.* 137, 122–130.

Karbalaei, S., Hanachi, P., Walker, T. R., and Cole, M. (2018). Occurrence, sources, human health impacts and mitigation of microplastic pollution. *Environ. Sci. Pollut. Res.* 25, 36046–36063. doi: 10.1007/s11356-018-3508-7

Ke, G.-R., Lai, C.-M., Liu, Y.-Y., and Yang, S.-S. (2010). Inoculation of food waste with the thermo-tolerant lipolytic actinomycete *Thermoactinomyces vulgaris* A31 and maturity evaluation of the compost. *Bioresour. Technol.* 101, 7424–7431. doi: 10.1016/j.biortech.2010.04.051

Kim, M. D., Song, M., Jo, M., Shin, S. G., Khim, J. H., and Hwang, S. (2010). Growth condition and bacterial community for maximum hydrolysis of suspended organic materials in anaerobic digestion of food waste-recycling wastewater. *Appl. Microbiol. Biotechnol.* 85, 1611–1618. doi: 10.1007/s00253-009-2316-x

Koch, D., and Mihalyi, B. (2018). Assessing the change in environmental impact categories when replacing conventional plastic with bioplastic in chosen application fields. *Chem. Eng. Trans.* 70, 853–858.

Koeck, D. E., Mechelke, M., Zverlov, V. V., Liebl, W., and Schwarz, W. H. (2016). Herbivorax saccincola gen. nov., sp. nov., a cellulolytic, anaerobic, thermophilic bacterium isolated via in sacco enrichments from a lab-scale biogas reactor. *Int. J. Syst. Evol. Microbiol.* 66, 4458–4463. doi: 10.1099/ijsem.0.001374

Lee, J., Hwang, B., Koo, T., Shin, S. G., Kim, W., and Hwang, S. (2014). Temporal variation in methanogen communities of four different full-scale anaerobic digesters treating food waste-recycling wastewater. *Bioresour. Technol.* 168, 59–63. doi: 10.1016/j.biortech.2014.03.161

Lhomme, E., Lattanzi, A., Dousset, X., Minervini, F., De Angelis, M., Lacaze, G., et al. (2015). Lactic acid bacterium and yeast microbiotas of sixteen French traditional sourdoughs. *Int. J. Food Microbiol.* 215, 161–170. doi: 10.1016/j.ijfoodmicro.2015.09.015

Li, N., and Zong, M.-H. (2010). Lipases from the genus Penicillium: production, purification, characterization and applications. *J. Mol. Catal. B Enzym.* 66, 43–54.

Li, Y. F., Nelson, M. C., Chen, P. H., Graf, J., Li, Y., and Yu, Z. (2015). Comparison of the microbial communities in solid-state anaerobic digestion (SS-AD) reactors operated at mesophilic and thermophilic temperatures. *Appl. Microbiol. Biotechnol.* 99, 969–980. doi: 10.1007/s00253-014-6036-5

Ma, S., Huang, Y., Wang, C., Fan, H., Dai, L., Zhou, Z., et al. (2017). Defluviitalea raffinosedens sp. nov., a thermophilic, anaerobic, saccharolytic bacterium isolated from an anaerobic batch digester treating animal manure and rice straw. *Int. J. Syst. Evol. Microbiol.* 67:1607. doi: 10.1099/ijsem.0.001664

Maharachchikumbura, S. S. N., Hyde, K. D., Jones, E. B. G., McKenzie, E. H. C., Bhat, J. D., Dayarathne, M. C., et al. (2016). Families of sordariomycetes. *Fungal Divers.* 79, 1–317.

Massardier-nageotte, V., Pestre, C., Cruard-pradet, T., and Bayard, R. (2006). Aerobic and anaerobic biodegradability of polymer films and physico-chemical characterization. *Polym. Degrad. Stab.* 91, 620–627. doi: 10.1016/j.polymdegradstab.2005.02.029

Micolucci, F., Gottardo, M., Cavinato, C., Pavan, P., and Bolzonella, D. (2016). Mesophilic and thermophilic anaerobic digestion of the liquid fraction of pressed biowaste for high energy yields recovery. *Waste Manag.* 48, 227–235. doi: 10.1016/j.wasman.2015.09.031

Micolucci, F., Gottardo, M., Pavan, P., Cavinato, C., and Bolzonella, D. (2018). Pilot scale comparison of single and double-stage thermophilic anaerobic digestion of food waste. *J. Clean. Prod.* 171, 1376–1385.

Mohee, R., Unmar, G. D., Mudhoo, A., and Khadoo, P. (2008). Biodegradability of biodegradable/degradable plastic materials under aerobic and anaerobic conditions. *Waste Manag.* 28, 1624–1629. doi: 10.1016/j.wasman.2007.07.003

Nair, N. R., Sekhar, V. C., and Nampoothiri, K. M. (2016). Augmentation of a Microbial Consortium for Enhanced Polylactide (PLA) Degradation. *Indian J. Microbiol.* 56, 59–63. doi: 10.1007/s12088-015-0559-z

Ng, E. L., Huerta Lwanga, E., Eldridge, S. M., Johnston, P., Hu, H. W., Geissen, V., et al. (2018). An overview of microplastic and nanoplastic pollution in agroecosystems. *Sci. Total Environ.* 627, 1377–1388. doi: 10.1016/j.scitotenv.2018.01.341

Olivera, C., Tondo, M. L., Girardi, V., Fattobene, L., Herrero, M. S., Pérez, L. M., et al. (2022). Early-stage response in anaerobic bioreactors due to high sulfate loads: Hydrogen sulfide yield and other organic volatile sulfur compounds as a sign of microbial community modifications. *Bioresour. Technol.* 350:126947. doi: 10.1016/j.biortech.2022.126947

Oranusi, S. U., and Dahunsi, S. O. (2013). Co-digestion of food waste and human excreta for biogas production. *Br. Biotechnol. J.* 3, 485–499.

Paul, M. B., Stock, V., Cara-Carmona, J., Lisicki, E., Shopova, S., Fessard, V., et al. (2020). Micro-and nanoplastics–current state of knowledge with the focus on oral uptake and toxicity. *Nanoscale Adv.* 2, 4350–4367. doi: 10.1039/d0na00539h

Paulson, J. N., Pop, M., and Bravo, H. C. (2011). Metastats: an improved statistical method for analysis of metagenomic data. *Genome Biol.* 12:17. doi: 10.1371/journal.pcbi.1000352

Peng, W., Wang, Z., Shu, Y., Lü, F., Zhang, H., Shao, L., et al. (2022). Fate of a biobased polymer via high-solid anaerobic co-digestion with food waste and following aerobic treatment: Insights on changes of polymer physicochemical properties and the role of microbial and fungal communities. *Bioresour. Technol.* 343:126079. doi: 10.1016/j.biortech.2021.126079

Plastics Europe (2020). Plastics-the facts 2020. *Plastic Eur.* 1, 1–64. Available online at: https://plasticseurope.org/knowledge-hub/plastics-the-facts-2020/

Puglisi, E., Romaniello, F., Galletti, S., Boccaleri, E., Frache, A., and Cocconcelli, P. S. (2019). Selective bacterial colonization processes on polyethylene waste samples in an abandoned landfill site. *Sci. Rep.* 9, 1–13. doi: 10.1038/s41598-019-50740-w

Qin, S., Wainaina, S., Awasthi, S. K., Mahboubi, A., Liu, T., Liu, H., et al. (2021). Fungal dynamics during anaerobic digestion of sewage sludge combined with food waste at high organic loading rates in immersed membrane bioreactors. *Bioresour. Technol.* 335:125296. doi: 10.1016/j.biortech.2021.125296

Raskin, L., Stromley, J. M., Rittmann, B. E., and Stahl, D. A. (1994). Group-specific 16S rRNA hybridization probes to describe natural communities of methanogens. *Appl. Environ. Microbiol.* 60, 1232–1240. doi: 10.1128/aem.60.4.1232-1240.1994

Rhodes, C. J. (2019). Solving the plastic problem: from cradle to grave, to reincarnation. *Sci. Prog.* 102, 218–248. doi: 10.1177/0036850419867204

Rujnić-Sokele, M., and Pilipović, A. (2017). Challenges and opportunities of biodegradable plastics: A mini review. *Waste Manag. Res.* 35, 132–140. doi: 10.1177/0734242X16683272

Rundberget, T., Skaar, I., and Flåøyen, A. (2004). The presence of *Penicillium* and *Penicillium mycotoxins* in food wastes. *Int. J. Food Microbiol.* 90, 181–188.

Ryckeboer, J., Mergaert, J., Vaes, K., Klammer, S., De Clercq, D., Coosemans, J., et al. (2003). A survey of bacteria and fungi occurring during composting and self-heating processes. *Ann. Microbiol.* 53, 349–410.

Sarasa, J., Gracia, J. M., and Javierre, C. (2009). Bioresource technology study of the biodisintegration of a bioplastic material waste. *Bioresour. Technol.* 100, 3764–3768.

Schloss, P. D., Westcott, S. L., Ryabin, T., Hall, J. R., Hartmann, M., Hollister, E. B., et al. (2009). Introducing mothur: Open-source, platform-independent, community-supported software for describing and comparing microbial communities. *Appl. Environ. Microbiol.* 75, 7537–7541. doi: 10.1128/AEM.01541-09

Shamsuddin, I. M., Jafar, J. A., Shawai, A. S. A., Yusuf, S., Lateefah, M., and Aminu, I. (2017). Bioplastics as better alternative to petroplastics and their role in national sustainability: a review. *Adv. Biosci. Bioeng.* 5:63.

Shrestha, A., van-Eerten Jansen, M. C. A. A., and Acharya, B. (2020). Biodegradation of bioplastic using anaerobic digestion at retention time as per industrial biogas plant and international norms. *Sustainability* 12:4231.

Silawat, N., Batav, N., Chouhan, S., Sairkar, P., Garg, R. K., and Singh, R. K. (2013). Fungal flora of vermicompost and organic manure: a case study of molecular diversity of *Mucor racemosus* using RAPD analysis. *Biosci. Biotechnol. Res. Asia* 10, 509–514.

Simankova, M. V., Chernych, N. A., Osipov, G. A., and Zavarzin, G. A. (1993). Halocella cellulolytica gen. nov., sp. nov., a new obligately anaerobic, halophilic, cellulolytic bacterium. *Syst. Appl. Microbiol.* 16, 385–389.

Sisto, R., Zhu, X., Lombardi, M., and Prosperi, M. (2018). Production of bioplastics for agricultural purposes: A supply chain study. *Riv. Stud. Sulla Sosten.* 119–136. doi: 10.3280/RISS2018-001010

Soh, A. L. A., Ralambotiana, H., Ollivier, B., Prensier, G., Tine, E., and Garcia, J.-L. (1991). *Clostridium thermopalmarium* sp. nov., a moderately thermophilic butyrate-producing bacterium isolated from palm wine in Senegal. *Syst. Appl. Microbiol.* 14, 135–139.

Song, J. H., Murphy, R. J., Narayan, R., Davies, G. B. H., Engineering, M., and Ub, M. (2009). Biodegradable and compostable alternatives to conventional plastics. 364, 2127–2139. doi: 10.1098/rstb.2008.0289

Sousa, D. Z., Smidt, H., Alves, M. M., and Stams, A. J. M. (2007). Syntrophomonas zehnderi sp. nov., an anaerobe that degrades long-chain fatty acids in co-culture with Methanobacterium formicicum. *Int. J. Syst. Evol. Microbiol.* 57, 609–615. doi: 10.1099/ijs.0.64734-0

Spaccini, R., Todisco, D., Drosos, M., Nebbioso, A., and Piccolo, A. (2016). Decomposition of bio-degradable plastic polymer in a real on-farm composting process. *Chem. Biol. Technol. Agric.* 3, 1–12.

Sposob, M., Moon, H.-S., Lee, D., Kim, T.-H., and Yun, Y.-M. (2020). Comprehensive analysis of the microbial communities and operational parameters of two full-scale anaerobic digestion plants treating food waste in South Korea: Seasonal variation and effect of ammonia. *J. Hazard. Mater.* 398:122975. doi: 10.1016/j.jhazmat.2020.122975

Steger, K., Eklind, Y., Olsson, J., and Sundh, I. (2005). Microbial community growth and utilization of carbon constituents during thermophilic composting at different oxygen levels. *Microb. Ecol.* 50, 163–171. doi: 10.1007/s00248-004-0139-y

Steger, K., Jarvis, Å, Vasara, T., Romantschuk, M., and Sundh, I. (2007). Effects of differing temperature management on development of *Actinobacteria* populations during composting. *Res. Microbiol.* 158, 617–624. doi: 10.1016/j.resmic.2007.05.006

Suwannarat, J., and Ritchie, R. J. (2015). Anaerobic digestion of food waste using yeast. *Waste Manag.* 42, 61–66.

Takai, K., and Horikoshi, K. (2000). Rapid detection and quantification of members of the archaeal community by quantitative PCR using fluorogenic probes. *Appl. Environ. Microbiol.* 66, 5066–5072. doi: 10.1128/AEM.66.11.5066-5072.2000

Thakur, S., Chaudhary, J., and Sharma, B. (2018). ScienceDirect Sustainability of bioplastics?: Opportunities and challenges. *Curr. Opin. Green Sustain. Chem.* 13, 68–75. doi: 10.1016/j.cogsc.2018.04.013

Tomita, K., Nakajima, T., Kikuchi, Y., and Miwa, N. (2004). Degradation of poly (L-lactic acid) by a newly isolated thermophile. *Polym. Degrad. Stab.* 84, 433–438.

Torp, M., and Skaar, I. (1998). "Moulds in food wastes for animal feeds-occurrence and potential mycotoxin production," in *Preliminary results in husdyrforsoeksmoetet 1998, aas (Norway), 10-11 Feb 1998* (Oslo: Forskningsparken i Aas AS).

Torres, A., Li, S. M., Roussos, S., and Vert, M. (1996). Screening of microorganisms for biodegradation of poly(lactic acid) and lactic acid-containing polymers. *Appl. Environ. Microbiol.* 62, 2393–2397. doi: 10.1128/aem.62.7.2393-2397.1996

Toussaint, B., Raffael, B., Angers-Loustau, A., Gilliland, D., Kestens, V., Petrillo, M., et al. (2019). Review of micro-and nanoplastic contamination in the food chain. *Food Addit. Contam. Part A* 36, 639–673.

Vajna, B., Szili, D., Nagy, A., and Márialigeti, K. (2012). An improved sequence-aided T-RFLP analysis of bacterial succession during oyster mushroom substrate preparation. *Microb. Ecol.* 64, 702–713. doi: 10.1007/s00248-012-0063-5

Vasileiadis, S., Puglisi, E., Trevisan, M., Scheckel, K. G., Langdon, K. A., McLaughlin, M. J., et al. (2015). Changes in soil bacterial communities and diversity in response to long-term silver exposure. *FEMS Microbiol. Ecol.* 91, 1–11. doi: 10.1093/femsec/fiv114

Wang, J., Liu, X., Li, Y., Powell, T., Wang, X., Wang, G., et al. (2019). Microplastics as contaminants in the soil environment: A mini-review. *Sci. Total Environ.* 691, 848–857. doi: 10.1016/j.scitotenv.2019.07.209

Wang, P., Qiao, Z., Li, X., Su, Y., and Xie, B. (2020). Functional characteristic of microbial communities in large-scale biotreatment systems of food waste. *Sci. Total Environ.* 746:141086. doi: 10.1016/j.scitotenv.2020.141086

Wang, P., Wang, H., Qiu, Y., Ren, L., and Jiang, B. (2018). Microbial characteristics in anaerobic digestion process of food waste for methane production–A review. *Bioresour. Technol.* 248, 29–36. doi: 10.1016/j.biortech.2017.06.152

Wang, W., Yan, L., Cui, Z., Gao, Y., Wang, Y., and Jing, R. (2011). Characterization of a microbial consortium capable of degrading lignocellulose. *Bioresour. Technol.* 102, 9321–9324.

White, T. J., Bruns, T., Lee, S., and Taylor, J. (1990). Amplification and direct sequencing of fungal ribosomal RNA genes for phylogenetics. *PCR Protoc. Guid. Appl.* 18, 315–322.

Yabe, S., Kato, A., Hazaka, M., and Yokota, A. (2009). Thermaerobacter composti sp. nov., a novel extremely thermophilic bacterium isolated from compost. *J. Gen. Appl. Microbiol.* 55, 323–328. doi: 10.2323/jgam.55.323

Yang, Z., Guo, R., Shi, X., He, S., Wang, L., Dai, M., et al. (2016). Bioaugmentation of Hydrogenispora ethanolica LX-B affects hydrogen production through altering indigenous bacterial community structure. *Bioresour. Technol.* 211, 319–326. doi: 10.1016/j.biortech.2016.03.097

Ye, Y., Gan, J., and Hu, B. (2015). Screening of phosphorus-accumulating fungi and their potential for phosphorus removal from waste streams. *Appl. Biochem. Biotechnol.* 177, 1127–1136. doi: 10.1007/s12010-015-1801-1

Zafar, U., Nzeram, P., Langarica-Fuentes, A., Houlden, A., Heyworth, A., Saiani, A., et al. (2014). Biodegradation of polyester polyurethane during commercial composting and analysis of associated fungal communities. *Bioresour. Technol.* 158, 374–377.

Zhang, C., Li, T., Su, G., and He, J. (2020). Enhanced direct fermentation from food waste to butanol and hydrogen by an amylolytic Clostridium. *Renew. Energy* 153, 522–529.

Zhang, H., Wang, W., Li, Z., Yang, C., Liang, S., and Wang, L. (2021). *Planifilum fulgidum* is the dominant functional microorganism in compost containing spent mushroom substrate. *Sustainability* 13:10002.

Zhang, J., Lv, C., Tong, J., Liu, J., Liu, J., Yu, D., et al. (2016). Optimization and microbial community analysis of anaerobic co-digestion of food waste and sewage sludge based on microwave pretreatment. *Bioresour. Technol.* 200, 253–261. doi: 10.1016/j.biortech.2015.10.037

Zhang, N., Castlebury, L. A., Miller, A. N., Huhndorf, S. M., Schoch, C. L., Seifert, K. A., et al. (2006). An overview of the systematics of the Sordariomycetes based on a four-gene phylogeny. *Mycologia* 98, 1076–1087. doi: 10.3852/mycologia.98.6.1076

Zhang, Y., Li, L., Kong, X., Zhen, F., Wang, Z., Sun, Y., et al. (2017). Inhibition effect of sodium concentrations on the anaerobic digestion performance of Sargassum species. *Energy Fuels* 31, 7101–7109.

Zheng, L., Xu, Y., Geng, H., and Dai, X. (2022). Enhancing short-term ethanol-type fermentation of waste activated sludge by adding saccharomycetes and the implications for bioenergy and resource recovery. *J. Environ. Sci.* 113, 179–189. doi: 10.1016/j.jes.2021.06.005

Ziganshin, A. M., Liebetrau, J., Pröter, J., and Kleinsteuber, S. (2013). Microbial community structure and dynamics during anaerobic digestion of various agricultural waste materials. *Appl. Microbiol. Biotechnol.* 97, 5161–5174. doi: 10.1007/s00253-013-4867-0

Ziganshina, E. E., Ibragimov, E. M., Vankov, P. Y., Miluykov, V. A., and Ziganshin, A. M. (2017). Comparison of anaerobic digestion strategies of nitrogen-rich substrates: Performance of anaerobic reactors and microbial community diversity. *Waste Manag.* 59, 160–171. doi: 10.1016/j.wasman.2016.10.038

frontiers | Frontiers in Microbiology

TYPE Original Research
PUBLISHED 18 January 2023
DOI 10.3389/fmicb.2022.1062414

OPEN ACCESS

EDITED BY
Paola Grenni,
National Research Council,
Italy

REVIEWED BY
Maria Ludovica Saccà,
Council for Agricultural and Economics Research (CREA), Italy
Ni Luh Suriani,
Udayana University,
Indonesia

*CORRESPONDENCE
Angela Sierra-Almeida
✉ angelasierra@udec.cl

†These authors have contributed equally to this work

SPECIALTY SECTION
This article was submitted to Terrestrial Microbiology, a section of the journal Frontiers in Microbiology

RECEIVED 05 October 2022
ACCEPTED 30 December 2022
PUBLISHED 18 January 2023

CITATION
Aguilera-Torres C, Riveros G, Morales LV, Sierra-Almeida A, Schoebitz M and Hasbún R (2023) Relieving your stress: PGPB associated with Andean xerophytic plants are most abundant and active on the most extreme slopes.
Front. Microbiol. 13:1062414.
doi: 10.3389/fmicb.2022.1062414

Relieving your stress: PGPB associated with Andean xerophytic plants are most abundant and active on the most extreme slopes

Carla Aguilera-Torres[1,2,3], Gustavo Riveros[4†], Loreto V. Morales[1,2†], Angela Sierra-Almeida[1,2*], Mauricio Schoebitz[4,5†] and Rodrigo Hasbún[6†]

[1]Grupo de Ecofisiología Térmica, Facultad de Ciencias Naturales y Oceanográficas, Departamento de Botánica, Universidad de Concepción, Concepción, Chile, [2]Cape Horn International Center (CHIC), Puerto Williams, Chile, [3]Rizoma, Centro de Estudios Agroecológicos y Botánicos, Valparaíso, Chile, [4]Laboratorio de Microbiología de Suelos, Departamento de Suelos y Recursos Naturales, Facultad de Agronomía, Universidad de Concepción, Concepción, Chile, [5]Laboratorio de Biopelículas y Microbiología Ambiental, Centro de Biotecnología, Universidad de Concepción, Concepción, Chile, [6]Laboratorio de Epigenética Vegetal, Facultad de Ciencias Forestales, Departamento de Silvicultura, Universidad de Concepción, Concepción, Chile

Introduction: Plants interact with plant growth-promoting bacteria (PGPB), especially under stress condition in natural and agricultural systems. Although a potentially beneficial microbiome has been found associated to plants from alpine systems, this plant- PGPB interaction has been scarcely studied. Nevados de Chillán Complex hold one of the southernmost xerophytic formations in Chile. Plant species living there have to cope with drought and extreme temperatures during the growing season period, microclimatic conditions that become harsher on equatorial than polar slopes, and where the interaction with PGPB could be key for plant survival. Our goal was to study the abundance and activity of different PGPB associated to two abundant plant species of Andean xerophytic formations on contrasting slopes.

Methods: Twenty individuals of *Berberis empetrifolia* and *Azorella prolifera* shrubs were selected growing on a north and south slope nearby Las Fumarolas, at 2,050 m elevation. On each slope, microclimate based on temperature and moisture conditions were monitored throughout the growing period (oct. – apr.). Chemical properties of the soil under plant species canopies were also characterized. Bacterial abundance was measured as Log CFU g^{-1} from soil samples collected from each individual and slope. Then, the most abundant bacterial colonies were selected, and different hormonal (indoleacetic acid) and enzymatic (nitrogenase, phosphatase, ACC-deaminase) mechanisms that promote plant growth were assessed and measured.

Results and Discussion: Extreme temperatures were observed in the north facing slope, recording the hottest days (41 vs. 36°C) and coldest nights (–9.9 vs. 6.6°C). Moreover, air and soil moisture were lower on north than on south slope, especially late in the growing season. We found that bacterial abundance was higher in soils on north than on south slope but only under *B. empetrifolia* canopy. Moreover, the activity of plant growth-promoting mechanisms varied between slopes, being on average higher on north than on south slope, but with plant species-dependent trends. Our work showed how the environmental heterogeneity at microscale in alpine systems (slope and plant species identity) underlies variations in the abundance and plant growth promoting activity of the microorganisms present under the plant canopy of the Andean xerophytic formations and highlight the importance of PGPB from harsh systems as biotechnological tools for restoration.

KEYWORDS

alpine, ACC deaminase, extreme temperatures, IAA, nitrogenase, soil bacteria, xerophytic plants

Introduction

Plant growth-promoting bacteria (hereafter PGPB) are a diverse group of microorganisms beneficial to free-living or endophytic plants and can inhabit different plant compartments (de Souza et al., 2015; Afzal et al., 2017). Different bacterial traits promote plant growth directly or indirectly through mechanisms that have been widely documented, especially in soil and plant rhizosphere bacteria (Gamalero and Glick, 2011; Ramakrishna et al., 2019). These mechanisms mainly include enzymatic activities, such as urease, phosphatases, β-glucosidase, catalase, and the production of bacterial phytohormones that promote plant growth (Glick, 2012). Among the most studied mechanisms are nitrogen fixation, phosphate solubilization, phytohormone production, siderophores, and enzymes activity such as ACC deaminase that promotes resistance to different stress factors (e.g., Drought, Ashry et al., 2022; salinity, Kumar et al., 2020; trace metals, Kong and Glick, 2017). For example, the bacterial enzyme nitrogenase catalyzes molecular nitrogen to ammonia, which is absorbed by the plants increasing crop yields (Franche et al., 2009). Likewise, bacteria with ACC deaminase enzyme activity can degrade 1-aminocyclopropane-1-carboxylate (ACC), an ethylene precursor, producing ammonia and α-ketobutyrate. The decrease in ethylene levels allows the plant to survive under stressful conditions (e.g., drought and salinity; Glick et al., 2007; Orozco-Mosqueda et al., 2021). Another interesting mechanism is phosphate solubilization by bacterial enzymes such as phosphatase, phytase, and C-P lyase, that solubilize organic phosphate into inorganic phosphate, which could be absorbed and used for plant metabolism (Rawat et al., 2021). Moreover, bacterial phytohormones such as indole acetic acid (IAA) stimulate plant cell division, enhancing growth in roots and aerial structures (Duca and Glick, 2020). All these bacterial mechanisms that promote plant growth depend on environmental factors (Olanrewaju et al., 2017).

The growth-promoting activity of soil PGPB is influenced by abiotic and biotic factors. For example, nitrogen fixation is favored by increasing phosphorus and carbon availability but decreases in the presence of trace metals (Liengen, 1999; Wakelin et al., 2010). Regarding phosphate solubilization, Mujahid et al. (2015) have reported that phosphate-solubilizing PGPB increase their halo in media with carbon and nitrogen sources. While Alemneh et al. (2022) correlated soil chemical properties and phosphate solubilization of PGPB, and determined that these did not benefit from soil carbon and nitrogen. We believe that the high availability of carbon and nitrogen in growing media, such as those observed by Mujahid et al. (2015) generate opposite trends in phosphate solubilization when compared to the availability of these nutrients in the soil. Moreover, the production of IAA correlates positively with the presence of heavy metals, and negatively with the availability of sugars, nitrogen, and phosphorus in the soil (Ahmad et al., 2005; Mendoza-Hernández et al., 2016; Alemneh et al., 2022). Finally, ACC-deaminase activity of several bacteria genus increases to deaminate ACC in the presence of copper, arsenic, and lead (Mendoza-Hernández et al., 2016). Alternatively, plant root exudates compound rich in sugars, which favor microbial metabolism, increasing growth-promoting activity and plant-PGPB interactions (Bais et al., 2006). In turn, root exudates releasing is also influenced by abiotic conditions to which plants and PGPB are exposed, such as soil moisture, nutrient availability, and temperature (Vives-Peris et al., 2018; Barbosa et al., 2020). For instance, the interaction between the coastal halophyte plant *Limonium sinense* with habitat-adapted, endophytic bacteria of the genus *Bacillus* favoring plant survival under salt stress and is mediated by root exudates (Xiong et al., 2020). Soil temperature and moisture have also been defined as drivers of bacterial growth-promoting activity (Rousk et al., 2018). The ideal temperature for phosphate solubilization is below 25°C (Mujahid et al., 2015), while higher temperatures coupled with higher soil acidity increase IAA production (Kanu and Dakora, 2009; Alemneh et al., 2022). Soil moisture, in turn, has been defined as an indispensable resource for the activity of nitrogen-fixing bacteria in cold climates such as the Arctic tundra (Rousk et al., 2018). Therefore, the abundance and activity of PGPB will depend on their environmental requirements and availability of resources such as those required by the plants with which they interact.

The benefits of PGPBs have been reported mainly in agricultural systems due to the global demand for food and cultivable land (Bhattacharyya and Jha, 2012; Ramakrishna et al., 2019). In contrast, the abundance and activity of PGPBs in natural systems have been scarcely explored, despite its great potential and novelty (Pérez-Jaramillo et al., 2018; Leontidou et al., 2020). For example, PGPBs associated to wild (or native plants) species have been reported in harsh environments, such as desert (Fuentes et al., 2020; Maldonado et al., 2022), alpine (Sezen et al., 2016; Adamczyk et al., 2019; Wang et al., 2020), and saline environments (Rueda-Puente et al., 2019). Additionally, some studies have explored the presence of PGPBs adapted to environments with extreme conditions, such as salinity, (e.g., PGPBs studied from the soils of Lonar Lake in India, Hingole and Pathak, 2016), drought (e.g., PGPBs from different desert regions of Egypt, Ashry et al., 2022), or low temperatures (e.g., isolated PGPBs from the Himalayas, Yadav et al., 2015). Undoubtedly, exploring "harsh" systems for different life forms offers a space to find microorganisms with great potential for plant production and restoration, due to their ability to cope with extreme conditions and to promote plant growth and survival.

Alpine systems represent a natural laboratory to explore the presence and activity of PGPBs because of their harsh climatic conditions for life (Körner, 2004; Li et al., 2020; Rahman et al., 2020). In alpine habitats, temperature, radiation, exposure, and precipitation vary with season, altitude, and exposure of slopes (Körner and Ohsawa, 2005), producing a spatial heterogeneity of environmental conditions (Siles and Margesin, 2016; Körner, 2021), which may affect from individual physiological responses to the distribution and community structure of plants (Chaturvedi and Shivaji, 2006; Rumpf et al., 2018; López-Angulo et al., 2019; Sklenář et al., 2021). Such environmental heterogeneity has been studied mainly along altitudinal gradients and contrasting slope exposures. Specifically, soils of pole-facing slopes tend to be wetter, colder and with higher organic matter than those of equatorial-facing slopes (Scherrer and Körner, 2011). These differences in environmental conditions propitiate greater plant species richness and cover in polar than equatorial facing slopes (Zeng et al., 2014; Måren et al., 2015; Viale et al., 2019). While the difference in plant diversity of high-elevation species between slopes has been widely studied (e.g., Zeng et al., 2014; Yang et al., 2020), differences for other organisms such as PGPBs have been almost unexplored. To date, bacterial diversity decreases with altitude (Adamczyk et al., 2019). Meanwhile, their relative abundance, especially in free-living psychrophiles, increases with elevation (Siles and Margesin, 2016; Rui et al., 2022). PGPBs natives to alpine systems are essential nowadays due to their ability to cope with low temperatures and to promote plant growth through different mechanisms under cold conditions and poor nutrient soils (Chaturvedi and Shivaji, 2006; Jaggi et al., 2020; Farooq et al., 2022). These constraint conditions for plants can be alleviated by PGPBs through the activity of enzymes and phytohormones that favor

plant nutrient uptake and stress resistance (Haselwandter et al., 1983; Widawati and Suliasih, 2006; Joshi et al., 2014; Yarzábal, 2014; Kadioglu et al., 2018; Pandey and Yarzábal, 2019; Fan et al., 2021). Some studies have reported PGPBs in alpine ecosystems (Yadav et al., 2015), described their diversity in terms of factors structuring bacterial communities (Tang et al., 2020; Wang et al., 2020; Rui et al., 2022), and quantified their plant growth-promoting activity (Haselwandter et al., 1983; Widawati and Suliasih, 2006; Viruel et al., 2011; Yadav et al., 2015; Kadioglu et al., 2018). Although the interaction with beneficial microorganisms could be part of the adaptive strategy of plants in alpine systems (Farooq et al., 2022), little is known about their abundance and activity of PGPB in contrasting microhabitats within these natural systems.

The Nevados de Chillán volcanic complex is in a Mediterranean – Temperate climate transition zone (Arroyo et al., 2004), characterized by a complex topography (González-Ferrán, 1995; Dixon et al., 1999), and great plant diversity and endemism (Rodríguez et al., 2008). The lower portion of the alpine zone is dominated by xerophytic vegetation, which is one of the southernmost xerophytic formations in Chile (Squeo et al., 2008). Plant species of this Andean xerophytic formation must cope with low soil moisture and large-daily thermal oscillations during the snow-free period in the area, which could be even more extreme depending on slope exposure. The success of xerophytic plant species in alpine systems could be mediated by PGPBs-plant associations. However, knowledge is scarce, with only one study reporting PGPB isolated from the shrub species *Parastrephia quadrangularis* in the Andean Puna (Acuña et al., 2019). Thus, our general goal was to study the abundance and activity of different plant growth-promoting bacteria (PGPB) associated with two abundant plant species of Andean xerophytic formations on contrasting slopes. We expected that the abundance and activity of different PGPB associated with plant species will be greater on drier and or more thermally extreme slope.

Materials and methods

The study area was the Fumarolas sector (36°55′15”S, 71°26′25”W), nearby Nevados de Chillán Ski Resort, located at 80 km east of Chillán (Ñuble region, Chile). Is located in the transition zone between central Chile's Mediterranean regions, with sclerophyllous and temperate forests plant elements of South Chile (Arroyo et al., 2004). This area is characterized by a past and current volcanic activity resulting in a manifold topography characterized by a complex relief and geology (González-Ferrán, 1995; Dixon et al., 1999). The combination of biogeographic situation, geomorphologic complexity, and climate change leads to an exceptional degree of botanical diversity and endemism (Rodríguez et al., 2008). In this area, the treeline is determined by *Nothofagus pumilio* and *N. antarctica* at approximately 2,100 m above sea level (Fajardo et al., 2011; Piper et al., 2016). Above there, the alpine zone comprises an elevation range from 2,100 to 2,700 m (Pfanzelt et al., 2008). Vegetation is short (<150 cm), and arranged in plant assemblages of shrubs, rosettes, grasses, and geophytes (Pfanzelt et al., 2008). For example, lower elevation portion (2100–2,300 m) comprises several shrubs (*Berberis empetrifolia*, *Azorella prolifera*) and herbaceous species (*Adesmia emarginata, Grausa lateritia*) assemblages, which coincides with one of the southmost xerophytic formations in Chile (Figure 1; Donoso, 1982; Squeo et al., 2001; Moreira and Cereceda, 2013). Upper elevation portion (2300–2,700 m) is dominated by herbaceous species (*Viola volcanica*, *Nassauvia revoluta*) and grasses (*Bromus, Festuca,* and *Poa* species), which forms a matrix of low plant cover between rocks and lava flows (Pfanzelt et al., 2008). In general, this Andean system is characterized by summer water shortage and great daily temperature fluctuations (Termas de Chillán climatic station, CN360042, 1708 m above sea level).[1] During the snow free period, i.e., between October and April approximately, daily minimum and maximum air temperatures oscillate between −10°C to more than 41°C, respectively (Table 1), depending on slope and date. Moreover, soil water potential decrease from −0.8 MPa in October to <−2 MPa in March, especially in north-facing slopes (Figure 2).

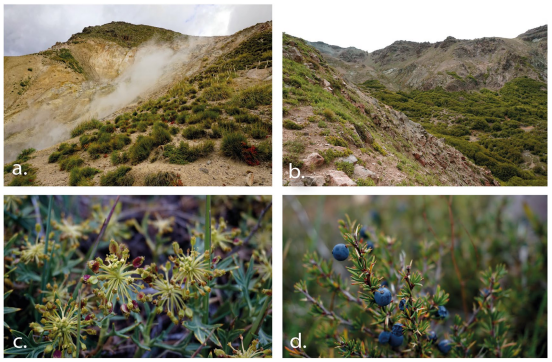

FIGURE 1
Study site located in the Nevados de Chillán Volcanic complex. Letters **(A,B)** indicate the north and south slopes, respectively. Selected species present on both slopes are indicated on the right side: **(C)**. *A. prolifera* and **(D)**. *B. empetrifolia*. Credits: Carla Aguilera-Torres.

Species selection

A pre-selection of six target species was conducted, based on Herbarium data at the Universidad de Concepción (CONC, Chile). This information was crossed with the national distribution of plant xerophytic formation report elaborated by National Forestry Service, CONAF [Gestión de Recursos Naturales (GRN), 2022]. The combined information added to field observations enabled to select within the study area two dominant species in the Andean xerophytic formations: *Berberis empetrifolia* Lam. (Berberidaceae) and *Azorella prolifera* (Cav.) G.M. Plunkett & A.N. Nicolas (Apiaceae; Figure 1). *B. empetrifolia* is a spiny and dwarf shrub of 50 cm tall, that has small narrow entire leaves, and small, yellow-colored flowers and later freshy blue-black berries. It is distributed from 29° to 56° S along Chile and Argentina, and from sea level to 3,500 m elevation (Rodríguez et al., 2018). *A. prolifera* is a shrub or subshrub that is native to Argentina, Bolivia and Chile, that forms cushions up to 100 cm high, yellowish-green, sometimes glaucous, very aromatic, petiolate leaves measuring up to 50 mm long, with yellow flowers, hermaphrodite in the center and male at the edge, arranged in simple umbels protruding above the foliage, its fruit is a winged reddish-yellow schizocarp. *A. prolifera* is distributed from 26° to 56° S, and from o to above 1,500 m of elevation (Rodríguez et al., 2018). Both species are key for other plants recruitment in the southern Andes (Nuñez et al., 1999) and exhibit high resistance to different types of stress (Durante et al., 2011; Golluscio et al., 2011; Varas et al., 2013; Sierra-Almeida et al., 2016).

1 https://climatologia.meteochile.gob.cl/ref

TABLE 1 Air temperature and moisture conditions measured on two contrasting slopes in the alpine zone of the Nevados de Chillán volcano complex.

Variable	North-facing slope	South-facing slope
Snow free period (d)	174	140
Mean temperature (°C)	11.9 ± 0.1^{a}	12.3 ± 0.1^{a}
GDD_0 (°C day^{-1})	2363.4 ± 153^{a}	1846.8 ± 78.5^{b}
Thermal breadth (°C)	22.1 ± 0.3^{a}	18.2 ± 0.3^{b}
Minimum temperature (°C)	2.6 ± 0.2^{a}	4.3 ± 0.2^{b}
Freezing intensity (°C)	-2.5 ± 0.2^{a} [−9.9]*	-2.3 ± 0.3^{a} [−6.6]*
Freezing duration (h)	4.1 ± 0.3^{a}	5.5 ± 0.6^{b}
Freezing frequency (%)	29.3^{a}	11.4^{b}
Maximum temperature (°C)	24.6 ± 0.4^{a}	22.5 ± 0.6^{b}
Heat intensity (°C)	33.5 ± 0.3^{a} [41.3]*	32.2 ± 0.2^{b} [35.8]*
Heat duration (°C)	3.2 ± 0.2^{a}	2.4 ± 0.3^{b}
Heat frequency (%)	48.9^{a}	27.9^{b}
Mean Relative Humidity (%)	51.9 ± 0.2^{a}	51 ± 0.3^{a}
Min Relative Humidity (%)	21.9 ± 0.6^{a}	28.4 ± 1.2^{b}
Max Relative Humidity (%)	84 ± 0.6^{a}	80.4 ± 1.3^{b}

*On the north-facing slope, freezing occurred on November 4, 2021, while heat occurred on January 17, 2022; on the south-facing slope, heat occurred on February 8 and freezing occurred on April 3, 2022. Values correspond to average ± SE ($n = 3$) for the entire snow free period between October 28, 2021, and April 19, 2022. Different upper cases indicate significant differences ($p < 0.05$). Extreme temperatures are shown between brackets as absolute values.

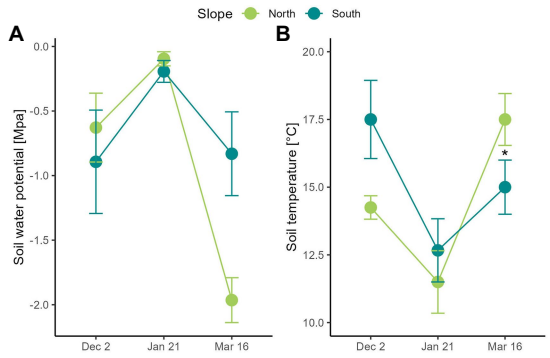

FIGURE 2
Soil climatic conditions measured in two contrasting slopes in the Nevados de Chillán Volcano complex. **(A)** Water potential (MPa) and **(B)** soil temperature (°C) was measured at 15 cm of soil depth on two contrasting slopes. Values correspond to average±SE ($n = 3$). Dashed grey lines indicate temperature thresholds for plant physiology: heat (30°C) – freezing (0°C). Blue arrows indicate snowfall. Asterisks show significant differences (Repeated measures ANOVA, $p < 0.05$).

Microclimatic characterization of contrasting slopes

Target species were present in two contrasting slopes (Figure 1): north- (1,984 m, 36°54′24.25”S 71°24′10.16”W) and south-exposure (2,089 m, 36°54′16.90”S 71°23′58.83”W). On each slope, three air temperature (°C) and relative humidity (%) sensors were placed at 15 cm above the soil surface (U23 Hobo Pro v2 6′, Onset Comp, United States). They were programmed to record every 30 min during the entire snow free period. On the north-facing slope, sensors were installed on October 28, 2021, whilst on the south slope, they were installed on December 02 because it was covered by snow before this date. Air temperature recording were used to estimate several parameters: seasonal mean, maximum and minimum air temperatures; intensity, frequency, and duration of freezing ($T < 0$°C) and heat events ($T > 30$°C); growing degree days (GDDs), used as a measure of heat accumulation (in °C) above a base temperature (i.e., 0°C) to represent an index of the cumulate energy available to growing plants (McMaster and Wilhelm, 1997). It was calculated as:

$$GDD_0 = [[(\text{maximum daily temperature} + \text{minimum daily temperature})/2]] - \text{base temperature}.$$

The daily GDDs were summed per the entire growing season on each slope. We used 0°C as a conservative base growing temperature (threshold temperature above which plants can perform metabolic functions), because plants from cold climate generally vary in their absolute base growing temperature, and this value encompasses this variability (Körner, 2011).

Soil temperature and water potential were recorded by using psychrometers (PST-55, C52 Wescor Inc., Utah, United States), which were placed at 15 cm of soil depth ($n = 3$ per slope). These sensors were buried at the same date as air sensors. Soil temperature and moisture were manually recorded once per month using a microvoltmeter (HR 33 T; Wescor Inc., Utah, United States). In April, measurements of soil temperature and water potential were not carried out because started snowfall. All sensors were removed from the sites on April 19, 2022.

Given that soil chemical properties affect the bacterial abundance and activity (Preem et al., 2012; Chodak et al., 2015), on April 16, soil samples were collected under the plant canopy for their chemical characterization. A total of 12 soil samples of 1 kg (3 replicates × 2 species × 2 slopes) were placed into plastic bags, marked, and immediately transported into a cooler to our lab group at the University of Concepción (Concepción). Then, soil samples were sent for complete chemical analysis to the Soil and Plant Analysis Laboratory at Universidad de Concepción (Chillán).

Bacterial abundance

On April 19, soil samples were collected from surrounding roots of *Azorella prolifera* and *Berberis empetrifolia*. Three soil samples of 0,5 kg were collected per species and slope (total 12 samples). Samples soils were placed into a cooler and immediately transported to our lab, where they were stored at −20°C until the start of microbiological studies. Abundance of bacteria were estimated by Colony-Forming Unit (CFU) per species (*A. prolifera* and *B. empetrifolia*) and slope (North and South). For this, 1 g of soil per species and slope exposure was taken and serially diluted in Phosphate-Buffered Saline (PBS) medium under sterile conditions. Subsequently, the 10^{-2} and 10^{-3} dilutions were sown on plates with plate count agar medium (DIFCO), which were incubated for 2 days at 25°C. The CFU of each dilution was then counted to determine the most abundant and morphologically different culturable strains for plant growth-promoting trait assays. The CFU were transformed to their natural logarithm (Log CFU g^{-1}).

PGPB activity

The five most abundant and distinct colonies by species and slope were selected according to their bacterial cell shape and structural appearance. They were subculture two or three times until pure strains

were obtained. Nineteen culturable bacterial strains were obtained and subjected to assays that evaluated the activity of four plant growth-mechanisms, including IAA production, ACC deaminase, phosphate solubilization and nitrogenase enzyme activities and then were compared between contrasting slopes.

a. To evaluate **indole acetic acid (IAA) production**, selected culturable strains were inoculated in generic nutrient broth [1 gD (+)-glucose, 15 g peptone, 6 g NaCl, 3 g yeast extract], with 0.15% (w/v) tryptophan in darkness for 96 h at 30°C with 120 rpm. IAA production was measured *via* high-performance liquid chromatography (HPLC; Primaide, Hitachi Co, Ltd., Tokyo, Japan; Gang et al., 2019). The calibration curve was prepared with serial solutions of IAA ranging from 0 to 50 ppm in methanol, 50 µl of the samples were injected onto a kromasil C-18 column equipped with a diode array detector, and retention times ranged from 5.7 to 7.9 min. All samples were analyzed in triplicate. The results were expressed in µg ml^{-1} of bacterial IAA.
b. The presence and activity of **ACC-deaminase enzyme** was studied following protocols described by Senthilkumar et al. (2021) and Penrose and Glick (2003) with modifications. Liquid DF minimal culture medium was prepared, where the bacteria of interest were inoculated at 28°C for 72 h; bacteria that showed turbidity were seeded in solid DF minimal medium to confirm the presence of ACC deaminase. In cultures that evidenced plate growth in solid DF medium, ACC deaminase enzymatic activity was measured by the production of α-ketobutyrate, which was determined by spectrophotometer (Spectroquant Prove 300) at 540 nm by comparison with the standard curve of α-ketobutyrate, which ranged from 0 to 100 µM (Honma and Shimomura, 1978). Higher concentrations of α-ketobutyrate were indicative of higher enzyme activity (Ali et al., 2014).
c. **To determine nitrogenase enzyme activity**, strains were incubated in a semi-solid nitrogen-free (NF) medium for 72 h at 28°C (Kifle and Laing, 2015). Samples showing evidence of turbidity were subjected to acetylene reduction assay (ARA; Hardy et al., 1968), where 10% of the atmosphere was removed with a syringe and replaced with acetylene. After 20 h, 4.4 ml of gas was taken for each vial to analyze the amount of ethylene formed through gas chromatography (GC 6890 N, Agilent Technologies), equipped with J&W HP-5 GC column, 30 m, 0.25 mm, 0.25 µm, H_2, N_2, and air detectors, with flow rates of 40, 24, and 450 ml/min, respectively. To determine the injection, detection and column temperatures, the ranges of Hara et al. (2009) were followed with modifications: Injection temperatures were 150°C, detection temperature was 150°C, and column temperature was 50°C. Retention times ranged from 1 to 1.5 min. 4–5 ml of samples were injected per 10 min. Each sample was prepared in triplicate for injection. The calibration curve was prepared with solutions composed of different ethylene concentrations expressed in nmol C_2H_4 $d^{-1}vial^{-1}$.
d. **Phosphate solubilization,** mineral phosphate solubilization was assayed according to Pikovskaya (1948), the mineral phosphate solubilization was assayed by seeding bacteria in a solid medium Pikovskaya (PVK) in plates containing insoluble tricalcium phosphate, that bacteria with phosphatase are capable of degrading. The plates were incubated at 28°C. The development of a clear zone around the colony was evaluated after 20 days. Samples were analyzed in triplicate.

Identification of bacterial strains by studying the 16S rRNA gene

To determine whether the selection of bacterial strains by cellular and structural appearance included different species, the following analysis were carried out. Ten bacterial strains randomly selected of 19 used for PGPB analysis were grown on semi-solid TBS medium. DNA extractions of individual colonies were performed using the DNeasy® Plant mini kit (QIAGEN, Dusseldorf, Germany) according to the manufacturer's instructions. The integrity of the DNA samples was visualized by agarose gel electrophoresis, the concentration was determined by spectrophotometry (A260/A280) using Infinite® M200 Pro NanoQuant (Tecan®, Tecan Trading AG, Switzerland) and the DNA samples were kept at −20°C. PCR was performed to amplify and sequence part of the 16S rRNA gene. PCR reactions contained 1X GoTaq® reaction buffer (1.5 mM $MgCl_2$), 200 mM dNTP, 0 2 µM of each primer (16S_27F, 5'-AGAGAGTTTGATCCTGCTCAG-3′ and 16S_805R, 5'-GACTACHVGGGGGTATCTAATCC-3′), 1 U of GoTaq DNA Polymerase (Promega, Madison, United States), 20 ng/μL^{-1} of DNA and filled to 20 µl with sterile filtered molecular grade water. Thermal conditions were achieved by cycling at 94°C for 3 min, followed by 35 cycles of DNA denaturation at 94°C for 60 s, primer annealing at 45°C for 40 s and DNA elongation at 72°C for 60 s, and a final extension at 72°C for 7 min. PCR products were run on 1% (w/v) agarose gels with SYBR Safe DNA Gel Stain (Thermo Fisher Scientific, Inc., Carlsbad, CA) in TAE buffer at 80 V for 45 min. The amplicons were visualized in a UV light transilluminator. The amplified DNA fragments were purified and directly sequenced in both directions (Macrogen, Seoul, South Korea). Sequencing results (ABI chromatograms) were analyzed in the free open-source software UGENE v.33. Nine out of 10 bacterial strains yielded analyzable chromatograms. The consensus fastq files were analyzed using the EzBioCloud 16S Database (Yoon et al., 2017). EzBiocloud is a species level resolution database made of 61 700 species/phylotypes, including 13 132 species/phylotypes with validly published names. A phylogenetic tree was constructed using the Seaview 4.0 program with the neighbor-joining method to determine relationships between bacterial strains. The resulting consensus tree was constructed using 1000 replicates.

Data analysis

Differences in soil conditions (i.e., temperature and water potential) throughout the growing season between north and south slopes were assessed by repeated measures ANOVAs ($p < 0.05$). Differences in mean, maximum, minimum air temperature and relative humidity, thermal breadth, intensity and duration of freezing and heat events between north and south-facing slopes, were assessed by *t* tests or non-parametric equivalent tests ($p < 0.05$) when data normality and homoscedasticity were not met. Differences in frequency of freezing and heat events and GDDs between slopes were assessed by Chi^2 tests. Differences in soil properties were assessed by Factorial ANOVAs, where species and slope were predictors. When parametric requirements were not met these differences were assessed by Kruskal-Wallis ANOVA by ranks. Differences in PGPB abundance (Log $CFUg^{-1}$) and in the activity of plant growth-promoting mechanisms (i.e., phytohormone and enzymes) were assessed by ANOVAs as well. All data were analyzed through the Statistica version 13.

Results

Microclimatic characterization of contrasting slopes

The North-facing slope was potentially more stressful than south-facing slope according to microclimatic data obtained during the complete snow free period (Table 1). Although air mean temperature was similar between slopes ($t = 0.02$, $p = 0.985$), GDD_0 were 22% ($\chi^2 = 3{,}133$, $p < 0.0001$) and thermal breadth was 3.9°C greater ($t = 7.3$, $p < 0.001$) in north- than in south-facing slope. In addition, considerable differences in extreme temperatures were observed (Table 1). For example, the mean minimum temperature was lower in north- than in south-facing slope (2.5°C ± 0.2 vs. 4.3°C ± 0.2, $t = 4.2$, $p < 0.0001$). The intensity of freezing events averaged −2.4°C for both slopes ($t = 0.11$, $p = 0.74$), but their frequency was 2.4 times greater in north- than in south-facing slope ($\chi^2 = 10.7$, $p = 0.001$), with the lowest temperature of −9.9°C recorded on November 4, whilst south-facing slope was covered by snow. The duration of freezing events was 25% longer in south- than north-facing slope ($t = 5$, $p = 0.028$), but in both microsites they lasted on average more than 4 h (Table 1). At the other extreme, the mean maximum air temperature was 2.2°C higher in north- than in south-facing slope (Table 1, $Z = 2.86$, $p = 0.004$). In north-facing slope, heat events were 1.8 times more frequent ($\chi^2 = 9.8$, $p = 0.002$), 1.3 times longer ($Z = 2.3$, $p = 0.022$) and 1.3°C hotter ($Z = 2.5$, $p = 0.011$) than in the south-facing slope. In addition, heat events with temperatures over 40°C were recorded only in the north-facing slope (Table 1). Regarding air relative humidity (RH), averaged 51% for both slopes ($t = 2.7$, $p = 0.077$), but minimum RH was 6.5% lower ($t = 3.9$, $p = 0.001$) and maximum RH was 4% higher ($t = 2.1$, $p = 0.034$) in north- than in south-facing slopes.

Soil temperature was similar on north and the south-facing slope (Figure 2; slope $F_{1,4} = 0.5$, $p = 0.519$) with variations reported throughout the growing season (*date* $F_{2,8} = 15.3$, $p = 0.002$). In contrast, soil water potential was on average −0.7 MPa and −0.5 MPa in December and January on both slopes, respectively (Figure 2). However, its decrease was 2.2 times greater in the north- than in the south-facing slope (*date x slope* $F_{2,8} = 9.3$, $p = 0.008$). Hence, soils of north-facing slopes reported water potential of −1.96 MPa in March, while on the south-facing slope it was of −0.89 MPa (Figure 2). No recordings were carried out in April because snow started to cover soil moisture sensors.

Soil chemical properties varied between plant species and slope exposure (Table 2). For example, soil pH under *Azorella prolifera* was on average greater than of under *Berberis empetrifolia* (6.3 *vs* 5.3, $H_{3,12} = 8.44$, $p < 0.038$), independent of slope. Regarding organic matter, slope differences were observed for soils under both species but in opposite directions (Table 2; $H_{3,12} = 9.15$, $p < 0.027$). Under *A. prolifera* canopy, organic matter was a half lower in the north than in the south slope ($Z = 1.96$, $p = 0.049$). In contrast, organic matter was almost once greater in the north than in the south slope ($Z = 1.96$, $p = 0.049$) in soil collected under *B. empetrifolia* canopy (Table 2). Available K was 3 times greater in south than north slope for soils under *A. prolifera* ($Z = 1.96$, $p = 0.049$), whilst for soils under *B. empetrifolia* available K was similar between slopes ($Z = 1.09$, $p = 0.275$). Exchange Al was similar between slopes in soils under *A. prolifera* ($Z = 0.86$, $p = 0.383$), but it was almost 3 times greater in soils from north than south slopes under *B. empetrifolia* ($Z = 1.96$, $p = 0.049$). Al and Ca saturation varied between species but were similar between slopes (Table 2). For example, Al saturation was on average 15 times greater in soils under *B. empetrifolia* than in soils under *A. prolifera* ($H_{3,12} = 9.26$, $p < 0.026$). In contrast, Ca saturation was on average 26,4% greater in soils under *A. prolifera* than under *B. empetrifolia* (Table 2, $F_{1,8} = 66.8$, $p < 0.0001$). In the case of K Saturation, it was greater in soils from south slope independent of plant species (Table 2; $H_{3,12} = 9.36$, $p < 0.025$), with slope differences of 2.6 and 3.7 times in soils under *A. prolifera* and *B. empetrifolia*. Mg saturation exhibited similar percentages between slopes for soils under *A. prolifera*, but it was 8.2% greater in north than in south slope in soils under *B. empetrifolia* (Table 2; $F_{1,8} = 10.9$, $p = 0.011$). Similar pattern was observed in Fe (Table 2). No differences in Fe were found between slopes for soils under *A. prolifera*, but Fe was 44.2% greater in north than in south slope in soils under *B. empetrifolia* (Table 2; $H_{1,6} = 3.86$, $p = 0.049$). Regarding S available, it was almost 9 times greater in south than in north slopes in soils under *A. prolifera*, but no differences between slopes were observed in soils under *B. empetrifolia* (Table 2; $F_{1,8} = 12.9$, $p = 0.007$).

Bacterial abundance and their identity from Andean xerophytic formations

Differences in CFU abundance between contrasting slopes depended on plant species where soil samples were obtained ($H_{3,20} = 7.91$, $p = 0.048$; Figure 3). While abundance in soils collected under *Azorella prolifera* was similar between slopes (Figure 3A; $Z = 1.43$, $p = 0.28$), CFU were more abundant in soils from north-facing slope when they were collected under *Berberis empetrifolia* canopy (Figure 3B; $Z = 0.57$, $p = 0.021$).

Slope differences in activity plant growth-promoting mechanisms

Of the 19 bacterial isolates present in the soils under the canopies of *A. prolifera* and *B. empetrifolia* on the north and south slopes, 89.47% of the isolates had activity in the production of IAA. Of the 17 isolates with activity in the indole acetic acid production mechanism, 52.95% of the isolates were from the northern slope and 47.05% were from the southern slope. For the ACC deaminase mechanism, 52.6% of the isolates had activity corresponding to 10 bacterial isolates, of which 70% corresponded to the northern slope and 30% to the southern slope. As for nitrogen fixation, 73.6%, corresponding to 14 bacterial isolates, had activity for this mechanism, where 64.28% corresponded to the northern slope and 35.73% had activity on the southern slope. 89.47% of the isolates corresponding to 17 bacterial isolates could solubilize phosphate, among the isolates with activity, we detected that 47.05% belonged to the northern slope and 52.95% (Supplementary Table S1; Supplementary material).The activity of four PGP mechanisms were compared between slopes. The hormonal PGP mechanism; Indole acetic acid (IAA) is presented in Figure 4. All isolates on the north slope of both *A. prolifera* and *B. empetrifolia* produced IAA, while on the south slope only 80% of the isolates produced this phytohormone. The highest value of IAA production was from an isolate from the north slope and *A. prolifera* soil (Supplementary Table S1; Supplementary material). When comparing the averages of IAA production on the north and south slopes for *A. prolifera* and *B. empetrifolia* species, we did not find differences between slopes, with averages IAA production of 1.4 μg ml^{-1} for *A. prolifera* (Figure 4A; $F_{1,22} = 16.49$, $p = 0.9$), and 1.6 μg ml^{-1} for *B. empetrifolia* (Figure 4B; $F_{1,25} = 0{,}89$, $p = 0.46$).

10.3389/fmicb.2022.1062414

TABLE 2 Chemical characterization of the soils collected under plant canopy of *Azorella prolifera* and *Berberis empetrifolia* species growing in contrasting slopes.

Chemical properties of the soil	*Azorella prolifera*		*Berberis empetrifolia*	
	North-facing	South-facing	North-facing	South-facing
pH (water)	6.4 ± 0.1^{a}	6.3 ± 0.3^{a}	5.3 ± 0.1^{b}	5.3 ± 0.2^{b}
Organic Matter (%)	0.9 ± 0.2^{a}	1.9 ± 0.1^{bc}	2.5 ± 0.2^{b}	1.6 ± 0.1^{c}
N-NO_3 (mg kg^{-1})	2.8 ± 0.4^{a}	2.3 ± 1.5^{a}	4 ± 1.3^{a}	8.4 ± 2.2^{a}
N-NH_4 (mg kg^{-1})	1.8 ± 0.4^{a}	1.3 ± 0.2^{a}	2.7 ± 0.3^{a}	1.7 ± 0.2^{a}
Available Nitrogen (mg kg^{-1})	4.6 ± 0.1^{a}	3.6 ± 1.6^{a}	6.7 ± 1.3^{a}	10.1 ± 2.4^{a}
Olsen P (mg kg^{-1})	4.3 ± 1.7^{a}	3.9 ± 0.5^{a}	4.3 ± 1.1^{a}	3.9 ± 0.2^{a}
Available K (mg kg^{-1})	53.5 ± 20.9^{a}	162 ± 3.6^{b}	150 ± 25.8^{bc}	97.9 ± 18.6^{c}
Exchangeable K (cmol kg^{-1})	0.2 ± 0.03^{a}	0.4 ± 0.01^{a}	0.4 ± 0.1^{a}	0.3 ± 0.1^{a}
Exchangeable Ca (cmol kg^{-1})	14.6 ± 2.7^{a}	12.2 ± 3.4^{a}	9.5 ± 3.4^{a}	1.2 ± 0.2^{a}
Exchangeable Mg (cmol kg^{-1})	1.4 ± 0.4^{a}	1.2 ± 0.5^{a}	3 ± 1.3^{a}	0.3 ± 0.05^{a}
Exchangeable Na (cmol kg^{-1})	0.06 ± 0.02^{a}	0.03 ± 0.01^{a}	0.04 ± 0.003^{a}	0.02 ± 0.003^{a}
Sum of bases (cmol kg^{-1})	16.3 ± 2.8^{a}	13.8 ± 3.7^{a}	12.9 ± 4.8^{a}	1.8 ± 0.3^{a}
Exchange Al (cmol kg^{-1})	0.1 ± 0.1^{ac}	0.08 ± 0.05^{a}	1.4 ± 0.3^{b}	0.5 ± 0.1^{c}
CEC (cmol kg^{-1})	16.5 ± 2.7^{a}	13.9 ± 3.6^{a}	14.4 ± 5^{a}	2.2 ± 0.4^{a}
Al saturation (%)	1.1 ± 0.8^{a}	1 ± 0.8^{a}	10.9 ± 2.4^{b}	20.9 ± 3.8^{b}
K saturation (%)	1.4 ± 0.1^{a}	3.6 ± 1.15^{b}	3 ± 0.5^{b}	11.2 ± 0.2^{c}
Ca saturation (%)	88 ± 3.6^{a}	85.8 ± 3.8^{a}	66 ± 1.2^{b}	55 ± 3.5^{b}
Mg saturation (%)	9.1 ± 2.6^{a}	9.3 ± 2.4^{a}	19.7 ± 1.5^{b}	11.5 ± 0.5^{a}
Available S (mg kg^{-1})	1 ± 0.5^{a}	8.8 ± 1.4^{b}	1.9 ± 0.4^{a}	4 ± 0.6^{a}
Fe (mg kg^{-1})	8.2 ± 1.4^{a}	15.3 ± 5.1^{a}	18.3 ± 2.3^{a}	10.2 ± 0.3^{b}
Mn (mg kg^{-1})	1.8 ± 0.3^{a}	3.5 ± 0.1^{a}	2.6 ± 1.1^{a}	1.5 ± 0.5^{a}
Zn (mg kg^{-1})	0.2 ± 0.03^{a}	0 ± 0^{a}	0.1 ± 0^{a}	0.2 ± 0.03^{a}
Cu (mg kg^{-1})	0.6 ± 0.1^{a}	1.3 ± 0.4^{a}	0.7 ± 0.1^{a}	0.4 ± 0^{a}
B (mg kg^{-1})	0.1 ± 0.03^{a}	0.2 ± 0.03^{a}	0.1 ± 0^{a}	0.1 ± 0.03^{a}

Values correspond to average ± SE ($n = 3$). Different lower-case letters indicate significant differences ($p < 0.05$).

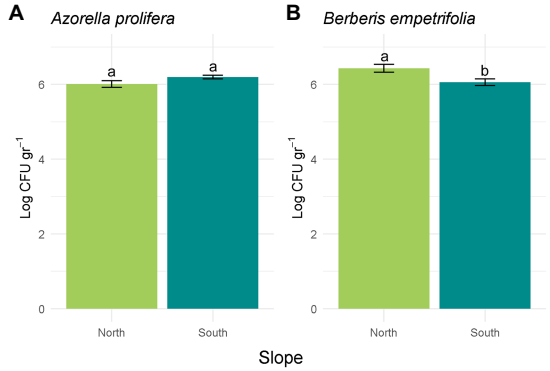

FIGURE 3
Bacterial abundance calculated in Log CFU g^{-1} for *A. prolifera* **(A)** and *B. empetrifolia* **(B)** soil. Values indicate average ± SE (n=3). Letters indicate significant differences between slopes (Wilcoxon test, p>0.05).

The activity of enzymatic PGP mechanisms was on average higher in north than south slopes (Figure 5). On the north slope 77.7% of the bacterial isolates under the canopies of *A. prolifera* and *B. empetrifolia* possessed ACC-deaminase enzymatic mechanism activity, whereas, on the south slope, only 30% of the bacterial isolates from this slope possessed ACC-deaminase activity (Supplementary Table S1; Supplementary material). The highest activity of ACC deaminase was observed in a bacterial strain isolated from *A. prolifera,* which was 5 times higher in soils from north- than south slopes (7.1 vs. 1 µM; Figure 5A; $F_{1,7} = 0.8$ $p = 0.01$). In the case of *B. empetrifolia,* ACC deaminase had a similar activity in soils from both slopes (3.39 vs. 2.42 µM; Figure 5B; $F_{1,8} = 0.04$, $p = 0.41$).

Among the north slope isolates, bacterial colonies with phosphate solubilizing mechanism were 88.8%, while on the south slope it was 90% (Supplementary Table S1; Supplementary material). However, the ability to solubilize phosphorus was higher on the north slope ($H_{3,20} = 9.66$, $p = 0.022$), particularly under the *A. prolifera* canopy, where, the solubilization Phosphorus index was 12% greater for culturable bacteria

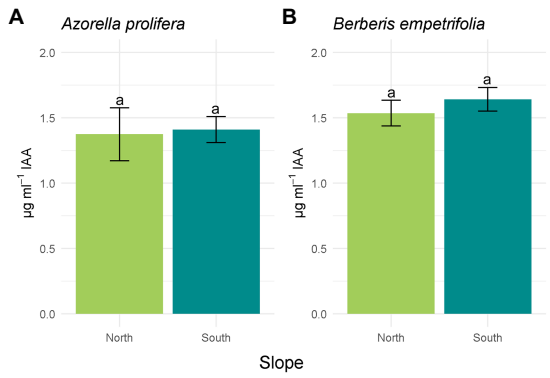

FIGURE 4
Indoleacetic acid (IAA) production of bacteria isolated from 2 species of Andean xerophytic formations on contrasting slopes: *Azorella prolifera* **(A)** and *Berberis empetrifolia* **(B)**. For each species, north slope is shown in green and south slope in light blue. Values indicate average±SE. Equal letters indicate no differences (p>0.05).

obtained in soils under from north than from south slope (Figure 5C; Z = 1.7, p = 0.01). In contrast, solubilization P index was similar between slopes for bacteria obtained from soil under *B. empetrifolia* (1,31 vs. 1,31; Figure 5D; Z = 0.21, p = 0.87).

Nitrogenase enzyme activity on the north slope occurred for all isolates, both for soils under *A. prolifera* canopy and *B. empetrifolia* soils. On the southern slope, on the other hand, nitrogenase activity only occurred for half of the bacterial isolates (Supplementary Table S1; Supplementary material). A greater nitrogenase activity was observed in bacteria obtained from north slope soils independent of plant species (Figures 5E,F). For example, for bacteria isolated from *A. prolifera* soils, ethylene production averaged 396 nmoles C_2H_4 $d^{-1}vial^{-1}$ on the south slope, whilst on the north slope it was 1,109 nmoles C_2H_4 $d^{-1}vial^{-1}$ (Figure 5E; $F_{1,25}$ = 0.95, p = 0.007). For bacteria isolated from *B. empetrifolia* soils, the nitrogenase activity was 3.3 times greater in the north than in the south slope (Figure 5F; $F_{1,25}$ = 3.5, p = 0.001).

Molecular identification of bacterial strains

Randomly selected bacterial strains used to determine species identity of colonies and correspond to five genus and six species (Table 3). Regarding phylogenetic tree, four clades were identified and correspond with genus detected (Figure 6). Only two bacterial strains were assigned to the same species (2HBER4 and 4SBER4) and would correspond to *Pseudomonas atacamensis*. These bacterial strains where isolated from *B. empetrifolia*. Five bacterial strains were assigned to species belonging to the genera *Pseudarthrobacter* and *Arthrobacter*, detecting only almost identical (2SAZO6 and 6SAZO5) both from under *A. prolifera* on the south slope. The other two entities are made up of single species, respectively.

Discussion

This work quantified the abundance and activity of bacteria present in the south-central zone of the Andes Mountains. In addition, we observed how environmental variability in water availability, thermal oscillation, and plant identity impacted the different indicators evaluated. An important finding in the present investigation was that a higher abundance and enzyme activity was observed on the drier slope compared to the southern slope. In addition, two of the three enzymatic mechanisms showed differences between slopes, but only for bacteria associated with *Azorella prolifera*, not for *Berberis empetrifolia*. Thus, species identity is key when exploring the beneficial potential of plant growth-promoting bacteria in alpine systems.

First, the ranges obtained for bacterial abundance seem to coincide with the literature. For example, works such as those of Sinegani and Younessi (2017) have obtained ranges close to 3 Log CFU g^{-1} for contaminated sites, and values between 6.3 and 8.3 Log CFU g^{-1} for pastures and agricultural systems, the most common being close to 6 Log CFU g^{-1}. Kieft et al. (1993) have obtained ranges between 2 and 6.7 Log CFU g^{-1} for soils of natural arid systems in the United States. In relation to the activity of PGPBs from Andean xerophytic formations reached low levels compared to those reported for agricultural systems. For example, our PGPBs produced indole acetic acid in a range of 1.4 µg ml^{-1} to 1.7 µg ml^{-1}, whilst in agricultural systems IAA productions fluctuate between 8.5 µg ml^{-1} and 69.7 µg ml^{-1} (Herlina et al., 2017). Likewise, while phosphate solubilization in agricultural systems fluctuates between 4 and 5 (Schoebitz et al., 2013; Pande et al., 2017), in our Andean xerophytic system it did not exceed 1.5. While the highest nitrogenase enzyme activity in our assay was 1.4 µmol C_2H_4 $d^{-1}vial^{-1}$, assays with industrial bacteria ranged between 6 and 108 µmol C_2H_4 d^{-1} $vial^{-1}$ (Li et al., 2017). Most studies evaluating the potential benefits of PGPBs are conducted in agricultural systems, with bacteria that have been optimized for years, so the low enzyme activity observed in bacteria from natural systems is not surprising. Interestingly, this pattern changes when we compare our results with the plant growth-promoting activity of bacteria from natural systems. For example, Kadioglu et al. (2018), isolated cold-tolerant bacteria with ACC deaminase activity from different native alpine plants in Erzurum (between 1,760 and 2,720 m above sea level). The activity of these bacteria ranged from 0.9 to 1.2 µM α-ketobutyrate, almost six times less than the activity obtained in our study. Most studies on the abundance and activity of PGPBs in alpine systems are generally from the Himalayas, where the bacteria interact with cultivated plants and in highly degraded soils (e.g., Majeed et al., 2018; Kumar et al., 2019). The level of disturbance in a system is also known to affect PGPB activity (Bergottini et al., 2015). This makes it difficult to draw comparisons that evidence the potential of the findings embodied in this study.

Bacterial abundance and growth-promoting mechanisms related to slopes

We observed that bacterial abundance and enzyme activity was higher on the north than on the south slope. The climatic conditions could be behind this trend. Generally, the north slope tends to be drier and warmer than the south slope, as previously described for its equatorially oriented slopes (Scherrer and Körner, 2011). In addition, more intense and frequent heat and freezing events occurred on the north slope (Table 1), with greater intra-seasonal thermal fluctuations than on the south slope. This means that plant-PGPB interactions should be more likely to be found on the north slope, and the benefits, represented as the activity of PGP mechanisms, should be greater on this "hard" slope.

Regarding the influence of each environmental factor on bacterial abundance, what might contribute to the differences observed on the

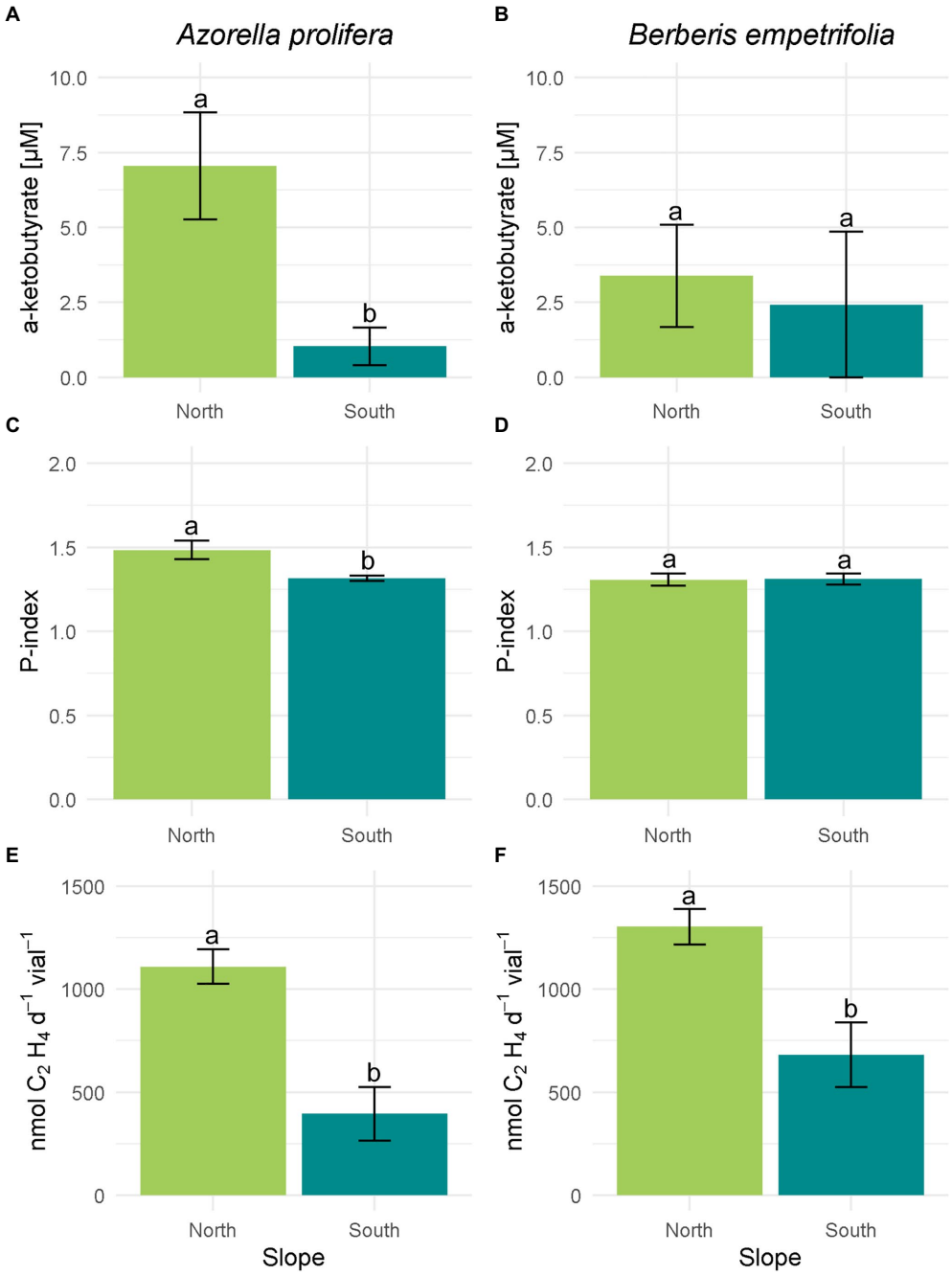

FIGURE 5
Enzymatic plant growth promoting mechanisms of bacteria isolated from 2 species of Andean xerophytic formations on contrasting slopes. For all mechanisms the columns were divided by species: *A. prolifera* on the left and *B. empetrifolia* on the rights. For each species the slopes are indicated with colors: green for the north slope and light blue for the south slope. ACC deaminase enzyme activity **(A,B)** are presented as µM of α-ketobutyrate. Phosphate solubilization **(C,D)** is presented as Index P. Nitrogen fixation **(E,F)** is given as nmoles C_2H_4 d^{-1} $vial^{-1}$. Values indicate average±SE. Different letters above error bars indicate significant differences between slopes (T test or nonparametric equivalent, $p<0.05$).

north slope. Studies have described the influence of each environmental factor independently, such as temperature (Chen et al., 2015), soil moisture (Naylor and Coleman-Derr, 2018), and soil chemical properties (Ai et al., 2020). For example, increasing temperature favors bacterial abundance, especially in cold regions (Chen et al., 2015). As for soil moisture, it affects in a more dynamic and integrated way, because it affects soil chemical properties and plant performance (Naylor and Coleman-Derr, 2018), which in turn affects bacteria. However, the identity and adaptations of bacteria determine whether they will survive and grow under extreme conditions (Pérez-Jaramillo et al., 2018). Furthermore, their response will depend on how stable the communities they compose are; stable bacterial communities do not change in drier soils (Stres et al., 2008). A clear example is a work of Chodak et al. (2015), who evaluated the response of drought-adapted bacteria that were subsequently rewetted, resulting in a stress-related decrease in gram-negative bacteria and an increase in gram-positive bacteria. Although the higher bacterial abundance observed on the north-facing slope responded to climatic factors, we believe that the response of bacterial abundance depends also

TABLE 3 Bacterial sequences obtained for 9 of the most abundant colonies isolated from soil under plant xerophytics species in the Nevados de Chillán Volcano Complex. See Materials and Methods for details.

ID	Plant species origin	Slope	Colony	Top-hit taxon in EzBioCloud 16S database	Similarity (%) in EzBioCloud 16S database	GenBank accession number
1SBER5	*Berberis empetrifolia*	South	5	Arthrobacter oryzae/A. pascens	99,37/99,21	OP776725
2HBER4	*Berberis empetrifolia*	North	4	Pseudomonas atacamensis	99,86	OP776726
2HBER10	*Berberis empetrifolia*	North	10	Rhodococcus qingshengii	99,44	OP776727
2SAZO6	*Azorella prolifera*	South	6	Arthrobacter globiformis/ Pseudarthrobacter scleromae	99,53/99,52	OP776728
3HBER9	*Berberis empetrifolia*	North	9	Leifsonia soli	99,85	OP776729
4HAZO6	*Azorella prolifera*	North	6	Arthrobacter oryzae/A. pascens	99,85/99,85	OP776730
4HBER2	*Berberis empetrifolia*	North	2	Pseudarthrobacter sulfonivorans/ Arthrobacter ginsengisoli/A. pascens	98,98/98,71/98,71	OP776731
4SBER4	*Berberis empetrifolia*	South	4	Pseudomonas atacamensis	99,85	OP776732
6SAZO5	*Azorella prolifera*	South	5	Arthrobacter oryzae/A. pascens	98,99/98.84	OP776733

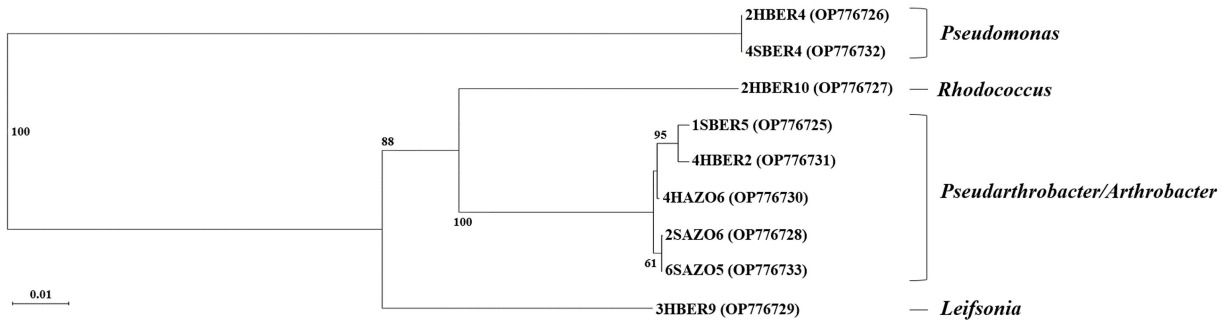

FIGURE 6
Phylogenetic tree based on sequences of the 16S genes (790 bp amplicon size) of 9 bacterial isolates obtained from *A. prolifera* and *B. empetrifolia* species from the north and south slopes of the Nevados de Chillán volcanic complex. 2HBER4, 2HBER10, 4HBER2, 3HBER9 correspond to isolates of the species *B. empetrifolia* on the south slope. 4SBER4, 1SBER5 correspond to isolates of the specie *B. empetrifolia* on the north slope. 4HAZO6 correspond to isolates of the specie *A. prolifera* on the south slope. 2SAZO6, and 6SAZO5 correspond to isolates of the species *A. prolifera* on north slope.

on the characteristics of the bacteria (i.e., adaptations and identity), their community and the plants with which they interact.

The identity of the most abundant and active bacteria coincides with that reported for other systems with extreme conditions. All bacterial genera identified in this study have been identified in climatically limiting environments such as the Himalayas (e.g., *Pseudomonas*, Selvakumar et al., 2008; *Rhodococcus*, Ruberto et al., 2005; *Leifsonia*, Reddy et al., 2008), the Andes mountain range (e.g., *Pseudomonas* Viruel et al., 2011; Vega-Celedón et al., 2021), Antarctica (e.g., *Arthrobacter*, Dsouza et al., 2015; *Pseudarthrobacter*; Shin et al., 2020; *Leifsonia*, Ganzert et al., 2011), as well as in extremely dry regions (e.g., *Pseudoarthrobacter* isolated from African deserts, Buckley et al., 2019). In terms of their activity, the detected genera have been characterized as PGPB. For example, the production of IAA by bacteria of the genus *Leifsonia* (Kang et al., 2016), or the ACC deaminase, phosphatase, and nitrogenase activity of *Pseudomonas* (Georgieva et al., 2018; Adhikari et al., 2021; Vega-Celedón et al., 2021), or bacteria of the genera *Arthrobacter* and *Pseudoarthrobacter* that have been reported with multiple growth-promoting activities (Lahsini et al., 2022). It is believed that the climatic limitations of our study area favored a select group of PGPB that possess adaptations that allow them to survive and grow in conditions that for other bacterial groups would be lethal.

The influence of climatic variability concerning temperature and water availability on the enzyme activity of PGPB has been limitedly studied. For example, for ACC deaminase enzyme activity, we know that it is an enzyme characteristic of saline and drought-exposed soils (Glick, 2004; Brockett et al., 2012). In general, both the number of ACC deaminase isolates, and their activity were higher on the north slope than on the south slope, which was much less active. Considering our results, it could be intuited that in more extreme environments there could be a higher activity of this enzyme. The phosphatase activity has been detected in psychrotolerant bacteria, which also solubilize phosphate under low-temperature conditions [e.g., *Pseudomonas* spp. isolated from Hilamaya, Adhikari et al. (2021)]. Our studied bacteria likely possess the same qualities, but studies are lacking to understand the influence of temperature on phosphate solubilization of our isolates. About nitrogen fixation, which is also higher on the north slope, we know that nitrogenase enzyme activity is favored in humid and cold south conditions (Rousk et al., 2018). However, our results showed that nitrogenase enzyme activity was higher on the drier and more temperature fluctuating north slope. Probably, a specific group of

nitrogen-fixing bacteria adapted to such microclimatic conditions prevails on the north slope. The exposure of the slope favored the activity of the three enzymatic mechanisms on the north slope. However, it was not enough to create differences between the two species, so we believe that plant identity played a key role in our results.

Bacterial abundance and growth-promoting mechanisms related to species identity

Bacterial abundance was influenced by slope exposure, and unexpectedly by species identity. Initially, we thought that trends in abundance and activity should respond only to slope exposure and should coincide for the two species since both were present under the same temperature and moisture conditions. By looking at the chemical properties of the soil, there were noticeable differences between species. A clear example was the alteration of pH by plant identity, which exacerbated the differences in bacterial abundance only in *B. empetrifolia* soils. Soils of *B. empetrifolia* and *A. prolifera* had differences in pH, with the former being more acidic. Soil pH is usually altered by root exudates of plant identity (Youssef and Chino, 1989). However, studies that have evaluated bacterial abundance as a function of pH claim that increasing pH should increase bacterial abundance (Rousk et al., 2018). On the other hand, research such as that of Yang et al. (2019), conducted in alpine systems disturbed by agricultural activity, mentions that the abundance of groups such as Actinobacteria (e.g., *Rhodococcus* associated with *B. empetrifolia* on the North Slope) is not influenced by changes in pH (Yang et al., 2019). While we believe that the combination of slope exposure coupled with pH changes in *B. empetrifolia* soils benefited the bacterial abundance of a group of microorganisms, studies are lacking to secure these insights.

Linking plant identity and associated abundant bacteria. We found that for the genus *Azorella*, it is the first time that bacteria of the genus *Pseudoarthrobacter* are detected. Previously, works such as those of Rodríguez-Echeverría et al. (2021) had detected abundant phyla such as actinobacteria for *A. compacta* and *A. madreporica*. However, among the bacteria identified, no actinobacteria were reported for *A. prolifera*. Vega-Celedón et al. (2021) had previously detected bacteria of the genus *Arthrobacter* associated with *B. microphylla* in Patagonia. Genera such as *Pseudomonas*, *Rhodococcus*, and *Leifsonia* had not been previously detected, so this is the first record in this regard.

In this study, plant identity influenced two of the three evaluated mechanisms of PGPB. Interestingly, bacterial isolates present on the north slope under the *A. prolifera* plant canopies differed in activity for two of the four mechanisms evaluated between the north and south slopes. At the same time, these bacterial isolates were the only ones that presented activity in all the hormonal and enzymatic mechanisms evaluated (Supplementary Table S1; Supplementary material). Phosphatase activity was high in soils under the *A. prolifera* canopy, which in parallel exhibited the lowest percentage of organic matter on the north slope. Coincidentally, Alemneh et al. (2022) reported a negative correlation between phosphate solubilization and soil carbon, which explains our results. Concerning ACC deaminase enzyme activity, we believe that it is not linked to soil chemical properties and is related to the plant in a more complex way. We know that the plant through its root exudates modifies its microbiome benefiting one group of microorganisms over others for its benefit (Glick et al., 2007). *A. prolifera* was likely more stressed than *B. empetrifolia* on the north slope, and for this reason, we only had differences in ACC deaminase activity for one species. As for nitrogenase enzyme activity, this was higher on the north slope for both species, so we believe that at least this mechanism is not influenced by species identity. Our results evidence a notorious relationship between plants and PGPB activity, where interactions do not seem to occur randomly.

The combination of slope exposure and plant identity evidenced a clear influence on PGPB enzyme activity, where the harshness of the alpine system favored PGPB and its benefits when conditions became more extreme on the north slope. Studies indicate that stressed plants modify their root exudates, altering their soil microbiome and favoring the presence of PGPB (Li et al., 2020; Glick and Gamalero, 2021; Chen et al., 2022). The composition of root exudates depends on soil chemical properties, plant genotype, and plant age (Vives-Peris et al., 2018). Perhaps, climatically limiting conditions "enhanced" *A. prolifera* root exudation, increasing the activity of PGPBs. Further studies need to consider plant responses by incorporating root exudates among predictors of bacterial abundance and activity.

Conclusion

Our work brings us closer to understanding what factors affect the abundance and activity of PGPB in hard systems such as those present in our system. Before our research, studies related to PGPB present in the soils of the Andes Mountains had evidenced their great biotechnological potential and their novelty for the detection of new species, in areas such as the Atacama Desert and the altiplano, with preliminary characterizations. The present work enriches the existing information related to the presence of PGPB from alpine systems in regions that had not been previously explored.

Our work showed how the environmental heterogeneity of the alpine systems, given by the contrasting slopes and its thermal and moisture oscillations, added to the identity of the species, generating variations in the abundance and plant growth promoting activity of the microorganisms present under the plant canopy of the xerophytic formations. It would be interesting to determine how and to what extent each factor contributes to the benefit provided by PGPBs. We believe that incorporating the influence of factors such as plant condition, plant identity, and microclimatic variations on changes in PGPB abundance and activity would highlight the importance of these interactions that do not occur randomly, especially when conditions become more extreme.

Data availability statement

The original contributions presented in the study are included in the article/Supplementary material, further inquiries can be directed to the corresponding author.

Author contributions

Plants may interact with soil bacteria that promote their survival and growth (PGPB) through a variety of mechanisms, especially under harsh climatic conditions. Plants that live in alpine systems have to be able to cope with harsh climatic conditions such as temperature extremes. Likely, plant-bacteria interactions are behind of plant strategies through they can grow in alpine systems. However, these interactions are poorly known. One of the southernmost xerophytic formations is in the Andes of central-southern Chile. In this system,

plants are exposed to drought and extreme temperatures during the growing season, being harsher on equatorial than polar slopes. Thus, we compared the abundance and activity of PGPB under two plant species canopy that live in contrasting slopes. We found that bacterial abundance and enzymatic activity of PGPB was higher on the driest and with greatest thermal oscillation slope. Unexpectedly, we also found that abundance and activity of bacteria depended on plant identity. We believe that microclimatic conditions such as humidity, temperature, soil nutrients, and plant identity explain our findings, which are not random, especially when conditions become more extreme.

Funding

This work was supported by CONAF-FIBN 047/2020 (RH), FONDECYT N°1220425 (MS), VRID-UDEC 2021000184INV (ASA) Grants, and ANID-Chile Technological Centres of Excellence with Basal Financing Project [CHIC–ANID PIA/BASAL PFB210018]. Carla Aguilera-Torres holds an ANID Master Fellowship.

Acknowledgments

María Dolores López and Felipe Noriega (Laboratorio de Química de Productos Naturales), José Becerra and Claudia Pérez (Laboratorio de Química de Productos Naturales), Matías Betancur (Laboratorio de Microbiología de Suelos), Adrián Garrido (Laboratorio de Epigenética Vegetal) and GET team for their help in the field work.

Conflict of interest

The authors declare that the research was conducted in the absence of any commercial or financial relationships that could be construed as a potential conflict of interest.

Publisher's note

Supplementary material

The Supplementary material for this article can be found online at: https://www.frontiersin.org/articles/10.3389/fmicb.2022.1062414/full#supplementary-material

References

Acuña, J. J., Campos, M., Mora, M. D. L. L., Jaisi, D. P., and Jorquera, M. A. (2019). ACCD-producing rhizobacteria from an Andean Altiplano native plant (*Parastrephia quadrangularis*) and their potential to alleviate salt stress in wheat seedlings. *Appl. Soil Ecol.* 136, 184–190. doi: 10.1016/j.apsoil.2019.01.005

Adamczyk, M., Hagedorn, F., Wipf, S., Donhauser, J., Vittoz, P., Rixen, C., et al. (2019). The soil microbiome of GLORIA Mountain summits in the Swiss Alps. *Front. Microbiol.* 10:1080. doi: 10.3389/fmicb.2019.01080

Adhikari, P., Jain, R., Sharma, A., and Pandey, A. (2021). Plant growth promotion at low temperature by phosphate-solubilizing pseudomonas Spp. isolated from high-altitude Himalayan soil. *Microb. Ecol.* 82, 677–687. doi: 10.1007/s00248-021-01702-1

Afzal, I., Iqrar, I., Shinwari, Z. K., and Yasmin, A. (2017). Plant growth-promoting potential of endophytic bacteria isolated from roots of wild *Dodonaea viscosa* L. *Plant Growth Regul.* 81, 399–408. doi: 10.1007/s10725-016-0216-5

Ahmad, F., Ahmad, I., and Khan, M. S. (2005). Indole acetic acid production by the indigenous isolates of *Azotobacter* and fluorescent *pseudomonas* in the presence and absence of tryptophan. *Turk. J. Biol.* 29, 29–34.

Ai, S., Chen, J., Gao, D., and Ai, Y. (2020). Distribution patterns and drivers of artificial soil bacterial community on cut-slopes in alpine mountain area of Southwest China. *Catena* 194:104695. doi: 10.1016/j.catena.2020.104695

Alemneh, A. A., Zhou, Y., Ryder, M. H., and Denton, M. D. (2022). Soil environment influences plant growth-promotion traits of isolated rhizobacteria. *Pedobiologia* 90:150785. doi: 10.1016/j.pedobi.2021.150785

Ali, S. Z., Sandhya, V., and Rao, L. V. (2014). Isolation and characterization of drought-tolerant ACC deaminase and exopolysaccharide-producing fluorescent pseudomonas sp. *Ann. Microbiol.* 64, 493–502. doi: 10.1007/s13213-013-0680-3

Arroyo, M. T. K., Squeo, F., Cavieres, L. A., and Marticorena, C. (2004). "Chilenische Anden" in *Gebirge der Erde. Landschaft, Klima, Pflanzenwelt*. eds. C. A. Burga, F. Klötzli and G. Grabherr (Ulmer, Stuttgart, Germany: Ulmer Eugen Verlag), 210–219.

Ashry, N. M., Alaidaroos, B. A., Mohamed, S. A., Badr, O. A. M., El-Saadony, M. T., and Esmael, A. (2022). Utilization of drought-tolerant bacterial strains isolated from harsh soils as a plant growth-promoting rhizobacteria (PGPR): utilization of drought-tolerant bacterial strains. *Saudi J. Biological Sciences* 29, 1760–1769. doi: 10.1016/j.sjbs.2021.10.054

Bais, H. P., Weir, T. L., Perry, L. G., Gilroy, S., and Vivanco, J. M. (2006). The role of root exudates in rhizosphere interactions with plants and other organisms. *Annu. Rev. Plant Biol.* 57, 233–266. doi: 10.1146/annurev.arplant.57.032905.105159

Barbosa, M. S., Rodrigues, E. P., Stolf-Moreira, R., Tischer, C. A., and de Oliveira, A. L. M. (2020). Root exudate supplemented inoculant of *Azospirillum brasilense* Ab-V5 is more effective in enhancing rhizosphere colonization and growth of maize. *Environmental Sustain.* 3, 187–197. doi: 10.1007/s42398-020-00103-3

Bergottini, V. M., Otegui, M. B., Sosa, D. A., Zapata, P. D., Mulot, M., Rebord, M., et al. (2015). Bio-inoculation of yerba mate seedlings (*Ilex paraguariensis* St. hill.) with native plant growth-promoting rhizobacteria: a sustainable alternative to improve crop yield. *Biol. Fertil. Soils* 51, 749–755. doi: 10.1007/s00374-015-1012-5

Bhattacharyya, P. N., and Jha, D. K. (2012). Plant growth-promoting rhizobacteria (PGPR): emergence in agriculture. *World J. Microbiol. Biotechnol.* 28, 1327–1350. doi: 10.1007/s11274-011-0979-9

Brockett, B. F. T., Prescott, C. E., and Grayston, S. J. (2012). Soil moisture is the major factor influencing microbial community structure and enzyme activities across seven biogeoclimatic zones in western Canada. *Soil Biol. Biochem.* 44, 9–20. doi: 10.1016/j.soilbio.2011.09.003

Buckley, E., Lee, K. C., Higgins, C. M., and Seale, B. (2019). Crossm whole-genome sequences of one Arthrobacter strain and desert. *Microbiology Resource Announcements* 8, 18–19. doi: 10.1128/MRA.00885-19

Chaturvedi, P., and Shivaji, S. (2006). *Exiguobacterium indicum* sp. Nov., a psychrophilic bacterium from the Hamta glacier of the Himalayan mountain ranges of India. *Int. J. Syst. Evol. Microbiol.* 56, 2765–2770. doi: 10.1099/ijs.0.64508-0

Chen, J., Luo, Y., Xia, J., Jiang, L., Zhou, X., Lu, M., et al. (2015). Stronger warming effects on microbial abundances in colder regions. *Sci. Rep.* 5, 1–10. doi: 10.1038/srep18032

Chen, C., Wang, M., Zhu, J., Tang, Y., Zhang, H., Zhao, Q., et al. (2022). Long-term effect of epigenetic modification in plant–microbe interactions: modification of DNA methylation induced by plant growth-promoting bacteria mediates promotion process. *Microbiome* 10, 36–19. doi: 10.1186/s40168-022-01236-9

Chodak, M., Golebiewski, M., Morawska-Ploskonka, J., Kuduk, K., and Niklinska, M. (2015). Soil chemical properties affect the reaction of forest soil bacteria to drought and rewetting stress. *Ann. Microbiol.* 65, 1627–1637. doi: 10.1007/s13213-014-1002-0

de Souza, R., Ambrosini, A., and Passaglia, L. M. P. (2015). Plant growth-promoting bacteria as inoculants in agricultural soils. *Genet. Mol. Biol.* 38, 401–419. doi: 10.1590/S1415-475738420150053

Dixon, H. J., Murphy, M. D., Sparks, S. J., Chávez, R., Naranjo, J. A., Dunkley, et al. (1999). La geología del volcán Nevados de Chillán, Chile. *Rev. Geol. Chile* 26, 227–253.

Donoso, C. (1982). Reseña ecológica de los bosques mediterráneos de Chile. *Bosque* 4, 117–146. doi: 10.4206/bosque.1982.v4n2-04

Dsouza, M., Taylor, M. W., Turner, S. J., and Aislabie, J. (2015). Genomic and phenotypic insights into the ecology of Arthrobacter from Antarctic soils. *BMC Genom.* 16, 1–18. doi: 10.1186/s12864-015-1220-2

Duca, D. R., and Glick, B. R. (2020). Indole-3-acetic acid biosynthesis and its regulation in plant-associated bacteria. *Appl. Microbiol. Biotechnol.* 104, 8607–8619. doi: 10.1007/s00253-020-10869-5

Durante, M., Maseda, P. H., and Fernández, R. J. (2011). Xylem efficiency vs. safety: acclimation to drought of seedling root anatomy for six Patagonian shrub species. *J. Arid Environ.* 75, 397–402. doi: 10.1016/j.jaridenv.2010.12.001

Fajardo, A., Piper, F. I., and Cavieres, L. A. (2011). Distinguishing local from global climate influences in the carbon status variation with altitude of a treeline species. *Glob. Ecol. Biogeogr.* 20, 307–318. doi: 10.1111/j.1466-8238.2010.00598.x

Fan, S., Sun, H., Yang, J., Qin, J., Shen, D., and Chen, Y. (2021). Variations in soil enzyme activities and microbial communities along an altitudinal gradient on the eastern Qinghai–Tibetan plateau. *Forests* 12, 1–14. doi: 10.3390/f12060681

Farooq, S., Nazir, R., Ganai, B. A., Mushtaq, H., and Dar, G. J. (2022). Psychrophilic and psychrotrophic bacterial diversity of Himalayan Thajwas glacial soil. *India. Biologia* 77, 203–213. doi: 10.1007/s11756-021-00915-6

Franche, C., Lindström, K., and Elmerich, C. (2009). Nitrogen-fixing bacteria associated with leguminous and non-leguminous plants. *Plant Soil* 321, 35–59. doi: 10.1007/s11104-008-9833-8

Fuentes, A., Herrera, H., Charles, T. C., and Arriagada, C. (2020). Fungal and bacterial microbiome associated with the rhizosphere of native plants from the Atacama desert. *Microorganisms* 8:209. doi: 10.3390/microorganisms8020209

Gamalero, E., and Glick, B. R. (2011). in *Mechanisms used by plant growth-promoting bacteria BT – Bacteria in agrobiology: Plant nutrient management*. ed. D. K. Maheshwari (Berlin Heidelberg: Springer), 17–46.

Gang, S., Sharma, S., Saraf, M., Buck, M., and Schumacher, J. (2019). Analysis of indole-3-acetic acid (IAA) production in Klebsiella by LC-MS/MS and the Salkowski method. *Bio-Protocol* 9, e3230–e3239. doi: 10.21769/bioprotoc.3230

Ganzert, L., Bajerski, F., Mangelsdorf, K., Lipski, A., and Wagner, D. (2011). Leifsonia psychrotolerans sp. nov., a psychrotolerant species of the family microbacteriaceae from Livingston Island, Antarctica. *Int. J. Syst. Evol. Microbiol.* 61, 1938–1943. doi: 10.1099/ijs.0.021956-0

Georgieva, T., Evstatieva, Y., Savov, V., Bratkova, S., and Nikolova, D. (2018). Assessment of plant growth promoting activities of five rhizospheric *pseudomonas* strains. *Biocatal. Agric. Biotechnol.* 16, 285–292. doi: 10.1016/j.bcab.2018.08.015

Gestión de Recursos Naturales (GRN). (2022). Mapa de Áreas con Presencia de Formaciones Xerofíticas. Reviewed from https://www.grn.cl/Mapa%20de%20Areas%20con%20Presencia%20de%20Formaciones%20Xerofiticas.pdf.

Glick, B. R. (2004). Bacterial ACC deaminase and the alleviation of plant stress. *Adv. Appl. Microbiol.* 56, 291–312. doi: 10.1016/S0065-2164(04)56009-4

Glick, B. R. (2012). Plant growth-promoting bacteria: mechanisms and applications. *Scientifica (Cairo)*. 2012:963401, 1–15. doi: 10.6064/2012/963401

Glick, B. R., and Gamalero, E. (2021). Recent developments in the study of plant microbiomes. *Microorganisms* 9, 1–18. doi: 10.3390/microorganisms9071533

Glick, B. R., Todorovic, B., Czarny, J., Cheng, Z., Duan, J., and McConkey, B. (2007). Promotion of plant growth by bacterial ACC deaminase. *Crit. Rev. Plant Sci.* 26, 227–242. doi: 10.1080/07352680701572966

Golluscio, R. A., Cavagnaro, F. P., and Valenta, M. D. (2011). Shrubs of the Patagonian steppe: adapted to tolerate drought or grazing? *Austral Ecol.* 21, 61–70.

González-Ferrán, O. (1995). *Volcanes de Chile*. Editorial IGM, Santiago de Chile. 640 pp.

Hara, S., Hashidoko, Y., Desyatkin, R. V., Hatano, R., and Tahara, S. (2009). High rate of N2 fixation by East Siberian cryophilic soil bacteria as determined by measuring acetylene reduction in nitrogen-poor medium solidified with gellan gum. *Appl. Environ. Microbiol.* 75, 2811–2819. doi: 10.1128/AEM.02660-08

Hardy, R. W. F., Holsten, R. D., Jackson, E. K., and Burns, R. C. (1968). The acetylene-ethylene assay for N2 fixation: laboratory and field evaluation 1. *Plant Physiol.* 43, 1185–1207. doi: 10.1104/pp.43.8.1185

Haselwandter, K., Hofmann, A., Holzmann, H. P., and Read, D. J. (1983). Availability of nitrogen and phosphorus in the nival zone of the Alps. *Oecologia* 57, 266–269. doi: 10.1007/BF00379589

Herlina, L., Pukan, K. K., and Mustikaningtyas, D. (2017). The endophytic bacteria producing IAA (Indole acetic acid) in *Arachis hypogaea*. *Cell Biology and Develop.* 1, 31–35. doi: 10.13057/cellbioldev/v010106

Hingole, S. S., and Pathak, A. P. (2016). Saline soil microbiome: a rich source of halotolerant PGPR. *J. Crop. Sci. Biotechnol.* 19, 231–239. doi: 10.1007/s12892-016-0035-2

Honma, M., and Shimomura, T. (1978). Metabolism of 1-aminocyclopropane-1-carboxylic acid. *Agric. Biol. Chem.* 42, 1825–1831. doi: 10.1080/00021369.1978.10863261

Jaggi, V., Brindhaa, N. T., and Sahgal, M. (2020). in *Microbial diversity in northwestern Himalayan Agroecosystems: Functions and applications BT - microbiological advancements for higher Altitude Agro-Ecosystems & Sustainability*. eds. R. Goel, R. Soni and D. C. Suyal (Singapore: Springer), 135–161.

Joshi, P., Joshi, G. K., Tanuja, , Mishra, P. K., Bisht, J. K., and Bhatt, J. C. (2014). Diversity of cold tolerant phosphate solubilizing microorganisms from North Western Himalayas. 1, 227–264. doi: 10.1007/978-3-319-05936-5_10

Kadioglu, G. B., Koseoglu, M. S., Ozdal, M., Sezen, A., Ozdal, O. G., and Algur, O. F. (2018). Isolation of cold tolerant and ACC Deaminase producing plant growth promoting Rhizobacteria from high altitudes. *Romanian Biotechnological Letters* 23, 13479–13486.

Kang, S. M., Asaf, S., Kim, S. J., Yun, B. W., and Lee, I. J. (2016). Complete genome sequence of plant growth-promoting bacterium *Leifsonia xyli* SE134, a possible gibberellin and auxin producer. *J. Biotechnol.* 239, 34–38. doi: 10.1016/j.jbiotec.2016.10.004

Kanu, S., and Dakora, F. D. (2009). Thin-layer chromatographic analysis of lumichrome, riboflavin and indole acetic acid in cell-free culture filtrate of Psoralea nodule bacteria grown at different pH, salinity and temperature regimes. *Symbiosis* 48, 173–181. doi: 10.1007/BF03179996

Kieft, T. L., Amy, P. S., Brockman, F. J., Fredrickson, J. K., Bjornstad, B. N., and Rosacker, L. L. (1993). Microbial abundance and activities in relation to water potential in the vadose zones of arid and semiarid sites. *Microb. Ecol.* 26, 59–78. doi: 10.1007/BF00166030

Kifle, M. H., and Laing, M. D. (2015). Isolation and screening of bacteria for their Diazotrophic potential and their influence on growth promotion of maize seedlings in greenhouses. *Front. Plant Sci.* 6:1225. doi: 10.3389/fpls.2015.01225

Kong, Z., and Glick, B. R. (2017). The role of plant growth-promoting bacteria in metal phytoremediation. *Adv. Microb. Physiol.* 71, 97–132. doi: 10.1016/bs.ampbs.2017.04.001

Körner, C. (2004). Mountain biodiversity, its causes and function. *Ambio* 33, 11–17. doi: 10.1007/0044-7447-33.sp13.11

Körner, C. (2011). Coldest places on earth with angiosperm plant life. *Alp. Bot.* 121, 11–22. doi: 10.1007/s00035-011-0089-1

Körner, C. (2021). Life under and in snow: protection and limitation. *Alpine Plant Life*. 89–118. doi: 10.1007/978-3-030-59538-8_5

Körner, C., and Ohsawa, M. (2005). "Mountain systems" in *Ecosystems and human well-being: Current state and trends*. eds. R. Hassan, R. Scholes and N. Ash, vol. *1* (Washington DC: Island press), 681–716.

Kumar, N., Kumar, A., Jeena, N., Singh, R., and Singh, H. (2020). Factors influencing soil ecosystem and agricultural productivity at higher altitudes. 55–70. doi: 10.1007/978-981-15-1902-4_4,

Kumar, A., Kumari, M., Swarupa, P., and Shireen. (2019). Characterization of pH dependent growth response of agriculturally important microbes for development of plant growth promoting bacterial consortium. *J. Pure and Applied Microbiol.* 13, 1053–1061. doi: 10.22207/JPAM.13.2.43

Lahsini, A., Sallami, A., Ait-ouakrim, E. H., El, H., Obtel, M., Douira, A., et al. (2022). Rhizosphere isolation and molecular identification of an indigenous abiotic stress-tolerant plant growth-promoting rhizobacteria from the rhizosphere of the olive tree in southern Morocco. *Rhizosphere* 23:100554. doi: 10.1016/j.rhisph.2022.100554

Leontidou, K., Genitsaris, S., Papadopoulou, A., Kamou, N., Bosmali, I., Matsi, T., et al. (2020). Plant growth promoting rhizobacteria isolated from halophytes and drought-tolerant plants: genomic characterisation and exploration of phyto-beneficial traits. *Sci. Rep.* 10, 14857–14815. doi: 10.1038/s41598-020-71652-0

Li, J., Li, C., Kou, Y., Yao, M., He, Z., and Li, X. (2020). Distinct mechanisms shape soil bacterial and fungal co-occurrence networks in a mountain ecosystem. *FEMS Microbiol. Ecol.* 96, 1–12. doi: 10.1093/femsec/fiaa030

Li, H. B., Singh, R. K., Singh, P., Song, Q. Q., Xing, Y. X., Yang, L. T., et al. (2017). Genetic diversity of nitrogen-fixing and plant growth promoting *pseudomonas* species isolated from sugarcane rhizosphere. *Front. Microbiol.* 8, 1–20. doi: 10.3389/fmicb.2017.01268

Liengen, T. (1999). Environmental factors influencing the nitrogen fixation activity of free-living terrestrial cyanobacteria from a high arctic area, Spitsbergen. *Can. J. Microbiol.* 45, 573–581. doi: 10.1139/w99-040

López-Angulo, J., Pescador, D. S., Sánchez, A. M., Luzuriaga, A. L., Cavieres, L. A., and Escudero, A. (2019). Alpine vegetation dataset from three contrasting mountain ranges differing in climate and evolutionary history. *Data Brief* 27:104816. doi: 10.1016/j.dib.2019.104816

Majeed, A., Muhammad, Z., and Ahmad, H. (2018). Plant growth promoting bacteria: role in soil improvement, abiotic and biotic stress management of crops. *Plant Cell Rep.* 37, 1599–1609. doi: 10.1007/s00299-018-2341-2

Maldonado, J. E., Gaete, A., Mandakovic, D., Aguado-Norese, C., Aguilar, M., Gutiérrez, R. A., et al. (2022). Partners to survive: *Hoffmannseggia doellii* root-associated microbiome at the Atacama Desert. *New Phytol.* 234, 2126–2139. doi: 10.1111/nph.18080

Måren, I. E., Karki, S., Prajapati, C., Yadav, R. K., and Shrestha, B. B. (2015). Facing north or south: does slope aspect impact forest stand characteristics and soil properties in a semiarid trans-Himalayan valley? *J. Arid Environ.* 121, 112–123. doi: 10.1016/j.jaridenv.2015.06.004

McMaster, G. S., and Wilhelm, W. W. (1997). Growing degree-days: one equation, two interpretations. *Agriculture, Forest and Meteorology.* 87, 291–300. doi: 10.1016/S0168-1923(97)00027-0

Mendoza-Hernández, J. C., Perea-Vélez, S., Arriola Morales, J., Martínez-Simón, S. M., and Pérez-Osorio, G. (2016). Assessing the effects of heavy metals in ACC deaminase and IAA production on plant growth-promoting bacteria. *Microbiol. Res.* 188-189, 53–61. doi: 10.1016/j.micres.2016.05.001

Moreira, A., and Cereceda, P. (2013). Diversidad y fragilidad del paisaje botánico de chile mediterráneo. *Revista Chagual, XI* 11, 30–40.

Mujahid, T. Y., Subhan, S. A., Wahab, A., Masnoon, J., Ahmed, N., and Abbas, T. (2015). Effects of different physical and chemical parameters on phosphate solubilization activity of plant growth promoting bacteria isolated from indigenous soil. *J. Pharmacy and Nutrition Sciences* 5, 64–70. doi: 10.6000/1927-5951.2015.05.01.10

Naylor, D., and Coleman-Derr, D. (2018). Drought stress and root-associated bacterial communities. *Front. Plant Sci.* 8, 1–16. doi: 10.3389/fpls.2017.02223

Nuñez, C. I., Aizen, M. A., and Ezcurra, C. (1999). Species associations and nurse plant effects in patches of high-Andean vegetation. *J. Veg. Sci.* 10, 357–364. doi: 10.2307/3237064

Olanrewaju, O. S., Glick, B. R., and Babalola, O. O. (2017). Mechanisms of action of plant growth promoting bacteria. *World J. Microbiol. Biotechnol.* 33, 197–116. doi: 10.1007/s11274-017-2364-9

Orozco-Mosqueda, M. D. C., Flores, A., Rojas-Sánchez, B., Urtis-Flores, C. A., Morales-Cedeño, L. R., Valencia-Marin, M. F., et al. (2021). Plant growth-promoting bacteria as bioinoculants: attributes and challenges for sustainable crop improvement. *Agronomy* 11, 1–15. doi: 10.3390/agronomy11061167

Pande, A., Pandey, P., Mehra, S., Singh, M., and Kaushik, S. (2017). Phenotypic and genotypic characterization of phosphate solubilizing bacteria and their efficiency on the growth of maize. *J. Genetic Engineering and Biotechn.* 15, 379–391. doi: 10.1016/j.jgeb.2017.06.005

Pandey, A., and Yarzábal, L. A. (2019). Bioprospecting cold-adapted plant growth promoting microorganisms from mountain environments. *Appl. Microbiol. Biotechnol.* 103, 643–657. doi: 10.1007/s00253-018-9515-2

Penrose, D. M., and Glick, B. R. (2003). Methods for isolating and characterizing ACC deaminase-containing plant growth-promoting rhizobacteria. *Physiol. Plant.* 118, 10–15. doi: 10.1034/j.1399-3054.2003.00086.x

Pérez-Jaramillo, J. E., Carrión, V. J., de Hollander, M., and Raaijmakers, J. M. (2018). The wild side of plant microbiomes. *Microbiome* 6, 143–149. doi: 10.1186/s40168-018-0519-z

Pfanzelt, S., Grau, J., and Rodríguez, R. (2008). A vegetation map of Nevados De Chillan volcanic complex, Bio-Bio region, Chile. *Gayana. Botánica* 65, 209–219. doi: 10.4067/s0717-66432008000200007

Pikovskaya, R. I. (1948). Mobilization of phosphorus in soil in connection with vital activity of some microbial species. *Mikrobiologiya* 17, 362–370.

Piper, F. I., Viñegla, B., Linares, J. C., Camarero, J. J., Cavieres, L. A., and Fajardo, A. (2016). Mediterranean and temperate treelines are controlled by different environmental drivers. *J. Ecol.* 104, 691–702. doi: 10.1111/1365-2745.12555

Preem, J.-K., Truu, J., Truu, M., Mander, Ü., Oopkaup, K., Lõhmus, K., et al. (2012). Bacterial community structure and its relationship to soil physico-chemical characteristics in alder stands with different management histories. *Ecol. Eng.* 49, 10–17. doi: 10.1016/j.ecoleng.2012.08.034

Rahman, I. U., Afzal, A., Iqbal, Z., Hart, R., Abd Allah, E. F., Alqarawi, A. A., et al. (2020). Response of plant physiological attributes to altitudinal gradient: plant adaptation to temperature variation in the Himalayan region. *Sci. Total Environ.* 706:135714. doi: 10.1016/j.scitotenv.2019.135714

Ramakrishna, W., Yadav, R., and Li, K. (2019). Plant growth promoting bacteria in agriculture: two sides of a coin. *Appl. Soil Ecol.* 138, 10–18. doi: 10.1016/j.apsoil.2019.02.019

Rawat, P., Das, S., Shankhdhar, D., and Shankhdhar, S. C. (2021). Phosphate-solubilizing microorganisms: mechanism and their role in phosphate Solubilization and uptake. *J. Soil Sci. Plant Nutr.* 21, 49–68. doi: 10.1007/s42729-020-00342-7

Reddy, G. S. N., Prabagaran, S. R., and Shivaji, S. (2008). *Leifsonia pindariensis* sp. nov., isolated from the Pindari glacier of the Indian Himalayas, and emended description of the genus Leifsonia. *Int. J. Syst. Evol. Microbiol.* 58, 2229–2234. doi: 10.1099/ijs.0.65715-0

Rodríguez, R., Grau, J., Baeza, C., and Davies, A. (2008). Lista comentada de las plantas vasculares de Nevados de Chillán, Chile. *Gayana Botanica* 65, 153–197. doi: 10.4067/S0717-66432008000200005

Rodríguez, R., Marticorena, C., Alarcón, D., Baeza, C., Cavieres, L., Finot, V. L., et al. (2018). Catálogo de las plantas vasculares de Chile. *Gayana Botánica* 75, 1–430. doi: 10.4067/S0717-66432018000100001

Rodríguez-Echeverría, S., Delgado-Baquerizo, M., Morillo, J. A., Gaxiola, A., Manzano, M., Marquet, P. A., et al. (2021). Azorella cushion plants and aridity are important drivers of soil microbial communities in Andean ecosystems. *Ecosystems* 24, 1576–1590. doi: 10.1007/s10021-021-00603-1

Rousk, K., Sorensen, P. L., and Michelsen, A. (2018). What drives biological nitrogen fixation in high arctic tundra: moisture or temperature. *Ecosphere* 9:2117. doi: 10.1002/ecs2.2117

Ruberto, L. A. M., Vazquez, S., Lobalbo, A., and Mac Cormack, W. P. (2005). Psychrotolerant hydrocarbon-degrading *Rhodococcus* strains isolated from polluted Antarctic soils. *Antarct. Sci.* 17, 47–56. doi: 10.1017/S0954102005002415

Rueda-Puente, E. O., Bianciotto, O., Farmohammadi, S., Zakeri, O., Elías, J. L., Hernández-Montiel, L. G., et al. (2019). "Plant growth-promoting bacteria associated to the halophyte Suaeda maritima (L.)" in *Abbas, Iran BT - Sabkha ecosystems*. eds. B. Gul, B. Böer, M. A. Khan, M. Clüsener-Godt and A. Hameed, vol. *VI* (New York: Springer International Publishing), 289–300.

Rui, J., Hu, J., Wang, F., Zhao, Y., and Li, C. (2022). Altitudinal niches of symbiotic, associative and free-living diazotrophs driven by soil moisture and temperature in the alpine meadow on the Tibetan plateau. *Environ. Res.* 211:113033. doi: 10.1016/j.envres.2022.113033

Rumpf, S. B., Hülber, K., Klonner, G., Moser, D., Schütz, M., Wessely, J., et al. (2018). Range dynamics of mountain plants decrease with elevation. *Proc. Natl. Acad. Sci. U. S. A.* 115, 1848–1853. doi: 10.1073/pnas.1713936115

Scherrer, D., and Körner, C. (2011). Topographically controlled thermal-habitat differentiation buffers alpine plant diversity against climate warming. *J. Biogeogr.* 38, 406–416. doi: 10.1111/j.1365-2699.2010.02407.x

Schoebitz, M., Ceballos, C., and Ciampi, L. (2013). Effect of immobilized phosphate solubilizing bacteria on wheat growth and phosphate uptake. *J. Soil Sci. Plant Nutr.* 13, 1–10. doi: 10.4067/s0718-95162013005000001

Selvakumar, G., Kundu, S., Joshi, P., Nazim, S., Gupta, A. D., Mishra, P. K., et al. (2008). Characterization of a cold-tolerant plant growth-promoting bacterium *Pantoea dispersa* 1A isolated from a sub-alpine soil in the North Western Indian Himalayas. *World J. Microbiol. Biotechnol.* 24, 955–960. doi: 10.1007/s11274-007-9558-5

Senthilkumar, M., Amaresan, N., and Sankaranarayanan, A. (2021). "Estimation of malondialdehyde (MDA) by Thiobarbituric acid (TBA) assay" in *Plant-microbe interactions* (Humana, New York, NY: Springer Protocols Handbooks)

Sezen, A., Ozdal, M., Kubra, K. O. C., and Algur, O. F. (2016). Isolation and characterization of plant growth promoting rhizobacteria (PGPR) and their effects on improving growth of wheat. *J. Appl. Biol. Sci.* 10, 41–46.

Shin, Y., Lee, B. H., Lee, K. E., and Park, W. (2020). *Pseudarthrobacter psychrotolerans* sp. nov., a cold-adapted bacterium isolated from Antarctic soil. *Int. J. Syst. Evol. Microbiol.* 70, 6106–6114. doi: 10.1099/ijsem.0.004505

Sierra-Almeida, A., Reyes-Bahamonde, C., and Cavieres, L. A. (2016). Drought increases the freezing resistance of high-elevation plant species from central Chilean Andes. *Oecologia* 181, 1011–1023. doi: 10.1007/s00442-016-3622-5

Siles, J. A., and Margesin, R. (2016). Abundance and diversity of bacterial, Archaeal, and fungal communities along an altitudinal gradient in alpine Forest soils: what are the driving factors? *Microb. Ecol.* 72, 207–220. doi: 10.1007/s00248-016-0748-2

Sinegani, A. A. S., and Younessi, N. (2017). Antibiotic resistance of bacteria isolated from heavy metal-polluted soils with different land uses. *J. Global Antimicrobial Resistance* 10, 247–255. doi: 10.1016/j.jgar.2017.05.012

Sklenář, P., Romoleroux, K., Muriel, P., Jaramillo, R., Bernardi, A., Diazgranados, M., et al. (2021). Distribution changes in Páramo plants from the equatorial high Andes in response to increasing temperature and humidity variation since 1880. *Alp. Bot.* 131, 201–212. doi: 10.1007/s00035-021-00270-x

Squeo, F. A., Arancio, G., and Gutiérrez, J. R. (2001). *Libro rojo de la flora nativa y de los sitios prioritarios para su conservación: Región de Coquimbo*. eds. G. Arancio and J. R. Gutiérrez (Gutiérrez La Serena, Chile: Ediciones Universidad de La Serena), 137–163.

Squeo, F. A., Arancio, G., Gutiérrez, J. R., Letelier, L., Arroyo, M. T. K., León-Lobos, P. Y., et al. (2008). *Flora amenazada de la Región de Atacama y estrategias para su conservación. Anexo acuerdos taller de la Ley de Bosque Nativo de la Macro Zona Norte. Ediciones de la Universidad de La Serena*, 71–72.

Stres, B., Danevčič, T., Pal, L., Fuka, M. M., Resman, L., Leskovec, S., et al. (2008). Influence of temperature and soil water content on bacterial, archaeal and denitrifying microbial communities in drained fen grassland soil microcosms. *FEMS Microbiol. Ecol.* 66, 110–122. doi: 10.1111/j.1574-6941.2008.00555.x

Tang, M., Li, L., Wang, X., You, J., Li, J., and Chen, X. (2020). Elevational is the main factor controlling the soil microbial community structure in alpine tundra of the Changbai Mountain. *Sci. Rep.* 10, 12442–12415. doi: 10.1038/s41598-020-69441-w

Varas, B., Castro, M. H., Rodriguez, R., Von Baer, D., Mardones, C., and Hinrichsen, P. (2013). Identification and characterization of microsatellites from calafate (*Berberis microphylla*, Berberidaceae). *Applications in Plant Sciences* 1:1200003. doi: 10.3732/apps.1200003

Vega-Celedón, P., Bravo, G., Velásquez, A., Cid, F. P., Valenzuela, M., Ramírez, I., et al. (2021). Microbial diversity of psychrotolerant bacteria isolated from wild flora of Andes mountains and Patagonia of Chile towards the selection of plant growth-promoting bacterial consortia to alleviate cold stress in plants. *Microorganisms* 9, 1–28. doi: 10.3390/microorganisms9030538

Viale, M., Bianchi, E., Cara, L., Ruiz, L. E., Villalba, R., Pitte, P., et al. (2019). Contrasting climates at both sides of the Andes in Argentina and Chile 7, 1–15. doi: 10.3389/fenvs.2019.00069,

Viruel, E., Lucca, M. E., and Siñeriz, F. (2011). Plant growth promotion traits of phosphobacteria isolated from Puna, Argentina. *Arch. Microbiol.* 193, 489–496. doi: 10.1007/s00203-011-0692-y

Vives-Peris, V., Molina, L., Segura, A., Gómez-Cadenas, A., and Pérez-Clemente, R. M. (2018). Root exudates from citrus plants subjected to abiotic stress conditions have a positive effect on rhizobacteria. *J. Plant Physiol.* 228, 208–217. doi: 10.1016/j.jplph.2018.06.003

Wakelin, S. A., Gupta, V. V. S. R., and Forrester, S. T. (2010). Regional and local factors affecting diversity, abundance and activity of free-living, N2-fixing bacteria in Australian agricultural soils. *Pedobiologia* 53, 391–399. doi: 10.1016/j.pedobi.2010.08.001

Wang, C., Michalet, R., Liu, Z., Jiang, X., Wang, X., Zhang, G., et al. (2020). Disentangling large- and small-scale abiotic and biotic factors shaping soil microbial communities in an alpine cushion plant system. *Front. Microbiol.* 11, 1–17. doi: 10.3389/fmicb.2020.00925

Widawati, S., and Suliasih, S. (2006). The population of phosphate solubilizing bacteria (PSB) from Cikaniki, Botol Mountain, and Ciptarasa area, and the ability of PSB to solubilize insoluble P in solid pikovskaya medium. *Biodiversitas J. Biological Diversity* 7, 109–113. doi: 10.13057/biodiv/d070203

Xiong, Y. W., Li, X. W., Wang, T. T., Gong, Y., Zhang, C. M., Xing, K., et al. (2020). Root exudates-driven rhizosphere recruitment of the plant growth-promoting rhizobacterium *Bacillus flexus* KLBMP 4941 and its growth-promoting effect on the coastal halophyte *Limonium* sinense under salt stress. *Ecotoxicol. Environ. Saf.* 194:110374. doi: 10.1016/j.ecoenv.2020.110374

Yadav, A. N., Sachan, S. G., Verma, P., and Saxena, A. K. (2015). Prospecting cold deserts of northwestern Himalayas for microbial diversity and plant growth promoting attributes. *J. Biosci. Bioeng.* 119, 683–693. doi: 10.1016/j.jbiosc.2014.11.006

Yang, J., El-Kassaby, Y. A., and Guan, W. (2020). The Effect of slope aspect on vegetation attributes in a mountainous dry valley, Southwest China. *Sci. Rep.*, 10, 1–11. doi: 10.1038/s41598-020-73496-0

Yang, F., Niu, K., Collins, C. G., Yan, X., Ji, Y., Ling, N., et al. (2019). Grazing practices affect the soil microbial community composition in a Tibetan alpine meadow. *Land Degrad. Dev.* 30, 49–59. doi: 10.1002/ldr.3189

Yarzábal, L. A. (2014). "Cold-tolerant phosphate-solubilizing microorganisms and agriculture development in mountainous regions of the world" in *Phosphate solubilizing microorganisms* eds. K. Mohammad Saghir, Z. Almas and M. Javed. (Cham: Springer), 113–135.

Yoon, S. H., Ha, S. M., Kwon, S., Lim, J., Kim, Y., Seo, H., et al. (2017). Introducing EzBioCloud: a taxonomically united database of 16S rRNA and whole genome assemblies. *Int. J. Syst. Evol. Microbiol.* 67, 1613–1617. doi: 10.1099/ijsem.0.001755

Youssef, R. A., and Chino, M. (1989). Root-induced changes in the rhizosphere of plants. I. pH changes in relation to the bulk soil. *Soil Sci. Plant Nutr.* 35, 461–468. doi: 10.1080/00380768.1989.10434779

Zeng, X. H., Zhang, W. J., Song, Y. G., and Shen, H. T. (2014). Slope aspect and slope position have effects on plant diversity and spatial distribution in the hilly region of mount Taihang, North China. *J. Food, Agriculture and Environ.* 12, 391–397. doi: 10.13287/j.1001-9332.202008.004

frontiers | Frontiers in Microbiology

TYPE Original Research
PUBLISHED 18 May 2023
DOI 10.3389/fmicb.2023.1167083

OPEN ACCESS

EDITED BY
Paola Grenni,
National Research Council, Italy

REVIEWED BY
Giulia Caneva,
Roma Tre University, Italy
Sandi Orlic,
Rudjer Boskovic Institute, Croatia

*CORRESPONDENCE
Samah Mohamed Rizk
✉ samah_rizk@agr.asu.edu.eg
Mahmoud Magdy
✉ m.elmosallamy@agr.asu.edu.eg

†These authors have contributed equally to this work

RECEIVED 15 February 2023
ACCEPTED 27 April 2023
PUBLISHED 18 May 2023

CITATION
Rizk SM, Magdy M, De Leo F, Werner O, Rashed MA-S, Ros RM and Urzì C (2023) Culturable and unculturable potential heterotrophic microbiological threats to the oldest pyramids of the Memphis necropolis, Egypt.
Front. Microbiol. 14:1167083.
doi: 10.3389/fmicb.2023.1167083

Culturable and unculturable potential heterotrophic microbiological threats to the oldest pyramids of the Memphis necropolis, Egypt

Samah Mohamed Rizk[1*†], Mahmoud Magdy[1*†], Filomena De Leo[2], Olaf Werner[3], Mohamed Abdel-Salam Rashed[1], Rosa M. Ros[3] and Clara Urzì[2]

[1]Genetics Department, Faculty of Agriculture, Ain Shams University, Cairo, Egypt, [2]Department of Chemical, Biological, Pharmaceutical, and Environmental Sciences, University of Messina, Messina, Italy, [3]Department of Plant Biology, Faculty of Biology, Murcia University, Murcia, Spain

A large percentage of the world's tangible cultural heritage is made from stone; thus, it deteriorates due to physical, chemical, and/or biological factors. The current study explored the microbial community inhabiting two prehistoric sites with high cultural value in the Memphis necropolis of Egypt (Djoser and Lahun Pyramids) using amplicon-based metabarcoding and culture-dependent isolation methods. Samples were examined by epifluorescent microscopy for biological signs before environmental DNA extraction and *in vitro* cultivation. The metabarcoding analysis identified 644 bacterial species (452 genera) using the 16S rRNA and 204 fungal species (146 genera) using ITS. In comparison with the isolation approach, an additional 28 bacterial species (13 genera) and 34 fungal species (20 genera) were identified. A total of 19 bacterial and 16 fungal species were exclusively culture-dependent, while 92 bacterial and 122 fungal species were culture-independent. The most abundant stone-inhabiting bacteria in the current study were *Blastococcus aggregatus*, *Blastococcus saxobsidens*, and *Blastococcus* sp., among others. The most abundant rock-inhabiting fungi were *Knufia karalitana* and *Pseudotaeniolina globosa*, besides abundant unknown Sporormiaceae species. Based on previous reports, microorganisms associated with biodeterioration were detected on color-altered sites at both pyramids. These microorganisms are potentially dangerous as physical and chemical deterioration factors and require proper conservation plans from a microbiological perspective.

KEYWORDS

tangible monuments, cultural heritage, microbial genomics, microbial isolation, biodeterioration, rock-inhabiting fungi, stone-inhabiting bacteria

1. Introduction

Tracks of human history and past civilizations are presently witnessed in archeological sites and stone monuments, which are considered an invaluable cultural heritage worldwide. A large percentage of the world's tangible cultural heritage is made from stone. However, it is slowly but irreversibly disappearing by transforming stone into sand and soil as a part of the natural recycling process, which is essential to sustain life on Earth (Allsopp et al., 2004; Gadd, 2017).

Thus, the deterioration of stone monuments represents a permanent loss of our cultural heritage.

The biodeterioration of stone is a complex process that involves biological, chemical, and environmental factors (Griffin et al., 1991; Nuhoglu et al., 2006). Although stone materials differ, their biodeterioration mechanisms are common, such as discoloration and biofilm formation (Gaylarde et al., 2012b; Martino, 2016), acid corrosion by organic and inorganic compounds (Sand and Bock, 1991; Gu et al., 2011), secondary mineral formation and crystallization redox reactions of cations (Warscheid and Braams, 2000), biological or chemical contaminants, and physical penetration by microbes (Gaylarde et al., 2006). Black crusts and dark discolorations are common symptoms of deterioration caused by microbes while biopitting, cracks, fissures, and exfoliation cause the rock's surface to appear darker and blackish brown (Gorbushina et al., 1993; Diakumaku et al., 1995; Cappitelli et al., 2007). Melanin-producing microbes are responsible for the esthetic changes that give rocks their dark brown color (Gorbushina, 2007; Sert et al., 2007). Biodeterioration as a term that is often used to describe any damage to any stone or other objects caused by microorganisms regardless of the climatic conditions or erosion factors (Urzi, 2004; Trovão et al., 2019) with much attention given to cultural heritage stone structures (Warscheid and Braams, 2000; Gorbushina et al., 2004; Scheerer et al., 2009; Hermosin et al., 2018).

Despite the harsh conditions resulting from low water availability and nutrient concentration, stone surfaces represent a complex ecosystem of several microhabitats, enabling a diverse range of microorganisms to proliferate (Urzi et al., 2001). The microbiota reported from such complex ecosystems includes algae, fungi (including lichens), cyanobacteria, and other bacteria of various phylogenetic affiliations (Urzì et al., 2000; Lindahl et al., 2013; Piñar et al., 2019). The inhabiting microorganisms may be chasmolithic, epilithic, or endolithic (Gadd et al., 2007; Fry, 2014). Such microorganisms have been reported worldwide, including the Antarctic and regions of extreme dryness and high solar irradiation (Onofri et al., 2004); they live between the limit of adaptability and near death while barely surviving and rarely reproducing (Friedmann and Weed, 1987).

Previously, in Egyptian monuments, an environmental extremotolerant genotype of the black yeast *Hortaea werneckii* GPS5 was isolated from a stone surface in the Great Pyramid of Giza's royal corridor (King Khufu's pyramid; Rizk and Magdy, 2022). Three xerophilic fungi, namely *Aspergillus amstelodami*, *Aspergillus chevalieri*, and *Aspergillus repens*, and six non-xerophilic species *Alternaria alternata*, *Aspergillus terreus*, *Cladosporium herbarum*, and *Penicillium chrysogenum* were isolated from Al-Shatby and El-Anfoushi archeological tombs in the Alexandria governorate (Alexandria city), respectively (Afifi and Geweely, 2011). Fungal damage (e.g., decayed wood, contaminated bones, and black spots on mud objects) was observed in Tuna El-Gabel's excavations near Al-Minya city, where different organic and inorganic materials belonging to the Ptolemaic era were found (Mansour and Ahmed, 2012). The identified fungal isolates were *A*, *alternata*, *Aspergillus flavus*, *Aspergillus niger*, *Bipolaris sorokiniana*, *Dichotomopilus indicus*, *Fusarium fujikuroi*, and *Rhizopus ehrenb*.

Aspergillus niger and *A*, *terreus* were the most common and dominant fungal deteriogens, followed by *Aspergillus fumigatus*, *Cladosporium cladosporioides*, and *C*, *herbarum* in Seti I tomb (Abydos city), Senusret I obelisk (Fayoum city), Great pyramid complex (Giza city), Mosque of judge Abd El-Basset (Cairo city), and Museum of Ismailia Antiquities (Ismailia City) where fungal biodeterioration signs were uncovered (e.g., black spots; Mohamed and Eid Ibrahim, 2018). Brown spots on the famous Tutankhamun's tomb walls were investigated for possible microbial origin (Vasanthakumar et al., 2013). Those authors found that fungal communities were composed primarily of Genera *Penicillium*, whereas the abundant bacterial taxa were members of the Firmicutes, Actinobacteria, and Bacteroidetes phyla. Actinobacteria demonstrated a great taxonomic diversity on stone surfaces. Despite the predominance of isolates of the genus *Streptomyces*, members of the genera *Geodermatophilus* and *Rhodococcus* were also reported (Groth et al., 1999). In addition to *Streptomyces* and *Nocardia*, *Micromonospora* species were also isolated from ancient stones from a tomb site in Tell Basta (Zagazig city, Egypt (Abdulla et al., 2008)).

Previously, culture-dependent (traditional isolation methods) were used to identify the organisms associated with the discoloration and degradation of historic buildings. By using this method, inactive forms and unculturable species are not considered, while active conditions are detected; thus, only a small fraction of the total diversity of microbes can be detected (Urzì et al., 2000, 2010; Urzi, 2004; de Los Ríos and Ascaso, 2005). Microbial biodiversity in sandstone surfaces was further investigated using next-generation sequencing (NGS) for profiling microbial populations in biodeterioration cultural heritage studies, which can provide a solution to the limitations imposed by the culture-dependent method (Gaylarde et al., 2012a; Ogawa et al., 2017; Soliman and Magdy, 2018; Trovão et al., 2019; Skipper et al., 2022).

The current study's general objective was to reveal part of the microbial diversity inhabiting two prehistoric sites in the Memphis necropolis of Egypt (Djoser and Lahun Pyramids) with high cultural values exposed to harsh and arid environmental conditions. The specific aims were the following: (i) to explore the nature, richness, and diversity of the bacterial and fungal microbiota inhabiting Djoser and Lahun Pyramids, (ii) to check if extremotolerant species with potential biodeterioration effects are present, and (iii) to compare the effectiveness of the amplicon-based metabarcoding analysis and traditional isolation methods to detect biodeterioration-associated microbes of the studied pyramids.

2. Materials and methods

2.1. Archeological sites

Geographically, the sampling area is generally characterized by light, warm, dry sandy soil that tends to be acidic with low nutrients (Mahmoud et al., 2015) and with an arid climate characterized by high UV exposure and day temperature that drop drastically during the night (The Egyptian Meteorological Authority, http://ema.gov.eg/wp/). Two pyramids were chosen for this study; they are among the oldest and largest ones in the Memphis necropolis of ancient Egypt. Deterioration was observed in many parts of both pyramidal complexes in the form of dark spots, coloration, and brittle rocks.

The pyramid of Djoser (DP), also known as the "Step Pyramid," is an archeological remain in the Saqqara district in Memphis necropolis, located in the northern part of the Nile Valley, northwest of the city of Memphis, situated at 29°52′10.17″N and 31°13′8.70″E in Giza governorate, Egypt The building was constructed during the 27th

century B.C. (3rd dynasty) of limestone by Imhotep, King Djoser's vizier (Mark, 2016). In an enormous courtyard surrounded by ceremonial structures and decorations, it is the focal point of a vast mortuary complex (Shaw, 2003). It is considered the first Egyptian pyramid and is known as the world's oldest structure, built entirely of stone (Hawkes, 1974). The Pyramid of Lahun (commonly spelled Al-Lāhūn; LP), also known as the "Senusret II Pyramid" or the "Mud-pyramid," is located on the west bank of the Nile valley near the opening of the Hawara Channel from the Nile Valley into the Fayum basin situated at 29°14′0″N and 30°58′0″E. The construction of the pyramid is believed to have been constructed by the pharaoh Senusret II ~ 2,000 BC (12th dynasty) and is considered the first large mudbrick Pyramid with a yellow limestone core. It was once covered entirely by white limestone (Redford, 2005). The wall had been encased in limestone that was decorated with niches, perhaps as a copy of Djoser's complex at Saqqara; although it is still impressively large, A natural outcrop of the pyramid can be seen now in its ruinous condition of the yellow limestone core can be seen protruding from the rubble of the mudbrick fill in some places (Eugene Cruz-Uribe, 2010).

TABLE 1 Nature and location description of the collected samples in Djoser (DP) and Lahun (LP) pyramids; sample codes are the same as in Figure 1.

Code	Nature and location of samples in pyramids
DP1	Scratch from the entrance tablet of an unidentified tomb near Mastaba "Khenut"
DP2	Scratch from the false door of the Mastaba "Khenut" southwest corner
DP3	Sand covers from Mastaba "Mehu" entrance
DP4	Sand covers the feet of four statues found in the "Heb-Sed" court
DP5	Brittle rock precipitations of the western Massifs on the pyramid's left side
DP6	Sand cover from the entrance ground
LP1	Sandy soil on the surface of the mud-rocks from the top of the pyramid
LP2	Sandy soil on the surface of the rocks from the south-eastern limestone stump
LP3	Soil from the queen's pyramid remains
LP4	Scratch of altered rock surface at the entrance shaft
LP5	Scratch of altered rock surface corridor to the burial chamber
LP6	Scratch of altered rock surface at the ceiling of the ventilation room

2.2. Sampling

Six samples per pyramid were collected around the archeological sites (Table 1; Figure 1); no special permission was required, as the sampling area is a free-walking zone, and the sampling was performed using a non-destructive method. Samples were collected using a sterilized scalpel and brush. Soft scratches of the brittle rock formations and sandy soil from the stone structures' that showed different biodeterioration types, such as biopitting, and black crusts or spots in samples (DP1, DP2, DP5 and DP6; LP3, LP4, LP5 and LP6). Erosion and mild color alteration, mostly gray to brown, as observed in samples (DP4, LP1 and LP2). The samples were placed into 50 mL Falcon tubes and preserved in sterile bags for further analysis. A portion of ~1 g was aliquoted from each sample and preserved in −20°C for the amplicon-based metabarcoding analysis.

2.3. Sample preparation and epifluorescence examination

Each sample was powdered in a mortar, and ~1 g was suspended (1,10) in a physiological solution (i.e., isotonic solution: 0.9% NaCl) with the addition of 0.001% Tween 80 and continuously agitated for 1 h at 30°C to facilitate a better separation and distribution of microorganisms living in/on the rock material (Urzi et al., 2001). Epifluorescent microscope examination was performed using a drop of sample suspension prepared at the previous step and a drop of 0.1% (w/v) of Acridine Orange solution. Direct observations of samples were carried out using a light/epifluorescent Leica DMR microscope equipped with a 50 W mercury lamp and a 450–490 nm excitation filter.

2.4. DNA extraction and metabarcoding analysis

Total environmental DNA (eDNA) was extracted directly from 0.25 g of each sample using the PowerSoil DNA Isolation Kit (MO BIO Laboratories Inc., CA, USA) and quantified using a Qubit fluorometer and the Qubit BR assay kit (Invitrogen, Life Technologies, USA). Due to the low concentration of the obtained eDNA from the current Material, for each pyramid, samples were bulked into two sets (including three field-collected samples each) to reach the minimum concentration level required for the metabarcoding library construction (Supplementary Tables S1, S2).

For the bacteria, the V3-V4 region rRNA of the bacterial 16S RNA gene was amplified using primers 338F (5′-ACT CCT ACG GG AGG CAG CAG-3′) and 806R (5′-GGA CTA CHV GGG TWT CTA AT-3′; Caporaso et al., 2010). For the fungi, the ITS1 of the nuclear ribosomal RNA genes was amplified using primers ITS1F (5'-TCC GTA GGT GAA CCT GCG G-3′) and ITS2R (5'-GCT GCG TTC TTC ATC GAT GC-3′) as recommended for the Miseq analysis (Blaalid et al., 2013). Four independent PCR assays were performed for each bulked DNA sample under the following conditions: a 20 μL PCR reaction using TransStart FastPfu DNA Polymerase mixture contained 4 μL of 5× FastPfu Buffer, 2 μL of 2.5 mM (each) dNTPs, 0.8 μL of 5 μM Bar-PCR primer F, 0.8 μL of 5 μM primer R, 0.4 μL of FastPfu polymerase, 0.2 μL of BSA and 10 ng of genomic DNA. PCR amplification was conducted in an ABI GeneAmp 9,700 thermocycler (IET, USA) under the following conditions: 98°C for 3 min, 27 cycles of 10 s at 98°C, 60°C for 30 s, and 72°C for 45 s, followed by 7 min at 72°C. PCR products were examined by 2% agarose gel electrophoresis and purified using Agencourt AMPure XP beads (Beckman, USA) and were sequenced by Illumina (MiSeq, PE 2 × 300 bp mode), following Illumina instructions. Using FLASH (Magoc and Salzberg, 2011) and Trimmomatic (Bolger et al., 2014), the pair-end reads were trimmed at any sites receiving an average quality score below 20 over a 50 bp sliding window, while reads shorter than 50 bp were discarded. The pair ends were merged with a minimum overlap length of 10 (0.2 maximum mismatch ratio). Barcodes and primer sequences at both ends were used to obtain valid sequences per sample, with 0 and 2 allowed mismatches, respectively.

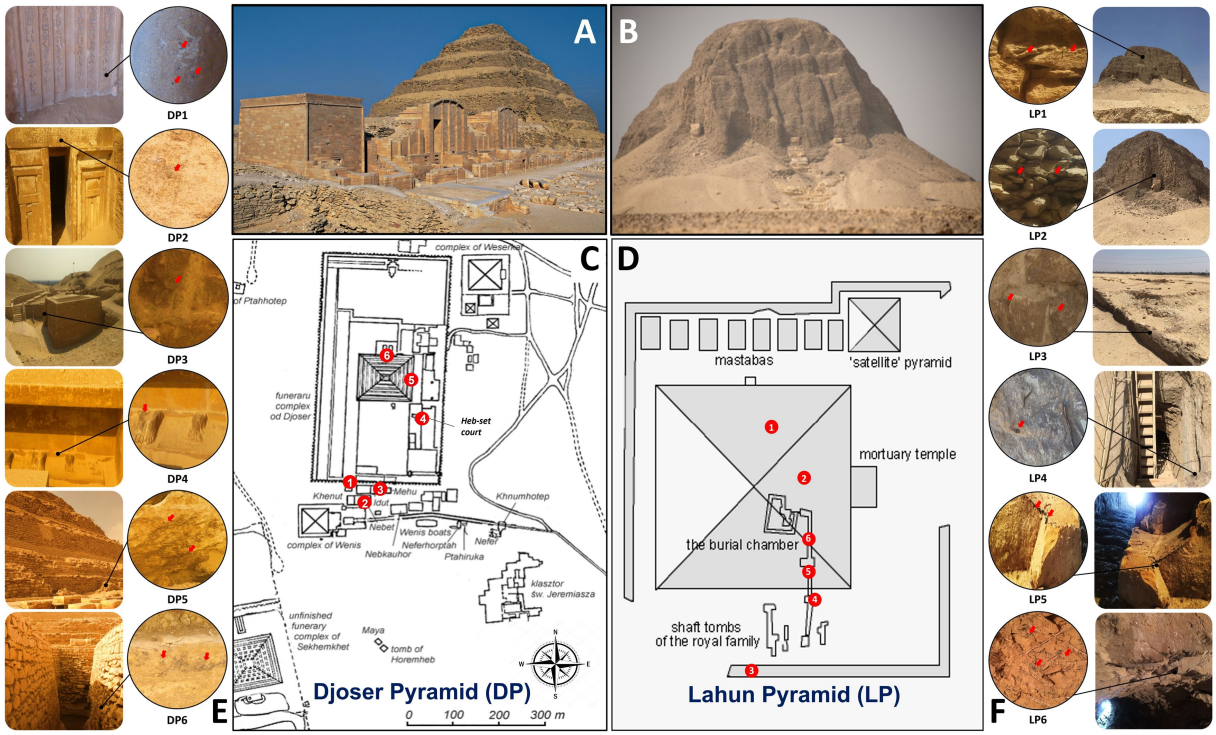

FIGURE 1
Sampling site information in Djoser pyramid (DP) and Lahun pyramid (LP). **(A,B)**: photographs of DP and LP, respectively, (by Samah Mohamed Rizk). **(C,D)**: schematic drawing of DP and LP complexes, respectively, showing the sampling sites by numbers (Table 1). **(E,F)**: sampling sites photographs showing their location in the pyramid and the sampling spot (by Samah Mohamed Rizk).

The metabarcoding analysis was performed using the online Majorbio Cloud Platform.[1] The operational taxonomic units (OTUs) were retrieved as follows: sequences with a single occurrence were discarded, and the remaining sequences were dereplicated and tested for chimeric sequences and artifacts using the UPARSE software (version 7.1 http://drive5.com/uparse/) at OTU sequence similarity of 0.97. The retained representative sequences were classified using the RDP Classifier[2] and mapped against the Silva (Release 138 http://www.arb-silva.de) database for 16S rRNA and Unite (Release 8.3 http://unite.ut.ee/index.php) for ITS using a confidence threshold of 0.7. Microbial composition statistics were estimated at each taxonomic level (domain, kingdom, phylum, class, order, family, genus, and species). Mothur (Schloss et al., 2009) was used to assess species richness and microbial diversity, while the Venn diagrams and bar plots for the microbial composition were analyzed and visualized using the vegan R package.[3] The species percentage per sample shown as a circos plot was elaborated using Circos-0.67.[4] The OTU abundance table was analyzed by PICRUSt and FUNGuild to predict the microbial function annotations. Heatmaps were constructed using Orange 3.24.1.[5]

1 http://en.majorbio.com/
2 http://rdp.cme.msu.edu/
3 https://github.com/vegandevs/vegan
4 http://circos.ca/
5 https://orange.biolab.si/

2.5. Culture-dependent isolation of microorganisms

2.5.1. Isolation and enumeration

For the isolation and the enumeration of cultivable chemoorganotrophic microorganisms in the 12 field-collected samples, the pour plate technique (Burdass et al., 2006) was applied by inoculating 1 mL of the sample suspension (prepared in the sample preparation step) following decimal dilutions $10P^{-1}P$:$10P^{5}P$. The sample suspension was poured in duplicates onto (1) BRII medium (Bunt and Rovira, 1955) modified as reported by Urzi et al. (2001) + 0.05% of the antifungal cycloheximide was utilized for chemoorganotrophic bacteria (Atlas, 2005); and (2) Geo medium (#714, List of Media for Microorganisms, DSMZ, Germany) + 0.05% cycloheximide was utilized for *Geodermatophilus* species (Atlas, 2005). The plates were then incubated at 28°C for up to 1 month. For the isolation and the enumeration of cultivable fungi, DRBC medium (Dichloran Rose Bengal Chloramphenicol agar; #CM0727, Oxoid, USA) supplemented with 100 ppm chloramphenicol to prevent bacterial growth (#SR0078, Oxoid, USA) was used. Incubation was carried out at 25°C for up to 1 month. At the end of incubation time, counts of viable microorganisms were referred to as colony-forming units *per* gram of sample (CFU/g) to detect the microbial community's enumeration in samples per each g for bacteria and fungi (Urzì et al., 2010).

2.5.2. Molecular identification of microbial isolates

DNA extraction from successfully isolated strains was performed using the PureLink Genomic DNA kit according to the kit protocol.

DNA quality was checked using 1% (w/v) agarose gel electrophoresis, visualized by pre-added RedSafe dye under UV light, and quantified using Qubit and the Qubit BR assay kit (Invitrogen, Life Technologies, USA).

For the isolated bacteria, the bacterial 16S rRNA gene was fully amplified using primers 27F (5′-AGA GTT TGA TCC TGG CTC AG-3′) and 1,492R [5′-GGT TAC CTT GTT ACG ACT T-3′ (Lillo et al., 2006)]. For the isolated fungi, the ITS1 of the nuclear ribosomal RNA genes was amplified using primers ITS1F (5′-TCC GTA GGT GAA CCT GCG G-3′) and ITS4R [5′-TCC TCC GCT TAT TGA TAT GC-3′ (White et al., 1990)]. PCR reactions were performed using the Red Mix (BioLine, UK) kit. Each 25 μL reaction tube included 5 pmol of each primer, and 40 ng of DNA template was added. The amplification was carried out using a Techne 512 thermocycler (Techne, UK). The PCR program was adjusted according to the primer pair melting temperature (Tm) as follows: the first denaturation step at 95°C for 3 min was followed by denaturation at 95°C for 2 s, annealing at 50°C for 30 s for 16S rRNA and at 55°C for 30 s for ITS, extension at 72°C for 30 s. The last three steps were repeated 35 times, with the last extension step of 72°C for 5 min. PCR products were tested using 1.5% agarose gel electrophoresis and prepared for purification using GeneJET PCR purification kit (K0702, Fermentas, USA) before automated Sanger sequencing.

Chromatograms were trimmed, assembled, and aligned using Geneious Prime (Kearse et al., 2012) and blasted for species identification using NCBI online Blast tool[6] against the ITS database using the default settings. Taxonomic ranking and phylogenetic relationships were retrieved from the taxonomy database.[7]

3. Results

3.1. Epifluorescence examination

With the aim to explore the biological presence in the samples collected from such hyper-arid locations, the samples were examined by direct epifluorescent microscopy. Evidence of bacterial cells and fungal spores among the particles of the soil collected from both pyramids was found. The examination showed a uniform green stain in the case of bacteria, whereas phototrophic cytoplasm showed a red autofluorescence due to the presence of chlorophylls; the nuclei of eukaryotic cells appeared green, while the cytoplasm of heterotrophs was orange (Supplementary Figure 1).

3.2. Environmental DNA extraction

The eDNA was extracted successfully for the 12 field-collected samples. The eDNA concentration ranged from 19 to 49 ng/μl with an average of 36.85 ± 10.97 ng/μl for the DP samples and from 26 to 60 ng/μl with an average of 40.33 ± 10.96 ng/μl for the LP samples.

6 https://www.ncbi.nlm.nih.gov/blast.cgi

7 https://www.ncbi.nlm.nih.gov/taxonomy

3.3. Metabarcoding analysis of the bacterial 16S rRNA

3.3.1. Raw reads information

After filtering, the four bulked samples (two sets per pyramid) recorded an average of 43,881 ± 3,318 sequence reads, with an average nucleotide number of 18 ± 1.5 million nucleotides. The mean read length ranged from 413 to 422 bp; the minimum recorded sequence read length was 226 (bulk LP_S1), while the maximum was 526 bp (bulk LP_S2; Supplementary Table 1). The total number of sequences was 232,423, with an average length of 417 bp. Using an alignment threshold of 97% similarity level, the number of classified sequences was 225,266 (96.92%), while only 7,157 sequences had 'no known relative' (3.08%).

3.3.2. Taxonomical composition

Based on the OTU identification pipeline and the Venn diagram plot, the total number of the identified OTUs in the metabarcoding samples (meta) was 940. Both pyramids shared 284 OTUs, while 104 and 552 were uniquely found in DP and LP, respectively. The OTUs identified from the two pyramids DP and LP were 388 and 836, respectively (Supplementary Figure 2).

The identified OTUs were classified into higher taxonomical ranks. Six hundred and forty four out of the 940 OTUs were classified as species belonging to 452 genera, forming 256 families from 142 orders, 57 classes, and 26 phyla, and all belonged to kingdom Bacteria. The relative proportion of the major bacterial classes was visualized by abundance for each pyramid. For both pyramids, the Actinobacteria and Bacilli were the most abundant classes; however, the percentage values' order was reversed between both pyramids. In the case of DP, the class Actinobacteria was the most abundant, followed by the Bacilli, Chloroflexia, Bacteroidia, Gammaproteobacteria, Alphaproteobacteria, and Deinococci classes, among others. On the contrary, in LP, the class Bacilli was the most abundant, followed by Actinobacteria, Bacteroidia, Gammaproteobacteria, Alphaproteobacteria, and Chloroflexia classes, among others (Figure 2A).

When the community composition was compared between both pyramids at the family level, OTUs belonging to three major families were highly represented in both communities (i.e., at least >1% abundance in both pyramids), namely: Geodermatophilaceae, Micrococcaceae, and Planococcaceae. Additionally, the OTUs belonging to the family Bacillaceae were highly represented in LP while weakly found (<1%) in DP. In contrast, OTUs belonging to orders Frankiales (non-ranked) and JG30-KF-CM45 (Thermomicrobiales), and families Hymenobacteraceae and Nocardioidaceae, among others, were highly represented in DP while much rarer (<1%) in LP (Figure 2B). By testing the taxonomical relationships among the detected families, five bacterial classes were highly represented. Class Actinobacteria was the most represented (five families), followed by Bacilli (two families), Bacteroidia, Chloroflexia, and Gammaproteobacteria (single family).

Based on the metabarcoding analysis, the top-represented bacterial genera were *Blastococcus*, *Planococcus*, *Kocuria*, and *Bacillus*, respectively. According to the applied database classification, the genus *Blastococcus*, family Geodermatophilaceae, was represented by *Blastococcus saxobsidens*, with a relative abundance ratio (rA) of 0.155 (DP) and 0.104 (LP), *Blastococcus*

aggregatus with an rA of 0.054 (DP) and 0.011 (LP), and an unclassified *Blastococcus* sp. with an rA of 0.034 (DP) and 0.011 (LP). The genus *Planococcus*, family Planococcaceae was represented by *Planococcus salinarum* with an rA of 0.167 (DP) and 0.126 (LP) and an unclassified *Planococcus* sp. with an rA of 0.024 (DP) and 0.224 (LP). *Kocuria rosea* represented the genus *Kocuria*, family Micrococcaceae with an rA of 0.109 and 0.234 for the DP and the LP samples, respectively. The genus *Bacillus*, family Bacillaceae was represented by *Bacillus persicus* with an rA of 0.001 (DP) and 0.129 (LP) and *Bacillus alkalitelluris*, with an rA of $0.008 \times 10P^{-1}P$ (DP) and 0.050 (LP; Figure 2C).

The overall functional composition profile was predicted for each pyramid based on the identified OTUs. Both profiles were very similar; the relative abundance was the highest for bacteria characterized by genes of unknown function, general function and amino acid transport and metabolism, energy production, and conversion, among others. In the latter, minor differences were found between both pyramids, as DP was slightly higher than LP (Supplementary Figure 3).

3.4. Metabarcoding analysis of the fungal its region

3.4.1. Raw reads information

After filtering, the four bulked samples recorded an average of 49,483 ± 7,111 sequence reads, with an average nucleotide number of 12.47 ± 1.67 million nt. The mean read length ranged from 251 to 254 bp; the minimum recorded sequence read length was 140 (bulk LP_S2), while the maximum was 515 bp (bulk DP_S1; Supplementary Table 2). Total valid sequences were 98.5 K and 133.5 K for the DP and the LP, respectively. Using an alignment threshold of 97% similarity level, the number of classified sequences was 301,603 (99.52%), while only 1,468 sequences had 'no known relative' (0.48%).

3.4.2. Taxonomical composition

Based on the OTU identification pipeline and the Venn diagram plot, the total number of the identified OTUs in the metabarcoding samples was 306. Both pyramids shared 48 OTUs,

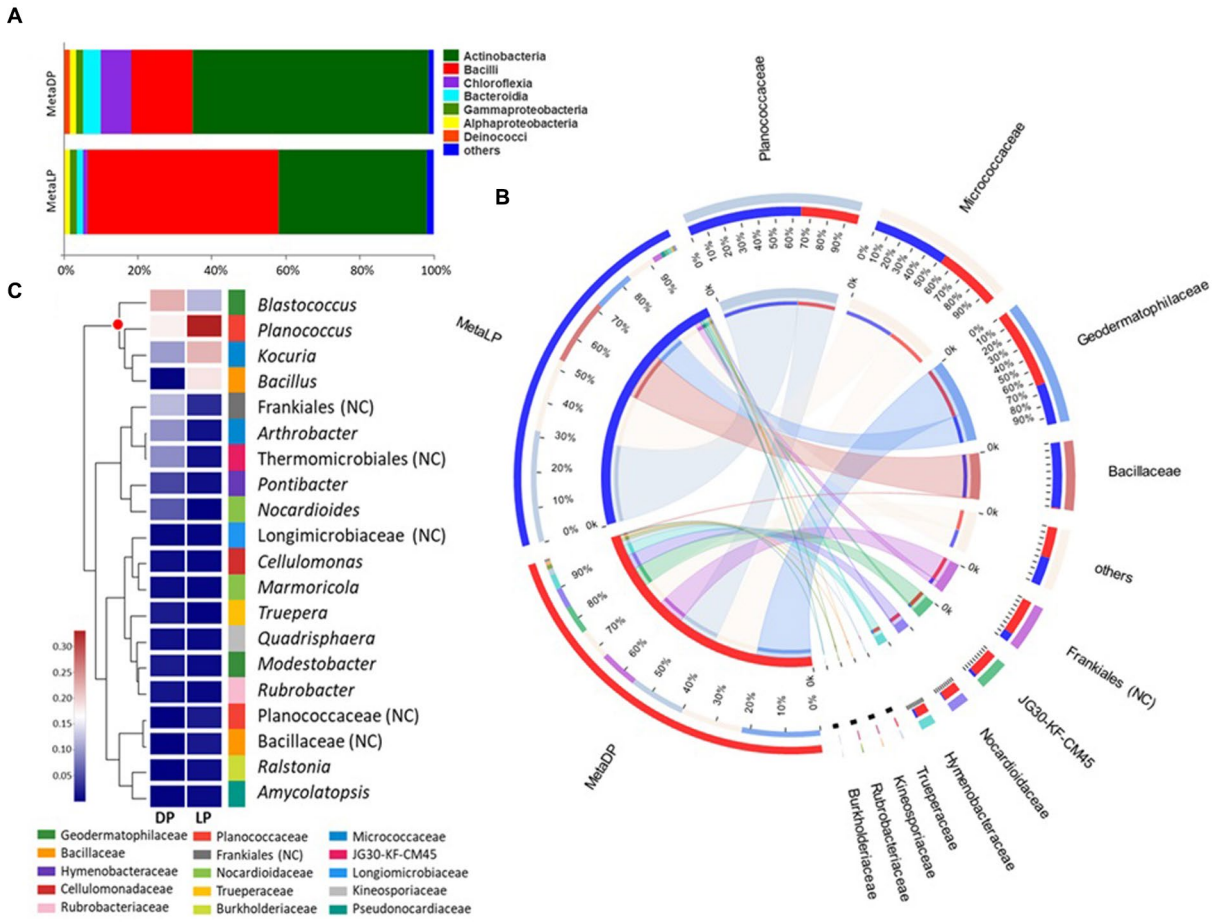

FIGURE 2
16S rRNA-based metabarcoding profiling of Djoser and Lahun pyramids. **(A)** Bacterial community composition bar-plot based on the identified OTUs for DP and LP in the metabarcoding samples. The percentage of community abundance at the class level is shown. **(B)** Circos plot for the comparative bacterial community composition based on the identified OTUs for both DP (MetaDP; red) and LP (MetaLP; blue) in the metabarcoding samples. The percentage of community abundance at the family level is shown for each pyramid. NC=not classified. **(C)** Bacterial community heatmap for the top 20 of the most abundant genera. The relative abundance ratio is shown for the two pyramids (DP and LP) using a colour scale given on the left of the figure. The family is indicated by colour mark for each genus. The top represented genera are clustered and marked by the red dot. NC=not classified.

while 43 and 215 OTUs were uniquely found in DP and LP, respectively. The OTUs identified from the two pyramids DP and LP were 91 and 263, respectively (Supplementary Figure 4). The identified OTUs were classified into higher taxonomical ranks; 204 out of the 306 OTUs were classified as species belonging to 146 genera, forming 99 families, 48 orders, 21 classes, and 6 phyla, all belonging to the kingdom Fungi. The relative proportion of the major fungal classes was visualized by abundance for each pyramid. For both pyramids, the class Dothideomycetes was the most abundant. However, in DP, it was up to 80% compared to LP with 37%. In the case of DP, this class was followed by the Eurotiomycetes and Sordariomycetes classes, among others. In LP, the Dothideomycetes were followed by the Pezizomycetes, Sordariomycetes, Saccharomycetes, Tremellomycetes, and Eurotiomycetes classes, among others (Figure 3A).

When the community composition was compared between both pyramids at the family level, one family was highly represented in both communities (i.e., at least >1% abundance in both pyramids), namely: Pleosporaceae. Additionally, the families Sporormiaceae and Trichomeriaceae were highly represented in DP while weakly found (<1%) in LP. In contrast, the families Cladosporiaceae, Mycosphaerellaceae, Pichiaceae, Sordariaceae, and Trichosporonaceae, among others, were highly represented in LP while weakly found (<1%) in DP (Figure 3B). Besides, OTUs classified to order Pezizales and others belonging to phylum Ascomycota were highly represented in LP while weakly found (<1%) in LP. The abundant families represented five classified fungal classes and two unclassified ones by testing the phylogenetic relationships among the detected families. The class Dothideomycetes was the most represented (four families), followed by Eurotiomycetes (two families), Pezizomycetes, Saccharomycetes, and Sordariomycetes (single-family).

In descending order, the top represented fungal genera based on the metabarcoding analysis were: *Knufia*, *Alternaria* an unclassified member of the Sporormiaceae family (GenBank accession: MN899880), and an unclassified member of Pezizales order (UNITE DOI:SH1569317.08FU). The genus *Knufia* was represented by *Knufia karalitana*, family Trichomeriaceae with an rA of 0.151 and 0.005 for the DP and the LP, respectively. *Alternaria chlamydospora* with an rA of 0.122 (DP) and 0.007 (LP) and *Alternaria oudemansii* with an rA of 0.301 (DP) and 0.009 (LP) represented the genus *Alternaria*, family Pleosporaceae. The unclassified species of the family Sporormiaceae showed rA values of 0.35 for the DP and 0.001 for the LP samples. The Pezizales unclassified species showed rA values of $0.007 \times 10P^{-2}P$ for the DP and 0.271 for the LP samples (Figure 3C).

The overall functional composition profile was predicted for each pyramid based on the identified OTUs. Both profiles were very different; the relative abundance was the highest for fungi characterized as an animal pathogen, dung saprotrophs, and unknown or undefined saprotroph types. For the DP, the fungi characterized as animal pathogens or dung saprotrophs were higher represented than for the LP, similar to those belonging to the "Animal-Pathogen—Endophytic—Lichen Parasite—Plant-Pathogen—Wood saprotroph" group. In contrast, the fungi of unknown or undefined saprotroph type and those characterized as plant pathogens were more prevalent in LP than DP samples (Supplementary Figure 5).

3.5. *In vitro* culture analysis and traditional isolation of microorganisms

3.5.1. Enumeration of most representative colonies

Variable numbers of cultivable bacteria and fungi among the DP samples were observed. The CFU/g ranged between 1.63 and 2.33 for bacteria and 1.78 to 2.41 for fungi (DP1 was excluded since no cultivable fungi were found). The highest number of bacterial and fungal isolates was observed in sample DP6, while the lowest was found in sample DP1. Total cultivable bacteria in DP samples were 61 on BRII and 144 on Geo media, with total cultivable fungal colonies of 211. The CFU/g ranged between 1.82 and 2.22 for bacteria and 2.00 and 2.48 for fungi compared to LP samples. The highest number of bacterial and fungal isolates was observed in sample LP1, while the lowest was found in sample LP2. Total cultivable bacteria in the LP samples were 96 on BRII and 106 on Geo media, with total cultivable fungal colonies of 278. The LP samples showed a higher number of successfully identified bacteria 32 than the DP of 20 and fungi of 40 for the LP to 26 for the DP samples (Table 2).

3.5.2. Molecular identification of microbial isolates

The isolation approach surveyed 28 bacterial species (13 genera) and 34 fungal species (20 genera). In the case of Djoser Pyramid, the bacterial 16S rRNA identified 13 strains among the successful isolates, and the fungal ITS region rRNA enabled the identification of 15 isolates that were amplified and analyzed. At the genus level, the most frequent bacteria belonged to 8 genera, namely: *Arthrobacter*, *Bacillus*, *Brevibacterium*, *Kocuria*, *Micrococcus*, *Pseudomonas*, *Streptomyces*, and *Xanthomonas* (Supplementary Table 3). Equally, the isolated fungi were assigned to 10 genera, namely: *Alternaria*, *Aspergillus*, *Cladosporium*, *Curvularia*, *Epicoccum*, *Fusarium*, *Glomerella*, *Penicillium*, *Phialocephala*, and *Ulocladium* (synonym of *Alternaria*; Supplementary Table S4). A black meristematic fungus was isolated from samples DP5 and DP6 and was assigned to the genus *Pseudotaeniolina*.

In the case of Lahun Pyramid, the bacterial 16S rRNA identified 21 strains among the successful isolates, and the fungal ITS region enabled the identification of 26 amplified and analyzed strains. At the genus level, the most frequent strains of bacteria belonged to 13 genera, namely: *Agrobacterium*, *Arthrobacter*, *Bacillus*, *Brevibacterium*, *Clostridium*, *Klebsiella*, *Kocuria*, *Micrococcus*, *Micromonospora*, *Pseudomonas*, *Rhizobium*, *Streptomyces*, and *Xanthomonas* (Supplementary Table 4). The identified fungi were assigned to 16 genera: *Alternaria*, *Aspergillus*, *Chaetomium*, *Cladosporium*, *Curvularia*, *Epicoccum*, *Fusarium*, *Monilinia*, *Mucor*, *Mycosphaerella*, *Podospora*, *Puccinia*, *Stachybotrys*, *Stemphylium*, *Trichoderma*, and *Ulocladium* (Supplementary Table 4).

3.5.3. Comparative phylogenetic and taxonomic analyses

The ranking of bacterial and fungal species and the relationship of the organisms isolated from both pyramids was defined based on the taxonomic unrooted phylogenetic tree (genus level). In the bacterial species case, the class Actinobacteria ranked first in both pyramids, while it varied for Proteobacteria, which ranked third in DP and second in LP, and vice versa for Firmicutes. Species belonging to

10.3389/fmicb.2023.1167083

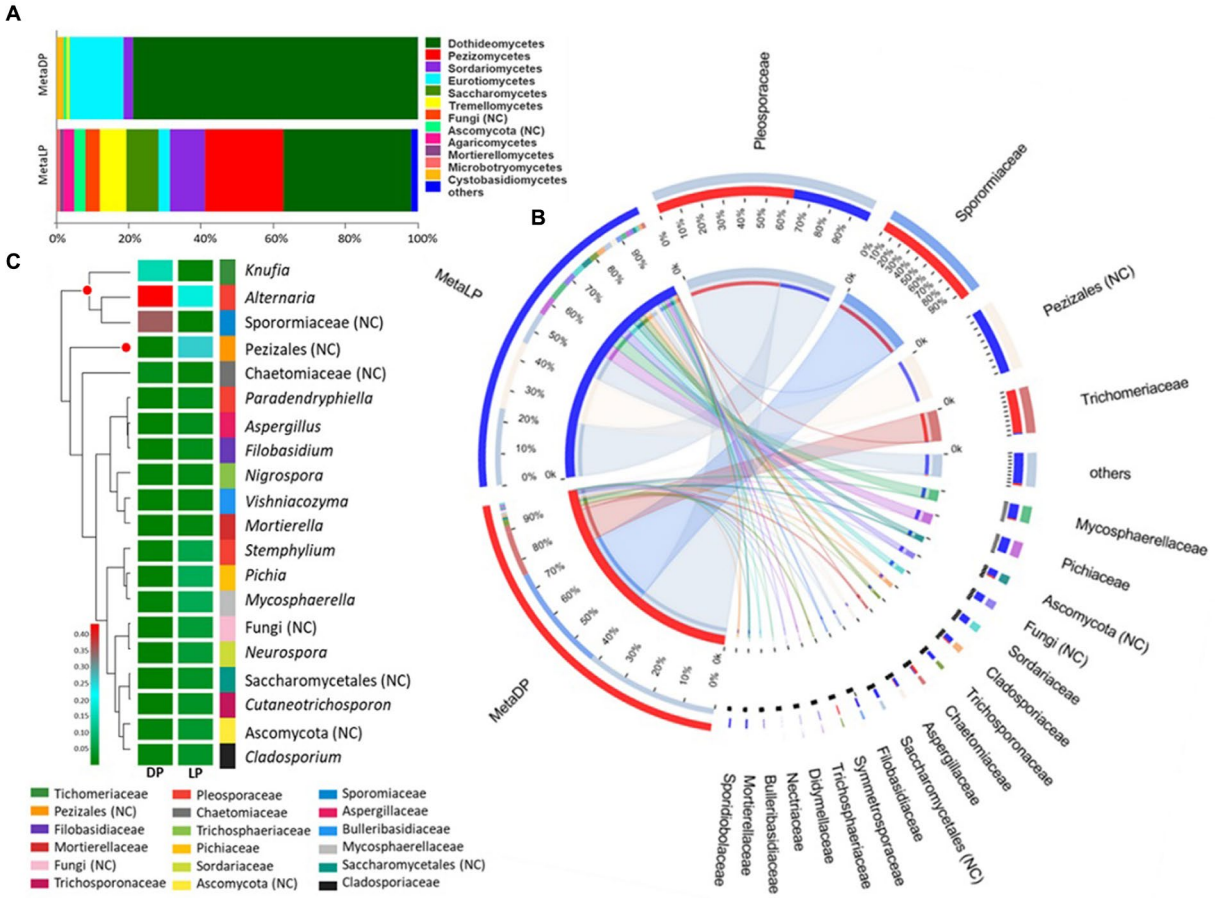

FIGURE 3
ITS-based metabarcoding profiling of Djoser and Lahun pyramids. **(A)** Fungal community composition bar-plot based on the identified OTUs for DP and LP in the metabarcoding samples. The percentage of community abundance on the class level is shown. **(B)** Circos plot for the comparative fungal community composition based on the identified OTUs for both DP (MetaDP; red) and LP (MetaLP; blue) in the metabarcoding samples. The percentage of community abundance at the family level is shown for each pyramid. NC=not classified. **(C)** Fungal community heatmap for the top 20 of the most abundant genera. The relative abundance ratio is shown for the two pyramids (DP and LP) using a color scale given on the left of the figure. The family is indicated by color for each genus. The top represented genera are clustered and marked by a red dot. NC=not classified.

the genus *Clostridium* (order Clostridiales, class Firmicutes) were only found in DP; oppositely, *Agrobacterium* and *Rhizobium* species (order Rhizobiales, class Proteobacteria), *Micromonospora* sp. (order Micromonosporales, class Actinobacteria) and *Klebsiella* (order Enterobacteriales, class Proteobacteria) were only found in LP. Species of order Micrococcales (class Actinobacteria), species of genera *Bacillus* (order Bacillales, class Firmicutes), *Streptomyces* (order Streptomycetales, class Actinobacteria), and *Xanthomonas* (order Xanthomonadales, class Proteobacteria) were higher represented in DP than in LP. On the contrary, species from the genus *Pseudomonas* (order Pseudomonadales, class Proteobacteria) were higher in LP than in the DP (Figure 4A).

In the case of the fungal species, the class Dothideomycetes ranked; first, Sordariomycetes ranked second, followed by Eurotiomycetes in both pyramids. Species of genera *Glomerella* (order Glomerellales, class Sordariomycetes) and *Phialocephala* (order Ophiostomatales, class Sordariomycetes) were only found in DP. Oppositely, species of genera *Monilinia* (order Helotiales, class Leotiomycetes), *Mucor* (order Mucorales, class Mucoromycetes), and *Puccinia* (order Pucciniales, class Pucciniomycetes) were only found in LP. *Cladosporium* (order Cladosporiales), *Mycosphaerella* (order Mycosphaerellales), and *Pseudotaeniolina* (order Capnodiales) species, all belong to the class Dothideomycetes were represented in DP more than LP, and equally for *Alternaria*, *Curvularia*, and *Stemphylium* species (order Pleosporales, class Dothideomycetes), but slightly lower than Capnodiales. On the contrary, *Aspergillus* species (order Eurotiales, class Eurotiomycetes) were somewhat higher in LP than DP, and *Fusarium*, *Stachybotrys*, and *Trichoderma* species (order Hypocreales, class Sordariomycetes) were higher represented in LP than in DP (Figure 4B).

3.6. Culturable versus unculturable microbial species identification

Except for few cases, most of the unculturable bacteria and fungi were of unknown species. When compared with the culturable species, no common species were detected by both methods, only unknown species identified at generic level. In case of bacteria, no taxa were detected by both methods from both pyramids, however, the culturable and unculturable methods yielded two unknown species belonging to *Rhizobium* and *Micromonospora* genera from

TABLE 2 Enumeration of the cultivable colonies isolated from Djoser (DP) and Lahun (LP) pyramids.

Samples	Bacteria (CFU/g)	Fungi (CFU/g)	Isolate counts						
			a	b	c	d	e	f	g
DP1	2.22	0.00	-	33	0	-	-	3	-
DP2	2.33	1.78	24	17	12	-	1	5	2
DP3	2.30	2.41	-	40	45	-	-	4	3
DP4	2.23	2.18	-	34	30	-	-	3	3
DP5	1.63	2.23	13	-	51	1	1	3	8
DP6	2.12	2.26	24	20	73	-	-	2	10
Total DP	-	-	61	144	211	1	2	20	26
LP1	2.12	2.48	40	-	90	2	4	5	8
LP2	1.83	2.10	26	-	38	-	2	5	7
LP3	2.22	2.00	-	50	30	1	-	6	5
LP4	2.00	2.06	30	-	35	-	-	6	5
LP5	1.82	2.18	-	20	45	-	2	4	10
LP6	2.08	2.12	-	36	40	-	4	6	5
Total LP	-	-	96	106	278	3	12	32	40

(a) Total cultivable bacterial colonies on BRII medium. (b) Total cultivable bacterial colonies on Geo medium. (c) Total cultivable fungal colonies on DRBC medium. (d) Count of occasionally found bacteria. (e) Count of occasionally found fungi. (f) Count of successfully identified bacteria using 16S. (g) Count of successfully identified fungi using ITS.

Lahun Pyramid, and two additional unknown species belonging to *Clostridium* and *Pseudomonas* genera were found common with the unculturable species detected from Djoser Pyramid. In case of fungi, unknown species belonging to *Cladosporium* and *Fusarium* genera were detected by both methods from both pyramids. The culturable and unculturable methods yielded one unknown species belonging to genus *Monilinia* from Lahun Pyramid, and three additional unknown species belonging to *Stemphylium*, *Trichoderma*, and *Mycosphaerella* genera were found common with the unculturable species detected from Djoser pyramid. Unknown species belong to Alternaria were detected using culturable and unculturable methods from Djoser Pyramid and found common with the unculturable species found from Lahun Pyramid (Figure 5).

4. Discussion

There is no doubt that microorganisms greatly influence stone transformation and decay in a currently termed biodeterioration process. Unfortunately, such modification is irreversible, causing significant damage to human-made stone structures, such as monuments of cultural value and historical significance. Many reports concentrated on the diversity of the microbiota inhabiting such complex and harsh stone microhabitats (Urzì et al., 2000; Scheerer et al., 2009; Sanz et al., 2017; Pena-Poza et al., 2018). Those microorganisms are considered the second factor after erosion (i.e., physical and chemical damage), while other studies considered them the primary cause of decay and deterioration (Warscheid and Braams, 2000; Liu et al., 2020). Microorganisms inhabiting stone feature the extremotolerance aspect to survive and reproduce under such harsh conditions (Rampelotto, 2013).

The recorded microbial communities varied in composition, and the dominant species at bacterial and fungal levels between the two largest pyramids of the Memphis necropolis of ancient Egypt. However, the commonly recorded species were the key to defining the stone-inhabiting bacteria (SIB) and rock-inhabiting fungi (RIF). A total of 19 bacterial and 16 fungal species were exclusively culture-dependent, while 92 bacterial and 122 fungal species were culture-independent. The culture-dependent identification (traditional) method is considered less informative and convenient than the culture-independent identification, as the former enabled the detection of ≤5% of the total microbial community (Dakal and Arora, 2012).

Nevertheless, the traditional method has many benefits; the most important is the availability of the detected species and/or strains for further studies, especially when they are newly identified; however, the metabarcoding identification method has shown more advantages, considering that, in most cases, the behavior of a species is better explained in relation to the entire microbial community within a particular substrate (Li et al., 2016).

The concentration of eDNA extracted from arid and hyper-arid soils, as in the case described here, is very low (Schneegurt et al., 2003), which poses a challenge to the application of metabarcoding. In our study, bulking the samples increased the eDNA concentration and improved the 16S rRNA and ITS library preparation and sequencing. While the metabarcoding revealed higher microbial diversity than expected, considering the harsh arid conditions of the sampling sites (Lang-Yona et al., 2018). The most common bacterial class shared between the two pyramids is Actinobacteria, which is deemed to be the dominant bacteria in outdoor and subterranean habitats, such as caves and tombs (Cuezva et al., 2012). Concerning the highly represented families in both pyramids, the Planococcaceae, gram-positive bacteria with no known characteristics exclusive to all family members, dominate. However, the known isolated species was *P. salinarum*, which was previously isolated from a marine solar saltern and can grow *in vitro* up to 13% w/v NaCl (Yoon et al., 2010). The species representing the family

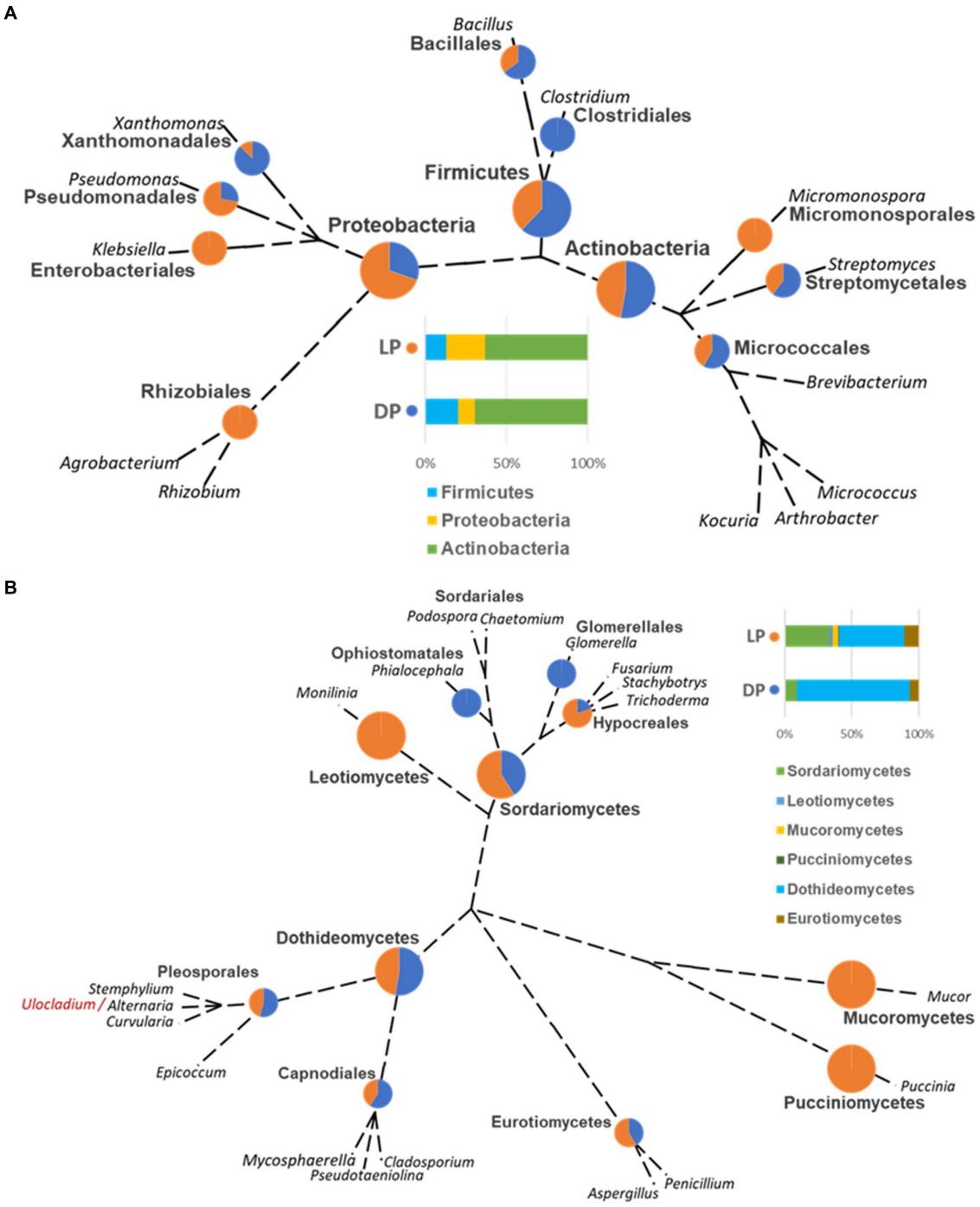

FIGURE 4
Unrooted phylogenetic tree based on the taxonomic ranking retrieved from the NCBI database (https://www.ncbi.nlm.nih.gov/taxonomy) for the bacterial **(A)** and fungal **(B)** species isolated from the Djoser pyramid (DP) and Lahun pyramid (LP). The abundance percentage of each order and class is demonstrated as a pie chart between both pyramids at each node. (Note: order Capnodiales node includes Mycosphaerellales and Cladosporiales species).

Micrococcaceae was *Kocuria rosea*, known as a common soil and water species found previously in extreme environments such as heavily polluted waters, deep-sea sediments, and spacecraft surfaces (Coil et al., 2016). The most abundant species belonged to the family Geodermatophilaceae, described as one of the most abundant stones inhabiting Actinobacteria (Urzi et al., 2001; Sghaier et al., 2016). Two known species of the family Geodermatophilaceae, *B. aggregatus* and *B. saxobsidens*, that cause an orange coloration were identified from both pyramids. The latter was found to resist harsh environmental conditions (e.g., UV light, ionizing radiation, desiccation, and heavy metals (Gtari et al., 2012; Montero-Calasanz et al., 2015)).

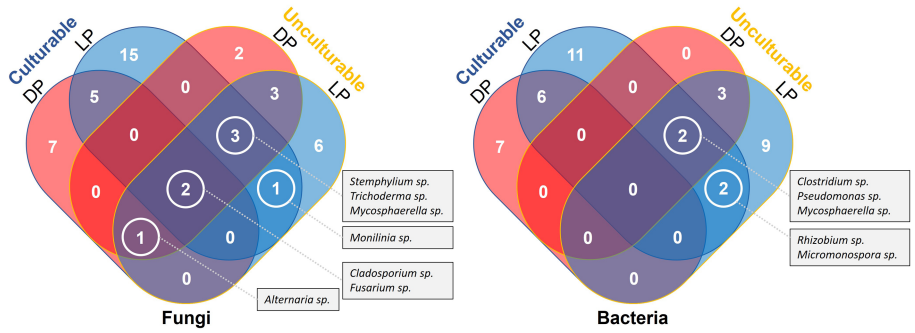

FIGURE 5
Venn Diagram illustrate a comparative listing of the culturable and culturable microbial species detected from both Djoser and Lahun Pyramids.

Compared with the isolated culture-dependent bacterial species, the species of Geodermatophilaceae and Planococcaceae did not grow in the currently used media. Therefore, different media compositions and protocols will be required to retrieve such isolates, especially for the two unknown species found highly represented in both pyramids (*Blastococcus* sp. and *Planococcus* sp.). Chemoorganotrophic bacteria utilize a wide range of nutrients and may serve other microorganisms by breaking down poorly degradable compounds, which could otherwise not be utilized (Saier et al., 2008). One example is the species belonging to the genus *Bacillus*, four of which were isolated from both pyramids and frequently identified on stone buildings (Kiel and Gaylarde, 2006). An exclusive bacterium to LP belonged to the genus *Micromonospora*, which was occasionally reported from decayed stone (Ciferri et al., 2000), along with isolates from *Micropolyspora*, and *Streptomyces*, which were previously reported from a tomb in Tella Baste, Zagazig city in Egypt (Abdulla et al., 2008). Other isolates were best known as common environmental species of natural presence on soil [e.g., *Arthrobacter* (Eschbach et al., 2003)].

One of the most functional bacterial gene groups in the surveyed sites of both pyramids was the amino acid transport and metabolism; it could be very efficient in the survival in the studied sites as amino acid metabolism is associated with abiotic stress tolerance mechanisms in bacteria (Batista-Silva et al., 2019). One group is the Mycosporine-like amino acids, a family of intracellular compounds biosynthesized by the shikimic acid pathway to synthesize aromatic amino acids and are expressed under biotic and abiotic stresses [e.g., high UV exposure (Bhatia et al., 2011)]. Identifying related pathways would help to understand the stone-inhabiting mechanisms.

Based on ITS metabarcoding functional analysis, most of the detected fungi are naturally present in the soil. At the same time, some are molds, plant-pathogen species, and/or wood-inhabiting fungi (e.g., *Chaetomium globosum*). It is worth mentioning that the family Pleosporaceae (class Dothideomycetes) was one of the most abundant families in the studied pyramids, followed by the family Trichomeriaceae (class Eurotiomycetes), which was represented by *A, chlamydospora* and *A, oudemansii* species, that were previously reported from similar studies (Ruibal et al., 2009; Piñar et al., 2019), and an extremotolerant RIF, *K, karalitana* (Isola et al., 2016), respectively.

Compared with fungal culture-dependent isolation, seven common genera were observed at both pyramidal sites. The most remarkable isolated fungal species was a black meristematic fungus, *Pseudotaeniolina globosa* De Leo, Urzì & De Hoog, which was an extremotolerant ecotype adapted to harsh and arid conditions and was attributed to the family Teratosphaeriacea, order Capnodiales (Rizk et al., 2021). Meristematic growth is infrequent in the fungal kingdom and can be interpreted as a specific response to external stress (Isola et al., 2016). RIF usually are extremotolerant microorganisms that can tolerate abiotic stress such as drought, prolonged water deficiency, osmotic stress, extreme temperatures, UV radiation, and outer-space conditions (Sterflinger, 2006; Onofri et al., 2012; Zakharova et al., 2013; Sterflinger et al., 2014; Selbmann et al., 2015). RIFs are known for the dark-colour aspect and are very active agents causing noticeable alteration patterns and exfoliation of stone monuments with endolithic activity (Onofri et al., 2014; De Leo et al., 2019). Comparing our results with similar studies, several fungal genera detected in the Djoser and Lahun pyramids were previously reported from cultural heritage material. For example, *Alternaria*, *Aspergillus*, *Cladosporium*, *Epicoccum*, *Fusarium*, *Mucor*, *Penicillium*, and *Trichoderma* were reported, among others, from storage room objects in the Tianjin Museum, China (Liu et al., 2018; Soliman and Magdy, 2018), Etruscan tombs in Italy and ancient tombs of the Baekje Dynasty in the Republic of Korea (Caneva et al., 2020).

To know the real potential of biodeterioration caused by the isolated species, a follow-up study is currently in progress to characterize the stone substrate where the microorganisms found are inoculated and subjected to specific environmental conditions as well as the examination of possible biocidal treatments using organic and natural products without deteriorating side effects.

5. Conclusion

Our survey of two of the oldest and largest pyramids in Memphis necropolis of ancient Egypt, Djoser and Lahun pyramids, revealed that both pyramids are inhabited by potential biodeterioration agents, some known for their ability to transform the stone surface and rock formation, and potentially as dangerous as physical and chemical erosions. Our results confirm that the best methodological approach to identifying and studying a complex microbial community is by combining microscopy and molecular identification for culture-dependent microbes. Metabarcoding methods are ideal for culture-independent microbes by extracting DNA and/or RNA directly

from the substratum and/or biomass. Based on both culturable and unculturable microbial identification methods, the identified SIB known to be related to biodeterioration were *B*, *aggregatus*, *B*, *saxobsidens*, and *Blastococcus* sp., while *B*, *alkalitelluris*, *B*, *persicus*, *P*, *salinarum*, and *Planococcus* sp. will need further investigation to examine their biodeterioration effect. Equally, the surveyed RIF in the current study were *K*, *karalitana* and *P*, *globosa*, in addition to a species belonging to the family Sporormiaceae, which will need further isolation and identification. These findings will require further inspection and biodeterioration-related analysis to fully understand the damaging effect on Djoser and Lahun pyramids and help to design prevention and conservation plans.

Data availability statement

The datasets presented in this study can be found in online repositories. The names of the repository/repositories and accession number(s) can be found in the article/Supplementary material.

Author contributions

MM, FL, OW, RR, and CU: conceptualization. SR and MM: data curation. MM: formal analysis. MM and MR: funding acquisition. SR and MM: investigation, methodology, and manuscript drafting. RR, OW, and CU: project administration. MM and RR: resources. OW, RR, FL, CU, and MR: revisions. All authors contributed to the article and approved the submitted version.

Funding

SR was partially supported by a PhD exchange scholarship funded by the Erasmus Mundus Action 2: EMMAG Program (2014–2016), and the experiments were funded by Science, Technology and Innovation Funding Authority (STDF) under grant no. 26383 (2018–2020).

Conflict of interest

The authors declare that the research was conducted in the absence of any commercial or financial relationships that could be construed as a potential conflict of interest.

Publisher's note

All claims expressed in this article are solely those of the authors and do not necessarily represent those of their affiliated organizations, or those of the publisher, the editors and the reviewers. Any product that may be evaluated in this article, or claim that may be made by its manufacturer, is not guaranteed or endorsed by the publisher.

Supplementary material

The Supplementary material for this article can be found online at: https://www.frontiersin.org/articles/10.3389/fmicb.2023.1167083/full#supplementary-material

References

Abdulla, H., May, E., Bahgat, M., and Dewedar, A. (2008). Characterisation of actinomycetes isolated from ancient stone and their potential for deterioration. *Pol. J. Microbiol.* 57, 213–220.

Afifi, H., and Geweely, N. (2011). Comparative study on fungal deterioration and ozone conservation of El-Anfoushi and Al-Shatby archeological tombs-Alexandria-Egypt. *J. Am. Sci.* 7, 776–784.

Allsopp, D., Seal, K. J., and Gaylarde, C. C. (2004). *Introduction to Biodeterioration. 2nd* Edn London, UK: CRC Press Chem Tec Publishing.

Atlas, R. M. (2005). *Handbook of Media for Environmental Microbiology. 2nd* Edn, Taylor & Francis, Boca Raton, Florida: CRC Press.

Batista-Silva, W., Heinemann, B., Rugen, N., Nunes-Nesi, A., Araújo, W. L., Braun, H., et al. (2019). The role of amino acid metabolism during abiotic stress release. *Plant Cell Environ.* 42, 1630–1644. doi: 10.1111/pce.13518

Bhatia, S., Sharma, K., Sharma, A., Garg, A., Kumar, S., and Purohit, A. (2011). Mycosporine and mycosporine-like amino acids: a paramount tool against ultra violet irradiation. *Phcog. Rev.* 5, 138–146. doi: 10.4103/0973-7847.91107

Blaalid, R., Kumar, S., Nilsson, R. H., Abarenkov, K., Kirk, P. M., and Kauserud, H. (2013). ITS 1 versus ITS 2 as DNA metabarcodes for fungi. *Mol. Ecol. Resour.* 13, 218–224. doi: 10.1111/1755-0998.12065

Bolger, A. M., Lohse, M., and Usadel, B. (2014). Trimmomatic: a flexible trimmer for Illumina sequence data. *Bioinformatics* 30, 2114–2120. doi: 10.1093/bioinformatics/btu170

Bunt, J. S., and Rovira, A. D. (1955). Microbiological studies of some subantarctic soils. *J. Soil Sci.* 6, 119–128. doi: 10.1111/j.1365-2389.1955.tb00836.x

Burdass, D., Grainger, J., and Hurst, J. (2006). Basic practical microbiology. Society for General Microbiology. Reading, United Kingdom.

Caneva, G., Isola, D., Lee, H. J., and Chung, Y. J. (2020). Biological risk for hypogea: shared data from Etruscan tombs in Italy and ancient tombs of the Baekje dynasty in Republic of Korea. *Appl. Sci.* 10:6104. doi: 10.3390/app10176104

Caporaso, J. G., Kuczynski, J., Stombaugh, J., Bittinger, K., Bushman, F. D., Costello, E. K., et al. (2010). QIIME allows analysis of high-throughput community sequencing data. *Nat. Methods* 7, 335–336. doi: 10.1038/nmeth.f.303

Cappitelli, F., Principi, P., Pedrazzani, R., Toniolo, L., and Sorlini, C. (2007). Bacterial and fungal deterioration of the Milan cathedral marble treated with protective synthetic resins. *Sci. Total Environ.* 385, 172–181. doi: 10.1016/j.scitotenv.2007.06.022

Ciferri, O., Tiano, P., and Mastromei, G. eds. (2000). *Of Microbes and Art*. Boston, MA: Springer US

Coil, D. A., Neches, R. Y., Lang, J. M., Brown, W. E., Severance, M., Cavalier, D., et al. (2016). Growth of 48 built environment bacterial isolates on board the international Space Station (ISS). *PeerJ* 4:e1842. doi: 10.7717/peerj.1842

Cuezva, S., Fernandez-Cortes, A., Porca, E., Pašić, L., Jurado, V., Hernandez-Marine, M., et al. (2012). The biogeochemical role of Actinobacteria in Altamira cave, Spain. *FEMS Microbiol. Ecol.* 81, 281–290. doi: 10.1111/j.1574-6941.2012.01391.x

Dakal, T. C., and Arora, P. K. (2012). Evaluation of potential of molecular and physical techniques in studying biodeterioration. *Rev. Environ. Sci. Biotechnol.* 11, 71–104. doi: 10.1007/s11157-012-9264-0

De Leo, F., Antonelli, F., Pietrini, A. M., Ricci, S., and Urzì, C. (2019). Study of the euendolithic activity of blackmeristematic fungi isolated from a marble statue in the Quirinale Palace's gardens inRome, Italy. *Facies* 65:18. doi: 10.1007/s10347-019-0564-5

de Los Ríos, A., and Ascaso, C. (2005). Contributions of in situ microscopy to the current understanding of stone biodeterioration. *Int. Microbiol.* 8:181.

Diakumaku, E., Gorbushina, A. A., Krumbein, W. E., Panina, L., and Soukharjevski, S. (1995). Black fungi in marble and limestones—an aesthetical, chemical and physical problem for the conservation of monuments. *Sci. Total Environ.* 167, 295–304. doi: 10.1016/0048-9697(95)04590-W

Eschbach, M., Mabitz, H., Rompf, A., and Jahn, D. (2003). Members of the genus Arthrobacter grow anaerobically using nitrate ammonification and fermentative processes: anaerobic adaptation of aerobic bacteria abundant in soil. *FEMS Microbiol. Lett.* 223, 227–230. doi: 10.1016/S0378-1097(03)00383-5

Eugene Cruz-Uribe (2010). Daily life in ancient Egypt: recreating Lahun (review). *J. World History* 21, 134–136. doi: 10.1353/jwh.0.0112

Friedmann, E. I., and Weed, R. (1987). Microbial trace-fossil formation, Biogenous, and abiotic weathering in the Antarctic Cold Desert. *Science* 236, 703–705. doi: 10.1126/science.11536571

Fry, J. C. (2014). "Culture-Dependent Microbiology," in *Microbial Diversity and Bioprospecting*. ed. A. T. Bull (Washington, DC, USA: ASM Press), 80–87.

Gadd, G. M. (2017). Geomicrobiology of the built environment. *Nat. Microbiol.* 2:16275. doi: 10.1038/nmicrobiol.2016.275

Gadd, G., Watkinson, S. C., and Dyer, P. S. (Eds.) (2007). *Fungi in the Environment. 1st* Edn New York: Cambridge University Press.

Gaylarde, P., Englert, G., Ortega-Morales, O., and Gaylarde, C. (2006). Lichen-like colonies of pure Trentepohlia on limestone monuments. *Int. Biodeterior. Biodegradation* 58, 119–123. doi: 10.1016/j.ibiod.2006.05.005

Gaylarde, C. C., Rodríguez, C. H., Navarro-Noya, Y. E., and Ortega-Morales, B. O. (2012a). Microbial biofilms on the sandstone monuments of the Angkor wat complex, Cambodia. *Curr. Microbiol.* 64, 85–92. doi: 10.1007/s00284-011-0034-y

Gaylarde, C. C., Rodriguez, C. H., Navarro-Noya, Y. E., and Ortega-Morales, B. O. (2012b). Microbial biofilms on the sandstone monuments of the Angkor wat complex, Cambodia. *Curr. Microbiol.* 64, 85–92. doi: 10.1007/s00284-011-0034-y

Gorbushina, A. A. (2007). Life on the rocks: life on the rocks. *Environ. Microbiol.* 9, 1613–1631. doi: 10.1111/j.1462-2920.2007.01301.x

Gorbushina, A. A., Heyrman, J., Dornieden, T., Gonzalez-Delvalle, M., Krumbein, W. E., Laiz, L., et al. (2004). Bacterial and fungal diversity and biodeterioration problems in mural painting environments of St. martins church (Greene–Kreiensen, Germany). *Int. Biodeterior. Biodegradation* 53, 13–24. doi: 10.1016/j.ibiod.2003.07.003

Gorbushina, A. A., Krumbein, W. E., Hamman, C. H., Panina, L., Soukharjevski, S., and Wollenzien, U. (1993). Role of black fungi in color change and biodeterioration of antique marbles. *Geomicrobiol J.* 11, 205–221. doi: 10.1080/01490459309377952

Griffin, P. S., Indictor, N., and Koestler, R. J. (1991). The biodeterioration of stone: a review of deterioration mechanisms, conservation case histories, and treatment. *Int. Biodeterior.* 28, 187–207. doi: 10.1016/0265-3036(91)90042-P

Groth, I., Vettermann, R., Schuetze, B., Schumann, P., and Saiz-Jimenez, C. (1999). Actinomycetes in karstic caves of northern Spain (Altamira and Tito Bustillo). *J. Microbiol. Methods* 36, 115–122. doi: 10.1016/S0167-7012(99)00016-0

Gtari, M., Essoussi, I., Maaoui, R., Sghaier, H., Boujmil, R., Gury, J., et al. (2012). Contrasted resistance of stone-dwelling Geodermatophilaceae species to stresses known to give rise to reactive oxygen species. *FEMS Microbiol. Ecol.* 80, 566–577. doi: 10.1111/j.1574-6941.2012.01320.x

Gu, J.-D., Ford, T. E., and Mitchell, R. (2011). "Microbial degradation of materials: general processes" in *Uhlig's corrosion handbook*. ed. R. W. Revie (Hoboken, NJ, USA: John Wiley & Sons, Inc.), 351–363.

Hawkes, J. H. (1974). *Atlas of Ancient Archaeology*. London Heinemann, New Hampshire (US): Heinemann.

Hermosin, B., Laiz, L., Jurado, V., Miller, A. Z., and Rogerio-Candelera, M. A. (2018). "Microorganisms and monuments: forty years of heritage conservation," in *Conserving Cultural Heritage*. eds. M. J. Mosquera and M. L. A. Gil (Taylor & Francis, London: CRC Press), 295–297.

Isola, D., Zucconi, L., Onofri, S., Caneva, G., de Hoog, G. S., and Selbmann, L. (2016). Extremotolerant rock inhabiting black fungi from Italian monumental sites. *Fungal Divers.* 76, 75–96. doi: 10.1007/s13225-015-0342-9

Kearse, M., Moir, R., Wilson, A., Stones-Havas, S., Cheung, M., Sturrock, S., et al. (2012). Geneious basic: an integrated and extendable desktop software platform for the organization and analysis of sequence data. *Bioinformatics* 28, 1647–1649. doi: 10.1093/bioinformatics/bts199

Kiel, G., and Gaylarde, C. C. (2006). Bacterial diversity in biofilms on external surfaces of historic buildings in Porto Alegre. *World J. Microbiol. Biotechnol.* 22, 293–297. doi: 10.1007/s11274-005-9035-y

Lang-Yona, N., Maier, S., Macholdt, D. S., Müller-Germann, I., Yordanova, P., Rodriguez-Caballero, E., et al. (2018). Insights into microbial involvement in desert varnish formation retrieved from metagenomic analysis: the desert varnish microbiome. *Environ. Microbiol. Rep.* 10, 264–271. doi: 10.1111/1758-2229.12634

Li, Q., Zhang, B., He, Z., and Yang, X. (2016). Distribution and diversity of Bacteria and Fungi colonization in stone monuments analyzed by high-throughput sequencing. *PLoS One* 11:e0163287. doi: 10.1371/journal.pone.0163287

Lillo, A., Ashley, F. P., Palmer, R. M., Munson, M. A., Kyriacou, L., Weightman, A. J., et al. (2006). Novel subgingival bacterial phylotypes detected using multiple universal polymerase chain reaction primer sets: novel periodontal bacterial phylotypes. *Oral Microbiol. Immunol.* 21, 61–68. doi: 10.1111/j.1399-302X.2005.00255.x

Lindahl, B. D., Nilsson, R. H., Tedersoo, L., Abarenkov, K., Carlsen, T., Kjøller, R., et al. (2013). Fungal community analysis by high-throughput sequencing of amplified markers – a user's guide. *New Phytol.* 199, 288–299. doi: 10.1111/nph.12243

Liu, X., Koestler, R. J., Warscheid, T., Katayama, Y., and Gu, J.-D. (2020). Microbial deterioration and sustainable conservation of stone monuments and buildings. *Nat. Sustain.* 3, 991–1004. doi: 10.1038/s41893-020-00602-5

Liu, Z., Zhang, Y., Zhang, F., Hu, C., Liu, G., and Pan, J. (2018). Microbial community analyses of the deteriorated storeroom objects in the Tianjin museum using culture-independent and culture-dependent approaches. *Front. Microbiol.* 9:802. doi: 10.3389/fmicb.2018.00802

Mansour, M., and Ahmed, H. (2012). Occurrence of fungi on some deteriorated ancient Egyptian materials and their controlling by ecofriendly products. *Egypt. J. Archaeol. Restoration Stud.* 2, 91–101. doi: 10.21608/ejars.2012.7465

Magoc, T., and Salzberg, S. L. (2011). FLASH: fast length adjustment of short reads to improve genome assemblies. *Bioinformatics* 27, 2957–2963. doi: 10.1093/bioinformatics/btr507

Mahmoud, S. H., Alazba, A. A., Adamowski, J., and El-Gindy, A. M. (2015). GIS methods for sustainable stormwater harvesting and storage using remote sensing for land cover data—location assessment. *Environ. Monit. Assess.* 187:598. doi: 10.1007/s10661-015-4822-x

Mark, E. (2016). Taoism. Ancient history encyclopedia https://www.ancient.eu.Taoism/#:~:text=Taoism20.

Martino, P. D. (2016). What about biofilms on the surface of stone monuments? *Open Conf. Proceed. J.* 6, 14–28. doi: 10.2174/2210289201607020014

Mohamed, S., and Eid Ibrahim, S. (2018). Characterization and management of fungal deterioration of ancient limestone at different sites along Egypt. *Egypt. J. Microbiol.* doi: 10.21608/ejm.2018.4735.1068

Montero-Calasanz, M. D. C., Hezbri, K., Göker, M., Sghaier, H., Rohde, M., Spröer, C., et al. (2015). Description of gamma radiation-resistant Geodermatophilus dictyosporus sp. nov. to accommodate the not validly named *Geodermatophilus obscurus* subsp. dictyosporus (Luedemann, 1968). *Extremophiles* 19, 77–85. doi: 10.1007/s00792-014-0708-z

Nuhoglu, Y., Oguz, E., Uslu, H., Ozbek, A., Ipekoglu, B., Ocak, I., et al. (2006). The accelerating effects of the microorganisms on biodeterioration of stone monuments under air pollution and continental-cold climatic conditions in Erzurum, Turkey. *Sci. Total Environ.* 364, 272–283. doi: 10.1016/j.scitotenv.2005.06.034

Ogawa, A., Celikkol-Aydin, S., Gaylarde, C., Baptista-Neto, J. A., and Beech, I. (2017). Microbiomes of biofilms on decorative siliceous stone: drawbacks and advantages of next generation sequencing. *Curr. Microbiol.* 74, 848–853. doi: 10.1007/s00284-017-1257-3

Onofri, S., de la Torre, R., de Vera, J.-P., Ott, S., Zucconi, L., Selbmann, L., et al. (2012). Survival of rock-colonizing organisms after 1.5 years in outer space. *Astrobiology* 12, 508–516. doi: 10.1089/ast.2011.0736

Onofri, S., Selbmann, L., Zucconi, L., and Pagano, S. (2004). Antarctic microfungi as models for exobiology. *Planet. Space Sci.* 52, 229–237. doi: 10.1016/j.pss.2003.08.019

Onofri, S., Zucconi, L., Isola, D., and Selbmann, L. (2014). Rock-inhabiting fungi and their role in deterioration of stone monuments in the Mediterranean area. *Plant Biosyst.—Int. J. Dealing With All Aspects Plant Biol.* 148, 384–391. doi: 10.1080/11263504.2013.877533

Pena-Poza, J., Ascaso, C., Sanz, M., Pérez-Ortega, S., Oujja, M., Wierzchos, J., et al. (2018). Effect of biological colonization on ceramic roofing tiles by lichens and a combined laser and biocide procedure for its removal. *Int. Biodeterior. Biodegradation* 126, 86–94. doi: 10.1016/j.ibiod.2017.10.003

Piñar, G., Poyntner, C., Tafer, H., and Sterflinger, K. (2019). A time travel story: metagenomic analyses decipher the unknown geographical shift and the storage history of possibly smuggled antique marble statues. *Ann. Microbiol.* 69, 1001–1021. doi: 10.1007/s13213-019-1446-3

Rampelotto, P. (2013). Extremophiles and extreme environments. *Life* 3, 482–485. doi: 10.3390/life3030482

Redford, D. B. (2005). *The Oxford Encyclopedia of Ancient Egypt*. UK: Oxford University Press.

Rizk, S. M., and Magdy, M. (2022). An indigenous inland genotype of the black yeast Hortaea werneckii inhabiting the great pyramid of Giza, Egypt. *Front. Microbiol.* 13. doi: 10.3389/fmicb.2022.997495

Rizk, S. M., Magdy, M., De Leo, F., Werner, O., Rashed, M. A.-S., Ros, R. M., et al. (2021). A new Extremotolerant ecotype of the fungus Pseudotaeniolina globosa isolated from Djoser pyramid, Memphis necropolis, Egypt. *JoF* 7:104. doi: 10.3390/jof7020104

Ruibal, C., Gueidan, C., Selbmann, L., Gorbushina, A. A., Crous, P. W., Groenewald, J. Z., et al. (2009). Phylogeny of rock-inhabiting fungi related to Dothideomycetes. *Stud. Mycol.* 64, 123–133. doi: 10.3114/sim.2009.64.06

Saier, M. H., Ma, C. H., Rodgers, L., Tamang, D. G., Yen, M. R., Laskin, A., et al. (2008). Protein secretion and membrane insertion systems in bacteria and eukaryotic organelles. *Adv. Appl. Microbiol.* 65, 141–197. doi: 10.1016/S0065-2164(08)00606-0

Sand, W., and Bock, E. (1991). Biodeterioration of mineral materials by microorganisms—biogenic sulfuric and nitric acid corrosion of concrete and natural stone. *Geomicrobiol J.* 9, 129–138. doi: 10.1080/01490459109385994

Sanz, M., Oujja, M., Ascaso, C., Pérez-Ortega, S., Souza-Egipsy, V., Fort, R., et al. (2017). Influence of wavelength on the laser removal of lichens colonizing heritage stone. *Appl. Surf. Sci.* 399, 758–768. doi: 10.1016/j.apsusc.2016.12.032

Scheerer, S., Ortega-Morales, O., and Gaylarde, C. (2009). "Chapter 5 microbial deterioration of stone monuments—an updated overview" in *Advances in Applied Microbiology* (Massachusetts, Cambridge: Academic Press), 97–139.

Schloss, P. D., Westcott, S. L., Ryabin, T., Hall, J. R., Hartmann, M., Hollister, E. B., et al. (2009). Introducing mothur: open-source, platform-independent, community-

supported software for describing and comparing microbial communities. *Appl. Environ. Microbiol.* 75, 7537–7541. doi: 10.1128/AEM.01541-09

Schneegurt, M. A., Dore, S. Y., and Kulpa, C. F. (2003). Direct extraction of DNA from soils for studies in microbial ecology. *Curr. Issues Mol. Biol.* 5, 1–8. doi: 10.21775/cimb.005.001

Selbmann, L., Zucconi, L., Isola, D., and Onofri, S. (2015). Rock black fungi: excellence in the extremes, from the Antarctic to space. *Curr. Genet.* 61, 335–345. doi: 10.1007/s00294-014-0457-7

Sert, H., Sümbül, H., and Sterflinger, K. (2007). Microcolonial fungi from antique marbles in Perge/side/Termessos (Antalya/Turkey). *Antonie Van Leeuwenhoek* 91, 217–227. doi: 10.1007/s10482-006-9111-9

Sghaier, H., Hezbri, K., Ghodhbane-Gtari, F., Pujic, P., Sen, A., Daffonchio, D., et al. (2016). Stone-dwelling actinobacteria *Blastococcus saxobsidens*, Modestobacter marinus and *Geodermatophilus obscurus* proteogenomes. *ISME J.* 10, 21–29. doi: 10.1038/ismej.2015.108

Shaw, I. (2003). *The Oxford History of Ancient Egypt*. New York: Oxford University Press, INC.

Skipper, P. J., Skipper, L. K., and Dixon, R. A. (2022). A metagenomic analysis of the bacterial microbiome of limestone, and the role of associated biofilms in the biodeterioration of heritage stone surfaces. *Sci. Rep.* 12, 1–18. doi: 10.1038/s41598-022-08851-4

Soliman, S., and Magdy, M. (2018). *Lahun Pyramid, More Surprising Treasures are Revealed: Fungal Diversity Analysis Using Amplicon-Based Metagenomic Approach*. Oxford Univ Press Great Clarendon St. Oxford Ox2 6DP, England, S21. doi: 10.1093/mmy/myy135

Sterflinger, K. (2006). "Black yeasts and meristematic Fungi: ecology, diversity and identification," in *Biodiversity and ecophysiology of yeasts the yeast handbook*. eds. G. Péter and C. Rosa (Berlin/Heidelberg: Springer-Verlag), 501–514.

Sterflinger, K., Lopandic, K., Pandey, R. V., Blasi, B., and Kriegner, A. (2014). Nothing special in the specialist? Draft genome sequence of Cryomyces antarcticus, the Most Extremophilic fungus from Antarctica. *PLoS One* 9:e109908. doi: 10.1371/journal.pone.0109908

Trovão, J., Portugal, A., Soares, F., Paiva, D. S., Mesquita, N., Coelho, C., et al. (2019). Fungal diversity and distribution across distinct biodeterioration phenomena in limestone walls of the old cathedral of Coimbra, UNESCO world heritage site. *Int. Biodeterior. Biodegradation* 142, 91–102. doi: 10.1016/j.ibiod.2019.05.008

Urzi, C. (2004). Microbial deterioration of rocks and marble monuments of the Mediterranean Basin: a review. *Corros. Rev.* 22, 441–458. doi: 10.1515/CORRREV.2004.22.5-6.441

Urzi, C., Brusetti, L., Salamone, P., Sorlini, C., Stackebrandt, E., and Daffonchio, D. (2001). Biodiversity of Geodermatophilaceae isolated from altered stones and monuments in the Mediterranean basin. *Environ. Microbiol.* 3, 471–479. doi: 10.1046/j.1462-2920.2001.00217.x

Urzì, C., De Leo, F., Bruno, L., and Albertano, P. (2010). Microbial diversity in Paleolithic caves: a study case on the phototrophic biofilms of the cave of bats (Zuheros, Spain). *Microb. Ecol.* 60, 116–129. doi: 10.1007/s00248-010-9710-x

Urzì, C., De Leo, F., De Hoog, S., and Sterflinger, K. (2000). "Recent advances in the molecular biology and ecophysiology of meristematic stone-inhabiting Fungi" in *Of microbes and art*. eds. O. Ciferri, P. Tiano and G. Mastromei (Boston, MA: Springer US), 3–19.

Vasanthakumar, A., DeAraujo, A., Mazurek, J., Schilling, M., and Mitchell, R. (2013). Microbiological survey for analysis of the brown spots on the walls of the tomb of king Tutankhamun. *Int. Biodeterior. Biodegradation* 79, 56–63. doi: 10.1016/j.ibiod.2013.01.014

Warscheid, T., and Braams, J. (2000). Biodeterioration of stone: a review. *Int. Biodeterior. Biodegradation* 46, 343–368. doi: 10.1016/S0964-8305(00)00109-8

White, T. J., Bruns, T., Lee, S., and Taylor, J. (1990). "Amplification and direct sequencing of fungal ribosomal RNA genes for Phylogenetics" in *PCR Protocols*. New York: Academic Press, 315–322.

Yoon, J.-H., Kang, S.-J., Lee, S.-Y., Oh, K.-H., and Oh, T.-K. (2010). *Planococcus salinarum* sp. nov., isolated from a marine solar saltern, and emended description of the genus Planococcus. *Int. J. Syst. Evol. Microbiol.* 60, 754–758. doi: 10.1099/ijs.0.013136-0

Zakharova, K., Tesei, D., Marzban, G., Dijksterhuis, J., Wyatt, T., and Sterflinger, K. (2013). Microcolonial Fungi on rocks: a life in constant drought? *Mycopathologia* 175, 537–547. doi: 10.1007/s11046-012-9592-1

frontiers | Frontiers in Microbiology

TYPE Original Research
PUBLISHED 14 September 2023
DOI 10.3389/fmicb.2023.1202266

OPEN ACCESS

EDITED BY
Katharina Kujala,
University of Oulu, Finland

REVIEWED BY
Roey Angel,
Academy of Sciences of the Czech Republic (ASCR), Czechia
Capucine Baubin,
University of Colorado Boulder, United States

*CORRESPONDENCE
Cecilia Demergasso
✉ cdemerga@ucn.cl
Julia W. Neilson
✉ jneilson@arizona.edu

RECEIVED 07 April 2023
ACCEPTED 31 July 2023
PUBLISHED 14 September 2023

CITATION
Demergasso C, Neilson JW, Tebes-Cayo C, Véliz R, Ayma D, Laubitz D, Barberán A, Chong-Díaz G and Maier RM (2023) Hyperarid soil microbial community response to simulated rainfall.
Front. Microbiol. 14:1202266.
doi: 10.3389/fmicb.2023.1202266

Hyperarid soil microbial community response to simulated rainfall

Cecilia Demergasso[1]*, Julia W. Neilson[2]*, Cinthya Tebes-Cayo[1,3], Roberto Véliz[1], Diego Ayma[4], Daniel Laubitz[5], Albert Barberán[2], Guillermo Chong-Díaz[3] and Raina M. Maier[2]

[1]Biotechnology Center "Profesor Alberto Ruíz", Universidad Católica del Norte, Antofagasta, Chile, [2]Department of Environmental Science, University of Arizona, Tucson, AZ, United States, [3]Department of Geology, Faculty of Engineering and Geological Sciences, Universidad Católica del Norte, Antofagasta, Chile, [4]Department of Mathematics, Faculty of Sciences, Universidad Católica del Norte, Antofagasta, Chile, [5]Steele Steele Children's Research Center, Department of Pediatrics, University of Arizona, Tucson, AZ, United States

The exceptionally long and protracted aridity in the Atacama Desert (AD), Chile, provides an extreme, terrestrial ecosystem that is ideal for studying microbial community dynamics under hyperarid conditions. Our aim was to characterize the temporal response of hyperarid soil AD microbial communities to *ex situ* simulated rainfall (5% g water/g dry soil for 4 weeks) without nutrient amendment. We conducted replicated microcosm experiments with surface soils from two previously well-characterized AD hyperarid locations near Yungay at 1242 and 1609 masl (YUN1242 and YUN1609) with distinct microbial community compositions and average soil relative humidity levels of 21 and 17%, respectively. The bacterial and archaeal response to soil wetting was evaluated by 16S rRNA gene qPCR, and amplicon sequencing. Initial YUN1242 bacterial and archaeal 16S rRNA gene copy numbers were significantly higher than for YUN1609. Over the next 4 weeks, qPCR results showed significant increases in viable bacterial abundance, whereas archaeal abundance decreased. Both communities were dominated by 10 prokaryotic phyla (Actinobacteriota, Proteobacteria, Chloroflexota, Gemmatimonadota, Firmicutes, Bacteroidota, Planctomycetota, Nitrospirota, Cyanobacteriota, and Crenarchaeota) but there were significant site differences in the relative abundances of Gemmatimonadota and Chloroflexota, and specific actinobacterial orders. The response to simulated rainfall was distinct for the two communities. The actinobacterial taxa in the YUN1242 community showed rapid changes while the same taxa in the YUN1609 community remained relatively stable until day 30. Analysis of inferred function of the YUN1242 microbiome response implied an increase in the relative abundance of known spore-forming taxa with the capacity for mixotrophy at the expense of more oligotrophic taxa, whereas the YUN1609 community retained a stable profile of oligotrophic, facultative chemolithoautotrophic and mixotrophic taxa. These results indicate that bacterial communities in extreme hyperarid soils have the capacity for growth in response to simulated rainfall; however, historic variations in long-term hyperaridity exposure produce communities with distinct putative metabolic capacities.

KEYWORDS

hyperarid, soil microbiome, soil wetting, extremophiles, oligotrophic microbes, Atacama Desert, mixotroph

Introduction

The Atacama Desert (AD) provides an ideal laboratory for studying microbial habitability under hyperarid conditions and identifying associated unique survival strategies. The AD soils reach ages exceeding 10 million years and have undergone an exceptionally long and protracted period of aridity (Hartley and Chong, 2002) that is rare on the rest of the planet. In addition, the occurrence and distribution of salts have allowed the characterization of the AD as a unique Saline Domain (Chong-Diaz et al., 2020). This extreme environment has attracted diverse research interests. For example, bio-signatures can offer insights into past or present life on surfaces such as early Mars, and guide astrobiology research on extraterrestrial surfaces (Cabrol et al., 2007; Hock et al., 2007; Certini et al., 2009; Certini and Ugolini, 2013; Warren-Rhodes et al., 2019). Related to this is interest in the strategies used by microbes to remain metabolically active over long time scales under hyperarid conditions, a topic that remains poorly understood (Davila et al., 2013; Leung et al., 2020).

Deserts are not only characterized by low precipitation levels, but precipitation events are erratic. Soil microorganisms in extreme, hyperarid deserts such as the AD and the Namib Desert in Namibia must survive protracted periods of aridity between isolated rainfall events. Data from the Namib Desert projected that surface soil microbial communities have active growth for just 184–363 h per year (Bosch et al., 2022). Similarly, soil relative humidity (RH) data recorded in the AD from 2015 to 2018 (sensors at 20 cm depth recording every 2 h) revealed average RH values of just 17–29% across eight hyperarid sites with no values recorded above 52% (Neilson et al., 2017). Areas in the AD that experience rainfall have soil RH values of 100%. Thus, AD soil microbial communities in hyperarid regions survive years to decades with no precipitation events (Neilson et al., 2017; Schulze-Makuch et al., 2018; Supplementary Figure S1 AD rainfall history). Temporal studies in deserts are rare, but it is clear that isolated rainfall events are a primary trigger controlling microbial activity (Huxman et al., 2004;Makhalanyane et al., 2015).

These extreme conditions support increasing interest in understanding the strategies for survival of the AD microbiome during prolonged periods of desiccation. Initial culture-independent techniques concluded that the hyperarid core of the AD was an environment completely devoid of life (Navarro-Gonzalez et al., 2003). But soon thereafter recoverable DNA and low cell numbers of bacteria from soils in the extreme arid core were reported showing differences between the composition of the microbial community in vegetated and unvegetated areas (Maier et al., 2004; Drees et al., 2006; Connon et al., 2007).

Later studies employing high throughput sequencing techniques facilitated the identification of associations between environmental factors, soil microbial community composition, and potential metabolic strategies under arid and hyperarid conditions. Two research studies evaluated associations between aridity gradients and microbial community composition along extensive transects. Moisture and soil electrical conductivity significantly correlated with microbial community diversity along a North–South (24–26° Latitude S) moisture gradient transect (Crits-Christoph et al., 2013). In a second study along a west–east elevational transect, moisture and temperature explained significant reductions in the diversity, evenness, and connectivity of AD soil microbial communities (Neilson et al., 2017). In the second study, the abundance of "key bacterial taxa" typically associated with the microbiome of fertile soils as well as Archaea decreased with decreasing moisture and increasing temperature. On the contrary, more abundant microbial phylotypes were phylogenetically associated with chemolithoautotrophs that obtain energy by oxidation of nitrite (NO_2^-), carbon monoxide (CO), iron (Fe) or sulfur (S) suggesting genetic potential for non-phototrophic primary production and geochemical cycling in these hyperarid ecosystems (Neilson et al., 2012, 2017). Strong evidence has also been found for contributions by hydrogen-oxidizing bacteria in four distinct desert soils (Australian, Namib, Gobi, and Mohave) whose activity is stimulated by hydration (Jordaan et al., 2020). Interestingly, the microbial composition of AD hyperarid soils was site-specific suggesting that specific environmental factors shape these communities.

A study of microbial activity in the AD using oxygen (O) and nitrogen (N) isotopes indicates that at least 20% of the nitrate in the driest region of the AD has been biologically cycled (Amundson et al., 2007). However, the low rate of biological N cycling, combined with very low organic matter (OM) cycling rates based on ^{14}C determination, reflected exceedingly small rates of microbial processing of carbon (C) and N. An assessment of biomolecular proxies for cell adaptation and growth suggests that for the driest areas of the AD this basal metabolic activity is used for cellular repair and maintenance and there is minimal or no *in situ* microbial growth (Wilhelm et al., 2018).

Some studies have amended AD surface soils (1–10 cm) with moisture and C substrates to evaluate the heterotrophic metabolic potential of AD soil microbial communities. Emissions of carbon dioxide (CO_2), N_2O, and methane (CH_4) after amendment revealed the retention of some biogeochemical-cycling capacity despite long-term deprivation (Hall et al., 2012). In addition, an exceptional rainfall event in 2017 allowed for an *in situ* analysis of hyperarid AD soil response to moisture and provided evidence of metabolically active microbial communities (Schulze-Makuch et al., 2018). In that study, biomolecules indicative of potentially active cells [e.g., presence of ATP, phospholipid fatty acids (PLFAs), metabolites, and enzymatic activity], as well as *in situ* replication rates of metagenome-assembled genomes (MAGs) were measured, despite extremely low microbial biomass and diversity. The researchers inferred that the microbial populations underwent selection and adaptation in response to their specific soil microenvironment and to the degree of aridity.

The objective of this study was to determine the capacity of AD soil microbial communities from two distinct hyperarid locations to respond to a simulated rainfall event under controlled laboratory conditions in the absence of any nutrient amendment. Specifically, the study evaluated the response of hyperarid soil microbiomes to a soil-wetting event in terms of (1) the growth capacity of bacterial and archaeal communities and (2) the dynamic changes in relative abundances of specific taxa. Functional contributions of key taxa from each community were evaluated to characterize the metabolic response of each community. Hyperarid sites YUN1242 and YUN1609 were selected for analysis based on previous environmental and microbial community characterization that showed them to have distinct microbial communities (Neilson et al., 2017). The model experiment was conducted over 30 days to quantitatively assess the temporal response of these two microbial communities to water addition using qPCR and amplicon sequencing. The qPCR analysis quantifies the metabolically active fractions of the bacterial and

archaeal communities in the respective soils, whereas changes in the relative abundance of microbial populations characterized by amplicon sequencing identify the specific taxa with the capacity to respond to a rainfall event. We hypothesize that hyperarid soil microbial communities from different geographic locations in the AD will have the same response to a simulated rainfall event. Results from this study will inform our understanding of the composition, physiology and activity of resilient microorganisms inhabiting arid soils, and will help guide the search for life in terrestrial and extraterrestrial sites.

Results

Soil characterization

The selected sites (Figure 1), labeled YUN1242, and YUN1609, were previously classified as long-term hyperarid soil based on nitrate and sulfate profiles (Neilson et al., 2017). Nitrate and sulfate levels over 15 and 340 mmol g^{-1} soil, respectively, in the soil samples revealed the long-term hyperaridity in the Atacama Desert (Supplementary Figure S2). Higher nitrate and sulfate levels in the YUN1609 soil profile compared with YUN1242 suggest greater long-term aridity at this site. Soil organic carbon (OC) ranged from 0.02 to 0.04% (Neilson et al., 2017).

The soils in both sites were alkaline (pH 8.9 in YUN1242, and pH 8.4 in YUN1609) and were characterized by an electrical conductivity of 311.5 and 589.3 µS·cm^{-1} (Table 1) and a soil moisture of 1.71% in YUN1242, and 1.09% in YUN1609. After the rain event in 2017, the soil gravimetric water content in each sample increased to 4.196 and 6.159%, respectively (Table 1). Our records show that gravimetric moisture contents remained at these levels for at least 12 days after the 2017 rain event (Table 1). Further, elevated RH levels of 40–50% were recorded at 10–20 cm depth for more than 90 days in an alluvial fan near YUN1242 (Pfeiffer et al., 2021).

Bacterial and archaeal total abundances during the incubation time

The average DNA concentrations retrieved from the experiments (Supplementary Figure S3) with YUN1242 and YUN1609 samples were significantly (p-value < 0.001) higher than those obtained from the blanks (Supplementary Figure S4). The initial (T0) 16S rRNA copy number per gram of soil was 3.09×10^5 and 1.78×10^6 for Bacteria, and 1.18×10^4 and 4.55×10^4 for Archaea in YUN1609 and YUN1242, respectively (Figure 2). Thus, bacterial and archaeal copy numbers were significantly higher for YUN1242 soils than YUN1609 at T0 (t-test value of ps, 0.018 and 0.023, respectively).

The bacterial abundance response to soil wetting for both YUN1242 and YUN1609 was significantly different from that of the archaea. For bacteria, pairwise multiple comparisons using FDR correction indicated a significant increase in abundance from T0 to T30 in both sampling sites (value of $p < 0.05$). This increase was relatively steady for YUN1242. In contrast, for YUN1609 bacterial abundance increased

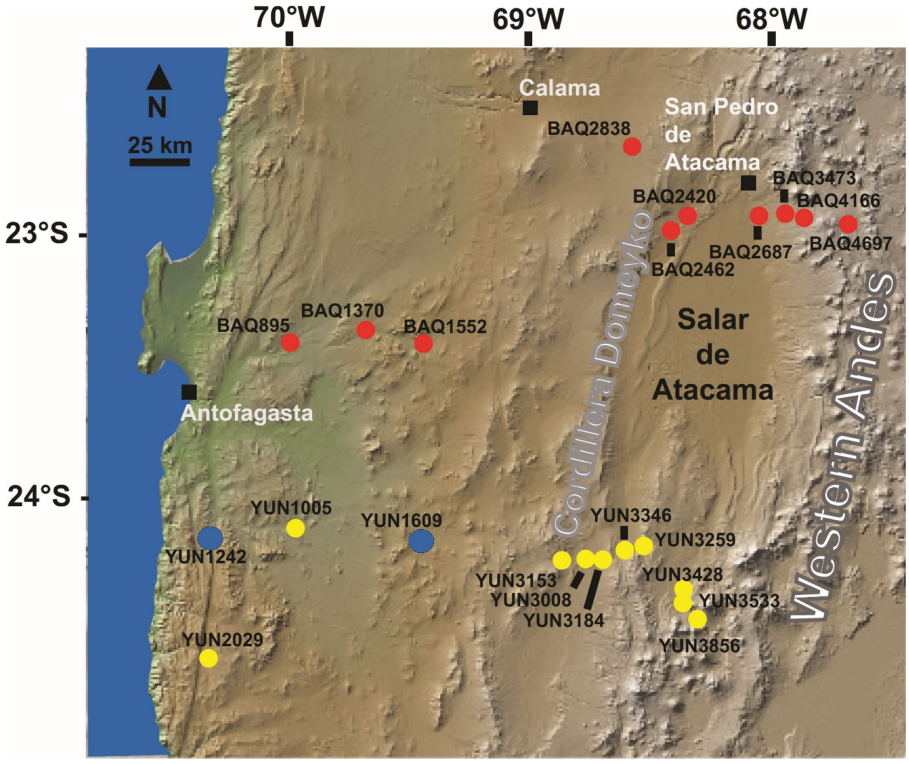

FIGURE 1
Map of the studied area indicating the locations of sampling sites YUN1242 and YUN1609 in blue at the Atacama Desert, Chile. The sites in yellow and red belong to two transects studied before (Neilson et al., 2017).

TABLE 1 Physicochemical parameters of the soil samples from January and June 2017, before and after the rain (6–7 June).

Date	Parameters	Unit	YUN1242	YUN1609
Before rain (1/25/2017)	Coordinates	Latitude (S)	24.141	24.144
		Longitude (W)	70.312	69.442
	Soil Temp.	°C	31.4	30.2
	Air RH /Temp.	%/°C	30.5/31.5	9.4/30.2
	pH		8.9	8.4
	ORP	mV	226.1	230.7
	EC	µS/cm	311.5	589.3
	UV A	µW/m^2	6503	3019
	UV B	µW/m^2	658.3	360.5
	UV C	µW/m^2	14	19.75
	PAR	µmol/m^{2}s	1948	2584
	Soil moisture	%	1.7380	1.0909
After rain (6/19/2017)	Soil moisture	%	4.196	6.159

RH, Relative humidity; ORP, Oxidation–reduction potential; EC, electrical conductivity; UV, ultraviolet radiation; PAR, photosynthetic active radiation.

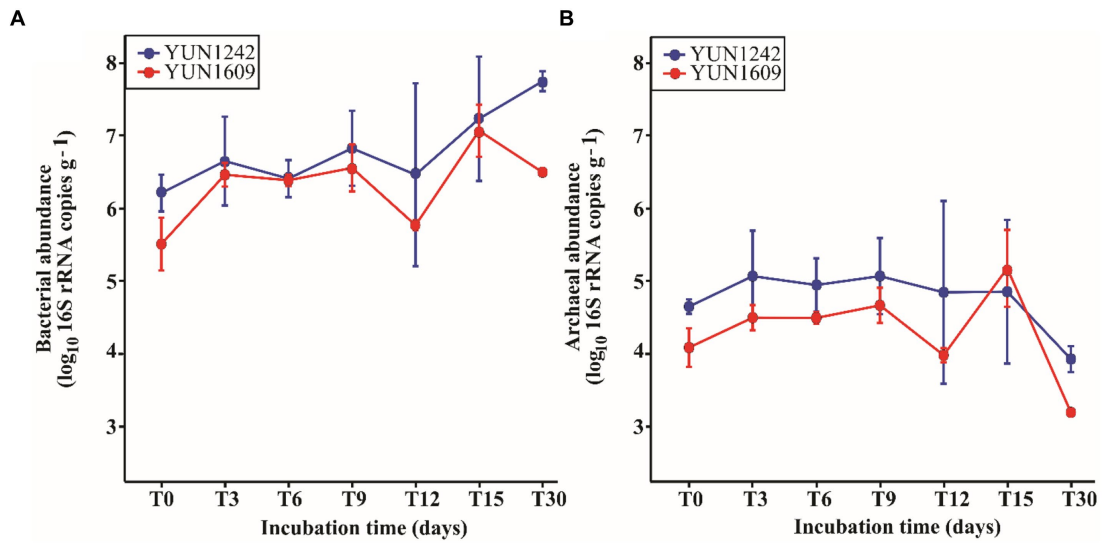

FIGURE 2
Profile of bacterial **(A)** and archaeal **(B)** 16S rRNA copies·g^{-1} (on a log 10 scale) in sampling sites YUN1242 and YUN1609 during the incubation at 5% soil moisture, 20°C, 12-h-light, and oxic environment. The means and standard deviations for observations per incubation time are represented via points and vertical lines, respectively. The raw data is in Supplementary Table S7.

significantly from T0 to T6 (value of $p = 0.010$), remained stable until T9, followed by a significant decrease until T12 (value of $p = 0.014$) and finally another significant increase from T12 to T30 (value of $p < 0.001$) (Figure 2 and Supplementary Table S1). Both sampling site and the incubation time were statistically significant factors (two-way repeated measures ANOVA using the log 10 bacterial total abundance as the response variable, value of $p < 0.005$).

A similar analysis of archaeal abundance indicated a significant decrease in archaeal abundance from T6 to T30 in YUN1242 (value of $p = 0.002$) and from T0 to T30 in YUN1609 (value of $p = 0.007$). Again, for YUN1242 the decrease was relatively gradual whereas for YUN1609 the copy number remained stable from T0 to T9, then decreased significantly at T12 (value of $p = 0.019$) followed by a significant rebound in abundance at T15 (value of $p = 0.041$), and then a sharp decrease again until T30 (value of $p = 0.005$) (Figure 2 and Supplementary Table S2).

Overall community diversity and taxonomic composition

A total of 410–45,284 16S rRNA gene sequences per sample were retrieved from the extracted DNA during the wetting experiments (for T3–T30 subsamples), 690–4,617 sequences per sample from the T0

samples, and 555–1,599 sequences in both blank and reagent control experiments (Supplementary Table S3).

The quality control and rarefaction (retain samples with ≥1,500 reads per sample) process provided 353,319 input sequences which resulted in 31,500 bacterial and archaeal Amplicon Sequence Variants [ASVs]. The ASVs were classified into 12 prokaryotic phyla accounting for 91% of the total sequences in the communities (Figure 3). All ASVs were classified at the kingdom level; 40.7% were assigned to genus and less than 2.3% to species.

The diversity of the YUN1242 microbial community was higher than the YUN1609 community, Shannon index averages over incubation time of 2.928 and 2.685 for YUN1242 and YUN1609, respectively (value of $p < 0.05$) (Supplementary Table S4A and Supplementary Figure S5A). The richness index showed a linear increase with time (value of $p < 0.05$) during the wetting experiments for the YUN1242 community, whereas the increase in richness for YUN1609 was not significant (value of $p = 0.0532$). Multiple linear regression analysis showed no significant difference in terms of their slopes (value of $p > 0.05$) (Supplementary Figure S6).

Eleven bacterial phyla (Actinobacteriota, Proteobacteria, Chloroflexota, Gemmatimonadota, Firmicutes, Bacteroidota, Planctomycetota, Nitrospirota, Cyanobacteriota, Acidobacteriota, Verrucomicrobiota) and one archaeal phylum (Crenarchaeota) jointly comprised 99% of the total community of both soils (samples and subsamples) (Figure 3A). The taxonomic analysis of the sequencing (control tubes) and DNA extraction (blank tubes) reagents revealed the presence of common contaminants observed in molecular techniques like *Streptococcus* (Salter et al., 2014). Although direct PCR of those tubes did not generate sequences that passed the quality score, nested PCR detected 14 contaminant ASVs that represented less than 1% of abundance on average (from 2 to 113 ASV counts) of target samples (Supplementary Information Box 1). The nested PCR approach was employed for more stringent contaminant detection as described in Supplementary Information Box 1. These contaminant sequences were eliminated in the original samples or from the re-wetting experiments.

Actinobacteriota dominated bacterial abundance ranging from 65 to 90% in the samples and subsamples from both sites (Figure 3A). Site had an important influence on Actinobacteriota distribution at the genus level. For example, the unclassified family *Nitriliruptoraceae* was predominant in the microbial communities from both sites (Figure 3B). *Rubrobacter* distribution was also similar in both sites. However, several groups were more abundant in one site or the other, e.g., the unclassified order *Gaiellales* was more abundant in YUN1609 than in YUN1242 whereas the *Streptomycetaceae* family was more abundant in YUN1242.

Chloroflexi was most represented by *Thermomicrobiales*, *Thermobaculales*, and unclassified Class Gitt-GS-136 sequences (Botero et al., 2004; Gupta et al., 2013). The *Gemmatimonadota* phylum was represented mainly by *Longimicrobia* (Figure 3B; Pascual et al., 2016) in YUN1242 and YUN1609 samples. The Proteobacteria (now Pseudomonadota) phylum was mainly represented by the order *Burkholderiales* and *Ferrovibrionales* in YUN1609, and *Rhizobiales* in YUN1242.

Noteworthy is that some bacterial phyla that are common in other dryland soils, such as Cyanobacteriota, Bacteroidota, Firmicutes, and Acidobacteriota (Leung et al., 2020) were under-represented in the samples, each of them limited to one predominant ASV.

An ASV occurrence diagram revealed that only 1.4% of the identified ASVs belonged to the core community (present at T0 and all subsequent time points for both YUN1242 and YUN1609). This core microbial community group was comprised primarily of *Rubrobacter*, *Thermobaculum*, unclassified *Nitriliruptoraceae*, *Gaiellales*, *Nocardioidaceae*, *Longimicrobiaceae*, and *Frankiales* (Supplementary Figure S7C and Supplementary Table S5). The change caused by wetting is further evidenced by the fact that 84 and 87.6% of the ASVs present from T3 to T30 in YUN1242, and T6 to T30 in YUN1609, respectively, were not detected in the corresponding T0 YUN1242 and YUN1609 samples (Supplementary Figures S7A,B). A particular group of interest are ASVs belonging to the genus *Streptomyces* in the YUN1242 community that were not detected in T0 samples but became dominant by T30 (Figures 3B, 4B, 5A). Similarly, in YUN1609, the *Sphingobacteriales* order appeared at T30 (Figure 5D).

The site factor explained a larger proportion of the variation in microbial communities' dissimilarity patterns (PERMANOVA site value of $p < 0.005$, $R^2 = 0.55$). Six phyla were most strongly correlated with the different similarity patterns between the two soil microbial communities (BEST rho = 0.997), Actinobacteriota, Gemmatimonadota, Chloroflexota, Crenarchaeota, Proteobacteria (now Pseudomonadota), and Bacteroidota. The ordination analysis (NMDS) of all data (before and after wetting) revealed two well-defined groups (Figure 4A). The relative abundances of four main bacterial phyla (Actinobacteriota, Gemmatimonadota, Chloroflexota, and Proteobacteria) explained the variation between the two groups (Spearman correlation over 0.50). The main difference between the groups is a higher abundance of Gemmatimonadota (average 3.73% vs. 0.13%), Chloroflexota (average 4.36% vs. 3.21%) and Actinobacteriota (average 86.70 vs. 84.27) in YUN1242 than in YUN1609 and a higher abundance of Proteobacteria (average 7.47 vs. 2.78), in YUN1609 than in YUN1242 (Figure 4A).

The distribution (NMDS) of the most abundant actinobacterial orders revealed the unique composition of the YUN1242 and YUN1609 (PERMANOVA site value of $p < 0.005$, $R^2 = 0.39$). Significant contributions to the differences in site community composition (Spearman's correlation >0.75) were explained by 0319-7L14, and *Gaiellales* for YUN1609 and by *Streptomycetales*, *Euzebyales*, and *Pseudonocardiales* for YUN1242 (Supplementary Figure S8).

Ordination analysis of the distribution of the ASVs from the most abundant actinobacterial genera revealed the distinct response to soil wetting of the YUN1242 and YUN1609. Figures 4B, 5A,B shows the temporal increase of *Streptomyces* and concurrent decrease of unclassified family *Nitriliruptoraceae*, in the community of the YUN1242 experiment, and the stability of the community up to almost the end of the experiment in YUN1609 (see also Figure 3B).

A temporal analysis of the relative abundance of key ASVs assigned to each taxon showed the differences in the response of taxa from both sites to wetting. The low DNA concentrations retrieved from the replicate soil samples limited the yield of quality sequences from every time point and every flask. As shown in Supplementary Table S4B, the experiment generated from 0 to 3 data points from each site for each time point. Therefore, we looked for temporal changes in ASVs patterns based on a comparison of the first and second halves of the experiment (defined in Supplementary Table S6). The YUN1242 community showed a simultaneous significant increase of *Streptomyces*, *Frankiales*, and

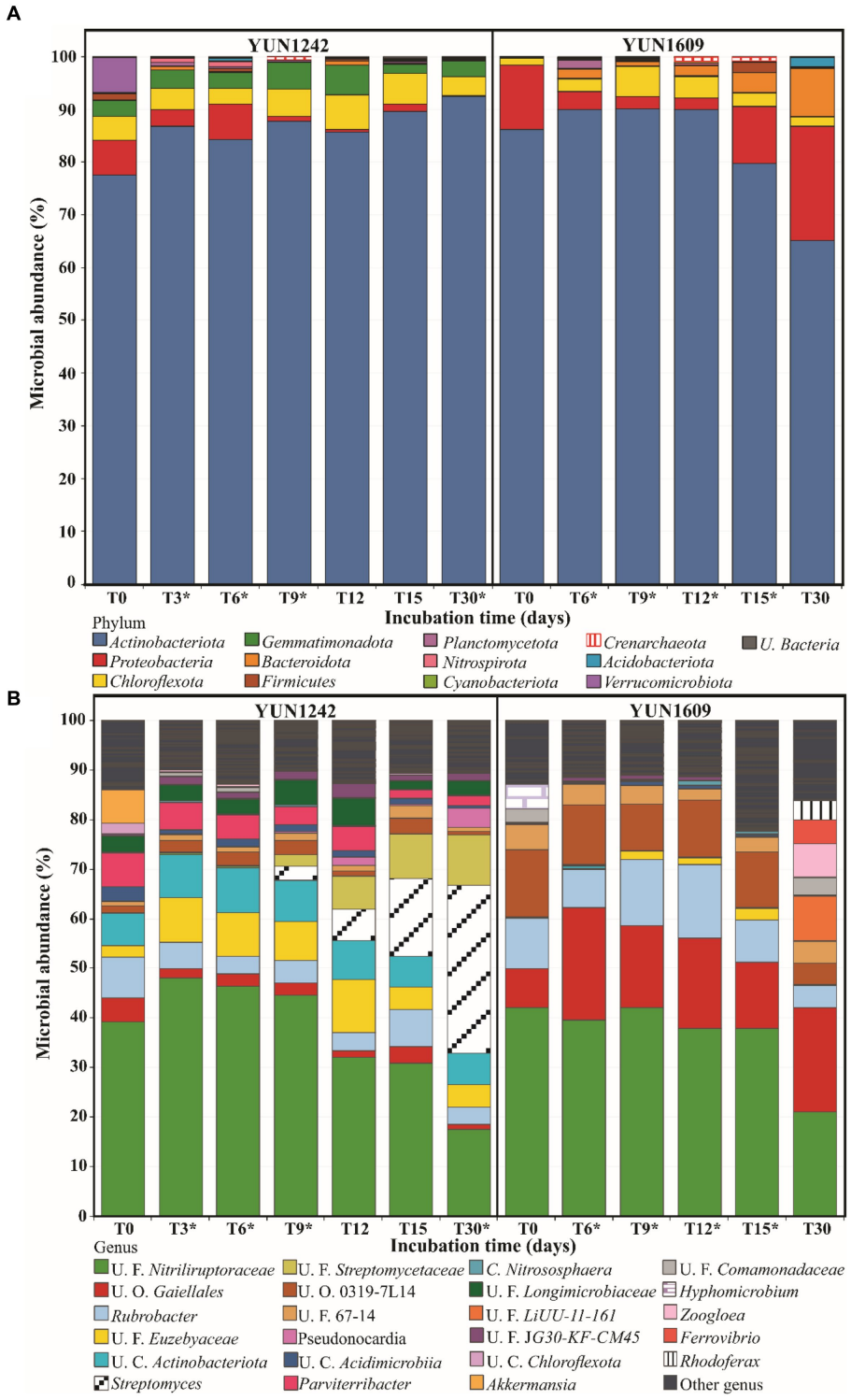

FIGURE 3
Average of relative microbial abundance at Phylum **(A)** and Genus **(B)** level versus the incubation time using YUN1242 and YUN1609 soils. * Indicates the microbial abundance's mean of replicates. Other genus = genus that have less than 1% of abundance in all the samples.

Nocardioidaceae (Figures 5A,C, and Supplementary Figure S9B respectively, and Supplementary Table S6), and a significant decrease of unclassified *Nitriliruptoraceae* family (Figure 5B and Supplementary Table S6) (One-way ANOVA value of $p < 0.01$), and *Parviterribacter* from *Thermoleophilia* class (Supplementary Figure S9A and Supplementary Table S6) (One-way ANOVA value of $p < 0.05$) during the 30-day incubation period. The *Streptomyces* growth was modeled as an exponential profile ($R^2 = 0.99$) up to day 15 (Supplementary Figure S10),

10.3389/fmicb.2023.1202266

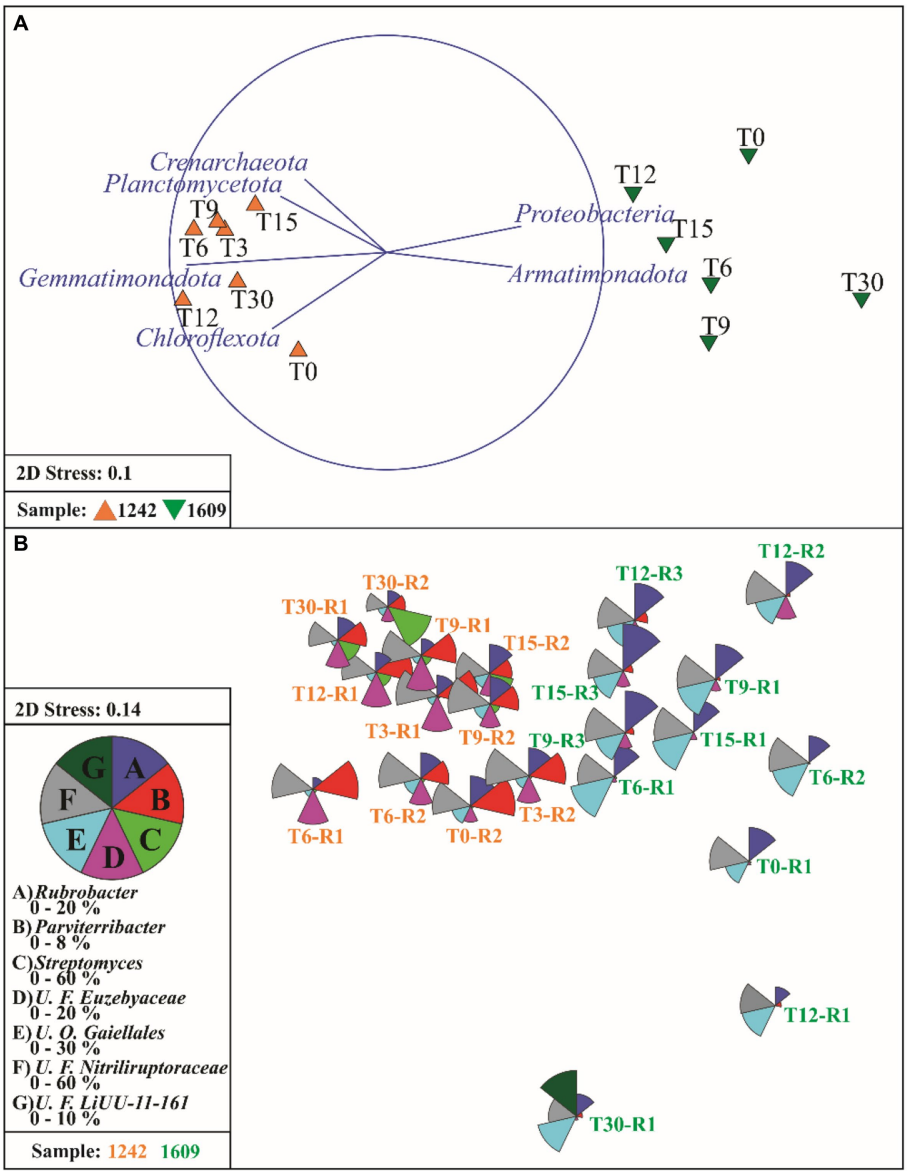

FIGURE 4
Non-metric multidimensional (NMDS) scaling of Bray-Curtis similarities for fourth root transformed phylum abundance data **(A)** and vectors of phyla which relative abundance has a Spearman correlation >0.50 with ordination axes. **(B)** NMDS plot of samples using the fourth root-transformed microbial genera abundance data, overlaid with the segmented bubble plot showing the percentage contribution of seven selected genera from *Actinobacteriota* phylum (*Streptomyces*, *Rubrobacter*, *Parviterribacter*, unclassified Families *Nitriliruptoracea* and *Euzebyaceae*, unclassified Order *Gaillales*) and one selected from *Bacteriodota, U. F. LiUU-11-161,* to the whole community. T0 to T30 indicates the incubation time in days. R1 to R3 indicates the replicate.

and it represented more than 15% (average 41%) of the total community at day 30 (Figure 3B). Other abundant taxa, like *Rubrobacter* did not show significant changes for either soil community (Supplementary Figure S11A). In the YUN1609 community, a significant increase was observed in the relative abundance of *Nocardioidaceae* (from Actinobacteriota phylum) during the wetting experiment (Figure 5C). In addition, *Sphingobacteriales*, *Burkholderiales* and *Ferrovibrionales* showed an exponential increase after 15-day incubation (Figure 5D), but we were not able to collect enough data to statistically test the significance of that increase because sufficient sequence reads for analysis (> 1,500) were retrieved from just one of the three T30 flasks for the YUN1609 sample. Similarly, the increase of *Pseudonocardiales*, mainly represented by *Pseudonocardia nigra* previously isolated from AD soils (Trujillo et al., 2017), was evidenced in YUN1242 sample in only one of the two replicate flasks (data not shown).

Differences between replicated experiments

Of additional interest were observed differences in the relative abundance patterns of specific phylotypes in replicates of the same

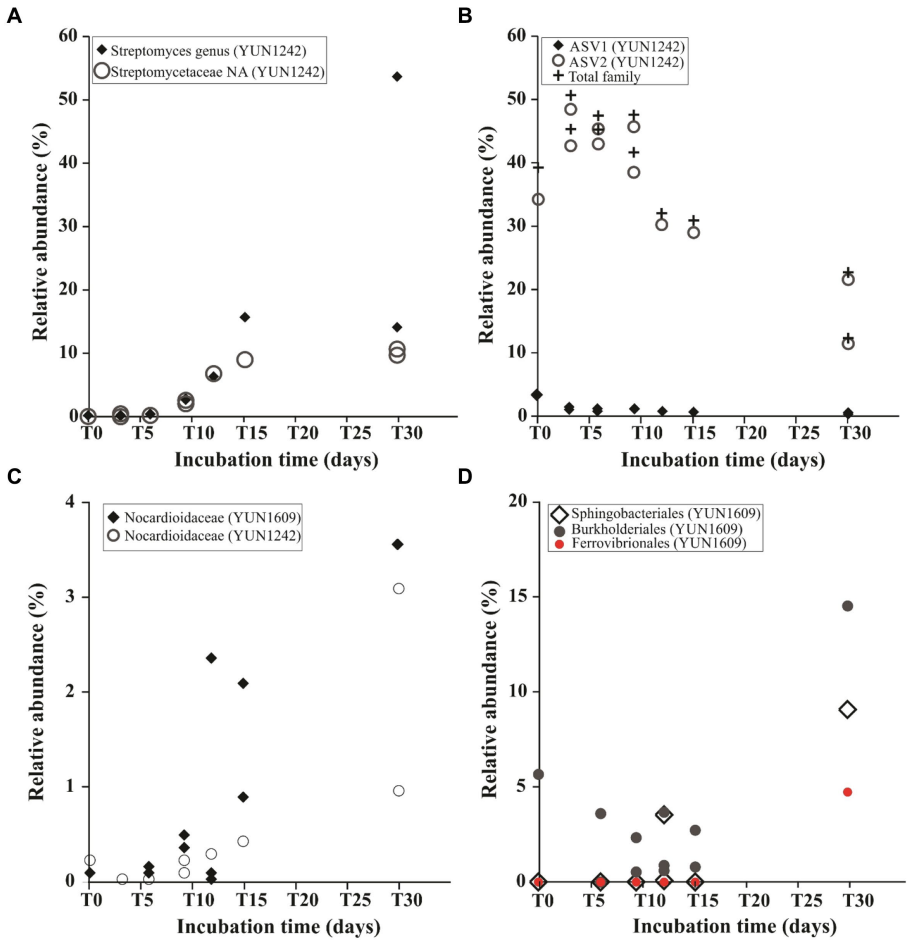

FIGURE 5
Relative abundance dynamics of taxa during the wetting experiments from the phylum *Actinobacteriota* **(A–C)**: *Streptomyces* genus and non-assigned (NA) *Streptomycetaceae* family in YUN1242 **(A)**; Predominant ASVs from *Nitriliruptoraceae* family in YUN1242 **(B)**; *Nocardioidaceae* in YUN1609 and YUN1242 samples **(C)**. Relative abundance dynamics of *Sphingobacteriales*, *Burkholderiales* and *Ferrovibrionales* in YUN1609 **(D)**. Note that each point represents the relative abundance in a single replicated flask.

treatment during the incubation experiment, i.e., (i) the relative abundance pattern of *Rubrobacter* (i.e., in ASV4) was significantly different (value of $p < 0.05$) in replicated flasks from YUN1242 experiment (Supplementary Figure S11A); (ii) the relative abundance profiles of *Gaillales* ASVs were significantly different (value of $p < 0.01$) in the replicated flasks (Supplementary Figure S11B and Supplementary Table S6) from the YUN1609 experiment; and (iii) a sudden increase in the relative abundance of Gemmatimonadota sequences was significantly observed in only one replicated flask of the YUN1242 experiment (Supplementary Figure S11C).

Discussion

The literature provides evidence for the occurrence of active microbial communities in the AD soils with the capacity to respond to rain events; however, the data is based on natural events over large time periods (Schulze-Makuch et al., 2018) under complex soil environmental conditions. The results of this study facilitate a detailed temporal analysis of the microbiome response of two hyperarid AD soil communities to a simulated rainfall event in the absence of nutrient amendment. The moisture conditions approximate a natural AD rainfall event.

General impact of site factor and soil moisture

The results confirm significant differences between the two hyperarid soil communities analyzed in this study. Initial bacterial and archaeal gene copy number and alpha diversity were significantly higher in the YUN1242 soil than YUN1609. Values for both soils were similar to previous reports from hyperarid regions of the AD; between BDL and 9.5×10^2 bacterial gene copies g^{-1} soil in 2016/2017 (Schulze-Makuch et al., 2018); 10^3 bacterial gene copies g^{-1} soil (Fletcher et al., 2011; Valdivia-Silva et al., 2016), and between 2.7 and 6.7×10^3 cells g^{-1} soil estimated by DAPI (Crits-Christoph et al., 2013). Archaea were less abundant than bacteria at both sites as has been reported in other arid and hyperarid soils (7% of the total prokaryotic soil biomass) (Bar-On et al., 2018).

Multiple factors can explain the greater abundance and diversity of bacteria and archaea at YUN1242 relative to YUN1609. Air RH was higher at the YUN1242 site (Table 1), a condition that can impact soil moisture levels under extreme hyperaridity (Neilson et al., 2017; Schulze-Makuch et al., 2018). In addition, higher NaCl content in the YUN1242 surface soils (Supplementary Figure S1) may contribute to

the higher water content measured at this site (Vitek et al., 2010; Neilson et al., 2017; Lee et al., 2018).

Finally, soil microbial community composition in the AD was previously found to be strongly correlated with soil electrical conductivity (EC) and historically the YUN1242 EC was four times higher than that of YUN1609 (Neilson et al., 2017). The difference observed between the EC previously reported from 2015 and 2017 YUN1242 samples could be assigned to soluble salts downward remobilization typically evidenced in AD soil profiles (Ericksen, 1981; Rech et al., 2003; Voigt et al., 2020). We hypothesized that today's microbial community correlate more to the history of high EC (2015) (Neilson et al., 2017), potentially associated to a more productive event, than the current (2017) (Table 1) EC level.

Following wetting, a significant increase in bacterial copy number was observed for both YUN1242 and YUN1609 soils (value of $p < 0.02$). The qPCR data confirm the presence of viable and metabolically active taxa in both soil microbial communities with the capacity for replication in response to simulated rainfall. In contrast, the archaeal gene copy number decreased in soils from both sites (Figure 2B). These results indicate that bacteria from the hyperarid, nutrient-poor soils of the AD are resilient and can have a growth response to wetting events that occur even in the absence of added nutrients. In contrast, the response of the archaea suggests lower resilience which is consistent with previous findings on the impact of aridity on archaea relative abundance (Neilson et al., 2017).

General microbial community functional capacity

The structure of the microbial communities at the phylum level remained stable after hydration (Figure 3). This response is distinct from that observed with biocrusts from a hyperarid region in the Negev Desert, where a drastic collapse of *Actinobacteriota* occurred (Angel and Conrad, 2013; Baubin et al., 2022). Despite community stability at the phylum level, dynamic, but distinct shifts were observed within the actinobacterial community for both the YUN1242 and YUN1609 soil microbiomes. Further, more than 12% of the ASVs present at day 15 were not detected in the T0 communities of either site. Previous research has shown that both dead and living microorganisms are present in the hyperarid soils of the AD as indicated by measurable extracellular DNA (eDNA) and intercellular DNA (iDNA), respectively (Schulze-Makuch et al., 2018). Thus, we assume that a significant portion of the T0 ASVs were associated with eDNA or dead microorganisms. This group represents an important component of the soil organic matter available as nutrients for the survival and growth of viable microbial populations. The analysis of fluctuations in relative abundances of specific phylotypes (growing, persisting, or declining) during the 30-days of the wetting experiment targets the viable and metabolically active ASVs in the microbial communities and provides predictions for the functional capacities and survival mechanisms of microbial communities colonizing hyperarid soils of the AD.

Both soil microbiomes included specialist taxa adapted to survival in saline and dry environments. Adaptations include the production of: (1) endogenous compatible solutes by *Nitriliruptoraceae* (Chen et al., 2020) that include small organic molecules such as sugars and amino-acids, involved in cell protection against osmotic pressure and desiccation (Vargas et al., 2006); and (2) biopolymers like polyhydroxyalkanoates (PHA) by *Rubrobacter* which are considered extremolytes (Kourilova et al., 2021). PHAs not only serve as a reserve of carbon, energy, and nitrogen for cell survival during starvation (Vargas et al., 2006), but also contribute to the organic matter associated with dead cell debris (Jansson and Hofmockel, 2020). The relative abundance of *Rubrobacter* is greatest in YUN1609; however, the total bacteria abundance (16S rRNA copy number) is greater in YUN1242 so the *Rubrobacter* absolute abundance is actually providing higher levels of PHA reserves for the YUN1242 than the YUN1609 communities.

Results showed a decrease in *Nitriliruptoriales* relative abundance in both communities beginning at T12 for YUN1242 and by T30 for YUN1609. This pattern demonstrates a common feature of desert soils in which the growth of one microbial group comes at the expense of the cell death of other members of the community (Angel and Conrad, 2013). Despite the observed decrease in *Nitriliruptoriales* relative abundance in YUN1242, the total abundance actually plateaued (Figure 6) due to the overall increase in the total bacterial cell number (qPCR analysis of 16S rRNA bacterial copy number). In contrast, the total abundance of *Nitriliruptoriales* decreased after T15 for YUN1609. It is likely that *Nitriliruptoriales* was less competitive in the respective communities due to a lower affinity for OC relative to the other oligotrophic taxa within the community (Figure 6). The compatible solutes produced by *Nitriliruptorales* provide more easily degraded OC for the community than the PHA, produced by *Rubrobacter*, whose degradation potential has been reported by a dozen phyla (Viljakainen and Hug, 2021; Figure 6).

In contrast, *Rubrobater* was more persistent in both communities after wetting. This is potentially due to the ability of this taxon to store carbon in PHAs (Kourilova et al., 2021) and to its reported ability to co-assimilate organic and inorganic carbon through a mixotrophic growth strategy. *Rubrobacter* uses the acetyl-CoA pathway (Leon-Sobrino et al., 2019) supported by available energy resources in desert soils such as light and hydrogen (Meier et al., 2021). In addition, the *Rubrobacter* genus has been described as a "CO tolerant capnophilic, nitrogen scavenging oligotroph" (Norman et al., 2017). Taxa from the *Rubrobacterales* order are considered active members of the Yungay soils microbial communities based on their identification in the iDNA fraction (Schulze-Makuch et al., 2018), and in the Namib desert where that family represented 7% of the active microbial community (Leon-Sobrino et al., 2019). Despite their resilience, a decrease in relative abundance was observed at the end of this experiment in YUN1609.

Increases in the *Nocardioidaceae* family were observed in both communities after T9. Members of this oligotrophic and motile family *Marmoricola* and *Marmoricola* like (Bartelme et al., 2020; Zhang et al., 2021) produce extracellular enzymes mainly involved in N-recycling such as aminopeptidases. Not only that but *Marmoricola* are also characterized by a higher affinity for OC (low *Km* for organic molecule transport), lower energy requirement for cell maintenance, and low respiration activity (Semenov, 1991). In addition, *Nocardioidaceae* along with other taxa present in the YUN1242 community following soil wetting (*Streptomyces, Frankiales*, and *Pseudonacardia*) are characterized by sporulation and mycelia production. Taken together these microbial properties are important because prior to wetting, soil

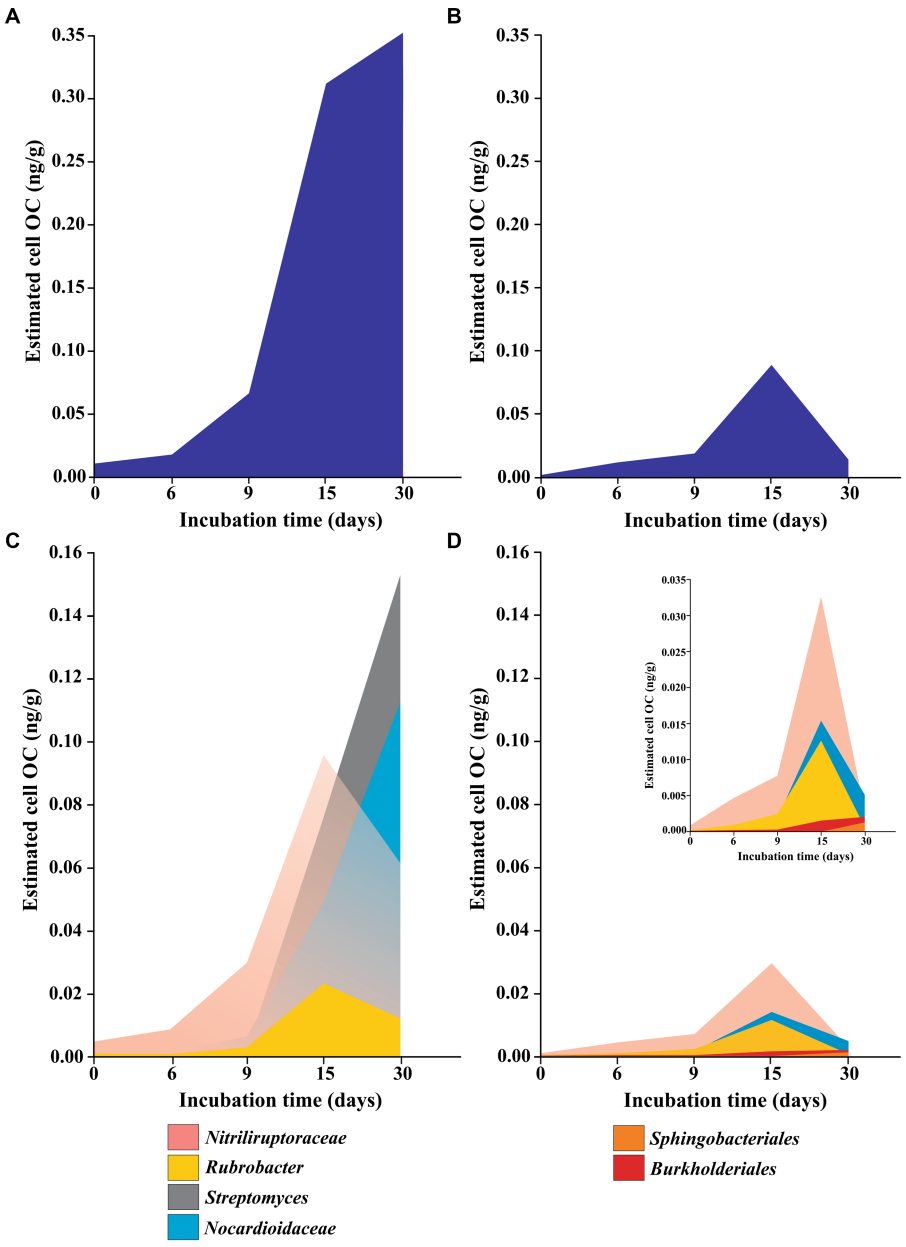

FIGURE 6
Approximation to total **(A,B)** and specific **(C,D)** cell organic carbon content (OC) of YUN1242 **(A,C)** and YUN1609 **(B,D)** estimated assuming 4.2 as the average 16S copy number per cell (Vetrovsky and Baldrian, 2013) and the relative abundance of each taxa. The insert in **(D)**, with a different Y axis scale, was included to improve the understanding. Only the main taxa responsible for microbial community dynamics were included.

dryness and heterogeneity create isolated conditions (Neilson et al., 2017; Petrenko et al., 2020) limiting symbiotic, commensalistic, and competitive interactions between taxa. Immediately after wetting, the resulting water films facilitate spore germination and mycelia formation, microbe-microbe interactions and create greater potential essential shared resource utilization within the microbial communities. Soil wetting can enhance the production of these extracellular enzymes to improve the utilization of OC available following the cell death of other microorganisms. Similar increases in the abundance of soil Actinobacteriota capable of producing aminopeptidase enzymes involved in N-cycling under drought (i.e., *Streptomyces*, *Marmoricola*, and other *Nocardioides*) have been previously reported (Zhang et al., 2021).

Specific functional potential of the YUN1242 microbiome

The initial YUN1242 community composition differed from YUN1609 by a greater relative abundance of Gemmatimonadota and Choroflexota phyla (Figures 3, 4A). In addition, within the Actinobacteriota phylum, YUN1242 was characterized by a greater relative abundance of *Euzebyales* order (*Nitriliruptoria* class,

Actinobacteriota) (Figure 3B). Interestingly, both *Euzebyales* and *Nitriliruptorales* are specialized to survive in saline environments (Neilson et al., 2017; Yin et al., 2018), however, unlike *Nitriliruptorales*, the *Euzebyales* relative abundance was sustained throughout the wetting experiment. The higher relative abundance of these taxa in YUN1242 is logical, considering the history of higher Cl^- and EC levels observed at this site relative to YUN1609 (Neilson et al., 2017).

After hydration, significant changes were observed in the YUN1242 microbial community within Actinobacteriota (Supplementary Figures S7, S9, S11). Increases in the relative abundances of *Streptomyces* and *Frankiales* were observed beginning at T9 and T12, respectively, with concurrent decreases in the relative abundances of *Nitriliruptorales* (initial relative abundance 37.8%) and *Parviterribacter* (initial relative abundance 4.2%). These results resemble what was previously observed in culturing experiments with AD hyperarid soils (Schulze-Makuch et al., 2018). *Parviterribacter* is reported to have a saprophytic lifestyle based on their preference for complex proteinaceous substrates and glucose as carbon sources observed in the strains isolated from Namibian desert soil (Foesel et al., 2016). Thus, this phylotype may have thrived during more active episodes following precipitation events. Cell death of *Nitriliruptorales* and *Parviterribacter* provides OC for the growth of *Streptomyces* and *Frankiales* during the experiment (Figures 4B, 5A and Supplementary Figure S9B). A recent calculation revealed that soil microbial biomass accounts for more than half the OC in soils from agricultural, grassland, and forest ecosystems (Liang et al., 2019), and it is hypothesized that microbial biomass comprises an even greater percentage of the OC reserves in deserts (Azua-Bustos et al., 2017).

The results suggest a mixotrophic growth strategy for *Streptomyces* and *Frankiales* within this hyperarid microbial community. The cell growth observed (Figure 2) in YUN1242 soils suggests an estimated 13-fold increase in OC content by T6 to T9 [an approximation of the cell OC content was estimated by the reported OC content per cell, 26.02 ± 1.08 fg C $cell^{-1}$ (Troussellier et al., 1997), and the 16S rRNA gene copy numbers determined by qPCR, assuming the occurrence of 4.2 16S rRNA gene copy per cell in all the taxa based on the average number reported (Vetrovsky and Baldrian, 2013; Figures 2, 6)]. The mixotrophy strategy combines heterotrophy (supplied by OC from microbial cell death) and autotrophy (chemolithotrophy, phototrophy) (Stoecker et al., 2017) for carbon acquisition when OC supplies are limited.

Obligate and facultative CO and H_2-supported autotrophic metabolisms have been confirmed in the *Streptomyces* genus (Kim and Goodfellow, 2002). Threshold values of $0.2\,\mu L\,L^{-1}$ of CO were estimated for *S. thermoautotrophicus* growth which is comparable to levels observed in various soils (Gadkari et al., 1990). The appearance of *Streptomyces* at T9 (0 to >30% of relative abundance) (Figures 3B, 5A) was potentially supported by the occurrence of carboxydotrophy/hydrogenotrophy in YUN1242. Reduced growth and cell death of *Nitriliruptorales* probably resulted from exhaustion of intracellular OC reserves and the inability to compete with the (Troussellier et al., 1997) faster growth of *Streptomyces* based on its mixotrophic growth strategy. An H_2-supported growth capacity previously reported for *Frankia* (Sellstedt and Richau, 2013) could also allow this phylotype to contribute to the mixotrophic metabolism of the microbial community, and explain the increase in *Frankia* relative abundance in the YUN1242 wetting experiment.

Nitrate reduction has been suggested as the main source of available N_2 in desert soils (Leon-Sobrino et al., 2019). Several members of the obligate aerobic genus *Streptomyces* can reduce nitrate (Fischer et al., 2014) which could allow *Streptomyces* to couple CO oxidation to nitrate reduction to nitrite (dissimilatory nitrate reduction) or dinitrogen (denitrification) (King and Weber, 2007; He et al., 2021). The capacity of *Frankia* for fixing N_2 suggests a syntrophic association in the proliferation of these two phylotypes. In addition, the Frankia genus demonstrates uptake hydrogenase activity (Tisa et al., 2016) that facilitates the recycling of the H_2 produced by nitrogenase during N_2 fixation, thus improving the efficiency of N_2 fixation (Gtari et al., 2012, 2019). H_2 oxidation provides energy (ATP), reducing equivalents, and removes O_2 which improves nitrogenase activity (Tamagnini et al., 2002). Thus, we propose a syntrophic association between *Streptomyces* growth respiring nitrate and *Frankia* N_2 fixation, and H_2 production.

The Gemmatimonadota and Choroflexota phyla add to the metabolic potential of the YUN1242 microbiome. Gemmatimonadota are associated with multiple assimilative and dissimilative N processes, including the ability to perform the terminal step in denitrification by NO_2 removal (Chee-Sanford et al., 2019). In addition, *Longimicrobiacea* (Gemmatimonadota) is an oligotrophic microorganism capable of storing intracellular polyphosphate granules, a potential phosphorous source for the growing community. This taxon has also been added to the list of bacterial phyla containing anoxygenic phototrophic species (Bull et al., 2018; Koblizek et al., 2020; Mujakic et al., 2021; Zeng et al., 2021). Chloroflexota (Figure 3) includes *Thermobaculum*, a non-phototrophic gram-positive, heterotrophic, thermophile (Botero et al., 2004; Kuhlman et al., 2006; Kiss et al., 2010; Kunisawa, 2011; Gupta et al., 2013). This phylotype has the potential to use CO and H_2 as energy sources for growth based on evidence from one of its closest relatives, *Thermomicrobium roseum*, that can persist mixotrophically on atmospheric gases (Wu et al., 2009; Houghton et al., 2015; Islam et al., 2019). Chloroflexota in general have a wide distribution of enzymes responsible for mixotrophic metabolisms using reduced gasses (Islam et al., 2019) and they have been reported to colonize new soils after volcanic eruptions (Hernandez et al., 2020; Sterling et al., 2022).

Specific metabolic potential of the YUN1609 soil microbiome

The YUN1609 soil microbial community was characterized by significantly lower T0 microbial biomass than YUN1242 (lower total bacterial and archaeal abundance). YUN1609 had a greater and more significant relative abundance of *Gaiellales* relative to YUN1242 (Figures 3B, 4B). From T0 to T15, carbon fixation is suggested to play a relevant role in the microbial community persistence and growth based on the CO_2 fixation capacity predicted by the genome analysis of the *Gaiella occulta* and the growth of marine isolates from this taxon in an inorganic medium (Chen et al., 2021). Nitrate reduction was also evidenced by culturing the type strain (Severino et al., 2019; Chen et al., 2021; Ai et al., 2022). The greater relative abundance of *Gaiellales* in the YUN1609 community relative to YUN1242 could be explained by the low salt tolerance of the type strain *Gaiella occulta* (Albuquerque et al., 2011). YUN1609 soils have a history of lower Cl^- and EC levels than YUN1242.

Furthermore, nitrate reduction was previously predicted for two taxa with higher abundance in YUN1609, the Unclassified Class 0319-7L14 (Zhang et al., 2019) and the Family 67–14 (Kantor et al., 2017). The

Unclassified Class 0319-7L14 isolated from Australian arid soils, was reported in an arid soil ecosystem in China, and in semiarid, unseeded control sites during mine waste revegetation in the US (Shange et al., 2012; Zhang et al., 2019; Ossanna et al., 2023). The Family 67–14 was isolated from a thiocyanate stock bioreactor (Kantor et al., 2017).

After T15, the appearance of new taxa outside Actinobacteriota phylum was observed. These included the Unclassified LiUU-11-161 (Eiler and Bertilsson, 2004) (*Sphingobateriales*/Bacteroidota), *Zoogloeae* (Rossello-Mora et al., 1995), uncultured *Commamonadaceae*, *Rhodoferax* genera (*Burkholderiales*), and *Ferrovibrio* (*Ferrovibrionales*/*Alphaproteobacteria*) (Dahal and Kim, 2018; Figure 3). A simultaneous decrease in *Nitriliruptorales* (Figure 3) relative abundance and in overall estimated viable cell OC was observed.

Rhodoferax and *Zoogloea* genera, are capable of carbon and N_2 fixation, respectively. Anaerobic, photoheterotrophic or photoautotrophic (using H_2 or reduced sulfur compounds [RSC]), aerobic heterotrophic, anaerobic fermenter, N_2 fixation (Willems, 2013), iron-reducing and microaerobic Fe(II) oxidation (Kato and Ohkuma, 2021) metabolisms, have been evidenced in *Rhodoferax* genus (Comamonadaceae/Burkholderiales). Capacity for nitrate reduction and N_2 fixation was reported in *Zoogloea* genus from *Rhodocyclaceae* family (Dahal et al., 2020). In addition, *Zoogloea* sp. N299 was described as an aerobic oligotrophic denitrifier isolated from autotrophic nitrate removal reactors (Huang et al., 2015). Nitrate reduction was reported as well in *Ferrovibrio* genus (Dahal and Kim, 2018). Furthermore, a key role in reductive sulfate assimilation and cycling has been also suggested for *Burkholderiales* in soil desert environments (Leon-Sobrino et al., 2019).

We argue that the proposed low level of carbon fixation activity sustained during the first 15 days of the experiment by *Gaillales* and *Rubrobacter* provided carbon reserves for the increase in the relative abundance of new taxa at the end of the experiment (*Nocardiodaceae*, *Zoogloea*, *Rhodoferax and Ferrivibionales*). The decrease in *Nitriliruptoraceae* provided potential OC reserves as explained for YUN1242. The new phylotypes increased the proposed functional capacity of this microbiome for nitrate reduction in aerobic/microaerobic conditions, nitrogen fixation, and iron oxidation/reduction. These slow-growing oligotrophic microorganisms that can use inorganic sources of energy appear to be able to compete for the scarce OC at the end of the experiment. However, the proposed mixotrophic metabolic capacity that evolved in the YUN1242 microbiome in response to soil wetting was not observed in this community. We maintain that the 4-fold lower microbial biomass content as estimated by 16S rRNA gene copy number at T0 may explain this difference in metabolic capacity.

It is important to note that some potential conclusions from this research were limited by the difficulties in obtaining sufficient DNA from all replicates at each time point and the significant differences observed between replicates at a few time points. The variation observed between replicate flasks could be explained by the occurrence of isolated assemblages in the hyperarid environments (Neilson et al., 2012) which were probably due to the restricted motility expected for microorganisms in soils of low a_w (Kim and Goodfellow, 2002; Jones et al., 2018). The results obtained from this research will guide future experiments to characterize the distinct metabolic capacities of these two communities.

Conclusion

The erratic precipitation events that control the metabolic activity of desert soil microbiomes are extremely rare in the core region of the AD. The results from this controlled, temporal analysis demonstrated the presence of viable cells in AD hyperarid soils with sufficient resources to support growth following a precipitation event despite such extended periods of desiccation. Thirty-day changes in the bacterial community composition of the studied sites revealed two distinct predicted strategies for survival. Initial bacterial and archaeal abundance and their associated nutrient reserves were significantly greater in the YUN1242 community. The YUN1242 microbiome evolved quickly from a community dominated by taxa that can accumulate resources to survive (*Nitriliruptoraceae*, *Parviterribacter*, and *Rubrobacter*) to one dominated by spore-forming, mixotrophic taxa able to use microbial biomass, and atmospheric gases to fix CO_2, and N_2, with O_2 and nitrate used as electron acceptors. In contrast, slow biomass accumulation of facultative autotrophic taxa characterized growth in the drier YUN1609 community. The proposed syntrophic association between Streptomyces growth respiring nitrate and Frankia N_2 fixation, and H_2 production in the YUN1242 suggests a capacity for critical microbe-microbe associations in this soil microbiome following a rainfall event. The results indicate that slight differences in available moisture for extreme hyperarid soil microbial communities can have significant impacts on community composition, functional potential, and responses to soil wetting. The microbial profiles and proposed metabolic strategies, including microbial interactions, defined by this study can be used as long-term biomarkers of hyperaridity, potential biosignature distribution on other planets, and for bioprospecting novel biological capacities.

Materials and methods

Sample collection

We studied previously characterized surface soils of a hyperarid region in the AD (Neilson et al., 2017). Hyperarid sites YUN1242 and YUN1609 were selected from five previously characterized hyperarid sites along the transect due to their distinct microbial communities. YUN1242 and YUN1609 had average soil relative humidity values of 20.9 and 17.2%, respectively. YUN1242 is located close to the coast with exposure to coastal fogs, whereas YUN1609 is over 90 km further inland beyond the coastal fog zone. Further, distinct microbial communities were observed at the two sites in samples collected in 2012 (Neilson et al., 2017). For example, Pseudonocardiaceae (20% relative abundance) and Euzebya (11%) comprised 33% relative abundance of the YUN1242 bacterial/archaeal community, whereas the relative abundances of these taxa in YUN1609 soils were just 0.2 and 0.3%, respectively. In contrast, the YUN1609 soils were dominated by Acidimicrobiales_koll13 (45% relative abundance) and Gaiellaceae (11%); two taxa with relative abundances of just 5 and 1% in the YUN1242 community.

The samples YUN1242, and YUN1609 were collected from the west–east southern Yungay (YUN) transect, on 25th January 2017 (Figure 1). Global Positioning System (Garmin GPSMAP 60CSX) coordinates, and elevations for all sites are listed in Table 1. Using a thermo-hygrometer (Hanna Instruments Inc., United States),

temperature and relative humidity parameters for each site were determined from a 50 cm deep soil pit. UVA, UVB, and UVC irradiances and photosynthetic active radiation (PAR) were measured with a portable photo-radiometer HD2302.0 (Delta OHM, Italy). In addition, three soil samples were collected, using sterilized instruments, from three different sidewalls at a 10–20 cm depth of each pit and stored in sterile transparent reclosable bags. The bags were sealed with tape, kept in a cooler and transported immediately to the lab (less than 100 km away from the site), and stored at environmental temperature (~20°C).

Soil analysis

The bags were unsealed in the lab and gravimetric moisture content was immediately measured. Moisture contents were determined in triplicate for each site. The soil sample (10 g) was added to a glass petri dish, incubated at 105°C for 24 h, and weighed after the dish was cooled down for 2 h. The procedure was repeated to obtain a constant result (<0.1%) between two successive weights (Blaska and Fisher, 2014). Soil pH, electrical conductivity (EC), and redox potential (ORP) were determined in a 1:1 slurry of 2 mm-sieved soil in distilled water after 1 h of shaking followed by 1 h of rest by using a Hanna HI 9829 multiparameter as described before (Neilson et al., 2017).

Wetting experiments

Immediately after having the result of the GWC of the samples (5 days after sampling), we started the experiment to determine the potential effects of wetting on both soil microbial communities. We sieved (<2 mm) 50 g of every soil sample, which were then added to sterile 250 mL flasks (Supplementary Figure S3). This procedure was repeated for each of the three soil samples collected from each site. Sterile water was introduced directly to the soil surface of the flasks until it reached 5% of moisture to simulate desert rainfall. The 5% moisture level was selected based on records of gravimetric moisture contents from desert soils following rainfall events and confirmed by samples collected from the two sample sites following the June 2017 rainfall event (Table 1). June 2017 moisture contents were 4.196 and 6.150% for sites YUN1242 and YUN1609, respectively. Afterwards, flasks were sealed with hydrophobic cotton and incubated for 30 days at 20°C under light-oxic conditions. The moisture was controlled by the measurements of weight difference at regular intervals throughout the experiment to maintain a 5% GWC considering the water retention observed in soils after rain events (Table 1; Pfeiffer et al., 2021).

Subsamples were retrieved from every flask on days 0, 3, 6, 9, 12, 15, and 30 of incubation and DNA was immediately extracted from 2 g of wet-weight soil from each sample, including a blank tube with the DNA-free reagents used, according to FastDNA SPIN kit for soil method (MPbio, United States). We quantified the DNA with a Fluorimeter (Quantus, Promega, United States), and the DNA integrity was measured by a Nanodrop NP1000 spectrophotometer (NanoDrop Technologies, United States) labeling the ratio of DNA/RNA 260/230 and the ratio of DNA/protein 260/280. The obtained concentration of all the subsamples ranged from 18 to 900 ng of DNA g-1 dry soil (Supplementary Figure S4). The extract concentration was less than 0.5 ng μL^{-1} in the control tests. Most of the extracted DNA showed acceptable quality (0.9–2.0 A 260/280).

qPCR analysis

The abundance of Bacteria and Archaea was quantified in duplicate by quantitative-polymerase chain reaction (qPCR) using Bacteria (UniBactF336: GACTCCTACGGGAGGCAGCA, UniBactR937: TTGTGCGGGCCCCCGTCAAT) and Archaea universal primers for 16S rRNA gene (ARC344F: ACGG GGNGCANCAGGCG, ARC915R: TGCTCCCCCGCCAATTCC) (Demergasso et al., 2010). The correlation coefficient for the standard curves was 0.99 and the PCR efficiency was on average 93%. In each periodic DNA extraction, control was also performed from the Kit reagents. A Rotor-Gene Q Real-Time Cycler (Qiagen, United States) was used for qPCR reactions and the data was processed using its software. Each reaction was 10 µL in volume and contained the following mixture: 5 µL of SensiMix SYBR No-Rox Kit (Bioline, United Kingdom), 2 µL nuclease-free water, 1 µL of the corresponding oligonucleotide primer (0.5 µM), and 1 µL of the template. The bacterial amplification program consisted of 40 cycles of 95°C for 30 s, 65°C for 30 s, and 72°C for 20 s while the archaeal program consisted of 40 cycles of 95°C for 40 s, 65°C for 40 s, and 72°C for 20 s. 16S rRNA gene copy number per g of each subsample was determined, as reported previously (Remonsellez et al., 2009), using the equation:

$$copies\ /\ g = \left(\left(copies\ /\ \mu l\right) * 100 * dilution\right) /\ g\ of\ \ initial\ wet\ weight$$

In addition, DNA was used for high-throughput sequencing.

That number of copies was considered equivalent to 4.2 times the number of cells [assuming 4.2 16S rRNA gene copies per cell (Vetrovsky and Baldrian, 2013) and was used for estimating the specific cell number of each taxon (taxon relative abundance [%] * total bacterial cell numbers), and the total and specific microbial OC (total bacterial + archaeal cell numbers * OC content per cell, and specific cell numbers * OC content per cell, respectively)]. We used 26.02 ± 1.08 fg C as the OC content per cell (Troussellier et al., 1997).

16S rRNA sequencing

Sequencing was performed with 42 subsamples (triplicates of the 7 time points during incubation of both soil pits) and 7 blanks (DNA extraction reagents) as well as 6 controls (sequencing reagents) according to the following procedure. The hypervariable V4 region of the 16S rRNA gene was amplified from each sample using unique for each sample barcoded reverse primers (806R: GTGYC AGCMGCCGCGGTAA) and a common forward primer (515F: GGACTACNVGGGTWTCTAAT). Both the reverse and the forward primers were extended with the sequencing primer pads, linkers, and Illumina adapters (Caporaso et al., 2012). The PCR was performed using MyFi™ Mix (Bioline Meridian, Cat. No. BIO-25050) on LightCycler 96 (Roche) in the final volume of 40 µL. Amplicons were quantified using the Quant-It PicoGreen dsDNA Assay kit (ThermoFisher Scientific, Cat. No. P7589), according to the manufacturer's protocol. Equal amounts of amplified DNA (120 ng) from each sample were pooled into a sequencing library followed by removing DNA fragments smaller than 120 bp (unused primers and dimer primers) with UltraClean PCR Clean-Up Kit (MoBio, Cat. No.

12500). The final amplicon concentration was quantified by qPCR with KAPA Library Quantification Kit for Illumina Platforms (KAPA Biosystems, Cat. No. KK4854) in the presence of the set of six DNA standards (KAPA Biosystems, Cat. No. KK4905). Subsequently, the library was diluted to a concentration of 4 nM, and denatured with 0.1 N NaOH. The library was sequenced at the Microbiome Core at the Steele Children's Research Center, University of Arizona, using the MiSeq platform (Illumina) and custom primers (Caporaso et al., 2012). Due to the limited sequence diversity among 16S rRNA amplicons, 5% of the PhiX Sequencing Control V3 (Illumina, Cat. No. FC-110-3001) was used to spike the library to increase diversity. The raw sequencing data were demultiplexed and barcodes trimmed using *idemp* script.[1]

The accuracy of microbial community surveys based on universal marker genes suffers from the presence of contaminant DNA sequences not truly present in the sample that can come from various sources, including reagents. Contaminant ASVs were identified using a nested-PCR approach as described in the Supplementary Information Box 1. Low levels of contaminant sequences from 2 to 113 ASV counts per sample were detected which represented an average of less than 1% of abundance in target samples (Supplementary Information Box 1).

Taxonomic and phylogenetic analysis

Demultiplexed fastq files were received and subjected to primer removal, filtered by sequence quality (for keeping Ph quality over 30, so paired reads are formed with 253 bp), denoised, merged, and chimaera removal using the DADA2 pipeline (Callahan et al., 2016). All filtered-merged sequences were assigned to amplicon sequence variants (ASV) by the DADA2 pipeline. The representative reads were mapped to the SILVA database (release 138) (Quast et al., 2013). Then we used the Phyloseq (version 1.42.0) pipeline to (a) eliminate taxa with one read, (b) remove taxa with less than 0.005% mean relative abundance across all read counts, (c) eliminate samples having less than 1,000 reads, and (d) remove the 14 bacterial sequences (n° of ASV 9, 20, 23, 19, 2, 18, 38, 29, 57, 58, 69, 72, 167, and 178) found in controls and blanks having less than, on average, 1% of abundance in targeted samples (Supplementary Data Box 1). We detected from 1,075 to 37,811 reads per sample for YUN1242 and 132 to 21,505 reads per sample for YUN1609 (Supplementary Table S3). We calculated histograms and rarefactions curves to standardize the sequence number using the rarefy_even_depth function from the Phyloseq package to standardize the sequence number. Most sequences were distributed around 1,500–5,000 reads counts (Supplementary Figure S12A) and we proceeded to rarefy the data to the smaller sample size of 1,500 reads (Supplementary Figure S12B). Finally, the read number by sequence, taxonomy table, and categorical variables (called sites, replicates, and days) associated with the samples were integrated and kept in a Primer-7 software package [Plymouth Marine Laboratory, Plymouth, United Kingdom (Clarke and Gorley, 2015)]. The ASV diagram was made using the website[2] previously described (Oliveros, 2007–2015).

The diversity (Shannon, H′), and richness (Margalef) indices were also calculated using the measures included in the PRIMER-7 software package based on the relatedness of the species within a sample.

Statistical analysis

Soil bacterial and archaeal total abundance (copies·g^{-1} of soil) were modeled as a function of the sampling site (YUN1242 and YUN1609) and incubation time (T0, T3, T6, T9, T12, T15, and T30) to determine significant differences between the levels of these factors (Supplementary Table S7). Modeling was carried out by using two-way repeated measures ANOVA. A log 10 transformation was used to meet ANOVA's assumptions. In the multiple testing, value of p correction via the Benjamini–Hochberg false discovery rate (FDR) was performed. Model fitting and pairwise multiple comparisons were performed using the statistical software R 3.6.0. (R Core Team, 2018) and car, tidyverse and rstatix packages.

In order to compare Shannon and Margalef indices between both samples (including all the subsamples obtained from a single site during the incubation time in one group), a box plot was created, and a t-test was applied using KaleidaGraph version 4.5.4 for Windows, Synergy Software, Reading, PA, United States.[3] Simple linear regression was used to fit the Margalef index distribution among incubation days for both samples (confidence bands were also calculated). Multiple linear regression was used to assess the difference in the slopes throughout an interaction term. The abundance of Amplicon Sequence Variances (ASVs) in different samples and at incubation time (days) was analyzed using Primer-7 (Primer -E) software (Clarke and Gorley, 2015). We used the fourth root transformation to homogenize the amounts of ASVs and thus reduce the dominance effect. A similarity matrix (resemblance) was constructed using the Bray-Curtis method (Bray and Curtis, 1957) included in Primer V7 software (Clarke and Gorley, 2015). We used non-metric multidimensional scaling (NMDS), included in Primer-7, to build a restricted arrangement of the ASVs or groups of other taxonomic levels based on the experiment design: (i) phylum abundance data; (ii) abundance of actinobacterial orders; (iii) microbial genera abundance data, overlaid with the segmented bubble plot (Clarke and Gorley, 2015) showing the percentage contribution of selected genera.

We performed a significance test using the permutational multivariate analysis of variance (PERMANOVA function) (Anderson, 2001) when Bray Curtis dissimilarity was tested with 10,000 permutations. Two factors were evaluated: Site (YUN1242 and YUN1609) and incubation time (0, 3, 6, 9, 12, 15, 30 days).

In addition, we analyzed the dynamics of the relative abundance of specific taxa during the wetting experiment. We performed one-way ANOVAs to evaluate the significance of the changes regarding the three identified factors, incubation time, sites, and replicates (flasks).

1 https://github.com/yhwu/idemp

2 https://bioinfogp.cnb.csic.es/tools/venny/

3 www.synergy.com

Data availability statement

The raw sequence data presented in the study are deposited in the DNA Data Bank of Japan (DDBJ) repository, accession numbers DRR465014 to DRR465087.

Author contributions

CD supervised the project and wrote the manuscript, aided by JN and CT-C. CD and JN conceived and designed the experiments. CD and CT-C carried out the field trips. Under the supervision of CD, CT-C sampled and monitored the wetting experiments, extracted DNA, and quantified the microbial abundance by qPCR. DA and CD did the statistical analysis of qPCR determination, aided by CT-C. DL did the sequencing. RV and CT-C performed the taxonomic and phylogenetic analyses. DA and CD did the statistical analysis of microbial diversity. All authors contributed to the review, editing, and revision of the article.

Funding

This research was partially supported by funding from BHP Minerals Americas Project 32002137 (2016-2020), and by the ANID Fondecyt Project N° 1231507. CT-C was supported by the ANID National Doctoral scholarship 21181422. The amplicon sequencing was paid for by the US National Institute of Environmental Health Sciences (NIEHS) grant P42ES004940.

Acknowledgments

We thank Daniel Laubitz of the Microbiome Core at the Steele Children's Research Center, University of Arizona for adaptations of the amplicon sequencing library preparation protocol to maximize the sequencing potential of the low DNA samples from the Atacama Desert.

Conflict of interest

The authors declare that the research was conducted in the absence of any commercial or financial relationships that could be construed as a potential conflict of interest.

Publisher's note

Supplementary material

The Supplementary material for this article can be found online at: https://www.frontiersin.org/articles/10.3389/fmicb.2023.1202266/full#supplementary-material

References

Ai, J., Guo, J. N., Li, Y. C., Zhong, X., Lv, Y., Li, J., et al. (2022). The diversity of microbes and prediction of their functions in karst caves under the influence of human tourism activities-a case study of Zhijin Cave in Southwest China. *Environ. Sci. Pollut. Res.* 29, 25858–25868. doi: 10.1007/s11356-021-17783-x

Albuquerque, L., Franca, L., Rainey, F. A., Schumann, P., Nobre, M. F., and da Costa, M. S. (2011). *Gaiella occulta* gen. nov., sp. nov., a novel representative of a deep branching phylogenetic lineage within the class Actinobacteria and proposal of Gaiellaceae fam. nov. and Gaiellales ord. nov. *Syst. Appl. Microbiol.* 34, 595–599. doi: 10.1016/j.syapm.2011.07.001

Amundson, R., Ewing, S. A., Michalski, G., Thiemens, M., Kendall, C., Nishiizumi, K., et al. (2007). The climatic and biotic thresholds on soil elemental cycling along an and to hyperarid rainfall gradient. *Geochim. Cosmochim. Acta* 71:A22.

Anderson, M. J. (2001). A new method for non-parametric multivariate analysis of variance. *Austral Ecol.* 26, 32–46. doi: 10.1111/j.1442-9993.2001.01070.pp.x

Angel, R., and Conrad, R. (2013). Elucidating the microbial resuscitation cascade in biological soil crusts following a simulated rain event. *Environ. Microbiol.* 15, 2799–2815. doi: 10.1111/1462-2920.12140

Azua-Bustos, A., Gonzalez-Silva, C., and Corsini, G. (2017). The hyperarid core of the Atacama Desert, an extremely dry and carbon deprived habitat of potential interest for the field of carbon science. *Front. Microbiol.* 8:993. doi: 10.3389/fmicb.2017.00993

Bar-On, Y. M., Phillips, R., and Milo, R. (2018). The biomass distribution on earth. *Proc. Natl. Acad. Sci.* 115, 6506–6511. doi: 10.1073/pnas.1711842115

Bartelme, R. P., Custer, J. M., Dupont, C. L., Espinoza, J. L., Torralba, M., Khalili, B., et al. (2020). Influence of substrate concentration on the culturability of heterotrophic soil microbes isolated by high-throughput dilution-to-extinction cultivation. *Msphere* 5:e00024-20. doi: 10.1128/mSphere.00024-20

Baubin, C., Ran, N., Siebner, H., and Gillor, O. (2022). Divergence of biocrust active bacterial communities in the Negev Desert during a hydration-desiccation cycle. *Microb. Ecol.* 86, 474–484. doi: 10.1007/s00248-022-02063-z

Blaska, P., and Fisher, Z. (2014). Moisture, water holding, drying and wetting in forest soils. *Open J. Soil Sci.* 4, 174–184. doi: 10.4236/ojss.2014.45021

Bosch, J., Marais, E., Maggs-Kölling, G., Ramond, J., Lebre, P. H., Eckardt, F., et al. (2022). Water inputs across the Namib Desert: implications for dryland edaphic microbiology. *Front. Biogeogr.* 14:2. doi: 10.21425/F5FBG55302

Botero, L. M., Brown, K. B., Brumefield, S., Burr, M., Castenholz, R. W., Young, M., et al. (2004). Thermobaculum terrenum gen. nov., sp nov.: a non-phototrophic gram-positive thermophile representing an environmental clone group related to the Chloroflexi (green non-sulfur bacteria) and Thermomicrobia. *Arch. Microbiol.* 181, 269–277. doi: 10.1007/s00203-004-0647-7

Bray, J., and Curtis, J. (1957). An ordination of the upland forest communities of Southern Wisconsin. *Ecol. Monogr.* 27, 325–349. doi: 10.2307/1942268

Bull, A. T., Andrews, B. A., Dorador, C., and Goodfellow, M. (2018). Special issue on microbiology of the Atacama Desert preface. *Anton. Leeuw. Int. J. Gen. Mol. Microbiol.* 111:1267. doi: 10.1007/s10482-018-1109-6

Cabrol, N. A., Wettergreen, D., Warren-Rhodes, K., Grin, E. A., Moersch, J., Chong Diaz, G., et al. (2007). Life in the Atacama: searching for life with rovers (science overview). *J. Geophys. Res. Biogeosci.* 112:G04S02. doi: 10.1029/2006jg000298

Callahan, B. J., McMurdie, P. J., Rosen, M. J., Han, A. W., Johnson, A. J. A., and Holmes, S. P. (2016). DADA2: high-resolution sample inference from Illumina amplicon data. *Nat. Methods* 13, 581–583. doi: 10.1038/Nmeth.3869

Caporaso, J. G., Lauber, C. L., Walters, W. A., Berg-Lyons, D., Huntley, J., Fierer, N., et al. (2012). Ultra-high-throughput microbial community analysis on the Illumina HiSeq and MiSeq platforms. *ISME J* 6, 1621–1624. doi: 10.1038/ismej.2012.8

Certini, G., Scalenghe, R., and Amundson, R. (2009). A view of extraterrestrial soils. *Eur. J. Soil Sci.* 60, 1078–1092. doi: 10.1111/j.1365-2389.2009.01173.x

Certini, G., and Ugolini, F. C. (2013). An updated, expanded, universal definition of soil. *Geoderma* 192, 378–379. doi: 10.1016/j.geoderma.2012.07.008

Chee-Sanford, J., Tian, D., and Sanford, R. (2019). Consumption of N2O and other N-cycle intermediates by *Gemmatimonas aurantiaca* strain T-27. *Microbiology Sgm* 165, 1345–1354. doi: 10.1099/mic.0.000847

Chen, R. W., He, Y. Q., Cui, L. Q., Li, C., Shi, S. B., Long, L. J., et al. (2021). Diversity and distribution of uncultured and cultured gaiellales and rubrobacterales in South China Sea Sediments. *Front. Microbiol.* 12:657072. doi: 10.3389/fmicb.2021.657072

Chen, D. D., Tian, Y., Jiao, J. Y., Zhang, X. T., Zhang, Y. G., Dong, Z. Y., et al. (2020). Comparative genomics analysis of Nitriliruptoria reveals the genomic differences and salt adaptation strategies. *Extremophiles* 24, 249–264. doi: 10.1007/s00792-019-01150-3

Chong-Diaz, G., Demergasso, C., Meza, J. U., and Vargas, M. (2020). The saline domain of northern Chile and its industrial mineral deposits. *Boletin De La Sociedad Geologica Mexicana* 72:A020720. doi: 10.18268/BSGM2020v72n3a020720

Clarke, K.R., and Gorley, R.N. (2015). *PRIMER v7: User Manual/Tutorial*. PRIMER-E: Plymouth.

Connon, S. A., Lester, E. D., Shafaat, H. S., Obenhuber, D. C., and Ponce, A. (2007). Bacterial diversity in hyperarid Atacama Desert soils. *J. Geophys. Res.* 112:G04S17. doi: 10.1029/2006JG000311

Crits-Christoph, A., Robinson, C. K., Barnum, T., Fricke, W. F., Davila, A. F., Jedynak, B., et al. (2013). Colonization patterns of soil microbial communities in the Atacama Desert. *Microbiome* 1:28. doi: 10.1186/2049-2618-1-28

Dahal, R. H., Chaudhary, D. K., Kim, D. U., and Kim, J. (2020). Zoogloea dura sp. nov., a N-2-fixing bacterium isolated from forest soil and emendation of the genus Zoogloea and the species Zoogloea oryzae and *Zoogloea ramigera*. *Int. J. Syst. Evol. Microbiol.* 70, 5312–5318. doi: 10.1099/ijsem.0.004416

Dahal, R. H., and Kim, J. (2018). Ferrovibrio soli sp. nov., a novel cellulolytic bacterium isolated from stream bank soil. *Int. J. Syst. Evol. Microbiol.* 68, 427–431. doi: 10.1099/ijsem.0.002527

Davila, A., Hawes, I., Ascaso, C., and Wierzchos, J. (2013). Salt deliquescence drives photosynthesis in the hyperarid Atacama Desert. *Environ. Microbiol. Rep.* 5, 583–587. doi: 10.1111/1758-2229.12050

Demergasso, C., Galleguillos, F., Soto, P., Serón, M., and Iturriaga, V. (2010). Microbial succession during a heap bioleaching cycle of low grade copper sulfides: does this knowledge mean a real input for industrial process design and control? *Hydrometallurgy* 104, 382–390. doi: 10.1016/j.hydromet.2010.04.016

Drees, K. P., Neilson, J. W., Betancourt, J. L., Quade, J., Henderson, D. A., Pryor, B. M., et al. (2006). Bacterial community structure in the hyperarid core of the Atacama Desert, Chile. *Appl. Environ. Microbiol.* 72, 7902–7908. doi: 10.1128/AEM.01305-06

Eiler, A., and Bertilsson, S. (2004). Composition of freshwater bacterial communities associated with cyanobacterial blooms in four Swedish lakes. *Environ. Microbiol.* 6, 1228–1243. doi: 10.1111/j.1462-2920.2004.00657.x

Ericksen, G. (1981). Geology and origin of the Chilean nitrate deposits. Geological Survey Professional Paper. (Washington: Geological Survey and Instituto de Investigaciones Geológicas de Chile).

Fischer, M., Falke, D., Pawlik, T., and Sawers, R. G. (2014). Oxygen-dependent control of respiratory nitrate reduction in mycelium of *Streptomyces coelicolor* A3(2). *J. Bacteriol.* 196, 4152–4162. doi: 10.1128/jb.02202-14

Fletcher, L. E., Conley, C. A., Valdivia-Silva, J. E., Perez-Montano, S., Condori-Apaza, R., Kovacs, G. T. A., et al. (2011). Determination of low bacterial concentrations in hyperarid Atacama soils: comparison of biochemical and microscopy methods with real-time quantitative PCR. *Can. J. Microbiol.* 57, 953–963. doi: 10.1139/w11-091

Foesel, B. U., Geppert, A., Rohde, M., and Overmann, J. (2016). Parviterribacter kavangonensis gen. nov., sp. nov. and Parviterribacter multiflagellatus sp. nov., novel members of Parviterribacteraceae fam. nov. within the order Solirubrobacterales, and emended descriptions of the classes Thermoleophilia and Rubrobacteria and their orders and families. *Int. J. Syst. Evol. Microbiol.* 66, 652–665. doi: 10.1099/ijsem.0.000770

Gadkari, D., Schricker, K., Acker, G., Kroppenstedt, R. M., and Meyer, O. (1990). *Streptomyces thermoautotrophicus* sp. nov., a thermophilic CO- and H(2)-oxidizing obligate chemolithoautotroph. *Appl. Environ. Microbiol.* 56, 3727–3734. doi: 10.1128/aem.56.12.3727-3734.1990

Gtari, M., Ghodhbane-Gtari, F., Nouioui, I., Beauchemin, N., and Tisa, L. S. (2012). Phylogenetic perspectives of nitrogen-fixing actinobacteria. *Arch. Microbiol.* 194, 3–11. doi: 10.1007/s00203-011-0733-6

Gtari, M., Nouioui, I., Sarkar, I., Ghodhbane-Gtari, F., Tisa, L. S., Sen, A., et al. (2019). An update on the taxonomy of the genus Frankia Brunchorst, 1886, 174(AL). *Anton. Leeuw. Int. J. Gen. Mol. Microbiol.* 112, 5–21. doi: 10.1007/s10482-018-1165-y

Gupta, R. S., Chander, P., and George, S. (2013). Phylogenetic framework and molecular signatures for the class Chloroflexi and its different clades; proposal for division of the class Chloroflexi class. nov into the suborder Chloroflexineae subord. nov., consisting of the emended family Oscillochloridaceae and the family Chloroflexaceae fam. nov., and the suborder Roseiflexineae subord. nov., containing the family Roseiflexaceae fam. nov. *Antonie Van Leeuwenhoek* 103, 99–119. doi: 10.1007/s10482-012-9790-3

Hall, S. J., Silver, W. L., and Amundson, R. (2012). Greenhouse gas fluxes from Atacama Desert soils: a test of biogeochemical potential at the Earth's arid extreme. *Biogeochemistry* 111, 303–315. doi: 10.1007/s10533-011-9650-7

Hartley, A. J., and Chong, G. (2002). Late Pliocene age for the Atacama Desert: implications for the desertification of western South America. *Geology* 30, 43–46. doi: 10.1130/0091-7613(2002)030<0043:Lpafta>2.0.Co;2

He, T., Wu, Q., Ding, C., Chen, M., and Zhang, M. (2021). Hydroxylamine and nitrite are removed effectively by *Streptomyces mediolani* strain EM-B2. *Ecotoxicol. Environ. Saf.* 224:112693. doi: 10.1016/j.ecoenv.2021.112693

Hernandez, M., Vera-Gargallo, B., Calabi-Floody, M., King, G. M., Conrad, R., and Tebbe, C. C. (2020). Reconstructing genomes of carbon monoxide oxidisers in volcanic deposits including members of the class ktedonobacteria, 1880. *Microorganisms* 8. doi: 10.3390/microorganisms8121880

Hock, A. N., Cabrol, N. A., Dohm, J. M., Piatek, J., Warren-Rhodes, K., Weinstein, S., et al. (2007). Life in the Atacama: a scoring system for habitability and the robotic exploration for life. *J. Geophys. Res. Biogeo.* 112:G04S08. doi: 10.1029/2006JG000321

Houghton, K. M., Morgan, X. C., Lagutin, K., MacKenzie, A. D., Vyssotskii, M., Mitchell, K. A., et al. (2015). Thermorudis pharmacophila sp nov., a novel member of the class Thermomicrobia isolated from geothermal soil, and emended descriptions of *Thermomicrobium roseum*, Thermomicrobium carboxidum, Thermorudis peleae and *Sphaerobacter thermophilus*. *Int. J. Syst. Evol. Microbiol.* 65, 4479–4487. doi: 10.1099/ijsem.0.000598

Huang, T. L., Zhou, S. L., Zhang, H. H., Bai, S. Y., He, X. X., and Yang, X. (2015). Nitrogen removal characteristics of a newly isolated indigenous aerobic denitrifier from oligotrophic drinking water reservoir, Zoogloea sp. N299. *Int. J. Mol. Sci.* 16, 10038–10060. doi: 10.3390/ijms160510038

Huxman, T. E., Smith, M. D., Fay, P. A., Knapp, A. K., Shaw, M. R., Loik, M. E., et al. (2004). Convergence across biomes to a common rain-use efficiency. *Nature.* 429, 651–654. doi: 10.1038/nature02561

Islam, Z. F., Cordero, P. R. F., Feng, J., Chen, Y. J., Bay, S. K., Jirapanjawat, T., et al. (2019). Two Chloroflexi classes independently evolved the ability to persist on atmospheric hydrogen and carbon monoxide. *ISME J.* 13, 1801–1813. doi: 10.1038/s41396-019-0393-0

Jansson, J. K., and Hofmockel, K. S. (2020). Soil microbiomes and climate change. *Nat. Rev. Microbiol.* 18, 35–46. doi: 10.1038/s41579-019-0265-7

Jones, D. L., Olivera-Ardid, S., Klumpp, E., Knief, C., Huil, P. W., Lehndorff, E., et al. (2018). Moisture activation and carbon use efficiency of soil microbial communities along an aridity gradient in the Atacama Desert. *Soil Biol. Biochem.* 117, 68–71. doi: 10.1016/j.soilbio.2017.10.026

Jordaan, K., Lappan, R., Dong, X. Y., Aitkenhead, I. J., Bay, S. K., Chiri, E., et al. (2020). Hydrogen-oxidizing bacteria are abundant in desert soils and strongly stimulated by hydration. *Msystems* 5:e01131-20. doi: 10.1128/mSystems.01131-20

Kantor, R. S., Huddy, R. J., Iyer, R., Thomas, B. C., Brown, C. T., Anantharaman, K., et al. (2017). Genome-resolved meta-omics ties microbial dynamics to process performance in biotechnology for thiocyanate degradation. *Environ. Sci. Technol.* 51, 2944–2953. doi: 10.1021/acs.est.6b04477

Kato, S., and Ohkuma, M. (2021). A single bacterium capable of oxidation and reduction of iron at circumneutral pH. *Microbiol. Spectr.* 9:e0016121. doi: 10.1128/Spectrum.00161-21

Kim, S. B., and Goodfellow, M. (2002). Streptomyces thermospinisporus sp. nov., a moderately thermophilic carboxydotrophic streptomycete isolated from soil. *Int. J. Syst. Evol. Microbiol.* 52, 1225–1228. doi: 10.1099/00207713-52-4-1225

King, G. M., and Weber, C. F. (2007). Distribution, diversity and ecology of aerobic CO-oxidizing bacteria. *Nat. Rev. Microbiol.* 5, 107–118. doi: 10.1038/nrmicro1595

Kiss, H., Cleland, D., Lapidus, A., Lucas, S., Del Rio, T. G., Nolan, M., et al. (2010). Complete genome sequence of "Thermobaculum terrenum' type strain (YNP1(T)). *Stand. Genomic Sci.* 3, 153–162. doi: 10.4056/sigs.1153107

Koblizek, M., Dachev, M., Bina, D., Nupur, , Piwosz, K., and Kaftan, D. (2020). Utilization of light energy in phototrophic Gemmatimonadetes. *J. Photochem. Photobiol. B* 213:112085. doi: 10.1016/j.jphotobiol.2020.112085

Kourilova, X., Schwarzerova, J., Pernicova, I., Sedlar, K., Mrazova, K., Krzyzanek, V., et al. (2021). The first insight into polyhydroxyalkanoates accumulation in multi-extremophilic Rubrobacter xylanophilus and Rubrobacter spartanus. *Microorganisms* 9:909. doi: 10.3390/microorganisms9050909

Kuhlman, K. R., Fusco, W. G., La Duc, M. T., Allenbach, L. B., Ball, C. L., Kuhlman, G. M., et al. (2006). Diversity of microorganisms within rock varnish in the Whipple Mountains, California. *Appl. Environ. Microbiol.* 72, 1708–1715. doi: 10.1128/AEM.72.2.1708-1715.2006

Kunisawa, T. (2011). The phylogenetic placement of the non-phototrophic, gram-positive thermophile "Thermobaculum terrenum' and branching orders within the phylum 'Chloroflexi' inferred from gene order comparisons. *Int. J. Syst. Evol. Microbiol.* 61, 1944–1953. doi: 10.1099/ijs.0.026088-0

Lee, C. J. D., McMullan, P. E., O'Kane, C. J., Stevenson, A., Santos, I. C., Roy, C., et al. (2018). NaCl-saturated brines are thermodynamically moderate, rather than extreme, microbial habitats. *FEMS Microbiol. Rev.* 42, 672–693. doi: 10.1093/femsre/fuy026

Leon-Sobrino, C., Ramond, J. B., Maggs-Kolling, G., and Cowan, D. A. (2019). Nutrient acquisition, rather than stress response over diel cycles, drives microbial transcription in a hyper-arid Namib Desert soil. *Front. Microbiol.* 10:1054. doi: 10.3389/fmicb.2019.01054

Leung, P. M., Bay, S. K., Meier, D. V., Chiri, E., Cowan, D. A., Gillor, O., et al. (2020). Energetic basis of microbial growth and persistence in desert ecosystems. *Msystems* 5:e00495-19. doi: 10.1128/mSystems.00495-19

Liang, C., Amelung, W., Lehmann, J., and Kastner, M. (2019). Quantitative assessment of microbial necromass contribution to soil organic matter. *Glob. Chang. Biol.* 25, 3578–3590. doi: 10.1111/gcb.14781

Maier, R. M., Drees, K. P., Neilson, J. W., Henderson, D. A., Quade, J., Betancourt, J. L., et al. (2004). Microbial life in the Atacama Desert. *Science* 306, 1289–1290. doi: 10.1126/science.306.5700.1289c

Makhalanyane, T. P., Valverde, A., Gunnigle, E., Frossard, A., Ramond, J.-B., and Cowan, D. A. (2015). Microbial ecology of hot desert edaphic systems. *FEMS Microbiology Reviews* 39, 203–221. doi: 10.1093/femsre/fuu011

Meier, D. V., Imminger, S., Gillor, O., and Woebken, D. (2021). Distribution of mixotrophy and desiccation survival mechanisms across microbial genomes in an arid biological soil crust community. *Msystems* 6:e00786-20. doi: 10.1128/mSystems.00786-20

Mujakic, I., Andrei, A. S., Shabarova, T., Fecskeova, L. K., Salcher, M. M., Piwosz, K., et al. (2021). Common presence of phototrophic gemmatimonadota in temperate freshwater lakes. *Msystems* 6:e01241-20. doi: 10.1128/mSystems.01241-20

Navarro-Gonzalez, R., Rainey, F. A., Molina, P., Bagaley, D. R., Hollen, B. J., de la Rosa, J., et al. (2003). Mars-like soils in the Atacama Desert, Chile, and the dry limit of microbial life. *Science* 302, 1018–1021. doi: 10.1126/science.1089143

Neilson, J. W., Califf, K., Cardona, C., Copeland, A., van Treuren, W., Josephson, K. L., et al. (2017). Significant impacts of increasing aridity on the arid soil microbiome. *mSystems* 2:e00195-16. doi: 10.1128/mSystems.00195-16

Neilson, J. W., Quade, J., Ortiz, M., Nelson, W. M., Legatzki, A., Tian, F., et al. (2012). Life at the hyperarid margin: novel bacterial diversity in arid soils of the Atacama Desert, Chile. *Extremophiles* 16, 553–566. doi: 10.1007/s00792-012-0454-z

Norman, J. S., King, G. M., and Friesen, M. L. (2017). Rubrobacter spartanus sp nov., a moderately thermophilic oligotrophic bacterium isolated from volcanic soil. *Int. J. Syst. Evol. Microbiol.* 67, 3597–3602. doi: 10.1099/ijsem.0.002175

Oliveros, J.C. (2007–2015). Venny. An interactive tool for comparing lists with Venn's diagrams. Available at: https://bioinfogp.cnb.csic.es/tools/venny/index.html

Ossanna, L., Serrano, K., Jennings, L., Dillon, J., Maier, R., and Neilson, J. W. (2023). Progressive belowground soil development associated with sustainable plant establishment during copper mine waste revegetation. *Appl. Soil Ecol.* 186:104813. doi: 10.1016/j.apsoil.2023.104813

Pascual, J., Garcia-Lopez, M., Bills, G. F., and Genilloud, O. (2016). Longimicrobium terrae gen. nov., sp nov., an oligotrophic bacterium of the under-represented phylum Gemmatimonadetes isolated through a system of miniaturized diffusion chambers. *Int. J. Syst. Evol. Microbiol.* 66, 1976–1985. doi: 10.1099/ijsem.0.000974

Petrenko, M., Friedman, S. P., Fluss, R., Pasternak, Z., Huppert, A., and Jurkevitch, E. (2020). Spatial heterogeneity stabilizes predator-prey interactions at the microscale while patch connectivity controls their outcome. *Environ. Microbiol.* 22, 694–704. doi: 10.1111/1462-2920.14887

Pfeiffer, M., Morgan, A., Heimsath, A., Jordan, T., Howard, A., and Amundson, R. (2021). Century scale rainfall in the absolute Atacama Desert: landscape response and implications for past and future rainfall. *Quat. Sci. Rev.* 254:106797. doi: 10.1016/j.quascirev.2021.106797

Quast, C., Pruesse, E., Yilmaz, P., Gerken, J., Schweer, T., Yarza, P., et al. (2013). The SILVA ribosomal RNA gene database project: improved data processing and web-based tools. *Nucleic Acids Res.* 41, D590–D596. doi: 10.1093/nar/gks1219

R Core Team. (2018). R: A language and environment for statistical computing. *R Foundation for Statistical Computing*. Vienna, Austria Available at: https://www.R-project.org/

Rech, J. A., Quade, J., and Hart, W. S. (2003). Isotopic evidence for the source of Ca and S in soil gypsum, anhydrite and calcite in the Atacama Desert, Chile. *Geochim. Cosmochim. Acta* 67, 575–586. doi: 10.1016/S0016-7037(02)01175-4

Remonsellez, F., Galleguillos, F., Moreno-Paz, M., Parro, V., Acosta, M., and Demergasso, C. (2009). Dynamic of active microorganisms inhabiting a bioleaching industrial heap of low-grade copper sulfide ore monitored by real-time PCR and oligonucleotide prokaryotic acidophile microarray. *Microb. Biotechnol.* 2, 613–624. doi: 10.1111/j.1751-7915.2009.00112.x

Rossello-Mora, R. A., Wagner, M., Amann, R., and Schleifer, K. H. (1995). The abundance of *Zoogloea ramigera* in sewage treatment plants. *Appl. Environ. Microbiol.* 61, 702–707. doi: 10.1128/aem.61.2.702-707.1995

Salter, S. J., Cox, M. J., Turek, E. M., Calus, S. T., Cookson, W. O., Moffatt, M. F., et al. (2014). Reagent and laboratory contamination can critically impact sequence-based microbiome analyses. *BMC Biol.* 12:87. doi: 10.1186/s12915-014-0087-z

Schulze-Makuch, D., Wagner, D., Kounaves, S. P., Mangelsdorf, K., Devine, K. G., de Vera, J. P., et al. (2018). Transitory microbial habitat in the hyperarid Atacama Desert. *Proc. Natl. Acad. Sci. U. S. A.* 115, 2670–2675. doi: 10.1073/pnas.1714341115

Sellstedt, A., and Richau, K. H. (2013). Aspects of nitrogen-fixing Actinobacteria, in particular free-living and symbiotic Frankia. *FEMS Microbiol. Lett.* 342, 179–186. doi: 10.1111/1574-6968.12116

Semenov, A. M. (1991). Physiological bases of oligotrophy of microorganisms and the concept of microbial community. *Microb. Ecol.* 22, 239–247. doi: 10.1007/BF02540226

Severino, R., Froufe, H. J. C., Barroso, C., Albuquerque, L., Lobo-da-Cunha, A., da Costa, M. S., et al. (2019). High-quality draft genome sequence of *Gaiella occulta* isolated from a 150 meter deep mineral water borehole and comparison with the genome sequences of other deep-branching lineages of the phylum Actinobacteria. *Microbiology* 8:e00840. doi: 10.1002/mbo3.840

Shange, R. S., Ankumah, R. O., Ibekwe, A. M., Zabawa, R., and Dowd, S. E. (2012). Distinct soil bacterial communities revealed under a diversely managed agroecosystem. *PLoS One* 7:e40338. doi: 10.1371/journal.pone.0040338

Sterling, J. J., Sakihara, T. S., Brannock, P. M., Pearson, Z. G., Maclaine, K. D., Santos, S. R., et al. (2022). Primary microbial succession in the anchialine ecosystem. *Integr. Comp. Biol.* 62, 275–287. doi: 10.1093/icb/icac087

Stoecker, D. K., Hansen, P. J., Caron, D. A., and Mitra, A. (2017). Mixotrophy in the marine plankton. *Annu. Rev. Mar. Sci.* 9, 311–335. doi: 10.1146/annurev-marine-010816-060617

Tamagnini, P., Axelsson, R., Lindberg, P., Oxelfelt, F., Wunschiers, R., and Lindblad, P. (2002). Hydrogenases and hydrogen metabolism of cyanobacteria. *Microbiol. Mol. Biol. Rev.* 66, 1–20, table of contents. doi: 10.1128/MMBR.66.1.1-20.2002

Tisa, L. S., Oshone, R., Sarkar, I., Ktari, A., Sen, A., and Gtari, M. (2016). Genomic approaches toward understanding the actinorhizal symbiosis: an update on the status of the Frankia genomes. *Symbiosis* 70, 5–16. doi: 10.1007/s13199-016-0390-2

Troussellier, M., Bouvy, M., Courties, C., and Dupuy, C. (1997). Variation of carbon content among bacterial species under starvation condition. *Aquat. Microb. Ecol.* 13, 113–119. doi: 10.3354/ame013113

Trujillo, M. E., Idris, H., Riesco, R., Nouioui, I., Igual, J. M., Bull, A. T., et al. (2017). Pseudonocardia nigra sp. nov., isolated from Atacama Desert rock. *Int. J. Syst. Evol. Microbiol.* 67, 2980–2985. doi: 10.1099/ijsem.0.002063

Valdivia-Silva, J. E., Karouia, F., Navarro-Gonzalez, R., and McKay, C. (2016). Microorganisms, organic carbon, and their relationship with oxidant activity in hyper-arid mars-like soils: implications for soil habitability. *PALAIOS* 31, 1–9. doi: 10.2110/palo.2015.010

Vargas, C., Jebbar, M., Carrasco, R., Blanco, C., Calderon, M. I., Iglesias-Guerra, F., et al. (2006). Ectoines as compatible solutes and carbon and energy sources for the halophilic bacterium *Chromohalobacter salexigens*. *J. Appl. Microbiol.* 100, 98–107. doi: 10.1111/j.1365-2672.2005.02757.x

Vetrovsky, T., and Baldrian, P. (2013). The variability of the 16S rRNA gene in bacterial genomes and its consequences for bacterial community analyses. *PLoS One* 8:e57923. doi: 10.1371/journal.pone.0057923

Viljakainen, V. R., and Hug, L. A. (2021). The phylogenetic and global distribution of bacterial polyhydroxyalkanoate bioplastic-degrading genes. *Environ. Microbiol.* 23, 1717–1731. doi: 10.1111/1462-2920.15409

Vitek, P., Edwards, H. G. M., Jehlicka, J., Ascaso, C., De los Rios, A., Valea, S., et al. (2010). Microbial colonization of halite from the hyper-arid Atacama Desert studied by Raman spectroscopy. *Philos. Trans. R. Soc. A Math. Phys. Eng. Sci.* 368, 3205–3221. doi: 10.1098/rsta.2010.0059

Voigt, C., Klipsch, S., Herwartz, D., Chong, G., and Staubwasser, M. (2020). The spatial distribution of soluble salts in the surface soil of the Atacama Desert and their relationship to hyperaridity. *Glob. Planet. Chang.* 184:103077. doi: 10.1016/j.gloplacha.2019.103077

Warren-Rhodes, K. A., Lee, K. C., Archer, S. D. J., Cabrol, N., Ng-Boyle, L., Wettergreen, D., et al. (2019). Subsurface microbial habitats in an extreme desert mars-analog environment. *Front. Microbiol.* 10:69. doi: 10.3389/fmicb.2019.00069

Wilhelm, M. B., Davila, A. F., Parenteau, M. N., Jahnke, L. L., Abate, M., Cooper, G., et al. (2018). Constraints on the metabolic activity of microorganisms in Atacama surface soils inferred from refractory biomarkers: implications for martian habitability and biomarker detection. *Astrobiology* 18, 955–966. doi: 10.1089/ast.2017.1705

Willems, A. (2013). "The family comamonadaceae" in *The prokaryotes: alphaproteobacteria and betaproteobacteria*. eds. E. Rosenberg, E. F. DeLong, S. Lory, E. Stackebrandt and F. Thompson (Berlin: Springer)

Wu, D. Y., Raymond, J., Wu, M., Chatterji, S., Ren, Q. H., Graham, J. E., et al. (2009). Complete genome sequence of the aerobic CO-oxidizing thermophile *Thermomicrobium roseum*. *PLoS One* 4:e4207. doi: 10.1371/journal.pone.0004207

Yin, Q., Zhang, L., Song, Z.-M., Wu, Y., Hu, Z.-L., Zhang, X.-H., et al. (2018). Euzebya rosea sp. nov., a rare actinobacterium isolated from the East China Sea and analysis of two genome sequences in the genus Euzebya. *Int. J. Syst. Evol. Microbiol.* 68, 2900–2905. doi: 10.1099/ijsem.0.002917

Zeng, Y. H., Nupur, , Wu, N., Madsen, A. M., Chen, X., Gardiner, A. T., et al. (2021). Gemmatimonas groenlandica sp. nov. is an aerobic anoxygenic phototroph in the phylum gemmatimonadetes. *Front. Microbiol.* 11:606612. doi: 10.3389/fmicb.2020.606612

Zhang, X. C., Myrold, D. D., Shi, L. L., Kuzyakov, Y., Dai, H. C., Hoang, D. T. T., et al. (2021). Resistance of microbial community and its functional sensitivity in the rhizosphere hotspots to drought. *Soil Biol. Biochem.* 161:108360. doi: 10.1016/j.soilbio.2021.108360

Zhang, B., Wu, X., Tai, X., Sun, L., Wu, M., Zhang, W., et al. (2019). Variation in actinobacterial community composition and potential function in different soil ecosystems belonging to the arid Heihe River basin of Northwest China. *Front. Microbiol.* 10:2209. doi: 10.3389/fmicb.2019.02209

frontiers | Frontiers in Microbiology

TYPE Correction
PUBLISHED 01 December 2023
DOI 10.3389/fmicb.2023.1327998

OPEN ACCESS

APPROVED BY
Frontiers Editorial Office,
Frontiers Media SA, Switzerland

*CORRESPONDENCE
Cecilia Demergasso
✉ cdemerga@ucn.cl
Julia W. Neilson
✉ jneilson@arizona.edu

RECEIVED 25 October 2023
ACCEPTED 13 November 2023
PUBLISHED 01 December 2023

CITATION
Demergasso C, Neilson JW, Tebes-Cayo C, Véliz R, Ayma D, Laubitz D, Barberán A, Chong-Díaz G and Maier RM (2023) Corrigendum: Hyperarid soil microbial community response to simulated rainfall. *Front. Microbiol.* 14:1327998. doi: 10.3389/fmicb.2023.1327998

Corrigendum: Hyperarid soil microbial community response to simulated rainfall

Cecilia Demergasso[1]*, Julia W. Neilson[2]*, Cinthya Tebes-Cayo[1,3], Roberto Véliz[1], Diego Ayma[4], Daniel Laubitz[5], Albert Barberán[2], Guillermo Chong-Díaz[3] and Raina M. Maier[2]

[1]Biotechnology Center "Profesor Alberto Ruíz", Universidad Católica del Norte, Antofagasta, Chile, [2]Department of Environmental Science, University of Arizona, Tucson, AZ, United States, [3]Department of Geology, Faculty of Engineering and Geological Sciences, Universidad Católica del Norte, Antofagasta, Chile, [4]Department of Mathematics, Faculty of Sciences, Universidad Católica del Norte, Antofagasta, Chile, [5]Steele Steele Children's Research Center, Department of Pediatrics, University of Arizona, Tucson, AZ, United States

KEYWORDS

hyperarid, soil microbiome, soil wetting, extremophiles, oligotrophic microbes, Atacama Desert, mixotroph

A corrigendum on
Hyperarid soil microbial community response to simulated rainfall

by Demergasso, C., Neilson, J. W., Tebes-Cayo, C., Véliz, R., Ayma, D., Laubitz, D., Barberán, A., Chong-Díaz, G., and Maier, R. M. (2023). *Front. Microbiol.* 14:1202266. doi: 10.3389/fmicb.2023.1202266

In the published article, there was an error regarding the affiliation for Diego Ayma. Instead of "Steele Steele Children's Research Center, Department of Pediatrics, University of Arizona, Tucson, AZ, United States," it should be "Department of Mathematics, Faculty of Sciences, Universidad Católica del Norte, Antofagasta, Chile."

The authors apologize for this error and state that this does not change the scientific conclusions of the article in any way. The original article has been updated.

Publisher's note

All claims expressed in this article are solely those of the authors and do not necessarily represent those of their affiliated organizations, or those of the publisher, the editors and the reviewers. Any product that may be evaluated in this article, or claim that may be made by its manufacturer, is not guaranteed or endorsed by the publisher.

Frontiers in Microbiology

Explores the habitable world and the potential of microbial life

The largest and most cited microbiology journal which advances our understanding of the role microbes play in addressing global challenges such as healthcare, food security, and climate change.

Discover the latest Research Topics

See more →

Frontiers

Avenue du Tribunal-Fédéral 34
1005 Lausanne, Switzerland
frontiersin.org

Contact us

+41 (0)21 510 17 00
frontiersin.org/about/contact